MULTI-OMICS APPROACHES TO STUDY PLACENTAL DEVELOPMENT AND DISEASE

EDITED BY: Geetu Tuteja and Michael J. Soares
PUBLISHED IN: Frontiers in Cell and Developmental Biology

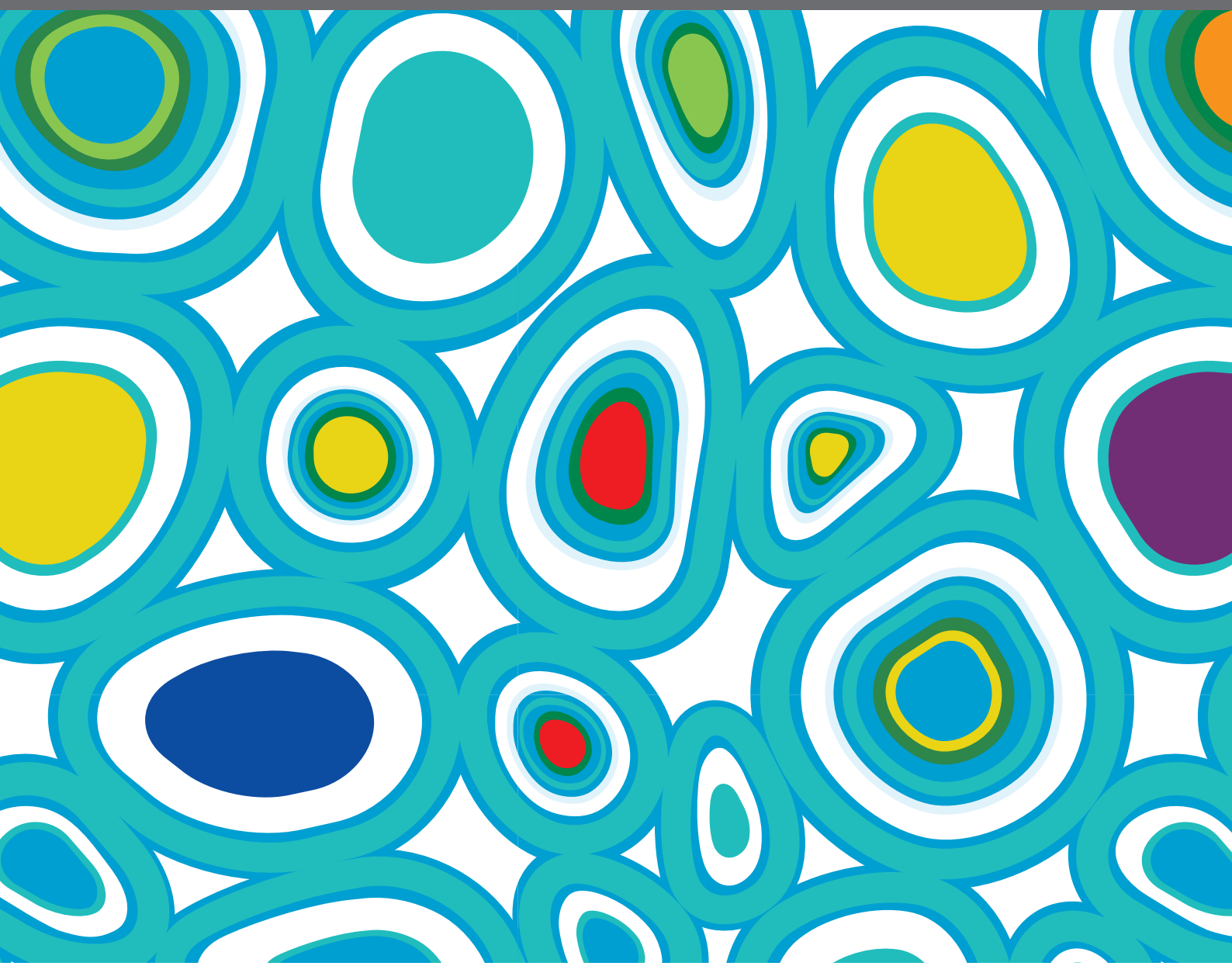

frontiers Research Topics

frontiers

ISSN 1664-8714
ISBN 978-2-88971-953-2
DOI 10.3389/978-2-88971-953-2

About Frontiers

Frontiers is more than just an open-access publisher of scholarly articles: it is a pioneering approach to the world of academia, radically improving the way scholarly research is managed. The grand vision of Frontiers is a world where all people have an equal opportunity to seek, share and generate knowledge. Frontiers provides immediate and permanent online open access to all its publications, but this alone is not enough to realize our grand goals.

Frontiers Journal Series

The Frontiers Journal Series is a multi-tier and interdisciplinary set of open-access, online journals, promising a paradigm shift from the current review, selection and dissemination processes in academic publishing. All Frontiers journals are driven by researchers for researchers; therefore, they constitute a service to the scholarly community. At the same time, the Frontiers Journal Series operates on a revolutionary invention, the tiered publishing system, initially addressing specific communities of scholars, and gradually climbing up to broader public understanding, thus serving the interests of the lay society, too.

Dedication to Quality

Each Frontiers article is a landmark of the highest quality, thanks to genuinely collaborative interactions between authors and review editors, who include some of the world's best academicians. Research must be certified by peers before entering a stream of knowledge that may eventually reach the public - and shape society; therefore, Frontiers only applies the most rigorous and unbiased reviews.
Frontiers revolutionizes research publishing by freely delivering the most outstanding research, evaluated with no bias from both the academic and social point of view. By applying the most advanced information technologies, Frontiers is catapulting scholarly publishing into a new generation.

What are Frontiers Research Topics?

Frontiers Research Topics are very popular trademarks of the Frontiers Journals Series: they are collections of at least ten articles, all centered on a particular subject. With their unique mix of varied contributions from Original Research to Review Articles, Frontiers Research Topics unify the most influential researchers, the latest key findings and historical advances in a hot research area! Find out more on how to host your own Frontiers Research Topic or contribute to one as an author by contacting the Frontiers Editorial Office: frontiersin.org/about/contact

MULTI-OMICS APPROACHES TO STUDY PLACENTAL DEVELOPMENT AND DISEASE

Topic Editors:
Geetu Tuteja, Iowa State University, United States
Michael J. Soares, University of Kansas Medical Center Research Institute, United States

Citation: Tuteja, G., Soares, M. J., eds. (2021). Multi-Omics Approaches to Study Placental Development and Disease. Lausanne: Frontiers Media SA. doi: 10.3389/978-2-88971-953-2

Table of Contents

04 ***Editorial: Multi-Omics Approaches to Study Placental Development and Disease***
Geetu Tuteja and Michael J. Soares

06 ***Knockdown of Splicing Complex Protein PCBP2 Reduces Extravillous Trophoblast Differentiation Through Transcript Switching***
Danai Georgiadou, Souad Boussata, Remco Keijser, Dianta A. M. Janssen, Gijs B. Afink and Marie van Dijk

19 ***Integrating High-Throughput Approaches and* in vitro *Human Trophoblast Models to Decipher Mechanisms Underlying Early Human Placenta Development***
Bum-Kyu Lee and Jonghwan Kim

30 ***RNA Network Interactions During Differentiation of Human Trophoblasts***
Tianjiao Chu, Jean-Francois Mouillet, Zhishen Cao, Oren Barak, Yingshi Ouyang and Yoel Sadovsky

43 ***Omics Approaches to Study Formation and Function of Human Placental Syncytiotrophoblast***
Adam Jaremek, Mariyan J. Jeyarajah, Gargi Jaju Bhattad and Stephen J. Renaud

66 ***Coordinated Expressional Landscape of the Human Placental miRNome and Transcriptome***
Rain Inno, Triin Kikas, Kristiina Lillepea and Maris Laan

86 ***Single Nucleus RNA Sequence (snRNAseq) Analysis of the Spectrum of Trophoblast Lineages Generated From Human Pluripotent Stem Cells* in vitro**
Teka Khan, Arun S. Seetharam, Jie Zhou, Nathan J. Bivens, Danny J. Schust, Toshihiko Ezashi, Geetu Tuteja and R. Michael Roberts

97 ***Transcriptomic Drivers of Differentiation, Maturation, and Polyploidy in Human Extravillous Trophoblast***
Robert Morey, Omar Farah, Sampada Kallol, Daniela F. Requena, Morgan Meads, Matteo Moretto-Zita, Francesca Soncin, Louise C. Laurent and Mana M. Parast

121 ***Characterization of the Primary Human Trophoblast Cell Secretome Using Stable Isotope Labeling With Amino Acids in Cell Culture***
Fredrick J. Rosario, Sammy Pardo, Trond M. Michelsen, Kathryn Erickson, Lorna Moore, Theresa L. Powell, Susan T. Weintraub and Thomas Jansson

132 ***Transcriptomics and Other Omics Approaches to Investigate Effects of Xenobiotics on the Placenta***
Cheryl S. Rosenfeld

145 ***Mechanistic Target of Rapamycin Complex 2 Regulation of the Primary Human Trophoblast Cell Transcriptome***
Fredrick J. Rosario, Amy Catherine Kelly, Madhulika B. Gupta, Theresa L. Powell, Laura Cox and Thomas Jansson

frontiers in Cell and Developmental Biology

EDITORIAL
published: 08 November 2021
doi: 10.3389/fcell.2021.798966

Editorial: Multi-Omics Approaches to Study Placental Development and Disease

Geetu Tuteja[1]* *and Michael J. Soares*[2,3,4,5]

[1]Department of Genetics, Development and Cell Biology, Iowa State University, Ames, IA, United States, [2]Institute for Reproduction and Perinatal Research, University of Kansas Medical Center, Kansas City, KS, United States, [3]Department of Pathology and Laboratory Medicine, University of Kansas Medical Center, Kansas City, KS, United States, [4]Center for Perinatal Research, Children's Mercy Research Institute, Kansas City, MO, United States, [5]Department of Obstetrics and Gynecology, University of Kansas Medical Center, Kansas City, KS, United States

Keywords: trophoblast, placenta, multi-omics, pregnancy, syncytiotrophoblast, extravillous trophoblast, invasion, differentiation

Editorial on the Research Topic

Multi-Omics Approaches to Study Placental Development and Disease

The placenta carries out diverse roles that are critical for the establishment and maintenance of pregnancy, including anchoring the fetus to the uterine wall, transporting nutrients and oxygen to the fetus, eliminating waste, shielding the fetus from the maternal immune system, and producing hormones. Defects in placental development can lead to pregnancy complications that impact both the mother and fetus, yet our understanding of the mechanisms regulating placental cell differentiation and other placental processes, especially at the systems level, remains limited. The research topic on "Multi-Omics Approaches to Study Placental Development and Disease" in *Frontiers in Cell and Developmental Biology* includes a series of 10 articles. Each article describes at least one omics-based approach used to aid in our understanding of placental development, and many articles provide novel candidates that could be further characterized for a functional role in the placenta.

For those who are not familiar with how omics-approaches have been used to study placental development, this issue includes three comprehensive review articles. One review article by Lee and Kim describes *cis*-regulation and *trans*-regulation studies in mouse and human placenta, and also describes recent *in vitro* human trophoblast model systems. The second review article by Jaremek et al. focuses on syncytiotrophoblast (STB), which facilitate human embryo implantation and later in development are the placenta cells that are in direct contact with maternal blood and facilitate nutrient transport. In addition to describing STB development, Jaremek et al. describe diverse omics-approaches that have been used to study STB, including metabolomics and proteomics. Rather than focusing on normal mechanisms of development, the third review article by Rosenfeld describes how endocrine disrupting chemicals and other environmental toxicants impact placental development by disrupting placental gene expression, DNA methylation patterns, and metabolomic profiles.

The placenta is composed of multiple types of trophoblast cells, and even the same type of trophoblast can have different properties during development. It is therefore important to identify and distinguish trophoblast cells that exhibit unique properties. To this end, this issue includes a research article by Morey et al. that profiles extravillous trophoblast from 1st trimester and term placenta to identify gene networks and novel candidates that could regulate early extravillous trophoblast differentiation or extravillous trophoblast maturation. In another article by Khan et al., single-nucleus RNA-seq was used on a trophoblast cell culture model, and two distinct populations of syncytiotrophoblast were identified, requiring further investigation as to how these populations relate to early human placentation.

OPEN ACCESS

Edited and reviewed by:
Rosalind M. John,
Cardiff University, United Kingdom

***Correspondence:**
Geetu Tuteja
geetu@iastate.edu

Specialty section:
This article was submitted to Developmental Epigenetics, a section of the journal Frontiers in Cell and Developmental Biology

Received: *20 October 2021*
Accepted: *25 October 2021*
Published: *08 November 2021*

Citation:
Tuteja G and Soares MJ (2021) Editorial: Multi-Omics Approaches to Study Placental Development and Disease. Front. Cell Dev. Biol. 9:798966. doi: 10.3389/fcell.2021.798966

In addition to understanding changes in expression of protein-coding genes during placental development or in pregnancy complications, it is also necessary to understand changes in the expression of non-coding RNAs, which are known to have regulatory functions and are less well studied in the placenta. This issue includes two studies that focus on identification of non-coding RNAs that could be important for placenta function. In the first article by Inno et al., microRNA expression was assessed in normal human placentas from all three trimesters, as well as placentas obtained from women with different pregnancy disorders. In addition to relating the microRNA data to mRNA expression, the study by Inno et al. highlights several specific microRNAs that may regulate placental development. In the second article by Chu et al., non-coding RNAs and mRNAs that are misregulated when primary human trophoblast differentiation was hindered were identified, and a co-expression network constructed to understand the relationship between different RNAs in the trophoblast differentiation system. It is of note that another article in this issue, by Rosario et al. could add yet another layer to our understanding of primary human trophoblast differentiation, as the secretome was assayed in these cells. Additional studies aimed at understanding the profiles of secreted proteins in the placenta are necessary, as transcriptome data alone will not give a full understanding of the complex regulatory processes taking place in the placenta.

While the previous studies use omics-approaches to identify novel candidates associated with placental development, omics-approaches can also be used to better understand the role of specific genes in the placenta. For example, Georgiadou et al. found that when PCBP2, an RNA splicing complex protein, was knocked-down in HTR-8/SVneo cells, global mRNA expression levels were not impacted, although, interestingly, the splicing pattern of genes involved in cellular organization, maintenance, and proliferation were impacted. In another article published by Rosario et al. in this issue, mTORC2, which regulates amino acid and folate transport in the placenta, was silenced in primary human trophoblast. Analysis of genes differentially regulated upon mTORC2 silencing led to the identification of a link between mTOR signaling, angiogenesis, micronutrient transport, and inflammation.

In summary, the application of omics-based technologies in the human placenta as well as trophoblast model systems have, and will continue, to provide a more complete picture of genes and pathways important for placental development and disease.

AUTHOR CONTRIBUTIONS

GT and MS wrote the editorial and approved the submitted version.

Conflict of Interest: The authors declare that the research was conducted in the absence of any commercial or financial relationships that could be construed as a potential conflict of interest.

Publisher's Note: All claims expressed in this article are solely those of the authors and do not necessarily represent those of their affiliated organizations, or those of the publisher, the editors and the reviewers. Any product that may be evaluated in this article, or claim that may be made by its manufacturer, is not guaranteed or endorsed by the publisher.

frontiers in Cell and Developmental Biology

ORIGINAL RESEARCH
published: 20 May 2021
doi: 10.3389/fcell.2021.671806

Knockdown of Splicing Complex Protein PCBP2 Reduces Extravillous Trophoblast Differentiation Through Transcript Switching

*Danai Georgiadou, Souad Boussata, Remco Keijser, Dianta A. M. Janssen, Gijs B. Afink and Marie van Dijk**

Reproductive Biology Laboratory, Amsterdam Reproduction and Development Research Institute, Amsterdam UMC, University of Amsterdam, Amsterdam, Netherlands

OPEN ACCESS

Edited by:
Geetu Tuteja, Iowa State University, United States

Reviewed by:
Daniel Vaiman, Institut National de la Santé et de la Recherche Médicale (INSERM), France
Masayuki Kobayashi, Akita Prefectural University, Japan

***Correspondence:**
Marie van Dijk
m.vdijk@amsterdamumc.nl

Specialty section:
This article was submitted to Cell Growth and Division, a section of the journal Frontiers in Cell and Developmental Biology

Received: *24 February 2021*
Accepted: *06 April 2021*
Published: *20 May 2021*

Citation:
Georgiadou D, Boussata S, Keijser R, Janssen DAM, Afink GB and van Dijk M (2021) Knockdown of Splicing Complex Protein PCBP2 Reduces Extravillous Trophoblast Differentiation Through Transcript Switching. Front. Cell Dev. Biol. 9:671806. doi: 10.3389/fcell.2021.671806

Mutations in the *LINC-HELLP* non-coding RNA (*HELLPAR*) have been associated with familial forms of the pregnancy-specific HELLP syndrome. These mutations negatively affect extravillous trophoblast (EVT) differentiation from a proliferative to an invasive state and disturb the binding of RNA splicing complex proteins PCBP1, PCBP2, and YBX1 to *LINC-HELLP*. In this study, by using both *in vitro* and *ex vivo* experiments, we investigate if these proteins are involved in the regulation of EVT invasion during placentation. Additionally, we study if this regulation is due to alternative mRNA splicing. HTR-8/SVneo extravillous trophoblasts and human first trimester placental explants were used to investigate the effect of siRNA-mediated downregulation of *PCBP1*, *PCBP2,* and *YBX1* genes on the differentiation of EVTs. Transwell invasion assays and proliferation assays indicated that upon knockdown of PCBP2 and, to a lesser extent, YBX1 and PCBP1, EVTs fail to differentiate toward an invasive phenotype. The same pattern was observed in placental explants where PCBP2 knockdown led to approximately 80% reduction in the number of explants showing any EVT outgrowth. Of the ones that still did show EVT outgrowth, the percentage of proliferating EVTs was significantly higher compared to explants transfected with non-targeting control siRNAs. To further investigate this effect of PCBP2 silencing on EVTs, we performed whole transcriptome sequencing (RNA-seq) on HTR-8/SVneo cells after PCBP2 knockdown. PCBP2 knockdown was found to have minimal effect on mRNA expression levels. In contrast, PCBP2 silencing led to a switch in splicing for a large number of genes with predominant functions in cellular assembly and organization, cellular function and maintenance, and cellular growth and proliferation and the cell cycle. EVTs, upon differentiation, alter their function to be able to invade the decidua of the mother by changing their cellular assembly and their proliferative activity by exiting the cell cycle. PCBP2 appears to be a paramount regulator of these differentiation mechanisms, where its disturbed binding to *LINC-HELLP* could contribute to dysfunctional placental development as seen in the HELLP syndrome.

Keywords: differentiation, invasion, splicing, placenta, extravillous trophoblast, HELLP syndrome, PCBP2

INTRODUCTION

The HELLP syndrome is a pregnancy complication occurring in approximately 0.5% of pregnancies and is characterized by Hemolysis, Elevated Liver enzymes, and Low Platelets in the mother. Symptoms specific to the HELLP syndrome can arise as a severe manifestation of preeclampsia, but they can also occur without *de novo* hypertension, which is an essential criterion for the diagnosis of preeclampsia. The HELLP symptoms can occur from the 20th week of pregnancy or even postpartum, but their cause originates in the first trimester. In those first months reduced invasion of extravillous trophoblasts (EVT) into the maternal decidua leads to hampered spiral artery remodeling causing insufficient blood flow to the fetus (Abildgaard and Heimdal, 2013). The dysfunction of the EVT can be due to a failure to undergo Epithelial Mesenchymal Transition (EMT) in which the trophoblasts transform from a proliferative epithelial trophoblast into an invasive mesenchymal type of cell (Davies et al., 2016). How this failure is triggered is still unknown.

Previously, by genome-wide linkage analysis of Dutch women with a familial form of the HELLP syndrome, we identified a long non-coding RNA on chromosome 12q23, *LINC-HELLP* (official gene symbol *HELLPAR*) (Van Dijk et al., 2012). It was shown that mutations in *LINC-HELLP* identified in HELLP families negatively affected EVT differentiation either by inducing proliferation rate or by causing cell cycle exit as shown by a decrease in both proliferation and invasion (van Dijk et al., 2015). Furthermore, as LincRNAs predominantly function through interactions with proteins, multiple interacting proteins were identified predominantly clustering in two functional networks, i.e., RNA splicing and the ribosome. The RNA splicing proteins further investigated were YBX1, PCBP1, and PCBP2. Binding of *LINC-HELLP* RNA to the YBX1 and PCBP2 proteins was confirmed to be influenced by the HELLP mutations carried (van Dijk et al., 2015).

YBX1 is one of three Y box binding protein family members containing a highly conserved cold shock protein domain and is able to bind to both DNA and RNA. It thereby has multiple functions such as regulating apoptosis, cell proliferation, differentiation, and stress response through regulation of transcription and translation, mRNA splicing, DNA repair, and mRNA packaging (Suresh et al., 2018).

PCBP1 and PCBP2 are two of the four widely expressed poly(C)-binding protein family members. PCBP1 is an intronless highly similar homolog of PCBP2, and both are abundantly expressed in different tissues and species. PCBP1 and PCBP2 each contain three RNA binding domains with high affinity for binding to C-rich polypyrimidine motifs (Makeyev and Liebhaber, 2002). Similar to YBX1, they also have been implicated in regulating cell proliferation and differentiation, as such behaving as oncogenes (Guo and Jia, 2018).

In the current study, we further investigated the role of the RNA splicing proteins YBX1, PCBP1, and PCBP2 in the regulation of EVT invasion during first trimester placenta development. For this we first performed siRNA mediated knockdown on EVT-like HTR-8/SVneo cells and first trimester placental explants followed by experiments measuring proliferation and invasion. The data show that specifically knockdown of PCBP2 leads to EVT differentiation failure. Next, we studied if this regulation of EVT invasion by PCBP2 is associated with alternative mRNA splicing, which is a prominent function of PCBP2 (Ji et al., 2016). We again performed knockdown experiments in HTR-8/SVneo cells followed by whole genome transcriptome sequencing (RNA-Seq). The data obtained was analyzed to detect both differential expression as well as differential transcript usage, showing that PCBP2 mainly affects splicing and not so much mRNA levels *per se*. Several transcripts of important EMT regulators are affected by PCBP2 providing evidence for the major role of PCBP2 in EVT differentiation in which its disturbed binding to *LINC-HELLP* could contribute to dysfunctional placental development.

MATERIALS AND METHODS

Cell Culture and Transfection

HTR-8/SVneo EVT cells were obtained from ATCC (LGC Standards, France) and cultured in RPMI media supplemented with FBS, HEPES, sodium pyruvate, glucose, and pen/strep at 37 °C, 5% CO_2. For transfection experiments, in 6 well plates 200,000 HTR-8/SVneo cells in 2 ml medium were transfected with 160 pmol *PCBP1, PCBP2,* or *YBX1* siRNAs (Qiagen, Germany, Flexitube Genesolution, a package of four preselected siRNAs targeting the different genes) or non-targeting siRNAs (Qiagen) using 10 μl XtremeGENE HP transfection reagent (Sigma). Forty-eight hours after transfection, the cells were harvested and stored at −80 °C for RNA or protein preparations or harvested to be used in invasion assays.

RNA Isolation and Quantitative PCR

RNA was isolated from transfected HTR-8/SVneo cells (described above) using the RNeasy Mini Kit (Qiagen) followed by cDNA synthesis using random hexamers and M-MLV reverse transcriptase (Promega). Quantitative PCRs were performed in triplicate on a Lightcycler 480 instrument using SYBR Green Supermix (Roche) according to the manufacturer's protocol in combination with primers specific for YBX1, PCBP1, PCBP2, and PSMD4 and YWHAZ as reference genes. For validation of transcript switching primers specific for FLNB exon 30 and reference exons, NCOR2 exon 8 and reference exons, and EXOC7 exon 7 and reference exons were used. Primer sequences can be found in **Supplementary Table 1**. The relative quantity (RQ) of gene expression was calculated using $RQ = 2^{-\Delta Ct}$, where ΔCt = Ct target gene − Ct reference genes (geometric mean).

Western Blot

HTR-8/SVneo cell lysates from transfected HTR-8/SVneo cells (described above) were prepared using RIPA buffer supplemented with cOmplete protease inhibitor cocktail (Roche) and PhosSTOP phosphatase inhibitor cocktail (Roche). Samples were prepared in LDS sample buffer (Life technologies), run on a NuPAGE 4–12% Bis-Tris Gel (Invitrogen), and subsequently blotted on an Immobilon PVDF membrane. Blotted proteins were visualized using Revert total Protein stain (Li-Cor)

according to protocol and measured on the Odyssey Imaging System (Li-Cor). For visualization of specific proteins, the blots were blocked with blocking buffer (Li-Cor) and incubated overnight at 4°C with primary antibodies YBX1 (1:200, Santa Cruz Biotechnology, sc-101198), PCBP1 (1:200, Santa Cruz Biotechnology, sc-137249), or PCBP2 (1:3,000, Santa Cruz Biotechnology, sc-101136). Next, Goat Anti-Mouse secondary antibodies (1:15,000, LI-COR, 926-32210) were used for 1 h at room temperature. Final imaging of the membrane was done on the Odyssey Imaging System.

Invasion and Proliferation Assays

To measure invasive capacity, 50,000 transfected and harvested HTR-8/SVneo cells were seeded in medium without FBS on 100 μl 16× diluted (final concentration approximately 0.6 mg/ml) Matrigel (Corning) coated 8.0 μm pore cell culture inserts. To induce invasion the inserts were placed in wells containing medium with FBS. Invasion took place for 48 h after which the membranes were fixed in 4% PFA and cells attached on the inside of the insert were removed. The membranes were mounted in Vectashield (VectorLabs) with DAPI (50 μM) (ThermoFisher) and coverslipped, after which the cells on the underside of the membrane were counted. To count the cells pictures were taken of nine random fields per membrane using a Leica Fluorescent microscope after which ImageJ was used to quantify the number of cells per picture. To measure proliferation, 48 h after siRNA transfection alamarBlue™ reagent (Invitrogen) was added to the cells according to protocol. Four hours later fluorescence was measured on a Synergy microplate reader.

First Trimester Placental Explants

Human first trimester placenta specimens ($n = 12$) were obtained from the HIS Mouse Facility of the Amsterdam UMC, location AMC, Amsterdam. All material has been collected from donors at the time of elective terminations of pregnancy from whom a written informed consent for the use of the material for research purposes had been obtained by the Bloemenhove clinic. Small fragments (15–20 mg wet weight) of placental villi from 5 to 12 weeks gestation were dissected from the placenta and placed in 48 well culture plates coated with 3 mg/ml collagen I (R&D systems). Transfection was done 24 h later with 80 pmol *PCBP1, PCBP2,* or *YBX1* siRNAs (Qiagen, Germany, Flexitube Genesolution, a package of four preselected siRNAs targeting the different genes) or non-targeting siRNAs (Qiagen) using 2.5 μl XtremeGENE HP transfection reagent (Sigma) in a total volume of 250 μl. Placental villous explants were cultured for a maximum of 5 days at 5% O_2 and 37 °C in serum free DMEM/F12 media supplemented with pen/strep. Images of the explants were taken on a Leica microscope daily to monitor changes in outgrowth. At day 4 or 5 explants were fixed in 4% PFA and embedded for immunohistochemistry.

Immunohistochemistry

Embedded first trimester placental explants were sectioned and subjected to standard immunohistochemistry procedures. Antigen retrieval was performed using microwave pre-treatment in sodium citrate buffer. Blocking was done in 5% BSA, followed by overnight primary antibody incubations in 1% BSA at 4 °C. The following primary antibodies were used: YBX1 (1:200, Santa Cruz Biotechnology, sc-101198), PCBP1 (1:200, Santa Cruz Biotechnology, sc-137249), and PCBP2 (1:200, Santa Cruz Biotechnology, sc-101136) that stain for the respective proteins, HLA-G (1:100, Novus Biologicals, NB500-302) that was used as a marker for EVTs, and phosphoH3(Ser10) (1:200, Sigma, 09–797) that was used as a marker for cell proliferation. Finally, Powervision Poly-HRP secondary antibodies were used followed by DAB staining and counterstaining using haematoxilin. ImageJ was used to count the number of proliferating extravillous trophoblasts.

RNA-Seq

RNA was isolated from transfected HTR-8/SVneo cells (described above) using the RNeasy Mini Kit (Qiagen). RNA-Seq libraries from 4 non-targeting control and 4 PCBP2 silenced samples all obtained in the same experiment were prepared using the KAPA RNA Hyperprep kit including ribodepletion (Roche). The 8 sample libraries were multiplexed across two sequencing lanes and paired-end (2 bp × 150 bp read length) sequencing was performed on an Illumina HiSeq4000 sequencer. The unmapped paired FASTQ files were processed with Cutadapt (v2.9) (Martin, 2011), and Sickle (v1.33) to remove adaptor sequences and trim low-quality bases. Quality control assessment was performed using FastQC (v0.11.9).

Gene Expression Analysis

STAR aligner (v2.7.3a) (Dobin et al., 2013) was used to align the reads against to the Human reference genome (GRCh38). The BAM alignments were position-sorted and indexed with Samtools (v1.10) and fragment counts were obtained with FeautureCounts (v2.0.0) (Liao et al., 2014). Reads were counted at the gene level and multi-mapped reads were discarded.

All statistical calculations were performed in R programming language (v3.6.3). Differential expression analysis was performed with R package EdgeR (v3.26.8) (Robinson et al., 2009). Only genes with an expression level greater than 0.2 count per million in at least four samples were included in the analysis. Genes exhibiting differential expression with $p < 0.05$ were included in further downstream analyses.

Differential Transcript Usage

Kallisto (v0.46.2) (Bray et al., 2016) was used to pseudo-align the paired FASTQ files, using an index based on the ENSEMBL GRCh38 Homo sapiens transcriptome. For statistical testing to identify differential transcript usage the transcript-level counts obtained from Kallisto were imported using tximport (v1.12.3) and analyzed with DRIMSeq (v1.12.0) Bioconductor packages (Soneson et al., 2015; Robinson and Nowicka, 2016) following the protocol described by Love et al. (2018) including the following filters for a transcript: it has a count of at least 10 in at least four samples, it has a relative abundance proportion of at least 0.1 in at least 4 samples, and the total count of the corresponding gene is at least 10 in all eight samples.

Ingenuity Pathway Analysis and MEME Motif Analysis

For functional enrichment analysis Ingenuity Pathway Analysis (Qiagen) was performed on the gene list obtained through the analysis of differential transcript usage. For the MEME motif analysis we constructed a data file containing all intronic regions (up to 500 bp) directly adjacent to the in- and excluded exons or transcription start sites of the genes in **Table 2** and the genes of **Table 3** that were found to also be differentially spliced in our study. MEME motif enrichment (v5.2.0) (Bailey et al., 2015) was then used to identify significant (E value < 0.05) motifs in our data file. The E-value of the motif is based on its log likelihood ratio, width, sites, the background frequencies, and the size of the training set. The final width of the motif identified was determined by increasing the maximum width until a peak in relative entropy (mean bit score) of the motif was obtained.

Statistics

Statistical analyses were performed using Graphpad Prism version 8 software using unpaired t-tests in case of two groups or with one-way or two-way ANOVA followed by a Dunnett's multiple comparison test when comparing multiple groups. P values ≤ 0.05 were considered significant.

RESULTS

In EVT-Like Cells RNA Splicing Complex Proteins Affect Differentiation

To study the effect of YBX1, PCBP1, and PCBP2 on EVT-like HTR-8/SVneo cell differentiation we transiently transfected the cells with siRNAs directed against the three mRNAs and compared their effect to the non-targeting control siRNAs. Significant knockdown was confirmed on mRNA (**Figure 1A**) and protein level (**Figure 1B**) by quantitative PCR and Western blot, respectively. In transwell invasion assays knockdown of YBX1, PCBP1, and PCBP2 led to a significant decrease in the number of invaded cells for siRNAs against YBX1 and PCBP2 (**Figure 1C**), while knockdown of PCBP1 had no clear effect. On the other hand, knockdown of PCBP2 only significantly increased the proliferation rate of these cells (**Figure 1D**), while PCBP1 and YBX1 knockdown did not lead to an apparent effect on proliferation. These results together indicate that *in vitro* knockdown of two out of three proteins negatively affect EMT, with PCBP2 providing the strongest effect.

PCBP2 Knockdown Diminishes Outgrowth of First Trimester Placental Explants

To investigate the *ex vivo* effects of knockdown of YBX1, PCBP1, and PCBP2 we transiently transfected human first trimester placental explants. Using non-targeting control siRNAs to transfect the explants leads to almost half of the explants showing EVT outgrowth. Outgrowth is slightly reduced to around 35% when transfecting *PCBP1* or *YBX1* siRNAs, while transfection with *PCBP2* siRNAs led to almost 90% of the explants not demonstrating any EVT outgrowth, which is a reduction compared to non-targeting control siRNAs of around 80% (**Figures 2A,B**). Knockdown in the explants was confirmed by immunohistochemistry using antibodies recognizing YBX1, PCBP1, and PCBP2 (**Figure 2C**). Predominant expression of all three proteins was observed in the villous cytotrophoblasts while the syncytiotrophoblast borders of the explants remained negative. Immunohistochemistry was also used to study the amount of proliferating EVTs in the explants that did show EVT outgrowth. EVTs were identified by staining with HLA-G antibody. In parallel sections we also stained for phosphoH3(Ser10) to identify proliferating cells undergoing mitosis (**Figure 2D**). We quantified the percentage of proliferating EVT and normalized, within different placenta samples, the results obtained in explants treated with *YBX1*, *PCBP1,* or *PCBP2* siRNAs to the results obtained transfecting with non-targeting control siRNAs. This showed that knockdown of PCBP2 led to a significant increase in proliferating EVTs compared to control, while YBX1 siRNAs led to a significant decrease in proliferation (**Figure 2E**). The combined results obtained *in vitro* and *ex vivo* clearly point out that knockdown of PCBP2 leads to failure of the EVTs to undergo proper EMT.

PCBP2 Silencing Does Not Have a Pronounced Effect on Differential Gene Expression

We performed whole transcriptome sequencing (RNA-Seq) on PCBP2 silenced HTR-8/SVneo cells and non-targeted controls, and the obtained data was analyzed. The data show a large number of differentially expressed genes between the control and PCBP2 knockdown samples, albeit at relatively low fold induction (**Figure 3**). Only 126 genes show more than $\pm$ 1 $\log_2$_fold change in expression levels in combination with an adjusted p value < 0.05 (**Supplementary Table 2**). Of these, only 14 genes have a $\log_2$_fold change of more than $\pm$ 1.5. Additionally, expression levels of these 14 genes are low and only two genes (*PCBP2* and *PLCE1-AS1*) have a logCPM above 0. From these results we concluded that the effect PCBP2 has on EVT differentiation cannot be explained by differential gene expression.

PCBP2 Silencing Leads to Transcript Switching of Proteins Involved in Cell Differentiation

Because PCBP2 is a known RNA splicing protein, we next sought to analyze differential transcript usage upon PCBP2 silencing. For this, we used DRIMSeq to identify differential splicing between PCBP2 knockdown and control samples. This identified a total number of 310 genes that show differential transcript usage (**Supplementary Table 3**). These genes were submitted into Ingenuity Pathway Analysis of which the pathway analysis results are presented in **Table 1**. The top scoring networks and functions show that PCBP2 silencing leads to differential splicing of genes with predominant functions in cellular assembly and

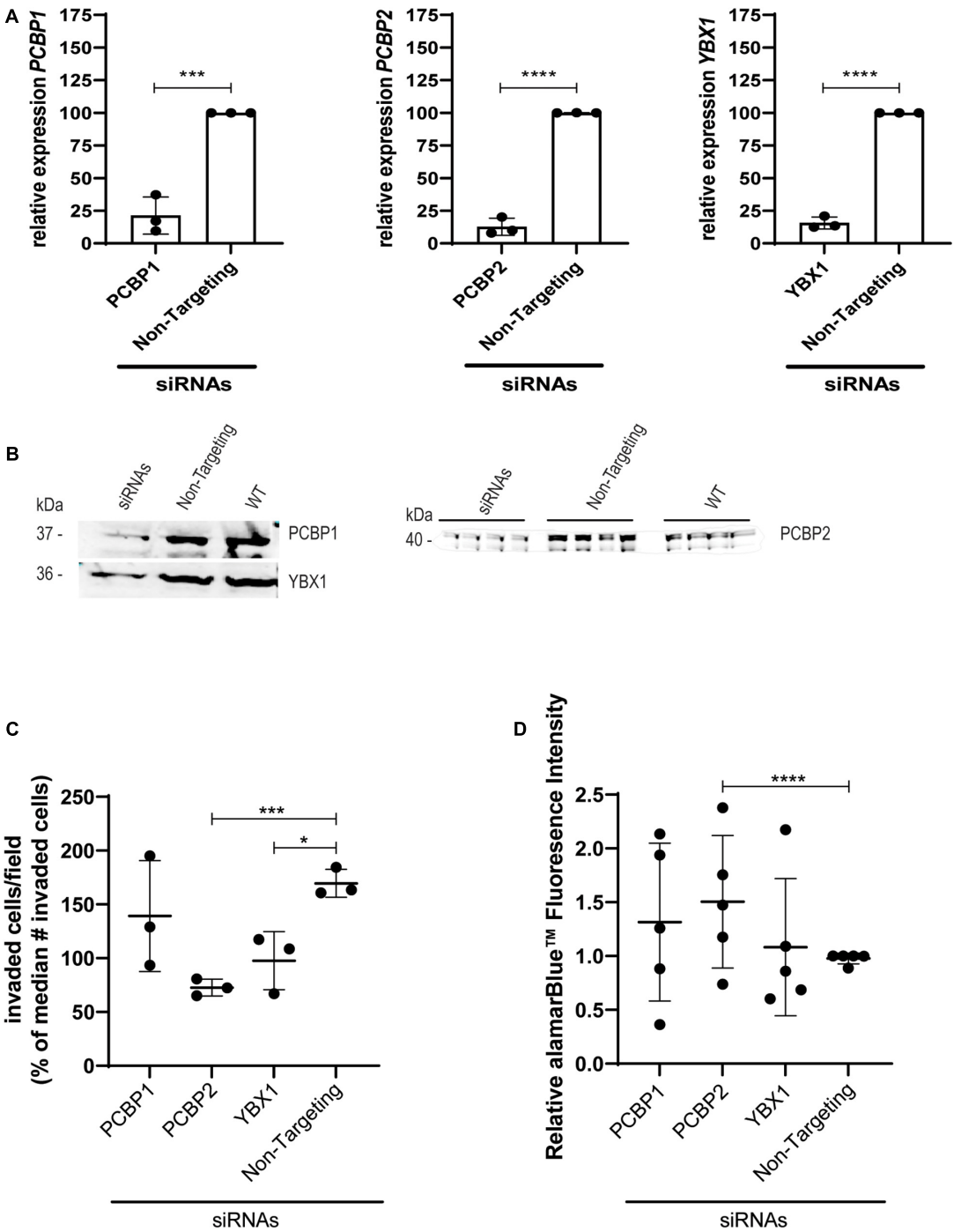

FIGURE 1 | Upon knockdown of YBX1, PCBP1, and PCBP2 EVT-like cells fail to differentiate toward an invasive phenotype. **(A)** qPCR results demonstrating successful mRNA downregulation of *PCBP1*, *PCBP2,* and *YBX1* in HTR-8/SVneo cells after transfection with respective siRNAs. An siRNA not targeting any known mammalian gene was used as a control. Normalization was done using the geometric mean of reference genes *PSMD4* and *YWHAZ*. Experiments were repeated 3 times using 3 replicates per treatment. **(B)** Successful siRNA-induced downregulation of target genes on protein level as shown by Western blot. Equal protein loading control was performed by total protein Revert stain (**Supplementary Figure 1**). **(C)** Transwell invasion assays show that PCBP2 and YBX1 downregulation leads to a significant decrease in invasive behavior of EVT-like cells. Experiments were repeated 3 times using 6 replicates per treatment. **(D)** Quantification of proliferation using alamarBlue™ solution. The proliferation rate of EVT-like cells with downregulated expression of PCBP2 was increased. Experiments were repeated five times using nine replicates per treatment. Data are presented as mean ± SD and tested with two-way ANOVA followed by Dunnett's multiple comparisons test or with a Student's *t*-test in case of two data sets. *Indicates $p < 0.05$; *** indicates $p < 0.001$; **** indicates $p < 0.0001$.

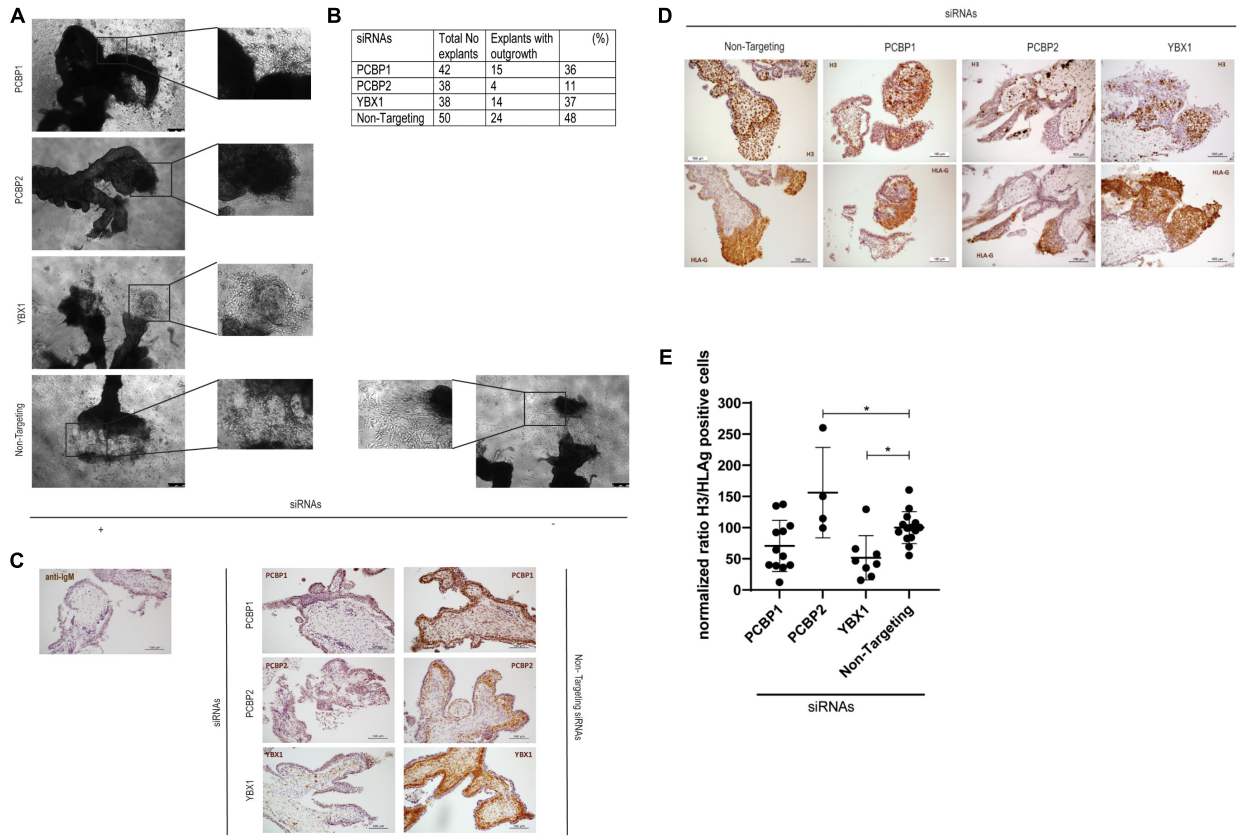

siRNAs	Total No explants	Explants with outgrowth	(%)
PCBP1	42	15	36
PCBP2	38	4	11
YBX1	38	14	37
Non-Targeting	50	24	48

FIGURE 2 | Downregulation of PCBP2 severely affects first trimester placental explant outgrowth. **(A)** Representative images of first trimester placental explants treated with siRNAs targeting *PCPB1*, *PCBP2*, *YBX1,* or non-targeting siRNAs that developed EVT outgrowth. **(B)** Number and percentage of explants that showed EVT outgrowth out of the total number of explants that were treated with the different siRNAs. PCBP2 downregulation leads to the strongest inhibition of explant outgrowth amongst the genes tested. **(C)** Representative images of immunohistochemical staining for PCBP1, PCBP2, and YBX1 proteins in first trimester placental explants transfected with the different siRNAs. The stainings demonstrate successful downregulation of the respective proteins. No staining was observed in mouse IgG control staining. Antibody-specific DAB staining is shown in brown, hematoxylin counterstain was used to stain nuclei blue. **(D)** Representative phosphoH3(Ser10) and HLA-G immunohistochemical stainings of first trimester placental explants after transfection with *PCBP1, PCBP2, YBX1,* or non-targeting siRNAs to identify proliferating cells undergoing mitosis and to indicate the location of EVTs, respectively. **(E)** Quantification of the ratio of H3/HLA-G representing proliferating EVTs indicates a significant induction of proliferating EVTs upon PCBP2 knockdown while YBX1 silencing leads to a reduction of proliferating EVTs. Within the different conditions each dot represents an explant with quantifiable outgrowths. In total this analysis was performed on explants derived from five different first trimester placentas. Data are presented as mean ± SD and tested with one-way ANOVA followed by Dunnett's multiple comparisons test. *Indicates $p < 0.05$.

organization, cellular function and maintenance, and cellular growth and proliferation and the cell cycle.

Validation of Transcript Switching by Two Distinct Approaches

We validated the DRIMSeq results by two different approaches, i.e., quantitative PCR and a comparison with published results. To be able to validate the differential splicing effects by quantitative PCR we added four additional criteria: the transcript specific adjusted p value had to be < 0.05, the PCBP2/non-targeting ratio of the transcript proportion had to be > 1.5 or < 0.67, the gene had to be represented by at least two significant transcripts to be able to pinpoint the exon spliced differently between the two transcripts, and the mean counts of the transcript had to be at least 300 in the DRIMSeq analysis in either the non-targeting control or PCBP2 knockdown samples. The latter criterion was introduced to have enough copies to yield large enough differences to detect by qPCR based on preliminary qPCR experiments on detecting the published transcript switch occurring in *RUNX1* (Ghanem et al., 2018). This yielded a list of 10 genes, presented in **Table 2**. We chose three genes to validate by qPCR: two genes that showed exon exclusion upon PCBP2 knockdown, i.e., *NCOR2* and *EXOC7*, and one gene showing inclusion, i.e., *FLNB*. For each gene we designed primers recognizing the included/excluded exon and a set of primers recognizing all transcripts of the specific gene expressed in HTR-8/SVneo cells. We were able to validate differential splicing upon PCBP2 knockdown in all three genes (**Figure 4**).

For our second validation approach we used the data on differential splicing mediated by PCBP2 described in two publications (Ji et al., 2016; Ghanem et al., 2018) and summarized in **Table 3**. In these two publications transcript switching was studied upon co-silencing PCBP2 and PCBP1, except for

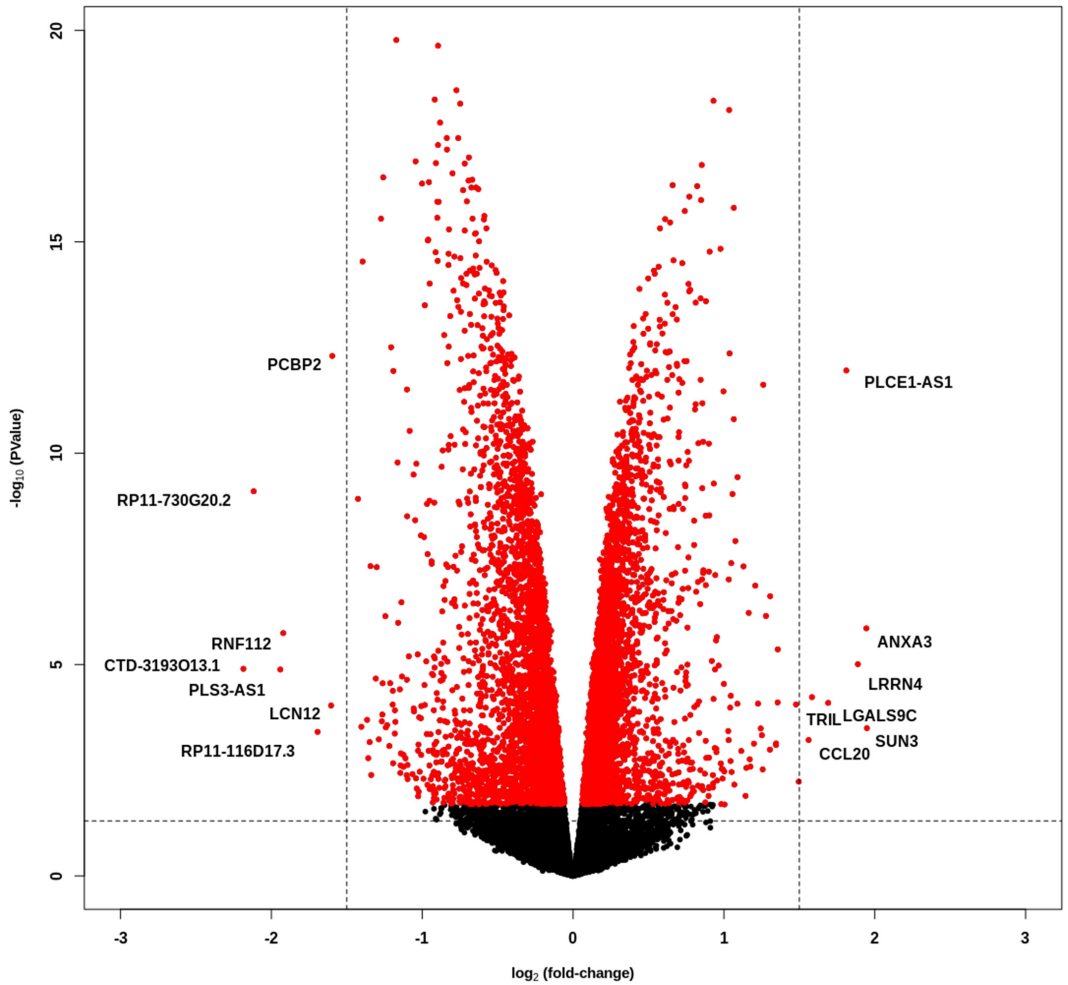

FIGURE 3 | PCBP2 knockdown does not lead to pronounced differential gene expression. Volcano plot of statistical significance against $\log_2$–fold change between PCBP2 knockdown and non-targeted control samples. The vertical dashed lines indicate a $\log_2$-fold change < -1.5 and > 1.5, respectively. Red dots denote genes with significant differential expression ($p < 0.05$).

TABLE 1 | Ingenuity Pathway Analysis of differentially spliced genes.

Total # of differentially spliced genes: 310		
Top 5 Molecular and Cellular Functions	**– log (*p*-value) range**	**# Molecules**
Cellular Development	2.7–9.1	106
Cellular Growth and Proliferation	2.7–9.1	104
Cell Death and Survival	2.7–9.1	120
Cellular Assembly and Organization	2.7–7.9	95
Cellular Function and Maintenance	2.7–7.9	111
Top 5 Networks	**Score**	**# Molecules**
Cancer, Dermatological Diseases and Conditions, Hereditary Disorder	59	31
Cellular Development, Hematological Disease, Hereditary Disorder	46	26
Cellular Assembly and Organization, Cellular Function and Maintenance, Cell Cycle	43	25
Cell Cycle, Cellular Assembly and Organization, Hematological System Development and Function	41	24
Cell-To-Cell Signaling and Interaction, Cell-mediated Immune Response, Cellular Function and Maintenance	34	21

TABLE 2 | Differentially spliced genes.

Total # of differentially spliced genes: 10 (transcript adjusted *p* value < 0.05; ratio transcript proportion > 1.5 or < 0.67; gene represented by ≥ 2 transcripts; mean counts > 300)

Gene	Transcript 1	Ratio proportion PCBP2/NT transcript 1	-log(adj p) transcript 1	Transcript 2	Ratio proportion PCBP2/NT transcript 2	-log(adj p) transcript 2	Function
GNAL	ENST00000585642.5	21.74	8.3	ENST00000590228.1	0.54	1.5	Stimulatory G protein alpha subunit which couples dopamine type 1 receptors and adenosine A2A receptors.
IFI16	ENST00000368131.8	2.14	6.2	ENST00000368132.7	0.56	9.2	Cytokine involved in DNA binding, transcriptional regulation, and protein-protein interactions; Inhibits cell growth in the Ras/Raf signaling pathway.
CMC1	ENST00000418849.2	1.82	3.9	ENST00000396610.6	0.56	1.7	Stabilizes the biogenesis of mitochondrial respiratory chain complex IV.
NCOR2	ENST00000404121.6	1.78	15.4	ENST00000356219.7	0.60	9.0	Nuclear receptor co-repressor involved in chromatin structure modification
ANKRD13D	ENST00000308440.11	1.73	1.8	ENST00000511455.7	0.39	3.0	Interacts with ubiquitin chains for rapid internalization
FLNB	ENST00000295956.9	1.57	20.6	ENST00000358537.7	0.46	33.7	Actin-binding protein regulating cytoskeleton dependent cell proliferation and migration; Skipping of exon 30 is associated with EMT
SMG1P4	ENST00000381448.8	1.56	2.4	ENST00000380598.4	0.11	2.4	Pseudogene of SMG1; SMG1 is involved in nonsense-mediated mRNA decay as part of the mRNA surveillance complex.
EXOC7	ENST00000332065.9	1.54	21.8	ENST00000589210.6	0.66	11.1	Part of exocyst complex which has a critical role in vesicular trafficking and the secretory pathway; Undergoes isoform switching mediated by ESRP1, a splicing factor that regulates EMT
SEC31A	ENST00000513858.5	1.53	4.0	ENST00000348405.8	0.53	10.4	Involved in vesicle budding from the endoplasmic reticulum and is required for ER-Golgi transport
TMEM237	ENST00000286196.9	1.52	3.0	ENST00000621467.4	0.64	2.3	Involved in WNT signaling; Required for ciliogenesis

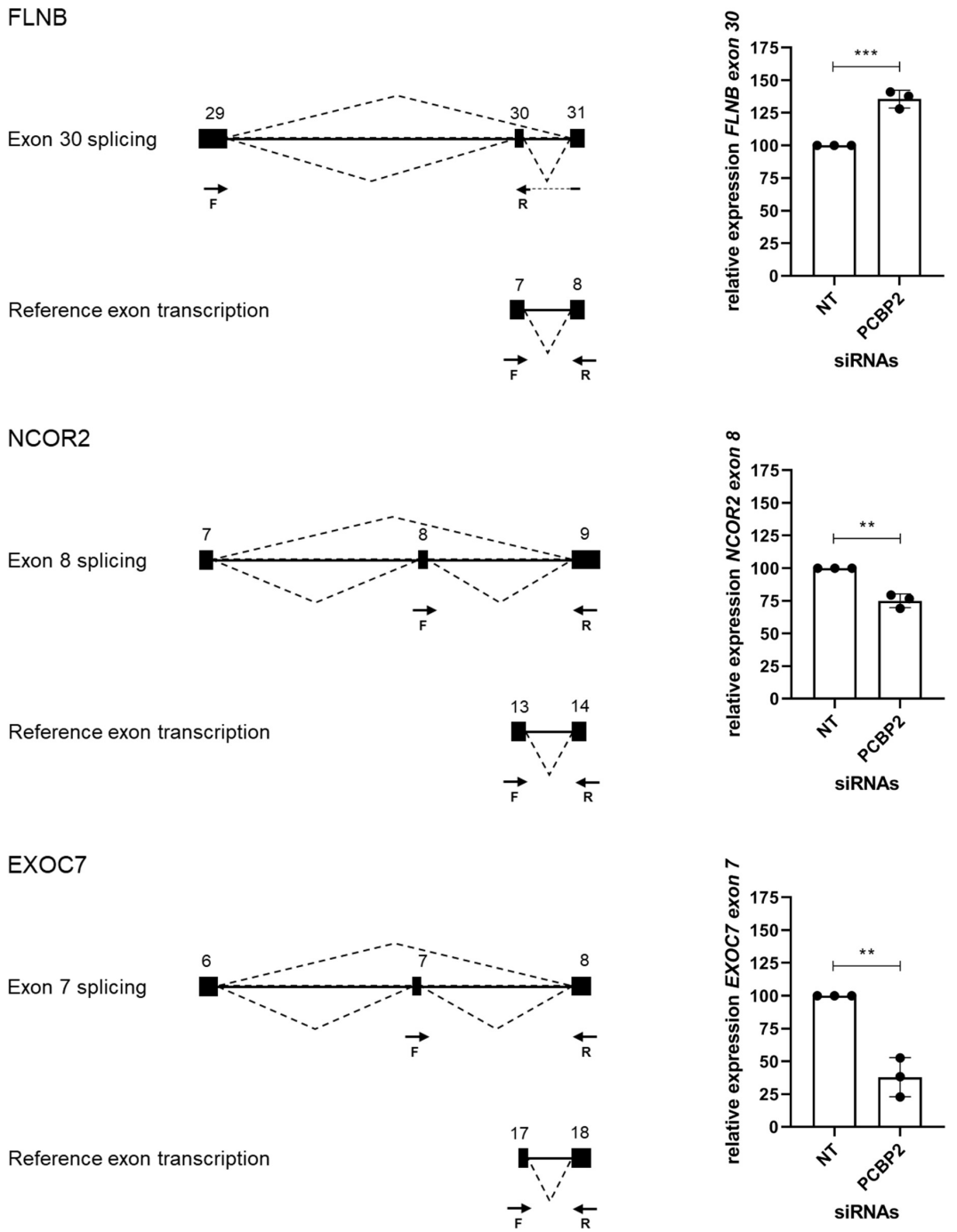

FIGURE 4 | Validation of PCBP2 knockdown effect on splicing. Validation by qPCR of three genes identified by RNA-Seq to undergo transcript switching upon silencing of PCBP2. Transcription of reference exons of each of the genes was used for normalization. The specific included or excluded exons are depicted in the diagrams which also indicate the location of the primers used (forward [F] and reverse [R]). *FLNB* shows significant inclusion of exon 30 upon PCBP2 silencing, while *NCOR2* and *EXOC7* show significant exclusion of exon 8 and 7, respectively. Experiments were repeated three times using 3–4 replicates per treatment. Data are presented as mean ± SD and tested with a Student's *t*-test. ** Indicates $p < 0.01$; *** indicates $p < 0.001$.

studying *RUNX1* transcript usage in which specific knockdown of PCBP2 was performed. For *TARS2* and *CTTN* transcript expression analysis both co-silencing as well as silencing PCBP2 only was studied. We were able to confirm both genes that were already described to be differentially spliced upon PCBP2 silencing, i.e., *RUNX1* and *CTTN*. Additionally, for two genes (*CDK2* and *WNK4*) we could confirm significant exon exclusion upon PCBP2 knockdown. It should be noted that the

TABLE 3 | Comparison between this study and published results.

Gene	Published skipped exon	Published gene silenced	Our result	Transcript	Ratio proportion PCBP2/NT	−log(adj p)
RUNX1	6	PCBP2[#]	Skipped exon 6	ENST00000399240.5	1.55	1.9
CDK2	5	PCBP1/2[$]	Skipped exon 5	ENST00000354056.4	1.62	3.6
SH2B1	9	PCBP1/2	No exon 9 exclusion			
TARS2	14	PCBP1/2; PCBP2 (n.s.)	No exon 14 exclusion			
CTTN	11	PCBP1/2; PCBP2	Skipped exon 11	ENST00000376561.7	1.51	5.9
VKORC1	2	PCBP1/2	No exon 2 exclusion			
TRPT1	7	PCBP1/2	No exon 7 exclusion			
TFR2	2	PCBP1/2	Not expressed			
AP1G2	3	PCBP1/2	No exon 3 exclusion			
WNK4	8	PCBP1/2	Skipped exon 8	ENST00000587705.5	4.42	1.7
ARHGAP4	9	PCBP1/2	Not expressed			
STAT2	18	PCBP1/2	No exon 18 exclusion			

[#]*Depletion of PCBP2 only;* [$]*Co-depletion of PCBP1 and PCBP2; n.s., not significant.*

differentially spliced transcripts of *RUNX1* and *WNK4* are not present in **Supplementary Table 3** as the relative abundance proportion of the transcripts was below the cutoff value of 0.1. Taken together, by two distinct methods we were able to validate the results obtained by DRIMSeq analysis of the RNA-Seq data.

PCBP2-Specific C-Rich Motif Adjacent to Skipped Exons

Ji et al. (2016) identified a motif (YYYYCWSCCY) that is highly enriched immediately adjacent (5′ and/or 3′) to the exons whose splicing was skipped upon co-depletion of PCBP1 and PCBP2. We therefore sought to identify a motif that might be more specific to PCBP2 only. This is because the data published by Ji et al. and the data presented in **Table 3** suggest that both PCBP1 and PCBP2 can affect the splicing of certain exons but that this might be specific to either PCBP1 or PCBP2 in certain cases. We constructed a data file containing all intronic regions affected by PCBP2 knockdown (up to 500 bp) directly adjacent to the significantly excluded exons of the genes in **Table 3** and added all intronic regions adjacent to all excluded exons of the genes of **Table 2**. To the data file we also added all intronic regions adjacent to included exons upon PCBP2 knockdown and added the 5′ and 3′ regions surrounding transcription start sites that were excluded upon PCBP2 knockdown. This data file was submitted to MEME motif enrichment analysis using a 0-order background model which provided us with a highly significant motif (CCCTSCYCTCCC), also depicted in **Figure 5A**. When studying the locations of the motif (**Supplementary Figure 2**) it was seen that in the group of genes that exclude an exon upon PCBP2 knockdown, the motif was found in 75% of the intronic regions < 100 bp 5′ and/or < 100 bp 3′ from the excluded exon (**Figure 5B**). The motif was additionally found in the adjacent regions in one of the two genes that included an exon upon PCBP2 silencing, but the motif was absent in the adjacent regions of the four genes with excluded transcription start sites upon PCBP2 knockdown. To be informed about the significance of the association between the presence of the motif adjacent to excluded exons compared to the presence of the motif adjacent to excluded transcription start sites and included exons a Fisher's exact test was performed. Although proportionally apparent, the test did not reach statistical significance ($p = 0.070$) due to the low total number of regions included in the dataset. The motif identified in our small dataset was compared to the motif identified by Ji et al. (2016) using the Tomtom motif comparison tool (Bailey et al., 2015). This analysis indicated that the two motifs significantly match (**Figure 5C**), providing evidence that the motif we identified is highly comparable, but different, which might explain the higher specificity to PCBP2 induced splicing. Finally, we extracted data from the ENCODE project generated by Van Nostrand et al. (2020), which demonstrates direct binding of PCBP2 to several of the motif locations presented in **Supplementary Figure 2**. The ENCODE data were produced by performing enhanced CLIP (crosslinking and immunoprecipitation) *in vivo* binding experiments in HepG2 cells to identify binding of PCBP2 to its RNA targets. Within this dataset, although generated in a different cell type, PCBP2 is shown to directly bind to the actual motifs identified by our MEME analysis (**Supplementary Figure 3**), providing further evidence for the validity of the PCBP2-specific motif identified.

DISCUSSION

In this study we show by *in vitro* and *ex vivo* experiments that proteins directly bound to the HELLP syndrome associated long non-coding RNA *LINC-HELLP* are involved in the regulation of EVT invasion during placentation. In both HTR-8/SVneo EVT-like cells and in human first trimester placental explants we show that, upon knockdown, PCBP2, and to a lesser extend PCBP1 and YBX1, are able to negatively affect EVT differentiation through EMT inhibition. This was shown by a reduction in transwell invasion and an increase in proliferation in HTR-8/SVneo cells. First trimester explants treated with *PCBP2* siRNAs predominantly failed to produce any EVT outgrowth. Of the ones that still did show EVT outgrowth, the percentage of proliferating EVTs was significantly higher compared to controls.

A

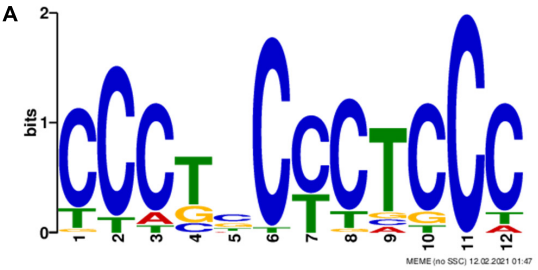

E = 7.1E-10

B

	Exon exclusion	Exon inclusion	Transcription start site exclusion
Number of genes	8	2	4
Motif present < 100bp 5' and / or 3'	6	1	0

C

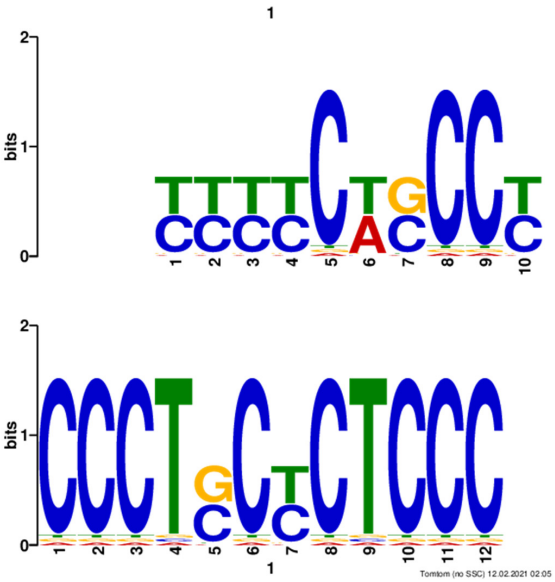

P = 1.46E-2

FIGURE 5 | PCBP2-specific C-rich motif adjacent to exons skipped upon PCBP2 knockdown. **(A)** MEME motif enrichment analysis revealed a highly significant motif (E-value: 7.1E-10) in the intronic regions surrounding in- or excluded exons or transcription start sites upon PCBP2 silencing. **(B)** The motif was found in 75% of genes in regions within 100 bp from the exon boundaries of exons excluded upon PCBP2 silencing (see locations of motif in **Supplementary Figure 2**). The adjacent regions of excluded transcription start sites did not contain the motif, while the regions adjacent to the included exon of one of the two genes contained the motif. **(C)** The motif identified in the data set of this study (lower motif) was compared to the motif identified by Ji et al. (2016) (upper motif) by the Tomtom motif comparison tool which showed that the motifs significantly matched (*p*-value: 1.46E-2), but that they are not the same.

We further investigated the effect of PCBP2 silencing on EVTs by performing whole transcriptome sequencing. Interestingly, PCBP2 knockdown only had a marginal effect on mRNA expression levels, providing evidence that the effect PCBP2 has on EVT differentiation does not occur through regulating downstream gene expression.

On the opposite, a large number of genes was found to show a switch in splicing upon PCBP2 silencing. Pathway analysis

on the genes showing differential transcript usage revealed that these genes are associated with functions in cellular assembly and organization, cellular function and maintenance, and cellular growth and proliferation and the cell cycle. The majority of genes presented in **Table 2** also conduct these functions. When EVTs differentiate from a proliferative epithelial cell to an invasive mesenchymal type of cell through Epithelial Mesenchymal Transition, they indeed alter their cellular assembly and their proliferative activity by exiting the cell cycle. Hereby they gain the capacity to invade the decidua of the mother.

Recently, Ruano et al. (2021) published the first systematic analysis of alternative splicing in third trimester placentas by microarray comparing preeclamptic and intra uterine growth restricted (IUGR) placentas to healthy controls. In their study, genes differentially spliced in preeclamptic placentas were predominantly associated with extracellular matrix organization pathways, genes differentially spliced in IUGR placentas were associated with hypoxia and hormone metabolism, while preeclampsia and IUGR both were associated with exocytosis. Especially the pathways associated with their third trimester preeclamptic placentas show overlap with the pathways identified in our PCBP2 silenced EVT-like cells. However, there are also some clear differences indicating that PCBP2, as can be expected, is not the sole regulator of alternative splicing occurring in placentas with pregnancy complications. The most interesting gene in this respect is *FLT1,* well known for its differential transcript usage in preeclampsia, where soluble transcripts of the gene are highly increased in preeclamptic pregnancies (Jebbink et al., 2011). Ruano et al. indeed show alternative splicing of *FLT1* in their third placental samples compared to controls, while *FLT1* is not differentially spliced in our dataset, indicating that PCBP2 does not regulate the splicing of *FLT1*.

For the majority of differentially spliced genes the actual effect on protein function is unknown and in pathway analysis it is merely assumed that the alternative transcript will lead to changes in function. However, for one of the genes validated by qPCR, *FLNB*, it actually has been proven that skipping of its exon 30 induces EMT as this exon encodes a hinge region that promotes EMT by releasing the FOXC1 transcription factor from an inhibitory complex (Li et al., 2018). In our study we confirm this result as we show that PCBP2 knockdown, reducing EMT, leads to inclusion of exon 30.

Additionally, in our study we identified a C-rich motif that is specifically located adjacent to exons that are excluded upon PCBP2 silencing. This motif is significantly comparable, but not the same, as the motif originally identified by Ji et al. (2016) who used co-depletion of PCBP1 and PCBP2. Our identified motif might therefore be more specific for binding and subsequent regulation by PCBP2.

To conclude, in this study we show that PCBP2, through mRNA splicing, might be a paramount regulator of extravillous trophoblast EMT differentiation, where its disturbed binding to *LINC-HELLP* could contribute to dysfunctional placental development as seen in the HELLP syndrome.

DATA AVAILABILITY STATEMENT

The datasets presented in this study can be found in online repositories. The names of the repository/repositories and accession number(s) can be found below: https://www.ncbi.nlm.nih.gov/, PRJNA691146.

ETHICS STATEMENT

The studies involving human participants were reviewed and approved by Medical Ethical Committee of the Academic Medical Center, Amsterdam. The patients/participants provided their written informed consent to participate in this study.

AUTHOR CONTRIBUTIONS

GA and MD designed the study. DG, SB, and DJ performed the experiments. DG, SB, DJ, and MD analyzed the data. RK and GA performed the RNA-Seq analysis. DG and MD wrote the manuscript. All authors reviewed and approved the final version of the manuscript.

ACKNOWLEDGMENTS

The authors thank the Amsterdam UMC location AMC HIS mouse facility and the donors and participating staff of the Bloemenhove clinic (Heemstede, Netherlands) for providing human first trimester placenta tissue specimens. The advice obtained from Aldo Jongejan (Department of Epidemiology and Data Science, Amsterdam UMC) on RNA-Seq analyses is greatly acknowledged. The RNA-Seq analyses were carried out on the Dutch national e-infrastructure with the support of SURF Cooperative.

SUPPLEMENTARY MATERIAL

The Supplementary Material for this article can be found online at: https://www.frontiersin.org/articles/10.3389/fcell.2021.671806/full#supplementary-material

REFERENCES

Abildgaard, U., and Heimdal, K. (2013). Pathogenesis of the syndrome of hemolysis, elevated liver enzymes, and low platelet count (HELLP): a review. *Eur. J. Obstet. Gynecol. Reprod. Biol.* 166, 117–123. doi: 10.1016/j.ejogrb.2012.09.026

Bailey, T. L., Johnson, J., Grant, C. E., and Noble, W. S. (2015). The MEME suite. *Nucleic Acids Res.* 43, W39–W49. doi: 10.1093/nar/gkv416

Bray, N. L., Pimentel, H., Melsted, P., and Pachter, L. (2016). Near-optimal probabilistic RNA-seq quantification. *Nat. Biotechnol.* 34, 525–527. doi: 10.1038/nbt.3519

Davies, E. J., Pollheimer, J., Yong, H. E. J., Kokkinos, M. I., Kalionis, B., Knöfler, M., et al. (2016). Epithelial-mesenchymal transition during extravillous trophoblast differentiation. *Cell Adhes. Migr.* 10, 310–321. doi: 10.1080/19336918.2016.1170258

Dobin, A., Davis, C. A., Schlesinger, F., Drenkow, J., Zaleski, C., Jha, S., et al. (2013). STAR: ultrafast universal RNA-seq aligner. *Bioinformatics* 29, 15–21. doi: 10.1093/bioinformatics/bts635

Ghanem, L. R., Kromer, A., Silverman, I. M., Ji, X., Gazzara, M., Nguyen, N., et al. (2018). Poly(C)-binding protein Pcbp2 enables differentiation of definitive erythropoiesis by directing functional splicing of the Runx1 transcript. *Mol. Cell. Biol.* 38:e00175–18. doi: 10.1128/mcb.00175-18

Guo, J., and Jia, R. (2018). Splicing factor poly(rC)-binding protein 1 is a novel and distinctive tumor suppressor. *J. Cell. Physiol.* 234, 33–41. doi: 10.1002/jcp.26873

Jebbink, J., Keijser, R., Veenboer, G., van der Post, J., Ris-Stalpers, C., and Afink, G. (2011). Expression of placental FLT1 transcript variants relates to both gestational hypertensive disease and fetal growth. *Hypertension* 58, 70–76. doi: 10.1161/HYPERTENSIONAHA.110.164079

Ji, X., Park, J. W., Bahrami-Samani, E., Lin, L., Duncan-Lewis, C., Pherribo, G., et al. (2016). αcP binding to a cytosine-rich subset of polypyrimidine tracts drives a novel pathway of cassette exon splicing in the mammalian transcriptome. *Nucleic Acids Res.* 44, 2283–2297. doi: 10.1093/nar/gkw088

Li, J., Choi, P. S., Chaffer, C. L., Labella, K., Hwang, J. H., Giacomelli, A. O., et al. (2018). An alternative splicing switch in FLNB promotes the mesenchymal cell state in human breast cancer. *Elife* 7:e37184. doi: 10.7554/eLife.37184

Liao, Y., Smyth, G. K., and Shi, W. (2014). FeatureCounts: an efficient general purpose program for assigning sequence reads to genomic features. *Bioinformatics* 30, 923–930. doi: 10.1093/bioinformatics/btt656

Love, M. I., Soneson, C., and Patro, R. (2018). Swimming downstream: statistical analysis of differential transcript usage following Salmon quantification. *F1000Res* 7:952. doi: 10.12688/f1000research.15398.3

Makeyev, A. V., and Liebhaber, S. A. (2002). The poly(C)-binding proteins: a multiplicity of functions and a search for mechanisms. *RNA* 8, 265–278. doi: 10.1017/S1355838202024627

Martin, M. (2011). Cutadapt removes adapter sequences from high-throughput sequencing reads. *EMBnet J.* 17, 10–12. doi: 10.14806/ej.17.1.200

Robinson, M. D., McCarthy, D. J., and Smyth, G. K. (2009). edgeR: a Bioconductor package for differential expression analysis of digital gene expression data. *Bioinformatics* 26, 139–140. doi: 10.1093/bioinformatics/btp616

Robinson, M. D., and Nowicka, M. (2016). DRIMSeq: a Dirichlet-multinomial framework for multivariate count outcomes in genomics. *F1000Res.* 5:1356. doi: 10.12688/f1000research.8900.2

Ruano, C. S. M., Apicella, C., Jacques, S., Gascoin, G., Gaspar, C., Miralles, F., et al. (2021). Alternative splicing in normal and pathological human placentas is correlated to genetic variants. *Hum. Genet.* doi: 10.1007/s00439-020-02248-x

Soneson, C., Love, M. I., and Robinson, M. D. (2015). Differential analyses for RNA-seq: transcript-level estimates improve gene-level inferences. *F1000Res.* 4:1521. doi: 10.12688/f1000research.7563.2

Suresh, P. S., Tsutsumi, R., and Venkatesh, T. (2018). YBX1 at the crossroads of non-coding transcriptome, exosomal, and cytoplasmic granular signaling. *Eur. J. Cell Biol.* 97, 163–167. doi: 10.1016/j.ejcb.2018.02.003

Van Dijk, M., Thulluru, H. K., Mulders, J., Michel, O. J., Poutsma, A., Windhorst, S., et al. (2012). HELLP babies link a novel lincRNA to the trophoblast cell cycle. *J. Clin. Invest.* 122, 4003–4011. doi: 10.1172/JCI65171

van Dijk, M., Visser, A., Buabeng, K. M. L., Poutsma, A., van der Schors, R. C., and Oudejans, C. B. M. (2015). Mutations within the LINC-HELLP non-coding RNA differentially bind ribosomal and RNA splicing complexes and negatively affect trophoblast differentiation. *Hum. Mol. Genet.* 24, 5475–5485. doi: 10.1093/hmg/ddv274

Van Nostrand, E. L., Freese, P., Pratt, G. A., Wang, X., Wei, X., Xiao, R., et al. (2020). A large-scale binding and functional map of human RNA-binding proteins. *Nature* 583, 711–719. doi: 10.1038/s41586-020-2077-3

Conflict of Interest: The authors declare that the research was conducted in the absence of any commercial or financial relationships that could be construed as a potential conflict of interest.

frontiers in Cell and Developmental Biology

REVIEW
published: 02 June 2021
doi: 10.3389/fcell.2021.673065

Integrating High-Throughput Approaches and *in vitro* Human Trophoblast Models to Decipher Mechanisms Underlying Early Human Placenta Development

Bum-Kyu Lee[1]* *and Jonghwan Kim*[2]*

[1] Department of Biomedical Sciences, Cancer Research Center, University at Albany-State University of New York, Rensselaer, NY, United States, [2] Department of Molecular Biosciences, Center for Systems and Synthetic Biology, The University of Texas at Austin, Austin, TX, United States

OPEN ACCESS

Edited by:
Geetu Tuteja,
Iowa State University, United States

Reviewed by:
Toshihiko Ezashi,
University of Missouri, United States
Mana Parast,
University of California, San Diego, United States

***Correspondence:**
Bum-Kyu Lee
blee6@albany.edu
Jonghwan Kim
jonghwankim@mail.utexas.edu

Specialty section:
This article was submitted to Developmental Epigenetics, a section of the journal Frontiers in Cell and Developmental Biology

Received: 26 February 2021
Accepted: 04 May 2021
Published: 02 June 2021

Citation:
Lee B-K and Kim J (2021) Integrating High-Throughput Approaches and in vitro Human Trophoblast Models to Decipher Mechanisms Underlying Early Human Placenta Development. Front. Cell Dev. Biol. 9:673065. doi: 10.3389/fcell.2021.673065

The placenta is a temporary but pivotal organ for human pregnancy. It consists of multiple specialized trophoblast cell types originating from the trophectoderm of the blastocyst stage of the embryo. While impaired trophoblast differentiation results in pregnancy disorders affecting both mother and fetus, the molecular mechanisms underlying early human placenta development have been poorly understood, partially due to the limited access to developing human placentas and the lack of suitable human *in vitro* trophoblast models. Recent success in establishing human trophoblast stem cells and other human *in vitro* trophoblast models with their differentiation protocols into more specialized cell types, such as syncytiotrophoblast and extravillous trophoblast, has provided a tremendous opportunity to understand early human placenta development. Unfortunately, while high-throughput research methods and omics tools have addressed numerous molecular-level questions in various research fields, these tools have not been widely applied to the above-mentioned human trophoblast models. This review aims to provide an overview of various omics approaches that can be utilized in the study of human *in vitro* placenta models by exemplifying some important lessons obtained from omics studies of mouse model systems and introducing recently available human *in vitro* trophoblast model systems. We also highlight some key unknown questions that might be addressed by such techniques. Integrating high-throughput omics approaches and human *in vitro* model systems will facilitate our understanding of molecular-level regulatory mechanisms underlying early human placenta development as well as placenta-associated complications.

Keywords: placenta, trophoblast, trophoblast stem cells, human placenta models, transcriptomes, epigenomes, omics approaches

INTRODUCTION

As a transient but multifunctional organ essential for the proper development of the fetus in placental mammals, the placenta plays a central role in multiple processes during pregnancy, such as gas and nutrient exchange, hormone production, and immunological protection (Rossant and Cross, 2001). Despite these important roles, the placenta has not received sufficient attention, remaining one of the least studied organs in the body (Cao and Fleming, 2016). It is noteworthy that a recent large-scale mouse knockout (KO) study has revealed that 68% of lethal mouse lines show morphological abnormality of the placenta (Perez-Garcia et al., 2018). The prevalence of placental deformities in KO of embryonic lethal genes emphasizes the significance of the placenta for the proper development of embryos, although this has not yet been systematically confirmed in humans.

The placenta originates from the trophectoderm (TE) of the blastocyst stage of the developing embryo, and it consists of multiple trophoblast cell types, including cytotrophoblasts (CT) and more specialized syncytiotrophoblasts (ST) and extravillous trophoblasts (EVT) in humans (Perez-Garcia et al., 2018). Abnormal trophoblast lineage development results in placental dysfunctions, which can cause morbidity and mortality in both mother and fetus. Defective placentas not only contribute to maternal insulin resistance, preeclampsia (PE), and gestational hypertension, but also result in premature growth of the fetus. These adverse effects often persist long after birth and predispose offspring to various chronic adult disorders, such as diabetes and cardiovascular and mental diseases (Hales and Barker, 2001; Barker and Thornburg, 2013; Courtney et al., 2018). Although the etiologies of pregnancy disorders are often multifactorial, prior research has suggested a direct link between the defect in trophoblast differentiation and pregnancy-related complications, such as PE and intrauterine growth restriction (IUGR) (Chen et al., 2002; Ergaz et al., 2005; Uzan et al., 2011).

Although the placenta is essential, limited access to the human placenta, particularly during the early stages of pregnancy, has hindered the molecular-level understanding of both normal and abnormal placenta development. For many years, trophoblast carcinoma cells, primary CT, and mouse or rat trophoblast stem cells (TSCs) have been used as *in vitro* models for trophoblast differentiation despite some drawbacks (Nagamatsu et al., 2004; Bilban et al., 2010; Latos and Hemberger, 2016; Dietrich et al., 2020), Mouse TSCs (mTSCs) have been extensively studied in combination with various research tools, including high-throughput approaches, revealing numerous key regulators, including transcription factors (TFs) and their regulatory mechanisms, and enhancing our understanding of general trophoblast development (Prudhomme and Morey, 2016; Lee et al., 2019; Ullah et al., 2020). Nevertheless, as human and mouse pregnancy do not share all physiological features, and recently established human TSCs (hTSCs) do not robustly express several previously known mTSC-specific key regulators such as *Cdx2, Eomes, Esrrb,* and *Sox2* (Okae et al., 2018), there is a pressing need to utilize human model systems to better understand human-specific trophoblast lineage differentiation and placentation.

Only recently, *bona fide* hTSCs, TS-like cells (TSLCs) that can mimic hTSCs in some aspects, and induced TSCs (iTSCs) have been established from various sources of human cells and started to gain attention for their utility (**Figure 1**). Some of these cells self-renew and retain a capacity to differentiate into multiple specialized cell types, such as ST and EVT (Okae et al., 2018; Castel et al., 2020; Dong et al., 2020; Liu et al., 2020). However, these *in vitro* human trophoblast model systems are relatively new and therefore have not been extensively studied yet. As various high-throughput omics approaches in the field of pluripotent stem cells (PSCs) have aided in understanding early embryo development by identifying critical *cis*- and *trans*-regulatory factors and their regulatory mechanisms (Loh et al., 2011), such omics approaches in combination with *in vitro* human placenta models will provide us with clues for the understanding of human placentation. In this review, we first provide a broad overview of multiple omics approaches used in the studies of mTSCs or other fields and key outcomes, and briefly describe differences between human and mouse placentation. Since most studies have been performed in mTSCs, the vast majority of data we reviewed here are from mouse studies, with occasional studies from human trophoblast and the placenta. Then, we introduce recently reported *in vitro* human trophoblast model systems and their applications, collectively emphasizing the pressing needs of similar omics approaches to be applied to human *in vitro* models to enable identification of previously unknown human trophoblast-specific key factors and their regulatory mechanisms underlying both normal and abnormal human placenta development.

Abbreviations: ATAC-seq, transposase-accessible chromatin followed by sequencing; BAP, BMP4, A83-01, and PD173074; BMP4, bone morphogenic protein 4; ChIP-seq, chromatin immunoprecipitation coupled with high-throughput sequencing; CT, cytotrophoblasts; EGF, epidermal growth factor; EMT, epithelial to mesenchymal transition; ESCs, embryonic stem cells; EVT, extravillous trophoblasts; HDAC, histone deacetylase; hEPSCs, human expanded potential stem cells; Hi-C, A method to study the three-dimensional architecture of genomes; IUGR, intrauterine growth restriction; iPSCs, induced pluripotent stem cells; iTSCs, induced trophoblast stem cells; KO, knockout; 5mC, DNA methylation at cytosine residues; 6mA, DNA methylation at adenine residues; NGS, next-generation sequencing; PE, preeclampsia; PSCs, pluripotent stem cells; ROCK, rho-associated protein kinase; RPL, recurrent pregnancy loss; RRBS, reduced representation bisulfite sequencing; S1P, phospholipid sphingosine 1-phosphate; ST, syncytiotrophoblasts; TE, trophectoderm; TFs, transcription factors; TGC, trophoblast giant cells; TGFB, transforming growth factor beta; TSCs, trophoblast stem cells; TSLCs, trophoblast stem (TS)-like cells.

VARIOUS OMICS STUDIES ON PLACENTA/TROPHOBLAST-SPECIFIC MODULATORS AND THEIR REGULATORY MECHANISMS

Transcriptional and epigenetic regulations govern global gene expression programs, thereby modulating cellular functions and identity *via* the interactions between *cis*-regulatory elements, such as promoters, enhancers, and insulators, and numerous *trans*-acting factors, including cell-type-specific TFs and

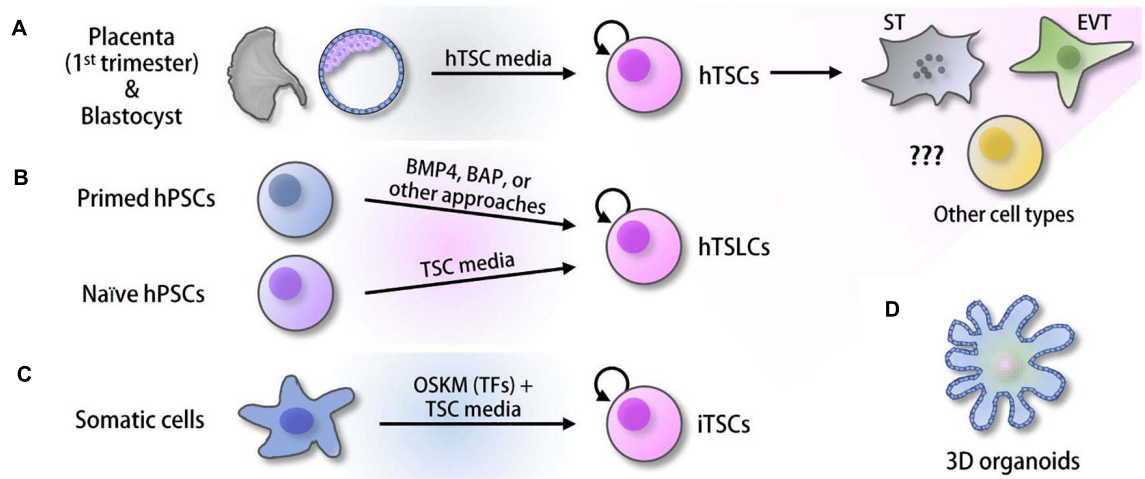

FIGURE 1 | Derivation of human *in vitro* placenta models. **(A)** Human trophoblast stem cells (hTSCs) derived from the trophectoderm (TE) of the blastocysts and first-trimester placenta (Okae et al., 2018). **(B)** Trophoblast stem-like cells (TSLCs) derived from various defined media (Xu et al., 2002; Amita et al., 2013; Li et al., 2013, 2019; Horii et al., 2016; Mischler et al., 2021). **(C)** Induced trophoblast stem cells (iTSCs) reprogrammed from somatic cells using ectopic expression of OCT4, SOX2, KLF4, and MYC (OSKM) followed by culture in hTSC media (Castel et al., 2020; Liu et al., 2020). **(D)** 3D organoids established from hTSCs and cytotrophoblast (CT) (Haider et al., 2018; Turco et al., 2018; Saha et al., 2020).

cofactors. Recent next-generation sequencing (NGS)-based genomics studies enable us to exhaustively determine cell-type-specific TFs, enhancer-TF interactions, and TF-TF interactions responsible for precise cellular functions in various contexts. Additionally, genome-wide profiling of histone modifications, DNA methylation landscapes, chromatin accessibility, and three-dimensional architectures has advanced our understanding of the mechanisms underlying cellular identity and animal development. In the field of trophoblast biology, due to the late establishment of human *in vitro* models, most omics studies have been performed in mTSCs in addition to *in vivo* functional studies in mouse KO models. In this section, we review some important omics approaches, such as chromatin immunoprecipitation coupled with high-throughput sequencing (ChIP-seq), transposase-accessible chromatin followed by sequencing (ATAC-seq), high-throughputpromotercapture (Hi-C), and other approaches mainly taken in mTSCs or other contexts. Integrative studies with *in vitro* human trophoblast models and various omics approaches will facilitate our understanding of the mechanisms underlying early human placenta development.

Mapping Cis-Regulatory Elements in mTSCs and Mouse Placenta

As ChIP-seq allows for the identification of pivotal *cis*-regulatory elements controlling tissue-specific gene expression, multiple ChIP-seq studies of an enhancer-binding protein (p300) or enhancer-associated histone marks (H3K27ac and H3K4me1) have identified comprehensive sets of enhancers in mTSCs and mouse placentas (Shen et al., 2012; Chuong et al., 2013; Tuteja et al., 2016; Lee et al., 2019). Integrative analyses of p300, H3K4me1, and H3K27ac ChIP-seq data sets have identified approximately 70K putative enhancers in mouse placenta, of which 4,431 enhancers were placenta-specific among 19 tissues tested (Shen et al., 2012). Placenta-specific enhancers often have stage-specific roles during placentation and may be implicated in certain placenta complications. For example, profiling of global enhancers and transcriptomes at the pinnacle and shortly after the trophoblast invasion revealed that many active enhancers contain three enriched motifs of trophoblast-specific TFs (AP1, ETS2, and TFAP2C), suggesting that these enhancer-TF networks may play essential roles in controlling the depth of trophoblast invasion during placenta development (Tuteja et al., 2016). Therefore, mapping enhancer-TFs networks will facilitate understanding of proper trophoblast invasion, which is essential for advancing treatments for pregnancy complications caused by aberrant trophoblast invasion, including placenta accreta (due to too much invasion) and PE as well as IUGR (due to too shallow or incomplete invasion) (Caniggia et al., 2000; Tantbirojn et al., 2008; Barrientos et al., 2017).

Interestingly, global mapping and comparison of enhancers between mouse and rat TSCs unveiled that endogenous retroviruses (ERVs) are strongly enriched within the species-specific enhancers among transposable elements. In particular, the ERV known as RLTR13D5 contributes to the mouse-specific enhancer landscape, suggesting differential insertions of transposable elements within the genome of various species may lead to placental diversity by altering the binding sites of TSC-specific TFs, such as ELF5, TFAP2C, and TEAD4 (Chuong et al., 2013). However, much remains unknown concerning the contribution of transposable element-associated enhancers

to placenta diversity. For example, it is not known whether ablation or mutation of ERVs is sufficient to cause substantial alteration in TF binding patterns during placentation. As noted above, due to the recent derivation of hTSCs and other human *in vitro* models, research on *cis*-regulatory elements in human trophoblast models is still rudimentary, awaiting intensive studies to unravel the core *cis*-regulatory elements required for human placenta development. Successful mapping of global hTSC-specific enhancers, as well as dynamic changes in enhancer usage during differentiation of hTSC toward ST and EVT, will help to explain the significant roles of enhancers in the maintenance and differentiation of hTSCs, and to identify TFs associated with the defined enhancers in hTSC and during ST or EVT differentiation *via* motif search, illuminating the mechanisms by which transcriptional regulatory landscape leads to trophoblast differentiation.

Trans-Acting Factors Implicated in mTSCs and Placenta Development

In addition to *cis*-regulatory elements, identifying trophoblast/placenta-specific TFs and their global target genes is crucial to understanding how they form regulatory networks to modulate placenta-specific gene expression programs and to further elucidate the etiology of placenta malfunction-related complications. Conventional loss-of-function studies in mouse models identified a handful of key TFs in trophoblast lineages, including *Cdx2* (Strumpf et al., 2005), *Tead4* (Yagi et al., 2007), *Gata3* (Ralston et al., 2010), *Elf5* (Donnison et al., 2005), *Tfap2c* (Auman et al., 2002), *Eomes* (Russ et al., 2000), *Esrrb* (Luo et al., 1997), *Ets2* (Yamamoto et al., 1998), *Ascl2* (Guillemot et al., 1994), *Gcm1* (Anson-Cartwright et al., 2000), and *Hand1*(Riley et al., 1998). Notably, the vast majority of these genes are embryonic lethal upon their deletion, and phenotypes typically include severe defects in placenta development. While some TFs (*Elf5*, *Esrrb*, and *Tfap2c*) are known to be essential for the maintenance of mTSCs and during mouse placenta development, others (such as *Hand1* for trophoblast giant cells (TGC) and *Ascl2* for spongiotrophoblast) (Guillemot et al., 1994; Riley et al., 1998) are known to play central roles in mTSC differentiation toward more specialized trophoblast cell types, suggesting that different classes of TFs may play unique roles during trophoblast specification. Aligning with this, a recent mTSC-specific super-enhancer mapping approach has identified numerous novel TSC-specific TF candidates and classified them into four groups based on their expression patterns during mTSC differentiation, revealing that different classes of TSC-specific TFs play distinct roles in the maintenance or differentiation of mTSCs (Lee et al., 2019).

A recent forward genetic screen identified *Zfp281* as a mTSC-specific regulator, and an integrative analysis of global ZFP281 targets with global histone modifications disclosed that ZFP281 interacts with MLL or COMPASS complex mediating H3K4me3, suggesting that ZFP281 recruits the complex onto the mTSC-specific targets (Ishiuchi et al., 2019). Notably, ZFP281 is also a member of the mouse embryonic stem cell (ESC) core pluripotency network (Wang et al., 2006). As multiple mTSC-specific TFs, such as ESRRB, SOX2, and TFAP2C, are also members of the pluripotency network, it is reasonable to speculate that these TFs may have context-specific functions by forming distinct regulatory networks in mTSCs or mouse ESCs (mESCs) with context-specific interacting partner proteins, controlling different downstream target genes. In agreement with their roles in mTSCs, numerous studies reported that overexpression of TSC-specific TFs, such as *Arid3a* (Rhee et al., 2014), *Cdx2* (Niwa et al., 2005), *Gata3* (Ralston et al., 2010), *Tead4* (Nishioka et al., 2009), *Zfp281* (Ishiuchi et al., 2019), and *Fosl1* (Lee et al., 2018), could induce trophoblast-specific gene expression programs in mESCs. Mapping of the global binding sites of CDX2, ARID3A, and GATA3 in concert with RNA-seq and ATAC-seq during cell fate conversion revealed that these TFs initially repress ESC-specific genes and subsequently activate TSC-specific genes (Rhee et al., 2017). Similarly, global mapping of TFAP2A, TFAP2C, GATA2, and GATA3 combined with transcriptome analysis upon cell fate conversion of human ESCs (hESCs) to hTSLCs elucidated the binding landscape of these TFs during fate conversion. Among the TFs, GATA3 preferentially co-occupies its targets with other TFs and promotes the activation of placental genes, suggesting that GATA3 is a pivotal factor, and GATA2/3 and TFAP2A/C networks modulate early specification of trophoblast progenitors (Krendl et al., 2017). These observations ironically suggest that ESCs can also serve as a useful tool to study trophoblast development in various ways. Unfortunately, while the roles of more than hundreds of TFs have been elucidated in the field of mouse and human ESCs (and PSCs), only a few TFs have been functionally characterized in human trophoblast lineage specifications (Lee et al., 2007; Soncin et al., 2018; Saha et al., 2020). For a better understanding of early human trophoblast lineage differentiation, identification and validation of master TFs will be the first essential step. Furthermore, studies on how these key TFs collaboratively control the self-renewal of hTSCs, modulate differentiation toward ST or EVT, interact with their chromosomal target genes, and form regulatory networks with other interacting partner proteins will be tremendously important for deeper mechanistic understating of both normal placentation and diseased placenta.

Epigenetic Regulations in mTSCs and Placenta

Histone Modifications

In addition to the enhancer-associated histone modifications (H3K27ac and H3K4me1) described above, genome-wide studies of active (H3K4me3 and H3K9ac) and repressive (H3K27me3 and H3K9me3) histone modifications suggested that epigenetic regulations also play important roles in development and early embryogenesis (Fogarty et al., 2015; Dahl et al., 2016; Liu et al., 2016; Xia et al., 2019). H3K4me3 is a well-known histone mark, generally observed at active promoters. H3K4 demethylase, KDM5B, is responsible for erasing these marks and plays a crucial role in mTSC differentiation toward specialized cell types by resetting the H3K4 methylation landscape at the promoters of mTSC self-renewal-related genes (Xu and Kidder, 2018). Bivalent domains that harbor both H3K4me3 and H3K27me3 marks are

enriched near the promoters of inactive developmental genes in ESCs, and these marks allow for rapid activation of such genes upon developmental cues (Bernstein et al., 2006; Mikkelsen et al., 2007). Interestingly, it is still controversial whether TSCs harbor bivalent modifications, as one study reported that mTSCs have rare H3K27me3 domains (Rugg-Gunn et al., 2010), while another study showed 5,172 bivalent genes in mTSCs (Liu et al., 2016). Surprisingly, H3K27me3 and H3K4me2 ChIP followed by quantitative PCR in mTSCs revealed that bivalent marks are observed in the developmental genes (*Atoh1*, *Sox1*, *Hoxa7*, *Gata4*, and *Sox7*) that are not expressed in placenta development, while placenta-specific genes, such as *Cdx2, Pax3,* and *Hand1*, were only marked by H3K4me2. It has not been reported in hTSCs whether ST- or EVT-specific genes have bivalent domains and subsequently lose their bivalent signature upon differentiation, as well as how histone writers and erasers are regulated during ST or EVT differentiation. Studies on the dynamics of bivalent domains in the maintenance of hTSCs and their differentiation to ST or EVT in conjunction with global gene expression profiles will answer this question, and such approaches will further reveal how and to what extent the bivalent loci regulate genes required for trophoblast lineage commitment.

DNA Methylation

In general, DNA methylation at cytosine residues (5mC) plays crucial roles in cell-type-specific gene expression and silences transposons and other repetitive sequences on the genome (Li and Zhang, 2014). The genome of the trophoblast lineage is globally hypomethylated relative to that of somatic cells. In human CT, DNMT1, which is responsible for the maintenance of 5mC, is downregulated by promoter methylation, while upregulated DNMT3L plays important roles in placenta development by facilitating the activation of *de novo* methyltransferase DNMT3A and DNMT3B (Suetake et al., 2004; Arima et al., 2006; Novakovic et al., 2010). Abnormal DNA methylation during placenta development is known to be associated with pregnancy-related diseases (Koukoura et al., 2012), and methylation is also a pivotal regulatory mechanism underlying the mono-allelic expression of imprinting genes. DNMT3L is required for establishing maternal gene imprinting (Hata et al., 2002). Imprinted genes play essential roles in feto-placental development by affecting placental growth, morphology, and nutrient uptake capacity, as reviewed in-depth of imprinting mechanisms in murine placenta (Hanna, 2020). One fundamental question regarding the roles of DNA methylation is how DNA methylation contributes to trophoblast lineage commitment. Global methylation was investigated in human trophoblasts, including side-population trophoblast (trophoblast stem cell population), CT (intermediate progenitors), and EVT from the first trimester of the human placenta using reduced representation bisulfite sequencing (RRBS) (Gamage et al., 2018). Comparison of methylomes and transcriptomes revealed 41 hypomethylated genes are upregulated in EVT compared to CT and implicated in epithelial to mesenchymal transition (EMT) and metastatic cancer pathways. The results suggest that these 41 genes are responsible for the acquisition of an invasive phenotype of EVT, which is consistent with the fact that villous CT differentiates into invasive EVT through the EMT process observed in numerous invasive cancers (DaSilva-Arnold et al., 2015), further implying shared mechanisms underlying heightened invasive capabilities between trophoblasts and cancer cells. Therefore, it will be of great interest to investigate how dynamic alterations of global methylomes drive trophoblast lineage commitment. *In vitro* human trophoblast models including hTSCs would be an ideal system to capture the dynamics of global methylomes during hTSC differentiation to ST or EVT.

In addition to 5mC, 5hmC regulated by the 10–11 translocation factor, TET1, is essential for maintaining the self-renewing status of mTSCs (Chrysanthou et al., 2018). Therefore, testing the roles of TET1 in hTSC or their differentiation might be interesting. An integrative analysis of DNA 5mC, 5hmC, transcriptomes, and TET1 occupancy in mTSCs and differentiated mTSCs revealed that the ratio of 5hmC–5mC correlates with their target gene activity. Interestingly, most TET1 sites demarcate potential trophoblast enhancers while overlapping with active histone marks and TFAP2C binding sites (Senner et al., 2020). Multiple genome-wide methylation studies have been performed in human diseased placentas from patients experiencing recurrent pregnancy loss (RPL), identifying numerous differentially methylated regions (DMRs) associated with dysregulated genes (Du et al., 2020). Therefore, DNA methylation may contribute significantly to placenta pathology. The differences in methylation between male and female origin placentas have also been linked with susceptibility to pregnancy complications (Gong et al., 2018). Recently, DNA N^6-methyladenine (6mA) modification was also reported in mammals (Xiao et al., 2018) and it was shown that 6mA contributes to epigenetic regulation by antagonizing the function of SATB1 during mTSC differentiation (Li et al., 2020). Conversely, recent comprehensive bioinformatics analyses of published data suggested that 6mA may not exist in mammals and this prior observation was due to false detection of 6mA (Douvlataniotis et al., 2020); therefore, more careful investigation is needed for the validation of 6mA contribution to mTSC differentiation and human trophoblast differentiation in the future.

Chromatin Landscape in mTSCs and Placenta

The ATAC-seq approach in mTSCs has identified 57,019 accessible chromatin regions (Nelson et al., 2017). Moreover, a subsequent comparison of mTSC-specific open loci with those in different stages of the developing embryo revealed that approximately 20% of mTSC-specific open loci are also accessible in the 8-cell stage embryo and enriched with placenta-related genes, suggesting that a significant portion of putative mTSC enhancers is already open in the 8-cell stage during embryogenesis (Nelson et al., 2017). Dynamic changes in chromatin landscape were observed upon mTSC differentiation; upon differentiation, chromatin accessibility drastically increased at the genes associated with trophoblast lineage specification, although surprisingly, chromatin accessibility was

not significantly changed for downregulated genes, suggesting the importance of chromatin openness changes for gene activation but not gene repression. Instead, the downregulated genes lost the occupancy of ESRRB, a TF for mTSC self-renewal, indicating that changes in chromatin accessibility are necessary but not sufficient for trophoblast gene regulation during differentiation (Nelson et al., 2017).

Recently, ATAC-seq for hTSCs derived from naïve hESCs has identified 12,132 open chromatin regions (Dong et al., 2020). A comparison of differentially accessible regions (DARs) between hTSCs and naïve hESCs revealed that the vast majority of DARs in hTSCs are located in loci that are distal from promoters, suggesting that long-range interactions between promoters and distal regulatory regions may be involved in transforming naïve hPSCs into hTSCs. However, comprehensive investigation of such long-range interactions has not yet been performed in hTSCs. Additionally, chromatin accessibility of EVT and ST has not been compared with that of hTSCs, and it remains unknown to what extent changes in accessibility facilitate cell fate specification in trophoblast lineages. Investigation of chromatin openness during differentiation of *in vitro* human trophoblast models will advance our understanding of how chromatin accessibility is altered in a different cellular context and contribute to the conversion of cellular identity during human trophoblast differentiation.

In addition to chromatin accessibility, chromatin architecture emerges as one of the key gene regulatory mechanisms to orchestrate spatiotemporal gene expression. Key cell-type-specific TFs are regulated by long-range looping between the promoter and enhancers. For instance, TEAD4 is robustly expressed in mTSCs (Nishioka et al., 2008, 2009). Circular chromosome conformation capture coupled with high-throughput sequencing (4C-seq) unveiled 64 putative long-range *Tead4* promoter interactomes in mTSCs. Comparison with enhancer histone signatures and open chromatin status revealed that five enhancer loci interact with the promoter of *Tead4* and significantly increase the activity of *Tead4* promoter in mTSCs, indicating that TSC-specific *Tead4* expression is regulated by inter-chromosomal promoter-enhancer interactions (Tomikawa et al., 2020). Of note, Hi-C in both mESCs and mTSCs revealed that enhancer-promoter interactions change dynamically between cell types and that the key mTSC-specific TFs tend to have promoter-enhancer interactions, particularly Tet1-regulated enhancers in mTSCs. These TFs are expressed relatively higher in mTSCs than in mESCs when they do not have promoter-enhancer interactions in mESCs, while mTSC-specific TFs that are suppressed in mESCs exhibit interactions between promoters marked with H3K27me3 in mESCs (Schoenfelder et al., 2018). Recent integrative analysis of H3K27me3 ChIP-seq with Hi-C and chromatin interaction analysis by paired-end sequencing (ChIA-PET) data discovered that long non-coding RNAs (lncRNAs), *Airn* and *Kcnq1ot1*, induce the spread of megabase-sized H3K27me3 domains in mTSCs by recruiting Polycomb repressive complex (PRC) to CpG islands (CGIs) in a lncRNA-dependent manner. This spreading of H3K27me3 is also reliant on the preexisting chromatin structure, abundance, and stability of *Airn* (Schertzer et al., 2019). Since these chromatin interaction studies in mTSCs revealed the dynamics and significance of chromatin structure in determining cell-type specificity, similar research using multiple human trophoblast models under the conditions of self-renewing and ST or EVT differentiation will also help to define how and to what extent chromatin architecture contributes to human placenta development.

The Differences Between Human and Mouse Placenta Development

Mouse and human placentas have many commonalities, as both of them are discoid and hemochorial placentas, and they also have many functionally conserved genes. However, there are also many apparent differences between them, such as size, shape, cellular organization, gestational length, and overall structure (Rossant, 2015; Schmidt et al., 2015). Accordingly, mouse placenta models do not always perfectly mimic human pregnancy disorders such as PE (Bodnar et al., 2005; Aubuchon et al., 2011). It is often difficult to extrapolate findings from studies on rodent placentation. A growing body of evidence indicates that human placenta development differs from that of mouse spatiotemporally. For example, human blastocysts show OCT4 expression restricted to the inner cell mass (ICM) about 2 days later than the mouse. While mouse blastocysts show mutually exclusive expression patterns between *Oct4* (in the ICM) and *Cdx2* (in the TE), *CDX2* in the human blastocyst is initially co-expressed with *OCT4*, the latter of which is not confined to the ICM until just before implantation (Niakan and Eggan, 2013). Core TE-specific TFs (*Id2*, *Elf5*, and *Eomes*) are exclusively expressed in mouse trophoblast lineages, whereas human orthologs are not present in human TE (Blakeley et al., 2015), but *ELF5* expression is observed in the trophoblast subpopulations of early implanted embryos (Hemberger et al., 2010; Soncin et al., 2018). In particular, genome-wide transcriptome comparison between human and mouse placentas not only unveiled that the itinerary of mouse placental development is parallel to only the first half of gestation in the human placenta, but also revealed significant differences in transcriptomes and identified VGLL1 as a human-specific marker for CT (Soncin et al., 2018).

Furthermore, immunohistochemistry in human placental tissues showed that a short isoform of *TP63* is specific to the human rather than the mouse placenta. *TP63* is mainly expressed in primary CT, and its expression level decreases when the cells undergo differentiation into either ST or EVT (Lee et al., 2007). Despite considerable differences between human and mouse placentation, only a few human placenta-specific TFs and *cis*-regulatory elements have been identified, and little is known about their mechanisms in regulating human trophoblast fate. It is still ambiguous to what extent key TFs share common targets and play conserved roles between humans and mice. Considering the differences between mouse and human placenta (Soncin et al., 2015), it is essential to identify human-specific *cis*-regulatory elements and TFs. All the above evidence highlights the necessity of the use of *in vitro* human placenta models. The multiple omics approaches in human *in vitro* trophoblast modes will reveal

human-specific regulatory elements and factors as well as distinct epigenetic regulations that can then later be validated for possible roles in human placenta development or pathology.

IN VITRO MODELS OF HUMAN PLACENTA DEVELOPMENT

Although rodent models, especially mouse *in vivo* and *in vitro* model systems, have been widely used in the field, animal model systems do not completely mimic the human placenta in various ways, as described above. Before establishing *bona fide* hTSCs, choriocarcinoma, immortalized cells, and primary CT in the placenta were used as *in vitro* models of human placenta development (Nagamatsu et al., 2004; Bilban et al., 2010; Dietrich et al., 2020). However, there were multiple drawbacks. Carcinoma cells do not completely recapitulate the multipotent human trophoblast, and they show an abnormal gene expression profile. Conversely, although multipotent, access to primary CT is limited, and they do not proliferate *in vitro* (Kliman et al., 1986; Soares et al., 2018). Due to these issues, more recent efforts have been made to establish human trophoblast models from human PSCs [hESCs or human induced pluripotent stem cells (hiPSCs)]. Since then, rapid advances in the field have established multiple human *in vitro* placenta models from various sources and using different protocols (**Figure 1**). In this section, we discuss recently available *in vitro* model systems of early human placenta development and also describe their applications and limitations.

BMP4-Induced hTSLCs

Since it has been reported that bone morphogenetic protein 4 (BMP4) can initiate differentiation of hESCs toward trophoblast lineages (Xu et al., 2002), multiple groups have attempted to convert hESCs to hTSLCs by treating them with BMP4 alone or in conjunction with small molecules, such as BAP (BMP4, A83-01, and PD173074) (Amita et al., 2013; Li et al., 2013; Horii et al., 2016). BMP4 treatment in the absence of FGF2 induces morphological changes of hESCs to epithelial cells that express KRT7 within 48 h (Amita et al., 2013). These cells robustly expressed trophoblast-specific markers, including HLA-G and secreted placenta hormones, such as chorionic gonadotropin, progesterone, and placental lactogen. Another study showed that CDX2+/TP63+CT-like cells, which have the potential to differentiate into ST- and EVT-like cells (bipotency), can be derived from hPSCs by the treatment of BMP4-containing defined media, based on the marker gene expression, hormone secretion, and invasion capacity (Horii et al., 2016). Although the exact mechanistic roles of BMP4 in the transformation of hPSCs to hTSLCs have not been well characterized, depletion of TP63 impaired the conversion of hPSCs to functional trophoblasts (Li et al., 2013), implying that BMP4 functions through TP63. These studies suggest that BMP4 may initiate the activation of trophoblast-specific gene expression in hPSCs that are known to harbor relatively loose chromatin structures (Melcer and Meshorer, 2010; Amita et al., 2013). Notably, BMP4-induced hTSLCs cannot proliferate for a prolonged time, and they ultimately differentiate into multiple uncharacterized cell populations, suggesting BMP4 treatment alone is not sufficient to convert hPSCs to self-renewing hTSCs with canonical bipotency. Nevertheless, these BMP4-induced hTSLCs have multiple advantages over other models. Since hiPSCs can be used as starting cells in addition to preexisting hESCs, generation of patient-specific hTSLCs is feasible by sequential establishment of hiPSCs from patients' somatic cells followed by conversion of the hiPSCs to hTSLCs. In turn, the approaches using trisomy 21 hPSCs and PE-derived hiPSCs successfully model trophoblast differentiation defects (Horii et al., 2016, 2021). Since many hiPSC lines have been established or can be established from human patients with various symptoms, similar approaches can be employed to understand previously unknown links between human diseases and the events during early placentation.

Bona Fide hTSCs

In 2018, Okae et al. established multiple self-renewing hTSCs lines harboring bipotency from the first-trimester placenta as well as human blastocysts (Okae et al., 2018). This long-standing goal of the field was achieved by the manipulation of multiple signaling pathways (activation of the epidermal growth factor (EGF) and Wnt signaling pathways, along with inhibition of the transforming growth factor beta (TGFB) pathway) combined with HDAC inhibitors and Rho-associated protein kinase (ROCK) inhibitor treatment. Although hTSCs present an excellent *in vitro* placenta model system and reliable protocols to differentiate them into ST and EVT are available, access to blastocysts or primary CT from the first-trimester placenta is still limited due to ethical issues. Interestingly, multiple research groups have recently reported the successful conversion of naïve hPSCs to hTSLCs (Cinkornpumin et al., 2020; Dong et al., 2020) using the defined culture condition used for the derivation of bona fide hTSCs (Okae et al., 2018). Notably, BMP4 treatment on naïve PSCs leads to adverse effects, such as promoting cell death, implying that naïve hPSCs must exit the naïve state to the primed state to efficiently respond to BMP4 for the conversion from hESCs to hTSLCs. Conversely, cultivating naïve hPSCs on Collagen IV in hTSC media allowed for the establishment of hTSLCs, whereas primed hPSCs cannot be transformed toward hTSLCs under the same conditions (Dong et al., 2020). Comparable to genuine hTSCs, naïve hPSC-derived hTSLCs can be maintained for over 20 passages without losing their bipotency, and they show overall gene expression signatures similar to hTSCs as well. Another group also reported that human expanded potential stem cells (hEPSCs) can be converted into hTSLCs under the bona fide hTSC culture condition (Gao et al., 2019). The hTSLCs derived from hEPSCs also showed bipotency; however, they did not show intact self-renewal capacity.

In contrast to the previous failures to generate self-renewing hTSLCs from primed hPSCs using BMP4 (Amita et al., 2013; Li et al., 2013; Horii et al., 2016), two independent groups have demonstrated the successful conversion of primed hESCs to hTSLCs. One group showed that the culture of hiPSCs on a nickel micromesh with triangular shapes results in cystic cells having characteristics of hTSCs in the absence of BMP4

(Li et al., 2019). These cells proliferated for over 205 days and showed bipotency, suggesting that it may be feasible to convert primed hPSCs to hTSLCs without BMP4. More recently, another study showed that the culture of hESCs in chemically defined media containing BMP4, SB43154, and S1P (the phospholipid sphingosine 1-phosphate) could convert primed hPSCs to two distinct subpopulations of hTSLCs (CDX2+ and CDX2- hTSLCs) (Mischler et al., 2021). Although additional functional validations are required to understand the true nature of all these hTSLCs, the results at least showed that different culture conditions can be used to transform naïve or primed hPSCs to hTSLCs, suggesting that there may be multiple molecular paths for the conversion of hPSCs toward hTSLCs.

iTSCs, TF-Mediated Conversion Models

In addition to the establishment of hTSLCs by applying defined culture conditions, recent studies showed that reprogramming of human somatic cells to human iTSCs by ectopic expression of TFs is feasible (Castel et al., 2020; Liu et al., 2020). Notably, unlike mouse iTSCs derived from the overexpression of multiple trophoblast-specific TFs (EOMES, GATA3, TFAP2C, and MYC or ETS2) in mouse fibroblasts (Benchetrit et al., 2015; Kubaczka et al., 2015), human iTSCs were established by reprogramming somatic cells with the induction of OCT4, SOX2, KLF4, and MYC (original TFs used to generate iPSCs; Takahashi and Yamanaka, 2006; Takahashi et al., 2007; Park et al., 2008) coupled with hTSC culture conditions. In this approach, expansion of the cells obtained from the intermediate stage of reprogramming in hTSC media was sufficient to reprogram somatic cells toward human iTSCs with the full differentiation potential of early trophoblasts without ectopic expression of trophoblast-specific TFs. This surprising result suggests that at least a small portion of cells during the intermediate stage of reprogramming harbor active trophoblast-specific gene expression programs, and the hTSC culture condition may stabilize hTSC-specific gene expression programs by repressing upregulation of other lineage-specific genes. It would be interesting to investigate the mechanisms underlying this observation and whether mouse iTSCs can be derived with the same procedure through which human iTSCs were derived from somatic cells.

3D Culture Models

Cells cultured on 2-dimensional (2D) surfaces do not always accurately recapitulate authentic tissue environments where cells are spatially surrounded by other cells in 3-dimensions (3D). Therefore, it is of great interest to study 3D-cultured cells that behave more closely to *in vivo* tissue (Simian and Bissell, 2017). Recently, multiple independent groups established placenta organoid models. One group generated trophoblast organoids *via* 3D culture of first-trimester villous CT (Haider et al., 2018). These trophoblast organoids showed globally similar gene expression profiles to the primary CT. Under self-renewing conditions, the organoids are composed of CT (outside) and ST (inside) that are spontaneously differentiated from CT, whereas CT can further differentiate into HLA-G + EVT at the outer CT layers upon withdrawal of Wnt stimulators. Another group also established genetically stable trophoblast organoids that can differentiate into both ST and EVT from EPCAM + proliferative trophoblasts (Turco et al., 2018). These organoids form villous-like structures where the basement membrane is located outside the organoids, whereas syncytial masses reside in the central cavity. These organoids can secrete placenta-specific hormones, growth factors, and glycoprotein, and can further differentiate into EVT. These trophoblast organoids are potentially useful models for studying critical elements required for placenta morphogenesis, feto-maternal communication, and transmission of pathogens. Most recently, hTSC-derived trophoblast organoids were also reported (Saha et al., 2020). Like CT-derived organoids, hTSC organoids had villous-like structures. Interestingly, depletion of TEAD4 in hTSCs prevented organoid formation. Accordingly, hTSCs derived from RPL placentas showing a reduced level of TEAD4 failed to efficiently form trophoblast organoids, suggesting a significant role of TEAD4 in human placenta development and RPL placentas.

CONCLUSION AND PERSPECTIVES

Recent genome-wide identification of *cis*-regulatory elements and *trans*-acting factors in mTSCs and placenta models revealed multiple essential factors and their action mechanisms underlying mTSC maintenance and trophoblast lineage specification. Also, in combination with conventional genetics approaches, global inspections of histone signatures, DNA methylation, chromatin openness, and 3D architecture in mTSC models unveiled that placenta development is orchestrated by multiple genetic and epigenetic modulators whose defects might be associated with pregnancy complications. Although both mouse *in vivo* and *in vitro* models have advanced our understanding of the mechanisms underlying placenta development, fundamental discrepancies between human and mouse placentas have been a major issue. Recent success in establishing multiple human *in vitro* placenta models, such as hTSCs, hTSLCs, iTSCs, and 3D trophoblast organoids, may fill the gap of knowledge by providing tremendous opportunities to study human trophoblast and placenta-specific gene regulation. In addition, they will serve as useful *in vitro* models for both normal and abnormal human placentation, especially in the early stages of development.

Despite recent advances in developing research and diagnostic tools, the placenta remains one of the least understood organs in the human body. Since multiple human *in vitro* model-based approaches have recently become available, numerous questions can be addressed: What factors or regulators are responsible for the specification of various cell types in the human placenta? How do they form regulatory networks modulating human trophoblast cell-type-specific gene expression programs? How do the malfunctions of the key regulators trigger placenta-associated complications? How do trophoblasts collaborate with maternal immune cells for a successful pregnancy without immunological

aggression? Is it possible to successfully derive multiple functional cell types from hTSCs, hTSLCs, iTSCs, or 3D organoid models? Recently developed multiple omics approaches with human *in vitro* placenta models, possibly from both normal and diseased placentas, will provide us with a more holistic view of genetic and epigenetic regulatory mechanisms in placentation and etiologies of placenta-associated pregnancy complications.

AUTHOR CONTRIBUTIONS

B-KL and JK wrote the manuscript. Both authors contributed to the article and approved the submitted version.

FUNDING

B-KL was supported by the start-up funding from University at Albany-State University of New York. JK was supported by the awards R01GM112722 and R01HD101512 from the National Institute of Health (NIH) and Preterm Birth Research Grant (1017294) from the Burroughs Wellcome Fund (BWF).

ACKNOWLEDGMENTS

We appreciate Lucy LeBlanc and Mijeong Kim for the critical reading of the manuscript.

REFERENCES

Amita, M., Adachi, K., Alexenko, A. P., Sinha, S., Schust, D. J., Schulz, L. C., et al. (2013). Complete and unidirectional conversion of human embryonic stem cells to trophoblast by BMP4. *Proc. Natl. Acad. Sci. U S A.* 110, E1212–E1221. doi: 10.1073/pnas.1303094110

Anson-Cartwright, L., Dawson, K., Holmyard, D., Fisher, S. J., Lazzarini, R. A., and Cross, J. C. (2000). The glial cells missing-1 protein is essential for branching morphogenesis in the chorioallantoic placenta. *Nat. Genet.* 25, 311–314. doi: 10.1038/77076

Arima, T., Hata, K., Tanaka, S., Kusumi, M., Li, E., Kato, K., et al. (2006). Loss of the maternal imprint in Dnmt3Lmat-/- mice leads to a differentiation defect in the extraembryonic tissue. *Dev. Biol.* 297, 361–373. doi: 10.1016/j.ydbio.2006.05.003

Aubuchon, M., Schulz, L. C., and Schust, D. J. (2011). Preeclampsia: animal models for a human cure. *Proc. Natl. Acad. Sci. U S A.* 108, 1197–1198. doi: 10.1073/pnas.1018164108

Auman, H. J., Nottoli, T., Lakiza, O., Winger, Q., Donaldson, S., and Williams, T. (2002). Transcription factor AP-2gamma is essential in the extra-embryonic lineages for early postimplantation development. *Development* 129, 2733–2747.

Barker, D. J., and Thornburg, K. L. (2013). Placental programming of chronic diseases, cancer and lifespan: a review. *Placenta* 34, 841–845. doi: 10.1016/j.placenta.2013.07.063

Barrientos, G., Pussetto, M., Rose, M., Staff, A. C., Blois, S. M., and Toblli, J. E. (2017). Defective trophoblast invasion underlies fetal growth restriction and preeclampsia-like symptoms in the stroke-prone spontaneously hypertensive rat. *Mol. Hum. Reprod.* 23, 509–519. doi: 10.1093/molehr/gax024

Benchetrit, H., Herman, S., van Wietmarschen, N., Wu, T., Makedonski, K., Maoz, N., et al. (2015). Extensive Nuclear Reprogramming Underlies Lineage Conversion into Functional Trophoblast Stem-like Cells. *Cell Stem Cell* 17, 543–556. doi: 10.1016/j.stem.2015.08.006

Bernstein, B. E., Mikkelsen, T. S., Xie, X., Kamal, M., Huebert, D. J., Cuff, J., et al. (2006). A bivalent chromatin structure marks key developmental genes in embryonic stem cells. *Cell* 125, 315–326. doi: 10.1016/j.cell.2006.02.041

Bilban, M., Tauber, S., Haslinger, P., Pollheimer, J., Saleh, L., Pehamberger, H., et al. (2010). Trophoblast invasion: assessment of cellular models using gene expression signatures. *Placenta* 31, 989–996. doi: 10.1016/j.placenta.2010.08.011

Blakeley, P., Fogarty, N. M., del Valle, I., Wamaitha, S. E., Hu, T. X., Elder, K., et al. (2015). Defining the three cell lineages of the human blastocyst by single-cell RNA-seq. *Development* 142, 3151–3165. doi: 10.1242/dev.123547

Bodnar, L. M., Ness, R. B., Markovic, N., and Roberts, J. M. (2005). The risk of preeclampsia rises with increasing prepregnancy body mass index. *Ann. Epidemiol.* 15, 475–482. doi: 10.1016/j.annepidem.2004.12.008

Caniggia, J. W., Lye, S. J., and Post, M. (2000). Oxygen and placental development during the first trimester: implications for the pathophysiology of pre-eclampsia. *Placenta* 21(Suppl. A), S25–S30. doi: 10.1053/plac.1999.0522

Cao, C., and Fleming, M. D. (2016). The placenta: the forgotten essential organ of iron transport. *Nutr. Rev.* 74, 421–431. doi: 10.1093/nutrit/nuw009

Castel, G., Meistermann, D., Bretin, B., Firmin, J., Blin, J., Loubersac, S., et al. (2020). Induction of Human Trophoblast Stem Cells from Somatic Cells and Pluripotent Stem Cells. *Cell Rep.* 33:108419. doi: 10.1016/j.celrep.2020.108419

Chen, C. P., Bajoria, R., and Aplin, J. D. (2002). Decreased vascularization and cell proliferation in placentas of intrauterine growth-restricted fetuses with abnormal umbilical artery flow velocity waveforms. *Am. J. Obstet. Gynecol.* 187, 764–769. doi: 10.1067/mob.2002.125243

Chrysanthou, S., Senner, C. E., Woods, L., Fineberg, E., Okkenhaug, H., Burge, S., et al. (2018). A Critical Role of TET1/2 Proteins in Cell-Cycle Progression of Trophoblast Stem Cells. *Stem Cell Rep.* 10, 1355–1368. doi: 10.1016/j.stemcr.2018.02.014

Chuong, E. B., Rumi, M. A., Soares, M. J., and Baker, J. C. (2013). Endogenous retroviruses function as species-specific enhancer elements in the placenta. *Nat. Genet.* 45, 325–329. doi: 10.1038/ng.2553

Cinkornpumin, J. K., Kwon, S. Y., Guo, Y., Hossain, I., Sirois, J., Russett, C. S., et al. (2020). Naive Human Embryonic Stem Cells Can Give Rise to Cells with a Trophoblast-like Transcriptome and Methylome. *Stem Cell Rep.* 15, 198–213. doi: 10.1016/j.stemcr.2020.06.003

Courtney, J. A., Cnota, J. F., and Jones, H. N. (2018). The Role of Abnormal Placentation in Congenital Heart Disease; Cause, Correlate, or Consequence? *Front. Physiol.* 9:1045. doi: 10.3389/fphys.2018.01045

Dahl, J. A., Jung, I., Aanes, H., Greggains, G. D., Manaf, A., Lerdrup, M., et al. (2016). Broad histone H3K4me3 domains in mouse oocytes modulate maternal-to-zygotic transition. *Nature* 537, 548–552. doi: 10.1038/nature19360

DaSilva-Arnold, S., James, J. L., Al-Khan, A., Zamudio, S., and Illsley, N. P. (2015). Differentiation of first trimester cytotrophoblast to extravillous trophoblast involves an epithelial-mesenchymal transition. *Placenta* 36, 1412–1418. doi: 10.1016/j.placenta.2015.10.013

Dietrich, B., Kunihs, V., Haider, S., Pollheimer, J., and Knöfler, M. (2020). 3-Dimensional JEG-3 choriocarcinoma cell organoids as a model for trophoblast expansion and differentiation. *Placenta* 104, 243–246. doi: 10.1016/j.placenta.2020.12.013

Dong, C., Beltcheva, M., Gontarz, P., Zhang, B., Popli, P., Fischer, L. A., et al. (2020). Derivation of trophoblast stem cells from naïve human pluripotent stem cells. *Elife* 9:52504. doi: 10.7554/eLife.52504

Donnison, M., Beaton, A., Davey, H. W., Broadhurst, R., L'Huillier, P., and Pfeffer, P. L. (2005). Loss of the extraembryonic ectoderm in Elf5 mutants leads to defects in embryonic patterning. *Development* 132, 2299–2308. doi: 10.1242/dev.01819

Douvlataniotis, K., Bensberg, M., Lentini, A., Gylemo, B., and Nestor, C. E. (2020). No evidence for DNA. *Sci. Adv.* 6:eaay3335. doi: 10.1126/sciadv.aay3335

Du, G., Yu, M., Xu, Q., Huang, Z., Huang, X., Han, L., et al. (2020). Hypomethylation of PRDM1 is associated with recurrent pregnancy loss. *J. Cell Mol. Med.* 24, 7072–7077. doi: 10.1111/jcmm.15335

Ergaz, Z., Avgil, M., and Ornoy, A. (2005). Intrauterine growth restriction-etiology and consequences: what do we know about the human situation and experimental animal models? *Reprod. Toxicol.* 20, 301–322. doi: 10.1016/j.reprotox.2005.04.007

Fogarty, N. M., Burton, G. J., and Ferguson-Smith, A. C. (2015). Different epigenetic states define syncytiotrophoblast and cytotrophoblast nuclei in the

trophoblast of the human placenta. *Placenta* 36, 796–802. doi: 10.1016/j.placenta.2015.05.006

Gamage, T. K. J. B., Schierding, W., Hurley, D., Tsai, P., Ludgate, J. L., Bhoothpur, C., et al. (2018). The role of DNA methylation in human trophoblast differentiation. *Epigenetics* 13, 1154–1173. doi: 10.1080/15592294.2018.1549462

Gao, X., Nowak-Imialek, M., Chen, X., Chen, D., Herrmann, D., Ruan, D., et al. (2019). Establishment of porcine and human expanded potential stem cells. *Nat. Cell Biol.* 21, 687–699. doi: 10.1038/s41556-019-0333-2

Gong, S., Johnson, M. D., Dopierala, J., Gaccioli, F., Sovio, U., Constância, M., et al. (2018). Genome-wide oxidative bisulfite sequencing identifies sex-specific methylation differences in the human placenta. *Epigenetics* 13, 228–239. doi: 10.1080/15592294.2018.1429857

Guillemot, F., Nagy, A., Auerbach, A., Rossant, J., and Joyner, A. L. (1994). Essential role of Mash-2 in extraembryonic development. *Nature* 371, 333–336. doi: 10.1038/371333a0

Haider, S., Meinhardt, G., Saleh, L., Kunihs, V., Gamperl, M., Kaindl, U., et al. (2018). Self-Renewing Trophoblast Organoids Recapitulate the Developmental Program of the Early Human Placenta. *Stem Cell Rep.* 11, 537–551. doi: 10.1016/j.stemcr.2018.07.004

Hales, C. N., and Barker, D. J. (2001). The thrifty phenotype hypothesis. *Br. Med. Bull.* 60, 5–20. doi: 10.1093/bmb/60.1.5

Hanna, C. W. (2020). Placental imprinting: Emerging mechanisms and functions. *PLoS Genet.* 16:e1008709. doi: 10.1371/journal.pgen.1008709

Hata, K., Okano, M., Lei, H., and Li, E. (2002). Dnmt3L cooperates with the Dnmt3 family of de novo DNA methyltransferases to establish maternal imprints in mice. *Development* 129, 1983–1993.

Hemberger, M., Udayashankar, R., Tesar, P., Moore, H., and Burton, G. J. (2010). ELF5-enforced transcriptional networks define an epigenetically regulated trophoblast stem cell compartment in the human placenta. *Hum. Mol. Genet.* 19, 2456–2467. doi: 10.1093/hmg/ddq128

Horii, M., Li, Y., Wakeland, A. K., Pizzo, D. P., Nelson, K. K., Sabatini, K., et al. (2016). Human pluripotent stem cells as a model of trophoblast differentiation in both normal development and disease. *Proc. Natl. Acad. Sci. U S A.* 113, E3882–E3891. doi: 10.1073/pnas.1604747113

Horii, M., Morey, R., Bui, T., Touma, O., Nelson, K. K., Cho, H. Y., et al. (2021). Modeling preeclampsia using human induced pluripotent stem cells. *Sci. Rep.* 11:5877. doi: 10.1038/s41598-021-85230-5

Ishiuchi, T., Ohishi, H., Sato, T., Kamimura, S., Yorino, M., Abe, S., et al. (2019). Zfp281 Shapes the Transcriptome of Trophoblast Stem Cells and Is Essential for Placental Development. *Cell Rep.* 27, 1742.e–1754.e. doi: 10.1016/j.celrep.2019.04.028

Kliman, H. J., Nestler, J. E., Sermasi, E., Sanger, J. M., and Strauss, J. F. (1986). Purification, characterization, and in vitro differentiation of cytotrophoblasts from human term placentae. *Endocrinology* 118, 1567–1582. doi: 10.1210/endo-118-4-1567

Koukoura, O., Sifakis, S., and Spandidos, D. A. (2012). DNA methylation in the human placenta and fetal growth (review). *Mol. Med. Rep.* 5, 883–889. doi: 10.3892/mmr.2012.763

Krendl, C., Shaposhnikov, D., Rishko, V., Ori, C., Ziegenhain, C., Sass, S., et al. (2017). GATA2/3-TFAP2A/C transcription factor network couples human pluripotent stem cell differentiation to trophectoderm with repression of pluripotency. *Proc. Natl. Acad. Sci. U S A.* 114, E9579–E9588. doi: 10.1073/pnas.1708341114

Kubaczka, C., Senner, C. E., Cierlitza, M., Araúzo-Bravo, M. J., Kuckenberg, P., Peitz, M., et al. (2015). Direct Induction of Trophoblast Stem Cells from Murine Fibroblasts. *Cell Stem Cell* 17, 557–568. doi: 10.1016/j.stem.2015.08.005

Latos, P. A., and Hemberger, M. (2016). From the stem of the placental tree: trophoblast stem cells and their progeny. *Development* 143, 3650–3660. doi: 10.1242/dev.133462

Lee, B. K., Jang, Y. J., Kim, M., LeBlanc, L., Rhee, C., Lee, J., et al. (2019). Super-enhancer-guided mapping of regulatory networks controlling mouse trophoblast stem cells. *Nat. Commun.* 10:4749. doi: 10.1038/s41467-019-12720-6

Lee, B. K., Uprety, N., Jang, Y. J., Tucker, S. K., Rhee, C., LeBlanc, L., et al. (2018). Fosl1 overexpression directly activates trophoblast-specific gene expression programs in embryonic stem cells. *Stem Cell Res.* 26, 95–102. doi: 10.1016/j.scr.2017.12.004

Lee, Y., Kim, K. R., McKeon, F., Yang, A., Boyd, T. K., Crum, C. P., et al. (2007). A unifying concept of trophoblastic differentiation and malignancy defined by biomarker expression. *Hum. Pathol.* 38, 1003–1013. doi: 10.1016/j.humpath.2006.12.012

Li, E., and Zhang, Y. (2014). DNA methylation in mammals. *Cold Spring Harb. Perspect. Biol.* 6:a019133. doi: 10.1101/cshperspect.a019133

Li, Y., Moretto-Zita, M., Soncin, F., Wakeland, A., Wolfe, L., Leon-Garcia, S., et al. (2013). BMP4-directed trophoblast differentiation of human embryonic stem cells is mediated through a ΔNp63+ cytotrophoblast stem cell state. *Development* 140, 3965–3976. doi: 10.1242/dev.092155

Li, Z., Kurosawa, O., and Iwata, H. (2019). Establishment of human trophoblast stem cells from human induced pluripotent stem cell-derived cystic cells under micromesh culture. *Stem Cell Res. Ther.* 10:245. doi: 10.1186/s13287-019-1339-1

Li, Z., Zhao, S., Nelakanti, R. V., Lin, K., Wu, T. P., Alderman, M. H., et al. (2020). N 6-methyladenine in DNA antagonizes SATB1 in early development. *Nature* 583, 625–630. doi: 10.1038/s41586-020-2500-9

Liu, X., Ouyang, J. F., Rossello, F. J., Tan, J. P., Davidson, K. C., Valdes, D. S., et al. (2020). Reprogramming roadmap reveals route to human induced trophoblast stem cells. *Nature* 586, 101–107. doi: 10.1038/s41586-020-2734-6

Liu, X., Wang, C., Liu, W., Li, J., Li, C., Kou, X., et al. (2016). Distinct features of H3K4me3 and H3K27me3 chromatin domains in pre-implantation embryos. *Nature* 537, 558–562. doi: 10.1038/nature19362

Loh, Y. H., Yang, L., Yang, J. C., Li, H., Collins, J. J., and Daley, G. Q. (2011). Genomic approaches to deconstruct pluripotency. *Annu. Rev. Genomics Hum. Genet.* 12, 165–185. doi: 10.1146/annurev-genom-082410-101506

Luo, J., Sladek, R., Bader, J. A., Matthyssen, A., Rossant, J., and Giguère, V. (1997). Placental abnormalities in mouse embryos lacking the orphan nuclear receptor ERR-beta. *Nature* 388, 778–782. doi: 10.1038/42022

Melcer, S., and Meshorer, E. (2010). Chromatin plasticity in pluripotent cells. *Essays Biochem.* 48, 245–262. doi: 10.1042/bse0480245

Mikkelsen, T. S., Ku, M., Jaffe, D. B., Issac, B., Lieberman, E., Giannoukos, G., et al. (2007). Genome-wide maps of chromatin state in pluripotent and lineage-committed cells. *Nature* 448, 553–560. doi: 10.1038/nature06008

Mischler, A., Karakis, V., Mahinthakumar, J., Carberry, C. K., San Miguel, A., Rager, J. E., et al. (2021). Two distinct trophectoderm lineage stem cells from human pluripotent stem cells. *J. Biol. Chem.* 296:100386. doi: 10.1016/j.jbc.2021.100386

Nagamatsu, T., Fujii, T., Ishikawa, T., Kanai, T., Hyodo, H., Yamashita, T., et al. (2004). A primary cell culture system for human cytotrophoblasts of proximal cytotrophoblast cell columns enabling in vitro acquisition of the extra-villous phenotype. *Placenta* 25, 153–165. doi: 10.1016/j.placenta.2003.08.015

Nelson, C., Mould, A. W., Bikoff, E. K., and Robertson, E. J. (2017). Mapping the chromatin landscape and Blimp1 transcriptional targets that regulate trophoblast differentiation. *Sci. Rep.* 7:6793. doi: 10.1038/s41598-017-06859-9

Niakan, K. K., and Eggan, K. (2013). Analysis of human embryos from zygote to blastocyst reveals distinct gene expression patterns relative to the mouse. *Dev. Biol.* 375, 54–64. doi: 10.1016/j.ydbio.2012.12.008

Nishioka, N., Inoue, K., Adachi, K., Kiyonari, H., Ota, M., Ralston, A., et al. (2009). The Hippo signaling pathway components Lats and Yap pattern Tead4 activity to distinguish mouse trophectoderm from inner cell mass. *Dev. Cell* 16, 398–410. doi: 10.1016/j.devcel.2009.02.003

Nishioka, N., Yamamoto, S., Kiyonari, H., Sato, H., Sawada, A., Ota, M., et al. (2008). Tead4 is required for specification of trophectoderm in pre-implantation mouse embryos. *Mech. Dev.* 125, 270–283. doi: 10.1016/j.mod.2007.11.002

Niwa, H., Toyooka, Y., Shimosato, D., Strumpf, D., Takahashi, K., Yagi, R., et al. (2005). Interaction between Oct3/4 and Cdx2 determines trophectoderm differentiation. *Cell* 123, 917–929. doi: 10.1016/j.cell.2005.08.040

Novakovic, B., Wong, N. C., Sibson, M., Ng, H. K., Morley, R., Manuelpillai, U., et al. (2010). DNA methylation-mediated down-regulation of DNA methyltransferase-1 (DNMT1) is coincident with, but not essential for, global hypomethylation in human placenta. *J. Biol. Chem.* 285, 9583–9593. doi: 10.1074/jbc.M109.064956

Okae, H., Toh, H., Sato, T., Hiura, H., Takahashi, S., Shirane, K., et al. (2018). Derivation of Human Trophoblast Stem Cells. *Cell Stem Cell* 22, 50.e–63.e. doi: 10.1016/j.stem.2017.11.004

Park, H., Zhao, R., West, J. A., Yabuuchi, A., Huo, H., Ince, T. A., et al. (2008). Reprogramming of human somatic cells to pluripotency with defined factors. *Nature* 451, 141–146. doi: 10.1038/nature06534

Perez-Garcia, V., Fineberg, E., Wilson, R., Murray, A., Mazzeo, C. I., Tudor, C., et al. (2018). Placentation defects are highly prevalent in embryonic lethal mouse mutants. *Nature* 555, 463–468. doi: 10.1038/nature26002

Prudhomme, J., and Morey, C. (2016). Epigenesis and plasticity of mouse trophoblast stem cells. *Cell Mol. Life Sci.* 73, 757–774. doi: 10.1007/s00018-015-2086-9

Ralston, A., Cox, B. J., Nishioka, N., Sasaki, H., Chea, E., Rugg-Gunn, P., et al. (2010). Gata3 regulates trophoblast development downstream of Tead4 and in parallel to Cdx2. *Development* 137, 395–403. doi: 10.1242/dev.038828

Rhee, C., Lee, B. K., Beck, S., Anjum, A., Cook, K. R., Popowski, M., et al. (2014). Arid3a is essential to execution of the first cell fate decision via direct embryonic and extraembryonic transcriptional regulation. *Genes Dev.* 28, 2219–2232. doi: 10.1101/gad.247163.114

Rhee, C., Lee, B. K., Beck, S., LeBlanc, L., Tucker, H. O., and Kim, J. (2017). Mechanisms of transcription factor-mediated direct reprogramming of mouse embryonic stem cells to trophoblast stem-like cells. *Nucleic Acids Res.* 45, 10103–10114. doi: 10.1093/nar/gkx692

Riley, P., Anson-Cartwright, L., and Cross, J. C. (1998). The Hand1 bHLH transcription factor is essential for placentation and cardiac morphogenesis. *Nat. Genet.* 18, 271–275. doi: 10.1038/ng0398-271

Rossant, J. (2015). Mouse and human blastocyst-derived stem cells: vive les differences. *Development* 142, 9–12. doi: 10.1242/dev.115451

Rossant, J., and Cross, J. C. (2001). Placental development: lessons from mouse mutants. *Nat. Rev. Genet.* 2, 538–548. doi: 10.1038/35080570

Rugg-Gunn, P. J., Cox, B. J., Ralston, A., and Rossant, J. (2010). Distinct histone modifications in stem cell lines and tissue lineages from the early mouse embryo. *Proc. Natl. Acad. Sci. U S A.* 107, 10783–10790. doi: 10.1073/pnas.0914507107

Russ, P., Wattler, S., Colledge, W. H., Aparicio, S. A., Carlton, M. B., Pearce, J. J., et al. (2000). Eomesodermin is required for mouse trophoblast development and mesoderm formation. *Nature* 404, 95–99. doi: 10.1038/35003601

Saha, B., Ganguly, A., Home, P., Bhattacharya, B., Ray, S., Ghosh, A., et al. (2020). TEAD4 ensures postimplantation development by promoting trophoblast self-renewal: An implication in early human pregnancy loss. *Proc. Natl. Acad. Sci. U S A.* 117, 17864–17875. doi: 10.1073/pnas.2002449117

Schertzer, M. D., Braceros, K. C. A., Starmer, J., Cherney, R. E., Lee, D. M., Salazar, G., et al. (2019). lncRNA-Induced Spread of Polycomb Controlled by Genome Architecture, RNA Abundance, and CpG Island DNA. *Mol. Cell* 75, 523.e–537.e. doi: 10.1016/j.molcel.2019.05.028

Schmidt, A., Morales-Prieto, D. M., Pastuschek, J., Fröhlich, K., and Markert, U. R. (2015). Only humans have human placentas: molecular differences between mice and humans. *J. Reprod. Immunol.* 108, 65–71. doi: 10.1016/j.jri.2015.03.001

Schoenfelder, S., Mifsud, B., Senner, C. E., Todd, C. D., Chrysanthou, S., Darbo, E., et al. (2018). Divergent wiring of repressive and active chromatin interactions between mouse embryonic and trophoblast lineages. *Nat. Commun.* 9:4189. doi: 10.1038/s41467-018-06666-4

Senner, C. E., Chrysanthou, S., Burge, S., Lin, H. Y., Branco, M. R., and Hemberger, M. (2020). TET1 and 5-Hydroxymethylation Preserve the Stem Cell State of Mouse Trophoblast. *Stem Cell Rep.* 15, 1301–1316. doi: 10.1016/j.stemcr.2020.04.009

Shen, Y., Yue, F., McCleary, D. F., Ye, Z., Edsall, L., Kuan, S., et al. (2012). A map of the cis-regulatory sequences in the mouse genome. *Nature* 488, 116–120. doi: 10.1038/nature11243

Simian, M., and Bissell, M. J. (2017). Organoids: A historical perspective of thinking in three dimensions. *J. Cell Biol.* 216, 31–40. doi: 10.1083/jcb.201610056

Soares, M. J., Varberg, K. M., and Iqbal, K. (2018). Hemochorial placentation: development, function, and adaptations. *Biol. Reprod.* 99, 196–211. doi: 10.1093/biolre/ioy049

Soncin, F., Khater, M., To, C., Pizzo, D., Farah, O., Wakeland, A., et al. (2018). Comparative analysis of mouse and human placentae across gestation reveals species-specific regulators of placental development. *Development* 145:156273. doi: 10.1242/dev.156273

Soncin, F., Natale, D., and Parast, M. M. (2015). Signaling pathways in mouse and human trophoblast differentiation: a comparative review. *Cell Mol. Life Sci.* 72, 1291–1302. doi: 10.1007/s00018-014-1794-x

Strumpf, D., Mao, C. A., Yamanaka, Y., Ralston, A., Chawengsaksophak, K., Beck, F., et al. (2005). Cdx2 is required for correct cell fate specification and differentiation of trophectoderm in the mouse blastocyst. *Development* 132, 2093–2102. doi: 10.1242/dev.01801

Suetake, I., Shinozaki, F., Miyagawa, J., Takeshima, H., and Tajima, S. (2004). DNMT3L stimulates the DNA methylation activity of Dnmt3a and Dnmt3b through a direct interaction. *J. Biol. Chem.* 279, 27816–27823. doi: 10.1074/jbc.M400181200

Takahashi, K., and Yamanaka, S. (2006). Induction of pluripotent stem cells from mouse embryonic and adult fibroblast cultures by defined factors. *Cell* 126, 663–676. doi: 10.1016/j.cell.2006.07.024

Takahashi, K., Tanabe, K., Ohnuki, M., Narita, M., Ichisaka, T., Tomoda, K., et al. (2007). Induction of pluripotent stem cells from adult human fibroblasts by defined factors. *Cell* 131, 861–872. doi: 10.1016/j.cell.2007.11.019

Tantbirojn, P., Crum, C. P., and Parast, M. M. (2008). Pathophysiology of placenta creta: the role of decidua and extravillous trophoblast. *Placenta* 29, 639–645. doi: 10.1016/j.placenta.2008.04.008

Tomikawa, J., Takada, S., Okamura, K., Terao, M., Ogata-Kawata, H., Akutsu, H., et al. (2020). Exploring trophoblast-specific Tead4 enhancers through chromatin conformation capture assays followed by functional screening. *Nucleic Acids Res.* 48, 278–289. doi: 10.1093/nar/gkz1034

Turco, M. Y., Gardner, L., Kay, R. G., Hamilton, R. S., Prater, M., Hollinshead, M. S., et al. (2018). Trophoblast organoids as a model for maternal-fetal interactions during human placentation. *Nature* 564, 263–267. doi: 10.1038/s41586-018-0753-3

Tuteja, G., Chung, T., and Bejerano, G. (2016). Changes in the enhancer landscape during early placental development uncover a trophoblast invasion gene-enhancer network. *Placenta* 37, 45–55. doi: 10.1016/j.placenta.2015.11.001

Ullah, R., Naz, A., Akram, H. S., Ullah, Z., Tariq, M., Mithani, A., et al. (2020). Transcriptomic analysis reveals differential gene expression, alternative splicing, and novel exons during mouse trophoblast stem cell differentiation. *Stem Cell Res. Ther.* 11:342. doi: 10.1186/s13287-020-01848-8

Uzan, J., Carbonnel, M., Piconne, O., Asmar, R., and Ayoubi, J. M. (2011). Pre-eclampsia: pathophysiology, diagnosis, and management. *Vasc. Health Risk Manag.* 7, 467–474. doi: 10.2147/VHRM.S20181

Wang, J., Rao, S., Chu, J., Shen, X., Levasseur, D. N., Theunissen, T. W., et al. (2006). A protein interaction network for pluripotency of embryonic stem cells. *Nature* 444, 364–368. doi: 10.1038/nature05284

Xia, W., Xu, J., Yu, G., Yao, G., Xu, K., Ma, X., et al. (2019). Resetting histone modifications during human parental-to-zygotic transition. *Science* 365, 353–360. doi: 10.1126/science.aaw5118

Xiao, C. L., Zhu, S., He, M., Chen, D., Zhang, Q., Chen, Y., et al. (2018). N 6-Methyladenine DNA Modification in the Human Genome. *Mol. Cell* 71, 306.e–318.e. doi: 10.1016/j.molcel.2018.06.015

Xu, J., and Kidder, B. L. (2018). KDM5B decommissions the H3K4 methylation landscape of self-renewal genes during trophoblast stem cell differentiation. *Biol. Open* 7:31245. doi: 10.1242/bio.031245

Xu, R. H., Chen, X., Li, D. S., Li, R., Addicks, G. C., Glennon, C., et al. (2002). BMP4 initiates human embryonic stem cell differentiation to trophoblast. *Nat. Biotechnol.* 20, 1261–1264. doi: 10.1038/nbt761

Yagi, R., Kohn, M. J., Karavanova, I., Kaneko, K. J., Vullhorst, D., DePamphilis, M. L., et al. (2007). Transcription factor TEAD4 specifies the trophectoderm lineage at the beginning of mammalian development. *Development* 134, 3827–3836. doi: 10.1242/dev.010223

Yamamoto, H., Flannery, M. L., Kupriyanov, S., Pearce, J., McKercher, S. R., Henkel, G. W., et al. (1998). Defective trophoblast function in mice with a targeted mutation of Ets2. *Genes Dev.* 12, 1315–1326. doi: 10.1101/gad.12.9.1315

Conflict of Interest: The authors declare that the research was conducted in the absence of any commercial or financial relationships that could be construed as a potential conflict of interest.

frontiers in Cell and Developmental Biology

ORIGINAL RESEARCH
published: 03 June 2021
doi: 10.3389/fcell.2021.677981

RNA Network Interactions During Differentiation of Human Trophoblasts

Tianjiao Chu[1], Jean-Francois Mouillet[1], Zhishen Cao[1], Oren Barak[1], Yingshi Ouyang[1] and Yoel Sadovsky[1,2]**

[1] *Department of Obstetrics, Gynecology and Reproductive Sciences, Magee-Womens Research Institute, University of Pittsburgh School of Medicine, Pittsburgh, PA, United States,* [2] *Department of Microbiology and Molecular Genetics, University of Pittsburgh School of Medicine, Pittsburgh, PA, United States*

In the human placenta, two trophoblast cell layers separate the maternal blood from the villous basement membrane and fetal capillary endothelial cells. The inner layer, which is complete early in pregnancy and later becomes discontinuous, comprises the proliferative mononuclear cytotrophoblasts, which fuse together and differentiate to form the outer layer of multinucleated syncytiotrophoblasts. Because the syncytiotrophoblasts are responsible for key maternal-fetal exchange functions, tight regulation of this differentiation process is critical for the proper development and the functional role of the placenta. The molecular mechanisms regulating the fusion and differentiation of trophoblasts during human pregnancy remain poorly understood. To decipher the interactions of non-coding RNAs (ncRNAs) in this process, we exposed cultured primary human trophoblasts to standard *in vitro* differentiation conditions or to conditions known to hinder this differentiation process, namely exposure to hypoxia (O_2 < 1%) or to the addition of dimethyl sulfoxide (DMSO, 1.5%) to the culture medium. Using next generation sequencing technology, we analyzed the differential expression of trophoblastic lncRNAs, miRNAs, and mRNAs that are concordantly modulated by both hypoxia and DMSO. Additionally, we developed a model to construct a lncRNA-miRNA-mRNA co-expression network and inferred the functions of lncRNAs and miRNAs via indirect gene ontology analysis. This study improves our knowledge of the interactions between ncRNAs and mRNAs during trophoblast differentiation and identifies key biological processes that may be impaired in common gestational diseases, such as fetal growth restriction or preeclampsia.

Keywords: trophoblast, differentiation, hypoxia, lncRNA, miRNA, gene ontology, RNA network

OPEN ACCESS

Edited by:
Geetu Tuteja,
Iowa State University, United States

Reviewed by:
Sha Sun,
University of California, Irvine, United States
Michelle Holland,
King's College London, United Kingdom

****Correspondence:***
Tianjiao Chu
tchu@mwri.magee.edu
Yoel Sadovsky
ysadovsky@mwri.magee.edu

Specialty section:
This article was submitted to Developmental Epigenetics, a section of the journal Frontiers in Cell and Developmental Biology

Received: *08 March 2021*
Accepted: *29 April 2021*
Published: *03 June 2021*

Citation:
Chu T, Mouillet JF, Cao Z, Barak O, Ouyang Y and Sadovsky Y (2021) RNA Network Interactions During Differentiation of Human Trophoblasts. Front. Cell Dev. Biol. 9:677981. doi: 10.3389/fcell.2021.677981

INTRODUCTION

The fusion of mononucleated cytotrophoblasts into multinucleated syncytiotrophoblasts is a central process in human trophoblast differentiation. Early in pregnancy, this fusion process is a part of the pre-lacunar and lacunar stages of implantation on days 6–12 after fertilization in human pregnancy (Boyd and Hamilton, 1970). Once villi are formed, the fusion of mononucleated cytotrophoblasts into overlying multinucleated syncytiotrophoblasts at the villous surface is

accompanied by a dramatic change in cell morphology, transcriptional output, and the production of growth factors and endocrine signals (Sadovsky and Jansson, 2015). Located at the surface of human placental villi, the syncytiotrophoblasts are uniquely positioned to regulate key functions of the placenta in terms of maternal-fetal gas exchange, the uptake of nutrients into the feto-placental compartment, the release of waste to the maternal blood, the production of hormones and the immune and mechanical protection of the developing fetus (Sadovsky and Jansson, 2015; Burton et al., 2016). The subjacent mononucleated cytotrophoblasts, which form a continuous layer early in pregnancy, later become a discontinuous layer of interspersed cytotrophoblasts that function as progenitors for replenishment of damaged or dead syncytium and homeostatic preservation of this critical layer (Jones and Fox, 1991). The syncytiotrophoblast exhibits polarity, with a microvillous plasma membrane facing the maternal blood on the apical side and a basal plasma membrane located adjacent to the cytotrophoblasts and the basement membrane. Considering its functions, it is not surprising that the syncytiotrophoblast microvillous membrane, which interfaces directly with the maternal blood, harbors receptors for diverse plasma proteins, growth factors, immunoglobulins, and other soluble ligands, all linked to intracellular trophoblast signaling cascades (Dearden and Ockleford, 1983; Sadovsky and Jansson, 2015).

Syncytium formation prior to 10–13 weeks of human pregnancy takes place in a hypoxic environment (Burton et al., 2002; Jauniaux et al., 2006; Burton and Jauniaux, 2018). Beyond that point, and once the maternal blood begins to perfuse the intervillous space, hypoxia may be harmful for proper placental function, leading to cytotrophoblast proliferation, attenuated fusion of cytotrophoblasts into syncytiotrophoblasts, reduced hormone and other biosynthetic functions, and overall syncytial damage and trophoblast death, leading to placental injury and diseases such as fetal growth restriction (Fox, 1970; Arnholdt et al., 1991; Pardi et al., 1993; Alsat et al., 1996; Levy et al., 2000; Pardi et al., 2002; Cartwright et al., 2007; McCarthy et al., 2007; Simon and Keith, 2008; Schoots et al., 2018). Seeking to characterize gene expression changes that define trophoblast differentiation, researchers have focused on the effect of hypoxia on the expression of protein-coding genes in term trophoblasts (Roh et al., 2005; Oh et al., 2011; Wakeland et al., 2017; Kwak et al., 2019).

Recent progress in untangling the complexity of the RNA world has shed light on diverse non-coding RNAs (ncRNAs) that play an essential role in shaping cellular differentiated functions. Among these RNAs, microRNAs (miRNAs) and long non-coding RNAs (lncRNAs) represent the two best characterized classes and perhaps those with the most important regulatory potential. Over 2000 miRNAs are encoded in the human genome. Most of these miRNAs act in the cytosol, where they target mRNAs though imperfect base-pairing to block their translation and accelerate their decay (Bartel, 2009). However, despite their relative simplicity, the full impact of miRNAs on gene expression remains incompletely understood. lncRNAs are more diverse, with an estimated 30,000–100,000 nuclear and cytoplasmic species expressed from the human genome (Iyer et al., 2015; Hon et al., 2017; Uszczynska-Ratajczak et al., 2018; Carlevaro-Fita and Johnson, 2019). Further, the action of lncRNAs is complex, spanning interactions with DNA, RNA, and proteins and involving 3D structural flexibility that enables protein scaffolding and the assembly of multi-subunit complexes and nuclear condensates that shape transcriptional and posttranscriptional functions (Carlevaro-Fita and Johnson, 2019; Statello et al., 2021).

Recent discoveries within the field of placental biology highlighted the putative role of lncRNAs and miRNAs in trophoblastic gene regulatory networks, their role in trophoblast differentiation and in response to hypoxic injury, and the impact of these processes on clinically relevant placental diseases (Canfield et al., 2019; Sheng et al., 2019; Saha and Ain, 2020). A systematic inquiry into network interactions of lncRNAs, miRNAs, and mRNAs in differentiating primary human trophoblasts (PHT cells) is lacking. Here, we used an *in vitro* model of cultured PHT cells to investigate harmonized changes of lncRNAs, miRNAs, and mRNAs during PHT cell differentiation. In addition to exposure of PHT cells to hypoxia (Nelson et al., 1999), diverse chemicals and culture conditions have been employed *in vitro* to modulate the differentiation of PHT cells. *Douglas et al.* found that cytotrophoblasts exposed to 1.5% DMSO retain their mononuclear morphology, culminating in drastic inhibition of hCG production (Thirkill and Douglas, 1997). Other approaches to limit trophoblast differentiation include the use of colchicine, an inhibitor of microtubule polymerization (Douglas and King, 1993), cobalt chloride, a hypoxia-mimicking agent (Daoud et al., 2005; Rimon et al., 2008), and the use of Ham's/Waymouth medium (Douglas and King, 1990; Chen et al., 2004; Bildirici et al., 2018). The deployment of these culture conditions led to the discovery of a repertoire of genes that have been implicated in trophoblast differentiation and to which hypoxia-induced placental injury has been attributed (Jiang and Mendelson, 2005; Chen et al., 2006; Soares et al., 2017).

We sought to hinder trophoblast differentiation using hypoxia or the addition of DMSO to the culture medium, two approaches that have led to reproducible results in our laboratory (Nelson et al., 1999; Yusuf et al., 2002; Roh et al., 2005; Oh et al., 2011; Mouillet et al., 2013; Bildirici et al., 2018; Beharier et al., 2020). We used next generation sequencing technology to identify differentially expressed lncRNAs, miRNAs, and mRNAs during these processes. Importantly, we interrogated the interactions among these RNAs and inferred the main biological processes represented by co-expression patterns.

MATERIALS AND METHODS

Placentas and Dispersed Primary Human Trophoblasts

All placentas used in our studies were obtained from uncomplicated pregnancies and term deliveries at Magee-Womens Hospital in Pittsburgh, under a protocol that was approved by the Institutional Review Board at the University of Pittsburgh. PHT cells were isolated using the

trypsin-DNase-dispase/Percollx method as described by Kliman et al. (1986), with modifications as we previously published (Nelson et al., 1999; Mouillet et al., 2010). PHT cells were cultured in DMEM (Sigma-Aldrich, St. Louis, MO) containing 10% bovine growth serum (HyClone, Logan, UT) and 1% P/S antibiotics (Sigma-Aldrich) at 37°C in a 5% CO_2-air atmosphere, until culture conditions were modified as below.

The data used for this study were derived from two independent sets of experiments, each including several paradigms (**Figure 1**). In the first experimental set, PHT cells from five independently collected placentas were first cultured for 4–6 h in standard conditions (20% O_2) to allow adhesion, using protocols established in our lab. Some of the cells were harvested at the end of the initial incubation period (time 0 in **Figure 1**) and were used as control. The remaining plates from the same culture were maintained for an additional 48 h in either standard culture conditions or in hypoxia (O_2 < 1%), using a dedicated hypoxia chamber, as we previously described (Mouillet et al., 2010). In the second experimental set, PHT cells from six independently collected placentas were first cultured for 4–6 h in standard conditions as above. The culture continued for an additional 48 h, with some of the cells exposed to DMSO 1.5% (Sigma-Aldrich), designed to mitigate cell differentiation as previously shown (Douglas and King, 1990) and reproducibly validated by us (Schaiff et al., 2000; Yusuf et al., 2001).

RNA Extraction, Library Preparation, and Sequencing

Total RNA was isolated from from placental specimens by using TRI Reagent (Sigma) according to the manufacturer's instructions and purified using EconoSpin spin columns (Epoch Life Science, Missouri City, TX). The quantity and quality of total RNA was determined with a NanoDrop 1000 spectrometer (Thermo Fisher, Waltham, MA) and an Agilent bioanalyzer (Agilent Technologies, Santa Clara, CA). From each extracted RNA sample, we used 10 μg of total RNA to generate two types of libraries—one for long RNAs (≥200 nt), including mRNAs and lncRNAs, and one for small RNAs. The libraries were prepared and sequenced by Ocean Ridge Biosciences (Palm Beach Gardens, FL) and by McGill University's Génome Québec Innovation Centre (Montréal, Canada). For the second set of experiments, the libraries were prepared and sequenced at the Health Sciences Sequencing Core at Children's Hospital of Pittsburgh. The miRNA samples were sequenced using the QIAseq miRNA sequencing protocol, which links a unique molecular identifier (UMI) to each miRNA to reduce sequencing bias. Data from all experiments were deposited to the Sequence Read Archive (SRA) at the National Center for Biotechnology Information with BioProject IDs: PRJNA674312, PRJNA674329, PRJNA674366, PRJNA704383, PRJNA704399, PRJNA704393.

Reverse Transcriptase and Quantitative PCR (RT-qPCR)

RNA was extracted from cells with TRI Reagent (Sigma). cDNA was synthesized from 1 μg of total RNA by using the High-Capacity cDNA Reverse Transcription kit (Applied Biosystems, Foster City, CA) according to the manufacturer's protocol. Template cDNA was PCR-amplified with the gene-specific primer sets (**Supplementary Figure 1B**). RT-qPCR was performed using SYBR Select (Applied Biosystems) in a ViiA 7 system (Applied Biosystems). Analysis of qPCR data was performed using the delta-delta Ct method (Livak and Schmittgen, 2001), normalized to glyceraldehyde-3-phosphate dehydrogenase expression.

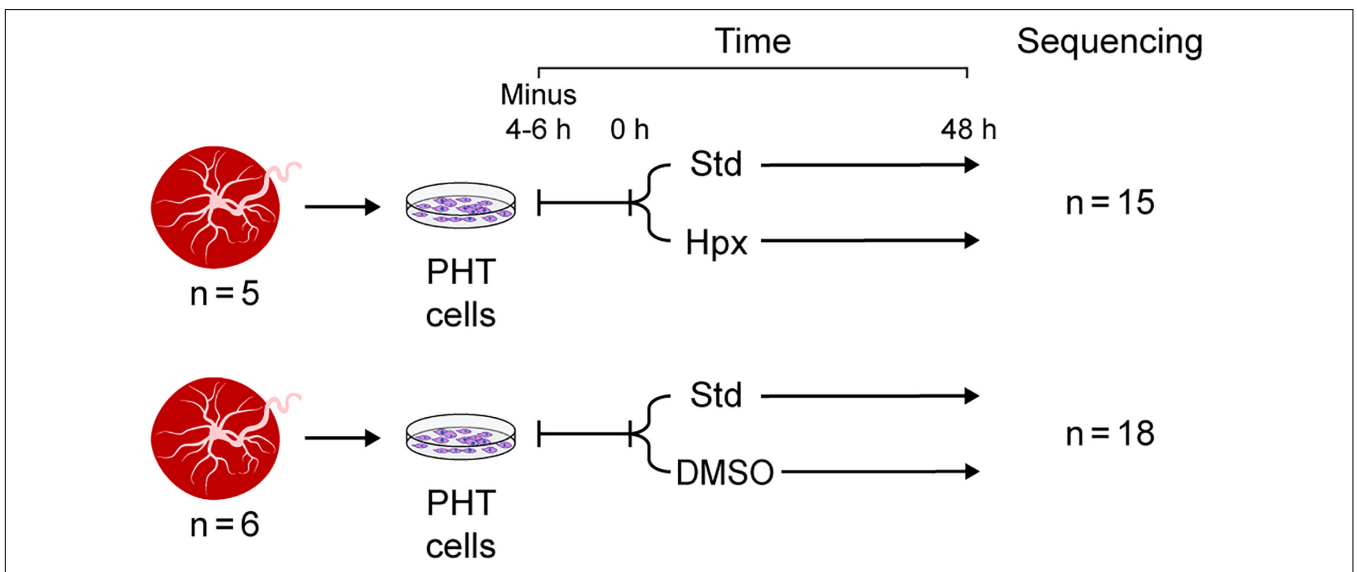

FIGURE 1 | Experimental design. Note that PHT cells were sequenced at 0 h (4–6 h after plating, serving as control) and at 48 h in standard culture conditions or in the two experimental exposure sets: hypoxia (Hpx) or DMSO added to the culture medium.

RNAseq Data Processing

The long RNA libraries were aligned to human reference genome GRCh38 using STAR (2.5.2b), an RNAseq alignment tool (Dobin et al., 2013), and annotated with GENCODE v25 (Frankish et al., 2019). The number of reads per gene was calculated for each RNAseq library, using STAR. We used the definition of lncRNA, which includes antisense RNA, sense intronic RNA, processed transcripts, and sense-overlapping RNAs (Derrien et al., 2012). The 15 small RNA libraries from the first set of experiments were analyzed using our validated miRNA sequencing data analysis pipeline (Chu et al., 2015). Briefly, after pre-processing the library reads, including the removal of adaptor sequences and dimerized primer sequences, we used Bowtie to align all remaining reads with of least 15 nucleotides to the human reference genome (GRCh38) (Langmead et al., 2009). The BEDTools program was used to intersect the alignments to a mature miRNA database maintained by miRBase (v21). The intersected alignments were summarized to obtain counts for all miRNAs. The 18 small RNA libraries from the second set of experiments were processed using the online Qiagen Primary QIAseq miRNA quantification tool[1] to handle the reads with UMIs. We found an extremely high correlation between miRNA counts with distinct UMIs and total miRNA reads. To ensure consistency across the two experimental sets, the total miRNA reads were used as the miRNA expression data.

The counts of long and short RNAs in the sequencing libraries were assumed to follow negative binomial distributions. The negative binomial test, implemented in the Bioconductor R package DESeq2 (Love et al., 2014), was used to identify differentially expressed lncRNAs, miRNAs, and mRNAs. Fisher exact test was used to perform gene ontology analysis and identify the biological processes that were over-represented in selected mRNAs. All *p*-values from multiple simultaneous multiples tests were adjusted using Benjamin and Hochberg's method to control the false discovery rate (Benjamini and Hochberg, 1995).

Model-Based Co-expression Analysis

We proposed a model-based method to identify mRNAs that were co-expressed with lncRNAs and/or miRNAs. Specifically, we assume that the two genes are co-expressed if their expressions Y and X are related through a (generalized) linear model:

$$g\left(E\left[Y \mid X, Z\right]\right) = aX + BZ,$$

where g is the link function, Z is the vector of confounding variables, B is a row vector representing the coefficients of Z, and a is a non-zero coefficient representing the co-expression relation between X and Y. We then examined whether X and Y were co-expressed by testing if $a = 0$. Note that when X, Y, and Z have a joint multivariate normal distribution, this is equivalent to testing whether X and Y have a zero partial correlation, given Z. As we used a negative binomial model to analyze the gene expression, Y is the count for one gene and X the log-transformed and normalized expression of the other gene. The vector B accounts for the experimental exposure and for placentas used for each batch of PHT cells.

[1] www.qiagen.com/

Analysis of Gene Ontology

Because the functions of lncRNAs and miRNAs are not available from the gene ontology database, we proposed an indirect approach through the gene co-expression analysis described above. Specifically, given a set of lncRNAs or miRNAs and using the model-based co-expression analysis, we identified all mRNAs that are co-expressed with each of the lncRNAs or miRNAs. The top-ranked mRNAs were then used for analysis of gene ontology to identify the enriched biological processes, attributed to altered expression of the set of lncRNAs or miRNAs.

The statistical analyses, detailed above, were performed using R (R Development Core Team, 2012) and Bioconductor (Gentleman et al., 2004). For analysis of lncRNA by RT-qPCR, the fold-change data were analyzed using Kruskal Wallis non-parametric test, with *post hoc* Tukey test for all pairwise comparisons. RT-qPCR data analysis was performed using Prism software (GraphPad Software, San Diego, CA).

RESULTS

Using an average read of 0.5 per library as a cutoff in the first set of experiments, we identified 33,719 long RNAs, including 8,035 lncRNA and 17,298 mRNA species, from the 15 long RNA libraries and 923 miRNAs from the 15 small RNA libraries. In the second set of experiments, we identified 30,421 long RNAs from the 15 long RNA libraries, including 6,988 lncRNA and 16,723 mRNA species, and 2,416 miRNAs from the 15 small RNA libraries. Overall, mRNAs had a higher read count per library than lncRNAs (**Figure 2**). For example, in the first experiment the median of average lncRNA reads per library was 6.2, compared to 457.5 reads for the mRNAs. In the second experiment, the corresponding values were 4.2 and 267.7, respectively. We also used RT-qPCR to validate the expression changes of 10 lncRNAs (**Supplementary Figure 1**), as we previously did for mRNA and miRNA transcript data (Mouillet et al., 2010; Xie et al., 2014).

To visualize the effect of exposure and potential confounding factors on the PHT transcriptome, we normalized and log transformed the long RNA and miRNA library data, using the regularized and variance-stabilizing transformation method in the Bioconductor package DESeq2. We then performed classical multidimensional scaling, respectively, for lncRNAs, miRNA, and mRNAs (**Figure 3**). These plots showed that the experimental conditions markedly influenced the PHT transcriptome. The exposure effect dominated for mRNAs in the two experimental sets and for lncRNAs in the second set and was clearly visible for lncRNAs in the first set and for miRNAs in both experimental sets. The plots also showed a batch effect on the expression of lncRNAs and miRNAs in the first experimental set (hypoxia), as samples 1 and 2 were processed by a different lab than samples 3–5. Our data also suggest an effect of the placenta on miRNAs in both experimental sets.

We tested the lncRNAs, miRNAs, and mRNAs that were differentially expressed between the conditions in the two experimental sets. For this, we used negative binomial regression models with two factors: the exposure factor

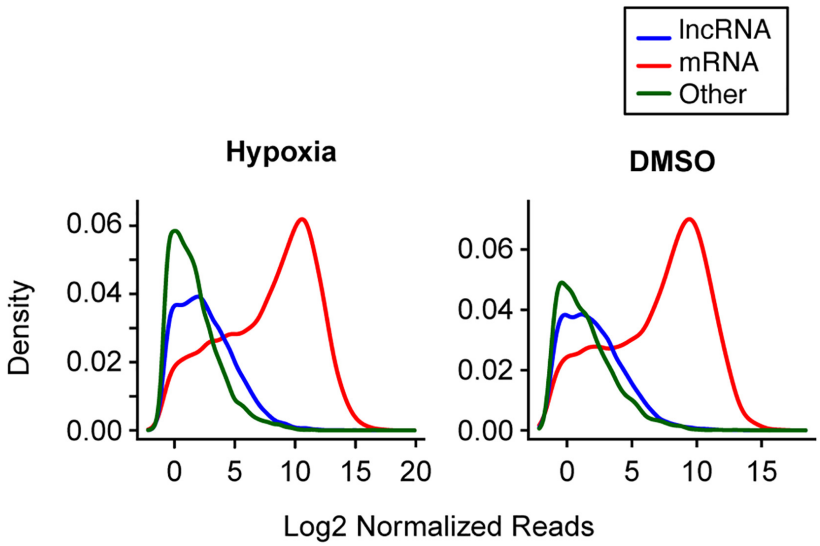

FIGURE 2 | The distribution of selected long RNA reads in PHT cells in the two experimental sets. The *X*-axis represents the average log2 normalized reads per library, and the *Y*-axis represents the estimated probability density. Note that analysis of multiple small RNA species was not performed, as the sequencing procedure was designed to enrich for miRNA (which represented 72.3% of small RNAs in hypoxia and 68.8% of RNAs in DMSO).

(hypoxia, DMSO) and the placenta factor, which refers to inter-individual variation in placental transcriptome and possible differences in processes related to placental collection and cell preparation. After controlling the false discovery rate at 0.05, the numbers of differentially expressed lncRNAs, miRNAs, and mRNAs are shown in **Table 1**. For convenience, herein genes differentially expressed under the hypoxic as opposed to the standard condition are termed "hypoxia-DE" genes, and genes differentially expressed with DMSO as distinguished from the standard condition are termed as "DMSO-DE" genes. We next examined the number of lncRNAs, miRNAs, and mRNA that exhibited concordant (**Figure 4**) or discordant (**Supplementary Figure 2**) expression change across the two experimental sets. We noticed a significant concordance (up or down) in RNA expression change between the two sets of experimental exposures, namely "hypoxia-DE" and "DMSO-DE" genes (**Figure 5**). This concordance was noted primarily for lncRNA and mRNA species (**Figures 5A,C**), with less concordance for up- or downregulated miRNAs (**Figure 5B**).

We also assessed the similarity of the two experimental sets by examining expression differences in mRNAs, lncRNAs, and miRNAs, between the 0 and 48 h time points, under standard conditions. We found an extremely high concordance (up or down) in the expression change of all three types of RNAs between the two experimental sets (**Supplementary Figure 3**). This confirms that the two experimental sets are comparable for similar conditions, thus supporting our experimental approach.

We provided additional support to our findings by comparing our gene expression changes with published human placental single cell RNAseq (scRNAseq) data, predicting that our data would be similar to gene expression changes between syncytiotrophoblasts and cytotrophoblasts. We performed this analysis using the PlacentaCellEnrich tool (Jain and Tuteja, 2021), available for protein coding genes, and examined changes among the 19 mRNAs with the highest concordant log2-fold increased expression and the 6 mRNAs with the highest concordant log2-fold decreased expression between standard conditions and hypoxia/DMSO. Among the selected 25 mRNAs (**Supplementary Table 1**) the vast majority of our results were consistent with the scRNAseq data, as predicted, with expression changes between standard conditions vs. hypoxia/DMSO that are similar to changes between syncytiotrophoblasts and cytotrophoblasts. Notably, discrepancies were more common for one of the databases, likely reflecting much lower mRNA expression levels and a lower magnitude of the log2-fold change for mRNAs that are downregulated during cell differentiation.

To define pathways that might be implicated in reduced trophoblast differentiation, we performed direct and indirect gene ontology analyses. We focused on genes with at least a moderate expression, defined as having a minimum of 25 reads per library. For mRNA, we focused on 3,338 hypoxia-DE genes, 2,232 DMSO-DE genes, and 988 DE genes that were concordantly altered in the two sets of experiments. **Table 2** shows the shared biological processes that were significantly enriched based on mRNA changes in "hypoxia-DE" and in "DMSO-DE" transcripts, irrespective of lncRNA or miRNA co-expression. **Supplementary Table 2** shows differentially expressed mRNAs that were concordantly expressed in the two exposure sets and that are co-expressed with at least one differentially expressed lncRNA and miRNA, where both lncRNA and miRNA exhibit concordant expression change (up- or downregulation) between the two exposure sets.

To further pursue the biological pathways reflecting mRNA expression changes that were associated with differentially expressed lncRNAs and/or differentially expressed miRNAs, we

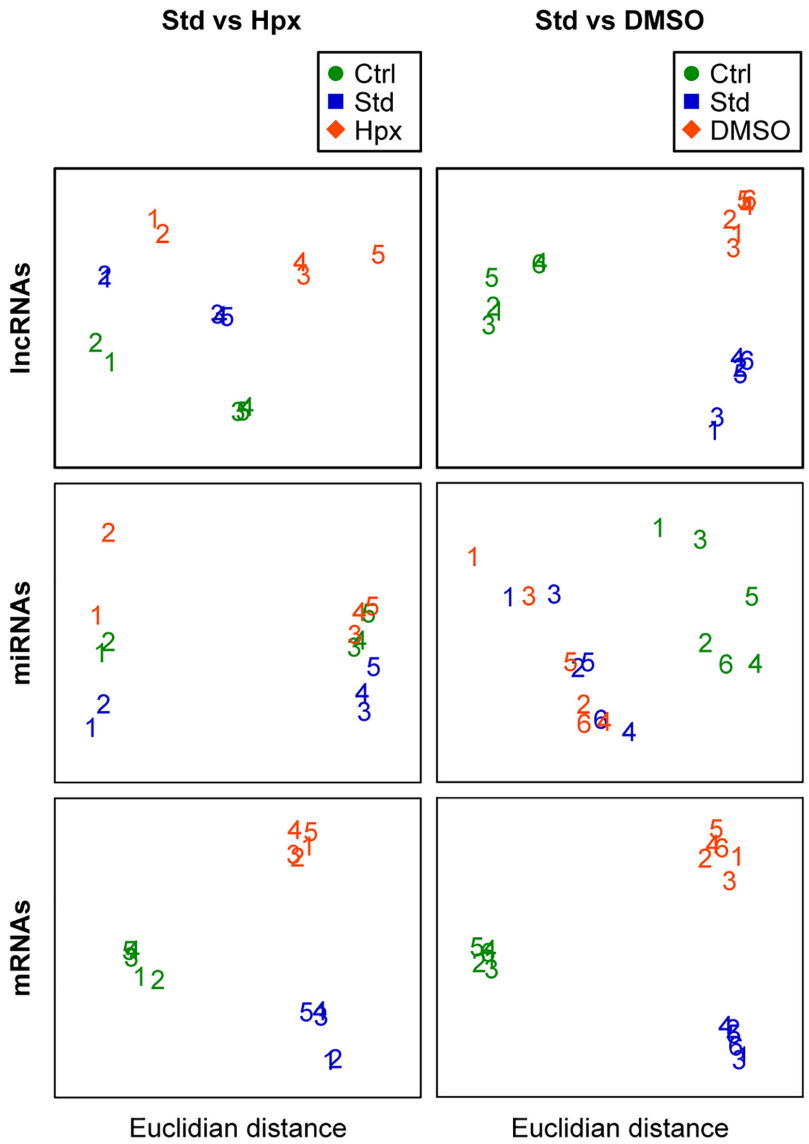

FIGURE 3 | Multidimensional scaling plots of RNAs in the two experimental sets. Classic multidimensional scaling plots of lncRNAs, miRNAs, and mRNAs were created using Euclidean distance as dissimilarity matrix across the samples. The cells were sequenced after plating (Ctrl), 48 h after culture in standard condition (Std) or after culture in hypoxia (Hpx) or in medium with added DMSO. The numbers in the plots represent each placental ID in the two exposure sets.

performed indirect gene ontology analysis as described in section "Materials and Methods." We first selected the 438 hypoxia-DE lncRNAs and 85 hypoxia-DE miRNAs, 167 DMSO-DE lncRNAs and 115 DMSO-DE miRNAs, as well as 66 concordant DE lncRNAs and 9 concordant DE miRNAs. We then performed model-based co-expression analysis for these associations on the basis of our negative binomial regression model. **Table 3** shows biological processes attributed to mRNAs that were expressed in a concordant manner in the two exposures, in association with changes with either lncRNA *or* with miRNA in the same conditions. Lastly, we identified the biological processes attributed to mRNAs that were differentially expressed in a concordant manner between the two exposures in association with changes with both lncRNA *and* with miRNA in the same conditions (**Table 4**). These associations are also shown in the Circos plot (**Figure 6**).

TABLE 1 | The numbers of differentially expressed RNA transcripts in the two experimental sets.

	Std vs. Hypoxia		Std vs. DMSO	
	Up	**Down**	**Up**	**Down**
mRNA	4,803	4,236	4,354	4,607
lncRNA	571	1,658	1,012	422
Other RNA	311	1,234	520	264
miRNA	69	58	94	156

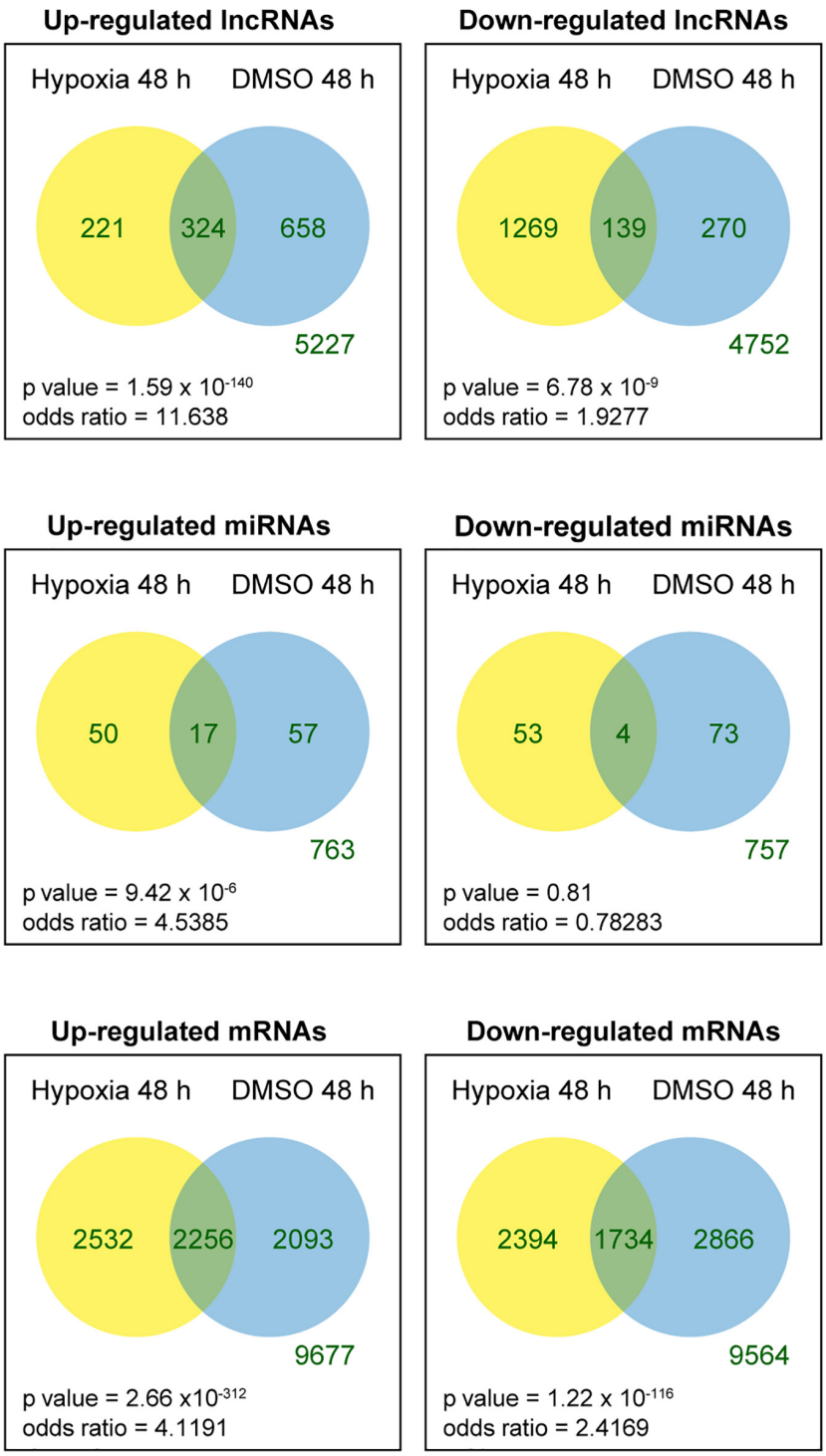

FIGURE 4 | Venn diagram of differentially expressed RNAs across the two experimental sets. Fisher exact tests were used to determine whether the genes that were up- or downregulated in one experimental set were more likely to be regulated in the same direction in the other experimental set.

DISCUSSION

To decipher RNA interactions during differentiation of primary term human trophoblasts, we interrogated two sets of experiments, where the normal differentiation process was hindered either by the physiologically relevant exposure to hypoxia or by using the chemical DMSO (Thirkill and Douglas, 1997; Nelson et al., 1999; Yusuf et al., 2002; Roh et al., 2005;

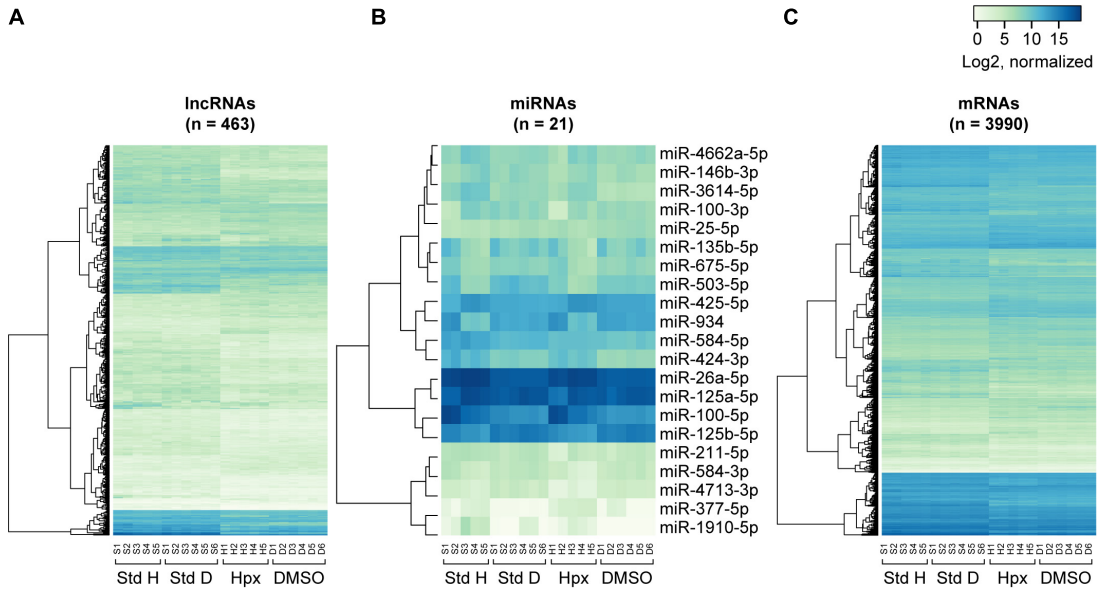

FIGURE 5 | Heatmaps of RNA expression clustering across the experimental paradigms. The heatmaps were constructed on the basis of normalized log2 gene expression for concordantly differentially expressed lncRNAs **(A)**, miRNAs **(B)**, and mRNAs **(C)** in the two exposure sets. Note that the first letter of the sample labels at the bottom of each plot represent experimental condition: "S" for 48 h in standard conditions, "H" for 48 h in hypoxic conditions, and "D" for 48 h in DMSO-containing medium. The number represents placental ID in each experiment. "Std H" and "Std D" refer to 48 h Std conditions in the hypoxia or DMSO experiments, respectively.

Oh et al., 2011). Because each of these exposures may influence the PHT transcriptome in a manner that is independent of the effect on differentiation, we focused on RNA interactions that are shared by both exposures. We surmised that identification of such interactions may suggest RNA regulatory pathways that govern trophoblast differentiation.

Our informatics-based data offered general insight into changes in the trophoblast transcriptome during differentiation. We noticed that the average number of reads for each lncRNA is about 1.3∼1.5% of the average mRNA read number. Based on Ensembl Gene 87 (Aken et al., 2017), the average length of a lncRNA molecule is 1 kb, and 1.7 kb for mRNA. Therefore, the average expression of lncRNA in PHT cells is between 2.2 and 2.5% of mRNA. This lower expression of lncRNA relative to mRNA was shown in other cell systems (Palazzo and Lee, 2015). Note that the reads per library for lncRNAs and mRNAs in the first experimental set are higher because of the larger average library size in that set. Further, our data show that the distribution of the reads per library of "other RNAs" is somewhat different between the two experiments (**Figure 2**). These two factors likely reflect differences in library size, preparation, and sequencing technology between the two experimental sets. Indeed, even among the "other RNAs," these factors tend to have a greater effect on smaller RNAs (**Supplementary Figure 4**). Importantly, these technical factors would not affect our analysis, because we tested the differential expression in the two experimental sets separately, and took library size into account in our statistical tests.

Importantly, we found that lncRNAs, miRNAs, and mRNAs respond to hypoxia and DMSO in different ways. Notably, mRNAs and lncRNAs exhibited a similar change in expression patterns despite of their vastly different expression levels: both RNA types clustered by the experimental conditions (**Figure 3**), both differentially expressed mRNAs and lncRNAs tended to have larger log2 fold expression change (**Figure 4**), and both exhibited significant concordance in DE transcripts between the two experimental sets (**Figure 5**). In contrast, DE miRNA clustering reflected not only the experimental exposure but also the placenta used for PHT cell dispersal and, in the case of hypoxia, even the laboratory performing the sequencing **Figure 3**). This observation could be explained by the smaller log2 fold expression change in differentially expressed miRNAs (**Figure 4**), a smaller number of miRNA with a concordant expression change between the two experimental sets (**Figure 5**), or differences in sequencing technology among the laboratories.

We identified mRNAs that were concordantly differentially expressed across both experimental sets and correlated with altered expression of ≥ 1 lncRNA *and* miRNA (**Supplementary Table 1**). Some of the identified transcripts were previously shown to be related to germane trophoblast processes and to complications of pregnancy. SDC1 (Syndecan1) was shown to have a positive correlation with trophoblast differentiation and exhibited lower expression in hypoxia/DMSO exposure compared to standard conditions (Prakash et al., 2011). Several identified differentially expressed mRNAs are known to regulate the invasion or adhesion of trophoblasts and other types of cells. KISS1 has a role in early placentation and implantation, ADAM12 (ADAM metallopeptidase domain 12) was shown to control trophoblast fusion through E-cadherin, and NECTIN3 (Nectin Cell Adhesion Molecule 3) is a member of a cell

TABLE 2 | Biological processes enriched in mRNAs that exhibited a concordant expression change during trophoblast differentiation[a] and ranked by adjusted *p*-value.

Process
Immune response
Female pregnancy
Signal transduction
Inflammatory response
Cell surface receptor signaling pathway
Immune system process
Chemokine-mediated signaling pathway
Cell-cell signaling
Response to drug
Retinoid metabolic process
Cytokine-mediated signaling pathway
Positive regulation of cytosolic calcium ion concentration
Positive regulation of T cell proliferation
Defense response
Regulation of calcium ion-dependent exocytosis
Calcium ion-regulated exocytosis of neurotransmitter
Multicellular organism development
Cell adhesion
Positive regulation of phagocytosis, engulfment
Chemotaxis
Single organismal cell-cell adhesion
Innate immune response
Keratinization
Cellular response to lipopolysaccharide
G-protein coupled receptor signaling pathway
Positive regulation of ERK1 and ERK2 cascade
Positive regulation of cell proliferation

[a] *Trophoblast differentiation was defined as expression change in control vs. hypoxia and in control vs. DMSO exposure.*

TABLE 3 | Biological processes enriched in mRNAs that were associated with lncRNA *or* miRNA during trophoblast differentiation, and ranked by adjusted *p*-value.

Association	Biological processes
mRNA associated with lncRNA[a]	Positive regulation of transcription from RNA pol II promoter
	Response to drug
	Inflammatory response
	Response to mechanical stimulus
	Positive regulation of gene expression
	Cellular oxidant detoxification
mRNA associated with miRNA[a]	Female pregnancy
	Cell adhesion
	Inflammatory response
	Extracellular matrix disassembly
	Cell-cell signaling
	Positive regulation of angiogenesis
	Response to drug

[a] *At least one DE lncRNA or one DE miRNA, respectively, were associated with mRNA in the two exposures.*

TABLE 4 | Biological processes enriched in mRNAs that were associated with lncRNA *and* miRNA during trophoblast differentiation[a], and ranked by adjusted *p*-value.

Process
Female pregnancy
Cholesterol metabolic process
Lipoprotein metabolic process
Positive regulation of cytosolic calcium ion concentration
Placenta development
Cell adhesion
Inflammatory response
Positive regulation of phagocytosis, engulfment
Retinoid metabolic process
Cytokine-mediated signaling pathway
Cellular response to hormone stimulus
Signal transduction
Immune response
Chemotaxis
Response to drug

[a] *At least one DE lncRNA and one DE miRNA were associated with altered mRNA expression in the two experimental exposures.*

adhesion family of proteins (Reymond et al., 2000; Aghababaei et al., 2015; Hu et al., 2019). Some of the genes with the most pronounced expression changes are related to preeclampsia, where hypoxia is commonly implicated in disease pathogenesis (Tal, 2012). Indeed, reduced placental expression of LGALS13 (Galectin 13), a member of the glycan-binding proteins that regulate innate and adaptive immune responses, was found in women with preeclampsia (Than et al., 2014). Similarly, the expression of SDC1, NPPB (natriuretic peptide B), GDF15 (growth differentiation factor 15), and ADAMTS6 (ADAM metallopeptidase with thrombospondin type 1 motif 6) all had a lower expression in our experimental exposures, and all are lower in preeclampsia (Junus et al., 2014; Chen et al., 2016; Gandley et al., 2016; Jiang et al., 2020). In contrast, our data are inconsistent with respect to the expression of PAPPA2, a regulator of trophoblast invasion and migration, or MNDA (myeloid cell nuclear differentiation antigen), which exhibited a lower expression level in our paradigms but is elevated in placentas from women with preeclampsia (Wagner et al., 2011; Kolialexi et al., 2017; Neuman et al., 2020).

A major innovative aspect of our work is the use of the model-based co-expression analysis. The Pearson correlation coefficient is often used as a measurement of co-expressed genes. When the data do not follow multivariate normal distribution, more robust methods, such as the Spearman correlation or the bi-weight mid-correlation, are recommended (Zhang and Horvath, 2005). These methods, however, may not be optimal for "real world" data, which are often influenced by confounding variables, such as the sample processing by separate laboratories in our first experimental sets, a factor known to strongly influence expression measurements. Thus, two genes may have significant correlation not because of shared biological pathways, but simply because the expression measurements were performed by a

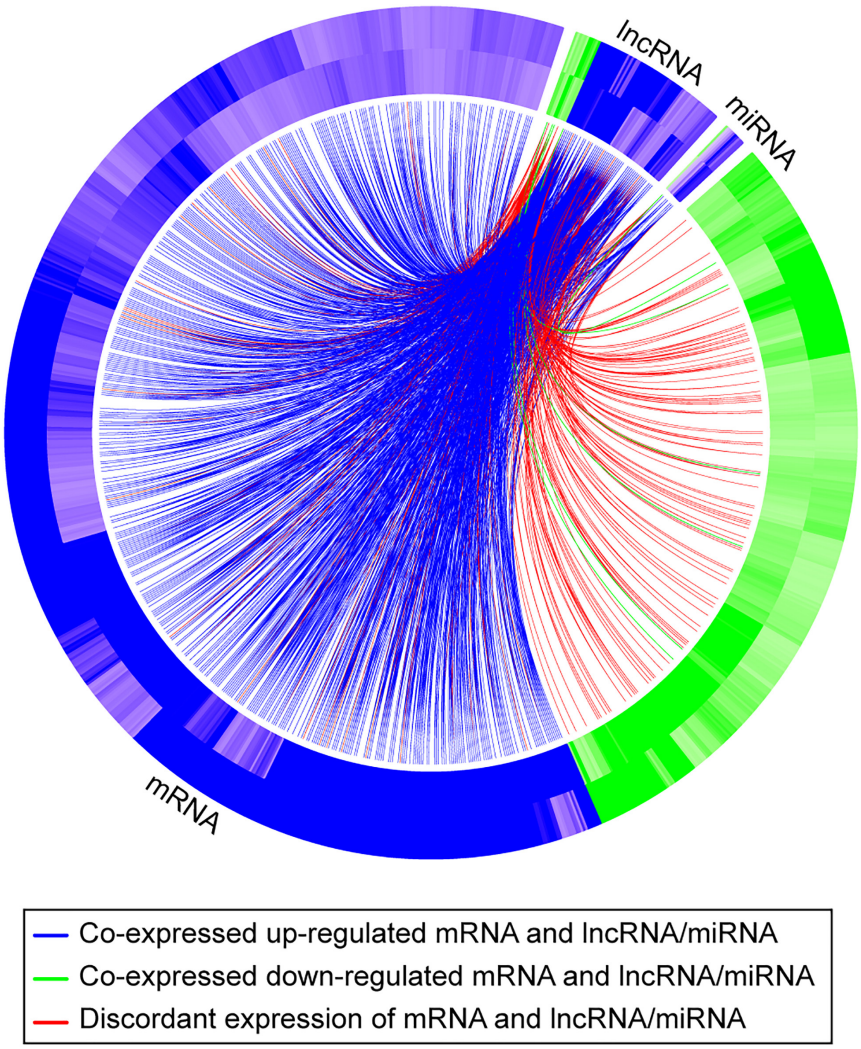

FIGURE 6 | A Circos plot depicting the association of mRNAs, lncRNAs, and miRNAs that exhibit a concordant expression change in the two exposures (hypoxia and DMSO). The outer band of the ring represents log2 fold changes in standard vs. hypoxia exposure, and the inner band of represents log2 fold changes in standard vs. DMSO exposure. Blue denotes that the RNA is upregulated; green denotes that the RNA is downregulated. The curved lines connect each lncRNA/miRNA to the co-expressed mRNAs, with blue (upregulation) and green (downregulation) lines representing positive correlations and red lines representing negative correlations.

certain laboratory or technology. Using the model-based method proposed in this paper, we can eliminate the "spurious" co-expression caused by known confounding factors. This is critical when data from multiple experiments are combined in a meta co-expression analysis. For example, consider a confounding factor Z with N(0,1) distribution, and two genes X, Y that are conditionally independent, given Z = z, with distribution N(z,1). It then follows that the Pearson correlation between X and Y is 0.5. As mentioned before, under this scenario, the model-based co-expression test is equivalent to testing whether X and Y have a zero partial correlation, given Z. It is easy to see that here, indeed, the partial correlation between X and Y, given Z, is 0. Thus, we correctly capture the independent relation between X and Y given the confounder Z, and eliminate the spurious correlation.

We recognize that this paper has several limitations. First, the data were collected over a period of 4 years, and two laboratories were used to perform RNAseq in the first experimental set. Although we have developed statistical models to address this shortcoming, it might have negatively affected the power of this study. Second, our results were derived from an informatic analysis of the gene expression data on the basis of RNA sequencing libraries. It will therefore require future experimental validation. This is particularly important as the regulation of mRNA by lncRNA and miRNA is a complex process, involving direct and indirect regulation and chromatin remodeling. For the same reason we did not consider the presence of or absence of miRNA-response elements in gene ontology analysis. Finally, our work is limited to *in vitro* approaches, which may not be fully consistent with changes that occur *in vivo*. In the future, we plan

to collect additional data from our experiments and from public databases to strengthen and validate our results.

DATA AVAILABILITY STATEMENT

The datasets presented in this study can be found in online repositories. The names of the repository/repositories and accession number(s) can be found below: https://www.ncbi.nlm.nih.gov/, PRJNA674312; https://www.ncbi.nlm.nih.gov/, PRJNA674329; https://www.ncbi.nlm.nih.gov/, PRJNA674366; https://www.ncbi.nlm.nih.gov/, PRJNA704383; https://www.ncbi.nlm.nih.gov/, PRJNA704399; https://www.ncbi.nlm.nih.gov/, PRJNA704393.

ETHICS STATEMENT

The studies involving human participants were reviewed and approved by the Institutional Review Board at the University of Pittsburgh. Written informed consent for participation was not required for this study in accordance with the national legislation and the institutional requirements.

AUTHOR CONTRIBUTIONS

TC, JFM, and YS: study design, manuscript writing. TC and YS: provided study materials. TC and ZC: data generation and analysis. TC, JFM, YO, OB, and YS: data interpretation. All authors contributed to the article and approved the submitted version.

FUNDING

This project was supported by Eunice Kennedy Shriver National Institute of Child Health and Human Development (NIH/NICHD) grants R01-HD065893 (to YS), Pennsylvania Department of Health Formula Research Funds (to TC and JFM).

ACKNOWLEDGMENTS

We thank Elena Sadovsky and Tiffany Coon for technical assistance, Lori Rideout for assistance with manuscript preparation, and Bruce Campbell for editing.

SUPPLEMENTARY MATERIAL

The Supplementary Material for this article can be found online at: https://www.frontiersin.org/articles/10.3389/fcell.2021.677981/full#supplementary-material

REFERENCES

Aghababaei, M., Hogg, K., Perdu, S., Robinson, W. P., and Beristain, A. G. (2015). ADAM12-directed ectodomain shedding of E-cadherin potentiates trophoblast fusion. *Cell Death Differ.* 22, 1970–1984. doi: 10.1038/cdd.2015.44

Aken, B. L., Achuthan, P., Akanni, W., Amode, M. R., Bernsdorff, F., Bhai, J., et al. (2017). Ensembl 2017. *Nucleic Acids Res.* 45, D635–D642. doi: 10.1093/nar/gkw1104

Alsat, E., Wyplosz, P., Malassiné, A., Guibourdenche, J., Porquet, D., Nessmann, C., et al. (1996). Hypoxia impairs cell fusion and differentiation process in human cytotrophoblast, in vitro. *J. Cell. Physiol.* 168, 346–353.

Arnholdt, H., Meisel, F., Fandrey, K., and Löhrs, U. (1991). Proliferation of villous trophoblast of the human placenta in normal and abnormal pregnancies. *Virchows Arch. B Cell Pathol. Incl. Mol. Pathol.* 60, 365–372. doi: 10.1007/bf02899568

Bartel, D. P. (2009). MicroRNAs: target recognition and regulatory functions. *Cell* 136, 215–233. doi: 10.1016/j.cell.2009.01.002

Beharier, O., Tyurin, V. A., Goff, J. P., Guerrero-Santoro, J., Kajiwara, K., Chu, T., et al. (2020). PLA2G6 guards placental trophoblasts against ferroptotic injury. *Proc. Natl. Acad. Sci. U.S.A.* 117, 27319–27328. doi: 10.1073/pnas.2009201117

Benjamini, Y., and Hochberg, Y. (1995). Controlling the false discovery rate: a practical and powerful approach to multiple testing. *J. R. Stat. Soc. Series B Stat. Methodol.* 57, 289–300.

Bildirici, I., Schaiff, W. T., Chen, B., Morizane, M., Oh, S. Y., O'brien, M., et al. (2018). PLIN2 is essential for trophoblastic lipid droplet accumulation and cell survival during hypoxia. *Endocrinology* 159, 3937–3949. doi: 10.1210/en.2018-00752

Boyd, J. D., and Hamilton, W. J. (1970). *The Human Placenta*. Cambridge: Heffer.

Burton, G. J., and Jauniaux, E. (2018). Pathophysiology of placental-derived fetal growth restriction. *Am. J. Obstet. Gynecol.* 218, S745–S761. doi: 10.1016/j.ajog.2017.11.577

Burton, G. J., Fowden, A. L., and Thornburg, K. L. (2016). Placental origins of chronic disease. *Physiol. Rev.* 96, 1509–1565. doi: 10.1152/physrev.00029.2015

Burton, G. J., Watson, A. L., Hempstock, J., Skepper, J. N., and Jauniaux, E. (2002). Uterine glands provide histiotrophic nutrition for the human fetus during the first trimester of pregnancy. *J. Clin. Endocrinol. Metab.* 87, 2954–2959. doi: 10.1210/jcem.87.6.8563

Canfield, J., Arlier, S., Mong, E. F., Lockhart, J., Vanwye, J., Guzeloglu-Kayisli, O., et al. (2019). Decreased LIN28B in preeclampsia impairs human trophoblast differentiation and migration. *FASEB J.* 33, 2759–2769. doi: 10.1096/fj.201801163R

Carlevaro-Fita, J., and Johnson, R. (2019). Global positioning system: understanding long noncoding RNAs through subcellular localization. *Mol. Cell* 73, 869–883. doi: 10.1016/j.molcel.2019.02.008

Cartwright, J. E., Keogh, R. J., and Tissot Van Patot, M. C. (2007). Hypoxia and placental remodelling. *Adv. Exp. Med. Biol.* 618, 113–126. doi: 10.1007/978-0-387-75434-5_9

Chen, B., Nelson, D. M., and Sadovsky, Y. (2006). N-myc down-regulated gene 1 modulates the response of term human trophoblasts to hypoxic injury. *J. Biol. Chem.* 281, 2764–2772. doi: 10.1074/jbc.M507330200

Chen, J., Thirkill, T. L., Lohstroh, P. N., Bielmeier, S. R., Narotsky, M. G., Best, D. S., et al. (2004). Bromodichloromethane inhibits human placental trophoblast differentiation. *Toxicol. Sci.* 78, 166–174. doi: 10.1093/toxsci/kfh046

Chen, Q., Wang, Y., Zhao, M., Hyett, J., Da Silva Costa, F., and Nie, G. (2016). Serum levels of GDF15 are reduced in preeclampsia and the reduction is more profound in late-onset than early-onset cases. *Cytokine* 83, 226–230. doi: 10.1016/j.cyto.2016.05.002

Chu, T., Mouillet, J. F., Hood, B. L., Conrads, T. P., and Sadovsky, Y. (2015). The assembly of miRNA-mRNA-protein regulatory networks using high-throughput expression data. *Bioinformatics* 31, 1780–1787. doi: 10.1093/bioinformatics/btv038

Daoud, G., Simoneau, L., Masse, A., Rassart, E., and Lafond, J. (2005). Expression of cFABP and PPAR in trophoblast cells: effect of PPAR ligands on linoleic acid uptake and differentiation. *Biochim. Biophys. Acta* 1687, 181–194. doi: 10.1016/j.bbalip.2004.11.017

Dearden, L., and Ockleford, C. (1983). "Structure of human trophoblast: correlation with function," in *Biology of Trophoblast*, eds Y. W. Loke and A. Whyte (Amsterdam: Elsevier).

Derrien, T., Johnson, R., Bussotti, G., Tanzer, A., Djebali, S., Tilgner, H., et al. (2012). The GENCODE v7 catalog of human long noncoding RNAs: analysis of their gene structure, evolution, and expression. *Genome Res.* 22, 1775–1789. doi: 10.1101/gr.132159.111

Dobin, A., Davis, C. A., Schlesinger, F., Drenkow, J., Zaleski, C., Jha, S., et al. (2013). STAR: ultrafast universal RNA-seq aligner. *Bioinformatics* 29, 15–21. doi: 10.1093/bioinformatics/bts635

Douglas, G. C., and King, B. F. (1990). Differentiation of human trophoblast cells in vitro as revealed by immunocytochemical staining of desmoplakin and nuclei. *J. Cell Sci.* 96(Pt 1), 131–141.

Douglas, G. C., and King, B. F. (1993). Colchicine inhibits human trophoblast differentiation in vitro. *Placenta* 14, 187–201. doi: 10.1016/s0143-4004(05)80260-7

Fox, H. (1970). Effect of hypoxia on trophoblast in organ culture. A morphologic and autoradiographic study. *Am. J. Obstet. Gynecol.* 107, 1058–1064. doi: 10.1016/0002-9378(70)90629-0

Frankish, A., Diekhans, M., Ferreira, A. M., Johnson, R., Jungreis, I., Loveland, J., et al. (2019). GENCODE reference annotation for the human and mouse genomes. *Nucleic Acids Res.* 47, D766–D773. doi: 10.1093/nar/gky955

Gandley, R. E., Althouse, A., Jeyabalan, A., Bregand-White, J. M., Mcgonigal, S., Myerski, A. C., et al. (2016). Low soluble Syndecan-1 precedes preeclampsia. *PLoS One* 11:e0157608. doi: 10.1371/journal.pone.0157608

Gentleman, R. C., Carey, V. J., Bates, D. M., Bolstad, B., Dettling, M., Dudoit, S., et al. (2004). Bioconductor: open software development for computational biology and bioinformatics. *Genome Biol.* 5:R80. doi: 10.1186/gb-2004-5-10-r80

Hon, C. C., Ramilowski, J. A., Harshbarger, J., Bertin, N., Rackham, O. J., Gough, J., et al. (2017). An atlas of human long non-coding RNAs with accurate 5' ends. *Nature* 543, 199–204. doi: 10.1038/nature21374

Hu, K. L., Chang, H. M., Zhao, H. C., Yu, Y., Li, R., and Qiao, J. (2019). Potential roles for the kisspeptin/kisspeptin receptor system in implantation and placentation. *Hum. Reprod. Update* 25, 326–343. doi: 10.1093/humupd/dmy046

Iyer, M. K., Niknafs, Y. S., Malik, R., Singhal, U., Sahu, A., Hosono, Y., et al. (2015). The landscape of long noncoding RNAs in the human transcriptome. *Nat. Genet.* 47, 199–208. doi: 10.1038/ng.3192

Jain, A., and Tuteja, G. (2021). PlacentaCellEnrich: a tool to characterize gene sets using placenta cell-specific gene enrichment analysis. *Placenta* 103, 164–171. doi: 10.1016/j.placenta.2020.10.029

Jauniaux, E., Poston, L., and Burton, G. J. (2006). Placental-related diseases of pregnancy: involvement of oxidative stress and implications in human evolution. *Hum. Reprod. Update* 12, 747–755. doi: 10.1093/humupd/dml016

Jiang, B., and Mendelson, C. R. (2005). O2 enhancement of human trophoblast differentiation and hCYP19 (aromatase) gene expression are mediated by proteasomal degradation of USF1 and USF2. *Mol. Cell. Biol.* 25, 8824–8833. doi: 10.1128/mcb.25.20.8824-8833.2005

Jiang, R., Wang, T., Zhou, F., Yao, Y., He, J., and Xu, D. (2020). Bioinformatics-based identification of miRNA-, lncRNA-, and mRNA-associated ceRNA networks and potential biomarkers for preeclampsia. *Medicine (Baltimore)* 99:e22985. doi: 10.1097/md.0000000000022985

Jones, C. J., and Fox, H. (1991). Ultrastructure of the normal human placenta. *Electron Microsc. Rev.* 4, 129–178. doi: 10.1016/0892-0354(91)90019-9

Junus, K., Wikström, A. K., Larsson, A., and Olovsson, M. (2014). Placental expression of proBNP/NT-proBNP and plasma levels of NT-proBNP in early- and late-onset preeclampsia. *Am. J. Hypertens.* 27, 1225–1230. doi: 10.1093/ajh/hpu033

Kliman, H. J., Nestler, J. E., Sermasi, E., Sanger, J. M., and Strauss, J. F. III (1986). Purification, characterization, and in vitro differentiation of cytotrophoblasts from human term placentae. *Endocrinology* 118, 1567–1582. doi: 10.1210/endo-118-4-1567

Kolialexi, A., Tsangaris, G. T., Sifakis, S., Gourgiotis, D., Katsafadou, A., Lykoudi, A., et al. (2017). Plasma biomarkers for the identification of women at risk for early-onset preeclampsia. *Expert Rev. Proteomics* 14, 269–276. doi: 10.1080/14789450.2017.1291345

Kwak, Y. T., Muralimanoharan, S., Gogate, A. A., and Mendelson, C. R. (2019). Human trophoblast differentiation is associated with profound gene regulatory and epigenetic changes. *Endocrinology* 160, 2189–2203. doi: 10.1210/en.2019-00144

Langmead, B., Trapnell, C., Pop, M., and Salzberg, S. L. (2009). Ultrafast and memory-efficient alignment of short DNA sequences to the human genome. *Genome Biol.* 10:R25. doi: 10.1186/gb-2009-10-3-r25

Levy, R., Smith, S. D., Chandler, K., Sadovsky, Y., and Nelson, D. M. (2000). Apoptosis in human cultured trophoblasts is enhanced by hypoxia and diminished by epidermal growth factor. *Am. J. Physiol. Cell Physiol.* 278, C982–C988. doi: 10.1152/ajpcell.2000.278.5.C982

Livak, K. J., and Schmittgen, T. D. (2001). Analysis of relative gene expression data using real-time quantitative PCR and the 2(-Delta Delta C(T)) Method. *Methods* 25, 402–408. doi: 10.1006/meth.2001.1262

Love, M. I., Huber, W., and Anders, S. (2014). Moderated estimation of fold change and dispersion for RNA-seq data with DESeq2. *Genome Biol.* 15:550. doi: 10.1186/s13059-014-0550-8

McCarthy, C., Cotter, F. E., Mcelwaine, S., Twomey, A., Mooney, E. E., Ryan, F., et al. (2007). Altered gene expression patterns in intrauterine growth restriction: potential role of hypoxia. *Am. J. Obstet. Gynecol.* 196, 70.E1–70.E6. doi: 10.1016/j.ajog.2006.08.027

Mouillet, J. F., Chu, T., Nelson, D. M., Mishima, T., and Sadovsky, Y. (2010). MiR-205 silences MED1 in hypoxic primary human trophoblasts. *FASEB J.* 24, 2030–2039. doi: 10.1096/fj.09-149724

Mouillet, J. F., Donker, R. B., Mishima, T., Cronqvist, T., Chu, T., and Sadovsky, Y. (2013). The unique expression and function of miR-424 in human placental trophoblasts. *Biol. Reprod.* 89:25. doi: 10.1095/biolreprod.113.110049

Nelson, D. M., Johnson, R. D., Smith, S. D., Anteby, E. Y., and Sadovsky, Y. (1999). Hypoxia limits differentiation and up-regulates expression and activity of prostaglandin H synthase 2 in cultured trophoblast from term human placenta. *Am. J. Obstet. Gynecol.* 180, 896–902. doi: 10.1016/s0002-9378(99)70661-7

Neuman, R. I., Alblas Van Der Meer, M. M., Nieboer, D., Saleh, L., Verdonk, K., Kalra, B., et al. (2020). PAPP-A2 and inhibin A as novel predictors for pregnancy complications in women with suspected or confirmed preeclampsia. *J. Am. Heart Assoc.* 9:e018219. doi: 10.1161/jaha.120.018219

Oh, S. Y., Chu, T., and Sadovsky, Y. (2011). The timing and duration of hypoxia determine gene expression patterns in cultured human trophoblasts. *Placenta* 32, 1004–1009. doi: 10.1016/j.placenta.2011.09.010

Palazzo, A. F., and Lee, E. S. (2015). Non-coding RNA: what is functional and what is junk? *Front. Genet.* 6:2. doi: 10.3389/fgene.2015.00002

Pardi, G., Cetin, I., Marconi, A. M., Lanfranchi, A., Bozzetti, P., Ferrazzi, E., et al. (1993). Diagnostic value of blood sampling in fetuses with growth retardation. *N. Engl. J. Med.* 328, 692–696. doi: 10.1056/nejm199303113281004

Pardi, G., Marconi, A. M., and Cetin, I. (2002). Placental-fetal interrelationship in IUGR fetuses–a review. *Placenta* 23(Suppl. A), S136–S141. doi: 10.1053/plac.2002.0802

Prakash, G. J., Suman, P., and Gupta, S. K. (2011). Relevance of syndecan-1 in the trophoblastic BeWo cell syncytialization. *Am. J. Reprod. Immunol.* 66, 385–393. doi: 10.1111/j.1600-0897.2011.01017.x

R Development Core Team (2012). *R: A Language and Environment for Statistical Computing*. Vienna: R Foundation for Statistical Computing.

Reymond, N., Borg, J. P., Lecocq, E., Adelaide, J., Campadelli-Fiume, G., Dubreuil, P., et al. (2000). Human nectin3/PRR3: a novel member of the PVR/PRR/nectin family that interacts with afadin. *Gene* 255, 347–355. doi: 10.1016/s0378-1119(00)00316-4

Rimon, E., Chen, B., Shanks, A. L., Nelson, D. M., and Sadovsky, Y. (2008). Hypoxia in human trophoblasts stimulates the expression and secretion of connective tissue growth factor. *Endocrinology* 149, 2952–2958. doi: 10.1210/en.2007-1099

Roh, C. R., Budhraja, V., Kim, H. S., Nelson, D. M., and Sadovsky, Y. (2005). Microarray-based identification of differentially expressed genes in hypoxic term human trophoblasts and in placental villi of pregnancies with growth restricted fetuses. *Placenta* 26, 319–328. doi: 10.1016/j.placenta.2004.06.013

Sadovsky, Y., and Jansson, T. (2015). "Placenta and placental transport function," in *Knobil and Neill's Physiology of Reproduction*, 4th Edn, eds T. M. Plant and A. J. Zeleznik (San Diego, CA: Academic Press).

Saha, S., and Ain, R. (2020). MicroRNA regulation of murine trophoblast stem cell self-renewal and differentiation. *Life Sci. Alliance* 3:202000674. doi: 10.26508/lsa.202000674

Schaiff, W. T., Carlson, M. G., Smith, S. D., Levy, R., Nelson, D. M., and Sadovsky, Y. (2000). Peroxisome proliferator-activated receptor-gamma modulates differentiation of human trophoblast in a ligand-specific manner. *J. Clin. Endocrinol. Metab.* 85, 3874–3881. doi: 10.1210/jcem.85.10.6885

Schoots, M. H., Gordijn, S. J., Scherjon, S. A., Van Goor, H., and Hillebrands, J. L. (2018). Oxidative stress in placental pathology. *Placenta* 69, 153–161. doi: 10.1016/j.placenta.2018.03.003

Sheng, F., Sun, N., Ji, Y., Ma, Y., Ding, H., Zhang, Q., et al. (2019). Aberrant expression of imprinted lncRNA MEG8 causes trophoblast dysfunction and abortion. *J. Cell. Biochem.* 120, 17378–17390. doi: 10.1002/jcb.29002

Simon, M. C., and Keith, B. (2008). The role of oxygen availability in embryonic development and stem cell function. *Nat. Rev. Mol. Cell Biol.* 9, 285–296. doi: 10.1038/nrm2354

Soares, M. J., Iqbal, K., and Kozai, K. (2017). Hypoxia and placental development. *Birth Defects Res.* 109, 1309–1329. doi: 10.1002/bdr2.1135

Statello, L., Guo, C. J., Chen, L. L., and Huarte, M. (2021). Gene regulation by long non-coding RNAs and its biological functions. *Nat. Rev. Mol. Cell Biol.* 22, 96–118. doi: 10.1038/s41580-020-00315-9

Tal, R. (2012). The role of hypoxia and hypoxia-inducible factor-1alpha in preeclampsia pathogenesis. *Biol. Reprod.* 87:134. doi: 10.1095/biolreprod.112.102723

Than, N. G., Balogh, A., Romero, R., Kárpáti, E., Erez, O., Szilágyi, A., et al. (2014). Placental Protein 13 (PP13) - A placental immunoregulatory galectin protecting pregnancy. *Front. Immunol.* 5:348. doi: 10.3389/fimmu.2014.00348

Thirkill, T. L., and Douglas, G. C. (1997). Differentiation of human trophoblast cells in vitro is inhibited by dimethylsulfoxide. *J. Cell. Biochem.* 65, 460–468.

Uszczynska-Ratajczak, B., Lagarde, J., Frankish, A., Guigó, R., and Johnson, R. (2018). Towards a complete map of the human long non-coding RNA transcriptome. *Nat. Rev. Genet.* 19, 535–548. doi: 10.1038/s41576-018-0017-y

Wagner, P. K., Otomo, A., and Christians, J. K. (2011). Regulation of pregnancy-associated plasma protein A2 (PAPPA2) in a human placental trophoblast cell line (BeWo). *Reprod. Biol. Endocrinol.* 9:48. doi: 10.1186/1477-7827-9-48

Wakeland, A. K., Soncin, F., Moretto-Zita, M., Chang, C. W., Horii, M., Pizzo, D., et al. (2017). Hypoxia Directs human extravillous trophoblast differentiation in a hypoxia-inducible factor-dependent manner. *Am. J. Pathol.* 187, 767–780. doi: 10.1016/j.ajpath.2016.11.018

Xie, L., Mouillet, J. F., Chu, T., Parks, W. T., Sadovsky, E., Knofler, M., et al. (2014). C19MC microRNAs regulate the migration of human trophoblasts. *Endocrinology* 155, 4975–4985. doi: 10.1210/en.2014-1501

Yusuf, K., Smith, S. D., Levy, R., Schaiff, W. T., Wyatt, S. M., Sadovsky, Y., et al. (2001). Thromboxane A(2) limits differentiation and enhances apoptosis of cultured human trophoblasts. *Pediatr. Res.* 50, 203–209. doi: 10.1203/00006450-200108000-00007

Yusuf, K., Smith, S. D., Sadovsky, Y., and Nelson, D. M. (2002). Trophoblast differentiation modulates the activity of caspases in primary cultures of term human trophoblasts. *Pediatr. Res.* 52, 411–415. doi: 10.1203/00006450-200209000-00018

Zhang, B., and Horvath, S. (2005). A general framework for weighted gene co-expression network analysis. *Stat. Appl. Genet. Mol. Biol.* 4:Article17. doi: 10.2202/1544-6115.1128 s

Conflict of Interest: YS was a consultant at Illumina, Inc.

The remaining authors declare that the research was conducted in the absence of any commercial or financial relationships that could be construed as a potential conflict of interest.

frontiers in Cell and Developmental Biology

REVIEW
published: 15 June 2021
doi: 10.3389/fcell.2021.674162

Omics Approaches to Study Formation and Function of Human Placental Syncytiotrophoblast

Adam Jaremek[1†], Mariyan J. Jeyarajah[1†], Gargi Jaju Bhattad[1] and Stephen J. Renaud[1,2]*

[1] Department of Anatomy and Cell Biology, Schulich School of Medicine and Dentistry, University of Western Ontario, London, ON, Canada, [2] Children's Health Research Institute, Lawson Health Research Institute, London, ON, Canada

Proper development of the placenta is vital for pregnancy success. The placenta regulates exchange of nutrients and gases between maternal and fetal blood and produces hormones essential to maintain pregnancy. The placental cell lineage primarily responsible for performing these functions is a multinucleated entity called syncytiotrophoblast. Syncytiotrophoblast is continuously replenished throughout pregnancy by fusion of underlying progenitor cells called cytotrophoblasts. Dysregulated syncytiotrophoblast formation disrupts the integrity of the placental exchange surface, which can be detrimental to maternal and fetal health. Moreover, various factors produced by syncytiotrophoblast enter into maternal circulation, where they profoundly impact maternal physiology and are promising diagnostic indicators of pregnancy health. Despite the multifunctional importance of syncytiotrophoblast for pregnancy success, there is still much to learn about how its formation is regulated in normal and diseased states. 'Omics' approaches are gaining traction in many fields to provide a more holistic perspective of cell, tissue, and organ function. Herein, we review human syncytiotrophoblast development and current model systems used for its study, discuss how 'omics' strategies have been used to provide multidimensional insights into its formation and function, and highlight limitations of current platforms as well as consider future avenues for exploration.

Keywords: pregnancy, placenta, trophoblast, syncytiotrophoblast, omics, cell models

OPEN ACCESS

Edited by:
Geetu Tuteja, Iowa State University, United States

Reviewed by:
Courtney W. Hanna, University of Cambridge, United Kingdom
Jennifer M. Frost, Queen Mary University of London, United Kingdom

***Correspondence:**
Stephen J. Renaud
srenaud4@uwo.ca

[†] These authors have contributed equally to this work and share first authorship

Specialty section:
This article was submitted to Developmental Epigenetics, a section of the journal Frontiers in Cell and Developmental Biology

Received: *28 February 2021*
Accepted: *24 May 2021*
Published: *15 June 2021*

Citation:
Jaremek A, Jeyarajah MJ, Jaju Bhattad G and Renaud SJ (2021) Omics Approaches to Study Formation and Function of Human Placental Syncytiotrophoblast. Front. Cell Dev. Biol. 9:674162. doi: 10.3389/fcell.2021.674162

INTRODUCTION

The placenta is a temporary organ that forms during pregnancy. It serves crucial functions to sustain pregnancy, promote fetal growth and development, and stimulate adaptive changes in maternal physiology and metabolism. These functions include (but are not limited to) hormone production and metabolism, hemodynamic adaptations, and serving as a physical barrier separating maternal and fetal circulations. The placental barrier enables nutrients, gases, and wastes to diffuse between maternal and fetal blood, yet protects the fetus from potentially harmful factors including toxins, pathogens, and maternal immune reactivity. Structural adaptations have evolved to enable the placental barrier to execute its versatile requirements as both protector and nurturer, culminating in the formation of a unique multinucleated syncytium consisting of millions of nuclei connected by a continuous cytoplasm, called syncytiotrophoblast (STB). In humans, STB

facilitates implantation and ultimately lines chorionic villi where it bathes in maternal blood. STB secretions and debris are deposited into the maternal circulation, where they have important roles in modulating maternal physiology as well as diagnostic potential for fetal-placental aberrations and pregnancy disease. Despite the importance of STB formation and function for fetal development and pregnancy outcome, limitations of cell and animal models have left much to be discovered. In the first part of this review, we will briefly highlight the ontogeny and diverse functions of human STB as well as models commonly used for its study. Then, we will discuss how various omics technologies have provided unprecedented insights into understanding STB formation and function, including current limitations, challenges, and opportunities for future investigation.

ONTOGENY OF STB

There are two types of STB that arise during different stages of human embryogenesis: a primitive STB that mediates implantation and decidual erosion during the second week after fertilization, and a definitive STB that lines chorionic villi from the third week and beyond. Whether these two STB subtypes are distinct entities or the gradual evolution of the same lineage as gestation progresses is unclear. The primitive STB first appears around the time of implantation as the blastocyst breaches the uterine surface epithelium, likely through intercellular fusion of underlying cytotrophoblasts (CTBs) at the embryonic pole of the blastocyst. The primitive STB rapidly expands into the decidua and erodes uterine stroma, glands, and capillaries. The cavities generated within the primitive STB, called lacunae, become filled with blood and glandular secretions from eroded decidual tissue, providing a source of early nutrition for the conceptus. The primitive STB provides the groundwork in which pillars of CTBs proliferate, forming primary villi. These primary villi traverse the entirety of the primitive STB and ultimately connect together to encircle the conceptus as the CTB shell, which serves to anchor the conceptus to the decidua basalis. Villi also branch extensively to create smaller floating villi that remain within spaces between villi (intervillous spaces), increasing the surface area of the villus tree. Chorionic villi are formed when extraembryonic mesoderm and blood vessels emanating from the allantois infiltrate the proximal cores of the primary villi during the third week of development. Thus, the villus core includes an inner meshwork of mesoderm-derived stroma consisting of fibroblasts and immune cells (notably macrophages) as well as blood vessels that are contiguous with the fetal circulation via the umbilical vessels. The core is lined by a trophoblast bilayer containing an outer STB layer and an inner CTB layer, which are physically separated from the stroma by a laminin-rich basement membrane. Blood vessels known as spiral arteries course through the decidua basalis and supply maternal blood to the intervillous spaces. Since STB lines the outer surface of the villi, it directly bathes in maternal blood and forms a key site of interaction between maternal and fetal tissue. A schematic illustrating the primitive and definitive STB is presented in **Figure 1**.

DIFFERENTIATION OF CTB INTO STB

Syncytiotrophoblast has a limited lifespan and must be regularly replenished throughout pregnancy with fresh cytoplasm and nuclei by controlled differentiation and fusion of underlying CTBs. Differentiation and fusion of CTBs into STB is a complex and highly orchestrated process that involves biochemical changes to support the immense endocrinological and secretory functions of STB as well as morphological changes to enable intercellular fusion. It is not yet clear whether the signal that initiates these biochemical and morphological events originates from the STB or from the underlying CTB layer. Additionally, while biochemical and morphological differentiation are coupled, they are thought to be executed by discrete pathways (Orendi et al., 2010). Biochemical differentiation requires that CTBs exit the cell cycle (Lu et al., 2017), and repress genes involved in maintaining a progenitor state, such as *ELF5*, *TP63*, *ID2*, and *TEAD4*. Simultaneously, factors implicated in nutrient transport, immunomodulation, and hormone biosynthesis and metabolism are induced. The integration of multiple signaling pathways and transcription factors (TFs) are implicated in the process of CTB differentiation, including suppression of WNT and activin/transforming growth factor beta (TGF-β) signaling as well as activation of cyclic adenosine monophosphate (cAMP)/protein kinase A (PKA) and mitogen-activated protein kinase (MAPK) pathways. CTB differentiation also involves the activity of many TFs and epigenetic regulators including PPARG, DLX3, GCM1, TFAP2A, OVOL1, and many others. A detailed characterization of TFs implicated in trophoblast differentiation is discussed in several comprehensive reviews (Knott and Paul, 2014; Baines and Renaud, 2017; Knöfler et al., 2019).

Morphologically, CTB fusion necessitates a modified epithelial-mesenchymal transition resulting in loss of junctional proteins such as E-cadherin, reorganization of cytoskeletal components, and intercellular mixing of intracellular contents (Ishikawa et al., 2014). The impetus for intercellular fusion is largely mediated by expression of cellular fusogens called syncytins. Syncytins are encoded by co-opted endogenous retroviral (ERV) envelope genes *ERVW-1* (encodes syncytin-1) and *ERVFRD-1* (encodes syncytin-2). Syncytin-1, which is expressed in STB, binds to the neutral amino acid transporter ASCT-2 expressed mainly by CTBs. Syncytin-2, on the other hand, is expressed in small clusters of CTBs and binds to MFSD2A, which is expressed by STB (Lavialle et al., 2013). Additionally, changes in the cytoskeleton are required to form the extensive microvilli that cover the apical surface of STB and increase the surface area of the STB up to sevenfold (Teasdale and Jean-Jacques, 1985).

STB LIFE CYCLE

Syncytiotrophoblast undergoes highly regulated turnover as aged or damaged syncytia are replaced by newly formed ones through fusion of underlying CTBs (Gauster et al., 2009). Since this occurs continuously from implantation until term, the nuclei present in STB are of different ages and exhibit

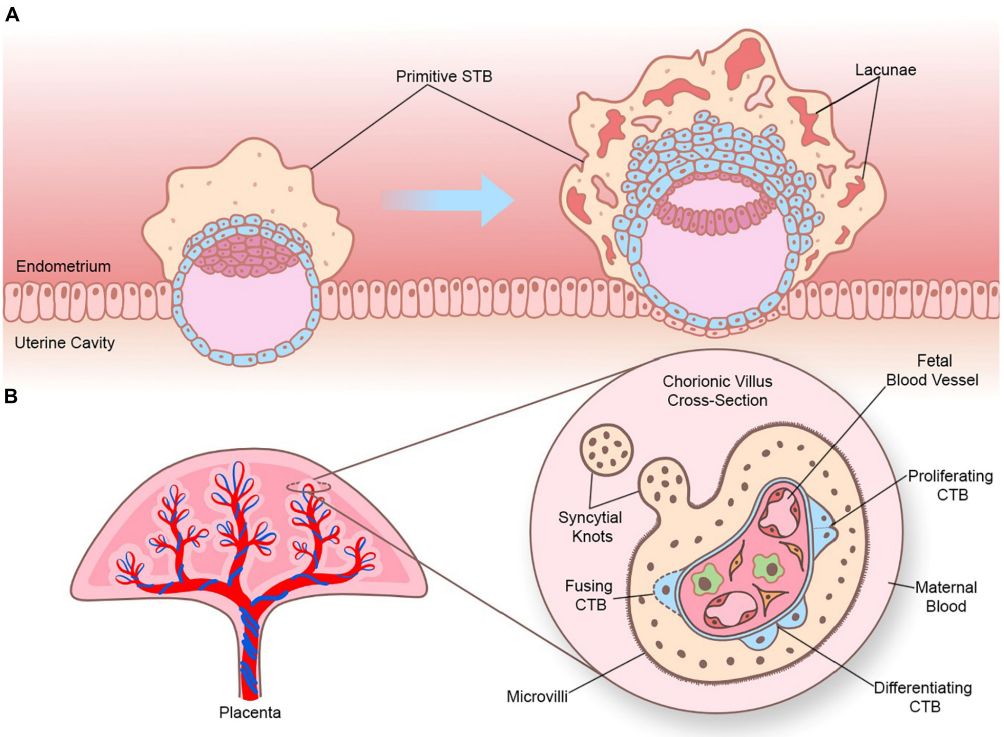

FIGURE 1 | Sequential development of STB. **(A)** Progression of a human embryo at approximately gestational days 7–8 (peri-implantation; left image) and days 9–10 (post-implantation; right image). Please note the invasive properties of the primitive STB at the forefront of the implanting human embryo and the gradual development of blood-filled lacunae. **(B)** Cross section of a chorionic villus in later gestation. Please note that the STB layer exhibits apical-basal polarity (as shown by the presence of microvilli) and bathes directly in maternal blood. An extruding syncytial knot is also shown. The villus core contains blood vessels that connect to the fetal circulation, as well as different cell types (such as Hofbauer cells and fibroblasts). CTBs are shown in various stages of their life cycle (proliferating, differentiating, and fusing).

a range of morphologies and packing densities that reflect progressive maturation. Within STB, clustering of nuclei occurs in regions known as syncytial sprouts and knots (Mayhew, 2014). Syncytial sprouts, which are predominant during the first-trimester, harbor nuclei that are primarily euchromatic with a distinct nucleolus. They form protrusions in the development of new villi, yet their connection with the villus surface can become attenuated and render them susceptible to detachment and release into the intervillous space (Burton, 2011). Syncytial knots, which often protrude from the surface of villi during the third trimester, contain more densely clustered nuclei that may be less transcriptionally active based on features such as dense condensations of heterochromatin and lack of apparent nucleoli (Burton and Jones, 2009). Although the nuclei resemble those classified as apoptotic, whether syncytial knots represent an apoptotic end-stage of the STB life cycle remains elusive as nuclear fragmentation is not observed (Mayhew, 2014). Nevertheless, knots are considered a means by which aged STB nuclei are sequestered to regions of the villus membrane where they do not interfere with exchange (Fogarty et al., 2013), and some normally detach to be shed into maternal circulation (Mayhew et al., 1999). The volume of syncytial knots relative to CTB volume increases during gestation, suggesting that early proliferation is geared toward growth with later proliferation toward renewal and repair (Mayhew and Barker, 2001).

Over the course of pregnancy, STB releases a variety of factors into maternal circulation that are critical for the maintenance of healthy pregnancy. This includes fragments derived from syncytial sprouts or knots, which range from small subcellular particles to large multinucleated fragments, that may play important roles in maintaining maternal immune tolerance to fetal tissues (Chamley et al., 2011). Furthermore, STB releases membrane-bound vesicles known as STB extracellular vesicles (STBEV) in the form of exosomes, microvesicles, or apoptotic bodies, from the villus surface into maternal circulation (Tannetta et al., 2017a). These vesicles contain a variety of biologically active molecules, such as proteins, RNAs, and lipids, that have regulatory roles in the maternal immune response to pregnancy and may interact with components of maternal circulation, such as endothelial cells or leukocytes, to facilitate maternal-fetal communication (Tannetta et al., 2017b). STB also releases cell-free 'fetal' DNA (cfDNA) into maternal blood that varies in concentration based on multiple factors including oxidative stress (Taglauer et al., 2014). Additional factors that are produced and released by STB include numerous steroid and peptide hormones, such as estrogen, progesterone, human chorionic gonadotropin (hCG), human placental lactogen

(hPL), and placental growth hormone (PGH) (Murphy et al., 2006). STB also produces a variety of growth factors, such as pregnancy-specific glycoproteins (PSGs), vascular endothelial growth factor (VEGF), placental growth factor (PlGF), TGF-β, and many other cytokines, chemokines, and signaling molecules (Kidima, 2015).

STB FORMATION IN PREGNANCY DISEASE

Abnormal formation or function of STB during pregnancy is implicated in the etiology of pregnancy complications, such as preeclampsia and fetal growth restriction (FGR). Preeclampsia is a serious disease characterized by vascular damage and hypertension in the mother during the latter half of pregnancy that can result in further organ deficiency and damage. Currently, the only definitive treatment is to remove the placenta and therefore deliver the baby, which can lead to complications associated with prematurity if performed prior to 37 weeks. FGR is the failure of a fetus to achieve its growth potential as predetermined by genetic and epigenetic factors (Burton and Jauniaux, 2018). Low birth weight as a result of FGR or premature delivery increases risk of perinatal death and morbidity and predisposes the child to lifelong risk of developing serious chronic diseases. Cultured CTBs from preeclampsia or FGR-affected placentas show impaired cell fusion and reduced expression of key fusion mediators (Langbein et al., 2008). In STB from these placentas, there is a greater number of apoptotic nuclei present (Ishihara et al., 2002). Preeclampsia is also associated with increased syncytial knotting as well as greater extrusion of STB fragments and pro-inflammatory STBEVs that are implicated in immune dysregulation and endothelial damage (Roland et al., 2016; Tannetta et al., 2017b). In addition, there is altered composition of placental proteins within STBEVs isolated from plasma of women with pregnancy-related disorders such as preeclampsia, which holds promise to be exploited as potential biomarkers for early diagnosis and monitoring (Levine et al., 2020). Current screening methods that use maternal serum biomarkers of STB stress, such as increased soluble vascular endothelial growth factor receptor 1 (sFLT1) and endoglin or reduced PlGF, are limited as these changes may not appear in later onset forms of disease with no early STB pathology (Redman and Staff, 2015).

MODELS TO STUDY STB DEVELOPMENT

Models commonly used to study human STB are listed in **Table 1**. Although this review will focus on human STB, it is noteworthy that animal models with a syncytialized placental barrier (including rodents and primates) have been instrumental in providing insight into STB formation and function. In many cases, factors identified as critical for STB formation in animal models have subsequently been shown to have a conserved function in human STB development.

Since the placenta is expelled at the end of pregnancy (i.e., early pregnancy termination or delivery) and is often considered clinical waste, it is possible to conduct experiments using placental tissue. Moreover, unlike many other tissues used for *ex vivo* analyses that are biopsied or removed only when diseased, it is possible to collect placental tissue from pregnancies deemed healthy. To study STB biology, villus explants can be cultured for defined time periods, which is advantageous to study STB function while preserving tissue integrity (Miller et al., 2005). CTBs can also be isolated and enriched from placental tissue (Kliman et al., 1986). Isolated CTBs spontaneously differentiate into STB following removal from intact tissue and are considered a reliable representation of STB generation. Since isolated CTBs have limited capacity for proliferation in culture, they are not well suited for mechanistically studying repression of proliferation during early stages of STB formation.

Choriocarcinoma cell-lines are a valuable tool to study STB biology due to their resiliency and extended lifespan in culture. BeWo cells were derived from a brain metastasis, serially cultivated, and are adapted to cell culture (Pattillo and Gey, 1968). Differentiation of BeWo cells into hormone-producing STB-like cells is stimulated following exposure to agents such as forskolin (Wice et al., 1990). Forskolin activates adenylate cyclase, which increases intracellular levels of cAMP, thereby stimulating cAMP-sensitive pathways implicated in STB generation such as PKA (Gerbaud et al., 2015). Other commonly used choriocarcinoma cells, including JEG-3, JAR, and ACH3P, produce hCG in response to forskolin, but do not fuse under standard culture conditions (Borges et al., 2003; Rothbauer et al., 2017). Thus, their utility as models of STB development is limited.

In 2018, culture conditions to maintain trophoblast stem cells (TSCs) from human embryos or first-trimester placentas were determined (Okae et al., 2018). These cells can be maintained as CTB-like cells or stimulated to form STB-like cells. Organoid cultures of human trophoblasts derived from first-trimester placenta have also been established, which provide a powerful model to study human STB biology while considering three-dimensional (3D) spatial configuration (Haider et al., 2018; Turco et al., 2018).

Human embryonic stem cells (hESCs) and pluripotent stem cells (hPSCs) cultured under defined culture conditions differentiate into cells with features consistent with trophoblasts, including STB (Xu et al., 2002; Amita et al., 2013; Li et al., 2019). In particular, recent reports indicate that naïve hPSCs can be used to model the entire trophoblast lineage trajectory from trophectoderm through CTBs to STB (Dong et al., 2020; Guo et al., 2021; Io et al., 2021). STB derived from hESCs and hPSCs offer the possibility of studying normal and pathological STB development from distinct genetic backgrounds. For instance, defective STB formation in placentas with trisomy-21 can be recapitulated using trisomy-21 hPSCs (Horii et al., 2016).

OMICS: AN OVERVIEW

'Omics' technologies provide a holistic and integrative approach toward the study of biological systems. To obtain a systems

TABLE 1 | Cell models used to study STB development and function.

Source	Cell model	Reference(s)	Notes
Placenta	Placental villus explants	Miller et al., 2005; Baczyk et al., 2006	Prepared by dissecting placental tissue and incubating in tissue culture wells for defined time periods. Denudation and regeneration of STB is also possible. Benefits include preservation of tissue integrity. Challenges include minimizing variation within and between experiments due to heterogeneity of explant preparation.
	Placental (CTB) organoids	Haider et al., 2018; Turco et al., 2018	Derived from early gestation placentas and can be expanded and cultured long-term. Provides a powerful model to study STB formation in 3D. Of note, the STB layer faces toward the inside of the organoid, so modeling transplacental passage of substrates may be limited.
	hTSCs	Okae et al., 2018	Derived from early gestation placentas or human blastocysts. Can be maintained as CTB-like cells in the presence of GSK-3, TGF-β, and HDAC inhibitors. Cells form STB-like cells after removing these inhibitors and adding forskolin.
	Primary CTBs	Kliman et al., 1986; Petroff et al., 2006	Isolated and enriched from placentas following delivery. Advantageous because they have undergone few population doublings or manipulations, and spontaneously form STB in culture. Cells have limited capacity to proliferate in culture, so they are less well suited to study early stages of syncytialization. Contamination with unwanted cell types and changes in CTB viability after isolation can pose a challenge.
Choriocarcinoma	BeWo	Pattillo and Gey, 1968	Cells have extended lifespans in culture. Beneficial for studying molecular aspects of cell fusion and hormone production, but possess genetic signatures distinct from normal trophoblast, so results should be interpreted with caution. Exposing BeWo cells to cAMP agonists stimulates STB-like cell fusion and hormone production. JEG-3, JAR, and ACH3P produce hormones (hCG) in response to cAMP agonists, but do not fuse, so their utility for modeling STB formation is limited. JEG-3 cells form STB-like cells when placed in 3D culture with microvascular cells.
	JEG-3	Kohler and Bridson, 1971	
	JAR	Pattillo et al., 1971	
	ACH3P	Hiden et al., 2007	
Early-stage embryos	hESCs	Xu et al., 2002; Amita et al., 2013	Using defined culture conditions, hESCs and hPSCs differentiate into cells possessing trophoblast-like properties, including STB-like cells. Beneficial for studying normal and pathological STB development from distinct genetic backgrounds, although there is contention about whether these cells truly represent trophoblast. Cells derived from naïve hESCs and hPSCs (rather than primed hESCs and hPSCs) appear to form bona fide trophoblast and can delineate the entire trophoblast developmental trajectory from pre- to post-implantation, including STB formation.
Reprogrammed somatic cells	Primed hPSCs	Chen et al., 2013; Horii et al., 2016; Wei et al., 2017	
	Naïve hPSCs	Dong et al., 2020; Guo et al., 2021; Io et al., 2021	

level understanding of biology and disease, large-scale data on DNA, RNA, protein, and/or metabolites are produced, which are then organized by computational tools to provide a framework for the hierarchical contribution of integrated cellular pathways (Debnath et al., 2010; Karahalil, 2016). The term 'omic' derives from the suffix –ome, which means 'whole', and is added to terms like gene, transcript, and protein to create names that encompass the entire set of biological molecules in a system, such as genome, transcriptome, and proteome. The addition of 'omics' to the terms (genomics, transcriptomics, and proteomics) refers to the comprehensive assessment of these molecules in a non-targeted and unbiased manner (Nalbantoglu and Karadag, 2019). An overview of omics approaches used to study STB biology is provided in **Figure 2**.

Genomics is the study of the genome and the genetic basis underlying disease. The emergence of high-throughput methods, such as genotype arrays and next-generation sequencing (NGS), have enabled large-scale analyses of DNA sequences to identify copy number variations, small insertions and deletions, as well as single nucleotide variations between individuals, tissues, or cells (Hasin et al., 2017). Epigenomics focuses on the genome-wide characterization of reversible, and sometimes heritable, modifications of DNA or DNA-associated proteins resulting in altered chromosome conformation or gene expression without changes in the DNA sequence. Epigenomics approaches include global assessment of DNA methylation through NGS following bisulfite treatment of DNA, profiling chromatin accessibility (e.g., assay for transposase-accessible chromatin coupled to sequencing, ATAC-seq), chromosome conformation capture technologies, or the characterization of DNA-binding protein distribution through chromatin immunoprecipitation followed by sequencing (ChIP-seq) (Buenrostro et al., 2015; Fröhlich, 2017; Hasin et al., 2017).

Transcriptomics is the study of the transcriptome that comprises the entire set of transcripts present in a cell or organism. Transcriptomics provides insight into particular types and levels of RNA molecules, including mRNA and non-coding RNA [e.g., short non-coding RNAs such as microRNA (miRNA) and long non-coding RNA], and is often used to evaluate changes in gene expression (Hasin et al., 2017). Transcriptomics approaches include hybridization-based strategies and high-throughput sequencing technologies,

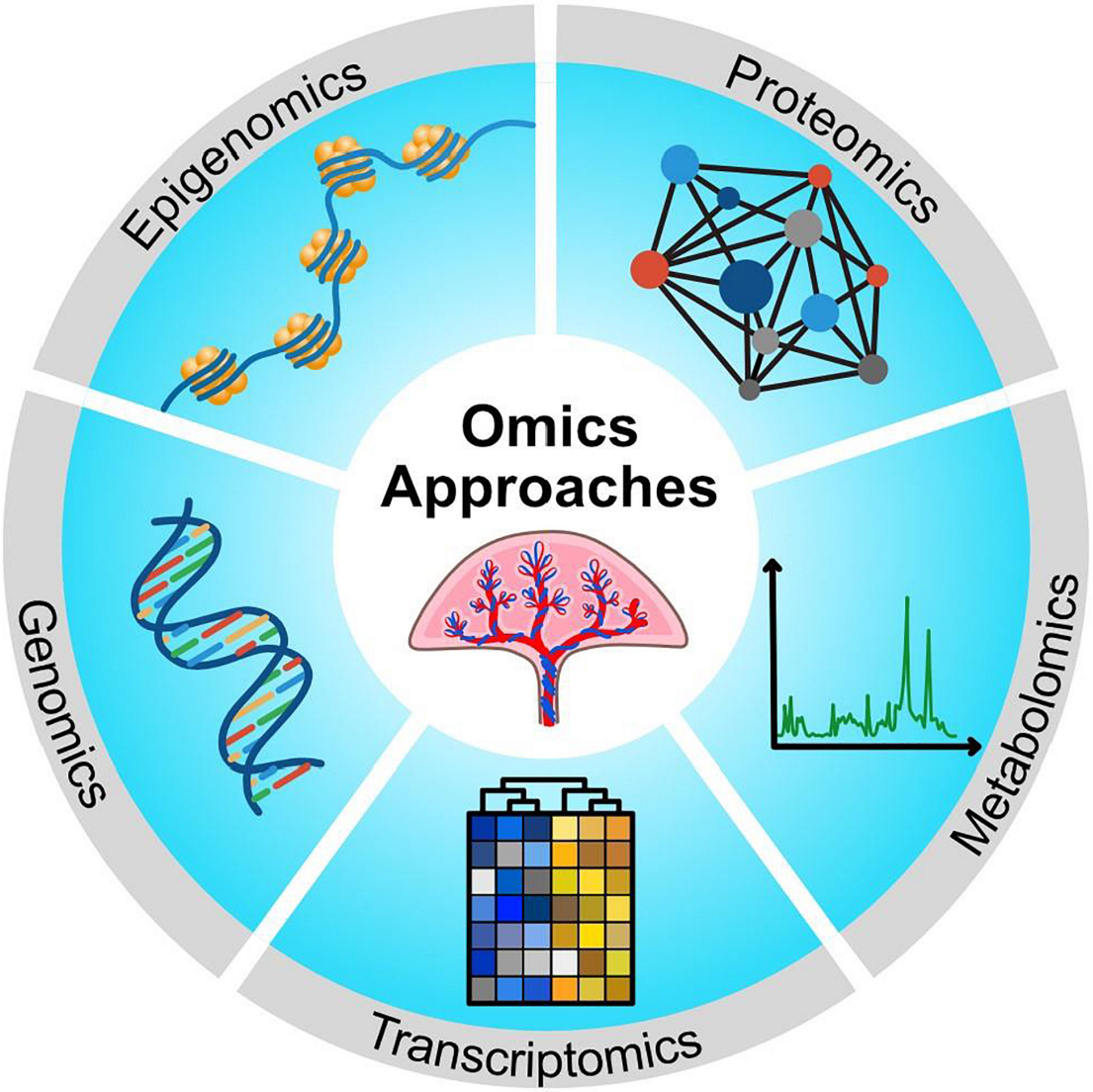

FIGURE 2 | Schematic showing multiple omics approaches that have been used to make new discoveries about STB biology.

including DNA microarrays, RNA sequencing (RNA-seq), single cell RNA-seq (scRNA-seq), and spatial identification of transcriptomes. Hybridization-based approaches can also be used in genomics research to genotype multiple DNA regions, or in epigenomics research (e.g., ChIP-on-chip).

The proteome is the set of all expressed proteins in a cell, tissue, or organism. Proteomics research encompasses protein expression profiles, post-translational modifications, and protein networks related to cellular function, and it endeavors to understand the biological functions of proteins, which holds promise in biomarker discovery (Debnath et al., 2010). Proteomics methods involve sample purification, protein digestion, and affinity capture or sample fractionation via gel-based methods, gas chromatography (GC), or liquid chromatography (LC). The gold standard for proteomic analyses is mass spectrometry (MS)-based techniques, which enable high-throughput detection of thousands of peptides from samples to provide insights into the proteome and how it varies under particular contexts (Debnath et al., 2010; Horgan and Kenny, 2011). Metabolomics is the study of the metabolome, which is the global profile of metabolites (e.g., amino acids, lipids, sugars, and hormones) that are detectable under certain conditions. Subsets of metabolites can also be measured, such as lipids (lipidomics), ions (ionomics), and hormones (hormonomics). Metabolomics methods usually take the form of nuclear magnetic resonance (NMR) spectroscopy or MS-based approaches to identify and quantify metabolite abundance.

Data obtained from omics experiments require detailed bioinformatic analysis and statistics to organize and interpret the information. Methods used for analysis of omics datasets include enrichment and network analyses, or other statistical tools. The

integration of multiple omics by interpreting data from several sources has enabled a more detailed understanding of biological processes (Culibrk et al., 2016; Karczewski and Snyder, 2018). Therefore, integrated multi-omics approaches allow researchers to delve into the molecular underpinnings of biological processes and diseases, such as healthy placental development or maldevelopment during pregnancy complications. Examples of studies that have used genomics, transcriptomics, and epigenomics approaches to study STB development are provided in **Table 2**. Examples of studies that have used proteomics approaches to study STB, or products produced by STB, are provided in **Table 3**.

OMICS TECHNOLOGIES FOR THE STUDY OF EARLY STB DEVELOPMENT

Using Omics to Characterize hESC and hPSC-Derived Models of Trophoblast

Omics technologies have fostered great progress toward the study of early human STB development. For instance, the use of omics has been instrumental in characterizing early hESC and hPSC models that recapitulate features of trophoblast differentiation when cultured in defined conditions. Xu et al. (2002) first demonstrated the ability of hESCs to differentiate into trophoblast-like cells via culture with BMP4. This was supported using DNA microarray to determine differentially expressed genes between BMP4-treated and untreated hESCs. By day 7 of treatment, cells expressed an array of trophoblast markers, including genes encoding hCG subunits, while transcripts associated with pluripotent cells (e.g., *OCT4*) were downregulated (Xu et al., 2002). Other studies have similarly used DNA microarray to evaluate global transcriptomic changes in BMP4-treated hESCs, consistently demonstrating gene expression patterns reminiscent of trophoblast (Marchand et al., 2011; Li et al., 2013).

Refinements in culture conditions have facilitated more detailed analyses of STB-like cells generated from hESCs. For example, Sudheer et al. (2012) used DNA microarray to show that BMP4 together with inhibition of both activin/nodal and FGF signaling stimulated pronounced differentiation into STB. Upregulated genes included those involved in hCG production, hormone biosynthesis (e.g., *CYP19A1*), and cell fusion (e.g., *ERVW-1*), whereas downregulated genes included those associated with mitosis (Sudheer et al., 2012). Yabe et al. (2016) used RNA-seq to compare hESC-derived STB isolated after 8 days of differentiation (using BMP4 and inhibitors of activin and FGF signaling) in two cell-size fractions, smaller syncytia (<40 μm) and larger syncytia (>70 μm), along with undifferentiated hESCs and primary CTBs isolated from term placenta. Notably, while the >70 μm hESC-derived STB showed a similar profile to primary CTB-derived STB, there were also major differences. For instance, several genes (e.g., *GABRP*) were highly expressed in >70 μm hESC-derived STB, but not in primary CTB-derived STB, whereas the reverse was true for others (e.g., *CSH1* as well as *PSG* and *LGALS* family members) (Yabe et al., 2016). To determine whether hESC-derived STB is more representative of STB from early or late pregnancy, Karvas et al. (2020) compared their transcriptome profile to publicly available transcriptome datasets of trophoblast from blastocysts through term. STB derived from hESCs closely resembled first-trimester STB, and transcripts expressed in hESC-derived STB that were not expressed in primary term trophoblasts (e.g., *ACTC1*, *GABRP*, *VTCN1*, and *WFDC2*) were identified as putative markers of STB in early pregnancy. Proteins encoded by these transcripts (which promote cell invasion in some cancers) showed reduced expression as gestation advanced, indicating that hESC-derived STB might represent the invasive STB population that forms soon after implantation (Karvas et al., 2020).

Sarkar et al. (2015) used proteomics methods to study the role of activin/nodal signaling during differentiation of hESCs to trophoblasts. Undifferentiated hESCs were labeled with stable isotopes and the plasma membrane and cytoplasmic fractions were compared through LC-MS/MS to fractions from cells treated for 6 days with SB431542 (an activin/nodal inhibitor). From 199 upregulated cell-surface proteins in treated cells, 83 had previously been identified in trophoblasts. KRT7 was upregulated and class I human leukocyte antigens were downregulated in SB431542-treated cells, suggesting differentiation into trophoblast (Sarkar et al., 2015). Analysis of the nuclear proteome in SB431542-treated cells showed downregulation of DNA methyltransferases such as DNMT1 while components of the BAF-A chromatin remodeling complex and SIN3 histone deacetylase (HDAC) complex were upregulated. There was also altered expression of β-catenin and CBF-1 TFs, suggesting involvement of WNT and Notch signaling in this process (Sarkar et al., 2016).

Multi-omics strategies have also been performed to study regulatory mechanisms implicated in hESC-mediated differentiation of trophoblast-like cells. Krendl et al. (2017) combined microarray, RNA-seq, scRNA-seq, ChIP-Seq, and DNA methylation analyses to profile the transcriptome and epigenome of trophoblasts derived from BMP4-treated hESCs and purified using the cell-surface marker aminopeptidase A. Furthermore, a TF circuit was identified involving GATA2, GATA3, TFAP2A, and TFAP2C that may regulate early trophoblast specification through activation of placenta-related genes and suppression of *OCT4* (Krendl et al., 2017). Liu et al. (2017a) investigated the role of *cis*-regulatory elements in this process by comparing chromatin accessibility of undifferentiated and BMP4-differentiated hESCs, which was derived from published DNase-seq datasets. This analysis was then integrated with transcriptome datasets to identify TFs binding within trophoblast-specific accessible chromatin domains (e.g., *BACH2*). The subset of these sites containing TF motifs was associated with genes controlling trophoblast invasion and placental development, and protein–protein interaction data were incorporated to construct a network highlighting candidate TFs that may be important in these processes (Liu et al., 2017a).

Similar to hESCs, transcriptome analyses of human induced PSCs (hiPSCs) cultured in defined conditions (such as with BMP4 or in micromesh culture) provide evidence that these cells possess STB-like gene expression profiles (Chen et al., 2013;

TABLE 2 | Examples of studies that used genomics, transcriptomics, and epigenomics to study STB.

Model	Method	Reference(s)	Summary
hESCs and primed hPSCs	DNA microarray	Xu et al., 2002; Sudheer et al., 2012; Chen et al., 2013; Wei et al., 2017; Tsuchida et al., 2020	Transcriptome analyses supported the notion that BMP4-treated hESCs/hPSCs differentiate into cells possessing trophoblast-like properties. BMP activation together with inhibition of both activin/nodal and FGF signaling stimulated pronounced differentiation into STB-like cells.
	WGS	Li et al., 2020	Found 6 genomic variations associated with differentiation-linked genes.
	RNA-seq	Yabe et al., 2016; Karvas et al., 2020	Characterized transcripts in hESC-derived STB, primary CTB-derived STB, and STB from early gestation placenta.
Naïve hPSCs	RNA-seq, scRNA-seq, ATAC-seq, Bisulfite-seq	Cinkornpumin et al., 2020; Dong et al., 2020; Guo et al., 2021; Io et al., 2021	Naïve hPSCs differentiate to form hTSCs with the capacity to form STBs. Naïve hPSC-derived hTSCs showed similar transcriptome signatures and chromatin accessibility to blastocyst-derived hTSCs and similar methylation patterns to placenta-derived hTSCs.
Human embryos	scRNA-seq	Lv et al., 2019; West et al., 2019	Single cell analyses identified underlying genetic networks and novel factors controlling STB development.
hTSCs	RNA-seq	Okae et al., 2018	hTSCs derived from first-trimester primary CTBs or human blastocysts can differentiate into STB. Transcriptome analyses provided evidence that hTSC-derived STB resemble primary CTB-derived STB.
CTB organoids	Bisulfite-seq, DNAm* microarray, RNA-seq	Haider et al., 2018; Turco et al., 2018	Revealed similarities between CTB organoids from first-trimester placentas and primary villus CTB and STB.
Primary CTBs	DNA microarray	Aronow et al., 2001; Rouault et al., 2016; Szilagyi et al., 2020	Classified global gene expression patterns during spontaneous differentiation into STB. Implicated new factors and genetic networks linked to signaling pathways that may be involved.
	RNA-seq	Azar et al., 2018	Coupled analysis of primary STB development to BeWo cell syncytialization and found similar genes differentially expressed during differentiation.
	ChIP-seq	Kwak et al., 2019	Illuminated global changes in binding of polymerase II and associated modified histones indicative of active or repressed chromatin during STB formation.
	miRNA microarray	Kumar et al., 2013	Identified members of the miR-17∼92 cluster and its paralog miR-106a-363 that promote CTB proliferation and were downregulated during differentiation.
	miRNA array	Ouyang et al., 2016	Characterized miRNA cargo in various STBEV subtypes.
BeWo	DNA microarray	Kudo et al., 2004; Kusama et al., 2018	Characterized transcriptome changes during forskolin-stimulated syncytialization and identified role of PKA and EPAC.
	RNA-seq	Renaud et al., 2015; Shankar et al., 2015; Zheng et al., 2017; Azar et al., 2018	Classified gene expression patterns during BeWo cell differentiation and uncovered novel genes and signaling pathways involved in this process.
	RRBS-seq	Shankar et al., 2015	Found altered CpG methylation near genes linked to STB differentiation.
	ChIP-seq	Shankar et al., 2015; Jaju Bhattad et al., 2020	Syncytialization is associated with a gain in transcriptionally active histone marks and altered histone H3 acetylation at select genomic sites.
	miRNA microarray	Dubey et al., 2018	Found that miR-92-1-5p was significantly downregulated during syncytialization.
JEG-3	DNA microarray	Msheik et al., 2019	Compared gene expression changes between JEG-3 cells and BeWo cells to identify genes potentially involved in fusion.
	RNA-seq	McConkey et al., 2016; Meinhardt et al., 2020	3D culture model of JEG-3 cells that form STB when cultured with endothelial cells. Affirmed role of YAP in promoting CTB stemness.
Placental tissue	RNA-seq	Saben et al., 2014	Transcriptome of term placenta compared to 7 other tissues revealed novel factors whose expression was localized to STB.
	scRNA-seq	Pavličev et al., 2017; Tsang et al., 2017; Liu et al., 2018; Vento-Tormo et al., 2018	Analyzed single cells from first-trimester and term placentas (and deciduas). Defined subclasses of CTBs, delineated differentiation trajectory into STB, and identified putative regulators. Inferred cell-cell interactions at the decidua-placental interface.
	DNA-seq	Poon et al., 2013; Zhang et al., 2019	No association between amount of cfDNA in maternal blood during early pregnancy and subsequent pregnancy complications. DNA isolated from placental EVs shared strong similarities with cfDNA.
	DNAm* microarray	Yuan et al., 2021	DNA methylation atlas of placental cells including laser capture dissected STB.

**DNAm, DNA methylation.*

TABLE 3 | Examples of studies that used proteomics, metabolomics, and secretomics to characterize STB function.

Model	Method	Reference(s)	Summary
hESC/hPSC models	LC-MS/MS	Sarkar et al., 2015, 2016	Analysis of cytoplasmic and nuclear proteome revealed various proteins and epigenetic regulators associated with differentiation of hESCs into trophoblast.
CTB organoids	LC-MS/MS	Turco et al., 2018	Organoids and placental villus explants produced PSGs, INSL4, hCG, KISS1, GDF15, hPL, and sorbitol.
Primary CTBs	Various types of MS	Heazell et al., 2008	Cultured CTBs and explants under different O_2 concentrations and found 264 unique metabolites in conditioned medium and tissue lysates.
		Epiney et al., 2012	Cultured primary CTBs isolated from first-trimester placentas, term placentas, and placentas from preeclampsia, reporting 33 proteins differentially expressed between cells from healthy and preeclamptic pregnancies.
		Ouyang et al., 2016	Characterized proteins in STBEV subtypes. Exosomes were enriched for surface proteins, and apoptotic bodies and microvesicles were enriched for cytoplasmic and focal adhesion proteins.
		Salomon et al., 2013	Cultured first-trimester primary CTBs at different O_2 tensions and characterized exosome release and composition.
Placental tissue	Various types of MS	Dunn et al., 2012	Characterized changes in metabolites between early and late-gestation placentas and between healthy and preeclamptic placentas. Differences in mitochondrial metabolites were apparent.
		Paradela et al., 2005; Zhang et al., 2010; Vandré et al., 2012	Analyzed the STB microvillus membrane and identified proteins associated with lipid raft microdomains, actin-based cytoskeletal structures, glucose transport, plasma membrane and lipid anchoring, nutrient transport, signal transduction, endo/exocytosis, and vesicular transport.
		Fisher et al., 2019	Compared changes in mitochondrial proteins between STB and CTB mitochondria.
		Burkova et al., 2019	Isolated exosomes using crude extraction and gel filtration protocols. Reported that crude extraction results in an overestimation of the number of detectable proteins.
	^{1}H-NMR and LC-MS/MS	Kedia et al., 2015; Walejko et al., 2018	Characterized differences in metabolites present at the basal plate and the chorionic plate. Reported that metabolite levels altered at the basal and chorionic plates following delivery.
	iTRAQ	Shi et al., 2013	Reported differential expression of mitochondrial proteins isolated from normotensive and preeclamptic placentas.
	SOMAscan	Michelsen et al., 2019	Sampled blood from uterine and umbilical arteries and veins. Proteins with altered levels in venous blood relative to arterial blood were deduced to be secreted or absorbed by STB.
Placental explants	Various types of MS	Horgan et al., 2010	Cultured placental explants from healthy control and FGR pregnancies at different O_2 concentrations and found 221 unique endogenous metabolites differentially produced.
		Baig et al., 2014	Identified 25 differentially expressed proteins in STB microvesicles in villus explants prepared from healthy and preeclamptic pregnancies.
		Tong et al., 2016	Characterized proteins present in macro-, micro-, and nano-sized EVs from placental explant cultures. Proteins were involved in vesicle transport, inflammation, and complement regulation.

Wei et al., 2017; Li et al., 2019; Mischler et al., 2021). Tsuchida et al. (2020) treated hiPSCs with BMP4 for 10 days, and cells positive for the pan-trophoblast marker KRT7 were purified and compared to undifferentiated hiPSCs by DNA microarray. Hierarchical clustering separated the two groups of cells into distinct clusters, with KRT7+ cells expressing markers representative of trophoblast lineages including STB. Furthermore, *XAGE2* and *KCNQ2*, which were upregulated in KRT7+ cells, exhibited distinct expression patterns in human placenta *in situ* (Tsuchida et al., 2020). Li et al. (2020) used whole-genome sequencing (WGS) along with published transcriptomic and epigenomic datasets to identify 6 genomic variations associated with genes upregulated following BMP4-mediated differentiation of hPSCs. One of these was a single nucleotide variation in the promoter region of *MEF2C* that increased the binding affinity of TFs to this region. This resulted in increased expression of MEF2C and its target genes, thereby promoting trophoblast differentiation (Li et al., 2020). The use of hiPSCs has also been exploited to study patient-specific STB developmental processes. For instance, hiPSCs generated from umbilical cords and exposed to culture conditions that promote trophoblast formation show stark differences in the transcriptome (as determined by RNA-seq) if the cords are collected from pregnancies

with early onset preeclampsia. In particular, expression of genes associated with O_2 responsiveness and STB formation is impaired in cells from preeclampsia, without marked changes in the DNA methylome (Sheridan et al., 2019; Horii et al., 2021).

Notably, the aforementioned studies applied hESC/hPSC differentiation paradigms that typically resulted in a heterogenous mixture of trophoblast-like cells rather than STB exclusively, with limited temporal control over differentiation events. Additionally, cells arising from these differentiation paradigms do not fulfill all criteria for trophoblast identity, suggesting either incomplete reprogramming to trophoblast or the possibility that cells other than trophoblast are formed, namely mesoderm or amnion (Bernardo et al., 2011; Roberts et al., 2014; Lee et al., 2016; Guo et al., 2021; Io et al., 2021). Nevertheless, the various omics approaches used in these studies were instrumental in characterizing these cells as having trophoblast-like properties and in discovering novel regulatory mechanisms that may be implicated in driving their differentiation. In many cases, results were validated using other trophoblast cell lines or placental tissue. Therefore, these studies have provided the groundwork for future improvements in the use of cell models for trophoblast development and advanced our understanding of early STB formation.

Omics-Based Analysis of STB Development Using Early Human Embryos

Omics experiments making use of early human embryos provide a compelling means of investigating primitive STB development. In particular, studies utilizing human embryos have made use of scRNA-seq technology to characterize development of early trophoblast lineages, including STB, although differences in cell isolation methodologies (particularly for STB due to its multinucleated nature) could lead to variability in gene expression levels. West et al. (2019) used scRNA-seq on trophoblast cells isolated from human embryos cultured for 8-, 10-, or 12-days post-fertilization. Genes enriched in STB were consistent with its known functions (e.g., transport) in addition to pathways reflecting the nature of primitive STB during implantation (e.g., invasion). CTBs with a partial STB signature most apparent at day 10 were also identified and inferred to be mitotically active intermediate CTBs primed to fuse into STB. At day 12, this population was in decline while there was a resurgence of undifferentiated and migratory CTBs, possibly reflecting the start of villus formation (West et al., 2019). Lv et al. (2019) also used scRNA-seq to profile the transcriptome of individual trophoblast cells isolated from human embryos, but embryos were co-cultured with or without endometrial cells for 6–10 days as a model of peri-implantation development. Interestingly, genes associated with trophoblast maturation were more robustly expressed when co-cultured with endometrial stromal cells, underscoring the importance of closely mimicking the *in vivo* environment when studying early developmental events. Separate cell clusters were enriched in STB, CTB, or extravillous trophoblast (EVT) marker genes. Moreover, three time-dependent genetic networks were characterized between days 6 and 10, including an early (possibly pre-implantation) stage associated with epithelial development, a middle (peri-implantation) stage featuring expression of fusion-related genes, and a late (post-implantation) stage featuring genes associated with cell migration. The authors then determined when STB segregated from cells expressing CTB and EVT markers, demonstrating that STB first appeared in co-cultures between days 7 and 8. Putative upstream regulators were screened to identify TBX3 as a novel TF required for STB formation, which was validated through knockdown experiments using JEG-3 cells (Lv et al., 2019). Collectively, these studies provide compelling insight into the developmental dynamics of early STB.

Using Omics to Characterize STB Development in hTSCs, Naïve hPSCs, and Organoids

Various omics approaches have also been applied to develop and profile hTSC, naïve hPSC, and organoid models that have been utilized to study STB development. For instance, Okae et al. (2018) used RNA-seq to compare CTBs and STB isolated from first-trimester placentas and identified genes predominant in each cell type. Functional annotation showed that genes overrepresented in CTBs were involved in WNT and epidermal growth factor (EGF) signal transduction pathways. It was ultimately determined that activation of WNT and EGF together with inhibition of TGF-β, HDAC, and ROCK allowed for extended culture of CTB-derived hTSCs. These hTSCs had the capacity to differentiate into STB after withdrawal of WNT and EGF signaling and exposure to forskolin. Similar cell-lines were also derived from human blastocysts. RNA-seq showed similar gene expression profiles between CTBs, EVTs, and STB generated from the stem cell-lines compared to those derived from primary first-trimester CTBs. Whole-genome bisulfite sequencing (bisulfite-seq) showed that CTB-derived and blastocyst-derived hTSCs had nearly identical DNA methylation patterns, although some differences were apparent with primary CTBs. Sequencing of miRNAs demonstrated similar global miRNA expression profiles between the three cell-types, including robust expression of miRNAs from the trophoblast-enriched chromosome 19 miRNA cluster (C19MC) (Okae et al., 2018).

While hTSCs offer exciting new ways to study STB development, generation of hTSCs through reprogramming increases access to hTSC lines from diverse genetic backgrounds, enabling integration of both normal and pathological states into the study of STB formation. Recent reports indicate that hTSCs can be derived from naïve hPSCs (reflecting pre-implantation epiblast) but not from conventional primed hPSCs (post-implantation epiblast) (Castel et al., 2020; Cinkornpumin et al., 2020; Dong et al., 2020; Guo et al., 2021; Io et al., 2021). These naïve hPSC-derived hTSCs can invariably differentiate into mature trophoblast lineages, including STB. Numerous omics methods have been used to characterize naïve hPSC-derived hTSCs. For example, Dong et al. (2020) showed through RNA-seq that naïve hTSCs had a transcriptomic

signature similar to blastocyst-derived hTSCs and to that of human trophectoderm at day 12 post-fertilization, and that they were capable of differentiating into STB. ATAC-seq was also performed, revealing similar chromatin accessibility landscapes between naïve and blastocyst-derived hTSCs and identifying TEAD4 binding motifs enriched at open chromatin sites during hTSC derivation, supporting the notion that TEAD4 is important for trophoblast specification (Dong et al., 2020). Cinkornpumin et al. (2020) conducted RNA-seq coupled with whole genome bisulfite-seq comparing naïve hPSC-derived hTSCs to blastocyst- or placenta-derived hTSCs, showing similar patterns of CpG methylation between placenta-derived hTSCs and naïve hPSC-derived hTSCs, a notable exception being hypermethylation near several imprinted genes (*PEG3*, *ZFAT*, and *PROSER2-AS1*) in transdifferentiated cells that was not apparent in placenta-derived hTSCs (Cinkornpumin et al., 2020). Io et al. (2021) established culture conditions to derive trophectoderm and subsequently hTSCs with the capacity to form STB from naïve hPSCs. Comparison of their transcriptome with scRNA-seq data of human embryos affirmed the trophoblast developmental spectrum from trophectoderm to post-implantation STB formation (Io et al., 2021). Guo et al. (2021) similarly performed transcriptomic analyses (RNA-seq and scRNA-seq) which was compared to published embryo culture datasets to illustrate the differentiation trajectory from naïve hPSCs into trophectoderm following inhibition of ERK/MAPK and Nodal signaling, with capacity to differentiate further into hTSCs, CTBs, and STB (Guo et al., 2021). Collectively, these studies delineate the developmental trajectory of naïve hPSCs into trophectoderm and offer the exciting potential of investigating early STB developmental dynamics.

Using a cocktail of growth factors and inhibitors proven to facilitate organoid growth of various adult epithelial cells, Haider et al. (2018) established long-term expanding 3D CTB organoid cultures from first-trimester placentas. While organoids are capable of expansion and self-renewal *in vitro*, they also spontaneously generate functionally active, hCG-secreting STB toward the luminal surface of the organoid. RNA-seq analysis comparing CTB organoids with primary villus CTBs (freshly isolated or differentiated for 72 h into STB) was conducted, demonstrating similarities in gene expression between organoids, villus CTBs, and *in vitro*-generated STB in monolayer culture (Haider et al., 2018). Similarly, Turco et al. (2018) independently established conditions for villus trophoblast organoids, which also form STB at the luminal surface of organoids. DNA microarray and whole-genome DNA methylation analysis showed similar profiles between organoids and first-trimester placental villi, including hypomethylation of the *ELF5* promoter and expression of *GATA3*, *EGFR*, *TFAP2A*, *TFAP2C*, and C19MC miRNAs. The secretome of these organoids was also analyzed using LC-MS/MS and showed a similar production of peptides as produced by placental villus explants, including PSGs, INSL4, hCG, KISS1, GDF15, hPL, and high levels of sorbitol (Turco et al., 2018). Overall, omics methods have allowed for the development of new models and have provided extensive mechanistic insights, such as identification of possible regulatory factors, to further our understanding of early STB development.

OMICS TECHNOLOGIES FOR THE STUDY OF VILLUS STB DEVELOPMENT

Studying Villus STB Development Using DNA Microarray Transcriptomics

The emergence of high-throughput omics methods has facilitated the comprehensive study of villus STB development, which is often modeled with primary CTBs or CTB-like choriocarcinoma cells (e.g., BeWo). The majority of these studies take advantage of transcriptomics, such as DNA microarray, to better understand the molecular underpinnings governing CTB differentiation and fusion into STB. Aronow et al. (2001) used DNA microarray to analyze gene expression patterns of villus CTBs isolated from term placentas and cultured for up to 6 days, with cells cultured for 12 h as reference. Their analyses categorized differentially expressed genes into varying kinetic patterns with respect to early or late induction or repression, with most groups displaying a rapid initiation of their transcriptional pattern. This suggested that CTBs are poised to rapidly commence differentiation into STB. Genes were separated into distinct functional categories, which often showed concomitant induction and repression of genes that were tightly coupled to morphological changes (Aronow et al., 2001). Rouault et al. (2016) used DNA microarray to evaluate the transcriptome of primary villus CTBs and *in vitro* generated STB, but also included villus samples from which the CTBs were isolated. CTB-enriched genes functionally represented processes such as DNA replication and repair, while STB-enriched genes were associated with cell morphology and lipid metabolism. *In silico* analysis showed that gene networks were linked to PPARG, RXRA, and NR2F1 signaling pathways, which have been implicated in CTB differentiation. While similar functional categories were observed for CTB versus STB in comparison to results from Aronow et al. (2001), each study identified unique differentially-expressed genes, which may be partly due to the variable microarray platforms used (Rouault et al., 2016).

Kudo et al. (2004) used DNA microarray to compare global gene expression in BeWo cells over a time-course of forskolin-stimulated syncytialization. Since the onset of BeWo cell differentiation can be precisely controlled through addition of forskolin, synchronized transcriptome changes at earlier time points of differentiation can be captured in comparison to primary CTB cultures. For instance, 2 h after forskolin treatment, many more genes exhibited increased expression compared to decreased expression, although this asymmetry decreased over time. Clustering of genes into temporal expression patterns provided new insights into the dynamics of BeWo cell differentiation, with those genes transiently increased at 2 h mostly encoding TFs or cell cycle-associated proteins, and genes stimulated during later stages of differentiation predominantly encoding proteins involved in cell communication and metabolism. Other genes involved in cell

adhesion and fusion had altered expression soon after forskolin exposure and prior to morphological changes (Kudo et al., 2004). Induction of BeWo cell differentiation through agents like forskolin activates two downstream molecules that both contribute to this process: PKA and exchange protein directly activated by cAMP (EPAC) (Chang et al., 2011). To identify new factors controlling syncytialization through activation of PKA or EPAC, Kusama et al. (2018) performed a DNA microarray using RNA extracted from BeWo cells stimulated using PKA- or EPAC-selective cAMP analogs, reporting far fewer transcript changes following exposure to cAMP-EPAC signaling than cAMP-PKA signaling. Two TFs upregulated following cAMP-PKA signaling (STAT5B and NR4A3) were further characterized through knockdown experiments, revealing that STAT5B contributes to STB formation while NR4A3 inhibits this process (Kusama et al., 2018).

Other studies have demonstrated that CTBs undergo both morphological differentiation (characterized by fusion of mononuclear cells) and biochemical differentiation (including production of hormones such as hCG and hPL) during syncytialization through independent mechanisms (Daoud et al., 2006, 2008). To identify genes specifically implicated in morphological differentiation, Msheik et al. (2019) performed genome-wide DNA microarray profiling comparing JEG-3 cells (which can differentiate biochemically but do not fuse in monolayer culture) with BeWo cells following forskolin treatment for 48 h. From the 32 genes that were altered in BeWo cells and not in JEG-3 cells (and thus may play roles in cell fusion), many participated in aspects of cell morphology including actin filament depolymerization, cell polarity, and protein kinase C signaling. Subsequent analyses were conducted on select genes, such as *SIK1*, which was rapidly upregulated in BeWo cells exposed to forskolin and whose silencing via CRISPR/Cas9 strongly abrogated cell fusion and, to a lesser extent, biochemical differentiation (Msheik et al., 2019). To address gaps in our understanding of villus CTB development, Szilagyi et al. (2020) employed an integrated omics approach. By consulting available gene expression data, a set of genes expressed predominantly in STB were identified. Global gene expression changes during a 7-day differentiation time-course of primary term CTBs were then evaluated using DNA microarray. By combining this data with publicly available DNase I footprinting datasets, several TFs involved in regulating differentially expressed genes (e.g., KLF10, ZNF394, and ZNF682) were identified. Moreover, the TFs were categorized into two distinct aspects of differentiation: those that governed a rapid downregulation of genes ubiquitously expressed in proliferating cells, and those involved in gradual upregulation of "placenta-specific" genes associated with STB differentiation (Szilagyi et al., 2020).

Studying Villus STB Development Using RNA-Seq and scRNA-Seq Transcriptomics

Studies that have used transcriptomics to further our understanding of villus STB development have also made use of RNA-seq technology to quantify global gene expression data. Saben et al. (2014) used RNA-seq to identify placenta-enriched transcripts by profiling the transcriptome of term placenta compared to those from 7 other tissues including adipose, breast, and heart. While many of the top expressed genes in placental tissue were to be expected, several novel genes were detected whose expression was localized *in situ* to STB, suggesting that they may play roles in STB development or function. For example, one such gene was *DLG5*, which regulates apical polarity complexes and epithelial-to-mesenchymal transition, and thus may be important for maintaining STB integrity (Saben et al., 2014). Our group previously utilized DNA microarray coupled to RNA-seq to identify the TF OVOL1 as a key regulator of STB development. Specifically, DNA microarray comparing BeWo cells cultured under control or differentiating conditions for 24 h was performed to profile changes in gene expression, which revealed *OVOL1* as the most highly upregulated gene encoding a TF. RNA-seq was then performed comparing BeWo cells expressing control shRNA and cells deficient in OVOL1 (i.e., expressing shRNA targeting *OVOL1*) cultured under differentiating conditions. Transcripts decreased in OVOL1-deficient cells included those vital for STB endocrine function. Furthermore, knockdown of OVOL1 in BeWo cells, primary CTBs, and BMP4-treated hESCs reduced expression of several ERV genes including *ERVW-1* and *ERVFRD-1*. By examining the microarray dataset for potential intermediary targets of OVOL1, it was discovered that genes encoding key factors that maintain CTBs in a progenitor state such as *MYC*, *ID1*, and *TP63* were downregulated following induced differentiation and were subsequently shown to be direct targets of OVOL1 regulation. Therefore, OVOL1 facilitates CTB differentiation and induction of STB-associated transcripts by repressing genes that maintain progenitor traits (Renaud et al., 2015).

To further uncover genes involved in CTB differentiation, RNA-seq was utilized by Zheng et al. (2017) comparing BeWo cells treated with vehicle control or forskolin for 0, 24, and 48 h. Differentially expressed genes were associated with terms such as syncytium formation, cell fate commitment, cell junction assembly, calcium ion transport, regulation of epithelial cell differentiation, and cell morphogenesis. In particular, RNA-seq findings facilitated identification of novel candidate genes possibly involved in CTB differentiation into STB, including *CACNA1S*, *NEO1*, *MYH9*, *TNS1*, and *AMOT* (Zheng et al., 2017). Azar et al. (2018) similarly performed RNA-seq on BeWo cells before and after forskolin treatment; however, this was coupled to RNA-seq analysis of primary term CTBs before and after spontaneous syncytium formation. Although there were distinct differences, transcriptome comparison of the models revealed a large overlap in the genes differentially expressed during the CTB to STB transition, lending support to the validity of both models in reflecting aspects of syncytialization. Further interrogation of the RNA-seq datasets revealed 11 genes coordinately regulated (6 upregulated: *CGB*, *TREML2*, *CRIP2*, *PAM*, *INHA*, and *FLRG*, and 5 downregulated: *SERPINF1*, *MMP19*, *EPOP*, *KRT17*, and *SAA1*) in both models following STB formation, and whose protein expression was confirmed via western blotting and immunohistochemistry (Azar et al., 2018).

McConkey et al. (2016) used RNA-seq to support their derivation of a 3D culture model of JEG-3 cells that release hCG, fuse, and express STB-specific markers when co-cultured with human brain microvascular endothelial cells. Indeed, the 3D co-cultures shared more similar transcriptomic profiles with primary human STB than their 2D-cultured counterparts. This included genes uniquely expressed in both 3D JEG-3 cultures and primary CTB-derived STB, including *CDKN1C*, *PSG1*, and *PSG5*. Moreover, similar to primary CTB-derived STB, JEG-3 cells grown in 3D are resistant to infection by viruses and Toxoplasma gondii, which further supports the use of this co-culture system to recapitulate STB development and function (McConkey et al., 2016). Furthermore, RNA-seq performed by Meinhardt et al. (2020) affirmed the role of the Hippo signaling-associated transcriptional coactivator YAP in promoting CTB stemness and inhibiting STB differentiation. Comparing the transcriptomes of primary CTBs overexpressing constitutively active YAP with YAP-knockout JEG-3 cells (generated using CRISPR-Cas9) and non-transfected primary CTBs, it was found that constitutive YAP expression upregulated various stemness, cell cycle, and mitosis-associated genes, but repressed STB-specific transcripts. On the other hand, numerous regulators of proliferation were downregulated in the YAP knockout clones while hormones and other STB markers were elevated. Follow-up experiments illustrated that YAP-TEAD4 complexes interact with genomic regions of stemness genes to promote their induction, while also forming complexes with the histone methyltransferase EZH2 prior to binding promoter regions of STB-specific genes and silencing their expression (Meinhardt et al., 2020).

Despite technical considerations associated with isolating viable single cells from a multinucleated syncytium, scRNA-seq has been applied to the study of villus STB development. Tsang et al. (2017) used this method to identify several cell-type specific gene signatures by profiling over 24,000 cells from normal term placentas and placentas from early-onset preeclampsia. Clustering analysis enabled the delineation of the known differentiation trajectory from villus CTB toward EVT or STB, with STB further bifurcating into populations with high expression of the hormone genes *GH2* and *CGB* or high expression of fusion-related genes. This study also identified multiple genes as putative regulators of STB development (e.g., *OMG, SLC1A2*, and *ADHFE1*) (Tsang et al., 2017). Vento-Tormo et al. (2018) used scRNA-seq to map the cell-cell communication network at the human decidual-placental interface by profiling the transcriptomes of 70,000 cells from first-trimester placentas and deciduas. They developed a repository of ligand-receptor interacting pairs and a statistical tool that could predict molecular interactions between cell populations based on the cell-type specificity of the complexes. In particular, this database predicted ligand-receptor interactions that are likely to control the differentiation trajectory of trophoblast into STB, including interactions of receptors present in CTBs that are involved in cellular proliferation and differentiation (EGF2, NRP2, and MET) with their corresponding ligands expressed by other cells of the placenta, such as Hofbauer cells or placental fibroblasts (Vento-Tormo et al., 2018). Liu et al. (2018) performed scRNA-seq on sorted placental cells from first and second trimester human placentas, including CTBs and STB isolated from placental villi at 8 weeks of pregnancy (STB fragments were manually sorted using a mouth pipette based on size). Bioinformatic analyses on the gene expression profiles identified three subclasses of CTBs: a highly proliferative subtype that may be responsible for replenishing the pool of CTBs (thus serving as hTSCs), a non-proliferative subtype with high expression of adhesion genes and the gene *ERVFRD-1* that was strongly suggested to be the fusion-competent progenitor cells of the STB, and a third non-proliferative subtype that did not express *ERVFRD-1* and whose function remains unknown. Expression profiles of imprinted genes and those encoding proteins involved in DNA methylation and chromatin modification were also compared between various cell-types and shown to be divergent between CTBs and STB (e.g., high expression of *DNMT1* in CTBs that maintains DNA methylation patterns during cell replication) (Liu et al., 2018).

Pavličev et al. (2017) performed scRNA-seq on term placenta complemented with RNA-seq analysis of undifferentiated endometrial cells and decidual cells. RNA-seq analysis of laser capture-dissected STB was included to circumvent limitations associated with generating single cell populations from a multinucleated syncytium. These data were amalgamated to infer putative cell-cell interactions by assessing complementary receptor-ligand pairs across different cell-types. STB-specific genes included those associated with endocrine function (*CSH2*, *CSHL1*, *GH2*, and *CGA*), PSGs, and genes associated with immunity (*HPGD* and class II human leukocyte antigens). Interactome analysis of receptor-ligand pairs revealed abundant potential for communication between STB and decidual cells. For example, STB and decidual cells express corresponding ligand-receptor pairs for WNT family members, prostaglandins, hormones, cytokines, and growth factors that may help modulate tissue-specific functions during pregnancy (Pavličev et al., 2017). The interactome analysis was inferred through gene expression profiles, so further analysis at the protein level is needed to affirm which interactions are pertinent to pregnancy maintenance and health.

Studying Villus STB Development Using Epigenomics Approaches

Epigenomics techniques have been used to provide more detailed insights into the dynamic epigenetic networks orchestrating villus STB development. Shankar et al. (2015) combined RNA-seq, genome-scale DNA methylation, and ChIP-seq to provide a comprehensive overview of the transcriptome and epigenome during BeWo syncytialization. RNA-seq revealed altered expression of about 3,000 genes during a 3-day forskolin treatment including *MMP9*, *SGK1*, and *TRPV2*. Global DNA methylation assessment via reduced representation bisulfite sequencing (RRBS-seq) showed altered methylation of numerous CpGs within and near genes linked to cell differentiation and commitment, with upregulated and downregulated genes showing decreased and increased methylation, respectively. Furthermore, integration of the RNA-seq dataset with genome-wide localization of key histone marks using ChIP-seq indicated that syncytialization was associated with a gain

in transcriptionally active marks (H3K4me3, K9ac, K27ac, and K36me3) among genes that were either expressed constitutively or upregulated following forskolin treatment, with no change in repressive histone modifications (Shankar et al., 2015). DNA methylation has also been assessed by BeadChip microarray in cultured primary CTBs exposed to different O_2 tensions, where it was found that low O_2 levels stimulated hypermethylation at specific sites within the genome that potentially decrease expression of genes vital for STB formation (Yuen et al., 2013). Recently, Yuan et al. (2021) used whole genome methylation microarray to provide a cell-specific DNA methylation atlas in placental cells following fluorescence-assisted cell sorting (for most lineages); STB was isolated using enzymatic digestion because of incompatibility with fluorescence-assisted cell sorting. In STB, differential methylation at specific CpGs localized to genes more prominently expressed in this lineage (e.g., *CGA*, *PAPPA2*, and *CYP19A1*) compared to other placental lineages, consistent with the notion that DNA methylation serves as a key epigenetic mechanism for gene regulation in the placenta (Yuan et al., 2021).

Our group investigated the role of particular epigenetic modifications and regulators during trophoblast differentiation into STB. Using multiple CTB models, we observed reduced global histone acetylation at multiple lysine residues during STB formation. ChIP-seq analysis comparing site-specific changes in histone H3 acetylation between undifferentiated and differentiating BeWo cells showed dynamic changes in chromosomal regions such as genes associated with CTB differentiation (e.g., *TEAD4* and *OVOL1*) as well as genes with novel regulatory roles in this process (e.g., *LHX4* and *SYDE1*). These findings prompted subsequent investigations into the functional roles of specific HDAC enzymes (that catalyze histone deacetylation) during STB formation, which identified HDAC1 and HDAC2 as critical mediators driving CTB differentiation (Jaju Bhattad et al., 2020). Kwak et al. (2019) used ChIP-seq to illuminate genome-wide changes in binding of polymerase II, a crucial component of the RNA transcription machinery, as well as associated modified histones indicative of active or repressed chromatin, in primary human CTBs isolated from mid-gestation placenta before and after differentiation into STB. Examples of genes showing increased polymerase II binding in STB compared to CTBs included the cell fusion gene *ERVV-2*, *CEBPB* (encodes the TF C/EBPβ), and other genes associated with immunomodulatory functions (e.g., *PSG* family members). Genes downregulated in STB included negative regulators of differentiation (e.g., *EGR1*) and genes encoding proinflammatory TFs (e.g., *NR4A2*/*NURR1*). Moreover, while promoter enrichment of repressive histone markers remained low in STB, increased and decreased polymerase II binding to promoters of a subset of genes during differentiation was closely correlated with increased and decreased active histone marks, respectively (Kwak et al., 2019).

Knowledge into the epigenetic control of human STB development has emerged from studies that assess regulatory miRNAs genome-wide. One such study by Kumar et al. (2013) used microarray-based miRNA profiling in primary term CTBs before and after STB differentiation. Several members of the miR-17∼92 cluster and its paralog miR-106a-363 were downregulated during STB differentiation. Subsequent experiments showed that these miRNAs directly target *CYP19A1* and *GCM1* that drive STB formation, and the TF c-Myc binds to genomic regulatory regions of these miRNAs to increase their expression in proliferating CTBs, thus preventing differentiation into STB (Kumar et al., 2013). Dubey et al. (2018) analyzed miRNA expression patterns in control and forskolin-treated BeWo cells using microarray-based miRNA profiling. Among miRNAs differentially expressed during syncytialization, miR-92a-1-5p was significantly downregulated, and overexpression of this miRNA in BeWo cells inhibited cell fusion and hCG secretion. *DYSF* and *PRKACA*, genes that promote STB formation, were identified as targets for inhibition by miR-92a-1-5p (Dubey et al., 2018). Future endeavors to define the epigenetic regulatory mechanisms governing STB formation could include genome-wide identification of enhancer elements. This can be achieved via multi-omics approaches integrating assays for chromatin accessibility (e.g., ATAC-seq) with ChIP-seq identifying genomic regions containing specific enhancer marks, or with chromosome conformation capture techniques (Abdulghani et al., 2019). Whole human genome STARR-seq has recently been described and shown promise in the global quantification of enhancer activity in the human genome (Liu et al., 2017b). Additionally, multi-modal analyses capable of jointly analyzing the transcriptome along with epigenetic features (e.g., DNA methylome and chromatin accessibility) have recently been developed (Clark et al., 2018). These types of analyses would provide a more thorough understanding of the epigenome and its associations with the transcriptome during STB development.

USING OMICS TO DEFINE THE STB METABOLOME AND SUB-PROTEOME

The placenta exhibits a high metabolic rate, consuming more than 40% of the O_2 used by the entire conceptus (Bonds et al., 1986). The high metabolic rate is needed for hormone biosynthesis and metabolism as well as nutrient transport, which are key functions of the STB. Several studies have exploited MS and NMR-based technologies using placental tissue to screen for changes in the proteome and metabolome in normal pregnancies and those in various other conditions such as obesity, neural tube defects, high altitude, preeclampsia, and gestational diabetes (Van Patot et al., 2010; Chi et al., 2014; Austdal et al., 2015; Yang et al., 2015; Mary et al., 2017; Qi et al., 2017; Fattuoni et al., 2018; Sun et al., 2018; Feng et al., 2019). Using GC-MS and ultra-performance LC-MS, Dunn et al. (2012) found changes in 156 metabolites between early and late-gestation placentas, including increased levels of diglycerides, phospholipids, sphingolipids, and vitamin D-related metabolites, as well as decreased levels of triglycerides in late gestation placental tissue. An additional 86 metabolites were altered in preeclampsia, with differences particularly evident in mitochondrial metabolites and those involved in oxidative and nitrative stress. The authors caution about differences in metabolite quantities based on the position from where the

sample was taken and delivery mode (cesarean versus labored), underscoring the importance of proper experimental design and rigor when performing metabolic assessments of the human placenta (Dunn et al., 2012). Furthermore, regional differences in metabolite concentrations have been measured when placental tissue samples are collected closer to the basal plate versus the chorionic plate. Specifically, using ^{1}H-NMR and LC-MS/MS, elevated levels of phosphatidylcholines, choline, sphingomyelins, and several amino acids (serine, alanine, taurine, and threonine) were detected in samples collected from the basal plate, whereas higher levels of formate and very low-density lipoproteins were identified in samples collected closer to the chorionic plate (Kedia et al., 2015; Walejko et al., 2018). Notably, levels of many of these metabolites changed rapidly following delivery (Walejko et al., 2018). Given the variable levels of metabolites depending on mode of delivery, time after delivery, and position from where the sample was taken, an abundance of caution must be exercised when interpreting placental metabolomics. Notably, these studies were conducted using whole placental tissue, so the contribution of STB to these findings is uncertain, especially given reports that CTBs are more metabolically active than STB (Kolahi et al., 2017).

To circumvent some of the variability associated with sampling, labor, and (to some extent) cellular heterogeneity of placental tissue, researchers have analyzed endogenous and secreted metabolites from placental explants and CTBs cultured for defined periods of time. For example, Heazell et al. (2008) prepared explants from term uncomplicated pregnancies and cultured them in different O_2 atmospheres for up to 96 h. Subsequently, conditioned medium and tissue lysates were analyzed using GC-MS, where 264 unique metabolite peaks were detected and 2-deoxyribose, threitol, and erythritol were elevated in explants cultured in 1% O_2 relative to 20% O_2 (Heazell et al., 2008). Horgan et al. (2010) used a similar strategy to determine whether O_2-dependent metabolic changes were evident in placental explants prepared from FGR pregnancies. They reported 1,676 metabolite features, and 221 unique endogenous metabolites differentially detected between placental explants prepared from healthy control and FGR pregnancies, notably those involved in glycerophospholipid and tryptophan metabolism (Horgan et al., 2010). Functional proteomic analyses have also been performed with primary CTBs after variable periods of culture following isolation from placentas and BeWo cells following forskolin treatment, although typically the extent of syncytialization is not reported (Hoang et al., 2001; Nampoothiri et al., 2007; Sun et al., 2007; Johnstone et al., 2011).

Sub-proteomics analyses have been used to characterize components of the STB microvillus membrane and mitochondria. Paradela et al. (2005) performed detergent-free LC-MS/MS to evaluate the composition of the STB microvillus membrane, identifying 57 proteins primarily associated with lipid raft microdomains such as annexins (ANXA1, ANXA2) and placental alkaline phosphatase, as well as proteins involved in actin-based cytoskeletal structures (CLIC5) and glucose transport (GLUT1) (Paradela et al., 2005). Zhang et al. (2010) used a similar detergent-free enrichment of STB microvillus membranes along with polyacrylamide gel electrophoresis, in-gel trypsin digestion, and nano-LC-MS/MS. They identified 292 proteins, including 161 proteins that are associated with the plasma membrane and are involved in lipid anchoring, nutrient transport, signal transduction, and vesicular trafficking (Zhang et al., 2010). Vandré et al. (2012) used cationic colloidal silica particles to isolate enriched preparations of microvilli containing the apical plasma membrane from placentas, and then performed LC-nanospray MS/MS. They identified 340 non-redundant proteins associated with pathways such as endocytosis, exocyst complex, and exocytosis, as well as those involved in vesicular transport such as flotillin-1, dysferlin, and myoferlin. Out of these 340 proteins, 208 were not previously detected in the studies conducted by Paradela et al. (2005) or Zhang et al. (2010), emphasizing the variability of this approach based on tissue sampling, extraction approaches, and analyses (Vandré et al., 2012).

Fisher et al. (2019) used sequential centrifugation to enrich mitochondrial fractions based on the distinct structural differences apparent between mitochondria in CTBs (larger mitochondria with defined cristae) and STB (smaller and punctate mitochondria with diffuse cristae). LC-MS/MS was then performed to evaluate proteomic differences between STB and CTB mitochondria. There were 24 proteins decreased and 5 proteins increased in STB mitochondria compared to CTB mitochondria (Fisher et al., 2019). Differences were validated using western blotting, and in many cases, were consistent with cell-type specific differences at the transcript level as determined by cross-referencing publicly available scRNA-seq datasets (Pavličev et al., 2017; Suryawanshi et al., 2018). Many of the proteins decreased in STB mitochondria are involved in key stages of electron transport complex assembly as well as carbohydrate, fatty acid, and amino acid metabolism, which is consistent with the notion that STB may be less metabolically active than CTBs. Proteomic analyses using iTRAQ labeling have also revealed differences in the levels of 26 mitochondrial proteins from placentas of preeclamptic pregnancies relative to normotensive controls, including those involved in fatty acid oxidation, reactive O_2 species generation, and the tricarboxylic acid cycle. Although this analysis was conducted using whole placental tissue, immunostaining subsequently localized selected mitochondrial proteins to STB, including TFRC, PRDX3, and HSPE1 (Shi et al., 2013).

USING OMICS TO DEFINE THE STB SECRETOME

Proteomic Characterization of Factors Released by STB

Syncytiotrophoblast releases numerous hormones and other substances into maternal (and possibly fetal) blood. Omics technologies have provided deeper insight into the plethora of substances produced and released by STB. Epiney et al. (2012) analyzed conditioned media from CTBs cultured up to 72 h that were isolated from first-trimester placentas, term placentas, or placentas from preeclampsia using LC-MS/MS.

They found 164 proteins in pooled supernatants, including 33 proteins that were differentially expressed between cells from healthy and preeclamptic pregnancies. Notably, higher levels of coagulation factor XIII were detected in control relative to preeclamptic samples, and levels were undetectable in first-trimester CTB samples. PSGs, CG-β, apolipoproteins (APOE), and the actin binding protein transgelin-2 (TAGLN2) also showed altered expression in samples from preeclamptic placentas (Epiney et al., 2012).

Michelsen et al. (2019) sampled blood in 35 pregnant women from four vessels: two maternal (radial artery and uterine vein) and two fetal (umbilical artery and vein). Slow off-rate modified aptamer (SOMAscan) technology was then used to determine levels of 1,310 proteins in maternal and fetal arterial and venous blood. Proteins that were increased in venous blood relative to arterial blood were surmised to be secreted by the placenta into the maternal or fetal circulation. There were 34 proteins secreted into the maternal circulation presumably by STB, including hormones and growth factors (PlGF, GDF15, FGF1, INHBA, and IGFBP7), annexins (ANXA1 and ANXA2), WNT signaling antagonists (DRP1 and DRP4), and chemokines (CXCL10). Increased levels of many of these proteins were identified as gestation progressed, including PlGF, GDF15, IGFBP7, and INHBA. Nine proteins exhibited decreased levels in uterine vein blood, including VEGF, APOB, and parathyroid hormone, suggesting that these proteins bind to STB and undergo further processing or degradation by the placenta. There were also 341 proteins with higher levels in umbilical vein blood compared to umbilical artery blood, indicating that the placenta may secrete these factors directly into fetal blood, although the cell-type responsible for producing these proteins is not yet clear. Although SOMAscan technology is limited to analyzing levels of 1,310 proteins out of the more than 20,000 in the human proteome, it provides insight into the abundance of proteins secreted by the placenta (Michelsen et al., 2019).

Proteomic Analysis of STBEVs

STBEVs are released by STB into maternal circulation and have the potential to provide important diagnostic information about placental health. Therefore, studies have used omics strategies to characterize the composition of STBEVs. Baig et al. (2014) prepared villus explants from healthy term placentas and placentas from preeclamptic women and then isolated microvesicles from conditioned media for gel electrophoresis, in-gel digestion, and LC-MS/MS after 72 h culture. The authors identified 421 proteins within STB microvesicles. There were 25 proteins differentially expressed in STB microvesicles between normal and preeclamptic women, including increased levels of annexins (ANXA2 and ANXA4), heat shock proteins (HSPB, HSPA8, and HSPA5), and cytoskeletal proteins (ACTB, ACTN1, TUBBA1C, TUBB4B, and TUBB) in preeclampsia, as well as decreased levels of integrins (ITGAV and ITGB1), complement regulatory proteins, and some histones (which may be due to defective DNA repair or increased DNA damage). Functional pathway analysis on the differentially expressed proteins revealed terms such as cell death and survival, cellular assembly and organization, immune response, lipid metabolism, endothelial dysfunction, and intercellular junctions (Baig et al., 2014).

Ouyang et al. (2016) isolated apoptotic bodies, microvesicles, and exosomes from primary CTBs (cultured up to 72 h) and used LC-electrospray ionization-MS/MS and miRNA Taqman card PCR to characterize phospholipids, proteins, and miRNA cargo in these STBEV subtypes. Phospholipidomic analysis revealed 11 major classes of phospholipids within STBEVs, with a notably higher content of phospholipids that promote membrane stability (e.g., phosphatidylcholine) in exosomes compared to apoptotic bodies and microvesicles. Proteomic analysis identified 1,684 proteins in STBEVs. In general, exosomes were enriched for surface proteins expressed by other cell-types, including tetraspanins (e.g., CD9 and CD63), syndecan-1, syntenin-1, integrins, and endosomal complex proteins (e.g., CHMP2A and CHMP3), but also contained proteins that are predominantly expressed in the placenta, including CD276, placental alkaline phosphatase, and the fusogens syncytin-1 and syncytin-2. Apoptotic bodies and microvesicles primarily contained cytoplasmic and focal adhesion proteins such as MYH9/10, PLEC, and TLN1. Interestingly, all three types of EVs contained similar profiles of miRNAs that are distinct from miRNAs in non-vesicular form. Notably, STBEVs contained abundant C19MC miRNAs, which confer immunomodulatory properties to non-placental cells including resistance to a broad range of viruses (Delorme-Axford et al., 2013; Ouyang et al., 2016). STBEVs also modulate inflammatory cytokine production from peripheral blood mononuclear cells (Southcombe et al., 2011), and contain a variety of cytokines and growth factors either on their surface (e.g., CRP, IL-6, and IL-8) or internally (e.g., CCL5, TGF-β, IL-10, IL-33, CXCL10, MIF, and TRAIL), further supporting an immunoregulatory function of STBEVs (Fitzgerald et al., 2018).

Tong et al. (2016) performed proteomic analysis of macro, micro, and nano-sized EVs from placental explant cultures collected from 56 first-trimester placentas. Macro, micro, and nano-sized EVs were collected and characterized by LC-MS/MS, and 1,585, 1,656, and 1,476 proteins were identified in each, respectively. Many (1125) of these proteins were detectable in all three fractions of EVs. Gene ontology pathway analysis revealed enrichment of proteins involved in vesicle transport/internalization and inflammation, including ANXA5, CALR, CD31, CD47, RPS4, SERPINE1 (also known as PAI1), as well as proteins implicated in complement regulation (C3, MCP, DAF, and protectin) (Tong et al., 2016). Salomon et al. (2013) assessed the impact of different O_2 tensions (8, 3, or 1% O_2) on exosome release and composition in first-trimester CTBs. In total, over 160 exosomal proteins were detected using LC-MS/MS. Lower O_2 tensions were associated with increased levels of EV-associated proteins, particularly those associated with hypoxia and IL-8 signaling. Other exosomal proteins were related to cellular movement (e.g., MMP-9, TGF-β, MAPK, and VEGF) (Salomon et al., 2013).

Burkova et al. (2019) isolated exosomes from term placental extracts using a crude extraction method with and without an additional gel filtration protocol. The authors report that crude extraction leads to contamination with additional

proteins, whereas gel filtration appears to avoid impurities. MALDI-MS/MS analysis of filtrated placental exosomes revealed expression of 12 proteins: tetraspanins (CD81 and CD63), annexins (ANXA1, ANXA2, and ANXA5), cytoplasmic proteins (actin, ACTN4), placental alkaline phosphatase, and serum proteins (transferrin, hemoglobin subunits, albumin, and immunoglobulins). The total number of detectable proteins was lower when compared to the number of proteins identified in other studies. It was suggested that crude extraction of proteins from exosomes can result in an overestimation of the number of detectable proteins, underscoring the importance of effective exosome extraction protocols and rigorous protein characterization (Burkova et al., 2019).

One limitation in STBEV omics research has been the variable extraction protocols resulting in differing findings about the number and identity of proteins detected in STBEVs. In order to identify consistencies among the various studies, Familari et al. (2017) performed a meta-analysis of 6 proteomic datasets from trophoblast-derived EVs. Only 3 proteins were identified in common with all 6 datasets: albumin, FN1, and PAI1. An additional 4 proteins – C3, hemoglobin delta, transferrin, and THBS1 – were identified in 5 of the 6 datasets. Notably, datasets used in this meta-analysis were not exclusively restricted to STB (for instance, immortalized EVT cell-lines were used in some studies), so the lack of consistency between studies may be due in part to the cell models selected for inclusion in the meta-analyses. Different methodologies for exosome extraction and proteomic approaches may also contribute to variability between studies (Familari et al., 2017).

OMICS APPROACHES USED TO CHARACTERIZE STB AS A SOURCE OF cfDNA

Syncytiotrophoblast is a major source of cfDNA in maternal blood, accounting for 5–10% of total circulating DNA in maternal serum (reviewed in Hahn and Holzgreve, 2002; Hudecova et al., 2014). DNA sequencing (DNA-seq) of cfDNA has revolutionized non-invasive prenatal diagnostic testing and is widely used to detect *de novo* mutations and common fetal aneuploidies like trisomy 21 (Bianchi, 2019; Guy et al., 2019). Intriguingly, the quantity of cfDNA is fivefold higher in the blood of women with preeclampsia compared to healthy control women (Lo et al., 1999; Rafaeli-Yehudai et al., 2018). However, Poon et al. (2013) suggest that cfDNA quantity may in fact not be useful as an early predictive marker of adverse pregnancy outcomes. These authors isolated maternal plasma from 1,949 women at 11–13 weeks of

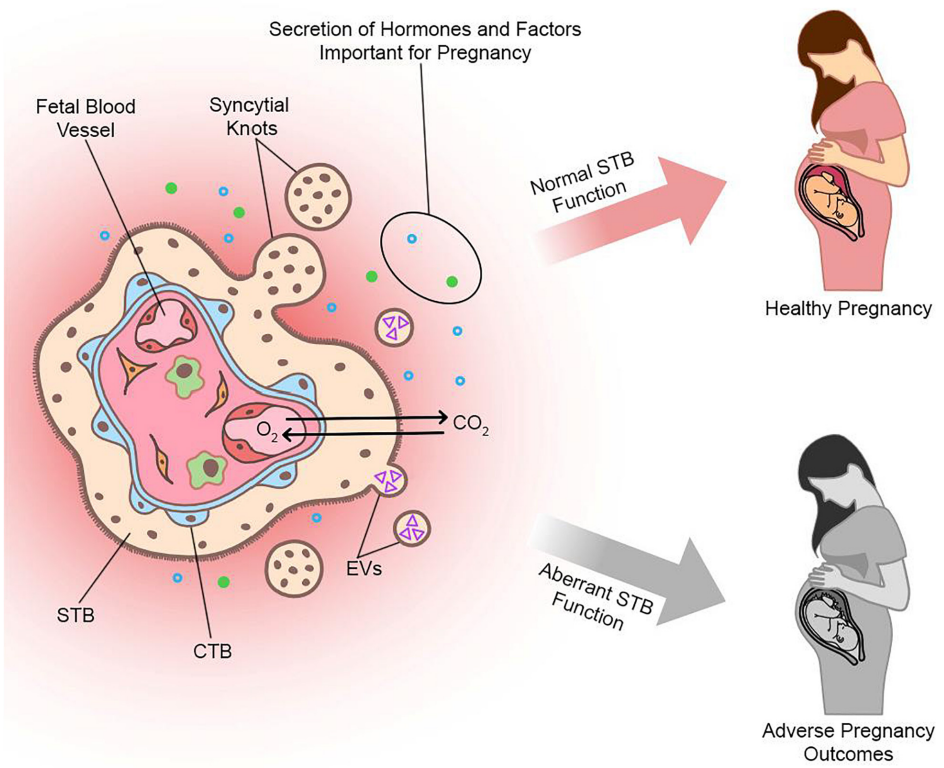

FIGURE 3 | Schematic illustrating the multifunctional importance of STB for healthy pregnancy. A cross section of a chorionic villus near term is shown. O_2, micronutrients, immunoglobulins, water, and various other substances pass across the STB layer to gain access to blood vessels in the villus core, through which they can be carried to the fetus. CO_2 and waste products diffuse across the STB layer from fetal to maternal blood. STB also produces and secretes a variety of factors into maternal blood, including peptide and steroid hormones, growth factors, EVs, and larger vesicles (e.g., syncytial knots). Given the diverse functions of STB for pregnancy success and its contiguity with maternal blood, aberrant STB function can contribute to adverse pregnancy outcomes.

gestation and conducted DNA-seq to determine the proportion of fetal and maternal cfDNA. Using this strategy, it was determined that the proportion of fetal to maternal cfDNA differed based on certain features in the patient population (e.g., ethnicity and smoking habits), but there was no association between the amount of fetal or maternal cfDNA during early pregnancy and subsequent development of a pregnancy complication (Poon et al., 2013). Furthermore, Zhang et al. (2019) demonstrated through DNA-seq that DNA isolated from placental EVs shared strong similarities with cfDNA. Given the superior stability of DNA encapsulated in lipid bilayers, EV-associated DNA may have potential clinical value for non-invasive prenatal testing of less common fetal aneuploidies or DNA modifications (Zhang et al., 2019).

A potential limitation when considering the clinical application of STB-derived DNA as a diagnostic indicator of pregnancy health is the confined placental mosaicism and chromosomal aberrations in trophoblast-derived tissue that may not be representative of the fetal genetic landscape (Peñaherrera et al., 2012; Kasak et al., 2015). Coorens et al. (2021) used whole-genome sequencing of bulk placental samples and laser capture dissected STB and found significant somatic mutagenesis that rivals childhood cancers in terms of base substitutions, copy number variation and overall mutagenic burden. Comparatively, non-trophoblast tissues (umbilical cord and villus core) did not possess frequent mutations or chromosomal irregularities. Despite the drastic alterations to the STB genome, the pregnancies themselves were seemingly normal with no obvious placental pathology or adverse pregnancy outcome (Coorens et al., 2021). Further studies are required to determine whether aberrations in the STB genome have functional consequences, and whether frequent mutagenesis of the STB genome will complicate its potential diagnostic utility to gauge pregnancy health.

CONCLUSIONS AND PERSPECTIVES

The use of omics-based approaches has provided unprecedented insights into the formation and function of STB. Where relevant, examples of how omics technologies have characterized changes in STB function in disease states were discussed (**Figure 3**). Several recent reviews, although not focused specifically on STB, have summarized the use of omics approaches in pregnancy complications. The reader is directed to these articles for a comprehensive discussion of omics approaches in pregnancy disease states (Herrera-Van Oostdam et al., 2019; Benny et al., 2020; Yong and Chan, 2020).

In assembling this review, several challenges became apparent that should be considered in future studies incorporating omics approaches to understand STB biology. One of these challenges is the lack of consistency between different studies. While it is not possible to mitigate all nuances between studies, consistency can be enhanced by including a detailed description of patient populations and sampling procedures (if applicable), rigorous analysis, validation with multiple techniques or models using independent samples, comprehensive discussion of limitations, and objective interpretation of results. The possibility of using a multi-omics approach is gaining traction to circumvent some of the limitations associated with a "one omics" strategy. For example, Turco et al. (2018) used DNA microarray, DNA-seq following bisulfite conversion, and LC-MS/MS approaches to characterize placental organoids developed in their lab, and Than et al. (2018) used transcriptomic and proteomic data from multiple publicly-available datasets combined with hypothesis-driven molecular approaches to reveal novel pathways associated with preeclampsia. Simultaneous measurements of two or more modalities on the same sample have also been described, which empower a more comprehensive interrogation of cell and tissue function (Zhu et al., 2020). The use of multi-omics approaches would also be greatly facilitated by better raw data accessibility, sharing, collaboration, and harmonization among the research community, potentially enabling more consistency across multiple studies.

Another challenge in understanding STB biology is the limited availability of cell and tissue models. Placental biopsies following delivery are frequently used to evaluate changes in placental function in normal and diseased states, but in many cases the specific role of STB is uncertain because biopsies contain many cell-types in addition to STB. Moreover, samples may vary even if collected from different regions of the same placenta (Konwar et al., 2019). This variation may contribute to differences in findings from study groups and reinforces the importance of consistent sampling procedures and cautious interpretation of data when inferring STB-specific functions from tissue. Cell, organoid, and explant models are available to study STB differentiation, but they all possess some limitations including heterogeneity (for example, not all primary CTBs form large syncytia in culture). In most cases, the complex 3D anatomical configuration along with the dynamic endocrinological, immunological, and hemodynamic environment characteristic of the *in vivo* milieu is not reflected in culture models. For instance, stark differences in trophoblast gene expression profiles are apparent when co-cultured with decidualized stromal cells compared to culture without these cells, highlighting the importance of modeling the *in vivo* environment as closely as possible (Lv et al., 2019).

Another limitation in the study of STB is its characteristic morphology and fragility that complicates cell isolation for *ex vivo* analyses. It is not yet possible to isolate and culture intact, purified STB from placentas, explants, or organoids to study STB in isolation or for use in functional studies. Although the recent upsurge in single cell omics has revolutionized the capacity to study specific cell lineages in complex tissue, STB poses a unique challenge for preparing single cells for analyses because of its enlarged, multinucleated nature. Future exploration incorporating single nucleus RNA-seq may enable a more robust characterization of STB at various stages of its life cycle, whereas spatial transcriptomics offers a promising avenue to study STB biology while preserving its native architectural integrity.

Omics technologies are advancing at a startling rate and are poised to continue providing unparalleled insights into STB development and function. Integration of multiple omics

strategies in combination with hypothesis-driven mechanistic approaches and improvements in available cell models will enable a better understanding of how this cell lineage functions in normal and diseased states. Given the importance of STB for pregnancy health and its unique position contiguous with maternal blood, studies of STB biology that incorporate omics approaches will be instrumental for driving discovery of novel biomarkers of placental stress or pregnancy disease.

AUTHOR CONTRIBUTIONS

AJ, MJ, and SR wrote and edited the manuscript. GJB edited the manuscript and contributed to preparation of the tables. All authors approved the final version of the manuscript.

FUNDING

This work was supported by grants awarded by the Natural Sciences and Engineering Research Council of Canada (5053, to SR). AJ was supported by the Queen Elizabeth II Graduate Scholarship in Science and Technology and a Canadian Institutes of Health Research Graduate Scholarship. MJ and GJB were each supported by fellowships from the Natural Sciences and Engineering Research Council of Canada.

ACKNOWLEDGMENTS

The authors would like to thank Tunyalux Langsub for illustrative assistance.

REFERENCES

Abdulghani, M., Jain, A., and Tuteja, G. (2019). Genome-wide identification of enhancer elements in the placenta. *Placenta* 79, 72–77. doi: 10.1016/j.placenta.2018.09.003

Amita, M., Adachi, K., Alexenko, A. P., Sinha, S., Schust, D. J., Schulz, L. C., et al. (2013). Complete and unidirectional conversion of human embryonic stem cells to trophoblast by BMP4. *Proc. Natl. Acad. Sci. U.S.A* 110, E1212–E1221. doi: 10.1073/pnas.1303094110

Aronow, B. J., Richardson, B. D., and Hangwerger, S. (2001). Microarray analysis of trophoblast differentiation: gene expression reprogramming in key gene function categories. *Physiol. Genomics* 6, 105–116. doi: 10.1152/physiolgenomics.2001.6.2.105

Austdal, M., Thomsen, L. C. V., Tangerås, L. H., Skei, B., Mathew, S., Bjørge, L., et al. (2015). Metabolic profiles of placenta in preeclampsia using HR-MAS MRS metabolomics. *Placenta* 36, 1455–1462. doi: 10.1016/j.placenta.2015.10.019

Azar, C., Valentine, M., Trausch-Azar, J., Druley, T., Nelson, D. M., and Schwartz, A. L. (2018). RNA-Seq identifies genes whose proteins are transformative in the differentiation of cytotrophoblast to syncytiotrophoblast, in human primary villous and BeWo trophoblasts. *Sci. Rep.* 8:5142. doi: 10.1038/s41598-018-23379-2

Baczyk, D., Dunk, C., Huppertz, B., Maxwell, C., Reister, F., Giannoulias, D., et al. (2006). Bi-potential behaviour of cytotrophoblasts in first trimester chorionic villi. *Placenta* 27, 367–374. doi: 10.1016/j.placenta.2005.03.006

Baig, S., Kothandaraman, N., Manikandan, J., Rong, L., Ee, K., Hill, J., et al. (2014). Proteomic analysis of human placental syncytiotrophoblast microvesicles in preeclampsia. *Clin. Proteomics* 11:40. doi: 10.1186/1559-0275-11-40

Baines, K. J., and Renaud, S. J. (2017). Transcription factors that regulate trophoblast development and function. *Prog. Mol. Biol. Transl. Sci.* 145, 39–88. doi: 10.1016/bs.pmbts.2016.12.003

Benny, P. A., Alakwaa, F. M., Schlueter, R. J., Lassiter, C. B., and Garmire, L. X. (2020). A review of omics approaches to study preeclampsia. *Placenta* 92, 17–27. doi: 10.1016/j.placenta.2020.01.008

Bernardo, A. S., Faial, T., Gardner, L., Niakan, K. K., Ortmann, D., Senner, C. E., et al. (2011). BRACHYURY and CDX2 mediate BMP-induced differentiation of human and mouse pluripotent stem cells into embryonic and extraembryonic lineages. *Cell Stem Cell* 9, 144–155. doi: 10.1016/j.stem.2011.06.015

Bianchi, D. W. (2019). Turner syndrome: New insights from prenatal genomics and transcriptomics. *Am. J. Med. Genet. Part C Semin. Med. Genet.* 181, 29–33. doi: 10.1002/ajmg.c.31675

Bonds, D. R., Crosby, L. O., Cheek, T. G., Hägerdal, M., Gutsche, B. B., and Gabbe, S. G. (1986). Estimation of human fetal-placental unit metabolic rate by application of the Bohr principle. *J. Dev. Physiol.* 8, 49–54.

Borges, M., Bose, P., Frank, H. G., Kaufmann, P., and Pötgens, A. J. G. (2003). A two-colour fluorescence assay for the measurement of syncytial fusion between trophoblast-derived cell lines. *Placenta* 24, 959–964. doi: 10.1016/S0143-4004(03)00173-5

Buenrostro, J. D., Wu, B., Chang, H. Y., and Greenleaf, W. J. (2015). ATAC-seq: A method for assaying chromatin accessibility genome-wide. *Curr. Protoc. Mol. Biol.* 2015, 21.29.1–21.29.9. doi: 10.1002/0471142727.mb2129s109

Burkova, E. E., Grigor'eva, A. E., Bulgakov, D. V., Dmitrenok, P. S., Vlassov, V. V., Ryabchikova, E. I., et al. (2019). Extra purified exosomes from human placenta contain an unpredictable small number of different major proteins. *Int. J. Mol. Sci.* 20:2434. doi: 10.3390/ijms20102434

Burton, G. J. (2011). Deportation of syncytial sprouts from the term human placenta. *Placenta* 32, 96–98. doi: 10.1016/j.placenta.2010.09.015

Burton, G. J., and Jauniaux, E. (2018). Pathophysiology of placental-derived fetal growth restriction. *Am. J. Obstet. Gynecol.* 218, S745–S761. doi: 10.1016/j.ajog.2017.11.577

Burton, G. J., and Jones, C. J. P. (2009). Syncytial knots, sprouts, apoptosis, and trophoblast deportation from the human placenta. *Taiwan. J. Obstet. Gynecol.* 48, 28–37. doi: 10.1016/S1028-4559(09)60032-2

Castel, G., Meistermann, D., Bretin, B., Firmin, J., Blin, J., Loubersac, S., et al. (2020). Induction of human trophoblast stem cells from somatic cells and pluripotent stem cells. *Cell Rep.* 33:108419. doi: 10.1016/j.celrep.2020.108419

Chamley, L. W., Chen, Q., Ding, J., Stone, P. R., and Abumaree, M. (2011). Trophoblast deportation: Just a waste disposal system or antigen sharing? *J. Reprod. Immunol.* 88, 99–105. doi: 10.1016/j.jri.2011.01.002

Chang, C.-W., Chang, G.-D., and Chen, H. (2011). A novel cyclic AMP/Epac1/CaMKI signaling cascade promotes GCM1 desumoylation and placental cell fusion. *Mol. Cell. Biol.* 31, 3820–3831. doi: 10.1128/mcb.05582-11

Chen, Y., Wang, K., Chandramouli, G. V. R., Knott, J. G., and Leach, R. (2013). Trophoblast lineage cells derived from human induced pluripotent stem cells. *Biochem. Biophys. Res. Commun.* 436, 677–684. doi: 10.1016/j.bbrc.2013.06.016

Chi, Y., Pei, L., Chen, G., Song, X., Zhao, A., Chen, T., et al. (2014). Metabonomic profiling of human placentas reveals different metabolic patterns among subtypes of neural tube defects. *J. Proteome Res.* 13, 934–945. doi: 10.1021/pr4009805

Cinkornpumin, J. K., Kwon, S. Y., Guo, Y., Hossain, I., Sirois, J., Russett, C. S., et al. (2020). Naive human embryonic stem cells can give rise to cells with a trophoblast-like transcriptome and methylome. *Stem Cell Rep.* 15, 198–213. doi: 10.1016/j.stemcr.2020.06.003

Clark, S. J., Argelaguet, R., Kapourani, C. A., Stubbs, T. M., Lee, H. J., Alda-Catalinas, C., et al. (2018). ScNMT-seq enables joint profiling of chromatin accessibility DNA methylation and transcription in single cells. *Nat. Commun.* 9:781. doi: 10.1038/s41467-018-03149-4

Coorens, T. H. H., Oliver, T. R. W., Sanghvi, R., Sovio, U., Cook, E., Vento-Tormo, R., et al. (2021). Inherent mosaicism and extensive mutation of human placentas. *Nature* 592, 80–85. doi: 10.1038/s41586-021-03345-1

Culibrk, L., Croft, C. A., and Tebbutt, S. J. (2016). Systems biology approaches for host-fungal interactions: an expanding multi-omics frontier. *Omi. A J. Integr. Biol.* 20, 127–138. doi: 10.1089/omi.2015.0185

Daoud, G., Le bellego, F., and Lafond, J. (2008). PP2 regulates human trophoblast cells differentiation by activating p38 and ERK1/2 and inhibiting FAK activation. *Placenta* 29, 862–870. doi: 10.1016/j.placenta.2008.07.011

Daoud, G., Rassart, É, Masse, A., and Lafond, J. (2006). Src family kinases play multiple roles in differentiation of trophoblasts from human term placenta. *J. Physiol.* 571, 537–553. doi: 10.1113/jphysiol.2005.102285

Debnath, M., Prasad, G. B. K. S., and Bisen, P. S. (2010). *Molecular Diagnostics: Promises and Possibilities*. Dordrecht: Springer Netherlands, 1–520. doi: 10.1007/978-90-481-3261-4

Delorme-Axford, E., Donker, R. B., Mouillet, J. F., Chu, T., Bayer, A., Ouyang, Y., et al. (2013). Human placental trophoblasts confer viral resistance to recipient cells. *Proc. Natl. Acad. Sci. U.S.A.* 110, 12048–12053. doi: 10.1073/pnas.1304718110

Dong, C., Beltcheva, M., Gontarz, P., Zhang, B., Popli, P., Fischer, L. A., et al. (2020). Derivation of trophoblast stem cells from naïve human pluripotent stem cells. *Elife* 9:e52504. doi: 10.7554/eLife.52504

Dubey, R., Malhotra, S. S., and Gupta, S. K. (2018). Forskolin-mediated BeWo cell fusion involves down-regulation of miR-92a-1-5p that targets dysferlin and protein kinase cAMP-activated catalytic subunit alpha. *Am. J. Reprod. Immunol.* 79:e12834. doi: 10.1111/aji.12834

Dunn, W. B., Brown, M., Worton, S. A., Davies, K., Jones, R. L., Kell, D. B., et al. (2012). The metabolome of human placental tissue: investigation of first trimester tissue and changes related to preeclampsia in late pregnancy. *Metabolomics* 8, 579–597. doi: 10.1007/s11306-011-0348-6

Epiney, M., Ribaux, P., Arboit, P., Irion, O., and Cohen, M. (2012). Comparative analysis of secreted proteins from normal and preeclamptic trophoblastic cells using proteomic approaches. *J. Proteomics* 75, 1771–1777. doi: 10.1016/j.jprot.2011.12.021

Familari, M., Cronqvist, T., Masoumi, Z., and Hansson, S. R. (2017). Placenta-derived extracellular vesicles: their cargo and possible functions. *Reprod. Fertil. Dev.* 29, 433–447. doi: 10.1071/RD15143

Fattuoni, C., Mandò, C., Palmas, F., Anelli, G. M., Novielli, C., Parejo Laudicina, E., et al. (2018). Preliminary metabolomics analysis of placenta in maternal obesity. *Placenta* 61, 89–95. doi: 10.1016/j.placenta.2017.11.014

Feng, Y., He, Y., Wang, J., Yuan, H., Zou, J., Yang, L., et al. (2019). Application of iTRAQ proteomics in identification of the differentially expressed proteins of placenta of pregnancy with preeclampsia. *J. Cell. Biochem.* 120, 5409–5416. doi: 10.1002/jcb.27819

Fisher, J. J., McKeating, D. R., Cuffe, J. S., Bianco-Miotto, T., Holland, O. J., and Perkins, A. V. (2019). Proteomic analysis of placental mitochondria following trophoblast differentiation. *Front. Physiol.* 10:1536. doi: 10.3389/fphys.2019.01536

Fitzgerald, W., Gomez-Lopez, N., Erez, O., Romero, R., and Margolis, L. (2018). Extracellular vesicles generated by placental tissues ex vivo: a transport system for immune mediators and growth factors. *Am. J. Reprod. Immunol.* 80:e12860. doi: 10.1111/aji.12860

Fogarty, N. M. E., Ferguson-Smith, A. C., and Burton, G. J. (2013). Syncytial knots (Tenney-parker changes) in the human placenta: evidence of loss of transcriptional activity and oxidative damage. *Am. J. Pathol.* 183, 144–152. doi: 10.1016/j.ajpath.2013.03.016

Fröhlich, E. (2017). Role of omics techniques in the toxicity testing of nanoparticles. *J. Nanobiotechnol.* 15:84. doi: 10.1186/s12951-017-0320-3

Gauster, M., Moser, G., Orendi, K., and Huppertz, B. (2009). Factors involved in regulating trophoblast fusion: potential role in the development of preeclampsia. *Placenta* 30, 49–54. doi: 10.1016/j.placenta.2008.10.011

Gerbaud, P., Taskén, K., and Pidoux, G. (2015). Spatiotemporal regulation of cAMP signaling controls the human trophoblast fusion. *Front. Pharmacol.* 6:202. doi: 10.3389/fphar.2015.00202

Guo, G., Stirparo, G. G., Strawbridge, S. E., Spindlow, D., Yang, J., Clarke, J., et al. (2021). Human naive epiblast cells possess unrestricted lineage potential. *Cell Stem Cell* 28, 1040–1056. doi: 10.1016/j.stem.2021.02.025

Guy, C., Haji-Sheikhi, F., Rowland, C. M., Anderson, B., Owen, R., Lacbawan, F. L., et al. (2019). Prenatal cell-free DNA screening for fetal aneuploidy in pregnant women at average or high risk: results from a large US clinical laboratory. *Mol. Genet. Genomic Med.* 7:e545. doi: 10.1002/mgg3.545

Hahn, S., and Holzgreve, W. (2002). Fetal cells and cell-free fetal DNA in maternal blood: New insights into pre-eclampsia. *Hum. Reprod. Update* 8, 501–508. doi: 10.1093/humupd/8.6.501

Haider, S., Meinhardt, G., Saleh, L., Kunihs, V., Gamperl, M., Kaindl, U., et al. (2018). Self-renewing trophoblast organoids recapitulate the developmental program of the early human placenta. *Stem Cell Rep.* 11, 537–551. doi: 10.1016/j.stemcr.2018.07.004

Hasin, Y., Seldin, M., and Lusis, A. (2017). Multi-omics approaches to disease. *Genome Biol.* 18, 1–15. doi: 10.1186/s13059-017-1215-1

Heazell, A. E. P., Brown, M., Dunn, W. B., Worton, S. A., Crocker, I. P., Baker, P. N., et al. (2008). Analysis of the metabolic footprint and tissue metabolome of placental villous explants cultured at different oxygen tensions reveals novel redox biomarkers. *Placenta* 29, 691–698. doi: 10.1016/j.placenta.2008.05.002

Herrera-Van Oostdam, A. S., Salgado-Bustamante, M., López, J. A., Herrera-Van Oostdam, D. A., and López-Hernández, Y. (2019). Placental exosomes viewed from an "omics" perspective: implications for gestational diabetes biomarkers identification. *Biomark. Med.* 13, 675–684. doi: 10.2217/bmm-2018-0468

Hiden, U., Prutsch, N., Gauster, M., Weiss, U., Frank, H. G., Schmitz, U., et al. (2007). The first trimester human trophoblast cell line ACH-3P: a novel tool to study autocrine/paracrine regulatory loops of human trophoblast subpopulations – TNF-α stimulates MMP15 expression. *BMC Dev. Biol.* 7:137. doi: 10.1186/1471-213X-7-137

Hoang, V. M., Foulk, R., Clauser, K., Burlingame, A., Gibson, B. W., and Fisher, S. J. (2001). Functional proteomics: examining the effects of hypoxia on the cytotrophoblast protein repertoire. *Biochemistry* 40, 4077–4086. doi: 10.1021/bi0023910

Horgan, R. P., Broadhurst, D. I., Dunn, W. B., Brown, M., Heazell, A. E. P., Kell, D. B., et al. (2010). Changes in the metabolic footprint of placental explant-conditioned medium cultured in different oxygen tensions from placentas of small for gestational age and normal pregnancies. *Placenta* 31, 893–901. doi: 10.1016/j.placenta.2010.07.002

Horgan, R. P., and Kenny, L. C. (2011). 'Omic' technologies: genomics, transcriptomics, proteomics and metabolomics. *Obstet. Gynaecol.* 13, 189–195. doi: 10.1576/toag.13.3.189.27672

Horii, M., Li, Y., Wakeland, A. K., Pizzo, D. P., Nelson, K. K., Sabatini, K., et al. (2016). Human pluripotent stem cells as a model of trophoblast differentiation in both normal development and disease. *Proc. Natl. Acad. Sci. U.S.A.* 113, E3882–E3891. doi: 10.1073/pnas.1604747113

Horii, M., Morey, R., Bui, T., Touma, O., Nelson, K. K., Cho, H. Y., et al. (2021). Modeling preeclampsia using human induced pluripotent stem cells. *Sci. Rep.* 11:5877. doi: 10.1038/s41598-021-85230-5

Hudecova, I., Sahota, D., Heung, M. M. S., Jin, Y., Lee, W. S., Leung, T. Y., et al. (2014). Maternal plasma fetal DNA fractions in pregnancies with low and high risks for fetal chromosomal aneuploidies. *PLoS One* 9:88484. doi: 10.1371/journal.pone.0088484

Io, S., Kabata, M., Iemura, Y., Semi, K., Morone, N., Minagawa, A., et al. (2021). Capturing human trophoblast development with naive pluripotent stem cells *in vitro*. *Cell Stem Cell* 28, 1023–1039. doi: 10.1016/j.stem.2021.03.013

Ishihara, N., Matsuo, H., Murakoshi, H., Laoag-Fernandez, J. B., Samoto, T., and Maruo, T. (2002). Increased apoptosis in the syncytiotrophoblast in human term placentas complicated by either preeclampsia or intrauterine growth retardation. *Am. J. Obstet. Gynecol.* 186, 158–166. doi: 10.1067/mob.2002.119176

Ishikawa, A., Omata, W., Ackerman, W. E., Takeshita, T., Vandré, D. D., and Robinson, J. M. (2014). Cell fusion mediates dramatic alterations in the actin cytoskeleton, focal adhesions, and E-cadherin in trophoblastic cells. *Cytoskeleton* 71, 241–256. doi: 10.1002/cm.21165

Jaju Bhattad, G., Jeyarajah, M. J., McGill, M. G., Dumeaux, V., Okae, H., Arima, T., et al. (2020). Histone deacetylase 1 and 2 drive differentiation and fusion of progenitor cells in human placental trophoblasts. *Cell Death Dis.* 11:311. doi: 10.1038/s41419-020-2500-6

Johnstone, E. D., Sawicki, G., Guilbert, L., Winkler-Lowen, B., Cadete, V. J. J., and Morrish, D. W. (2011). Differential proteomic analysis of highly purified placental cytotrophoblasts in pre-eclampsia demonstrates a state of increased oxidative stress and reduced cytotrophoblast antioxidant defense. *Proteomics* 11, 4077–4084. doi: 10.1002/pmic.201000505

Karahalil, B. (2016). Overview of systems biology and omics technologies. *Curr. Med. Chem.* 23, 4221–4230.

Karczewski, K. J., and Snyder, M. P. (2018). Integrative omics for health and disease. *Nat. Rev. Genet.* 19, 299–310. doi: 10.1038/nrg.2018.4

Karvas, R. M., McInturf, S., Zhou, J., Ezashi, T., Schust, D. J., Roberts, R. M., et al. (2020). Use of a human embryonic stem cell model to discover GABRP, WFDC2, VTCN1 and ACTC1 as markers of early first trimester human trophoblast. *Mol. Hum. Reprod.* 26, 425–440. doi: 10.1093/molehr/gaaa029

Kasak, L., Rull, K., Vaas, P., Teesalu, P., and Laan, M. (2015). Extensive load of somatic CNVs in the human placenta. *Sci. Rep.* 5, 1–10. doi: 10.1038/srep08342

Kedia, K., Nichols, C. A., Thulin, C. D., and Graves, S. W. (2015). Novel "omics" approach for study of low-abundance, low-molecular-weight components of a complex biological tissue: regional differences between chorionic and basal plates of the human placenta. *Anal. Bioanal. Chem* 407, 8543–8556. doi: 10.1007/s00216-015-9009-3

Kidima, W. B. (2015). Syncytiotrophoblast functions and fetal growth restriction during placental malaria: updates and implication for future interventions. *Biomed. Res. Int.* 2015:451735. doi: 10.1155/2015/451735

Kliman, H. J., Strauss, J. F., Nestler, J. E., Sermasi, E., Strauss, J. F., and Sanger, J. M. (1986). Purification, characterization, and in vitro differentiation of cytotrophoblasts from human term placentae. *Endocrinology* 118, 1567–1582. doi: 10.1210/endo-118-4-1567

Knöfler, M., Haider, S., Saleh, L., Pollheimer, J., Gamage, T. K. J. B., and James, J. (2019). Human placenta and trophoblast development: key molecular mechanisms and model systems. *Cell. Mol. Life Sci.* 76, 3479–3496. doi: 10.1007/s00018-019-03104-6

Knott, J. G., and Paul, S. (2014). Transcriptional regulators of the trophoblast lineage in mammals with hemochorial placentation. *Reproduction* 148, R121–R136. doi: 10.1530/REP-14-0072

Kohler, P. O., and Bridson, W. E. (1971). Isolation of hormone-producing clonal lines of human choriocarcinoma. *J. Clin. Endocrinol. Metab.* 32, 683–687. doi: 10.1210/jcem-32-5-683

Kolahi, K. S., Valent, A. M., and Thornburg, K. L. (2017). Cytotrophoblast, not syncytiotrophoblast, dominates glycolysis and oxidative phosphorylation in human term placenta. *Sci. Rep.* 7:42941. doi: 10.1038/srep42941

Konwar, C., Del Gobbo, G., Yuan, V., and Robinson, W. P. (2019). Considerations when processing and interpreting genomics data of the placenta. *Placenta* 84, 57–62. doi: 10.1016/j.placenta.2019.01.006

Krendl, C., Shaposhnikov, D., Rishko, V., Ori, C., Ziegenhain, C., Sass, S., et al. (2017). GATA2/3-TFAP2A/C transcription factor network couples human pluripotent stem cell differentiation to trophectoderm with repression of pluripotency. *Proc. Natl. Acad. Sci. U.S.A.* 114, E9579–E9588. doi: 10.1073/pnas.1708341114

Kudo, Y., Boyd, C. A. R., Sargent, I. L., Redman, C. W. G., Lee, J. M., and Freeman, T. C. (2004). An analysis using DNA microarray of the time course of gene expression during syncytialization of a human placental cell line (BeWo). *Placenta* 25, 479–488.

Kumar, P., Luo, Y., Tudela, C., Alexander, J. M., and Mendelson, C. R. (2013). The c-Myc-Regulated MicroRNA-17∼92 (miR-17∼92) and miR-106a∼363 Clusters Target hCYP19A1 and hGCM1 To inhibit human trophoblast differentiation. *Mol. Cell. Biol.* 33, 1782–1796. doi: 10.1128/mcb.01228-12

Kusama, K., Bai, R., and Imakawa, K. (2018). Regulation of human trophoblast cell syncytialization by transcription factors STAT5B and NR4A3. *J. Cell. Biochem.* 119, 4918–4927. doi: 10.1002/jcb.26721

Kwak, Y. T., Muralimanoharan, S., Gogate, A. A., and Mendelson, C. R. (2019). Human trophoblast differentiation is associated with profound gene regulatory and epigenetic changes. *Endocrinology* 160, 2189–2203. doi: 10.1210/en.2019-00144

Langbein, M., Strick, R., Strissel, P. L., Vogt, N., Parsch, H., Beckmann, M. W., et al. (2008). Impaired cytotrophoblast cell-cell fusion is associated with reduced syncytin and increased apoptosis in patients with placental dysfunction. *Mol. Reprod. Dev.* 75, 175–183. doi: 10.1002/mrd.20729

Lavialle, C., Cornelis, G., Dupressoir, A., Esnault, C., Heidmann, O., Vernochet, C., et al. (2013). Paleovirology of "syncytins", retroviral env genes exapted for a role in placentation. *Philos. Trans. R. Soc. B Biol. Sci.* 368:20120507. doi: 10.1098/rstb.2012.0507

Lee, C. Q. E., Gardner, L., Turco, M., Zhao, N., Murray, M. J., Coleman, N., et al. (2016). What Is Trophoblast? A Combination of Criteria Define Human First-Trimester Trophoblast. *Stem Cell Reports* 6, 257–272. doi: 10.1016/j.stemcr.2016.01.006

Levine, L., Habertheuer, A., Ram, C., Korutla, L., Schwartz, N., Hu, R. W., et al. (2020). Syncytiotrophoblast extracellular microvesicle profiles in maternal circulation for noninvasive diagnosis of preeclampsia. *Sci. Rep.* 10, 1–11. doi: 10.1038/s41598-020-62193-7

Li, H., Liu, Y., Liu, H., and Sun, X. (2020). Effect for human genomic variation during the bmp4-induced conversion from pluripotent stem cells to trophoblast. *Front. Genet.* 11:230. doi: 10.3389/fgene.2020.00230

Li, Y., Moretto-Zita, M., Soncin, F., Wakeland, A., Wolfe, L., Leon-Garcia, S., et al. (2013). BMP4-directed trophoblast differentiation of human embryonic stem cells is mediated through a ΔNp63+ cytotrophoblast stem cell state. *Development.* 140, 3965–3976. doi: 10.1242/dev.092155

Li, Z., Kurosawa, O., and Iwata, H. (2019). Establishment of human trophoblast stem cells from human induced pluripotent stem cell-derived cystic cells under micromesh culture. *Stem Cell Res. Ther.* 10:245. doi: 10.1186/s13287-019-1339-1

Liu, Y., Ding, D., Liu, H., and Sun, X. (2017a). The accessible chromatin landscape during conversion of human embryonic stem cells to trophoblast by bone morphogenetic protein 4. *Biol. Reprod.* 96, 1267–1278. doi: 10.1093/biolre/iox028

Liu, Y., Fan, X., Wang, R., Lu, X., Dang, Y. L., Wang, H., et al. (2018). Single-cell RNA-seq reveals the diversity of trophoblast subtypes and patterns of differentiation in the human placenta. *Cell Res.* 28, 819–832. doi: 10.1038/s41422-018-0066-y

Liu, Y., Yu, S., Dhiman, V. K., Brunetti, T., Eckart, H., and White, K. P. (2017b). Functional assessment of human enhancer activities using whole-genome STARR-sequencing. *Genome Biol.* 18:219. doi: 10.1186/s13059-017-1345-5

Lo, Y. D., Leung, T. N., Tein, M. S., Sargent, I. L., Zhang, J., Lau, T. K., et al. (1999). Quantitative abnormalities of fetal DNA in maternal serum in preeclampsia. *Clin. Chem.* 45, 184–188. doi: 10.1093/clinchem/45.2.184

Lu, X., Wang, R., Zhu, C., Wang, H., Lin, H. Y., Gu, Y., et al. (2017). Fine-tuned and cell-cycle-restricted expression of fusogenic protein syncytin-2 maintains functional placental syncytia. *Cell Rep.* 21, 1150–1159. doi: 10.1016/j.celrep.2017.10.019

Lv, B., An, Q., Zeng, Q., Zhang, X., Lu, P., Wang, Y., et al. (2019). Single-cell RNA sequencing reveals regulatory mechanism for trophoblast cell-fate divergence in human peri-implantation conceptuses. *PLoS Biol.* 17:e3000187. doi: 10.1371/journal.pbio.3000187

Marchand, M., Horcajadas, J. A., Esteban, F. J., McElroy, S. L., Fisher, S. J., and Giudice, L. C. (2011). Transcriptomic signature of trophoblast differentiation in a human embryonic stem cell model. *Biol. Reprod.* 84, 1258–1271. doi: 10.1095/biolreprod.110.086413

Mary, S., Kulkarni, M. J., Malakar, D., Joshi, S. R., Mehendale, S. S., and Giri, A. P. (2017). Placental proteomics provides insights into pathophysiology of pre-eclampsia and predicts possible markers in plasma. *J. Proteome Res.* 16, 1050–1060. doi: 10.1021/acs.jproteome.6b00955

Mayhew, T. M. (2014). Turnover of human villous trophoblast in normal pregnancy: what do we know and what do we need to know? *Placenta* 35, 229–240. doi: 10.1016/j.placenta.2014.01.011

Mayhew, T. M., and Barker, B. L. (2001). Villous trophoblast: Morphometric perspectives on growth, differentiation, turnover and deposition of fibrin-type fibrinoid during gestation. *Placenta* 22, 628–638. doi: 10.1053/plac.2001.0700

Mayhew, T. M., Leach, L., McGee, R., Wan Ismail, W., Myklebust, R., and Lammiman, M. J. (1999). Proliferation, differentiation and apoptosis in villous trophoblast at 13-41 weeks of gestation (including observations on annulate lamellae and nuclear pore complexes). *Placenta* 20, 407–422. doi: 10.1053/plac.1999.0399

McConkey, C. A., Delorme-Axford, E., Nickerson, C. A., Kim, K. S., Sadovsky, Y., Boyle, J. P., et al. (2016). A three-dimensional culture system recapitulates placental syncytiotrophoblast development and microbial resistance. *Sci. Adv.* 2:e1501462. doi: 10.1126/sciadv.1501462

Meinhardt, G., Haider, S., Kunihs, V., Saleh, L., Pollheimer, J., Fiala, C., et al. (2020). Pivotal role of the transcriptional co-activator YAP in trophoblast stemness of the developing human placenta. *Proc. Natl. Acad. Sci. U.S.A.* 117, 13562–13570. doi: 10.1073/pnas.2002630117

Michelsen, T. M., Henriksen, T., Reinhold, D., Powell, T. L., and Jansson, T. (2019). The human placental proteome secreted into the maternal and fetal circulations in normal pregnancy based on 4-vessel sampling. *FASEB J.* 33, 2944–2956. doi: 10.1096/fj.201801193R

Miller, R. K., Genbacev, O., Turner, M. A., Aplin, J. D., Caniggia, I., and Huppertz, B. (2005). Human placental explants in culture: approaches and assessments. *Placenta* 26, 439–448. doi: 10.1016/j.placenta.2004.10.002

Mischler, A., Karakis, V., Mahinthakumar, J., Carberry, C. K., Miguel, A. S., Rager, J. E., et al. (2021). Two distinct trophectoderm lineage stem cells from human pluripotent stem cells. *J. Biol. Chem.* 296:100386. doi: 10.1016/j.jbc.2021.100386

Msheik, H., El Hayek, S., Bari, M. F., Azar, J., Abou-Kheir, W., Kobeissy, F., et al. (2019). Transcriptomic profiling of trophoblast fusion using BeWo and JEG-3 cell lines. *Mol. Hum. Reprod.* 25, 811–824. doi: 10.1093/molehr/gaz061

Murphy, V. E., Smith, R., Giles, W. B., and Clifton, V. L. (2006). Endocrine regulation of human fetal growth: the role of the mother, placenta, and fetus. *Endocr. Rev.* 27, 141–169. doi: 10.1210/er.2005-0011

Nalbantoglu, S., and Karadag, A. (2019). "Introductory chapter: Insight into the OMICS technologies and molecular medicine," in *Molecular Medicine*, ed. S. Nalbantoglu (London: IntechOpen), doi: 10.5772/intechopen.86450

Nampoothiri, L. P., Neelima, P. S., and Rao, A. J. (2007). Proteomic profiling of forskolin-induced differentiated BeWo cells: an in-vitro model of cytotrophoblast differentiation. *Reprod. Biomed. Online* 14, 477–487. doi: 10.1016/S1472-6483(10)60896-6

Okae, H., Toh, H., Sato, T., Hiura, H., Takahashi, S., Shirane, K., et al. (2018). Derivation of human trophoblast stem cells. *Cell Stem Cell* 22, 50–63.e6. doi: 10.1016/j.stem.2017.11.004

Orendi, K., Gauster, M., Moser, G., Meiri, H., and Huppertz, B. (2010). The choriocarcinoma cell line BeWo: syncytial fusion and expression of syncytium-specific proteins. *Reproduction* 140, 759–766. doi: 10.1530/REP-10-0221

Ouyang, Y., Bayer, A., Chu, T., Tyurin, V. A., Kagan, V. E., Morelli, A. E., et al. (2016). Isolation of human trophoblastic extracellular vesicles and characterization of their cargo and antiviral activity. *Placenta* 47, 86–95. doi: 10.1016/j.placenta.2016.09.008

Paradela, A., Bravo, S. B., Henríquez, M., Riquelme, G., Gavilanes, F., González-Ros, J. M., et al. (2005). Proteomic analysis of apical microvillous membranes of syncytiotrophoblast cells reveals a high degree of similarity with lipid rafts. *J. Proteome Res.* 4, 2435–2441. doi: 10.1021/pr050308v

Pattillo, R. A., and Gey, G. O. (1968). The Establishment of a cell line of human hormone-synthesizing trophoblastic cells in vitro. *Cancer Res.* 28, 1231–1236.

Pattillo, R. A., Ruckert, A. C. F., Hussa, R. O., Bernstein, R., and Delfs, E. (1971). The JAr cell line – continuous human multi-hormone production and controls. *Vitr. Cell. Dev. Biol. Plant* 6, 398–399.

Pavličev, M., Wagner, G. P., Chavan, A. R., Owens, K., Maziarz, J., Dunn-Fletcher, C., et al. (2017). Single-cell transcriptomics of the human placenta: inferring the cell communication network of the maternal-fetal interface. *Genome Res.* 27, 349–361. doi: 10.1101/gr.207597.116

Peñaherrera, M. S., Jiang, R., Avila, L., Yuen, R. K. C., Brown, C. J., and Robinson, W. P. (2012). Patterns of placental development evaluated by X chromosome inactivation profiling provide a basis to evaluate the origin of epigenetic variation. *Hum. Reprod.* 27, 1745–1753. doi: 10.1093/humrep/des072

Petroff, M. G., Phillips, T. A., Ka, H., Pace, J. L., and Hunt, J. S. (2006). Isolation and culture of term human trophoblast cells. *Methods Mol. Med* 121, 203–217. doi: 10.1385/1-59259-983-4:201

Poon, L. C. Y., Musci, T., Song, K., Syngelaki, A., and Nicolaides, K. H. (2013). Maternal plasma cell-free fetal and maternal DNA at 11-13 weeks' gestation: relation to fetal and maternal characteristics and pregnancy outcomes. *Fetal Diagn. Ther.* 33, 215–223. doi: 10.1159/000346806

Qi, W. H., Zheng, M. Y., Li, C., Xu, L., and Xu, J. E. (2017). Screening of differential proteins of placenta tissues in patients with pre-eclampsia by iTRAQ proteomics techniques. *Minerva Med.* 108, 389–395. doi: 10.23736/S0026-4806.17.05080-7

Rafaeli-Yehudai, T., Imterat, M., Douvdevani, A., Tirosh, D., Benshalom-Tirosh, N., Mastrolia, S. A., et al. (2018). Maternal total cell-free DNA in preeclampsia and fetal growth restriction: Evidence of differences in maternal response to abnormal implantation. *PLoS One* 13:e0200360. doi: 10.1371/journal.pone.0200360

Redman, C. W. G., and Staff, A. C. (2015). Preeclampsia, biomarkers, syncytiotrophoblast stress, and placental capacity. *Am. J. Obstet. Gynecol.* 213(4 Suppl.), S9.e1–S9.e4. doi: 10.1016/j.ajog.2015.08.003

Renaud, S. J., Chakraborty, D., Mason, C. W., Karim Rumi, M. A., Vivian, J. L., and Soares, M. J. (2015). OVO-like 1 regulates progenitor cell fate in human trophoblast development. *Proc. Natl. Acad. Sci. U.S.A.* 112, E6175–E6184. doi: 10.1073/pnas.1507397112

Roberts, R. M., Loh, K. M., Amita, M., Bernardo, A. S., Adachi, K., Alexenko, A. P., et al. (2014). Differentiation of trophoblast cells from human embryonic stem cells: to be or not to be? *Reproduction* 147, D1–D12. doi: 10.1530/REP-14-0080

Roland, C. S., Hu, J., Ren, C. E., Chen, H., Li, J., Varvoutis, M. S., et al. (2016). Morphological changes of placental syncytium and their implications for the pathogenesis of preeclampsia. *Cell. Mol. Life Sci.* 73, 365–376. doi: 10.1007/s00018-015-2069-x

Rothbauer, M., Patel, N., Gondola, H., Siwetz, M., Huppertz, B., and Ertl, P. (2017). A comparative study of five physiological key parameters between four different human trophoblast-derived cell lines. *Sci. Rep* 7, 5892. doi: 10.1038/s41598-017-06364-z

Rouault, C., Clément, K., Guesnon, M., Henegar, C., Charles, M. A., Heude, B., et al. (2016). Transcriptomic signatures of villous cytotrophoblast and syncytiotrophoblast in term human placenta. *Placenta* 44, 83–90. doi: 10.1016/j.placenta.2016.06.001

Saben, J., Zhong, Y., McKelvey, S., Dajani, N. K., Andres, A., Badger, T. M., et al. (2014). A comprehensive analysis of the human placenta transcriptome. *Placenta* 35, 125–131. doi: 10.1016/j.placenta.2013.11.007

Salomon, C., Kobayashi, M., Ashman, K., Sobrevia, L., Mitchell, M. D., and Rice, G. E. (2013). Hypoxia-induced changes in the bioactivity of cytotrophoblast-derived exosomes. *PLoS One* 8:e79636. doi: 10.1371/journal.pone.0079636

Sarkar, P., Mischler, A., Randall, S. M., Collier, T. S., Dorman, K. F., Boggess, K. A., et al. (2016). Identification of epigenetic factor proteins expressed in human embryonic stem cell-derived trophoblasts and in human placental trophoblasts. *J. Proteome Res.* 15, 2433–2444. doi: 10.1021/acs.jproteome.5b01118

Sarkar, P., Randall, S. M., Collier, T. S., Nero, A., Russell, T. A., Muddiman, D. C., et al. (2015). Activin/nodal signaling switches the terminal fate of human embryonic stem cell-derived trophoblasts. *J. Biol. Chem.* 290, 8834–8848. doi: 10.1074/jbc.M114.620641

Shankar, K., Kang, P., Zhong, Y., Borengasser, S. J., Wingfield, C., Saben, J., et al. (2015). Transcriptomic and epigenomic landscapes during cell fusion in BeWo trophoblast cells. *Placenta* 36, 1342–1351. doi: 10.1016/j.placenta.2015.10.010

Sheridan, M. A., Yang, Y., Jain, A., Lyons, A. S., Yang, P., Brahmasani, S. R., et al. (2019). Early onset preeclampsia in a model for human placental trophoblast. *Proc. Natl. Acad. Sci. U.S.A.* 116, 4336–4345. doi: 10.1073/pnas.1816150116

Shi, J., Feng, H., Lee, J., and Chen, W. N. (2013). Comparative proteomics profile of lipid-cumulating oleaginous yeast: an iTRAQ-coupled 2-D LC-MS/MS analysis. *PLoS One* 8:e85532. doi: 10.1371/journal.pone.0085532

Southcombe, J., Tannetta, D., Redman, C., and Sargent, I. (2011). The immunomodulatory role of syncytiotrophoblast microvesicles. *PLoS One* 6:e20245. doi: 10.1371/journal.pone.0020245

Sudheer, S., Bhushan, R., Fauler, B., Lehrach, H., and Adjaye, J. (2012). FGF inhibition directs BMP4-mediated differentiation of human embryonic stem cells to syncytiotrophoblast. *Stem Cells Dev.* 21, 2987–3000. doi: 10.1089/scd.2012.0099

Sun, L., Yang, N., De, W., and Xiao, Y. (2007). Proteomic analysis of proteins differentially expressed in preeclamptic trophoblasts. *Gynecol. Obstet. Invest.* 64, 17–23. doi: 10.1159/000098399

Sun, X., Qu, T., He, X., Yang, X., Guo, N., Mao, Y., et al. (2018). Screening of differentially expressed proteins from syncytiotrophoblast for severe early-onset preeclampsia in women with gestational diabetes mellitus using tandem mass tag quantitative proteomics. *BMC Pregnancy Childbirth* 18:437. doi: 10.1186/s12884-018-2066-9

Suryawanshi, H., Morozov, P., Straus, A., Sahasrabudhe, N., Max, K. E. A., Garzia, A., et al. (2018). A single-cell survey of the human first-trimester placenta and decidua. *Sci. Adv.* 4:eaau4788. doi: 10.1126/sciadv.aau4788

Szilagyi, A., Gelencser, Z., Romero, R., Xu, Y., Kiraly, P., Demeter, A., et al. (2020). Placenta-specific genes, their regulation during villous trophoblast differentiation and dysregulation in preterm preeclampsia. *Int. J. Mol. Sci.* 21:628. doi: 10.3390/ijms21020628

Taglauer, E. S., Wilkins-haug, L., and Bianchi, D. W. (2014). Review: cell-free fetal DNA in the maternal circulation as an indication of placental health and disease. *Placenta* 35, S64–S68. doi: 10.1016/j.placenta.2013.11.014

Tannetta, D., Collett, G., Vatish, M., Redman, C., and Sargent, I. (2017a). Syncytiotrophoblast extracellular vesicles – circulating biopsies reflecting placental health. *Placenta* 52, 134–138. doi: 10.1016/j.placenta.2016.11.008

Tannetta, D., Masliukaite, I., Vatish, M., Redman, C., and Sargent, I. (2017b). Update of syncytiotrophoblast derived extracellular vesicles in normal pregnancy and preeclampsia. *J. Reprod. Immunol.* 119, 98–106. doi: 10.1016/j.jri.2016.08.008

Teasdale, F., and Jean-Jacques, G. (1985). Morphometric evaluation of the microvillous surface enlargement factor in the human placenta from mid-gestation to term. *Placenta* 6, 375–381. doi: 10.1016/S0143-4004(85)80014-X

Than, N. G., Romero, R., Tarca, A. L., Kekesi, K. A., Xu, Y., Xu, Z., et al. (2018). Integrated systems biology approach identifies novel maternal and placental pathways of preeclampsia. *Front. Immunol.* 9:1661. doi: 10.3389/fimmu.2018.01661

Tong, M., Kleffmann, T., Pradhan, S., Johansson, C. L., Desousa, J., Stone, P. R., et al. (2016). Proteomic characterization of macro-, micro- and nano-extracellular vesicles derived from the same first trimester placenta: relevance for feto-maternal communication. *Hum. Reprod.* 31, 687–699. doi: 10.1093/humrep/dew004

Tsang, J. C. H., Vong, J. S. L., Ji, L., Poon, L. C. Y., Jiang, P., Lui, K. O., et al. (2017). Integrative single-cell and cell-free plasma RNA transcriptomics elucidates placental cellular dynamics. *Proc. Natl. Acad. Sci. U.S.A.* 114, E7786–E7795. doi: 10.1073/pnas.1710470114

Tsuchida, N., Kojima, J., Fukuda, A., Oda, M., Kawasaki, T., Ito, H., et al. (2020). Transcriptomic features of trophoblast lineage cells derived from human induced pluripotent stem cells treated with BMP 4. *Placenta* 89, 20–32. doi: 10.1016/j.placenta.2019.10.006

Turco, M. Y., Gardner, L., Kay, R. G., Hamilton, R. S., Prater, M., Hollinshead, M. S., et al. (2018). Trophoblast organoids as a model for maternal–fetal interactions during human placentation. *Nature* 564, 263–281. doi: 10.1038/s41586-018-0753-3

Van Patot, M. C. T., Murray, A. J., Beckey, V., Cindrova-Davies, T., Johns, J., Zwerdlinger, L., et al. (2010). Human placental metabolic adaptation to chronic hypoxia, high altitude: hypoxic preconditioning. *Am. J. Physiol. Regul. Integr. Comp. Physiol.* 298, R166–R172. doi: 10.1152/ajpregu.00383.2009

Vandré, D. D., Ackerman, W. E. IV, Tewari, A., Kniss, D. A., and Robinson, J. M. (2012). A placental sub-proteome: the apical plasma membrane of the syncytiotrophoblast. *Placenta* 33, 207–213. doi: 10.1016/j.placenta.2011.12.010

Vento-Tormo, R., Efremova, M., Botting, R. A., Turco, M. Y., Vento-Tormo, M., Meyer, K. B., et al. (2018). Single-cell reconstruction of the early maternal–fetal interface in humans. *Nature* 563, 347–353. doi: 10.1038/s41586-018-0698-6

Walejko, J. M., Chelliah, A., Keller-Wood, M., Gregg, A., and Edison, A. S. (2018). Global metabolomics of the placenta reveals distinct metabolic profiles between maternal and fetal placental tissues following delivery in non-labored women. *Metabolites* 8:10. doi: 10.3390/metabo8010010

Wei, Y., Zhou, X., Huang, W., Long, P., Xiao, L., Zhang, T., et al. (2017). Generation of trophoblast-like cells from the amnion in vitro: a novel cellular model for trophoblast development. *Placenta* 51, 28–37. doi: 10.1016/j.placenta.2017.01.121

West, R. C., Ming, H., Logsdon, D. M., Sun, J., Rajput, S. K., Kile, R. A., et al. (2019). Dynamics of trophoblast differentiation in peri-implantation–stage human embryos. *Proc. Natl. Acad. Sci. U.S.A.* 116, 22635–22644. doi: 10.1073/pnas.1911362116

Wice, B., Menton, D., Geuze, H., and Schwartz, A. L. (1990). Modulators of cyclic AMP metabolism induce syncytiotrophoblast formation in vitro. *Exp. Cell Res.* 186, 306–316. doi: 10.1016/0014-4827(90)90310-7

Xu, R. H., Chen, X., Li, D. S., Li, R., Addicks, G. C., Glennon, C., et al. (2002). BMP4 initiates human embryonic stem cell differentiation to trophoblast. *Nat. Biotechnol.* 20, 1261–1264. doi: 10.1038/nbt761

Yabe, S., Alexenko, A. P., Amita, M., Yang, Y., Schust, D. J., Sadovsky, Y., et al. (2016). Comparison of syncytiotrophoblast generated from human embryonic stem cells and from term placentas. *Proc. Natl. Acad. Sci. U.S.A.* 113, E2598–E2607. doi: 10.1073/pnas.1601630113

Yang, J. I., Kong, T. W., Kim, H. S., and Kim, H. Y. (2015). The proteomic analysis of human placenta with pre-eclampsia and normal pregnancy. *J. Korean Med. Sci.* 30, 770–778. doi: 10.3346/jkms.2015.30.6.770

Yong, H. E. J., and Chan, S. Y. (2020). Current approaches and developments in transcript profiling of the human placenta. *Hum. Reprod. Update* 26, 799–840. doi: 10.1093/humupd/dmaa028

Yuan, V., Hui, D., Yin, Y., Peñaherrera, M. S., Beristain, A. G., and Robinson, W. P. (2021). Cell-specific characterization of the placental methylome. *BMC Genomics* 22:6. doi: 10.1186/s12864-020-07186-6

Yuen, R. K. C., Chen, B., Blair, J. D., Robinson, W. P., and Michael Nelson, D. (2013). Hypoxia alters the epigenetic profile in cultured human placental trophoblasts. *Epigenetics* 8, 192–202. doi: 10.4161/epi.23400

Zhang, Q., Schulenborg, T., Tan, T., Lang, B., Friauf, E., and Fecher-Trost, C. (2010). Proteome analysis of a plasma membrane-enriched fraction at the placental feto-maternal barrier. *Proteomics Clin. Appl.* 4, 538–549. doi: 10.1002/prca.200900048

Zhang, W., Lu, S., Pu, D., Zhang, H., Yang, L., Zeng, P., et al. (2019). Detection of fetal trisomy and single gene disease by massively parallel sequencing of extracellular vesicle DNA in maternal plasma: a proof-of-concept validation. *BMC Med. Genomics* 12:151. doi: 10.1186/s12920-019-0590-8

Zheng, R., Li, Y., Sun, H., Lu, X., Sun, B. F., Wang, R., et al. (2017). Deep RNA sequencing analysis of syncytialization-related genes during BeWo cell fusion. *Reproduction* 153, 35–48. doi: 10.1530/REP-16-0343

Zhu, C., Preissl, S., and Ren, B. (2020). Single-cell multimodal omics: the power of many. *Nat. Methods* 17, 11–14. doi: 10.1038/s41592-019-0691-5

Conflict of Interest: The authors declare that the research was conducted in the absence of any commercial or financial relationships that could be construed as a potential conflict of interest.

frontiers in Cell and Developmental Biology

ORIGINAL RESEARCH
published: 21 July 2021
doi: 10.3389/fcell.2021.697947

Coordinated Expressional Landscape of the Human Placental miRNome and Transcriptome

*Rain Inno, Triin Kikas, Kristiina Lillepea and Maris Laan**

Human Genetics Research Group, Institute of Biomedicine and Translational Medicine, Faculty of Medicine, University of Tartu, Tartu, Estonia

Placenta is a unique organ that serves its own function, and contributes to maternal gestational adaptation and fetal development. Coordination of its transcriptome to satisfy all the maternal-fetal needs across gestation is not fully understood. MicroRNAs are powerful transcriptome modulators capable to adjust rapidly the expression level and dynamics of large gene sets. This MiR-Seq based study presents a multi-omics investigation of the human placental miRNome and its synergy with the transcriptome. The analysis included 52 placentas representing three trimesters of normal pregnancy, and term cases of late-onset preeclampsia (LO-PE), gestational diabetes and affected fetal growth. Gestational-age dependent differential expression (FDR < 0.05) was detected for 319 of 417 tested miRNAs (76.5%). A shared list of target genes of dynamic miRNAs suggested their coordinated action. The most abundant miR-143-3p revealed as a marker for pregnancy progression. The data suggested critical, but distinct roles of placenta-specific imprinted C19MC and C14MC miRNA clusters. Paternally encoded primate-specific C19MC was highly transcribed during first trimester, potentially fine-tuning the early placental transcriptome in dosage-sensitive manner. Maternally encoded eutherian C14MC showed high expression until term, underlining its key contribution across gestation. A major shift in placental miRNome (16% miRNAs) was observed in LO-PE, but not in other term pregnancy complications. Notably, 13/38 upregulated miRNAs were transcribed from C19MC and only one from C14MC, whereas 11/28 downregulated miRNAs represented C14MC and none C19MC. miR-210-3p, miR-512-5p, miR-32-5p, miR-19a-3p, miR-590-3p, miR-379-5p were differentially expressed in LO-PE and cases of small-for-gestational-age newborns, supporting a shared etiology. Expression correlation analysis with the RNA-Seq data (16,567 genes) of the same samples clustered PE-linked miRNAs into five groups. Large notable clusters of miRNA–gene pairs showing directly and inversely correlated expression dynamics suggested potential functional relationships in both scenarios. The first genome-wide study of placental miR-eQTLs identified 66 placental SNVs associated with the expression of neighboring miRNAs, including PE-linked miRNAs miR-30a-5p, miR-210-3p, miR-490-3p and miR-518-5p. This study provided a rich

OPEN ACCESS

Edited by:
Geetu Tuteja,
Iowa State University, United States

Reviewed by:
Simão Teixeira da Rocha,
University of Lisbon, Portugal
Gerrit J. Bouma,
Colorado State University, United States

***Correspondence:**
Maris Laan
maris.laan@ut.ee

Specialty section:
This article was submitted to Developmental Epigenetics, a section of the journal Frontiers in Cell and Developmental Biology

Received: *20 April 2021*
Accepted: *28 June 2021*
Published: *21 July 2021*

Citation:
Inno R, Kikas T, Lillepea K and Laan M (2021) Coordinated Expressional Landscape of the Human Placental miRNome and Transcriptome. Front. Cell Dev. Biol. 9:697947. doi: 10.3389/fcell.2021.697947

catalog of miRNAs for further in-depth investigations of their individual and joint effect on placental transcriptome. Several highlighted miRNAs may serve as potential biomarkers for pregnancy monitoring and targets to prevent or treat gestational disorders.

Keywords: human placenta, miR-seq, gestational dynamics, pregnancy complications, preeclampsia, transcriptome (RNA-seq), miR-eQTL, genetic association study

INTRODUCTION

The placenta is a temporary mammalian organ that connects the maternal and fetal circulatory systems. Molecules produced by the placenta contribute to fetal developmental programming and support the maternal organism to cope with the pregnancy (Aplin et al., 2020). Alterations in placental gene expression may lead to its aberrant function and pregnancy complications (Sõber et al., 2015, 2016; Yong and Chan, 2020; Kikas et al., 2021).

MicroRNAs (abbreviated as miRNAs) are critical modulators of post-transcriptional levels of mRNAs, fine-tuning the composition of cellular proteome. Upon binding to 3′UTRs of mRNA transcripts, miRNAs guide their target to degradation or temporary translational inhibition. The transcript level of each mRNA is modulated by several jointly acting miRNAs and each miRNA contributes to fine-tuning the expression level of hundreds or even thousands of genes. The roles of several miRNAs (miR-155, miR-210-3p, miR-518b-3p) are well known in placental function, trophoblast growth and proliferation (Chiofalo et al., 2017; Apicella et al., 2019; Ghafouri-Fard et al., 2020). Increased expression of some specific miRNAs, such as miR-210 reflect placental distress in hypoxic or other malfunctioning conditions (Pineles et al., 2007; Zhang et al., 2012). Notably, there are large imprinted clusters of miRNA genes, C19MC (Chr. 19; 46 miRNA genes; only maternal allelic expressed) and C14MC (Chr. 14; 52 miRNA genes, only paternal allelic expression) that are nearly exclusively expressed in the placenta. C19MC has evolved in the primate lineage and C14MC among eutherians (Morales-Prieto et al., 2013; Tamaru et al., 2020). C14MC is one of the largest mammalian miRNA clusters and is located within an imprinted chromosomal region DLK1-DIO3, harboring also either paternally or maternally imprinted genes (*DLK1, RTL1, MEG3*, *MEG8* and *DIO3*) and C/D small nucleolar RNAs (SNORDs) (Seitz et al., 2004; Pilvar et al., 2019). A further co-regulator of placental transcriptome is the miR-371–373 gene cluster with also restricted expression to trophoblast lineage and embryonic stem cells (Chr.19; four miRNA genes) (Wu et al., 2014). Despite the potential important role of miRNAs in shaping the placental transcriptome throughout gestation, there is limited data on how the level of individual miRNAs as well as the whole placental miRNome is correlated with the placental transcriptome (Awamleh et al., 2019; Kennedy et al., 2020).

Single nucleotide variants (SNVs) that regulate the transcriptional activity of adjacent genes are termed as Expression Quantitative Trait Loci (eQTLs) (GTEx Consortium, 2015; The GTEx Consortium, 2020). Placental eQTLs and their potential functional link to pregnancy traits have only recently gained attention (Kikas et al., 2020, 2021). Unlike protein-encoding genes, there is no published data on SNVs regulating the expression levels of miRNAs in placenta, referred as miRNA eQTLs (miR-eQTLs).

The current study aimed at comprehensive profiling of the human placental miRNome and its expression dynamics. More specifically, miR-Seq datasets of 52 placentas were analyzed for differential expression between the three trimesters of pregnancy, as well as between cases with late gestational complications compared to uneventful pregnancies at term. The functional effect of 66 differentially expressed miRNAs (DEmiRs) in preeclamptic placentas was explored using expressional correlation analysis with the corresponding RNA-Seq based transcriptome dataset. For the first time, a genome-wide approach was applied to map placental miR-eQTLs and to investigate their link to pregnancy outcomes.

MATERIALS AND METHODS

Ethics Statement

The study utilized samples from Estonian REPROMETA (full study name "REPROgrammed fetal and/or maternal METAbolism"; recruitment 2006–2011) and HAPPY PREGNANCY (full: "Development of novel non-invasive biomarkers for fertility and healthy pregnancy"; 2013–2015) data sets. Both studies were approved by the Ethics Review Committee of Human Research of the University of Tartu, Estonia (Permissions No 146/18, 27.02.2006; 150/33, 18.06.2006; 158/80, 26.03.2007; 221/T-6, 17.12.2012; 286/M-18, 15.10.2018). All study participants were recruited, and the study material was collected at the Women's Clinic of Tartu University Hospital, Estonia. Written informed consent to participate in the study was obtained from each individual prior to recruitment. The study was carried out in compliance with the Helsinki Declaration and all methods were carried out in accordance with approved guidelines. All participants were of white European ancestry and living in Estonia.

Samples Utilized for the Placental miRNome Analysis

Genome-wide profiling of placental miRNome was performed for 52 placental samples representing first (n = 5) or second (n = 7) trimester of gestation, and term pregnancy (n = 40) (**Table 1**). Term placental samples were drawn before or shortly after delivery during the REPROMETA study (**Supplementary Methods**). The analyzed 40 term pregnancy cases (delivery after 37th gestational week, g.week) represented normal gestation, preeclampsia (PE), gestational diabetes (GD), and delivery of

a small- or large-for-gestational-age newborn (SGA and LGA, newborns <10th or >90th birth weight centile, respectively). Each clinical subgroup included eight cases, matched for the gestational age, delivery mode and proportions of male/female newborns. First and second trimester placental samples had been collected from women who underwent elective surgical termination of pregnancy or medically induced abortion due to maternal medical risks. In all analyzed cases, fetal anomalies and gross chromosomal aberrations were excluded. The definition of clinical subgroups, details of collection and processing of placental samples, and DNA and RNA extraction protocols are provided in **Supplementary Methods** and recent publications (Sõber et al., 2015; Reiman et al., 2017; Kikas et al., 2019, 2020).

Small-RNA Sequencing and Data Processing

Initial small-RNA libraries were prepared from 1 μg total RNA (TruSeq Small RNA kit, Illumina), followed by miRNA enrichment (Caliper LabChipXT, PerkinElmer) according to manufacturer's protocols. Small RNA-Seq libraries were sequenced on Illumina HiSeq 2000. Library preparation and sequencing were conducted in FIMM Sequencing Laboratory, University of Helsinki, Finland. Quality control of the raw reads was performed using FastQC (ver. 0.11.7) and MultiQC (ver. 1.7) (Ewels et al., 2016). Trimmomatic (ver. 0.38) was implemented to remove adapters and trim the quality of reads with the following settings - ILLUMINACLIP:2:30:9, LEADING:3, CROP:50, TRAILING:3, SLIDINGWINDOW:4:20, MINLEN:16. Reads were aligned to human genome reference GRCh38 using bowtie (ver. 1.2.2, settings: -n 1 -l 20 -q -m 40 -k 1 -t –best –strata) (Langmead et al., 2009). miRNA quantification was performed using featureCounts from the Rsubread package (ver. 1.20.6) (Liao et al., 2019) for R with miRNA annotations from miRBase 22.1 as reference (Kozomara et al., 2019).

Bioinformatic Analysis of the Placental miR-Seq Dataset

From 2,652 quantified placental miRNAs only those with median raw read counts over 50 across all analyzed samples (n = 417; 15.7%) were included in statistical analyses. All subsequent computational profiling and differential expression analyses were implemented using read counts normalized with DESeq2 (ver. 1.22.2) package for R with default settings (Love et al., 2014; **Supplementary Table 1**). In addition, counts per million reads mapped (CPM) were quantified for the graphical presentation of miRNA expression in subgroups. False-discovery rate (FDR) in differential expression tests was applied according to Benjamini and Hochberg (1995). Test results with FDR $P < 0.05$ were considered as statistically significant. Placental miRNome was compared for the following subgroups: first (n = 5) vs. second trimester (n = 7), second trimester vs. normal term (n = 8) pregnancy; late gestational complications (PE, GD, SGA, LGA) vs. normal term pregnancy (each group n = 8); term pregnancy 46, XX (n = 21) vs. 46, XY (n = 19). Comparisons of miRNA expression between the three trimesters of gestation were carried out without and with adjustment for sex as cofactor. miRTarBase database (Huang et al., 2020) was used to assemble the lists of experimentally validated target genes for differentially expressed miRNAs (DEmiRs) across normal pregnancy, and

TABLE 1 | Clinical characteristics of the pregnancies profiled for the placental miRNome.

	Early pregnancy		Term pregnancy					
Pregnancy related parameters (units)/	**I trimester**	**II trimester**	**All samples**	**Healthy**	**Preeclampsia**	**Gestational diabetes**	**SGA at birth**	**LGA at birth**
Sample size (*n*)	5	7	40	8	8	8	8	8
Maternal age (years)	24 (19–33)	24 (15–39)	29 (18–39)	33 (18–37)	27 (19–39)	33 (22–36)	25 (20–32)	30 (18–39)
Maternal height (cm)	161 (160–165)	170 (160–173)	166 (153–179)	165 (158–175)	170 (163–173)	167 (158–175)	166 (153–172)	167 (160–179)
Pre-pregnancy BMI (kg/m^2)	21 (20–26)	22 (17–25)	24 (16–43)	24 (17–30)	26 (20–34)	26 (18–43)	21 (17–24)	24 (19–31)
Nulliparity (*n*, %)	1 (20%)	5 (65.5%)	21 (52.5%)	3 (37.5%)	6 (75%)	3 (37.5%)	7 (87.5%)	2 (25%)
Smokers (*n*)	4	Unknown	7 (17.5%)	2 (25%)	2 (25%)	1 (12.5%)	2 (25%)	0
Gestational age at birth/abortion (days)	60 (51–81)	121 (108–140)	274 (260–291)	284 (260–291)	266 (260–271)	276 (268–284)	271 (264–289)	281 (275–288)
Vaginal/CS delivery	n.a	n.a	19/21	5/3	2/6	3/5	6/2	3/5
Fetal sex (M/F)	2/3	4/3	19/21	5/3	4/4	3/5	3/5	4/4
Birth weight (g)	n.a	n.a	3756 (2004–4986)	3756 (3102–4220)	2803 (2170–3570)	4284 (3940–4680)	2517 (2004–2698)	4744 (4420–4986)
Birth length (cm)	n.a	n.a	51 (45–55)	51 (49–55)	48 (45–49)	53 (51–54)	46 (45–48)	53 (52–55)
Birth head circumference (cm)	n.a	n.a	35 (32–39)	36 (33–36)	34 (32–36)	36 (34–38)	32 (32–34)	38 (37–38)
Birth chest circumference (cm)	n.a	n.a	35 (28–39)	35 (33.5–38)	31 (28.5–35)	36 (34–38)	31 (28–34)	37 (36–39)
Placental weight (g)	n.a	n.a	545 (200–1060)	575 (420–770)	463 (340–720)	588 (500–1060)	420 (200–470)	818 (610–970)

Data are represented as medians with ranges, except where indicated differently. Nulliparity refers to no previous childbirth. Birth data apply to the newborn. BMI, body mass index; CS, C-section; LGA, large-for-gestational-age; SGA, small-for-gestational-age; n.a., not applicable.

for miRNAs encoded by the C19MC and C14MC clusters. Only target genes with high confidence were considered for the gene enrichment analysis (see below). Expression correlations of miR-143-3p, miR-92a-3p, miR-26a-5p, as well as C19MC and C14MC microRNAs with high confidence target genes were calculated using Kendall correlation coefficient (parameter tau).

mRNA/lincRNA expression data was derived from the RNA-Seq datasets that had been previously generated for the same placental samples as utilized for miR-Seq. Placental RNA-seq library preparation, sequencing and raw data processing are detailed in **Supplementary Methods** and in previous studies (Sõber et al., 2015, 2016; Reiman et al., 2017; Pilvar et al., 2019).

Analysis of inter-relatedness between the expression of miRNAs and mRNA/lincRNA genes in 40 term placentas also utilized the above-mentioned published RNA-Seq data. Expressional correlation of miRNA/mRNA transcripts was evaluated using Spearman's correlation coefficient (parameter rho). Correlation analysis included 66 miRNAs showing differential expression in PE in the miR-Seq dataset and 16,567 genes with raw median read counts >50 in the RNA-Seq dataset. Spearman's rho values for 1,093,422 miRNA-gene pairs were estimated in R and visualized as a heatmap, using R package heatmap.2 (Gregory et al., 2015). Lists of genes showing confident expressional correlation with miRNA hierarchical cluster groups G1-G5 were formed using the following criteria: median Spearman's rho across 40 term placentas <-0.3 and for individual samples <-0.1 (negatively correlated genes); or median rho > 0.3 and for individual samples higher than rho > 0.1 (positively correlated genes). These gene lists were used as input for the gene enrichment analysis for *in silico* functional profiling.

All gene enrichment analyses based on miRNA hierarchical cluster groups were implemented in g:Profiler (ver. 1760) with default settings (Reimand et al., 2016). The recommendation for a more conservative analysis to compute functional enrichment in a custom gene list instead of all human genes in Ensembl database was followed to avoid overestimating statistically significant results (Reimand et al., 2016; Raudvere et al., 2019).

miR-eQTL Analysis

To avoid potential confounding effect of gestational expression dynamics, the discovery analysis of placental miR-eQTLs included only term placental samples (n = 40). SNV genotypes were derived from the previously published genome-wide genotyping dataset of the same placental samples [Illumina HumanOmniExpress-12-v1 BeadChip (>733,000 SNVs; median spacing 2.1 kb)] (Kasak et al., 2015; Pilvar et al., 2019). The analysis was targeted to ±100 kb window extending to both directions from the start and end of miRNA genes, annotated based on miRBase (ver. 22.1). The genomic regions flanking the analyzed 417 miRNAs included 6,274 common SNVs (MAF > 0.1). In total, 17,302 linear regression association tests were carried out between SNV genotypes and miRNA expression levels, quantified as normalized miRNA read counts. All tests with miR-eQTLs were implemented in PLINK v1.07 using fetal sex and gestational age as cofactors (Purcell et al., 2007). The results were corrected for multiple testing using the Benjamini–Hochberg method, with cut-off FDR < 0.05. All of the miR-eQTLs were tested for Hardy–Weinberg equilibrium (**Supplementary Table 2**).

Cohorts for the Genetic Association Testing Between miR-eQTLs and Term Pregnancy Traits

The REPROMETA study recruited 366 pregnant couples before or shortly after delivery of a singleton newborn at term (**Supplementary Table 3**). The cases represented pregnancies with uncomplicated gestation, PE, GD, SGA or LGA. Maternal and newborn clinical and epidemiologic data were documented retrospectively from self-reported questionnaires and medical records, collected biological materials included placental tissue (available for 326 cases) and parental blood samples.

The HAPPY PREGNANCY study recruited prospectively 2,334 pregnant women during their first antenatal visit. Longitudinal clinical and epidemiological data covers reproductive history, parental lifestyle, the course and outcome of pregnancy. The collected biological material included placental tissue (available for 1,772 cases), maternal blood and urine samples.

In both studies, the diagnosis of PE and GD followed the international guidelines at the time of recruitment (Metzger, 2010; American College of Obstetricians and Task Force on Hypertension in Pregnancy, 2013). Fetal growth was evaluated using the gestational age and sex adjusted weight centiles based on the Estonian Medical Birth Registry data (Sildver et al., 2015). Details of the REPROMETA and HAPPY PREGNANCY studies are provided in **Supplementary Methods** and in recent publications (Kikas et al., 2019, 2020).

Genetical Association Testing Between miR-eQTLs and Pregnancy Traits

Genetic association testing between the identified miR-eQTLs and pregnancy traits (placental weight; newborn's weight and height, head and chest circumference; diagnosis of PE or GD) was carried out using either linear or logistic regression (additive model) adjusted for fetal sex and gestational age as cofactors. Results were corrected for multiple testing using the Benjamini-Hochberg method, with cut-off FDR < 0.05. Initially, all miR-eQTLs were tested in the discovery dataset (n = 40, **Table 1**). Three SNVs (rs12985296, rs7046565, and rs12420868) were further analyzed in the REPROMETA (n = 326) and HAPPY PREGNANCY (n = 1,772) samples, including all cases with available placental tissue for genotyping (**Supplementary Table 3**).

Genotypes were generated with the TaqMan SNP Genotyping Assays (**Supplementary Methods** and **Supplementary Table 4**) using recommended experimental conditions (Applied Biosystems, Life Technologies). All association tests were carried out in PLINK v1.07 using (Purcell et al., 2007). Meta-analysis of REPROMETA and HAPPY PREGNANCY datasets

was implemented in R package meta (ver. 4.15-1) (Balduzzi et al., 2019), under fixed-effect model.

RESULTS

Highly Variable Expression Levels of Placental miRNAs

The dataset of 52 placental miRNomes was generated for the samples collected from first and second trimester and term pregnancy cases (n = 5, 7 and 40, respectively; **Table 1**). All subsequent analyses included 417 of total 2,652 identified miRNAs (15.7%, **Table 2A**), filtered for transcript levels that allow confident statistical testing (median raw read counts >50 across analyzed samples; **Supplementary Table 1**).

Placental miRNome in uncomplicated pregnancies was assessed in 20 samples: five cases representing first trimester [median 60 (51–81) gestational days, g.days], seven second trimester [121 (108–140) g.days], and eight term pregnancy [284 (260–291) g.days] cases. Overall, a broad variability in expression levels of individual placental miRNAs were measured in all trimesters (**Figure 1A** and **Supplementary Figure 1**). Median expression level of 417 analyzed miRNAs did not differ across the three trimesters of pregnancy (Kruskal–Wallis test, $p = 0.24$). However, a non-significant decreasing trend of median values was observed from 140 CPM (range 1–79,604) in first trimester, to 132 CPM (4–123,631) in second trimester and 103 CPM (7–172,159) in term placental samples.

A handful of miRNAs were identified with extremely high (CPM > 25,000) transcript levels throughout gestation (**Figures 1A,B**). Among these, miR-143-3p showing gradually increasing transcript levels from early pregnancy until term appeared as a potential marker for pregnancy progression and placental maturation. In total 47 high-confidence target genes for miR-143-3p were identified in the miRTarBase database (**Supplementary Table 5**). Majority, 93% of them clustered to the Gene Ontology (GO) pathway 'cellular response to stimulus' (GO:0051716; FDR = 7.2×10^{-10}; **Supplementary Table 6**). More specific enriched (FDR < 0.05) functional categories relevant to pregnancy included, e.g., 'PI3K-Akt signaling pathway' (KEGG:04151; 34% of target genes), 'Endocrine resistance' (KEGG:01522; 31%), 'collagen metabolic process' (GO:0032963; 12%),

TABLE 2 | General profile and expression dynamics of placental miRNAs.

Category	miRNA categories				
	All miRNAs	**C19MC[a] chr19q13.42**	**C14MC[b] chr14q32.31**	**miR-371–373[c] chr19q13.42**	**Other known or detected miRNAs**
(A) Comparative general profile of miRNA categories					
Gene cluster size (kb)	n.a.	∼100 kb	∼250 kb	∼1.1 kb	n.a.
Placenta-specific	n.a.	All	All	All	n.a.
Parent of origin expression	Most biallelic	Paternal	Maternal	Unknown	Most biallelic
All miRNA genes[d] (n)	1,792	46	52	4	1,690
All mature miRNA transcripts[d] (n)	2,656	67	94	8	2,487
All identified placental mature miRNA transcripts in this study (n)	2,652	67	93	8	2,484
Placental mature miRNA transcripts with adequate expression level for confident statistical testing (n)[e]	417	65	58	2	292
(B) Expressional patterns from first to second trimester – from second trimester to term pregnancy (miRNA mature transcripts: n, %)[e,f]					
Down – Down	30 (7.2%)	2 (3.1%)	8 (13.8%)	0 (0%)	20 (6.8%)
Down – No change	67 **(16.1%)**	21 **(32.3%)**	1 (1.7%)	2 **(100%)**	**43 (14.7%)**
Down – Up	28 (6.7%)	14 **(21.5%)**	0 (0%)	0 (0%)	14 (4.8%)
Up – Up	35 (8.4%)	0 (0%)	0 (0%)	0 (0%)	**35 (12.0%)**
Up – No change	41 (9.8%)	0 (0%)	7 (12.1%)	0 (0%)	34 (11.6%)
Up – Down	26 (6.2%)	0 (0%)	11 **(19.0%)**	0 (0%)	15 (5.1%)
No change – Down	54 **(13.0%)**	2 (3.1%)	26 **(44.8%)**	0 (0%)	26 (8.9%)
No change – Up	38 (9.1%)	4 (6.2%)	0 (0%)	0 (0%)	34 (11.6%)
No change – No change	98 **(23.5%)**	22 **(33.8%)**	5 (8.6%)	0 (0%)	**71 (24.3%)**

[a] *Primate-specific miRNA cluster.*
[b] *Eutherian-specific miRNA cluster.*
[c] *Homologous with the mouse miR-290–295 cluster (Wu et al., 2014).*
[d] *Data from miRBase version 22.1 (Kozomara et al., 2019).*
[e] *Median raw read counts over 50 across all analyzed samples; empirically determined transcript level for robust differential expression testing.*
[f] *Major patterns of expression dynamics are highlighted in bold; the expected proportion given an equal representation of each pattern is ∼11%.*
n.a., not applicable.

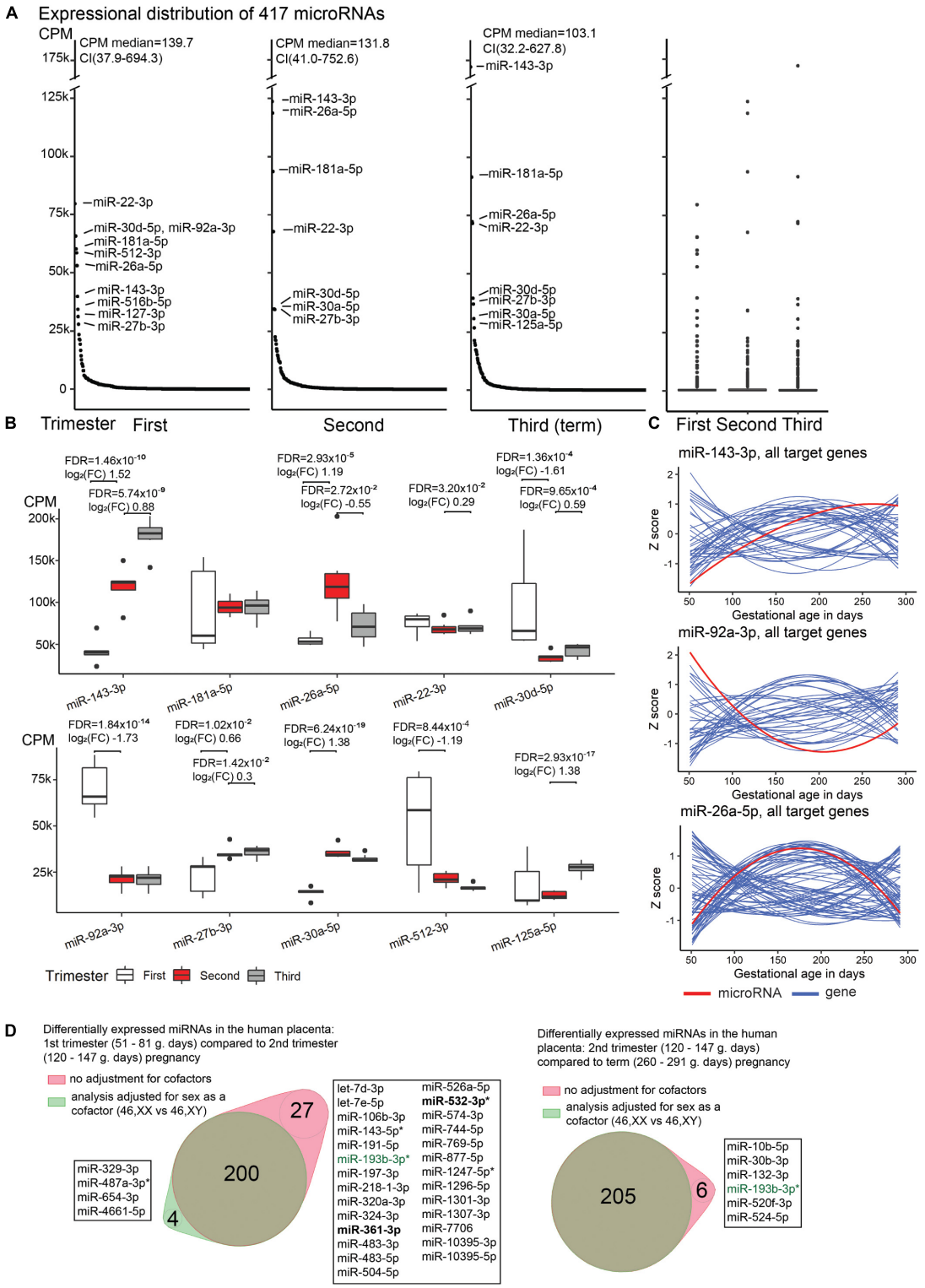

FIGURE 1 | Expressional distribution of placental miRNome. **(A)** Transcript levels of the analyzed 417 miRNAs in the first (median 60; range 51–81 g.days) and second trimester (121; 108–140 g.days) and term placental samples (284; 260–291 g.days). miRNA expression was quantified in counts per million reads mapped (CPM). Highly expressed miRNAs (CPM > 25,000) are indicated. Full details are provided in **Supplementary Table 1**. **(B)** Trimester-specific expression levels of placental miRNAs with the highest transcript levels. Differential expression testing between the three trimesters of pregnancy was implemented in DESeq2 (ver. 1.22.2) (Love et al., 2014) package for R with default settings. Log_2(FC), log_2 fold change in CPM; FDR, false discovery rate, calculated based on

(Continued)

FIGURE 1 | Continued
Benjamini–Hochberg method. **(C)** Gestational expression dynamics of some most highly transcribed placental miRNAs miR-143-3p, miR-92a-3p, miR-26a-5p compared to the transcript levels of their high-confidence target genes predicted in the miRTarBase (n = 47, 39, 74, respectively). Transcriptome data were derived from the published RNA-Seq datasets of the same placental samples representing first (n = 5) and second (n = 7) trimester, and normal term pregnancy (n = 8) (Sõber et al., 2015; Pilvar et al., 2019). miRNA and gene expression levels are presented in Z-scores; expression data for miRNA is shown in red and for target genes in blue. **(D)** Differentially expressed placental miRNAs between first (M/F, n = 2/3) and second trimester (n = 4/3), second trimester and term pregnancy (n = 5/3) samples, with or without incorporating fetal sex (46, XY vs. 46, XX) as a cofactor. X-linked miRNAs are highlighted in bold and differentially expressed miRNAs in preeclampsia are indicated with asterisk (*). miR-193-3p (green) showed sex-modulated transcript levels in both comparisons. F, female; M, male.

'regulation of glucose transmembrane transport' (GO:0010827; 12%), 'growth factor binding' (GO:0019838; 12%). Other examples of gestational age-dependent highly expressed miRNAs were miR-92a-3p, miR-30d-5p and miR-512-3p (specifically increased in first trimester), miR-26a-5p (second trimester), miR-125a-5p (at term). Some major miRNAs exhibited constant expression throughout gestation (e.g., miR-181a-5p, miR-22-3p).

Comparative assessment of the transcript levels of miR-143-3p, miR-92a-3p and miR-26a-5p with the expression of predicted target genes in the corresponding RNA-Seq dataset revealed a substantial group of mRNA/lincRNAs with reverse expression compared to the miRNA (**Figure 1C** and **Supplementary Table 7**). However, significant expressional correlations identified for miR-143-3p and miR-92a-3p (Kendall rank correlation coefficient, $p < 0.05$) included nearly equal proportions of reversely and directly correlated target genes (9/7 and 8/5, respectively; binominal test, $p > 0.58$). There was an under-representation of genes showing tight negative vs. positive correlation with the miR-26a-5p transcript levels (8/21; $p = 0.024$). Interestingly, positively correlated loci represented cancer driver genes (*MYC, PRKCD, RB1, CDK6*), molecules involved in immune response (*MALT1, PIK3CG*), as well as cellular and hormonal signaling (*HGF, PTPN13, IGF1, SMAD1, ESR1, CTGF*). These functional groups are well-known to be involved in placental development and role in supporting the pregnancy.

Expression Dynamics of miRNAs Is Linked to Placental Development and Function

The majority, 319 of 417 (76.5%) of tested miRNAs, exhibited significant gestational expression dynamics (**Table 2B** and **Supplementary Tables 8**, **9**). In total, 227 (54.4%) miRNAs were differentially expressed between first and second trimester [FDR < 0.05; $\log_2$(FC) from −4.91 to 2.84; 125 down- and 102 upregulated], and 211 miRNAs (50.1%) between second trimester and term pregnancy placental samples [FDR < 0.05; $\log_2$(FC) from −2.41 to 2.52; 110 down- and 101 upregulated]. More than a quarter of tested miRNAs (n = 119/417; 28.5%) represented DEmiRs in both comparisons, indicating their potential critical contribution in fine-tuning placental transcriptome profile in gestational age-dependent manner until term (**Figure 2A** and **Supplementary Table 10**).

The 319 placental miRNAs exhibiting trimester-dependent differential expression were explored for their predicted target genes in the miRTarBase database (**Supplementary Table 11**). An overrepresentation of target genes for upregulated compared to downregulated miRNAs was observed – 1305 vs. 773 genes in first vs. second trimester and 1207 vs. 888 in second trimester vs. term comparisons (χ^2-test, $p = 6.2 \times 10^{-4}$). Only a small fraction of genes (14.1–17.7%; **Supplementary Table 11**) represented trimester-specific targets of dynamic miRNAs, despite nearly two thirds of DEmiRs (200 of 319) being detected significant increase or decrease only in one trimester (**Figure 2A**). The shared list of target genes of dynamic miRNAs supported the coordinated action of the placental miRNome in modulating the expression of key placental genes during gestation.

In silico functional profiling of genes targeted by placental miRNAs with progressively increasing transcript levels from early pregnancy to term revealed a significant enrichment of GO pathways representing broad basic cellular and tissue functions (FDR < 0.05; **Table 3** and **Supplementary Tables 12**, **13**). Examples of modulated processes were 'protein binding' (GO:0005515; >90% of target genes) and 'cytosol' (GO:0005829; ∼48%), 'cytoplasmic stress granule (GO:0010494; ∼31% of the pathway genes) and 'extracellular matrix structural constituent conferring tensile strength' GO:0030020; 43.5%). Target genes for downregulated miRNAs in second compared to first trimester placentas represent more focused functional groups, possibly supporting the placental role in fine-tuning the fetal development in mid-gestation. These include, e.g., 'membrane-enclosed lumen' (GO:0031974; 54.4% of target genes) and 'cellular response to chemical stimulus' (GO:0070887; 52.9%); as well as 'thymocyte apoptotic process' (GO:0070242; 41.2% of pathway genes), 'DNA alkylation' (GO:0006305; 24.4%), 'PML body' (GO:0016605; 22.6%), 'regulation of cell size' (GO:0008361; 16.5%) and 'regulation of calcium ion transport' (GO:0051924; 15.6%). Loci that represent targets for downregulated miRNAs at term cluster in biological pathways relevant to the preparation for the delivery, such as 'positive regulation of smooth muscle contraction' (GO:0045987; 42.1% of pathway genes), 'phosphatidylinositol-3-phosphate biosynthetic process' (GO:0036092; 39.4%) and 'regulatory RNA binding' (GO:0061980; 38.7%).

The tested 417 placental miRNAs were assigned to one of nine subgroups representing their temporal expression dynamics pattern across three trimesters of pregnancy (**Table 2B** and **Supplementary Figure 2**). The most prevalent expression dynamics pattern represented miRNAs exhibiting specifically high transcript levels in early pregnancy (n = 67 miRNAs, ∼16%). The second frequent pattern reflected miRNAs that were downregulated only at term (n = 54, ∼13%). High

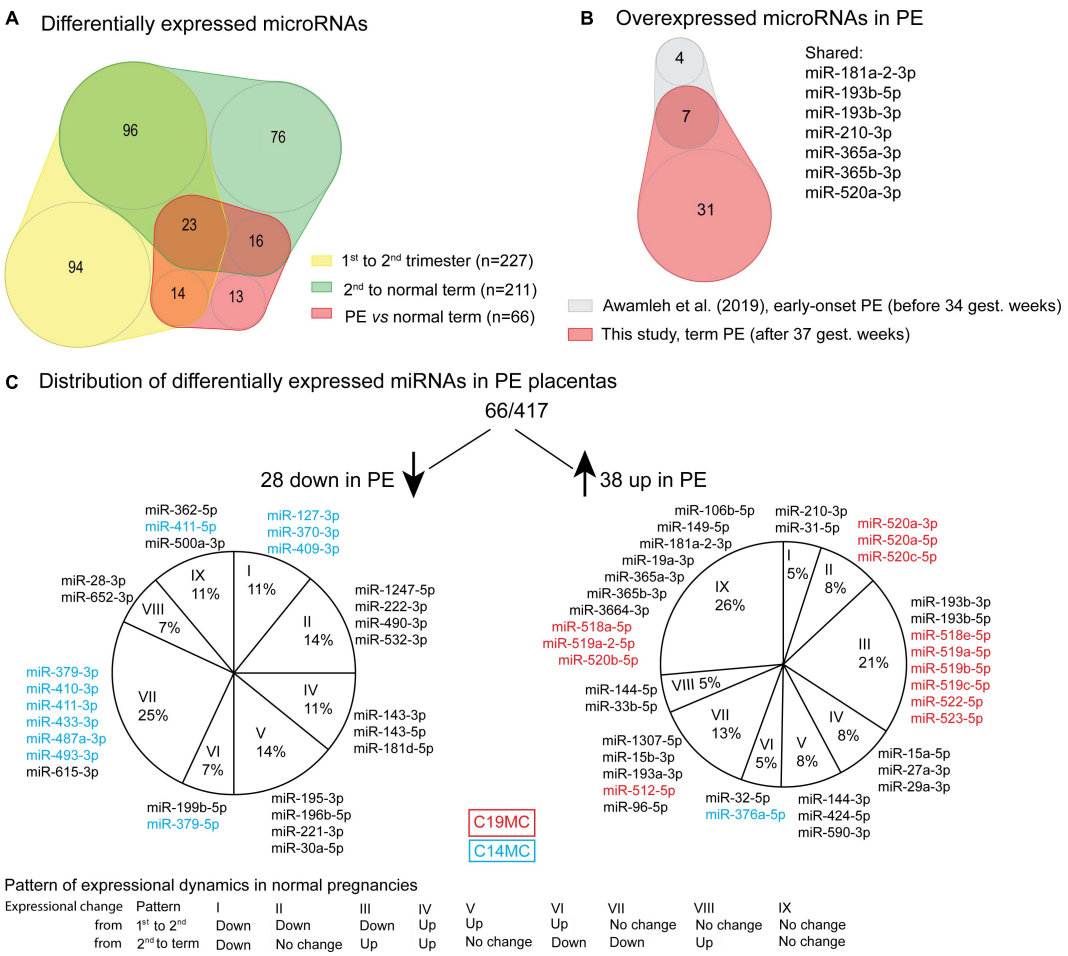

FIGURE 2 | Differentially expressed miRNAs in preeclampsia (PE). **(A)** Overlap of differentially expressed miRNAs in PE (**Supplementary Table 21**) with miRNAs showing gestational dynamics (**Supplementary Tables 8**, **9**). **(B)** Significantly upregulated miRNAs overlapping between term PE placentas in the current study and early-onset PE placentas in miR-Seq study by Awamleh et al. (2019). **(C)** Distribution of differentially expressed miRNAs in PE placentas according to their gestational dynamics patterns (**Table 2B**). miRNAs transcribed from placental-specific C14MC and C19MC clusters are highlighted in blue and red color, respectively.

miRNA expression restricted to second trimester was the rarest observed expressional pattern (n = 26, ~6%). A stable expressional window from early pregnancy to term was identified for 98 miRNAs (23.5%) with 900 predicted target genes (**Supplementary Tables 14**, **15**). Among these, the most significantly enriched biological pathways (FDR $< 1.0 \times 10^{-17}$) are also implicated in basic cellular and tissue functions, 'protein binding' (GO:0005515; 89.5 of target genes), 'cellular response to organic substance' (GO:0071310; 43.8%) and 'nuclear lumen' (GO:0031981; 43.5%) (**Supplementary Table 16**).

Fetal Sex Is Not a Major Modulator of Placental miRNome

When incorporating sex as a cofactor (46, XX; 46, XY) in differential expression testing between the three gestational trimesters, the list of DEmiRs remained largely the same (**Figure 1D** and **Supplementary Tables 8**, **9**). In second trimester [(M)ale/(F)emale, n = 4/3) compared to normal term placentas (M/F, n = 5/3), only six out of 211 (2.8%) DEmiRs were 'lost' after correction for fetal sex. The analysis of first (M/F, n = 2/3) compared to second trimester pregnancy samples with or without fetal sex as a cofactor resulted in 200 shared miRNAs, whereas four and 27 miRNAs were additionally detected in one sub-analysis. Only a single miRNA, miR-193-3p, was highlighted in both tests comparing trimester-specific miRNomes and may represent a locus with sex-specific expression level. The nature of other minor differences in the identified miRNAs lists cannot be speculated as testing small sample sets may result in spurious outcomes.

To evaluate further the role of fetal sex on placental miRNome, term pregnancy samples representing 46, XY (n = 19, 260–291 g.days) vs. 46, XX (n = 21, 262–288 g.days) cases were compared (**Supplementary Table 17**). Statistically significant differential expression was identified

TABLE 3 | Top Gene Ontology (GO) pathways of predicted target genes regulated by miRNAs showing gestational dynamics.

Gene Ontology		Pathway genes	Target genes in enrichment query[a]		Enrichment
Term	**Name**	**%**	***n***	**%**	***P*-value[b]**
Target genes for miRNAs significantly UPregulated in transition from first to second trimester[c]					
GO:0005515	Protein binding	11.5%	991	90.9%	7.5×10^{-76}
GO:0048522	Positive regulation of cellular process	19.9%	728	66.8%	4.0×10^{-160}
GO:0005829	Cytosol	12.7%	525	48.2%	1.5×10^{-25}
GO:0003730	mRNA 3′-UTR binding	32.7%	18	1.7%	9.9×10^{-4}
GO:0051881	Regulation of mitochondrial membrane potential	28.3%	17	1.6%	2.0×10^{-2}
GO:0010494	Cytoplasmic stress granule	33.3%	15	1.4%	7.2×10^{-3}
GO:0030212	Hyaluronan metabolic process	48.1%	13	1.2%	2.2×10^{-4}
GO:0061980	Regulatory RNA binding	41.9%	13	1.2%	1.6×10^{-3}
GO:0010586	miRNA metabolic process	40.7%	11	1.0%	1.7×10^{-2}
GO:0030020	Extracellular matrix structural constituent conferring tensile strength	43.5%	10	0.9%	2.2×10^{-2}
Target genes for miRNAs significantly DOWNregulated in transition from first to second trimester[c]					
GO:0031974	Membrane-enclosed lumen	8.0%	353	54.4%	9.7×10^{-23}
GO:0070887	Cellular response to chemical stimulus	15.6%	343	52.9%	7.1×10^{-97}
GO:0072659	Protein localization to plasma membrane	13.1%	26	4.0%	2.6×10^{-2}
GO:0019867	Outer membrane	13.5%	24	3.7%	3.6×10^{-2}
GO:0051480	Regulation of cytosolic calcium ion concentration	13.9%	23	3.5%	3.4×10^{-2}
GO:0051924	Regulation of calcium ion transport	15.6%	22	3.4%	7.5×10^{-3}
GO:0008361	Regulation of cell size	16.5%	21	3.2%	4.8×10^{-3}
GO:0016605	PML body	22.6%	19	2.9%	9.1×10^{-5}
GO:0035296	Regulation of tube diameter	19.0%	15	2.3%	2.6×10^{-2}
GO:0006305	DNA alkylation	24.4%	11	1.7%	3.3×10^{-2}
Target genes for miRNAs significantly UPregulated in transition from second trimester to term[c]					
GO:0005515	Protein binding	10.6%	909	90.1%	7.1×10^{-64}
GO:0048518	Positive regulation of biological process	17.0%	694	68.8%	1.1×10^{-133}
GO:0005829	Cytosol	11.8%	488	48.4%	5.8×10^{-24}
GO:0046914	Transition metal ion binding	14.5%	109	10.8%	7.8×10^{-7}
GO:2000060	Positive regulation of ubiquitin-dependent protein catabolic process	22.7%	20	2.0%	4.0×10^{-2}
GO:0000045	Autophagosome assembly	23.2%	19	1.9%	4.8×10^{-2}
GO:0010494	Cytoplasmic stress granule	31.1%	14	1.4%	1.7×10^{-2}
GO:0030020	Extracellular matrix structural constituent conferring tensile strength	43.5%	10	1.0%	1.2×10^{-2}
GO:1902751	Positive regulation of cell cycle G2/M phase transition	43.5%	10	1.0%	1.2×10^{-2}
GO:0070242	Thymocyte apoptotic process	52.9%	9	0.9%	4.6×10^{-3}
Target genes for miRNAs significantly DOWNregulated in transition from second trimester to term[c]					
GO:0005515	Protein binding	8.0%	684	91.3%	1.9×10^{-52}
GO:0048518	Positive regulation of biological process	13.2%	537	71.7%	3.1×10^{-113}
GO:0043233	Organelle lumen	9.0%	395	52.7%	3.5×10^{-22}
GO:0019898	Extrinsic component of membrane	14.5%	29	3.9%	2.1×10^{-2}
GO:0007204	Positive regulation of cytosolic calcium ion concentration	16.1%	25	3.3%	1.4×10^{-2}
GO:0003730	mRNA 3′-UTR binding	25.5%	14	1.9%	8.4×10^{-3}
GO:0036092	Phosphatidylinositol-3-phosphate biosynthetic process	39.4%	13	1.7%	6.1×10^{-5}
GO:0030301	Cholesterol transport	25.0%	13	1.7%	2.4×10^{-2}
GO:0061980	Regulatory RNA binding	38.7%	12	1.6%	2.7×10^{-4}
GO:0045987	Positive regulation of smooth muscle contraction	42.1%	8	1.1%	2.0×10^{-2}

[a] *Top 10 pathways per each gene list analysis are shown, sorted by the highest percentage of representation among the query genes. Full results of in silico functional enrichment analyses of gene lists are in* ***Supplementary Tables 12, 13****.*

[b] *P-value corrected for multiple testing by g: SCS method (Reimand et al., 2007).*

[c] *Query lists of miRNA target gene were extracted from the miRTarBase database (Huang et al., 2020).*

for three miRNAs: X-linked miR-361-5p, autosomal miR-378a-3p and miR-130b-3p. Additionally, miR-101-5p showed placental sex-modulated expression when the analysis was adjusted for pregnancy complications. These miRNAs did not overlap with the candidates identified in trimester-specific analysis. Overall, the analysis outcome

suggested that fetal sex is not a major modulator of placental miRNome.

C14MC and C19MC Clusters Have Key Role in Human Placental miRNome and Transcriptome

A notably high fraction, 125 of 417 (∼30%) expressed miRNAs belonged to the primate-specific miRNA cluster C19MC (detected mature placental miRNAs, n = 65; 15.6%) or to the eutherian-specific clusters C14MC (n = 58; 13.9%) and miR-371–373 (n = 2, 0.5%) (**Table 2A** and **Supplementary Table 1**). These clusters showed markedly different patterns of gestational expression dynamics. About ∼2/3 of C19MC and the miR-371–373 clusters are specifically highly transcribed in early pregnancy with a significant drop in second trimester and a slight increase at term (**Figure 3A**, **Table 2B**, and **Supplementary Tables 8**, **9**). The C14MC cluster showed diverse expression in first trimester, but more coordinated transcript levels in later gestational ages. The majority of C14MC miRNAs showed high expression in second trimester and significant downregulation before term. Only five C14MC, but 22 C19MC miRNAs exhibited stable expression levels from early pregnancy until delivery.

Among confident target genes in miRTarBase database reported for the C19MC and C14MC miRNAs, 63/76 and 215/262 loci were expressed in the current RNA-Seq dataset (**Supplementary Tables 18**, **19**). Indicating the distinct roles of C19MC and C14MC in shaping human placental transcriptome across gestation, only 21 of these target genes overlap. Most target genes are modulated explicitly by either C19MC or C14MC miRNAs. Assessment of gestational expression dynamics of C19MC and C14MC miRNAs and their predicted target genes supports their mutual functional relationship (**Figures 3A,B**). The major cluster of C19MC miRNAs have the lowest transcript levels at ∼180–200 g.days and a substantial proportion of their predicted target genes show increased expression during mid-gestation. Interestingly, the minor cluster of C19MC miRNAs is strongly positively correlated with over 1/3 of the analyzed genes. The majority of C14MC target genes belong to distinct co-expression groups that form clusters based on either negative or positive transcriptional correlation with miRNAs. Large notable clusters of miRNA–gene pairs showing directly and inversely correlated expression dynamics suggested potential functional relationships in both scenarios.

The top GO terms with significant enrichment of C19MC target genes (FDR $< 1.0 \times 10^{-5}$, **Supplementary Table 20**) were indicative of processes related to transcriptional activation and cellular signaling that are critical in early pregnancy, such as 'response to organic substance' (GO:0010033), 'transcription regulatory region DNA binding' (GO:0044212), 'kinase binding' (GO:0019900). Notably, most significantly enriched KEGG and REAC categories comprise of genes implicated in various cancers or are responsible for signaling pathways of cancer driver genes. The C14MC miRNAs were implicated in more basic cellular functions that are essential throughout pregnancy, such as 'cellular response to chemical stimulus' (GO:0070887), 'protein binding' (GO:0005515), 'intracellular organelle lumen' (GO:0070013). However, some target genes of C14MC reflect specific placental features, such as 'DNA-methyltransferase activity' (GO:0009008) potentially linked to

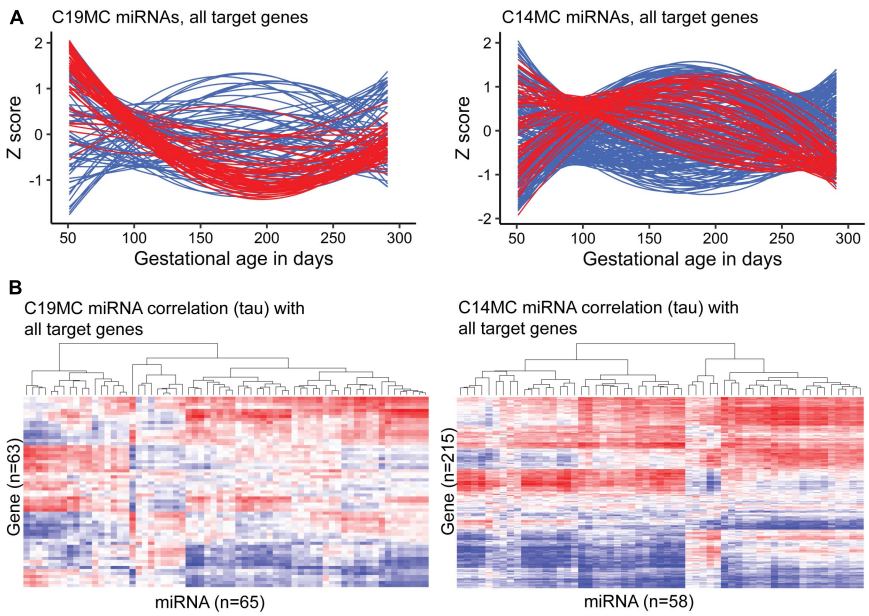

FIGURE 3 | Expression dynamics of C19MC and C14MC miRNA clusters across gestation compared to the transcript levels of their miRTarBase target genes. Placental transcript levels were confidently quantified for 63/76 and 215/262 predicted target genes of C19MC and C14MC, respectively. **(A)** miRNA and gene expression levels during pregnancy presented in Z-scores; expression data for miRNAs is shown in red and for target genes in blue. **(B)** Heatmap and hierarchical clustering of miRNA–target gene expression data based on the calculated correlation coefficient Kendall tau.

epigenetic programming or 'regulation of cell size' (GO:0008361) possibly referring to the development of large multinucleated placental cell types.

Major Shift in Placental miRNome in Preeclampsia and Link to Affected Fetal Growth

Placental miRNomes representing term cases of late-onset preeclampsia (LO-PE), gestational diabetes (GD), small- and large-for-gestational-age newborns (SGA, LGA) were tested for differential expression in comparison to uncomplicated pregnancies (n = 8 in each group; all cases after 37th g.week; **Table 1**). Only PE placentas demonstrated a major shift in their miRNome profile that affected 66 of 417 (15.8%) miRNAs (FDR < 0.05; **Figure 2** and **Supplementary Tables 21**, **22**). None of these miRNAs was detected to be modulated by fetal sex (**Supplementary Table 17**). Seven significantly upregulated miRNAs overlapped with the placental DEmiRs reported in early-onset PE cases (EO-PE, before 34th g.week) (Awamleh et al., 2019; **Figure 2B**). Several of these showed large changes in their expression level: miRNAs miR-210-3p (FC = 2.64), miR-193b-3p (2.53), miR-193b-5p (2.29), miR-365b-3p (1.93), miR-365a-3p (1.92), miR-520a-3p (1.82) (**Figure 4** and **Supplementary Table 21**). Notably, 13 of 38 (34%) upregulated DEmiRs were transcribed from the C19MC cluster and only one from C14MC, whereas 11 of 28 (39%) downregulated miRNAs were transcribed from the C14MC and none from the C19MC cluster (**Figure 2C**).

Differentially expressed miRNome in PE was comprised of both dynamic and stable miRNAs. No specific pattern of normal gestational dynamics was preferentially altered (**Figures 2A,C**). Several miRNAs normally downregulated at term were characterized by increased transcript levels in PE placentas corresponding to their typical mid-gestation values (e.g., miR-210-3p, miR-31-5p, miR-96-5p, miR-193a-3p, miR-519a/b-5p; **Figure 4**). On other occasions, miRNA expression in PE placentas was significantly downregulated compared to other analyzed samples (e.g., miR-196b-5p, miR-411-3p, miR-1247-5p). PE miRNome also showed aberrant upregulation of several miRNAs that are normally stably expressed across gestation (e.g., miR-365a/b-3p).

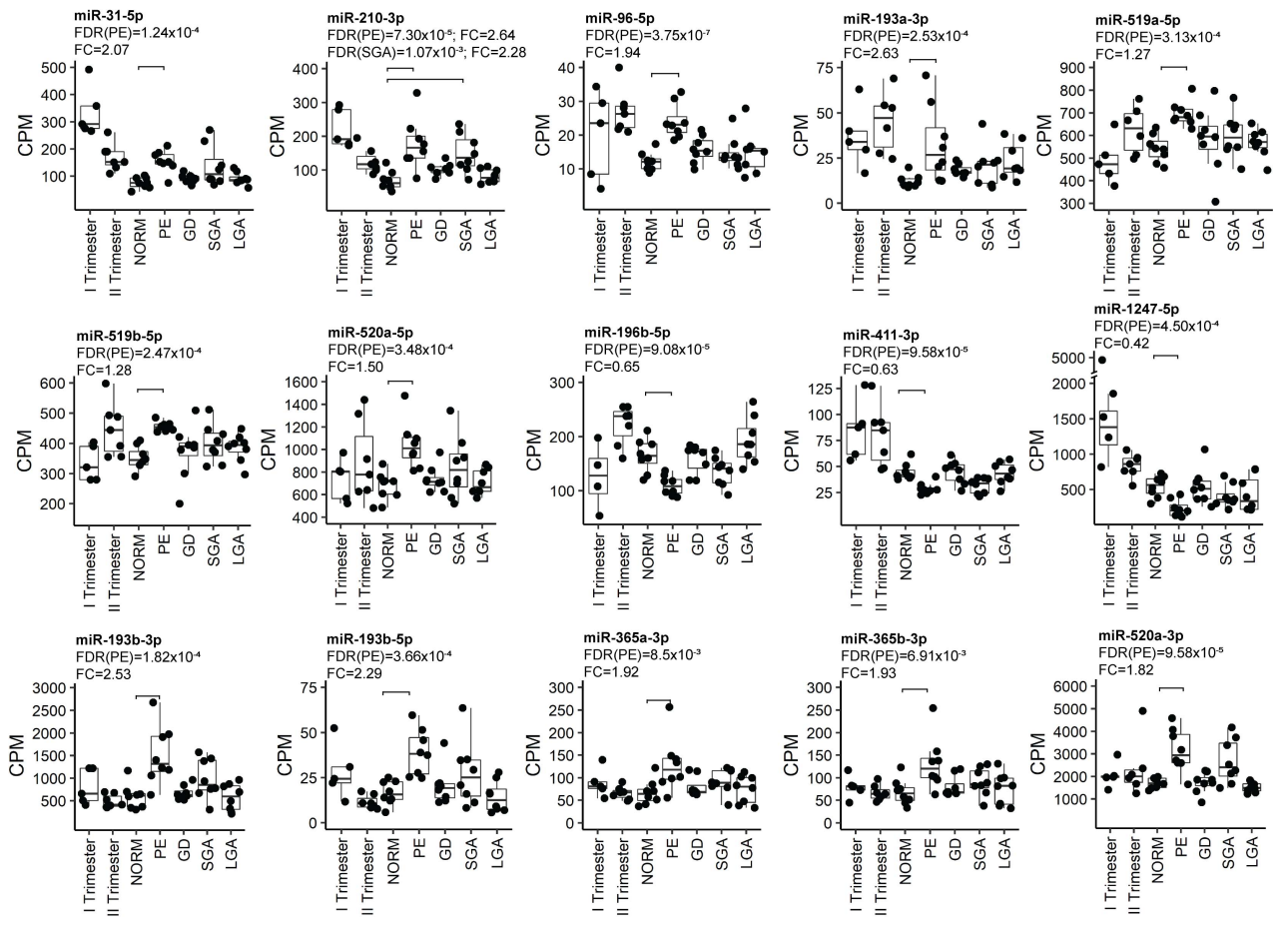

FIGURE 4 | Examples of the most significant differentially expressed miRNAs in PE. miRNA expression was quantified in counts per million mapped reads (CPM). FDR, false discovery rate, calculated based on Benjamini–Hochberg method; GD, gestational diabetes; NORM, normal term pregnancy; PE, preeclampsia; LGA, large-for-gestational-age; FC, fold change in CPM; SGA, small-for-gestational-age.

Six miRNAs with altered transcript levels in LO-PE represented also DEmiRs in term SGA placentas – upregulated miR-210-3p, miR-512-5p, miR-32-5p, miR-19a-3p and miR-590-3p, and downregulated miR-379-5p (**Supplementary Table 23**). No miRNAs exhibited significant expressional changes in the GD and LGA cases compared to normal term placenta (**Supplementary Tables 24**, **25**).

Differentially Expressed miRNAs in PE Exhibit a Coordinated Effect on the Transcriptome

Correlation analysis between the expression levels of 66 placental DEmiRs identified in PE and placental transcriptome was performed using the corresponding miR-Seq and RNA-Seq datasets of 40 term pregnancy samples. Hierarchical clustering based on the expressional correlation with the transcript levels of 16,567 genes assigned the tested miRNAs into five groups G1-G5, each containing 6–22 miRNAs (**Figure 5** and **Supplementary Data 1**). In these groups, there was a highly non-random distribution of miRNAs from C19MC (G1:10 miRNAs, G5:3) and C14MC (G4:9, G3:2, G5:1) clusters (χ^2-test, $p = 1.5 \times 10^{-5}$), providing further support to their distinct roles in modulating placental transcriptome. The C14MC cluster outlier miRNA that didn't properly fit in either groups G4 or G5 was miR-376a-5p. Furthermore, this miRNA already stood out in the differential expression analysis with an opposite behavior compared to the rest of the C14MC miRNAs (**Figure 2C**).

Six of 10 miRNAs with the highest number of negatively correlated placental transcripts belonged to miRNA group G2, e.g., miR-490-3p (median Spearman's rho across 40 placentas <–0.3, 4375 genes vs. rho > 0.3, 55 genes), miR-27a-3p (2957 vs. 25), miR-362-5p (2823 vs. 427) (**Supplementary Tables 22**, **26**). Among the C19MC miRNAs that are significantly upregulated in PE placentas, the largest proportion of negatively correlated genes was detected for miR-522-5p (1780 negative vs. 148 positive correlations) and miR-518a-5p (1731 vs. 154) clustering to group G1. In general, groups G1 and G2 showed confident negative correlation with a large number of genes (median rho <–0.3 and for all individual samples <–0.1: 342 and 239 genes, respectively; **Supplementary Table 27**). In contrast, groups G3-G5 were positively correlated with a substantial proportion of the placental transcriptome (median rho > 0.3 and for all individual samples >0.1; 1077, 484, and 2537, respectively). This included also C14MC cluster miRNAs that are significantly downregulated in PE.

Gene enrichment analysis was performed to clarify the potential functional link between the PE-linked miRNAs clustered into groups G1–G5 and their most significantly correlated placental transcripts (**Figure 5** and **Supplementary Tables 28–32**). Group G2 miRNAs appeared as potential key modulators of genes implicated in basic cellular processes, such as organelle function and ribosomal biogenesis, DNA and RNA metabolism, cell cycle and senescence (**Table 4**). However, expression of miRNAs in groups G1, G3, and G4 was correlated with functionally more specific gene categories, encoding proteins involved in extracellular matrix formation (G1, G4), DNA replication and immunoglobulin complex (G3), synaptic and ion channel activity, adrenergic signaling, renin and insulin secretion (G4).

Positive expressional correlation between miRNAs in group G5 and thousands of genes may reflect either true functional relationship or alternatively, co-correlated expression of miRNAs and some housekeeping genes through shared upstream regulatory modulators. Notably, ∼50% of them belonged to the functional category 'nucleus' (GO:0005634; enrichment $P = 5.0 \times 10^{-3}$), being responsible for various DNA, chromatin and RNA-related processes. Another large category represented 'immune system process' (GO:0002376, 19.5% of query genes, $P = 1.8 \times 10^{-4}$).

The Expression of Several Placental MicroRNAs Is Modulated by Specific SNVs, miR-eQTLs

Finally, the effect of SNVs on the placental miRNome was investigated. Placental Expression Quantitative Trait Loci (eQTLs) for 417 miRNAs were mapped by genetic association testing between their transcript levels in 40 term placental samples and genotypes of 6,274 common SNVs located ±100 kb from the miRNA genes. In total 66 miR-eQTLs for 16 miRNAs were detected (FDR < 0.05; 3.8% of tested miRNAs; **Figure 6**, **Supplementary Table 33**, and **Supplementary Data 2**). Four of 16 placental miRNAs modulated by eQTLs had also been identified as DEmiRs in PE (miR-30a-5p, miR-210-3p, miR-490-3p, miR-518-5p). Despite the limited sample size, the effect of miR-eQTL on some miRNAs was observed in all three trimesters of pregnancy (e.g., pairs rs447001 and miR-130b-3p/5p, rs2427554 and miR-941, rs12642661 and miR-1269a). The most extreme identified SNV-miRNA pair was rs7046565 (A/G) and miR-3927-3p. The major allele AA-homozygosity completely suppressed the expression of miR-3927-3p. This effect was also detected in second trimester placental samples (**Figure 6**).

Among 66 identified placental miR-eQTLs, 18 eQTLs were unique to placental miRNAs and 48 have also been reported in the GTEx database as expressional modulators of 53 coding genes (The GTEx Consortium, 2020). In our placental RNA-Seq dataset, 32 of them were expressed. Statistically significant associations (FDR < 0.05) were detected with transcript levels of the *KLHL3* (rs10515496), *SNX11* (rs11651097), *ANO9* and *PTDSS2* (rs12420868) genes (**Supplementary Table 34**). However, each of these statistical associations were weaker than the originally detected effect on the adjacent miR-874-3p, miR-152-3p, and miR-210-3p, respectively.

Individual Placental miR-eQTLs Did Not Show a Significant Effect on Term Pregnancy Traits

Three miR-eQTLs (SNVs: rs12420868, rs12985296, rs7046565) showing some nominal associations in the discovery dataset (n = 40, **Supplementary Table 35**) were targeted to replication testing with pregnancy traits in the REPROMETA (n = 326) and HAPPY PREGNANCY (n = 1,772) pregnancy-related cohorts (**Supplementary Table 3**

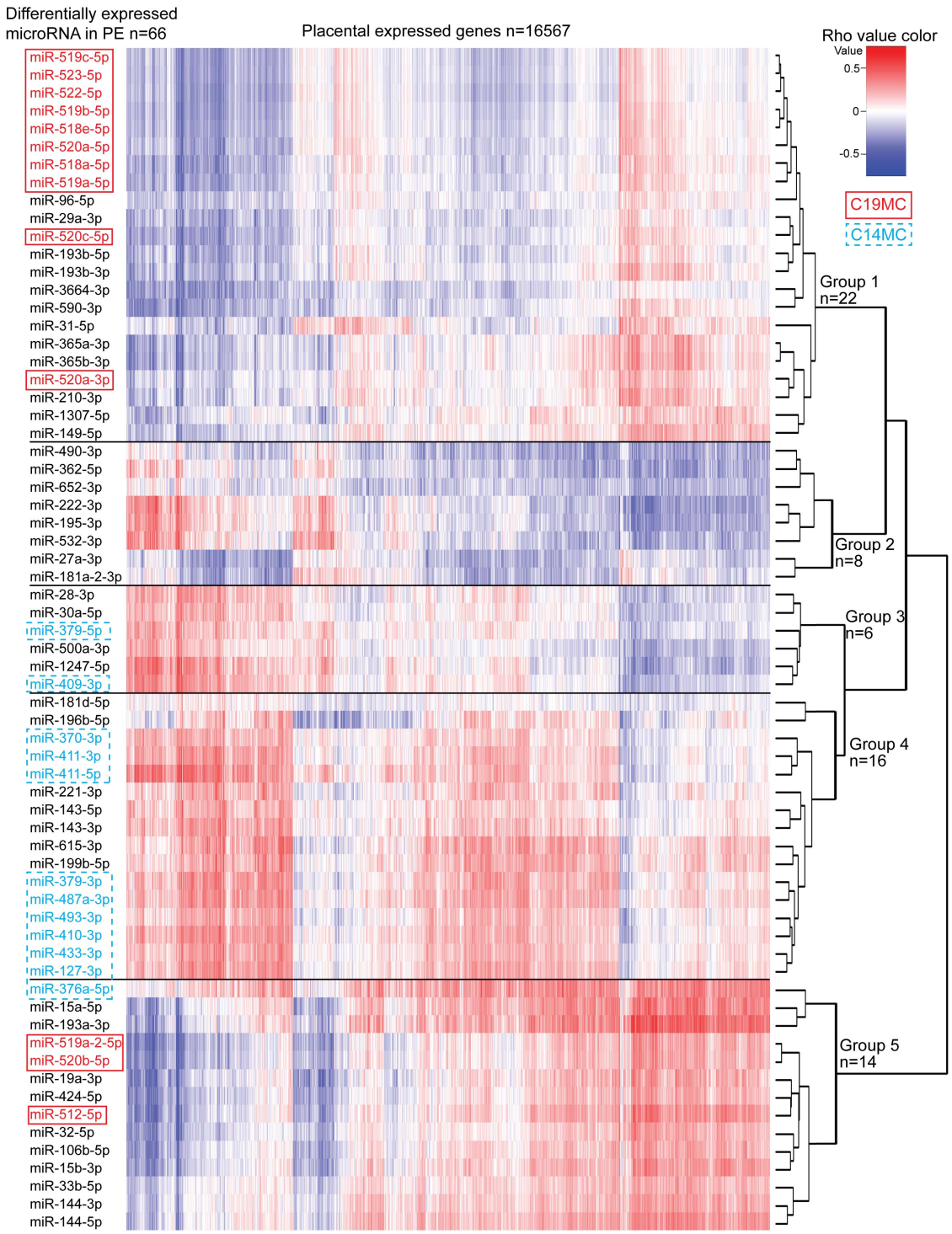

FIGURE 5 | Correlation analysis between miRNAs altered in preeclampsia and the whole transcriptome of 40 term placental samples. Expressional correlation of 66 miRNAs with mRNA transcripts of 16,567 genes (RNA-Seq data from Sõber et al., 2015) was evaluated using Spearman's correlation coefficient (parameter rho). Spearman's rho was estimated for 1,093,422 miRNA-gene pairs (**Supplementary Data 1**). The heatmap shows the hierarchical clustering of miRNAs based on the expressional correlation with mRNA transcripts of coding/lincRNA genes. Each row represents one miRNA and each column one gene. Expressional correlation is presented from –1 (maximum negative correlation, blue color) to 1 (maximum positive correlation, red). The value 0 indicates no correlation. miRNAs groups G1-G5 were formed based on their clustering. More details on genes with correlated expression in each miRNA group G1–G5 are presented in **Supplementary Tables 28–32**.

TABLE 4 | Functional enrichment of genes showing correlated expression in term placentas with 66 preeclampsia linked DEmiRs.

miRNA group/	Gene Ontology		Pathway genes	Correlated genes in enrichment query		Enrichment
correlation direction[a]	Term	Name	%	n	% n	*P*-value[b]
Group 1/negative[c]	GO:0031012	Extracellular matrix	7.1%	18	7.0%	1.1×10^{-2}
(258 genes)	GO:0005201	Extracellular matrix structural constituent	10.9%	10	3.9%	4.1×10^{-2}
Group 2/negative[c]	GO:0043232	Intracellular non-membrane-bounded organelle	2.6%	85	39.5%	2.4×10^{-2}
(215 genes)	GO:0007049	Cell cycle	3.3%	47	21.9%	1.9×10^{-2}
	GO:0051301	Cell division	5.0%	25	11.6%	3.0×10^{-3}
	GO:0042254	Ribosome biogenesis	7.1%	19	8.8%	3.8×10^{-4}
	GO:0000280	Nuclear division	6.1%	19	8.8%	4.1×10^{-3}
	GO:0006260	DNA replication	7.4%	18	8.4%	4.3×10^{-4}
	GO:0071103	DNA conformation change	8.0%	17	7.9%	3.3×10^{-4}
	GO:0007059	Chromosome segregation	6.8%	17	7.9%	3.2×10^{-3}
	GO:0006413	Translational initiation	7.7%	14	6.5%	6.4×10^{-3}
	GO:0044391	Ribosomal subunit	7.3%	13	6.0%	2.8×10^{-2}
	GO:0003735	Structural constituent of ribosome	8.5%	13	6.0%	5.2×10^{-3}
	GO:0022626	Cytosolic ribosome	11.4%	12	5.6%	5.3×10^{-4}
	GO:0006614	SRP-dependent co-translational protein targeting to membrane	12.2%	11	5.1%	8.7×10^{-4}
Group 3/negative (122 genes)	GO:0006260	DNA replication	4.5%	11	9.0%	4.8×10^{-2}
Group 3/positive	GO:0042571	Immunoglobulin complex, circulating	100%	5	0.6%	3.2×10^{-3}
(825 genes)	GO:0030054	Cell junction	10%	93	11.3%	4.0×10^{-2}
Group 4/positive[c]	GO:0032501	Multicellular organismal process	4.1%	184	47.5%	5.8×10^{-4}
(387 genes)	GO:0044459	Plasma membrane part	5.4%	88	22.7%	7.5×10^{-5}
	GO:0007399	Nervous system development	5.0%	78	20.2%	1.4×10^{-2}
	GO:0045202	Synapse	6.7%	36	9.3%	2.1×10^{-2}
	GO:0043062	Extracellular structure organization	8.2%	23	5.9%	4.3×10^{-2}
	GO:0005216	Ion channel activity	9.6%	18	4.7%	4.3×10^{-2}
	GO:0016849	Phosphorus-oxygen lyase activity	37.5%	6	1.6%	1.1×10^{-2}
	GO:0009975	Cyclase activity	35.3%	6	1.6%	1.7×10^{-2}
Group 5/negative	GO:0005886	Plasma membrane	2.6%	80	42.3%	1.0×10^{-4}
(189 genes)	GO:0048018	Receptor ligand activity	8.3%	13	6.9%	1.5×10^{-3}
Group 5/positive	GO:0005634	Nucleus	18.7%	1069	49.6%	5.0×10^{-3}
(2155 genes)	GO:0048519	Negative regulation of biological process	19.5%	726	33.7%	1.9×10^{-3}
	GO:0003676	Nucleic acid binding	19.9%	645	29.9%	7.8×10^{-4}
	GO:0002376	Immune system process	21.2%	421	19.5%	1.8×10^{-4}
	GO:0007017	Microtubule-based process	24.1%	141	6.5%	1.1×10^{-2}
	GO:0044772	Mitotic cell cycle phase transition	27.4%	121	5.6%	4.5×10^{-5}
	GO:0060271	Cilium assembly	28.2%	80	3.7%	3.5×10^{-3}
	GO:0006413	Translational initiation	39.2%	71	3.3%	1.7×10^{-9}
	GO:0003735	Structural constituent of ribosome	47.1%	72	3.3%	1.1×10^{-14}
	GO:0007059	Chromosome segregation	27.6%	69	3.2%	3.9×10^{-2}
	GO:0022626	Cytosolic ribosome	59.0%	62	2.9%	6.0×10^{-19}
	GO:0000184	Nuclear-transcribed mRNA catabolic process, nonsense-mediated decay	50.4%	59	2.7%	1.9×10^{-13}

(Continued)

TABLE 4 | Continued

miRNA group/ correlation direction[a]	Gene Ontology Term	Name	Pathway genes %	Correlated genes in enrichment query n	% n	Enrichment *P*-value[b]
	GO:0006614	SRP-dependent co-translational protein targeting to membrane	60.0%	54	2.5%	1.1×10^{-16}
	GO:0006261	DNA-dependent DNA replication	32.8%	45	2.1%	1.0×10^{-2}
	GO:0006334	Nucleosome assembly	42.3%	44	2.0%	2.5×10^{-6}
	GO:0048525	Negative regulation of viral process	40.0%	26	1.2%	2.3×10^{-2}
	GO:0045071	Negative regulation of viral genome replication	48.6%	18	0.8%	2.2×10^{-2}

[a] *miRNA clusters as formed in the correlation analysis between placental miRNome and transcriptome in 40 term pregnancy samples (heatmap,* ***Figure 5****). Transcriptome data of the samples utilized for miR-Seq was derived from the published RNA-Seq dataset (Söber et al., 2015). The number of genes entering correlation testing with the transcript level of 417 miRNAs was 16,567. Number of genes from the RNA-Seq dataset showing correlated expression with the specific miRNA Group are indicated in brackets. Full details are presented in* ***Supplementary Tables 27–32****.*

[b] *P-value corrected for multiple testing by g: SCS method (Reimand et al., 2007).*

[c] *No functional enrichment pathways were identified for genes showing positive expressional correlation with miRNAs in Groups 1 and 2, and genes showing negative correlation in Group 4.*

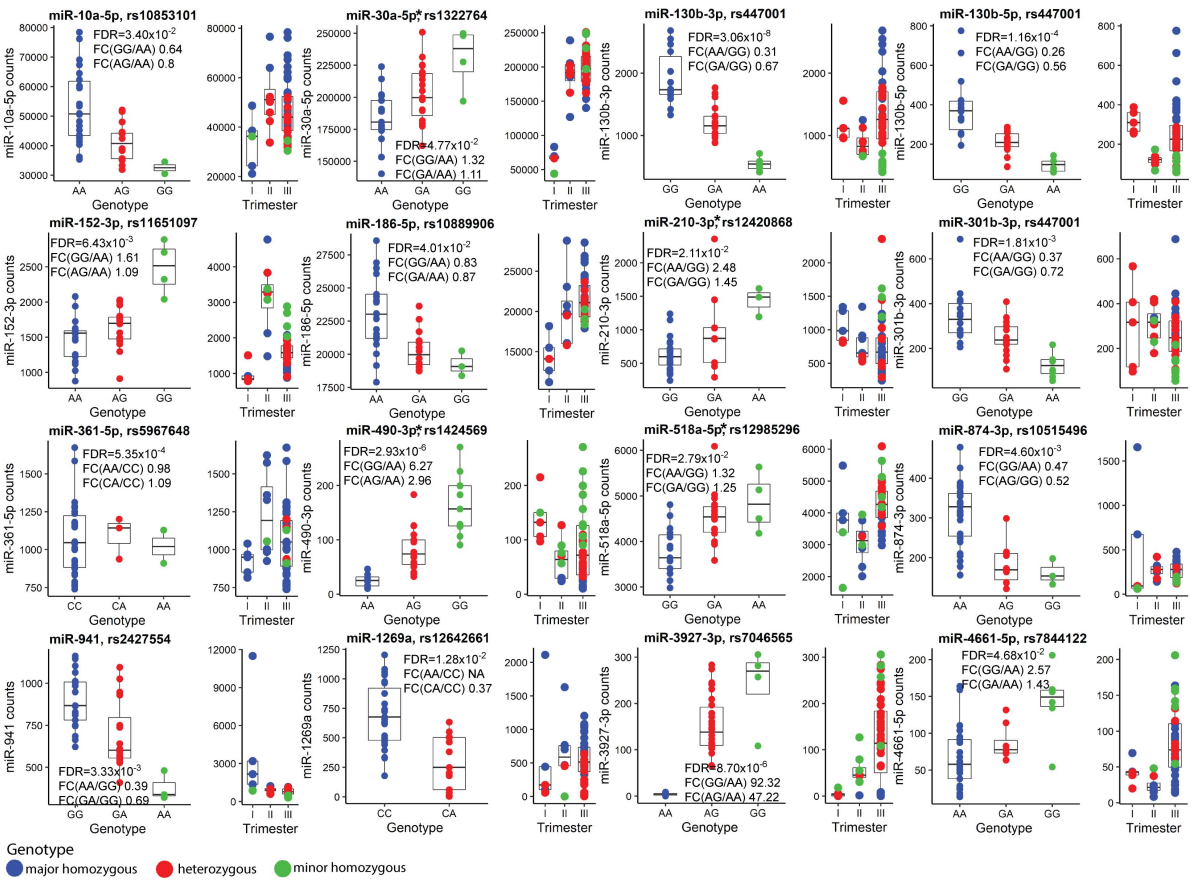

FIGURE 6 | Placental miRNA expression Quantitative Trait Loci (miR-eQTLs). Discovery analysis of single nucleotide variants (SNVs) modulating the expression of flanking miRNAs was carried out in 40 term placental samples and the most significant miR-eQTLs are presented. In each subgraph, miRNA normalized read counts (*y*-axis) are shown for samples stratified based on SNV genotypes (*x*-axis). Blue, red and green colors represent placentas homozygous for the major allele, heterozygous or homozygous for the minor allele of SNV, respectively. Additionally, distribution of genotype-stratified samples in the trimesters are shown. miRNAs that are also differentially expressed in term preeclampsia are indicated with an asterisk (*). Further details are presented in **Supplementary Tables 1**, **21**, **33** and **Supplementary Data 1**. FDR, false discovery rate; FC, fold change.

and **Supplementary Methods**). No statistically significant associations were identified with the height, weight, head and chest circumference of newborns, placental weight and PE or GD incidence in independent cohorts or their meta-analyses (all tests, FDR > 0.05; **Supplementary Table 36**). A non-significant trend was detected between rs12420868 (eQTL for miR-210-3p) and newborns' head circumference (meta-analysis: nominal $P < 0.05$; **Supplementary Figure 3**).

DISCUSSION

To our knowledge, this investigation represents the most comprehensive multi-omics analysis of human placental miRNome conducted to date. For the first time, this study used miR-Seq to profile simultaneously miRNA expression dynamics across normal gestation from the first trimester to term, and in late-onset pregnancy complications (PE, SGA, LGA and GD). Previous large study integrating placental miRNA and mRNA profiling was focused on a narrow gestational window (∼29–32 g.weeks) and investigated placentas representing idiopathic preterm birth and early-onset PE, intrauterine growth restriction (IUGR) or their combination (Awamleh et al., 2019). Additional innovations in the current study included expressional correlation analysis of miRNA-mRNA transcript pairs across the whole transcriptome and the first report of placental genetic variants that modulate miRNA expression levels.

The study data reveals that the major determinant of placental miRNA transcript levels is gestational age. According to their gestational expression dynamics, placental miRNAs cluster into distinct patterns containing potentially functionally linked miRNAs (**Table 3**). Only about one quarter of placental miRNAs show constant expression throughout pregnancy. miRNAs with significant gestational dynamics include also those with the highest placental expression (**Figures 1A–C**). For some top-transcribed miRNAs (miR-143-3p, miR-26a-5p, miR-27b-3p, miR-181a-5p), altered placental and umbilical cord transcript levels have been reported in gestational hypertension, PE and IUGR pregnancies (Hromadnikova et al., 2015, 2017; Muralimanoharan et al., 2016; Huang et al., 2019; Gusar et al., 2020). miR-181a-5p and miR-27b-3p target mRNAs of the *REN* and *ACE* genes, potentially contributing to fine-tuning of the placental renin-angiotensin system (RAS) essential for normal placentation (Arthurs et al., 2019; Huang et al., 2019). Alternations of RAS components have been associated with preterm birth and preeclampsia (Herse et al., 2007; Nonn et al., 2021).

Only limited miRNAs appeared to be potentially modulated by fetal sex (**Figure 1D** and **Supplementary Tables 8**, **9**, **17**). Among these, circulating levels of X-linked miR-361-3p have been reported to differ between obese adolescent females and males (Karere et al., 2021). Interestingly, placental expression of miR-130b-3p was potentially modulated by both, sex and a neighboring SNV, miR-eQTL (**Figure 6**).

The current multi-dimensional study supported distinct expressional regulation and functional roles of placenta-specific imprinted miRNA clusters C19MC and C14MC in human pregnancy. Paternally expressed young, primate-specific C19MC cluster is highly expressed in early pregnancy, potentially fine-tuning in dosage-sensitive manner the expression level of critical genes that are implicated in deep intrauterine trophoblast invasion and remodeling of uterine spiral arteries at the maternal-fetal interface, enabling unique close contact between maternal and fetal blood streams in humans. Target loci of C19MC include well-established cancer genes (37% of target genes), mediators of various molecular binding, signaling cellular response processes, supporting the suggested co-evolution of genes and processes involved in placentation and mammalian tumorigenesis (Kshitiz et al., 2019). Monoallelic expression of these target genes in early pregnancy may prevent pathological invasiveness of the developing placenta. Interestingly, C19MC miRNAs show a small, but confident increase in their expression level again at term and demonstrate significant upregulation in preeclamptic (PE) placentas (**Figures 1D**, **2C**). It can be speculated that C19MC expression may be upregulated in hypoxic conditions, known to be present in trophoblast development in early pregnancy (Chang et al., 2018), in PE placenta (Redman et al., 2021) and possibly, also in normal term placenta due to its senescence close to parturition (Seno et al., 2018). The maternally expressed C14MC is common for all eutherian mammals. Its high expression level until delivery refers to its role as a 'guardian' of normal placental development and unique functions to support the fetus and the mother until delivery. Correlation analysis of miRNA–mRNA expression indicated that C19MC and C14MC miRNAs do not function as uniform miRNA clusters, but contain functional subgroups of miRNAs targeting different sets of genes (**Figure 3**). Notably, a large fraction of confident target genes of C19MC and especially C14MC show strong positive correlation between their transcript levels and these miRNA clusters. This observation was further extended in the expression correlation analysis of 66 PE-linked miRNAs and the whole placental transcriptome (**Figure 5**). Positive expression correlation with a large number of confident target genes was also observed for the most highly expressed placental miRNAs (**Figure 1**). It has been suggested that for several genes, increased mRNA expression has to be followed by activated expression of its regulatory miRNAs in order to maintain the optimal transcript levels (Nunez et al., 2013). In cancer cells, positive miRNA-gene correlations are surprisingly prevalent and consistent across cancer types, and show more distinct patterns than negative correlations (Tan et al., 2019). This is consistent with the data from the current study on the correlated expression patterns of placental miRNome and transcriptome. Coordinated expression of miRNAs and mRNAs could be explained by shared transcription factors. Alternatively, increased levels of some regulatory miRNAs can upregulate a gene by inhibiting its upstream suppressor.

It is well known that aberrant expression of functionally critical miRNAs may lead to a major and potentially pathogenic change in the whole transcriptome. Among the analyzed late

pregnancy complications, a major shift in placental miRNome was only observed in PE, but not in GD, SGA or LGA cases (**Figure 2A** and **Supplementary Tables 21, 23–25**). The range of expressional alterations of miRNAs in PE placentas was usually not as extensive as the detected gestational age-dependent variation of transcript levels (**Figure 4** and **Supplementary Tables 1**, **8**, **9**). This outcome was similar to the RNA-Seq based study of late-onset pregnancy complications, whereby only PE, but not GD, SGA or LGA cases showed notable shift in the placental transcriptome (Sõber et al., 2015). None of the miRNAs or their groups stood out a major driver of PE-linked miRNome. More than a third (23 of 66) of miRNAs identified as DEmiRs in PE have been previously described in the context of pregnancy complications or placental function (**Supplementary Table 37** and references therein). Interestingly, a similar fraction of placental DEmiRs in PE (24 of 66) have been reported in the context of cancer, especially the miRNAs in group G4 (11 of 16; **Figure 5**).

Placental miR-Seq has been previously utilized to analyze miRNome in EO-PE (<34 g.week) and/or IUGR (Awamleh et al., 2019). In total 11 of 57 reported DEmiRs (19%) in PE/PE + IUGR (seven miRNAs) or only IUGR (four miRNAs) overlapped with the identified 66 (17%) LO-PE DEmiRs in this study (**Supplementary Table 21**). Seven miRNAs altered in both EO- and LO-PE represent a robust placental molecular signature of preeclampsia, and also validated by RT-qPCR (Awamleh et al., 2019; **Figure 2B**). Differently from the limited overlap of affected genes identified in EO-PE and LO-PE placentas in RNA-Seq studies (Sõber et al., 2015; Kaartokallio et al., 2016; Ashar-Patel et al., 2017), placental miRNome appears to undergo a similar expressional shift in both conditions. This observation supports the recently suggested scenario that EO-PE and LO-PE are linked with placental syncytiotrophoblast stress (Redman et al., 2021).

There are several lines of evidence that alterations in placental miRNome contribute to the shared molecular etiology of PE and affected fetal growth. In our dataset, six of 66 PE-altered miRNAs showed also differential expression in SGA cases (**Supplementary Table 23**). Similarly, six of 57 placental DEmiRs in EO-PE were reported to be shared with EO-PE/IUGR and preterm IUGR conditions (miR-193b-3p, miR-193b-5p, miR-210-3p, miR-520a-3p, miR-365a-3p, miR-365ba-3p) (Awamleh et al., 2019). Additional four PE-linked placental miRNAs in the current study were also reported as DEmiRs in preterm IUGR (miR-193a-3p, miR-376a-5p, miR-500a-3p, miR-362-5p) (**Supplementary Table 21**).

It is largely unknown whether the active contribution of altered miRNome profile may indeed increase the risk to PE and impaired fetal growth. Studies are needed to clarify whether the observed alterations in placental miRNome represent a passive consequence of the PE and IUGR/SGA condition or a direct response to unfavorable physiological conditions. In this study, we demonstrated that 66 PE-linked miRNAs cluster to five groups with potentially different coordinated impact in modulating the placental transcriptome (**Figure 5** and **Table 4**). Reverse correlation between expression levels of a certain set of miRNAs (Group 2) and a large number of genes may potentially indicate their joint synergetic action in fine-tuning transcript levels of functionally linked loci. The nature of strong positive correlation between groups of miRNAs (Groups 3–4) and transcript levels has to be still determined.

Finally, the study compiled the first list of 66 placental miR-eQTLs, some of which are regulating miRNAs implicated in preeclampsia (**Figure 6**). The identified miR-eQTLs showed stronger association with the expression of flanking 16 miRNAs rather than 30 neighboring mRNA genes (**Supplementary Table 34**). It has been proposed that co-localization of GWAS and eQTL signals may uncover the role of gene expression modulating variants (Hormozdiari et al., 2016). So far, only two of the identified placental miR-eQTLs have been reported in the GWAS catalog: rs10853101 (miR-10a-5p) associated with the risk to diverticular disease and rs1424569 (hsa-miR-490-3p) with cardiac PR interval. In perspective, the phenotype effects of placental miR-eQTLs individually or as a component in polygenic risk scores for pregnancy-related traits (Moen et al., 2018; Ursini et al., 2018; Lamri et al., 2020; Steinthorsdottir et al., 2020) are still to be clarified. The pilot association testing of miR-eQTLs with newborn traits in the current study may have suffered from inadequate statistical power due to highly polygenic contribution (each variant with small effect), as well as combined effect of maternal and fetal genetics in modulating anthropometric parameters at birth (Beaumont et al., 2020).

Also the limitations in this study have to be acknowledged. As a robust differential expression analysis was aimed, low-expressed miRNAs that may give spurious results were filtered out. The applied criterion 'median raw read counts >50 across all 52 samples' may have excluded some first or second trimester specific miRNAs due to underrepresentation of these samples in the total set. Another limitation was low sample size of first and second trimester placentas, restricting miRNA-mRNA expressional correlation analysis and miR-eQTL association testing to term samples.

In summary, the current study reported a large, multilayered and thorough investigation of placental miRNome and its synergy with placental transcriptome during pregnancy, as well as in normal and complicated term deliveries. The dataset represents a rich catalog for further in-depth studies of specific placental miRNAs, their contribution to shaping normal and pathological placental transcriptome and consequently, their individual and joint functional impact to the pregnancy course. Several highlighted miRNAs represent potential biomarkers for pregnancy monitoring and in perspective, possible targets to even prevent or treat gestational complications.

DATA AVAILABILITY STATEMENT

The datasets presented in this study can be found in online repositories. The names of the repository/repositories and accession number(s) can be found below: European Genome-phenome Archive (EGA, https://www.ebi.ac.uk/), Accession EGAS00001005378.

ETHICS STATEMENT

The studies involving human participants were reviewed and approved by The Ethics Review Committee of Human Research of the University of Tartu, Estonia (Permissions Nos 146/18, 27.02.2006; 150/33, 18.06.2006; 158/80, 26.03.2007; 221/T-6, 17.12.2012; and 286/M-18, 15.10.2018). The patients/participants provided their written informed consent to participate in this study.

AUTHOR CONTRIBUTIONS

ML contributed to the conception and the provision of study materials. RI and ML contributed to the design. RI, TK, and KL contributed to the experimental conduct. RI contributed to the data analysis. RI, KL, TK, and ML contributed to the data interpretation. RI and ML contributed to the manuscript writing. RI, TK, KL, and ML contributed to the critical reading and commenting of the article, and final approval of manuscript. All authors contributed to the article and approved the submitted version.

FUNDING

The study was supported by the Estonian Research Council grants IUT34-12 and PRG1021 for ML.

ACKNOWLEDGMENTS

We are grateful to all the participants of the REPROMETA and HAPPY PREGNANCY studies. Kristiina Rull and the clinical personnel at the Women's Clinic, Tartu University Hospital are thanked for the recruitment and collection of clinical data. Siim Sõber and Mario Reiman are acknowledged for the bioinformatics advice and Eve Laasik for the laboratory assistance.

SUPPLEMENTARY MATERIAL

The Supplementary Material for this article can be found online at: https://www.frontiersin.org/articles/10.3389/fcell.2021.697947/full#supplementary-material

REFERENCES

American College of Obstetricians and Task Force on Hypertension in Pregnancy (2013). Hypertension in Pregnancy. *Obstet. Gynecol.* 122 1122–1131. doi: 10.1097/01.AOG.0000437382.03963.88

Apicella, C., Ruano, C. S. M. M., Méhats, C., Miralles, F., and Vaiman, D. (2019). *The Role of Epigenetics in Placental Development and the Etiology of Preeclampsia*. Available Online at: /pmc/articles/PMC6600551/?report=abstract (accessed August 16, 2019).

Aplin, J. D., Myers, J. E., Timms, K., and Westwood, M. (2020). Tracking placental development in health and disease. *Nat. Rev. Endocrinol.* 16, 479–494. doi: 10.1038/s41574-020-0372-6

Arthurs, A. L., Lumbers, E. R., and Pringle, K. G. (2019). MicroRNA mimics that target the placental renin–angiotensin system inhibit trophoblast proliferation. *MHR Basic Sci. Reprod. Med.* 25, 218–227. doi: 10.1093/molehr/gaz010

Ashar-Patel, A., Kaymaz, Y., Rajakumar, A., Bailey, J. A., Karumanchi, S. A., and Moore, M. J. (2017). FLT1 and transcriptome-wide polyadenylation site (PAS) analysis in preeclampsia. *Sci. Rep.* 7:13129. doi: 10.1038/s41598-017-11639-6

Awamleh, Z., Gloor, G. B., and Han, V. K. M. (2019). Placental microRNAs in pregnancies with early onset intrauterine growth restriction and preeclampsia: potential impact on gene expression and pathophysiology. *BMC Med. Genom.* 12:91. doi: 10.1186/s12920-019-0548-x

Balduzzi, S., Rücker, G., and Schwarzer, G. (2019). How to perform a meta-analysis with R: a practical tutorial. *Evid. Based. Ment. Health* 22, 153–160. doi: 10.1136/ebmental-2019-300117

Beaumont, R. N., Kotecha, S. J., Wood, A. R., Knight, B. A., Sebert, S., McCarthy, M. I., et al. (2020). Common maternal and fetal genetic variants show expected polygenic effects on risk of small- or large-for-gestational-age (SGA or LGA), except in the smallest 3% of babies. *PLoS Genet.* 16:e1009191. doi: 10.1371/journal.pgen.1009191

Benjamini, Y., and Hochberg, Y. (1995). Controlling the false discovery rate: a practical and powerful approach to multiple testing. *J. R. Stat. Soc. Ser. B* 57, 289–300. doi: 10.1111/j.2517-6161.1995.tb02031.x

Chang, C. W., Wakeland, A. K., and Parast, M. M. (2018). Trophoblast lineage specification, differentiation and their regulation by oxygen tension. *J. Endocrinol.* 236, R43–R56. doi: 10.1530/JOE-17-0402

Chiofalo, B., Laganà, A. S., Vaiarelli, A., La Rosa, V. L., Rossetti, D., Palmara, V., et al. (2017). Do miRNAs play a role in fetal growth restriction? a fresh look to a busy corner. *Biomed. Res. Int.* 2017:6073167. doi: 10.1155/2017/6073167

Ewels, P., Magnusson, M., Lundin, S., and Käller, M. (2016). MultiQC: summarize analysis results for multiple tools and samples in a single report. *Bioinformatics* 32, 3047–3048. doi: 10.1093/bioinformatics/btw354

Ghafouri-Fard, S., Shoorei, H., and Taheri, M. (2020). The role of microRNAs in ectopic pregnancy: a concise review. *Non-Coding RNA Res.* 5:67. doi: 10.1016/j.ncrna.2020.04.002

Gregory, W. R., Ben, B., Lodewijk, B., Rober, G., Wolfgang, L. A. H., Thomas, L., et al. (2015). *gplots: Various R Programming Tools for Plotting Data*. Available online at: https://www.researchgate.net/publication/303186599_gplots_Various_R_programming_tools_for_plotting_data (accessed January 30, 2021).

GTEx Consortium (2015). Human genomics. the genotype-tissue expression (GTEx) pilot analysis: multitissue gene regulation in humans. *Science* 348, 648–660.

Gusar, V., Timofeeva, A., Chagovets, V., Kan, N., Vasilchenko, O., Prozorovskaya, K., et al. (2020). Preeclampsia: the interplay between oxygen-sensitive miRNAs and erythropoietin. *J. Clin. Med.* 9:574. doi: 10.3390/jcm9020574

Herse, F., Dechend, R., Harsem, N. K., Wallukat, G., Janke, J., Qadri, F., et al. (2007). Dysregulation of the circulating and tissue-based renin-angiotensin system in preeclampsia. *Hypertension* 49, 604–611. doi: 10.1161/01.HYP.0000257797.49289.71

Hormozdiari, F., van de Bunt, M., Segrè, A. V., Li, X., Joo, J. W. J., Bilow, M., et al. (2016). Colocalization of GWAS and eQTL signals detects target genes. *Am. J. Hum. Genet.* 99, 1245–1260. doi: 10.1016/j.ajhg.2016.10.003

Hromadnikova, I., Kotlabova, K., Hympanova, L., and Krofta, L. (2015). Cardiovascular and cerebrovascular disease associated microRNAS are dysregulated in placental tissues affected with gestational hypertension, preeclampsia and intrauterine growth restriction. *PLoS One* 10:e0138383. doi: 10.1371/journal.pone.0138383

Hromadnikova, I., Kotlabova, K., Ivankova, K., Vedmetskaya, Y., and Krofta, L. (2017). Profiling of cardiovascular and cerebrovascular disease associated microRNA expression in umbilical cord blood in gestational hypertension, preeclampsia and fetal growth restriction. *Int. J. Cardiol.* 249, 402–409. doi: 10.1016/j.ijcard.2017.07.045

Huang, H. Y., Lin, Y. C. D., Li, J., Huang, K. Y., Shrestha, S., Hong, H. C., et al. (2020). MiRTarBase 2020: updates to the experimentally validated microRNA-target interaction database. *Nucleic Acids Res.* 48, D148–D154. doi: 10.1093/nar/gkz896

Huang, X., Wu, L., Zhang, G., Tang, R., and Zhou, X. (2019). Elevated MicroRNA-181a-5p contributes to trophoblast dysfunction and preeclampsia. *Reprod. Sci.* 26, 1121–1129. doi: 10.1177/1933719118808916

Kaartokallio, T., Wang, J., Heinonen, S., Kajantie, E., Kivinen, K., Pouta, A., et al. (2016). Exome sequencing in pooled DNA samples to identify maternal pre-eclampsia risk variants. *Sci. Rep.* 6:29085. doi: 10.1038/srep29085

Karere, G. M., Cox, L. A., Bishop, A. C., South, A. M., Shaltout, H. A., Mercado-Deane, M. G., et al. (2021). Sex differences in MicroRNA expression and cardiometabolic risk factors in hispanic adolescents with obesity. *J. Pediatr.* doi: 10.1016/j.jpeds.2021.03.070 Online ahead of print.

Kasak, L., Rull, K., Vaas, P., Teesalu, P., and Laan, M. (2015). Extensive load of somatic CNVs in the human placenta. *Sci. Rep.* 5:8342. doi: 10.1038/srep08342

Kennedy, E. M., Hermetz, K., Burt, A., Everson, T. M., Deyssenroth, M., Hao, K., et al. (2020). Placental microRNA expression associates with birthweight through control of adipokines: results from two independent cohorts. *Epigenetics* 16, 770–782. doi: 10.1080/15592294.2020.1827704

Kikas, T., Inno, R., Ratnik, K., Rull, K., and Laan, M. (2020). C-allele of rs4769613 Near FLT1 represents a high-confidence placental risk factor for preeclampsia. *Hypertens* 76, 884–891. doi: 10.1161/HYPERTENSIONAHA.120.15346

Kikas, T., Laan, M., and Kasak, L. (2021). Current knowledge on genetic variants shaping placental transcriptome and their link to gestational and postnatal health. *Placenta* doi: 10.1016/j.placenta.2021.02.009 Online ahead of print.

Kikas, T., Rull, K., Beaumont, R. N., Freathy, R. M., and Laan, M. (2019). The effect of genetic variation on the placental transcriptome in humans. *Front. Genet.* 10:550. doi: 10.3389/fgene.2019.00550

Kozomara, A., Birgaoanu, M., and Griffiths-Jones, S. (2019). miRBase: from microRNA sequences to function. *Nucleic Acids Res.* 47, D155–D162. doi: 10.1093/nar/gky1141

Kshitiz, Afzal, J., Maziarz, J. D., Hamidzadeh, A., Liang, C., Erkenbrack, E. M., et al. (2019). Evolution of placental invasion and cancer metastasis are causally linked. *Nat. Ecol. Evol.* 3, 1743–1753. doi: 10.1038/s41559-019-1046-4

Lamri, A., Mao, S., Desai, D., Gupta, M., Paré, G., and Anand, S. S. (2020). Fine-tuning of genome-wide polygenic risk scores and prediction of gestational diabetes in south asian women. *Sci. Rep.* 10:8941. doi: 10.1038/s41598-020-65360-y

Langmead, B., Trapnell, C., Pop, M., and Salzberg, S. L. (2009). Ultrafast and memory-efficient alignment of short DNA sequences to the human genome. *Genome Biol.* 10:R25. doi: 10.1186/gb-2009-10-3-r25

Liao, Y., Smyth, G. K., and Shi, W. (2019). The R package Rsubread is easier, faster, cheaper and better for alignment and quantification of RNA sequencing reads. *Nucleic Acids Res.* 47:e47. doi: 10.1093/nar/gkz114

Love, M. I., Huber, W., and Anders, S. (2014). Moderated estimation of fold change and dispersion for RNA-seq data with DESeq2. *Genome Biol.* 15:550. doi: 10.1186/s13059-014-0550-8

Metzger, B. E. (2010). International association of diabetes and pregnancy study groups recommendations on the diagnosis and classification of hyperglycemia in pregnancy. *Diabetes Care* 33, 676–682. doi: 10.2337/dc10-0719

Moen, G. H., LeBlanc, M., Sommer, C., Prasad, R. B., Lekva, T., Normann, K. R., et al. (2018). Genetic determinants of glucose levels in pregnancy: genetic risk scores analysis and GWAS in the Norwegian STORK cohort. *Eur. J. Endocrinol.* 179, 363–372. doi: 10.1530/EJE-18-0478

Morales-Prieto, D. M., Ospina-Prieto, S., Chaiwangyen, W., Schoenleben, M., and Markert, U. R. (2013). Pregnancy-associated miRNA-clusters. *J. Reprod. Immunol.* 97, 51–61. doi: 10.1016/j.jri.2012.11.001

Muralimanoharan, S., Maloyan, A., and Myatt, L. (2016). Mitochondrial function and glucose metabolism in the placenta with gestational diabetes mellitus: role of miR-143. *Clin. Sci.* 130, 931–941. doi: 10.1042/CS20160076

Nonn, O., Fischer, C., Geisberger, S., El-Heliebi, A., Kroneis, T., Forstner, D., et al. (2021). Maternal angiotensin increases placental leptin in early gestation via an alternative renin-angiotensin system pathway: suggesting a link to preeclampsia. *Hypertens* 77, 1723–1736. doi: 10.1161/HYPERTENSIONAHA.120.16425

Nunez, Y. O., Truitt, J. M., Gorini, G., Ponomareva, O. N., Blednov, Y. A., Harris, R. A., et al. (2013). Positively correlated miRNA-mRNA regulatory networks in mouse frontal cortex during early stages of alcohol dependence. *BMC Genom.* 14:725. doi: 10.1186/1471-2164-14-725

Pilvar, D., Reiman, M., Pilvar, A., and Laan, M. (2019). Parent-of-origin-specific allelic expression in the human placenta is limited to established imprinted loci and it is stably maintained across pregnancy. *Clin. Epigenet.* 11:94. doi: 10.1186/s13148-019-0692-3

Pineles, B. L., Romero, R., Montenegro, D., Tarca, A. L., Han, Y. M., Kim, Y. M., et al. (2007). Distinct subsets of microRNAs are expressed differentially in the human placentas of patients with preeclampsia. *Am. J. Obstet. Gynecol.* 196:261.e1–6. doi: 10.1016/j.ajog.2007.01.008

Purcell, S., Neale, B., Todd-Brown, K., Thomas, L., Ferreira, M. A. R., Bender, D., et al. (2007). PLINK: a tool set for whole-genome association and population-based linkage analyses. *Am. J. Hum. Genet.* 81, 559–75. doi: 10.1086/519795

Raudvere, U., Kolberg, L., Kuzmin, I., Arak, T., Adler, P., Peterson, H., et al. (2019). g:Profiler: a web server for functional enrichment analysis and conversions of gene lists (2019 update). *Nucleic Acids Res.* 47, 191–198. doi: 10.1093/nar/gkz369

Redman, C. W. G., Staff, A. C., and Roberts, J. M. (2021). Syncytiotrophoblast stress in preeclampsia: the convergence point for multiple pathways. *Am. J. Obstet. Gynecol.* doi: 10.1016/j.ajog.2020.09.047 Online ahead of print.

Reiman, M., Laan, M., Rull, K., and Sõber, S. (2017). Effects of RNA integrity on transcript quantification by total RNA sequencing of clinically collected human placental samples. *FASEB J.* 31, 3298–3308. doi: 10.1096/fj.201601031RR

Reimand, J., Arak, T., Adler, P., Kolberg, L., Reisberg, S., Peterson, H., et al. (2016). g:Profiler-a web server for functional interpretation of gene lists (2016 update). *Nucleic Acids Res.* 44, W83–W89. doi: 10.1093/nar/gkw199

Reimand, J., Kull, M., Peterson, H., Hansen, J., and Vilo, J. (2007). g:Profiler–a web-based toolset for functional profiling of gene lists from large-scale experiments. *Nucleic Acids Res.* 35, W193–W200. doi: 10.1093/nar/gkm226

Seitz, H., Royo, H., Bortolin, M. L., Lin, S. P., Ferguson-Smith, A. C., and Cavaillé, J. (2004). A large imprinted microRNA gene cluster at the mouse Dlk1–Gtl2 domain. *Genome Res.* 14, 1741–1748. doi: 10.1101/gr.2743304

Seno, K., Tanikawa, N., Takahashi, H., Ohkuchi, A., Suzuki, H., Matsubara, S., et al. (2018). Oxygen concentration modulates cellular senescence and autophagy in human trophoblast cells. *Am. J. Reprod. Immunol.* 79:e12826. doi: 10.1111/aji.12826

Sildver, K., Veerus, P., and Lang, K. (2015). *Sünnikaalukõverad Eestis ja Sünnikaalu Mõjutavad Tegurid: Registripõhine Uuring*. Available online at: https://eestiarst.ee/sunnikaalukoverad-eestis-ja-sunnikaalu-mojutavad-tegurid-registripohine-uuring/ (accessed April 20, 2020).

Sõber, S., Reiman, M., Kikas, T., Rull, K., Inno, R., Vaas, P., et al. (2015). Extensive shift in placental transcriptome profile in preeclampsia and placental origin of adverse pregnancy outcomes. *Sci. Rep.* 5:13336. doi: 10.1038/srep13336

Sõber, S., Rull, K., Reiman, M., Ilisson, P., Mattila, P., and Laan, M. (2016). RNA sequencing of chorionic villi from recurrent pregnancy loss patients reveals impaired function of basic nuclear and cellular machinery. *Sci. Rep.* 6:38439. doi: 10.1038/srep38439

Steinthorsdottir, V., McGinnis, R., Williams, N. O., Stefansdottir, L., Thorleifsson, G., Shooter, S., et al. (2020). Genetic predisposition to hypertension is associated with preeclampsia in European and Central Asian women. *Nat. Commun.* 11:5976. doi: 10.1038/s41467-020-19733-6

Tamaru, S., Kajihara, T., Mizuno, Y., Mizuno, Y., Tochigi, H., and Ishihara, O. (2020). Endometrial microRNAs and their aberrant expression patterns. *Med. Mol. Morphol.* 53, 131–140. doi: 10.1007/s00795-020-00252-8

Tan, H., Huang, S., Zhang, Z., Qian, X., Sun, P., and Zhou, X. (2019). Pan-cancer analysis on microRNA-associated gene activation. *EBioMedicine.* 43, 82–97. doi: 10.1016/j.ebiom.2019.03.082

The GTEx Consortium (2020). The GTEx consortium atlas of genetic regulatory effects across human tissues. *Science* 369, 1318–1330. doi: 10.1126/science.aaz1776

Ursini, G., Punzi, G., Chen, Q., Marenco, S., Robinson, J. F., Porcelli, A., et al. (2018). Convergence of placenta biology and genetic risk for schizophrenia article. *Nat. Med.* 24, 792–801. doi: 10.1038/s41591-018-0021-y

Wu, S., Aksoy, M., Shi, J., and Houbaviy, H. B. (2014). Evolution of the miR-290-295/miR-371-373 cluster family seed repertoire. *PLoS One* 9:108519. doi: 10.1371/journal.pone.0108519

Yong, H. E. J., and Chan, S. Y. (2020). Current approaches and developments in transcript profiling of the human placenta. *Hum. Reprod. Update* 26, 799–840. doi: 10.1093/humupd/dmaa028

Zhang, Y., Fei, M., Xue, G., Zhou, Q., Jia, Y., Li, L., et al. (2012). Elevated levels of hypoxia-inducible microRNA-210 in pre-eclampsia: new insights into molecular mechanisms for the disease. *J. Cell. Mol. Med.* 16, 249–259. doi: 10.1111/j.1582-4934.2011.01291.x

Conflict of Interest: The authors declare that the research was conducted in the absence of any commercial or financial relationships that could be construed as a potential conflict of interest.

frontiers in Cell and Developmental Biology

ORIGINAL RESEARCH
published: 21 July 2021
doi: 10.3389/fcell.2021.695248

Single Nucleus RNA Sequence (snRNAseq) Analysis of the Spectrum of Trophoblast Lineages Generated From Human Pluripotent Stem Cells *in vitro*

Teka Khan[1,2†], Arun S. Seetharam[3,4†], Jie Zhou[1,5], Nathan J. Bivens[6], Danny J. Schust[5], Toshihiko Ezashi[1,2], Geetu Tuteja[4] and R. Michael Roberts[1,2,7*]*

[1] Christopher S Bond Life Sciences Center, University of Missouri, Columbia, MO, United States, [2] Division of Animal Sciences, Bond Life Sciences Center, University of Missouri, Columbia, MO, United States, [3] Department of Ecology, Evolution, and Organismal Biology, Iowa State University, Ames, IA, United States, [4] Genetics, Development and Cell Biology, Iowa State University, Ames, IA, United States, [5] Department of Obstetrics and Gynecology, University of Missouri School of Medicine, Columbia, MO, United States, [6] DNA Core Facility, University of Missouri, Columbia, MO, United States, [7] Department of Biochemistry, University of Missouri, Columbia, MO, United States

OPEN ACCESS

Edited by:
Ruby Yun-Ju Huang,
National Taiwan University, Taiwan

Reviewed by:
Shurong Liu,
Sun Yat-sen University, China
Yu Zhao,
Capital Medical University, China

***Correspondence:**
Geetu Tuteja
geetu@iastate.edu
R. Michael Roberts
robertsrm@missouri.edu

[†] These authors have contributed equally to this work and share first authorship

Specialty section:
This article was submitted to Molecular Medicine, a section of the journal Frontiers in Cell and Developmental Biology

Received: 14 April 2021
Accepted: 21 June 2021
Published: 21 July 2021

Citation:
Khan T, Seetharam AS, Zhou J, Bivens NJ, Schust DJ, Ezashi T, Tuteja G and Roberts RM (2021) Single Nucleus RNA Sequence (snRNAseq) Analysis of the Spectrum of Trophoblast Lineages Generated From Human Pluripotent Stem Cells in vitro. Front. Cell Dev. Biol. 9:695248. doi: 10.3389/fcell.2021.695248

One model to study the emergence of the human trophoblast (TB) has been the exposure of pluripotent stem cells to bone morphogenetic protein 4 (BMP4) in presence of inhibitors of ACTIVIN/TGFB; **A**83–01 and FGF2; **P**D173074 (BAP), which generates a mixture of cytotrophoblast, syncytiotrophoblast, and cells with similarities to extravillous trophoblast. Here, H1 human embryonic stem cells were BAP-exposed under two O_2 conditions (20% and 5%, respectively). At day 8, single nuclei RNA sequencing was used for transcriptomics analysis, thereby allowing profiling of fragile syncytial structures as well as the more resilient mononucleated cells. Following cluster analysis, two major groupings, one comprised of five (2,4,6,7,8) and the second of three (1,3,5) clusters were evident, all of which displayed recognized TB markers. Of these, two (2 and 3) weakly resembled extravillous trophoblast, two (5 and 6) strongly carried the hallmark transcripts of syncytiotrophoblast, while the remaining five were likely different kinds of mononucleated cytotrophoblast. We suggest that the two populations of nuclei within syncytiotrophoblast may have arisen from fusion events involving two distinct species of precursor cells. The number of differentially expressed genes between O_2 conditions varied among the clusters, and the number of genes upregulated in cells cultured under 5% O_2 was highest in syncytiotrophoblast cluster 6. In summary, the BAP model reveals an unexpectedly complex picture of trophoblast lineage emergence that will need to be resolved further in time-course studies.

Keywords: human embryonic stem cells, BMP4, syncytiotrophoblast, placenta, trophoblast, extravillous trophoblast, snRNASeq

INTRODUCTION

Early human gestation, especially the approximately 14 days between conception and the anticipated onset of the next menstruation period, is associated with high rates of pregnancy loss (Wilcox et al., 1988). It is the time in pregnancy when the trophoblast (TB) lineage emerges, implantation begins, and a trophoblast interface is established with the mother that allows for physical and nutritional support of the conceptus. Critically, it is also the period when signals from the conceptus trigger the phenomenon of maternal recognition of pregnancy, which prevents the mother from a return to ovarian cyclicity and provides the conceptus some measure of control over maternal physiology and its own future. TB, as the dominant lineage of the emerging placenta, has a major responsibility for all these functions. However, for a range of ethical and practical reasons, these first critical weeks of pregnancy have been largely inaccessible to experimental study. As a consequence, there has been interest in developing models that mimic some of these early events of placental TB emergence *in vitro*.

One approach that has been used to address our poor understanding of these enigmatic early days of pregnancy is extended embryo culture beyond the blastocyst stage (reviewed by Zhou et al. (2021), In Press), made possible because of the availability of "spare" human embryos from *in vitro* fertilization clinics and improved culture media that permitted development until at least day (d) 13 (Deglincerti et al., 2016; Shahbazi et al., 2016). These embryos, although separated from maternal influence, appear to follow a differentiation pathway quite similar to that inferred from the limited number of histological studies performed on *in vivo* material many years before (Hertig et al., 1956; Boyd and Hamilton, 1970). Single-cell RNA sequence (scRNAseq) analysis performed on such embryos at d 8, 10, and 12 of culture revealed the presence of emergent TB populations for syncytioTB and extravillous-like cytoTB that appeared to be similar to, but nonetheless distinct from, TBs that populate the villous placental structures that arise a little later in pregnancy (West et al., 2019). Extended human embryo culture has also provided insights into the mechanisms of TB lineage divergence around the time of implantation (Lv et al., 2019; West et al., 2019; Zhou et al., 2019).

A second model to study the TBs of early pregnancy has been to generate them from pluripotent stem cells, specifically human embryonic stem cells (hESCs) and induced pluripotent stem cells after exposure to BMP4. This pathway of directed differentiation was first reported by Xu et al. (2002) and continues be used extensively, albeit with a range of modifications [Reviewed in Roberts et al. (2018); Horii et al. (2019, 2020)] and especially the exclusion of FGF2 (Das et al., 2007). Among the refinements has been to include two pharmaceutical reagents, the ACTIVIN signaling inhibitor **A**83–01, and the FGF2 signaling inhibitor **P**D1730, so-called **BAP** medium (Amita et al., 2013; Yang et al., 2015). Under this regimen, virtually all cells become positive for the pan-trophoblast marker KRT7 by 48 h. HLA-G positive cells, indicative of extravillousTBs, appear soon after and reach a maximum by d 5–6, while the production of human chorionic gonadotropins (hCG) from syncytioTB begins at about d 5 and increases markedly thereafter. The colonies can be maintained in culture for approximately 8–9 days before regions of syncytium begin to loosen from the Matrigel substratum. The BAP model has allowed different-sized cell types, the largest being syncytium (syncytioTB) and the smallest mononucleated cytoTBs, to be partially characterized and compared (Yabe et al., 2016). Microarray analysis has also been performed on HLA-G positive cells isolated on magnetic beads, which demonstrated a resemblance in terms of its markers to extravillousTB derived from placenta (Telugu et al., 2013).

While microarray and RNAseq data from hESC colonies differentiated in response to BMP4 have shown the differentiated cells to be comprised only of TB, with no evidence for contributions from the main germ line lineages, particularly mesoderm (Schulz et al., 2008; Marchand et al., 2011; Telugu et al., 2013; Yabe et al., 2016; Jain et al., 2017), it has become clear that they displayed a different transcriptome profile from primary TBs isolated from the villous placenta. This realization led us to hypothesize that BAP best modeled the primitive placental structure that forms when the blastocyst first implants and establishes residency in the uterine wall. Although the original microarray and RNAseq studies were informatory about the general nature of the TB that formed in response to directed differentiation, they provided little detail about the identity of the different sub-lineages that formed, their relationships to each other, and how they originated. Here we have employed a single nuclei RNAseq approach, which allowed an analysis of fragile syncytioTB structures as well as the more resilient cytoTBs, to display an unexpected heterogeneity of TB sub-lineages in d 8 cultures.

MATERIALS AND METHODS

Human Embryonic Stem Cell Culture and Trophoblast Differentiation

Human ESCs (H1; WA01) originated from WiCell Research Institute. They were cultured and maintained in Matrigel (BD Bioscience)-coated 6-well tissue culture plates (Thermo Scientific) on mTeSR1 medium (Stemcell Technologies) under two different O_2 concentration conditions, i.e., 20% and 5% at 37°C, as described previously (Yabe et al., 2016). The medium was replaced daily and cells (50,000/well) passaged approximately every 5–6 days. The protocol first described by Amita et al. (2013) was used to drive differentiation of the ESC to TB. Briefly, the mTeSR1 culture medium, which contains a high concentration of FGF2 (100 ng/ml), was replaced with DMEM/F12 medium (Thermo Scientific)

Abbreviations: ANOVA, Analysis of variance; AP, **A**83–01, **P**D1730; BAP, **B**one morphogenic protein-4, **A**83–01, **P**D1730; bp, Base pair; CytoTB, Cytotrophoblast; GEMs, Gel Bead-in-Emulsion; hESCS, Human embryonic stem cells; UMAP, Uniform manifold approximation and projection; UMIs, Unique Molecular Identifiers; KOSR, Knock-out serum replacement; MEFs, Mouse embryonic fibroblast; NWRB, Nuclear wash and resuspension buffer; PCA, Principle component analyses; scRNAseq, Single cell RNA sequence; SNN, Shared nearest neighbor; snRNA, Single nucleus RNA sequence; SyncytioTB, Syncytiotrophoblast; TB, Trophoblast; t-SNE, t-distributed stochastic neighbor embedding; VST, Variance stabilizing transformation.

containing knock-out serum replacement (KOSR, Invitrogen) and low FGF2 (4 ng/ml) that had been conditioned by mouse embryonic fibroblast (MEFs) (**Supplementary Figure 1**). After 24 hours, the conditioned medium was replaced with daily changes of DMEM/F12/KOSR medium minus FGF2 but containing BMP4 (10 ng/ml), A83-01 (1 μM), and PD1730740 (0.1 μM), so-called BAP treatment, for 3 days and then the same medium without BMP4 for the following 4 days (AP treatment) (**Supplementary Figure 1A**). The content of hCG in the culture medium was measured on d 7 and d 8 by ELISA as described by Amita et al. (2013). The hCG concentration was normalized to 10^5 nuclei for each replicate cultured under the 20% O_2 and 5% O_2 conditions. One-way ANOVA was applied by using GraphPad Prism.

Nuclei Isolation

On d 8 of differentiation, each culture well was rinsed twice with DMEM/F12 and the colonies were partially dispersed by using gentle cell disassociation reagent (GDR) (Stemcell Technologies) (0.6 ml/well; 7 min at 37°C). The colonies were fully dislodged from the substratum by gentle scraping, and nuclei were isolated from the disassociated cells by the protocol provided by 10X Genomics with minor modifications (10x Genomics, 2019). Briefly, 1 ml of chilled lysis buffer (10 mM Tris-HCl, pH 7.4; 10 mM NaCl; 3 mM $MgCl_2$; and 0.1% Non-idet^{TM} P40 Substitute in Nuclease-Free Water) was added to each well through a wide-bore pipet tip. After gently pipetting several times, the suspension was kept on ice for 5 min to achieve maximum lysis of cells and centrifuged (500 ×*g*: 5 min at 4°C). The pellet was resuspended in 1 ml of nuclear wash and resuspension buffer (NWRB) (1X PBS with 1.0% w/v bovine serum albumin and 0.2 U/μl RNase inhibitor), cell debris were removed by filtration through a 40 μm Nylon cell strainer (Falcon), and the solution was recentrifuged as above. The supernatant solution was removed, and the final nuclear pellet was suspended in 1 ml of NWRB. The complete workflow is documented in **Supplementary Figure 1**.

Single Nuclear 3′ RNA-Seq Library Preparation

Libraries were constructed by following the manufacturer's (10x Genomics, 2019) protocol with reagents supplied in the 10x Genomics Chromium Next Gel Bead-in-Emulsion (GEMs) Single Cell 3′ Kit v3.1. Briefly, the concentrations of nuclei and intact cells in the nuclear preparation were measured with an Invitrogen Countess II automated cell counter. An aliquot of the nuclear suspension (1,000 nuclei per microliter), reverse transcription master mix, and partitioning oil were loaded on a Chromium Next GEM G chip with a nuclear capture target of 5,000 nuclei per library. Post-Chromium controller GEMs were transferred to a PCR strip tube, and reverse transcription was performed on an Applied Biosystems Veriti thermal cycler at 53°C for 45 min. cDNA was amplified for 14 cycles and purified by using Axygen AxyPrep MagPCR Clean-up beads. cDNA fragmentation, end-repair, A-tailing, and ligation of sequencing adaptors was performed according to manufacturer specifications. The final library was quantified with the Qubit HS DNA kit, and the fragment size was analyzed by means of an Agilent Fragment Analyzer system. Libraries were pooled and sequenced on an Illumina NovaSeq S1 flow cell with a goal to generate 50,000 reads per nucleus with a sequencing configuration of 28 base pair (bp) on read1 and 91 bp on read 2 using unique dual indexes.

Single-Nuclei Sequencing Analysis

The University of Missouri Informatics Research Core Facility pre-processed the data with the 10XGenomics/CellRanger software (v4.0.0) (Zheng et al., 2017), including demultiplexing, fastq file generation, read alignment, and UMI quantification. CellRanger was run with default options against the ENSEMBL GRCh38 reference genome (Schneider et al., 2017) with both pre-mRNA and mRNA feature files. The data were then processed by means of Seurat (v3.2.2) (Stuart et al., 2019), following the recommended practices for scRNAseq data with replicates. All steps used default options unless noted otherwise. Briefly, an expression matrix (count table) containing Unique Molecular Identifiers (UMIs) per nucleus per gene was imported for each replicate as the 10× data object. Only nuclei with greater than 200 but less than 7,500 genes and less than 15% of genes originating from mitochondrial sources were retained. Once the nuclei were quality filtered, the data were imported as a Seurat object, and all mitochondrial and ribosomal protein-coding genes were removed from the expression matrix. The replicates for each condition were integrated by using the FindIntegrationAnchors and IntegrateData commands. The count matrix was scaled and normalized by variance stabilizing transformation (VST) with Seurat's ScaleData and NormalizeData commands, respectively. The 2,000 most variable features were then selected with the FindVariableFeatures command for the Principle Component Analyses (PCA), which was performed by the RunPCA command. The PCs generated by the PCA were assessed with ElbowPlot and JackStraw analyses by using up to 20 different components. The resulting PCs were used for Jaccard-weighted, shared nearest neighbor (SNN) distance calculations and graph generation. The graph was then subjected to Louvain clustering and Uniform Manifold Approximation and Projection (UMAP) for dimension reduction in order to visualize nuclear transcriptomic profiles in two-dimensional space. After changing the default assay to RNA in the Seurat object, FindMarkers was run to determine the marker genes (genes with a fold change of greater than or equal to 1.5 with an adjusted p-value of less than 0.05) in each cluster by comparing each gene's expression level against other clusters.

Cluster identities were approximated by using single-cell RNA-Seq data from first trimester human placenta (Vento-Tormo et al., 2018). We used cell-type specific genes as described in PlacentaCellEnrich (Jain and Tuteja, 2021) within the TissueEnrich Bioconductor package (Jain and Tuteja, 2019).

To perform differential expression analysis between O_2 conditions, metadata in the Seurat object was updated with a new column containing both information about the cluster and the condition. This column was set as Seurat objects identity, and differential expression analyses were performed by using the FindMarkers command. No down-sampling of any cluster was performed since the corresponding clusters had roughly the same number of cells. Genes were considered upregulated in a

condition if the fold change was greater than or equal to 1.5, and the adjusted p-value was less than 0.05.

The GitHub repository documenting all the analyses steps is available at https://github.com/Tuteja-Lab/BAP.hESC.d8_snRNAseq. Sequencing data have been deposited in the Gene Expression Omnibus under accession ID GSE171768.

RESULTS

Heterogeneity of Cell Types

Exposure of either human embryonic stem cells or human induced pluripotent cells to BAP conditions for five days or more results in the initiation of syncytioTB formation evident as ruffled areas within the colonies and a steep increase in *CGA* and *CGB* expression and hCG production over subsequent days (Amita et al., 2013; Yabe et al., 2016). As previously described, these cells show downregulation of pluripotency genes, and upregulation of trophoblast marker genes compared to undifferentiated cells (**Supplementary Table 1**). CGA-expressing TBs are known to be confined to what has previously been demonstrated to be the syncytial patches, with little or no staining outside these areas (Das et al., 2007; Schulz et al., 2008; Amita et al., 2013; Yang et al., 2015), while other trophoblast markers, such as HLA-G, are confined to areas outside the syncytium. The heterogeneity of cell types is further demonstrable by the heterogeneity of staining within colonies and differences in intensities of staining for particular trophoblast markers. Together, these data indicate that snRNAseq analysis might be a fruitful approach to examining lineage divergence and cell type diversity.

Isolation of Nuclei

H1 ESCs were acclimated to 20% and 5% O_2 conditions prior to BAP-directed differentiation to TB (**Supplementary Figure 1A**). Sufficient hCG was released into the medium to be detected after d 5. By d7 and d8 copious amounts of hCG were being produced by cultures grown under both O_2 conditions (**Supplementary Figure 1B**), although previous studies had detected a significant lag between d6 and d8 under low O_2, possibly reflective of a slower rate of differentiation than at 20% (Schulz et al., 2008; Amita et al., 2013). At d 8, the colonies were dissociated as completely as possible without destroying syncytial clumps, and nuclei were isolated (**Supplementary Figure 1D**). This experiment was repeated a second time, also under the same two O_2 conditions, in order to provide two replicates for each treatment group (**Supplementary Figure 1A**). The concentrations of nuclei used to prepare libraries for subsequent snRNAseq analysis were comparable, and the content of intact cells in all four preparations was 5% or less (**Supplementary Figure 1F**).

snRNA-seq Analysis of Trophoblast Cells

After sequencing and data processing, nuclei were retained for analysis if they had between 200 and 7,500 unique genes detected, and less than 15% mitochondrial reads (**Supplementary Figure 2** and **Supplementary Table 2**). With the possible exception of the first replicate from cultures under 20% O_2 conditions, the majority of mitochondrial contamination was associated with nuclei that contained a relatively low number of nuclear transcripts (**Supplementary Figure 3**). From the four preparations, this resulted in a total of 5,355 nuclei passing quality control filters (**Supplementary Table 2**). In addition to transcripts from mitochondrial genes, sequencing also revealed, as expected, the presence of ribosomal subunit RNAs in all nuclei. Accordingly, all data were filtered to remove mitochondrial and ribosomal RNA transcripts before further analysis with Seurat software.

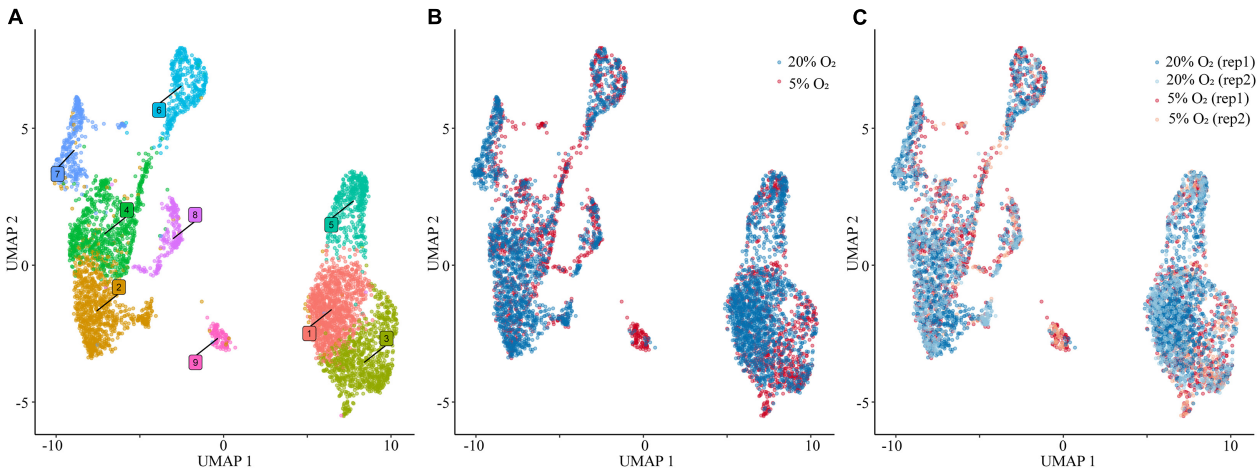

FIGURE 1 | Single nuclear RNA sequencing. **(A)** Visualization of nuclei included in the analysis, colored according to assignment by clustering analysis. **(B)** Plot of the nuclei obtained from the cells cultured under 20% O_2 (blue) and 5% O_2 (red) concentration conditions. **(C)** Nuclei plot obtained from each replicate of cells cultured under 20% O_2 (blue) and 5% O_2 (red) conditions. For all panels: 5,355 total nuclei were plotted in two dimensions based on transcriptome similarity using uniform manifold approximation and projection (UMAP) for all of the analyses using Seurat. Each dot represents an individual nuclei. 20% O_2, nuclei obtained from the cells cultured under 20% O_2; 5% O_2, nuclei obtained from the cells cultured under 5% O_2; rep, replicate.

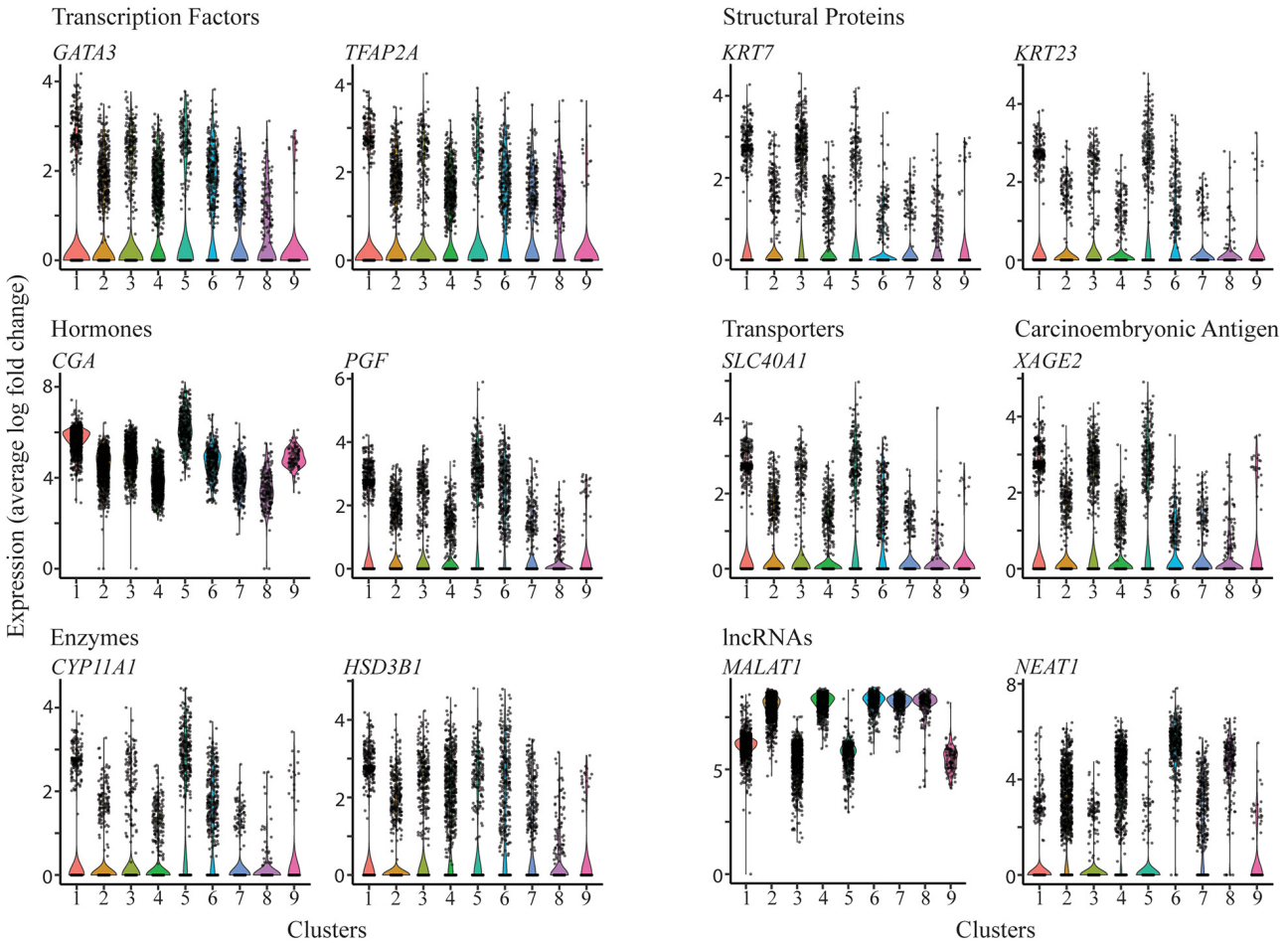

FIGURE 2 | Expression profiles of selected genes across the clusters. Violin plots showing expression for genes encoding transcription factors (**upper left panel**), structural proteins (**upper right panel**), hormones (**mid left panel**), transporters and carcinoembryonic antigen (**mid right panels**), enzymes involved in steroid biosynthesis (**lower left panel**), and long non-coding RNAs (**lower right panel**).

Following cluster analysis and projection of data in uniform manifold approximation and projection (UMAP) expression space, two major groupings, one comprised of five (2,4,6,7,8) and the second of three (1,3,5) clusters, were evident (**Figure 1**). Cluster 9 appeared to be separated from these two groupings. The gene expression signatures that distinguished the clusters are shown in **Supplementary Table 3** and illustrated graphically for each cluster in **Supplementary Figure 4**. The four different nuclear preparations replicated each other well (**Figure 1B**). Cluster 9 was again the exception and was comprised almost entirely by contributions from cells differentiated under 5% O_2. All nine clusters contained nuclei that expressed genes that have traditionally been used in various combinations as markers for TB. These genes included, among others, ones encoding transcription factors, e.g., *GATA3, TFAP2A*, structural proteins, e.g., *KRT7, KRT23*, hormones, e.g., *CGA, PGF*, transporters, e.g., *SLC40A1*, the carcinoembryonic antigen XAGE2, and enzymes involved in steroid biosynthesis, e.g., *CYP11A1, HSD3B1*. However, it is also clear that the expression of any particular gene was variable between individual nuclei within clusters and that mean expression values differed across clusters (**Figure 2**). In addition, all clusters had high levels of the placenta-enriched, long non-coding RNAs, *MALAT1* and *NEAT1* (**Figure 2**). Both of the latter were expressed most robustly in the grouping on the left (a) comprised of clusters 2, 4, 6, 7, and 8 compared to the right grouping (b) (clusters 1, 3, and 5) (**Figure 2**).

There was no significant expression of most marker genes examined for mesoderm, including *DLL3, FOXC1, RIPPLY, T/BRA, FOXA2, MIXL1,* endoderm, including *AFP, GATA4, GDF1, GDF3, MIXL2*, and ectoderm, including *FGF5, OTX2, SOX1, PAX6*. A few such marker genes, e.g., *TWIST2, GATA6, NES*, were detected at low levels (**Supplementary Figure 5**), but at least one of them (*TWIST2*) has a previously described functional association with TB (Ng et al., 2012). These data are generally consistent with the view expressed previously that the BAP-driven conversion of ESCs to TBs is largely, if not entirely, complete and leads to little or no differentiation of the ESCs along the main germline lineages (Amita et al., 2013; Yabe et al., 2016; Roberts et al., 2018).

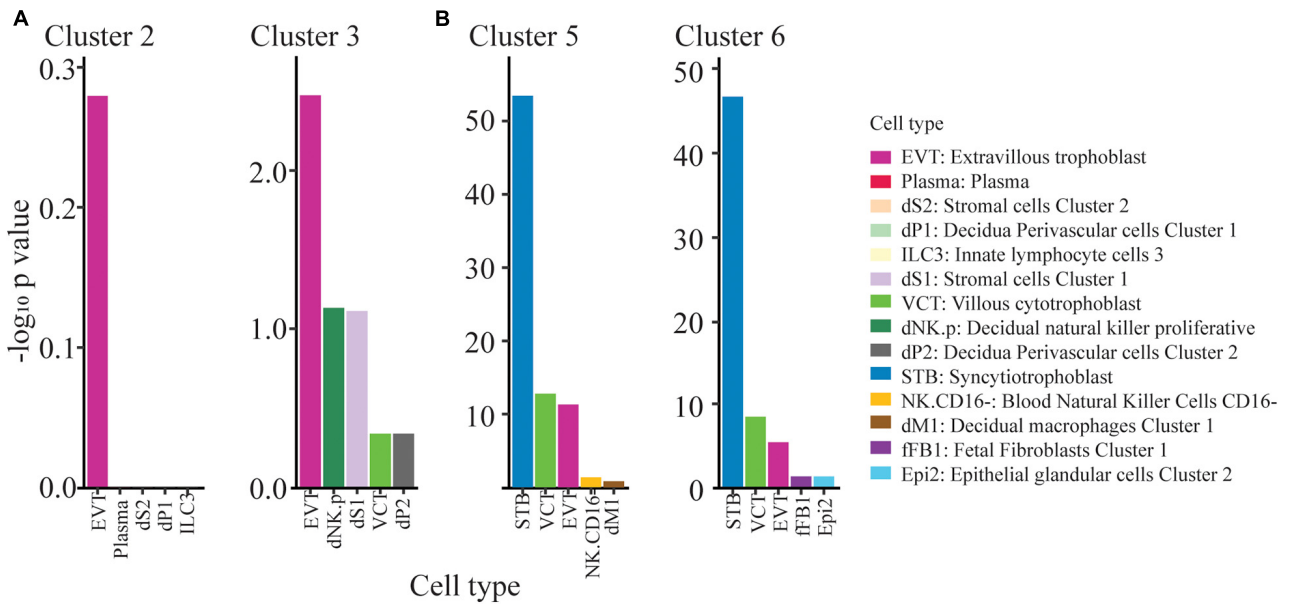

FIGURE 3 | ExtravillousTB and syncytioTB gene enriched clusters. **(A)** Clusters 2 and 3 show weak enrichment for ExtravillousTB specific markers. **(B)** Clusters 5 and 6 show strong enrichment for SyncytioTB specific markers. Top 5 cell type results from PlacentaCellEnrich have been shown here for clusters 2,3,5, and 6. The y-axis corresponds to $-\log_{10}$ of the adjusted p-value.

Trophoblast Nature of the Clusters

The question then arose as to the kind of TB represented in clusters 1–9. We used the PlacentaCellEnrich program (Jain and Tuteja, 2021) to determine if marker genes from clusters 1-9 were enriched for genes with cell-type specific expression in first trimester placenta, according to data from Vento-Tormo et al. (2018). This analysis provided strong evidence that clusters 5 and 6, were enriched for nuclei with a profile similar to that of placental syncytioTB, while cluster 3 embodied some features of extravillousTB from first trimester placenta (**Figure 3**). Cluster 2 showed most similarity to extravillousTB, although the adjusted P value when compared to the scRNAseq analysis of first trimester placenta conducted by Vento-Tormo et al. (2018) was not significant indicating that the similarities were low and therefore the cluster identity is unclear. Data for the remaining clusters 1, 4, 7, 8, and 9 were more equivocal, as they were not dominated by a particular set of TB markers, but rather expressed a majority of them (**Figure 2**). They may represent less well-differentiated cytoTB populations.

Clusters 5 and 6, which carry the more definitive hallmark features of placental syncytioTB, occupy the b and a cluster grouping (**Figure 1A**), respectively. However, they also differ markedly in the expression of several genes considered to be highly expressed in placental syncytioTB (**Figure 4A**, **Supplementary Table 4**). Of the 57 genes labeled as syncytioTB-specific in cluster 5 and the 55 genes labeled as syncytioTB-specific in cluster 6, only 18 were in common. Examples of genes up-regulated in cluster 5 compared to cluster 6 include *KRT8, S100P,* and *XAGE2* (**Figure 4B**). The reverse was observed for *ERVV-1*, and *TBX3* (**Figure 4C**), for example. A second endogenous retroviral gene, *ERVW-1*, had much higher expression in cluster 6 than in cluster 5 (expression values 12.76 versus 4.27, respectively). In general, more transcription factors were identified with higher expression in cluster 6 (44 transcription factors) compared to cluster 5 (15 transcription factors).

Cluster 2 (in the major grouping a; **Figure 1A**) and Cluster 3 (group b; **Figure 1A**) each showed most similarity to first trimester human placental extravillousTB. Although the similarity was weak, the clusters also lacked indications of a major contribution of other TB cell types (**Figure 3**). The two are also clearly distinct from each other (**Figure 1A**). Among the transcripts that distinguish Cluster 2 from 3 are ones that encode TLE4, a transcriptional co-repressor that regulates WNT-mediated beta-catenin signaling, the procadherin PCDH9, and MAML2, a co-activator that binds to the intracellular domain of NOTCH receptors (**Supplementary Figure 6**). Cluster 3 noticeably possesses a group of upregulated genes that are overexpressed relative to Cluster 2 and whose functions are linked to the structure and organization of the cytoskeleton. Among these are *ACTG1, TMSB10,* and *TAGLN,* as well as three calcium binding proteins (*S100A11, S100A6*, and *S100A10*) (**Supplementary Figure 6**).

Effects of O_2 Atmosphere

We identified differentially expressed genes between oxygen conditions in clusters 1–8. Cluster 9 is dominated by nuclei from 5% O_2, which did not allow evaluation of differentially expressed genes. The number of differentially expressed genes for clusters 1–8 ranged from 37 to 188 (**Supplementary Table 5**). Of the TB clusters with most similarity to extravillousTB (cluster 2 and cluster 3), and the TB clusters predicted to be syncytioTB (cluster

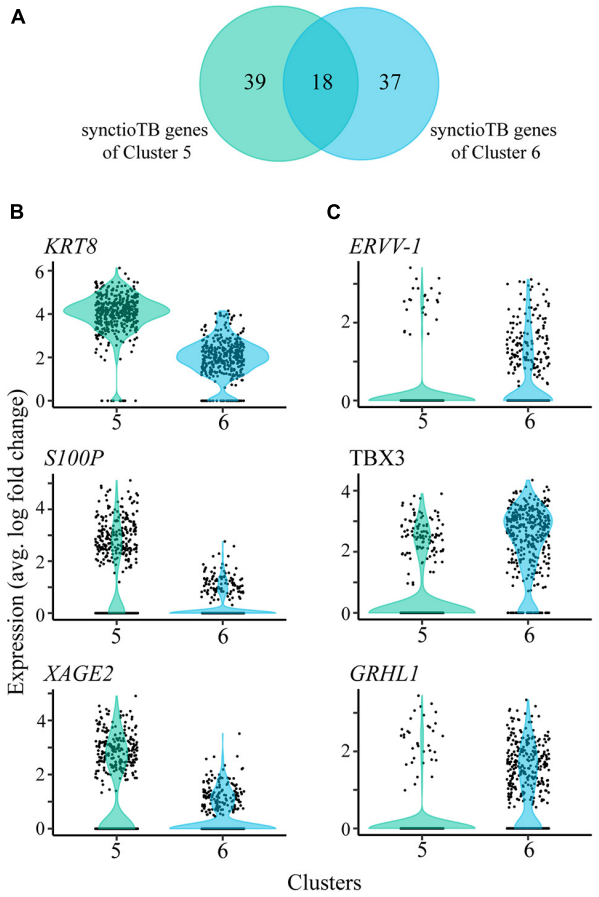

FIGURE 4 | SyncytioTB-specific gene expression profiles. **(A)** Comparison of the SyncytioTB specific genes in clusters 5 and 6. The two clusters have many differentially expressed genes, with some that are more highly expressed in cluster 5 **(B)** and others that are more highly expressed in cluster 6 **(C).**

5 and cluster 6), cluster 5 has the least number of differentially expressed genes (**Supplementary Table 5**). However, all of these clusters include genes associated with metabolism that were up-regulated in the 5% O_2 cultures (SLC2A3). Additionally, there are several other up-regulated transcripts in common in clusters 2,3,5, and 6, such as *CLIC3* and *FN1* (up-regulated in the 5% O_2 cultures) and *APOE*, *COL3A1,* and *LUM* (up-regulated in the 20% O_2 cultures; **Figure 5**, **Supplementary Figure 7**, **Supplementary Table 5**).

Because hypoxia inducible factor (HIF) is important in regulating gene expression in low O_2 conditions, we determined if previously published HIF targets (Ortiz-Barahona et al., 2010; Dengler et al., 2014) were upregulated in cells cultured under 5% O_2. Indeed, we found that in all clusters, HIF targets that were differentially expressed in the data were almost always upregulated in nuclei from 5% O_2 rather than in nuclei from 20% O_2 (**Supplementary Table 6**). Certain HIF targets, such as *EGLN3* and *MMP2*, were upregulated in multiple clusters, whereas others, such as *ADM* and *VEGFA* were only upregulated in one cluster. The significance of these observations remains to be determined.

DISCUSSION

The goals of this research were two. The primary objective was to study the heterogeneity in cells differentiated by the BAP protocol and determine whether there was evidence for the presence of different TB sub-lineages within the population. A second was to determine whether the oxygen atmosphere under which the colonies had been cultured influenced the state of differentiation following eight days of exposure to BAP conditions. Since syncytium, identified by its expression of CGA and CGB, comprises a significant and increasing fraction of the differentiating colonies after about d 5 (Yabe et al., 2016), and because such cellular structures are large and fragile, they were not amenable to scRNAseq analysis. Accordingly, we chose to analyze transcripts present in isolated nuclei, where the issues of cell breakage and size are less likely to confound outcomes. snRNAseq has recently been used to examine transcripts during mouse placental labyrinth development (Marsh and Blelloch, 2020), where the evaluation of syncytial structures by single-cell procedures had proved to be difficult. It is also clear that the single-cell analysis performed on first trimester human placenta by Vento-Tormo et al. (2018) likely lacks a mature syncytioTB component (Roberts et al., 2021).

We note that the number of differentially expressed genes between O_2 conditions was variable across clusters. While many genes were identified in syncytioTB cluster 6 (169 differentially expressed genes), only 44 were identified in syncytioTB cluster 5. These results could be due to the proportion of nuclei associated with each cluster in each condition. Investigating additional stages of differentiation would allow assessing changes in overall cell populations between oxygen conditions. Much more significant differences are expected to occur in early differentiation where high O_2 appears to speed events (Amita et al., 2013), while low O_2 permits later stage catch-up as observed here with hCG production (**Supplementary Figure 1B**).

The data have confirmed what has previously been contested, namely that the BMP4-driven differentiation of pluripotent stem cells results in complete or near-complete conversion to TB. However, a surprise from the analysis was the unexpectedly large number of well-defined clusters and, particularly, the presence of two major groupings (a and b) (**Figure 1A**), each containing distinct syncytioTB, and what appear to be diverse cytoTB components. One particular distinction between grouping a and b was the high expression of the long non-coding RNAs *NEAT1* and *MALAT1* in a, with the latter particularly abundant and, like *CGA*, expressed in almost every nucleus analyzed. Although cluster 9 is distinct from the two groupings, the expression of *NEAT1* and *MALAT1* in this cluster was more similar to grouping b. Other long non-coding RNAs, *H19, SPRY4*, and *HOTAIR* that, like *NEAT1* (Gremlich et al., 2014) and *MALAT1* (Tseng et al., 2009), have been linked to placental TB development and placental pathologies (Basak and Ain, 2019), were expressed relatively weakly and lacked meaningful discriminatory power to distinguish clusters.

It was clear that among the resulting clusters recognized in the Seurat analysis were ones that bore strong similarity to syncytioTB (5 and 6) and weaker similarity to extravillousTB

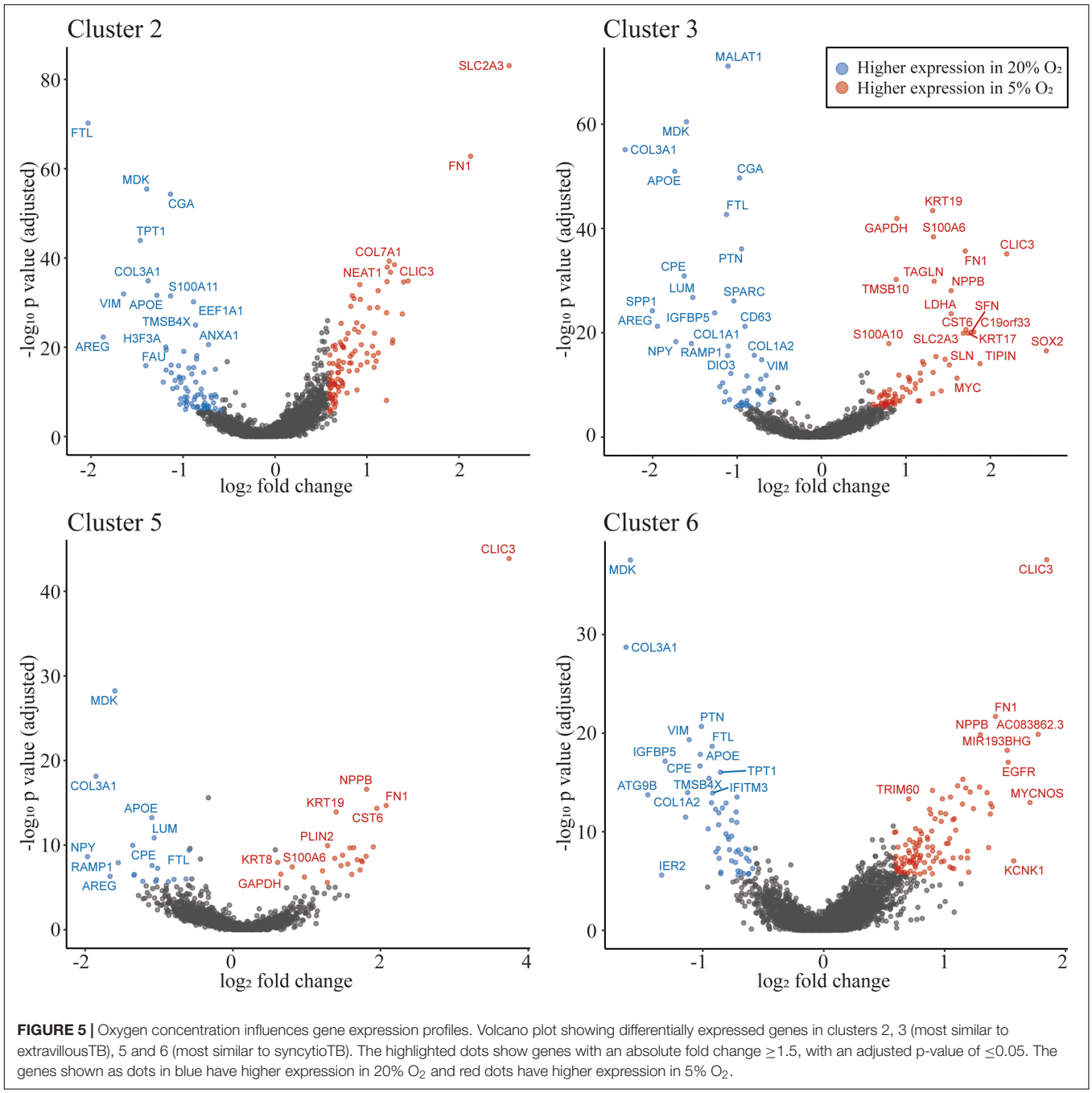

FIGURE 5 | Oxygen concentration influences gene expression profiles. Volcano plot showing differentially expressed genes in clusters 2, 3 (most similar to extravillousTB), 5 and 6 (most similar to syncytioTB). The highlighted dots show genes with an absolute fold change ≥1.5, with an adjusted p-value of ≤0.05. The genes shown as dots in blue have higher expression in 20% O_2 and red dots have higher expression in 5% O_2.

(2 and 3) of first trimester placental TB. The enrichment for extravillousTB was non-significant in cluster 2, and there were only four genes (*PAPPA2, GCSH*, *ADAM12*, and *ASPSCR1*) contributing to the enrichment. Nevertheless, cluster 2, although clearly expressing TB markers, did not have similarities to any other placenta cell populations (**Figure 3B**). Other clusters, for example 4 and 1, that clearly did not conform strongly to either of these two sub-lineages but were sandwiched between them in the Seurat plots (**Figure 1A**), also expressed classical human TB markers and likely represented forms of cytoTB. We suspect that the upper regions of these two putative cytoTB clusters represent cells providing a source of syncytioTB and that their lower regions are precursors of extravillousTB. Even the more enigmatic clusters, 7, 8, and 9, display multiple TB markers, but what cell types they represent in the tissue culture colonies from which they were derived remains as yet unclear. Even within the clusters, there is additional heterogeneity. For example, the lower tip of cluster 3 and cluster 9 uniquely express *SOX2* (**Supplementary Figure 8**), suggesting a shared origin. In scRNAseq studies on human placentas weeks 8 and 24 of gestation (Liu et al., 2018), in first trimester (weeks 6–11) material (Suryawanshi et al., 2018), and even in blastocyst-like structures

engineered from reprogrammed fibroblasts (Liu et al., 2021), it also has become clear that there are multiple distinguishable populations of cytoTBs. In the study of Liu et al. there were also three extravillousTB types (Liu et al., 2018). Moreover, cellular phenotypes as defined in terms of transcript content changed markedly between week 8 and week 24 of gestation (Liu et al., 2018). Perhaps it should be no surprise that multiple kinds of TBs comprise these cell populations derived directly from ESCs, which we have hypothesized likely represent the very early stages of *in vivo* placentation. A planned time-course experiment beginning when differentiation is initiated should enable us to infer cluster origins and interrelationships in a more complete manner.

Our ability to define two distinct syncytioTB clusters (5 and 6) is of particular interest. Do these nuclei represent different kinds of syncytioTB or nuclei with different cytoTB origins in a single type of syncytioTB? The fact that the transcripts for the presumed fusogens, ERVW-1 and ERVV-1, were primarily marker genes for nuclei in cluster 6 and less well expressed in cluster 5 could be evidence that syncytioTB formation requires the interaction of two select populations of presumptive syncytioTBs, one of which expresses the necessary syncytins (ERVs) on their surfaces, the other possibly bearing the appropriate "receptor" factors. Similarly, the absence of *MFSD2A*, which encodes the proposed receptor for ERVFRD-1, another proposed fusogen (Roberts et al., 2021), is puzzling. Perhaps another fusion partner for ERVFRD-1 exists or syncytialization of these TBs occurs without the involvement of ERVFRD-1, which has quite low expression in these preparations of ESC-derived TB.

Another observation of note is that *CGA*, whose translation product partners with one of the CGB isoforms to form the active placental hormone hCG, is expressed in most, if not all, nuclei (**Figure 2**), yet the protein itself can normally be detected only in syncytioTB and what appear to be its immediate precursor syncytioTB when H1 ESCs are differentiated to syncytioTB (Amita et al., 2013; Yabe et al., 2016). There seems to be three possible explanations: (1) *CGA* mRNA is not translated in cells that are not progressing to syncytioTB; (2) the protein product CGA is highly unstable in the context of cells outside the syncytial area and in absence of expression of its partner CGB with which it forms the hCG heterodimer; (3) *CGA* transcripts are unable to exit the nucleus for translation except in syncytioTB. Gene expression changes that are primarily regulated at the protein level have been noted previously in the mouse placenta and other cell types (Abdulghani et al., 2019). In fact, a general rule is that mRNA concentrations are relatively poor guides to protein levels (Ghaemmaghami et al., 2003; Ghazalpour et al., 2011; Schwanhausser et al., 2011). A number of other highly expressed transcripts, for example those for *GABRP* and *VTCN1*, are also abundant across clusters yet their proteins are restricted to emerging syncytioTB in BAP colonies. They are also expressed in placenta where they are localized to villous syncytioTB, primarily to the first trimester of pregnancy (Karvas et al., 2020). Interestingly, expression of the CD274 molecule, perhaps better known as B7-H1 or programmed cell death 1 ligand 1, also appears to be controlled at the translational level in placental TB cells (Holets et al., 2009). Both VTCN1 and CD274 bind to receptors on lymphocytes. In cancer cells and possibly in TB they are considered regulators of immune tolerance (Holets et al., 2006; Schust et al., 2021).

In summary, the BAP model, which we have proposed represents TB associated with the implanting conceptus, reveals a relatively complex picture of TB emergence, including the appearance of at least two kinds of syncytioTB nuclei plus multiple cytoTB populations. Conducting similar analyses at earlier time points should elucidate how these lineages arose and diverged and perhaps provide insights into what occurs during the very earliest stages of human embryonic development. Such studies may also be revealing about how syncytioTB arises, mechanisms of cell fusion, and the possible roles of the non-coding RNAs *MALAT1* and *NEAT1,* and various transcription factors in directing events.

DATA AVAILABILITY STATEMENT

The datasets presented in this study can be found in online repositories. The names of the repository/repositories and accession number(s) can be found below: https://www.ncbi.nlm.nih.gov/geo/, GSE171768. The GitHub repository documenting all the analyses is available at https://github.com/Tuteja-Lab/BAP.hESC.d8_.

AUTHOR CONTRIBUTIONS

TK, AS, JZ, NB, and TE performed the experiments. RR and TE conceived the project. RR, TE, TK, AS, and GT designed the study and were responsible for data interpretation. RR, TK, AS, and GT wrote the manuscript with contributions from all authors. RR, TE, GT, and DS sponsored the project through grants. All authors contributed to the article and approved the submitted version.

FUNDING

The authors' research is supported by grants 1R01HD094937 and 1R21A1145071 from the National Institutes of Health.

ACKNOWLEDGMENTS

We acknowledge the assistance of Mingyi Zhou and Ellen Kesler of the University of Missouri DNA Core for preparing libraries and generation of sequence. Christopher Bottoms of the University of Missouri Informatics Research Core assisted with initial data processing.

SUPPLEMENTARY MATERIAL

The Supplementary Material for this article can be found online at: https://www.frontiersin.org/articles/10.3389/fcell.2021.695248/full#supplementary-material

REFERENCES

Abdulghani, M., Song, G., Kaur, H., Walley, J. W., and Tuteja, G. (2019). Comparative Analysis of the Transcriptome and Proteome during Mouse Placental Development. *J. Proteome. Res.* 18, 2088–2099. doi: 10.1021/acs.jproteome.8b00970

Amita, M., Adachi, K., Alexenko, A. P., Sinha, S., Schust, D. J., Schulz, L. C., et al. (2013). Complete and unidirectional conversion of human embryonic stem cells to trophoblast by BMP4. *Proc. Natl. Acad. Sci. USA* 110, E1212–E1221.

Basak, T., and Ain, R (2019). Long non-coding RNAs in placental development and disease. *Non-Coding RNA Invest.* 3, 1–26.

Boyd, J. D., and Hamilton, W. J. (1970). *The human placenta*. Cambridge, MA: Heffer and Sons.

Das, P., Ezashi, T., Schulz, L. C., Westfall, S. D., Livingston, K. A., and Roberts, R. M. (2007). Effects of fgf2 and oxygen in the bmp4-driven differentiation of trophoblast from human embryonic stem cells. *Stem Cell Res.* 1, 61–74. doi: 10.1016/j.scr.2007.09.004

Deglincerti, A., Croft, G. F., Pietila, L. N., Zernicka-Goetz, M., Siggia, E. D., and Brivanlou, A. H. (2016). Self-organization of the in vitro attached human embryo. *Nature* 533, 251–254. doi: 10.1038/nature17948

Dengler, V. L., Galbraith, M., and Espinosa, J. M. (2014). Transcriptional regulation by hypoxia inducible factors. *Crit. Rev. Biochem. Mol. Biol.* 49, 1–15. doi: 10.3109/10409238.2013.838205

10x Genomics (2019). *Chromium Single Cell V(D)J Reagent Kits With Feature Barcoding Technology for Cell Surface Protein, Document Number CG000186 Rev A, (2019, July 25)*. Pleasanton, CA: 10x Genomics.

Ghaemmaghami, S., Huh, W. K., Bower, K., Howson, R. W., Belle, A., Dephoure, N., et al. (2003). Global analysis of protein expression in yeast. *Nature* 425, 737–741.

Ghazalpour, A., Bennett, B., Petyuk, V. A., Orozco, L., Hagopian, R., Mungrue, N., et al. (2011). Comparative analysis of proteome and transcriptome variation in mouse. *PLoS Genet.* 7:e1001393. doi: 10.1371/journal.pgen.1001393

Gremlich, S., Damnon, F., Reymondin, D., Braissant, O., Schittny, J. C., Baud, D., et al. (2014). The long non-coding RNA NEAT1 is increased in IUGR placentas, leading to potential new hypotheses of IUGR origin/development. *Placenta* 35, 44–49. doi: 10.1016/j.placenta.2013.11.003

Hertig, A. T., Rock, J., and Adams, E. C. (1956). A description of 34 human ova within the first 17 days of development. *Am. J. Anat.* 98, 435–493. doi: 10.1002/aja.1000980306

Holets, L. M., Carletti, M. Z., Kshirsagar, S. K., Christenson, L. K., and Petroff, M. G. (2009). Differentiation-induced post-transcriptional control of B7-H1 in human trophoblast cells. *Placenta* 30, 48–55. doi: 10.1016/j.placenta.2008.10.001

Holets, L. M., Hunt, J. S., and Petroff, M. G. (2006). Trophoblast CD274 (B7-H1) is differentially expressed across gestation: influence of oxygen concentration. *Biol. Reprod.* 74, 352–358. doi: 10.1095/biolreprod.105.046581

Horii, M., Bui, T., Touma, O., Cho, H. Y., and Parast, M. M. (2019). An Improved Two-Step Protocol for Trophoblast Differentiation of Human Pluripotent Stem Cells. *Curr. Protoc. Stem. Cell. Biol.* 50:e96.

Horii, M., Touma, O., Bui, T., and Parast, M. M. (2020). Modeling human trophoblast, the placental epithelium at the maternal fetal interface. *Reproduction* 160, R1–R11.

Jain, A., and Tuteja, G. (2019). TissueEnrich: Tissue-specific gene enrichment analysis. *Bioinformatics* 35, 1966–1967. doi: 10.1093/bioinformatics/bty890

Jain, A., and Tuteja, G. (2021). PlacentaCellEnrich: a tool to characterize gene sets using placenta cell-specific gene enrichment analysis. *Placenta* 103, 164–171. doi: 10.1016/j.placenta.2020.10.029

Jain, A., Ezashi, T., Roberts, R. M., and Tuteja, G. (2017). Deciphering transcriptional regulation in human embryonic stem cells specified towards a trophoblast fate. *Sci. Rep.* 7:17257.

Karvas, R. M., McInturf, S., Zhou, J., Ezashi, T., Schust, D. J., Roberts, R. M., et al. (2020). Use of a human embryonic stem cell model to discover GABRP, WFDC2, VTCN1 and ACTC1 as markers of early first trimester human trophoblast. *Mol. Hum. Reprod.* 26, 425–440. doi: 10.1093/molehr/gaaa029

Liu, X., Tan, J. P., Schröder, J., Aberkane, A., Ouyang, J. F., Mohenska, M., et al. (2021). Modelling human blastocysts by reprogramming fibroblasts into iBlastoids. *Nature* 2021, 1–6.

Liu, Y., Fan, X., Wang, R., Lu, X., Dang, Y. L., Wang, H., et al. (2018). Single-cell RNA-seq reveals the diversity of trophoblast subtypes and patterns of differentiation in the human placenta. *Cell Res.* 28, 819–832. doi: 10.1038/s41422-018-0066-y

Lv, B., An, Q., Zeng, Q., Zhang, X., Lu, P., Wang, Y., et al. (2019). Single-cell RNA sequencing reveals regulatory mechanism for trophoblast cell-fate divergence in human peri-implantation conceptuses. *PLoS Biol.* 17:e3000187. doi: 10.1371/journal.pbio.3000187

Marchand, M., Horcajadas, J. A., Esteban, F. J., McElroy, S. L., Fisher, S. J., and Giudice, L. C. (2011). Transcriptomic signature of trophoblast differentiation in a human embryonic stem cell model. *Biol. Reprod.* 84, 1258–1271. doi: 10.1095/biolreprod.110.086413

Marsh, B., and Blelloch, R. (2020). Single nuclei RNA-seq of mouse placental labyrinth development. *eLife* 9:e60266.

Ng, Y. H., Zhu, H., and Leung, P. C. (2012). Twist modulates human trophoblastic cell invasion via regulation of N-cadherin. *Endocrinology* 153, 925–936. doi: 10.1210/en.2011-1488

Ortiz-Barahona, A., Villar, D., Pescador, N., Amigo, J., and del Peso, L. (2010). Genome-wide identification of hypoxia-inducible factor binding sites and target genes by a probabilistic model integrating transcription-profiling data and in silico binding site prediction. *Nucleic Acids Res.* 38, 2332–2345. doi: 10.1093/nar/gkp1205

Roberts, R. M., Ezashi, T., Schulz, L. C., Sugimoto, J., Schust, D. J., Khan, T., et al. (2021). Syncytins expressed in human placental trophoblast. *Placenta* 2021:006

Roberts, R. M., Ezashi, T., Sheridan, M. A., and Yang, Y. (2018). Specification of trophoblast from embryonic stem cells exposed to BMP4. *Biol. Reprod.* 99, 212–224. doi: 10.1093/biolre/ioy070

Schneider, V. A., Graves-Lindsay, T., Howe, K., Bouk, N., Chen, H.-C., Kitts, P. A., et al. (2017). Evaluation. *Genome. Res.* 27, 849–864.

Schulz, L. C., Ezashi, T., Das, P., Westfall, S. D., Livingston, K. A., and Roberts, R. M. (2008). Human embryonic stem cells as models for trophoblast differentiation. *Placenta* 29, S10–S16.

Schust, D. J., Bonney, E. A., Sugimoto, J., Ezashi, T., Roberts, R. M., Choi, S., et al. (2021). The Immunology of Syncytialized Trophoblast. *Int. J. Mol. Sci.* 22, 1767. doi: 10.3390/ijms22041767

Schwanhausser, B., Busse, D., Li, N., Dittmar, G., Schuchhardt, J., Wolf, J., et al. (2011). Global quantification of mammalian gene expression control. *Nature* 473, 337–342. doi: 10.1038/nature10098

Shahbazi, M. N., Jedrusik, A., Vuoristo, S., Recher, G., Hupalowska, A., Bolton, V., et al. (2016). Self-organization of the human embryo in the absence of maternal tissues. *Nat. Cell. Biol.* 18, 700–708. doi: 10.1038/ncb3347

Stuart, T., Butler, A., Hoffman, P., Hafemeister, C., Papalexi, E., Mauck, W. M. III, et al. (2019). Comprehensive integration of single-cell data. *Cell* 177, 1888–1902.

Suryawanshi, H., Morozov, P., Straus, A., Sahasrabudhe, N., Max, K. E. A., Garzia, A., et al. (2018). A single-cell survey of the human first-trimester placenta and decidua. *Sci. Adv.* 4:eaau4788. doi: 10.1126/sciadv.aau4788

Telugu, B. P., Adachi, K., Schlitt, J. M., Ezashi, T., Schust, D. J., Roberts, R. M., et al. (2013). Comparison of extravillous trophoblast cells derived from human embryonic stem cells and from first trimester human placentas. *Placenta* 34, 536–543. doi: 10.1016/j.placenta.2013.03.016

Tseng, J. J., Hsieh, Y. T., Hsu, S. L., and Chou, M. M. (2009). Metastasis associated lung adenocarcinoma transcript 1 is up-regulated in placenta previa increta/percreta and strongly associated with trophoblast-like cell invasion in vitro. *Mol. Hum. Reprod.* 15, 725–731. doi: 10.1093/molehr/gap071

Vento-Tormo, R., Efremova, M., Botting, R. A., Turco, M. Y., Vento-Tormo, M., Meyer, K. B., et al. (2018). Single-cell reconstruction of the early maternal-fetal interface in humans. *Nature* 563, 347–353.

West, R. C., Ming, H., Logsdon, D. M., Sun, J., Rajput, S. K., Kile, R. A., et al. (2019). Dynamics of trophoblast differentiation in peri-implantation-stage human embryos. *Proc. Natl. Acad. Sci. USA* 116:22635. doi: 10.1073/pnas.1911362116

Wilcox, A. J., Weinberg, C. R., O'Connor, J. F., Baird, D. D., Schlatterer, J. P., Canfield, R. E., et al. (1988). Incidence of early loss of pregnancy. *N. Engl. J. Med.* 319, 189–194.

Xu, R. H., Chen, X., Li, D. S., Li, R., Addicks, G. C., Glennon, C., et al. (2002). BMP4 initiates human embryonic stem cell differentiation to trophoblast. *Nat. Biotechnol.* 20, 1261–1264. doi: 10.1038/nbt761

Yabe, S., Alexenko, A. P., Amita, M., Yang, Y., Schust, D. J., Sadovsky, Y., et al. (2016). Comparison of syncytiotrophoblast generated from human embryonic stem cells and from term placentas. *Proc. Natl. Acad. Sci. USA* 113, E2598–E2607.

Yang, Y., Adachi, K., Sheridan, M. A., Alexenko, A. P., Schust, D. J., Schulz, L. C., et al. (2015). Heightened potency of human pluripotent stem cell lines created by transient BMP4 exposure. *Proc. Natl. Acad. Sci. USA* 112, E2337–E2346.

Zheng, G. X., Terry, J. M., Belgrader, P., Ryvkin, P., Bent, Z. W., Wilson, R., et al. (2017). Massively parallel digital transcriptional profiling of single cells. *Nat. Commun*. 8:14049. doi: 10.1038/ncomms14049

Zhou, F., Wang, R., Yuan, P., Ren, Y., Mao, Y., Li, R., et al. (2019). Reconstituting the transcriptome and DNA methylome landscapes of human implantation. *Nature* 572, 660–664. doi: 10.1038/s41586-019-1500-0

Zhou, J., West, R. C., Ehlers, E. L., Ezashi, T., Schulz, L. C, Roberts, R. M., et al. (2021). Modeling human peri-implantation placental development and function. *Biol. Reprod.* 105, 40–51. doi: 10.1093/biolre/ioab080

Conflict of Interest: The authors declare that the research was conducted in the absence of any commercial or financial relationships that could be construed as a potential conflict of interest.

frontiers in Cell and Developmental Biology

ORIGINAL RESEARCH
published: 03 September 2021
doi: 10.3389/fcell.2021.702046

Transcriptomic Drivers of Differentiation, Maturation, and Polyploidy in Human Extravillous Trophoblast

*Robert Morey[1,2,3], Omar Farah[1,3], Sampada Kallol[1,3], Daniela F. Requena[1,3], Morgan Meads[1,3], Matteo Moretto-Zita[1,3], Francesca Soncin[1,3], Louise C. Laurent[2,3] and Mana M. Parast[1,3]**

[1] Department of Pathology, University of California, San Diego, La Jolla, CA, United States, [2] Department of Obstetrics, Gynecology, and Reproductive Sciences, Division of Maternal-Fetal Medicine, University of California, San Diego, La Jolla, CA, United States, [3] Sanford Consortium for Regenerative Medicine, University of California, San Diego, La Jolla, CA, United States

OPEN ACCESS

Edited by:
Geetu Tuteja,
Iowa State University, United States

Reviewed by:
Kaiyu Kubota,
National Agriculture and Food Research Organization (NARO), Japan
Alexander Beristain,
University of British Columbia, Canada

***Correspondence:**
Mana M. Parast
mparast@health.ucsd.edu

Specialty section:
This article was submitted to Developmental Epigenetics, a section of the journal Frontiers in Cell and Developmental Biology

Received: 29 April 2021
Accepted: 27 July 2021
Published: 03 September 2021

Citation:
Morey R, Farah O, Kallol S, Requena DF, Meads M, Moretto-Zita M, Soncin F, Laurent LC and Parast MM (2021) Transcriptomic Drivers of Differentiation, Maturation, and Polyploidy in Human Extravillous Trophoblast. Front. Cell Dev. Biol. 9:702046. doi: 10.3389/fcell.2021.702046

During pregnancy, conceptus-derived extravillous trophoblast (EVT) invades the endomyometrium, anchors the placenta to the maternal uterus, and remodels the spiral arteries in order to establish maternal blood supply to the fetoplacental unit. Recent reports have described early gestation EVT as polyploid and senescent. Here, we extend these reports by performing comprehensive profiling of both the genomic organization and transcriptome of first trimester and term EVT. We define pathways and gene regulatory networks involved in both initial differentiation and maturation of this important trophoblast lineage at the maternal–fetal interface. Our results suggest that like first trimester EVT, term EVT undergoes senescence and endoreduplication, is primarily tetraploid, and lacks high rates of copy number variations. Additionally, we have highlighted senescence and polyploidy-related genes, pathways, networks, and transcription factors that appeared to be important in normal EVT differentiation and maturation and validated a key role for the unfolded protein response in this context.

Keywords: extravillous trophoblast, placenta, polyploid, senescence, cytotrophoblast

INTRODUCTION

The human placenta is essential for successful pregnancy and unique in its transitory nature. It performs a multitude of functions, including gas and nutrient exchange, synthesis of pregnancy-specific signaling molecules, and induction of maternal immunological tolerance. The placenta is also unique in its invasive nature. Early in development, the placenta displays tumor-like properties as one of its component cell types, the extravillous trophoblast (EVT), aggressively invades the endomyometrium of the maternal uterus, and remodels the spiral arteries (Pijnenborg et al., 1980). EVTs arise from the proliferative epithelial stem cells of the placenta, the cytotrophoblast (CTB),

and exit the cell cycle as they differentiate and invade. EVTs share many of the molecular hallmarks of cancer cells (Ferretti et al., 2007), one of which is the frequent occurrence of structural genomic rearrangements and aneuploidy (Sansregret and Swanton, 2017). Trophoblast giant cells (TGCs), the mouse equivalent to EVTs, are known to be highly polyploid (Barlow and Sherman, 1972; Zybina et al., 2011), meaning that they possess more than two sets of chromosomes and undergo endoreduplication, a process by which cells undergo DNA replication in the absence of subsequent cell division (Fox and Duronio, 2013). Further studies have shown that TGCs harbor consistent regions of copy number variation (CNV) that may function as an important mode of genome regulation (Hannibal et al., 2014; Hannibal and Baker, 2016). Compared with rodents, there are only a small number of previous studies examining human trophoblast polyploidy or genomic CNVs (Zybina et al., 2002, 2004; Weier et al., 2005; Meinhardt et al., 2015). One such study in the human placenta showed an enrichment of CNVs, suggesting that, as in the mouse, the human placenta contains an atypical genome architecture that is important for the normal function of the organ (Kasak et al., 2015). Recently, however, another study focused on invasive EVT in first trimester human placenta and reported that, unlike mouse TGCs, these cells did not contain CNVs but were predominantly tetraploid, and potentially undergo senescence and endoreduplication (Velicky et al., 2018). However, to date, similar analysis of term EVT has not been done.

At the same time, several groups, including ours, have characterized the transcriptome of human first trimester EVT using microarray-based profiling (Apps et al., 2011; Telugu et al., 2013; Tilburgs et al., 2015; Wakeland et al., 2017). These studies have shown that, compared with their CTB precursors, EVTs down-regulate pathways involving cell cycle, oxidative phosphorylation, p53, and fatty acid metabolism while upregulating those involved in immune response, hypoxia- and hypoxia-inducible factor, mTOR signaling, and epithelial–mesenchymal transition (EMT), of which the latter has been most extensively studied during EVT differentiation (Apps et al., 2011; Telugu et al., 2013; Dasilva-Arnold et al., 2015; Tilburgs et al., 2015; Davies et al., 2016; Wakeland et al., 2017). Nevertheless, there is a paucity of data, both on the gene expression profile of term EVT and on gene regulatory networks associated with EVT differentiation, maturation, and polyploidy.

Here, we aimed to extend the recent studies discussed above by performing comprehensive profiling of the genomic organization and transcriptome of first trimester and term EVT. To this end, we have used single-cell and bulk whole genome sequencing (WGS) data, along with SNP genotyping, to investigate CNVs in first trimester and term EVT, compared with CTB and umbilical cord mesenchymal stem cells. We also used RNA sequencing to characterize the transcriptomes of both first trimester and term CTB and EVT, in order to identify pathways involved in EVT differentiation and maturation, as well as those that play a role in establishment of polyploidy in these cells. We also use the newly developed method of human trophoblast stem cell (hTSC) derivation and differentiation (Okae et al., 2018) to evaluate development of polyploidy in *in vitro*-differentiated EVT, and to validate the unfolded protein response (UPR) as a newly identified pathway involved in EVT function. Finally, we also analyze our RNA-seq data to identify the TF networks involved in normal EVT formation and function.

MATERIALS AND METHODS

Placenta Samples, Cell Isolation, and EVT Differentiation

Human placental tissues were collected under a UCSD Human Research Protections Program Committee Institutional Review Board-approved protocol; all patients provided informed consent for collection and use of these tissues. Cells were isolated from a total of 46 normal placentae, 27 first trimester and 19 term (**Supplementary Table 1**). Gestational age (GA) is stated in weeks and days since the last menstrual period. For first trimester placentae, "normal" refers to elective termination of pregnancy in the absence of structural fetal abnormalities; for third trimester placentae (term), "normal" is defined by a non-hypertensive, non-diabetic singleton pregnancy, where the placenta is normally grown and shows no gross or histological abnormalities.

Isolation of CTB and EVT from 20 term placentae (37–41 weeks GA) was performed as previously described in Li et al. (2013). Briefly, the placentae were obtained immediately after C-section and placed on ice. Tissue from the basal plate (for EVT) and chorionic portion (for CTB) was dissected and minced, rinsed in 1 × PBS (Corning), and digested for 20 min in 1 × Ca/Mg-free Hanks' Balanced Salt Solution (HBSS; Gibco), 1 × trypsin (Gibco), collagenase, and DNase (Roche) three times, discarding the supernatant after each digestion. A Percoll® gradient (Sigma-Aldrich) centrifugation separation was then performed. Cells were then subjected to positive selection using magnetic activated cell sorting (MACS; Miltenyi Biotec) and a PE-conjugated antibody against HLA-G (EXBIO MEM-G/9). The bound fraction was collected and tested for purity using flow cytometry. EVT preparations that contained greater than 90% HLA-G^+ cells were considered as adequate and used in downstream experiments. The unbound fraction was collected, and CTB was selected using APC-conjugated antibody against EGFR (Biolegend #352906) and tested for purity using flow cytometry. CTB preparations yielding greater than 90% EGFR positivity were considered adequate and used in downstream experiments. Isolation of primary first trimester (9–14 weeks GA) trophoblast cells from 27 placenta samples was performed as previously described in Wakeland et al. (2017) and Soncin et al. (2018). Briefly, chorionic villi were minced, washed in HBSS (Gibco), and digested three times with DNase I (Roche), and trypsin (Gibco). The cells were then pelleted, separated on a Percoll gradient (Sigma-Aldrich) and subjected to sequential MACS selection similar to the term placental samples.

Human trophoblast stem cell lines were derived from early first trimester (6–7 weeks GA) placentae as previously described by Okae et al. (2018). Briefly, placental villi were minced, enzymatically digested, and then filtered. After Percoll® separation, the cells in the trophoblast fraction were

MACS-purified with a PE-conjugated anti-ITGA6 antibody (Biolegend #313612; cell line 1,049) or an APC-conjugated anti-EGFR antibody (Biolegend #352906; cell line 1,048). The 1270C hTSC line was derived directly from the trophoblast fraction (after Percoll gradient) of the chorionic side of the placental tissue (manually separated from the basal side). Cells were then plated on collagen IV-coated 6-well plates for at least 1 h on TS media as described previously in Okae et al. (2018). Cells were first grown in modified basal media (advanced DMEM/F12, N2/B27 supplements, 2 mM glutamine, 10 μM 1-thioglycerol, 0.05% BSA, and 1% KSR). The media was then changed to modified complete media (basal media with the addition of 2 μM CHIR99021, 500 nM A83-01, 1 μM SB431542, 5 μM Y-27632, 0.8 mM valproic acid sodium, 100 ng/ml FGF2, 50 ng/ml EGF, 20 ng/ml Noggin, and 50 ng/ml HGF) and grown to 80% confluency. Cells were passaged using TrypLE incubated for 15 min at 37°C. To characterize the trophoblast stem cell identity of these cells, their transcriptome was compared with that of cells derived by Okae et al. (2018), as well as to primary CTB and EVT; our TSCs were found to cluster with both the embryo- and placenta-derived Okae TSC (**Supplementary Figure 4**). EVT differentiation was performed by plating 0.75×10^5 cells in a 6-well plate precoated with 20 μg/ml fibronectin using the EVT differentiation media described in Okae et al. (2018; DMEM/F12 supplemented with 0.1 mM 2-mercaptoethanol, 0.3% BSA, 1% ITS-X supplement, 100 ng/ml NRG1, 7.5 μM A83-01, 2.5 μM Y27632, 2% Matrigel, and 4% KnockOut Serum Replacement). On day 3, the medium was replaced with EVT medium lacking NRG1, and Matrigel was added to a final concentration of 0.5%. On day 5, the cells reached 80% confluency and were dissociated using TrypLE for 13 min at 37°C. The cells were assessed for differentiation efficiency by flow cytometric analysis using antibodies against HLA-G (EXBIO MEM-G/9) and EGFR (Biolegend #352906). For experiments evaluating the UPR pathway during EVT differentiation, the media was supplemented with 30 μM 4u8C (Sigma-Aldrich) or equivalent (vol/vol) amount of DMSO carrier.

Human umbilical cord (UC) was collected aseptically under a protocol approved by the Human Research Protections Program Committee of the UCSD Institutional Review Board (IRB number: 181917X). All patients provided informed consent for collection and use of these tissues, and all experiments were performed within guidelines and regulations set forth by the IRB. Umbilical cord mesenchymal stem cells (UC-MSCs) were derived from minced UC tissue per a published protocol (Ishige et al., 2009; Yang et al., 2014). UC samples were collected and processed within 24 h of delivery. Briefly, UCs were minced, washed to remove blood, and then cultured in basal medium [aMEM with nucleosides (ThermoFisher), containing 10% MSC-qualified FBS (Omega Scientific)]. Cultures were maintained in a humidified atmosphere with 5% CO_2 at 37°C. Approximately 3 weeks after plating, adherent fibroblast-like cells were detached using TrypLE Express for 5 min at 37°C (ThermoFisher) and filtered to remove any tissue fragments. The collected cells were then reseeded and maintained in growth medium containing b-FGF. After 2 weeks of growth with medium replacement every 3 days, the cells were checked for purity by flow cytometry analysis (BD FACSCanto 2 HTS). Cells were assessed for the expression of CD73 (FITC Mouse Anti-Human CD73—BD #561254) and the absence of CD31 (APC-Cy^{TM}7 Mouse Anti-Human CD31—BD #563653) and CD45 (APC Mouse Anti-Human CD45—BD #560973). UC-MSC samples displayed CD73 expression in over 90% of cells and lacked expression of CD31 and CD45. Sex of first trimester samples was determined based on PCR for SRY.

WGS Reanalysis

Whole genome sequencing fastq files from matched, isolated EGFR$^+$ and HLA-G$^+$ trophoblasts from two patients (11–12 weeks GA) were downloaded from BioProject (accession no. PRJNA445189; Velicky et al., 2018). The fastq files were trimmed (trim_galore v.0.4.1) using a quality score cut-off of 30. The samples were then mapped to GRCh38 using Bowtie2 (v.2.2.7; Langmead and Salzberg, 2012). ERDS 1.1 was used to call CNVs on patient 1 using the erds_pipeline.pl script (Zhu et al., 2012) with default parameters. CNV's found in both the EGFR$^+$ and HLA-G$^+$ samples were filtered out. Variants were called using GATK (v 4.0.11.0) on EGFR$^+$ and HLA-G$^+$ samples from both patients. Briefly, after merging replicate samples, duplicates were marked using Picard (v.2.18.15), base quality scores were recalibrated, and variants were called using HaplotypeCaller. Joint genotyping followed by SNP and InDel recalibration was then performed according to GATK best practices. Low quality variants (GQ $<$ 20.0) were then removed, and resulting vcf files were used to run PURPLE (PURity and PLoidy Estimator; Cameron et al., 2019). To run PURPLE, Amber3 (v.3.1) and Colbalt (v.1.8) were first run in "reference/tumor" mode with the EGFR$^+$ sample used as the reference sample and the matched HLA-G$^+$ sample used as the "tumor" sample.

Single-Cell RNA-seq Reanalysis and InferCNV

Single-cell data were downloaded from the European Genome-Phenome Archive (EGA; https://www.ebi.ac.uk/ega/) hosted by the European Bioinformatics Institute (EBI; accession no. EGAS00001002449). Data from only the "normal" placenta samples (PN1, PN2, PN3C, PN3P, and PN4; 38 weeks GA) were used in the InferCNV (inferCNV of the Trinity CTAT Project, https://github.com/broadinstitute/inferCNV) analysis (Patel et al., 2014). PN2 was determined to be an outlier and was removed prior to cell cycle analysis. Prior to running InferCNV, data were analyzed using Scanpy (v.1.4.3; Wolf et al., 2018). Briefly, quality control was performed, and data were filtered and batch corrected before dimensionality reduction and Louvain clustering. Cell cycle analysis was done using Scanpy's "score_genes_cell_cycle" command and gene sets determined previously (Macosko et al., 2015). Clusters were then annotated by ranking marker genes obtained by performing a modified *t*-test between each cluster and the remaining cells. Sub-clustering was performed on clusters that were not readily identifiable. Two EVT clusters were annotated and used downstream in the inferCNV algorithm as the "tumor" cells. All other annotated cells were considered part of the

"normal" reference cells. Anscombe_transform normalization was used before running inferCNV to remove noisy variation at low counts, and the parameter HMM_type "i3" was used to perform inferCNV.

SNP Genome-Wide Genotyping and CNV Detection

DNA was isolated from placental cell pellets from two first trimester and three term placentae (Qiagen DNeasy Blood and Tissue kit) and quantified (Qubit dsDNA BR Assay Kits, Thermo Fisher Scientific) according to the manufacturer's protocol. DNA was genotyped using Illumina InfiniumOmni2-5-8v1-4 BeadChips (∼2,381,000 markers with a median spacing of 0.65 kb) at the IGM Genomics Center at UC San Diego. Samples were called in GenomeStudio (Illumina) with an average overall call rate of 99.4%. The CTB sample from one patient (1,391) was removed from the analysis due to a low call rate (91.3%). CNVs were identified using the cnvPartition Plug-in (v.3.2.0) in GenomeStudio. The cnvPartition confidence threshold was set at 100, with a minimum number of SNPs per CNV region of 10. The R (v.3.6.1) package, allele-specific copy number analysis of tumors (ASCAT; v.2.5.2; Van Loo et al., 2010), was used to estimate the ploidy of EVT samples. LogR ratios and BAF values were exported from GenomeStudio, and no GC wave correction was performed. EVT samples were considered "tumor" samples, and matched UC-MSCs were used as "reference" samples.

Single-Cell CNV Detection

Matched EVTs, CTBs, and UC-MSCs from three term placentae were obtained as detailed above and following isolation were flash frozen. Cells were thawed and immediately resuspended into a single-cell suspension with 1 × PBS and 0.04% BSA and filtered through a Flowmi cell strainer (Belart) before beginning the 10 × Genomics single-cell DNA library prep. Briefly, between 100 and 500 cells in each sample were encapsulated in a hydrogel matrix and lysed, and then the genomic DNA was denatured and captured on a second microfluidic chip in Gel Beads containing unique cell indexes. After creation of amplified barcoded DNA fragments, sequencing libraries were created and sequenced on a NovaSeq at the IGM Genomics Center at UC San Diego. Cell Ranger (v 1.1.0; 10 × Genomics) DNA CNV pipeline was run to associate individual reads back to the individual cell. The reads were mapped to GRCh38, and downstream analysis was performed in LoupeBrowser. Each sample had on average over 1 million mapped and deduplicated reads per cell and a median estimated CNV resolution of less than 1 Mb.

Flow Cytometric-Based Ploidy Analysis

Matched EVT and CTB and matched EVT, CTB, and UC-MSC were isolated from two first trimester and three term placentae, respectively; three hTSC lines were collected at day 0 and day 5 of EVT differentiation. Cells were washed first with PBS and then cold ethanol. Following the ethanol wash, the cells were allowed to rehydrate in PBS before pelleting and resuspending in 1 ml of a 3 μM DAPI in staining buffer (100 mM Tris, pH 7.4, 150 mM NaCl, 1 mM $CaCl_2$, 0.5 mM $MgCl_2$, and 0.1% Non-idet P-40) solution. Cells were incubated in the DAPI solution for 15 min at room temperature before filtering and running on a BD FACSCanto II Cell Analyzer.

FISH

Isolated term placental cell samples from three patients (CTBs, EVTs, and UC-MSCs from each patient) were sent to the Cytogenomics Laboratory at UCSD's Center for Advanced Laboratory Medicine. Fluorescence *in situ* hybridization (FISH) was performed using enumeration probes for chromosomes 2, 6, 18, and 20 (D2Z2, D6Z1, D18Z1, D20Z1; Abbott Molecular, Inc.). Each probe was examined in 200 interphase nuclei.

RNA Isolation and RNA-seq Library Construction and Analysis

RNA from 10 first trimester CTB, 10 term CTB, 10 first trimester EVT, and 6 term EVT (split evenly between male and female) were isolated using the mirVana miRNA isolation kit (Ambion). RNA concentration was measured by Qubit RNA BR assay kit (ThermoFisher), and the quality of isolated RNA was checked using a bioanalyzer (Agilent). All samples were found to have a RIN above 7.5. RNA-seq libraries were prepared using the TruSeq Stranded mRNA sample preparation kit (Illumina) at the IGM Genomics Center at UC San Diego. Libraries were pooled and sequenced on NovaSeq 6000 S1Flow Cell (Illumina) to an average depth of 41 million uniquely mapped reads. Quality control was performed using FastQC (v.0.11.8) and multiQC (v.1.6). Reads were mapped to GRCh38.p10 (GENCODE release 26) using STAR (v.2.7.3a; Dobin et al., 2013) and annotated using featureCounts (subread v.1.6.3, GENCODE release 26 primary assembly annotation; Liao et al., 2014). The STAR parameters used were: –runMode alignReads –outSAMmode Full –outSAMattributes Standard –genomeLoad LoadAndKeep –clip3pAdapterSeq AGATCGGAAGAGC –clip3pAdapterMMp 1 – outFilterScoreMinOverLread 0.3 –outFilterMatchNminOverLread 0.3. The featureCounts parameters were: -s 2 -p -t exon -T 13 -g gene_id. Ensembl genes without at least three samples with 5 or more reads were removed from analysis. Normalization and differential expression analysis was performed using the R (v.3.6.3) package DESeq2 (v.1.28.1; Love et al., 2014). Sample sex was accounted for in the DESeq2 design, and, unless otherwise stated, genes with an adjusted p-value < 0.05 and $\log_2$ fold change > 1 were considered differentially expressed. BiomaRt (v.2.42.1) was used to convert Ensembl gene ID's to HUGO gene names, and Gene Set Enrichment Analysis (GSEA) was done with the R (v.3.6.3) package FGSEA (v.1.14.0) using 10,000 permutations and the Hallmark (v.7.0) pathways gene set, the GO term C5 (v.7.0) gene set, and the transcription factor c3.tft (v.7.2) gene set downloaded from MSigDB. Genes were ranked based on their Wald test statistic after performing differential expression. Additionally, where indicated, founder gene sets for the Hallmark pathway gene sets were downloaded from MSigDB (v.7.2). The cell senescence signature was downloaded from the Human Ageing Genomic Resources[1] (Tacutu et al., 2018).

[1]https://genomics.senescence.info/download.html#cellage

Cell cycle-related genes for each phase of the cell cycle were previously determined (Macosko et al., 2015). Characterization using principal component analysis (PCA) of the three hTSC lines derived for this study and two previously reported hTSCs (Okae et al., 2018) was done by merging the raw counts from six placental samples (three EVT and three CTB) and four hTSC samples (duplicates of blastocyst derived hTSCs and placental derived hTSCs) from Okae et al., with the nine hTSC samples (triplicates of each hTSC line) and 36 placental samples from this study, filtered as specified above. The combined RNA-seq data were then processed and transformed using DESeq2's variance stabilizing transformation method before performing PCA. Gene list enrichment analysis was done with Enrichr (Kuleshov et al., 2016). Visualization was performed with the R package ggplot2 or with the python packages seaborn, matplotlib, or plotly.

Gene regulatory networks were created by first performing GSEA using the transcription factor prediction gene set c3.tft (v.7.2) from the Molecular Signatures Database. Transcription factors (TFs) used as input into the gene regulatory network inference algorithm were selected based on adjusted p-value (<0.05). Arboreto (v 0.1.5; Moerman, 2019) was run using the GRNBoost2 algorithm. The input into the algorithm consisted of the differentially expressed genes (DEGs, adjusted p-value < 0.05 and $\log_2$ fold change > 1) from a given comparison and the significantly enriched TFs for the same comparison. For each target gene, the algorithm uses a tree-based regression model to predict its expression profile using the expression values of the set of input TFs. The algorithm outputs TF targets with a calculated importance score. The top 1,500 genes by $\log_2$ fold change were then used to create a protein–protein interaction network using the stringApp [v.1.5.1, confidence (score) cutoff = 0.4, max additional interactors = 0, use smart delimiters] application in Cytoscape (v.3.8.0). The networks were then clustered using MCL clustering with the clusterMaker2 application (v.1.3.1, inflation value = 2.0, assumption that edges were undirected, and loops were adjusted before clustering). The importance scores from the genes in each cluster were then summed to find the TFs with the highest importance for each subcluster.

RNA Isolation for qPCR of hTSC and EVT Derivatives

RNA was isolated using NucleoSpin® kit (Macherey-Nagel, Duren, Germany), and 300 ng of RNA was reverse transcribed to prepare cDNA using PrimeScript™ RT reagent kit (TAKARA, Mountain Vew, CA, United States) following the manufacturer's instructions. qRT-PCR was performed using Power SYBR® Green RT-PCR Reagents Kit (Applied Biosystems, Carlsbad, CA, United States) and primers listed in **Supplementary Table 2**. Data were normalized to beta-actin and shown as fold-change over day 0 (undifferentiated hTSC). Statistical analysis was performed using t-test. Data are expressed as mean ± SD of 2^{-ddCt} values. The level of statistical significance was set at $p < 0.05$.

Western Blot

Human trophoblast stem cell 1,049 cells were differentiated into EVT in 10 cm dishes for 5 days. Cell lysate was collected every day for 5 days using RIPA buffer (Fisher Scientific, United States) containing protease and phosphatase inhibitors (Roche Applied Science, United States) according to the manufacturer's protocol. Protein concentration was quantified by BCA protein assay (Thermo Scientific, United States). Thirty μg of total protein was loaded onto a 10% denaturing polyacrylamide gel for separation and then transferred to PVDF membranes by electrophoresis. Membranes were blocked with 5% non-fat dried milk in Tris-buffered saline containing 0.1% (v/v) Tween 20 (Sigma-Aldrich) for 1 h and then incubated overnight with primary antibodies: rabbit anti-STAT1 (Cell Signaling Technology or CST #9175) or mouse anti-ACTB (Sigma-Aldrich #A5441). Followed by 1-h incubation with HRP-conjugated secondary antibodies (donkey anti-rabbit IgG, CST #7074S or anti-mouse IgG, CST #7076S), signals were developed using SuperSignal West Dura Extended Duration substrate (Thermo Fisher, United States) and captured on film.

Immunostaining and *in situ* Hybridization

First trimester placental tissues were fixed in 4% paraformaldehyde in phosphate-buffered saline for 10 min and then permeabilized with 0.5% Triton X-100 for 2 min. Tissues were stained with mouse anti-HLAG antibody (clone 4H84; Abcam) and rabbit anti-STAT1 (CST #9175), using Alexa Fluor-conjugated secondary antibodies (Thermo Fisher), counterstained with DAPI (Invitrogen), and then visualized using a Leica DM IRE2 inverted fluorescence microscope.

Term placenta samples were fixed in neutral-buffered formalin and embedded in paraffin wax. Immunohistochemistry (IHC) and *in situ* hybridization (ISH) were performed on 5-μm sections of these tissues on a Ventana Discovery Ultra automated stainer (Ventana Medical Systems) at the UC San Diego Advanced Tissue Technology Core laboratory. For IHC, standard antigen retrieval was performed for 40 min at 95°C as per the manufacturer's protocol (Ventana Medical Systems), and the section was stained using mouse anti-HLAG antibody (clone 4H84; Abcam). Staining was visualized using 3,3′-diaminobenzidine (DAB; Ventana Medical Systems), and slides were counterstained with Hematoxylin. For ISH, we used the RNAscope method with probes specific to human GCM1 from ACD-Bio. Following amplification steps, the probes were visualized using DAB, and slides were counterstained with hematoxylin. IHC and ISH slides were analyzed by conventional light microscopy on an Olympus BX43 microscope (Olympus).

RESULTS

Term EVT Lacks Recurrent CNVs at Specific Genomic Regions

To address the question whether human EVTs are characterized by specific CNVs or contain whole genome amplifications (polyploidy), we first reanalyzed WGS data from recently published $EGFR^+$ (CTB, $n = 2$) and $HLA\text{-}G^+$ (EVT, $n = 2$) trophoblasts isolated from first trimester placentae (11 and

12 weeks GA; Velicky et al., 2018). To identify CNVs, we applied the Estimation by Read Depth with Single-nucleotide variants (ERDS) algorithm (Zhu et al., 2012), which was recently found to have high sensitivity and accuracy (Trost et al., 2018) and is an orthogonal method to those previously published (Velicky et al., 2018). Our reanalysis found fewer duplications in the HLA-G^+ samples than in the $EGFR^+$ samples; in addition, no duplications encompassed genes previously identified to be contained within amplified genomic regions of murine TGCs (Hannibal and Baker, 2016). Of the 35 genes found to have a duplication unique to the HLA-G^+ sample, 3 (TTC34, PKP1, and MBD5) were identified in similar previously published data from second trimester whole human placental tissue (Kasak et al., 2015; data not shown). Read depth CNV detection algorithms use intra-chromosomal comparisons and therefore do not provide aneuploidy/polyploidy detection. Therefore, to determine the ploidy of the HLA-G^+ samples, we applied the PURPLE (PURity and PLoidy Estimator) algorithm to the WGS data (Cameron et al., 2019; Priestley et al., 2019), which reported both HLA-G^+ samples to be diploid, with no evidence of significant duplications (**Supplementary Figure 1A**). We do note that the Patient 2 and Patient 1 samples were properly identified as female (two copies of the X chromosome) and male (one copy of the X chromosome), respectively.

Next, to find potential CNV genomic hotspots in term EVT, we isolated matched EVTs, CTBs, and UC-MSCs from three term placentae (**Supplementary Table 1**) and performed CNV calling on data from genome-wide SNP genotyping arrays. For comparison, we performed a similar analysis with matched CTB and EVT from two first trimester placentae. After removing one of the first trimester CTB samples due to inadequate data quality, we found nine CNVs unique to EVT samples (not found in either the matched CTB or the matched UC-MSC samples; **Figure 1A**). Of these nine CNVs, six were found in the first trimester EVT sample that lacked a matched CTB sample (numbered in **Figure 1A**), and three were duplications unique to the term EVT samples (green lines marked by * in **Figure 1A**), although not common between term EVT; none of the nine CNVs overlapped with previously identified CNV regions (Kasak et al., 2015). We next sought to determine the ploidy of our EVT samples by running ASCAT (Van Loo et al., 2010) on the data from genome-wide SNP genotyping arrays. We compared the EVT samples to their matched diploid UC-MSCs and again found no evidence of polyploidy in our term EVT samples (**Supplementary Figure 1B**).

To exclude the presence of a subpopulation of EVT cells showing polyploidy or a significantly higher load of CNVs, we performed single-cell CNV analysis on over 600 matched EVT, CTB, and UC-MSC cells isolated from one term placenta. The estimated ploidy in each of the three samples was the same, at 1.95. Although some cells contained duplications, we were not able to verify the existence of a polyploid subpopulation (**Figure 1B**). Finally, we interrogated a recently published term placentae single-cell RNA-seq dataset (Tsang et al., 2017) using InferCNV. After identifying EVT cells based on expression of HLAG, we used InferCNV to compare their expression intensity to a set of reference "normal" cells in the same placental samples. We again found no evidence of polyploidy. We did find cells with numerous smaller CNVs in many of the EVT cells, but none that were common across multiple EVT (data not shown). We note that this experiment was performed on one placenta (#2757), and that the placenta was not the same as those used for other analyses.

These data suggest that, while EVT may display CNVs, high frequency CNVs common across EVT within and between different individual placentae might not exist. Moreover, based on reanalysis of existing trophoblast WGS and single-cell RNA-seq data, as well as newly generated bulk SNP genotyping array and single-cell CNV data, we did not observe evidence of polyploidy in term EVT. However, as these techniques are not optimally designed to detect polyploidy, we proceeded with additional analyses to more directly assess this feature.

Flow Cytometry and Cytogenetic Analysis Confirm the Presence of Polyploid EVT at Term

Given that the techniques used thus far were performed on bulk cell preparations (and thus might miss genetic alterations present in a subpopulation of component cells), and/or were not designed to detect polyploidy (e.g., single-cell CNV analysis), we next sought to evaluate term EVT using approaches that can reliably detect polyploidy on the single-cell level. First, to confirm the presence of a population of tetraploid first trimester EVT cells, as shown in Velicky et al. (2018), we performed DNA ploidy analysis by flow cytometry on matched CTB and EVT from two first trimester placentae. As reported previously (Zybina et al., 2002; Velicky et al., 2018), the CTBs were predominantly diploid (76% of cells) compared with EVT, of which the majority (57%) were tetraploid (**Figure 2A**). We also noted a small subpopulation of cells that contained a DNA content above 4N (5.6% in CTB and 14.4% in EVT). We next asked if isolated EVTs from term placentae contain similar proportions of hyperdiploid cells. We found that, although, on average, a lower percentage of term EVT were tetraploid (44%), this was still a significantly larger proportion of tetraploidy than matched CTB and UC-MSC from the same placentae (p-value < 0.01; **Figures 2A,B**). Interestingly, compared with first trimester CTB and term MSC, term CTB showed an almost 3-fold increase in the proportion of >4N cells, and this proportion (∼15%) remained stable in matched term EVT (∼17%; **Figures 2A,B**). Additionally, we performed *in vitro* differentiation of three hTSC lines into HLA-G^+ EVT-like cells to assess how closely our *in vitro* differentiated EVT-like cells recapitulated the increased DNA content in primary EVT samples. We found no increase in the percentage of hyperdiploid cells following EVT differentiation of all three hTSC lines; in one cell line (1,049), there was a decrease in the number of diploid cells (and thus an increase in the ratio of polyploid to diploid cells) following differentiation (**Figure 2A**).

Finally, using the same matched term placental cell isolates, we subjected CTBs, EVTs, and UC-MSCs to FISH analysis using

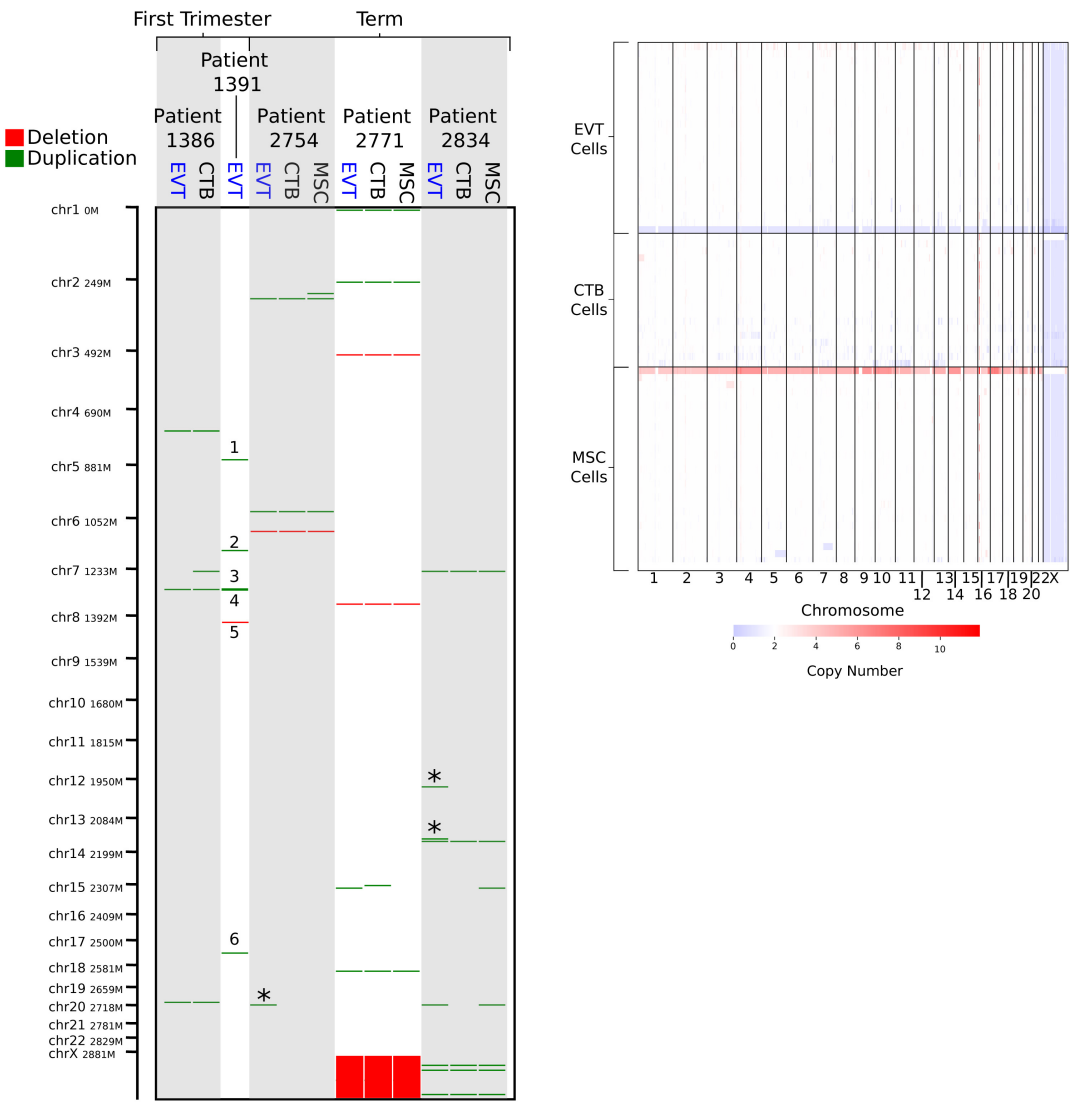

FIGURE 1 | Copy number variation (CNV) analysis using genome-wide SNP genotyping array and single-cell CNV data. **(A)** CNV analysis on matched cytotrophoblast (CTB), extravillous trophoblast (EVT), and umbilical cord-derived mesenchymal stem cells (MSC) from three term placentae, and matched CTB and EVT from two first trimester placentae, using genome-wide SNP genotyping array (CTB sample from Patient 1,391 was removed due to poor data quality). Deletions are shown in red and duplications in green. "*" indicates duplications that are unique to term EVT. Numbered CNVs are those potentially unique to first trimester EVT, though no matched CTB sample was available for Patient 1,391 for direct comparison. Patient 2,771 is female, and all other patients are male. **(B)** CNV calls from single-cell CNV analysis on matched CTB, EVT, and MSC from a single term placenta sample (Patient 2,757—male). Red on the heatmap represents increase in copy number and blue a loss in copy number. White represents a copy number of two.

enumeration probes for chromosomes 2, 6, 18, and 20. We again found that our EVT samples had a much higher percentage of tetraploid cells than their matched CTB and UC-MSC samples (**Figures 2C,D**). We also noted that approximately 7% of EVT cells were called triploid, but no triploid cells were found in any of the CTB or UC-MSC samples (data not shown). Taken together, these data suggest that similar to first trimester EVT, and in contrast to first trimester CTB and third trimester CTB and MSC, term EVTs contain a large subpopulation of polyploid cells. Additionally, the similar proportion of >4N polyploid CTB and EVT at term suggests that this may be a shared feature among term trophoblasts.

Global Gene Expression Analysis Reveals Unique and Common Pathways Involved in EVT Differentiation and Maturation

To further probe the differences between diploid CTB and polyploid EVT, we profiled the transcriptomes of both first

A

	MSC			CTB (EGFR$^+$)			EVT (HLA-G$^+$)		
Patient (First Trimester)	2N	4N	>4N	2N	4N	>4N	2N	4N	>4N
1389	-	-	-	77.2	13.7	5.2	15.3	65.9	14.3
1383	-	-	-	75.6	16.2	6.0	18.4	47.7	14.4
Average (1st Trimester)	-	-	-	76.4	15.0	5.6	16.9	56.8	14.4
Standard Error (1st Trimester)	-	-	-	0.8	1.3	0.4	1.6	9.1	0.05
Patient (Term)									
2754	54.5	18.1	8.7	50.5	21.1	24.0	29.8	43.9	18.1
2771	62.4	16.2	4.9	62.3	19.8	14.1	32.6	38.4	18.8
2834	75.0	16.2	4.0	67.0	19.0	8.8	33.5	49.3	15.4
Average (3rd Trimester)	64.0	16.8	5.9	59.9	20.0	15.6	32.0	43.9	17.4
Standard Error (3rd Trimester)	6.0	0.6	1.4	4.9	0.6	4.5	1.1	3.1	1.0
In Vitro Differentiated hTSC									
1270 day 0/CTB	-	-	-	34.6	29.7	21.4	-	-	-
1270 day 5/EVT	-	-	-	-	-	-	33.6	29.2	18.5
1049 day 0/CTB	-	-	-	45.1	25.7	17.6	-	-	-
1049 day 5/EVT	-	-	-	-	-	-	25.3	26.2	20.3
1048 day 0/CTB	-	-	-	27.7	28.3	27.7	-	-	-
1048 day 5/EVT	-	-	-	-	-	-	22.6	23.8	19.4
Average (Differentiated day 0)	-	-	-	35.8	27.9	22.2	-	-	-
Standard Error (Differentiated day 0)	-	-	-	5.1	1.2	3.0	-	-	-
Average (Differentiated day 5)	-	-	-	-	-	-	27.2	26.4	19.4
Standard Error (Differentiated day 5)	-	-	-	-	-	-	3.3	0.8	2.9

B

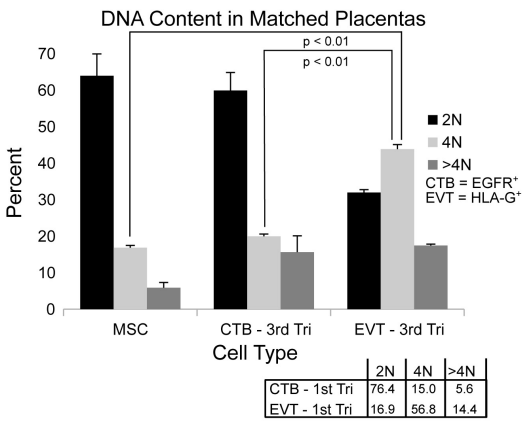

	2N	4N	>4N
CTB - 1st Tri	76.4	15.0	5.6
EVT - 1st Tri	16.9	56.8	14.4

C

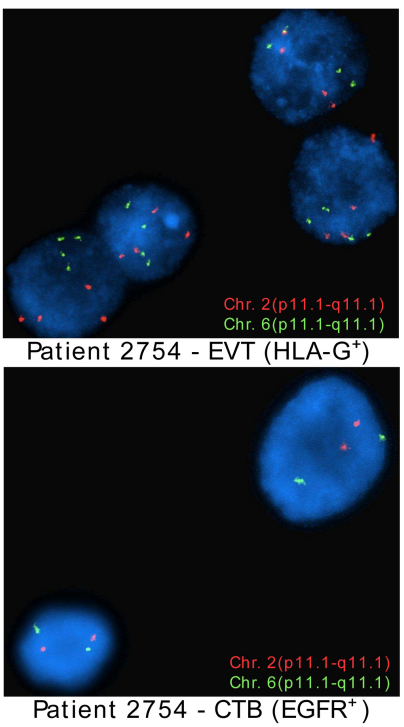

D

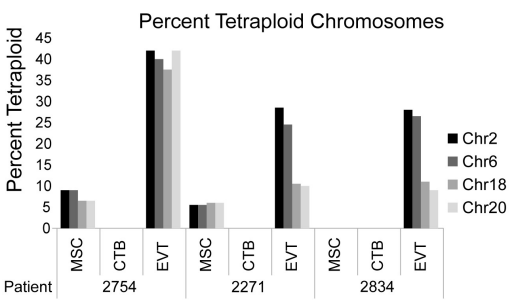

FIGURE 2 | DNA content flow cytometry and cytogenetics analysis. **(A)** Table showing results of DNA content flow cytometry analysis in umbilical cord-derived mesenchymal stem cells (MSC) from term placentae, cytotrophoblast (CTB) and extravillous trophoblast (EVT) from first trimester or term placentae CTB and EVT, and human trophoblast stem cells (hTSCs) that are either undifferentiated (day 0) or differentiated (through a 5-day protocol) into EVT *in vitro*. **(B)** DNA content as determined by flow cytometry from matched CTB, EVT, and MSC from three term placentae. Box in the bottom right corner shows the mean percentage of cells in each ploidy group of matched CTB and EVT from two first trimester placentae as determined by flow cytometry. **(C)** Example images from FISH analysis of matched EVT and CTB from one term placenta. Images show probes targeting chromosome 2 (red) and chromosome 6 (green). **(D)** Bar graph showing the percentage of cells determined by FISH to be tetraploid (chromosomes 2, 6, 18, and 20) in MSC, CTB, and EVT from three term placentae.

trimester and term CTB and EVT. We isolated CTB and EVT from 10 first trimester placentae, CTB from 10 term placentae, and EVT from 6 term placentae (**Supplementary Table 1**), with equal numbers of male and female placentae, and performed RNA-seq. PCA showed that samples clustered into the four expected groups (first trimester CTB, term CTB, first trimester EVT, and term EVT), based on cell-type along the first principal component, and on GA along the second principal component (**Figure 3A**). There did not appear to be any obvious transcriptional differences based on sex. However, because we had sequenced a sufficient number of patient samples and had equal numbers of male and female placentae, we performed differential gene expression analysis between male and female EVT (adjusted p-value < 0.05, Log_2 fold change > 1, and normalized mean expression in group > 100) from both GAs. We found a small number of sex-specific DEGs in first trimester EVT, with just 5 genes up-regulated in female EVT, including XIST and EPPK1, the latter a negative regulator of epithelial cell migration, and 11 genes up-regulated in male EVT, all of which were located on the Y chromosome except for PLXDC2 (**Supplementary Figure 2A**). Interestingly, term EVT showed a larger number of sex-specific DEGs, with 27 genes up-regulated in the female samples and 24 in the male samples (**Supplementary Figure 2B**). Several of the genes on the Y chromosome were up-regulated in both male term EVT and male first trimester EVT, but no significant gene ontology enrichment was identified in any groups.

To identify differences among these four groups of cells (first trimester CTB and EVT and term CTB and EVT), we first performed differential expression analysis, ranked genes based on their Wald test statistic, and conducted GSEA. CTBs are the proliferative epithelial cells of the placenta and differentiate early in pregnancy into EVT; therefore, we first sought to identify pathways that were significantly enriched between first trimester CTB and EVT (**Figure 3B**). Similar to previously published microarray data (Apps et al., 2011;Telugu et al., 2013;Tilburgs et al., 2015), all seven of the pathways that make up the immune process category in the Hallmark gene set (Liberzon et al., 2015) were significantly up-regulated in EVT vs. CTB in the first trimester (adjusted p-value < 0.05; **Figure 3B**). Furthermore, similar to what we previously found using gene expression microarrays (Wakeland et al., 2017), pathways such as hypoxia, UPR, and mTOR signaling were significantly up-regulated, and pathways such as oxidative phosphorylation, P53, fatty acid metabolism, and those related to cell cycle control were significantly down-regulated, in first trimester EVT (**Figure 3B**).

We next analyzed the pathways that were significantly enriched in term EVT compared with term CTB (**Figure 3C**). Perhaps unexpectedly, nearly all the pathways up-regulated in term EVT were also significantly up-regulated in first trimester EVT (**Figure 3C**, highlighted by *). Likewise, most pathways down-regulated in term EVT were also similarly altered in the first trimester comparison (**Figure 3C**, highlighted by *). However, in addition to the E2F targets, G2M checkpoint, and P53 pathways, term EVT also showed down-regulation of the three remaining pathways in the proliferation process category (namely: MYC targets V1, MYC targets V2, and mitotic spindle) in the Hallmark gene set (Liberzon et al., 2015).

Next, we examined the EVT maturation process by comparing gene expression between first trimester and term EVT samples (**Figure 3D**). We again saw many of the same pathways enriched in term EVT, compared with first trimester EVT, as in the comparison with term CTB (**Figure 3D**, highlighted by *). We noted that compared with first trimester EVT, term EVT down-regulated all of the proliferation process category pathways (E2F targets, G2M checkpoint, MYC targets, and mitotic spindle), except the P53 pathway gene set (**Figure 3D**).

To better understand how specific pathways were regulated during EVT development, we next looked at the pathways that were unique or common through both steps of the EVT maturation process (first trimester CTB → first trimester EVT → term EVT; **Figure 4A**). Of the common down-regulated pathways in EVT, the cell proliferation pathways E2F targets and G2M checkpoint had the lowest scores. We therefore repeated GSEA using just the founder gene sets (Liberzon et al., 2015) for these two pathways. We found that in both comparisons, term EVT showed significant downregulation for the neighborhood of CCNA2 (Cyclin A2), PCNA, and RRM2 in the GNF2 expression compendium (**Supplementary Figure 3A** and **Figure 5**; all comparisons with NES > 3.34 and adj. p-value < 0.006). These three genes are expressed just before the onset or during the S phase of the cell cycle, consistent with the absence of cells in the S phase in term EVT.

Two of the Hallmark pathways that were found to be uniquely up-regulated only in the first trimester EVT (compared with term EVT) were the PI3K/AKT/mTOR signaling and UPR pathways (**Figures 3B**, **4A**). These two pathways appeared to switch directions during this two-step process: first up-regulated during the initial conversion of first trimester CTB to EVT and then down-regulated in the subsequent maturation step from first trimester EVT to term EVT. The PI3K/AKT/mTOR pathway has been shown to be involved in the initial transition of CTB to EVT reviewed in Pollheimer and Knofler (2005) and Ferretti et al. (2007), specifically by promoting EMT. The other significantly up-regulated pathway, UPR (**Supplementary Figure 3B**), is mediated by endoplasmic reticulum (ER) stress and is a method used by cells to detect, eliminate, and avoid further accumulation of misfolded proteins in the ER lumen, which build up due to several environmental cues, including hypoxia, a known EVT differentiation cue (Wakeland et al., 2017). Moreover, UPR is a stress response phenotype, triggered by similar inducers to senescence, and recently found to be present in all types of senescence (Pluquet et al., 2015). We have previously identified this pathway among those up-regulated during the transition from CTB to proximal column EVT (Wakeland et al., 2017); however, it has not been further validated in EVT differentiation and/or function. We therefore repeated GSEA using just the founder gene sets (Liberzon et al., 2015) for the UPR pathway and found that the Reactome activation of chaperone genes by XBP1S (adj. p-value < 0.02) was significantly enriched. Furthermore, we found that the GO term IRE1 mediated UPR to be significantly up-regulated in first trimester EVT compared with first trimester CTB (adj. p-value < 0.04). Therefore, to

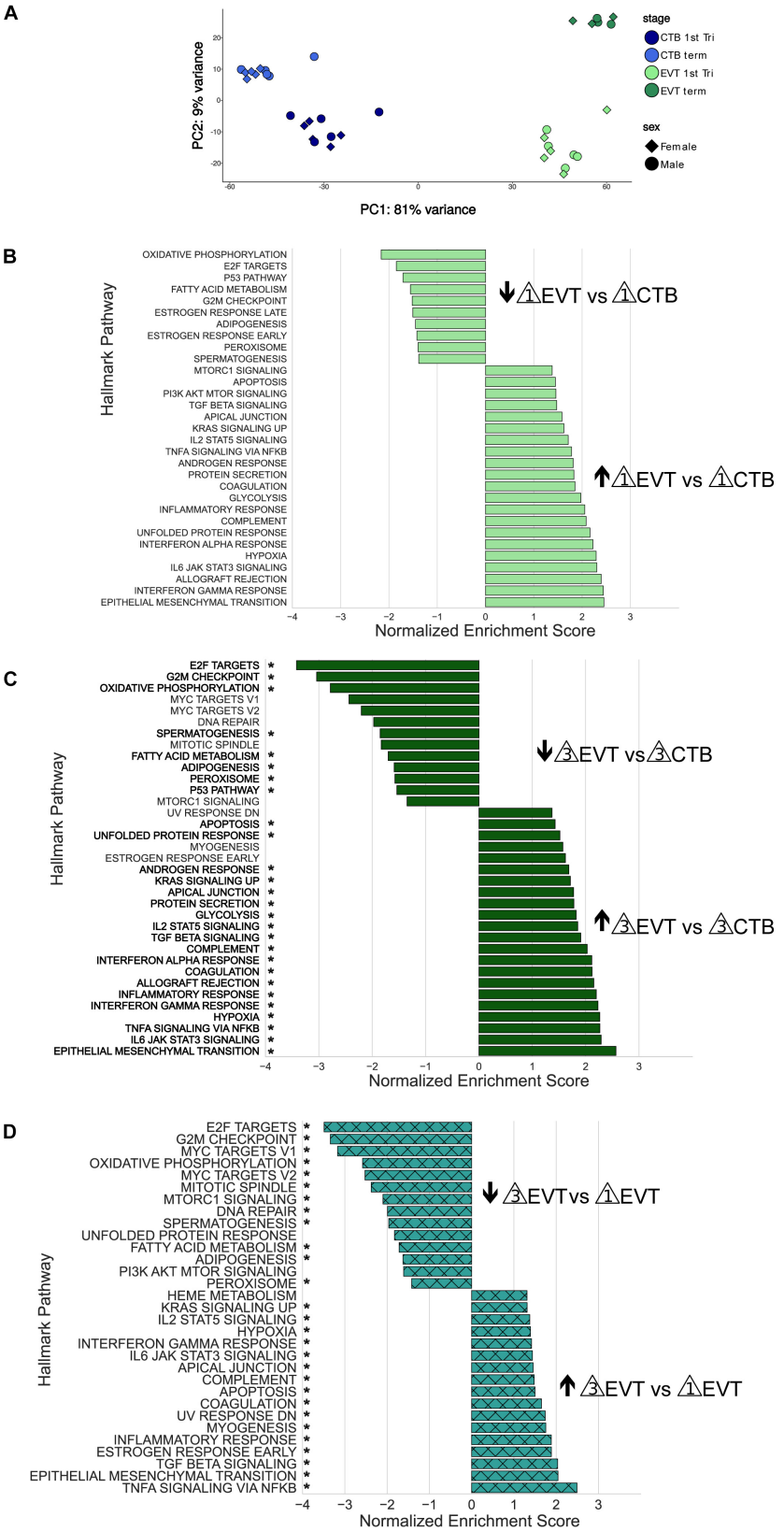

FIGURE 3 | Principal component analysis and Gene Set Enrichment Analysis (GSEA) of RNA-seq data. **(A)** Principal component analysis showing the first two components using all genes post-filtering of all 36 placenta samples (see **Supplementary Table 1**). Each sample group contained equal numbers of males and

(Continued)

FIGURE 3 | Continued
females. **(B)** GSEA using the Hallmark pathway gene set of first trimester EVT compared with first trimester CTB. Genes were ranked based on their Wald test statistic after performing differential expression on first trimester EVT and first trimester CTB. Normalized enrichment scores (NES) indicate pathways either up-regulated (NES > 0) or down-regulated (NES < 0) in first trimester EVT vs. first trimester CTB. Only pathways with an adjusted *p*-value < 0.05 are shown. **(C)** GSEA using the Hallmark pathway gene set of term EVT compared with term CTB. Genes were ranked based on their Wald test statistic after performing differential expression on term EVT and term CTB. Normalized enrichment scores (NES) indicate pathways either up-regulated (NES > 0) or down-regulated (NES < 0) in term EVT vs. term CTB. Only pathways with an adjusted *p*-value < 0.05 are shown. Pathway names with an "*" are those that were also found to be significantly enriched in first trimester EVT vs. first trimester CTB. **(D)** GSEA using the Hallmark pathway gene set of term EVT compared with first trimester EVT. Genes were ranked based on their Wald test statistic after performing differential expression on term EVT and first trimester EVT. Normalized enrichment scores (NES) indicate pathways either up-regulated (NES > 0) or down-regulated (NES < 0) in term EVT vs. first trimester EVT. Only pathways with an adjusted *p*-value < 0.05 are shown. Pathway names with an "*" are those that were also found to be significantly enriched in term EVT vs. term CTB.

assess the importance of the UPR pathway in EVT, we asked whether suppression of the IRE1-alpha arm, which is responsible for activating XBP1(S), would affect EVT formation *in vitro*. We derived two separate hTSC lines from early first trimester placentas; these lines appeared transcriptionally very similar to hTSC lines previously derived from early gestation placentas (Okae et al., 2018; **Supplementary Figure 4**). We then applied the IRE1-alpha arm inhibitor 4u8c to both hTSC lines during differentiation into EVT and found an ∼25% decrease in the percentage of HLA-G$^+$ cells at the end of the protocol in two separate hTSC lines (**Figure 4B**). However, qPCR did not show alteration of expression of any other EVT marker with 4u8C suppression (**Supplementary Figures 5A,B**). In addition, only total (and not spliced) XBP1 was increased with EVT differentiation (**Supplementary Figure 5C**). These results suggest that at least the IRE1-alpha arm of the UPR pathway is needed for proper surface expression of HLA-G but is not required for EVT differentiation *per se*. Overall, these data provide, for the first time, a global look at pathways involved in EVT differentiation and maturation, identifying pathways that are uniquely and commonly up- or down-regulated in either step.

Transcriptome Analysis Suggests Cell Cycle Arrest, Cellular Senescence, and Endoreduplication as Key Features of EVT

The induction of cellular senescence leads to irreversible growth arrest and has been proposed as a ploidy-limiting mechanism (Hayflick, 1965; Johmura and Nakanishi, 2016). Our initial transcriptomic analysis using GSEA (**Figures 3B–D**), along with the evaluation of expression of mitosis and cellular proliferation-associated genes (**Figure 5**), suggested that term EVTs are not cycling. We found that genes associated with all phases of the cell cycle exhibited decreased expression in term EVT, with the largest difference seen in genes associated with mitosis (**Figure 5**). An active cell cycle is characterized by expression of cyclins and cyclin-dependent kinases (CDKs). G1 phase cyclins and CDKs were differentially expressed between EVT and CTB samples, with the lowest overall expression in term EVT, suggesting G1 cell cycle arrest (**Figure 6A**). Additionally, two of the three retinoblastoma family genes, *RB1* and *RBL2*, both shown to play pivotal roles in the negative control of the cell cycle by binding to E2F TFs and thus preventing S phase entry (Giacinti and Giordano, 2006), were significantly up-regulated (adj. *p*-value < 0.01) in EVT compared with CTB (**Figure 6B**). Additionally, the genes encoding the "activating" E2Fs, which are known to interact with RB proteins to restrict cell cycle advancement (Shay et al., 1991) were significantly lower in term EVT than in CTB (adj. *p*-value < 0.01; **Figure 6C**). Interestingly, mitosis-associated cyclin B (CCNB1) was highly expressed in first trimester EVT (Velicky et al., 2018), but was roughly 100-fold lower in term EVT, suggesting the absence of mitosis in term EVT (**Supplementary Figure 6A**). Moreover, expression of the mitosis-linked genes, *CDK1*, *MKI67*, and *AURKA* (Zybina et al., 2004), was >10-fold lower in term EVT than in the other three groups (**Supplementary Figure 6A**). Additionally, we performed cell cycle scoring on term single-cell RNA-seq data (Tsang et al., 2017) and found that the EGFR$^+$ cluster contained a much higher fraction of cells in the G1 and S phases compared with the HLA-G$^+$ cluster, which was contained predominantly in the G2/M phase, as previously reported (Velicky et al., 2018; **Supplementary Figure 6B**). Next, to investigate whether polyploid EVT displayed a senescence-like transcriptomic profile, we performed PCA using genes (n = 1,225) reported to comprise a human senescence transcriptomic signature (Tacutu et al., 2018). We found that term EVT samples were uniquely clustered away from the other cell types, with first trimester EVT samples closer to both CTB groups than to the term EVT group (**Figure 6D**). A similar clustering was not present in a PCA plot using a random set of 1,225 genes (data not shown). Furthermore, the gene (*GLB1*) encoding the senescence-associated marker Beta-Galactosidase (SAβG; adj. *p*-value < 0.001), along with several other senescence-associated secretory phenotype (SASP) and metabolic genes (Basisty et al., 2020), was most highly expressed in either first trimester or term EVT (**Figure 6E**). Taken together, these results suggest that EVTs are undergoing cell cycle arrest and senescence.

A recent study has suggested that first trimester EVTs induce endocycles and enter a senescent state (Velicky et al., 2018). Endoreduplication consists of DNA replication without cell or nuclear division. It is thought to be triggered by inhibition of CDK1 by p57 (CDKN1C) and suppression of checkpoint protein kinase (CHEK1) by p21 (CDKN1A), preventing induction of apoptosis (Ullah et al., 2008). In our data, we noted the strongest reciprocal expression of p57 and CDK1, as well as p21 and CHEK1, in term EVT (*p*-value < 0.05; **Figures 6F,G**). Endoreduplication is also characterized by downregulation of CDK1, Cyclin A, and Cyclin B, with simultaneous persistence of Cyclin E expression (Ullah et al., 2009). In our data, CDK1

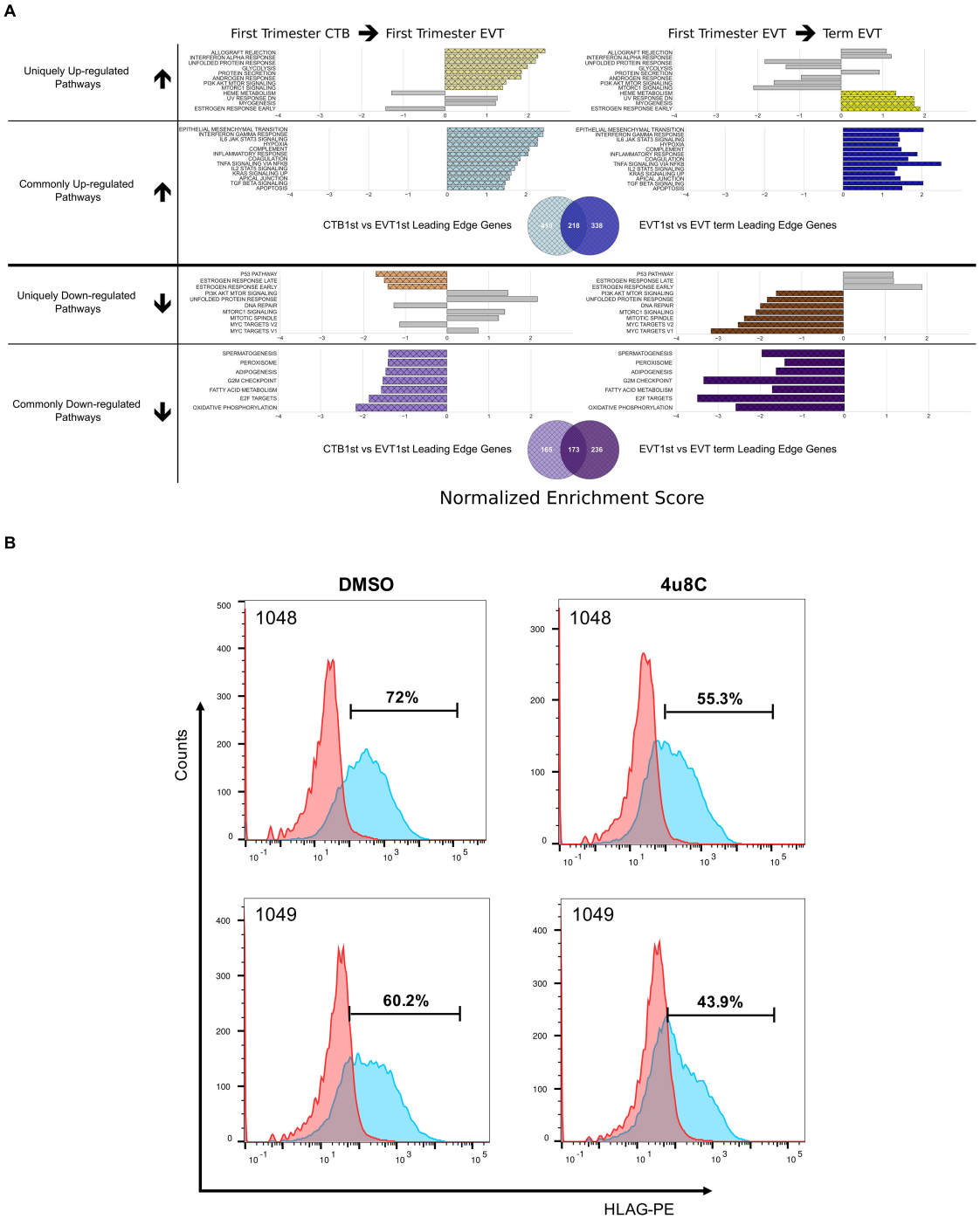

FIGURE 4 | Pathways enriched in the EVT differentiation and maturation process. **(A)** Pathways enriched either in one (unique) or both (common) steps of EVT differentiation (first trimester CTB → first trimester EVT) and maturation (first trimester EVT → term EVT). Colored bars in grid show significantly enriched pathways (adjusted p-value < 0.05) that are either uniquely up- or down-regulated in first trimester EVT when compared with first trimester CTB (left side) or uniquely up- or down-regulated in term EVT when compared with first trimester EVT (right side). Likewise, common up- and down-regulated pathways are shown in both comparisons. The gray bars on each unique pathway bar graphs represent the enrichment score of the comparison on the opposite side of the graph to highlight the similarity or difference of the corresponding comparison. The gray bars may show enrichment in the same direction as the colored bars; however, the pathway is considered uniquely regulated because the gray bars represent enrichment that did not achieve statistical significance. The Venn diagrams below each set of bar graphs show the number of unique and shared leading-edge genes in the commonly up-regulated or commonly down-regulated Hallmark pathways. **(B)** Validation of the IRE1-alpha arm of the unfolded protein response (UPR) pathway regulating surface HLA-G expression in EVT. Two hTSC lines were differentiated to EVT *in vitro* in the presence of either the IRE1-alpha inhibitor, 4u8c, or DMSO carrier alone. Graph shows the percentage of HLA-G^{+} cells at the end of the 5-day treatment, with ∼25% decrease in these cells in the presence of the inhibitor.

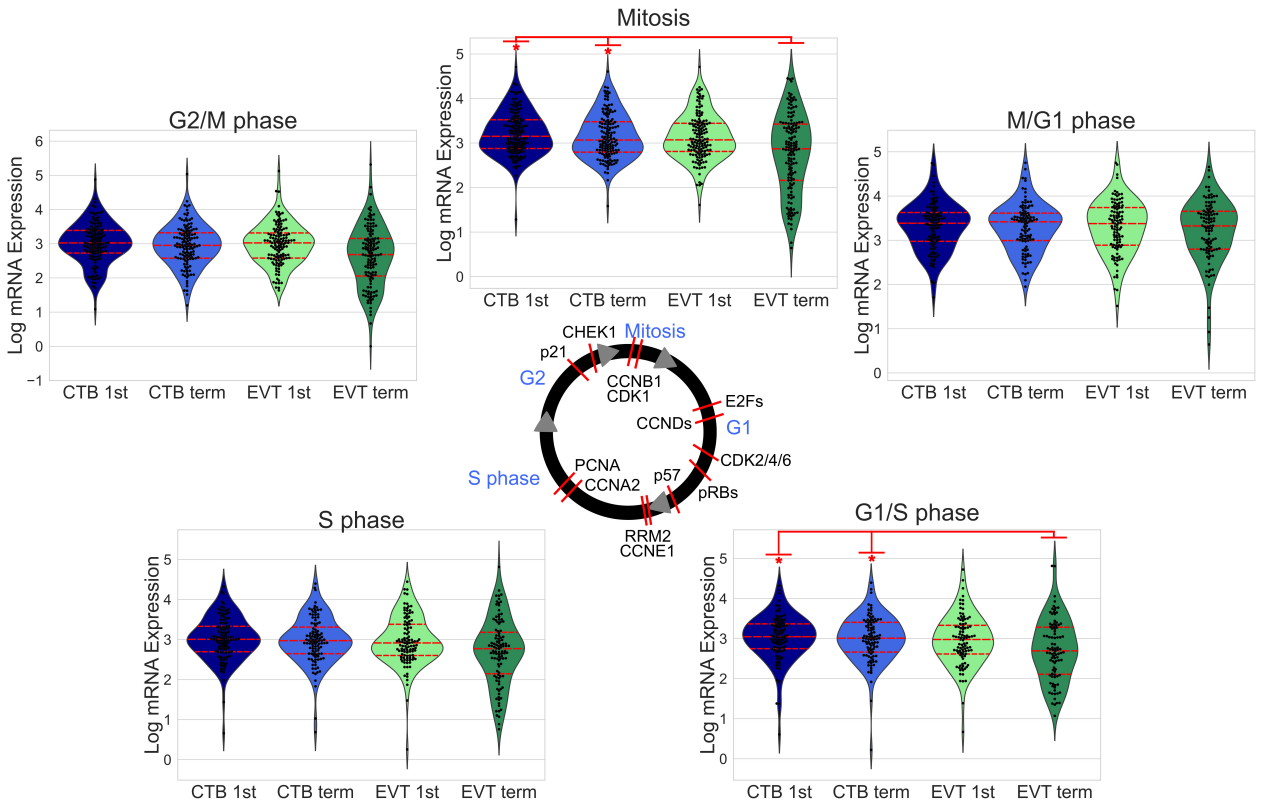

FIGURE 5 | Cell cycle-related gene expression in first trimester and term CTB and EVT. Expression of known cell cycle phase-related genes (Macosko et al., 2015) is shown. The median value of each gene in each group was used to create swarm/violin plots. Inner red dotted lines in swarm/violin plots represent the quartiles of the distribution (*p*-value: * <0.05 by *t*-test). Red lines on cell cycle figure represent location during cell cycle with reported peak expression of the labeled gene (protein names have been used in certain cases to represent multiple genes or because they are more commonly used).

was uniquely decreased in term EVT (**Figure 6F**); however, both Cyclin B (CCNB1) and Cyclin E1 (CCNE1) were highly expressed in first trimester EVT, with CCNB1 expression plummeting and CCNE1 persisting, albeit at a lower level, in term EVT (**Supplementary Figures 6A,C**). Although Cyclin A (CCNA1) had a similar expression profile to Cyclin E1, it was expressed at an extremely low level throughout (data not shown). This pattern of gene expression is most consistent with endoreduplication occurring in some first trimester EVT but becoming more ubiquitous/pronounced in term EVT.

TF Drivers Characteristic of EVT

To better understand the TF regulatory drivers of first trimester and term EVT, we performed GSEA using the TF prediction gene sets from the Molecular Signatures Database. To determine which enriched TFs were critical in each set of DEGs, and to infer gene regulatory networks, we used a tree-based regression model to calculate an "importance score" for each TF gene target pair using GRNBoost2 in the Arboreto software library (Moerman, 2019). Next, we created STRING networks for each of the top 1,500 DEGs in each of the different cell type comparisons and clustered the networks into subnetworks. We were then able to use the TF gene target importance scores to infer which TFs were critical to each of the subnetworks. In this process, more than one subnetwork may be assigned to a given TF. We first asked which TFs had the highest importance scores when assessing the differentiation of CTB to EVT, initially focusing on the paired first trimester cells and evaluating genes up-regulated in EVT over CTB. Following network clustering, these genes clustered into several subnetworks, with the largest containing close to 1,000 genes with *TNF*, *FN1*, and *ALB* as the genes with the highest centrality scores (**Figure 7**, top), and the top four TFs being *STAT1*, *IRF7*, *GABPB1*, and *ETS2* (**Figure 7**, top).

Next, we evaluated the TF network up-regulated in EVT compared with CTB at term. Following clustering, we compared the largest subnetwork in this comparison to the largest subnetwork up-regulated in first trimester EVT (compared with first trimester CTB) and found that approximately 25% of the genes were the same. The top four TFs unique to the largest term EVT subnetwork were MEF2A, RREB1, NFATC3, and FOXO4 (**Figure 7**, bottom). Additionally, *FN1*, the highest expressed gene in our EVT samples, and *TNF* appeared to again have the highest centrality scores in this subnetwork (**Figure 7**, bottom). The top ranked TFs in terms of importance scores shared in these two

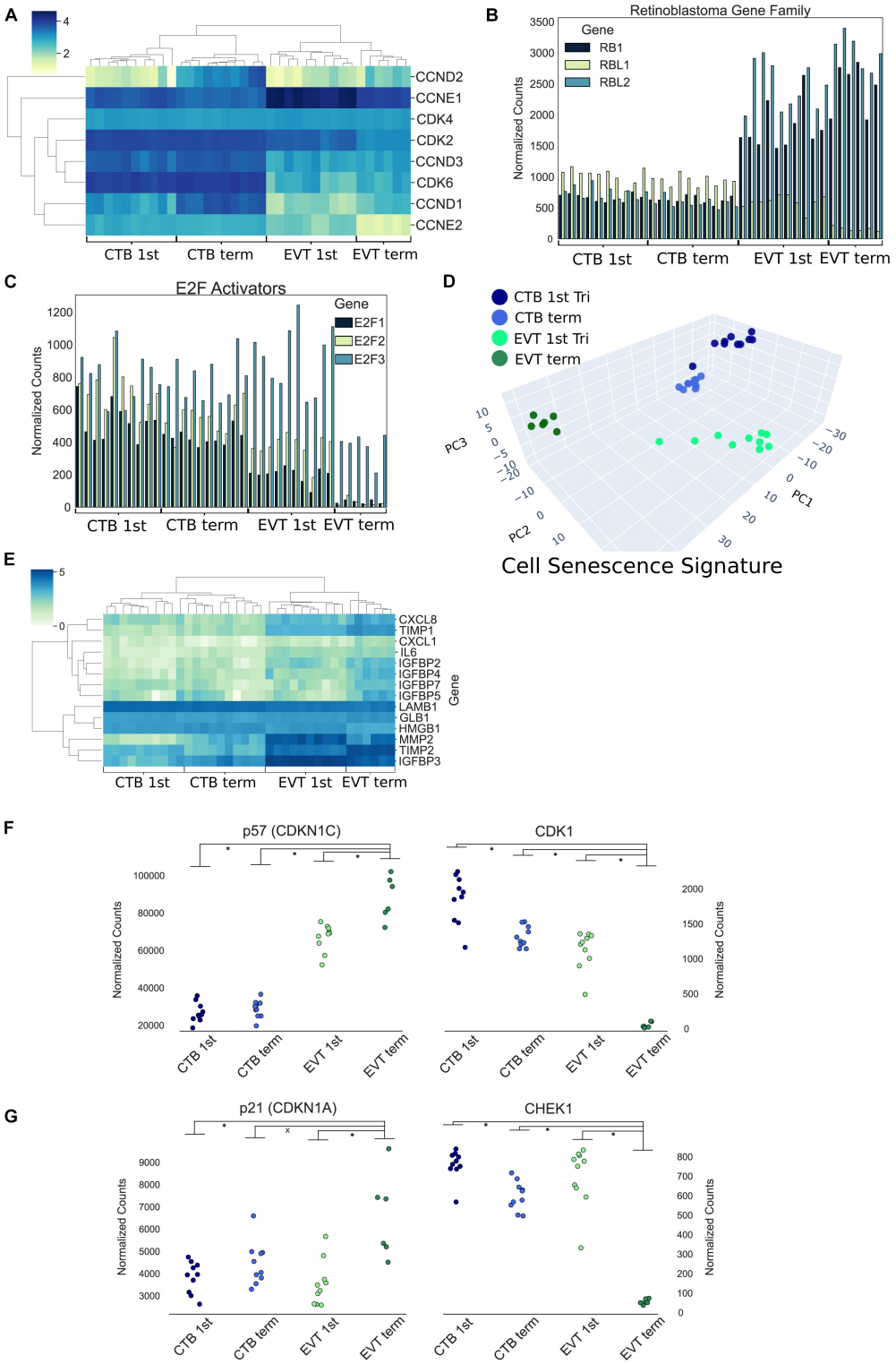

FIGURE 6 | Cell cycle and endoreduplication gene expression. **(A)** Heatmap of G1 phase cyclins and cyclin-dependent kinases using log transformed normalized gene counts. **(B)** Bar graph showing retinoblastoma family genes (*RB1*, *RBL1*, and *RBL2*) normalized gene expression. **(C)** Bar graph displaying E2F activators (E2F1, E2F2, and E2F3) normalized gene expression. **(D)** Three-dimensional principal component analysis using genes (n = 1,225) associated with human cellular senescence signature. **(E)** Heatmap of previously identified (Basisty et al., 2020) senescence-associated secretory phenotype (SASP)-associated genes using log transformed normalized gene counts. **(F)** Normalized expression of p57 (CDKN1C) and CDK1 (p-value: * <0.01 by t-test). **(G)** Normalized expression of p21 (CDKN1A) and CHEK1 (p-value: * <0.05 by t-test).

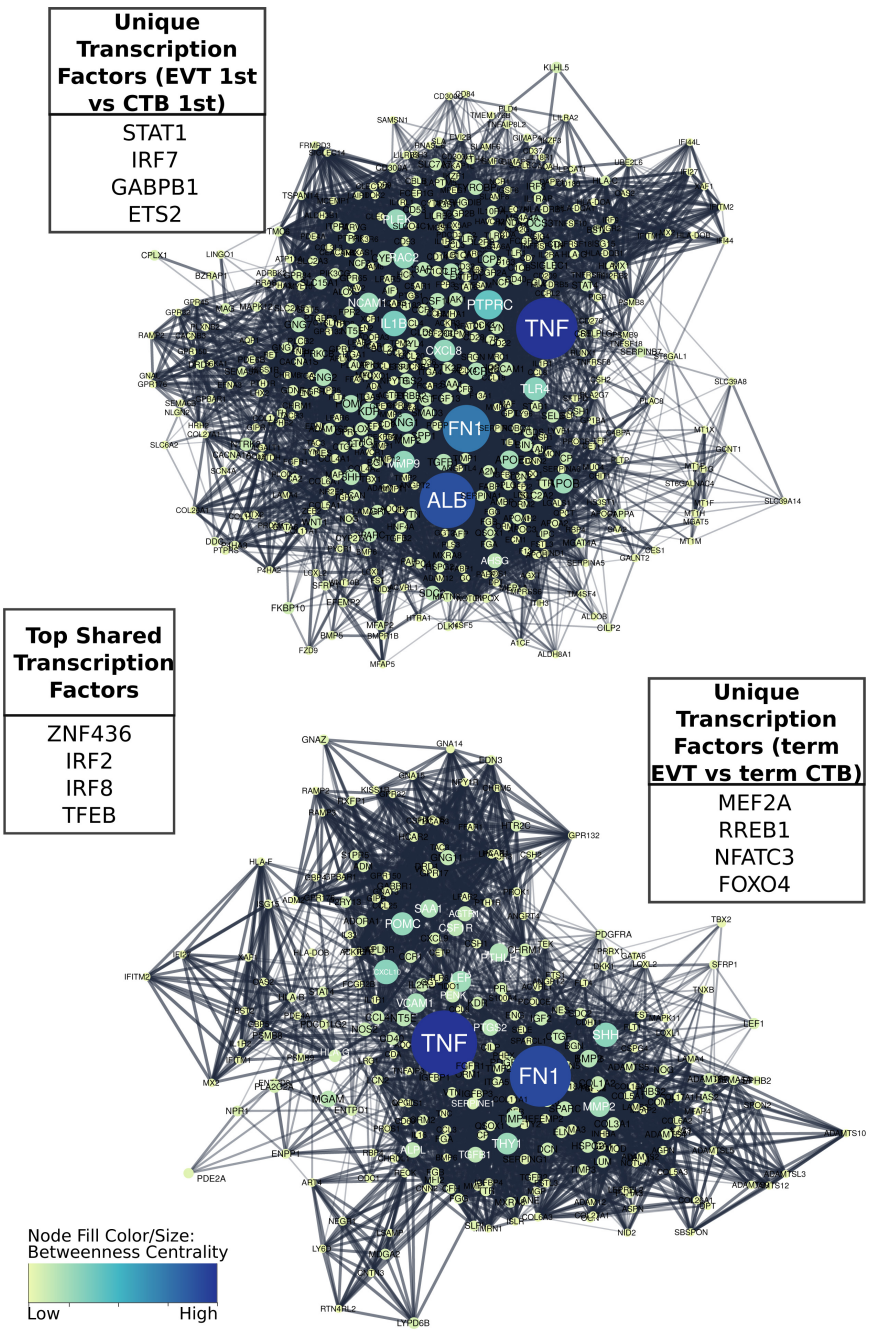

FIGURE 7 | Comparison of gene regulatory networks involved in development of first trimester and term EVT. Networks were created by first generating protein to protein interaction STRING networks of up-regulated genes, either in first trimester EVT compared with first trimester CTB (top), or in term EVT compared with term CTB (bottom), then clustering networks into subnetworks. The largest subnetwork from each comparative analysis is shown. Displayed "unique" transcription factors (TFs; top left and bottom right tables) were those found to have the highest summed importance scores in terms of the labeled subnetwork. Displayed "top shared" TFs (middle table) were the top four transcription factors in terms of importance for both subnetworks. Subnetwork node sizes and colors are determined by the nodes calculated betweenness centrality scores.

largest subnetworks in both first trimester and term EVT were ZNF436, IRF2, IRF8, and TFEB (**Figure 7**, center).

We next asked which TFs were important for EVT maturation. Using the genes that were up-regulated in term EVT, compared with first trimester EVT, we found that the four TFs with the highest importance scores were GCM1, NFAT5, MEF2A, and STAT4 (**Figure 8A**). GCM1 had decreased expression in term EVT compared with first trimester EVT but was also the TF with the highest importance score in the largest subnetwork (**Figure 8A**). This subnetwork was enriched for genes in the

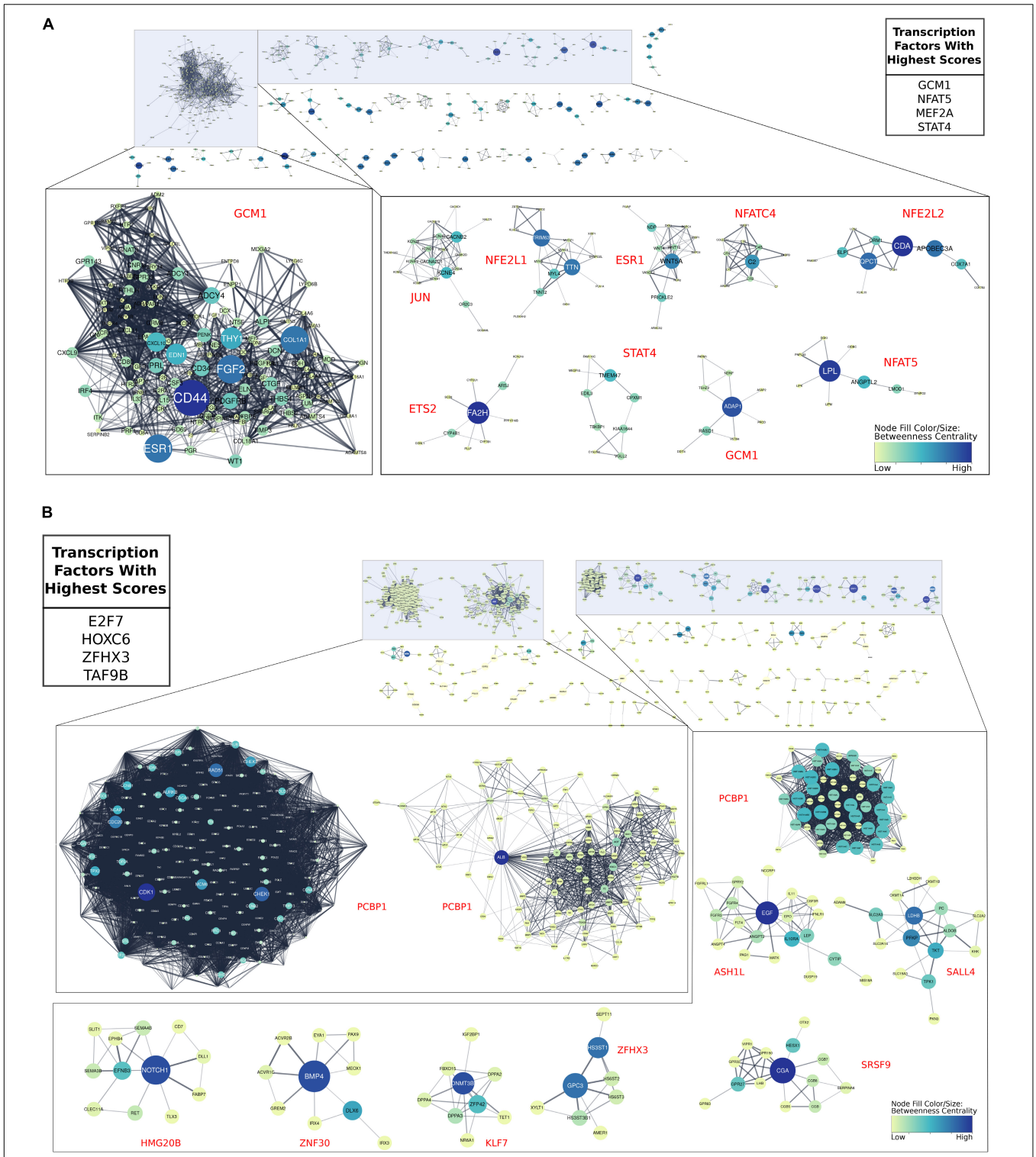

FIGURE 8 | Gene regulatory networks involved in EVT maturation. All gene regulatory subnetworks were created by clustering STRING networks of up- and down-regulated genes in term EVT compared with first trimester EVT. **(A)** All subnetworks created from genes up-regulated in term EVT compared with first trimester EVT. The top 10 largest subclusters are enlarged. The top four transcription factors (TFs) with the highest summed scores for all genes in the comparison are shown in the top right table. **(B)** All subnetworks created from down-regulated genes in term EVT compared with first trimester EVT. The top 10 largest subclusters are enlarged. The top four TFs with the highest summed scores for all genes in the comparison are shown in the top left table. For both analyses, the red TF names alongside each subnetwork are those with the highest importance scores in that subnetwork. Subnetwork node sizes and colors are determined by the nodes calculated betweenness centrality scores.

PI3K/AKT/mTOR pathway and extracellular matrix organization (adj. p-value < 0.01). We then analyzed which TFs had the highest importance scores when comparing genes down-regulated in term EVT, compared with first trimester EVT. The top four TFs were E2F7, HOXC6, ZFHX3, and TAF9B (**Figure 8B**). Additionally, we found that PCBP1 was the TF with the highest importance score in the three largest subnetworks in this comparison (**Figure 8B**). The identification of TFs involved in EVT differentiation and maturation provides the first step toward the ability to model this important placental cell type *in vitro* and to begin to decipher the various functions these cells serve at the maternal–fetal interface.

To validate some of these findings, we chose to focus on two TFs: STAT1, because it was identified in the top four TFs of the largest TF subnetwork in first trimester EVT (**Figure 7**, top), and GCM1, because it was within the top four TFs with the highest importance scores in term, compared with first trimester EVT, and the TF with the highest importance score in the largest subnetwork (**Figure 8A**). We first evaluated GCM1 expression and confirmed that this gene is most enriched in first trimester EVT with levels decreased at term (**Figure 9A**). We performed ISH on first trimester and term placental sections and confirmed enrichment of this gene to be highest in first trimester HLA-G$^+$ EVT (**Figures 9B,C**). We next confirmed STAT1 gene expression in first trimester and term CTB and EVT and found that in fact it is enriched in EVT, with similar levels at the different gestational timepoints (**Figure 9D**). We stained first trimester placental tissues with antibodies to HLA-G and STAT1 and found that STAT1 expression was confined to HLA-G$^+$ cells (**Figure 9E**). We also differentiated one of our primary hTSC lines into EVT and found that STAT1 expression significantly increases over this differentiation time course (**Figure 9F**). These data confirm that our analyses have indeed identified novel TF drivers of EVT differentiation and/or function. Future studies are needed to further validate the numerous additional findings from our TF network analyses, and to functionally assess the role of each of these TF's in EVT.

DISCUSSION

Abnormal placental development has been linked to numerous pregnancy complications, including pre-eclampsia, intrauterine growth restriction, miscarriage, and stillbirth (Khong, 1986; Khong et al., 1987; Hustin et al., 1990; Brosens et al., 2002; Fisher, 2015; Knofler et al., 2019). The placenta develops by forming primary villi consisting of rapidly proliferating CTB. These cells fuse to form an outer layer of villous syncytiotrophoblast. At the same time, the CTBs start to differentiate into EVT within the trophoblast columns of the early gestation placenta, anchoring the placenta to the uterine wall (Turco and Moffett, 2019). EVTs mature as they move distally within the trophoblast column, and subsequently invade into the decidua and myometrium as interstitial EVT, or remodel decidual arterioles as endovascular EVT (Pijnenborg et al., 1980, 2006). While much has been done to characterize early gestation EVT, fewer studies have focused on mature EVT. In this study, we set out to characterize these cells from normal term placentae, including their genome and transcriptome; given this tissue source, the majority of these cells are likely mature interstitial (and not endovascular) EVTs. Additionally, by comparison to both first trimester and term CTB, as well as first trimester EVT, we assembled gene regulatory networks to better understand the pathways and TFs involved in the maturation and unique genomic architecture of EVT.

Characterization of EVT Genome

Extravillous trophoblasts share numerous cellular characteristics with tumor cells, including EMT (Viovac and Aplin, 1996). In addition, multiple studies have suggested that EVTs are tumor-like in their carriage of genomic aberrations (Zybina et al., 2002, 2004; Weier et al., 2005; Velicky et al., 2018). Specifically, earlier studies (Zybina et al., 2002, 2004) suggested that EVTs show moderate genome amplification (up to 8N) but are not highly polyploid, unlike mouse TGCs; the latter not only show significant polyploidy (with some cells $>$ 900N) but also contain functionally relevant under- or over-represented genomic regions (Hannibal et al., 2014; Hannibal and Baker, 2016). Another study suggested the presence of aneuploidy and hyperdiploidy in trophoblast, with the greatest proportion in HLA-G$^+$ EVT (Weier et al., 2005). Most recently, Velicky et al. (2018) have reported that the majority of first trimester EVTs were hyperdiploid, possibly through endoreduplication, and undergoing senescence through this process. Several recent studies have also examined the existence of CNVs in the placenta (Kasak et al., 2015; Meinhardt et al., 2015; Coorens et al., 2021), but with inconsistent conclusions. One study identified amplification of the *ERBB2* gene and found it to be particularly prominent in EVT (Meinhardt et al., 2015). Other studies have used bulk placental samples with parental controls and identified widespread copy number changes; however, these studies either excluded EVT from samples or could not confirm the presence of somatic genomic rearrangements in placenta-specific cell types at term (Kasak et al., 2015; Coorens et al., 2021).

Here, to gain a better understanding of the genomes of normal human EVT, we applied multiple cellular and bioinformatic methods. First, we reanalyzed a previously published WGS dataset from CTB and EVT purified from first trimester placentae (Velicky et al., 2018), applying CNV detection algorithms not used in the original analysis. We did not find CNVs that had been reported in mouse TGCs but did find three duplications previously reported in bulk second trimester human placental samples (Kasak et al., 2015; Coorens et al., 2021). Additionally, we performed genome-wide CNV analysis of our own samples using high-resolution SNP genotyping arrays and identified three duplications in our term EVT samples, none of which were common between samples or previously reported (Kasak et al., 2015; Coorens et al., 2021). Although we could not identify any common EVT-specific CNVs among preparations from different placentae, including those from a previous publication, definitive assessment of this observation will require a substantially larger sample size. We also applied ploidy-detection algorithms on Velicky et al. (2018)'s WGS data as well as our SNP genotyping data but found no evidence of polyploidy. Lastly, to rule out the presence of a subpopulation of EVT cells showing a high

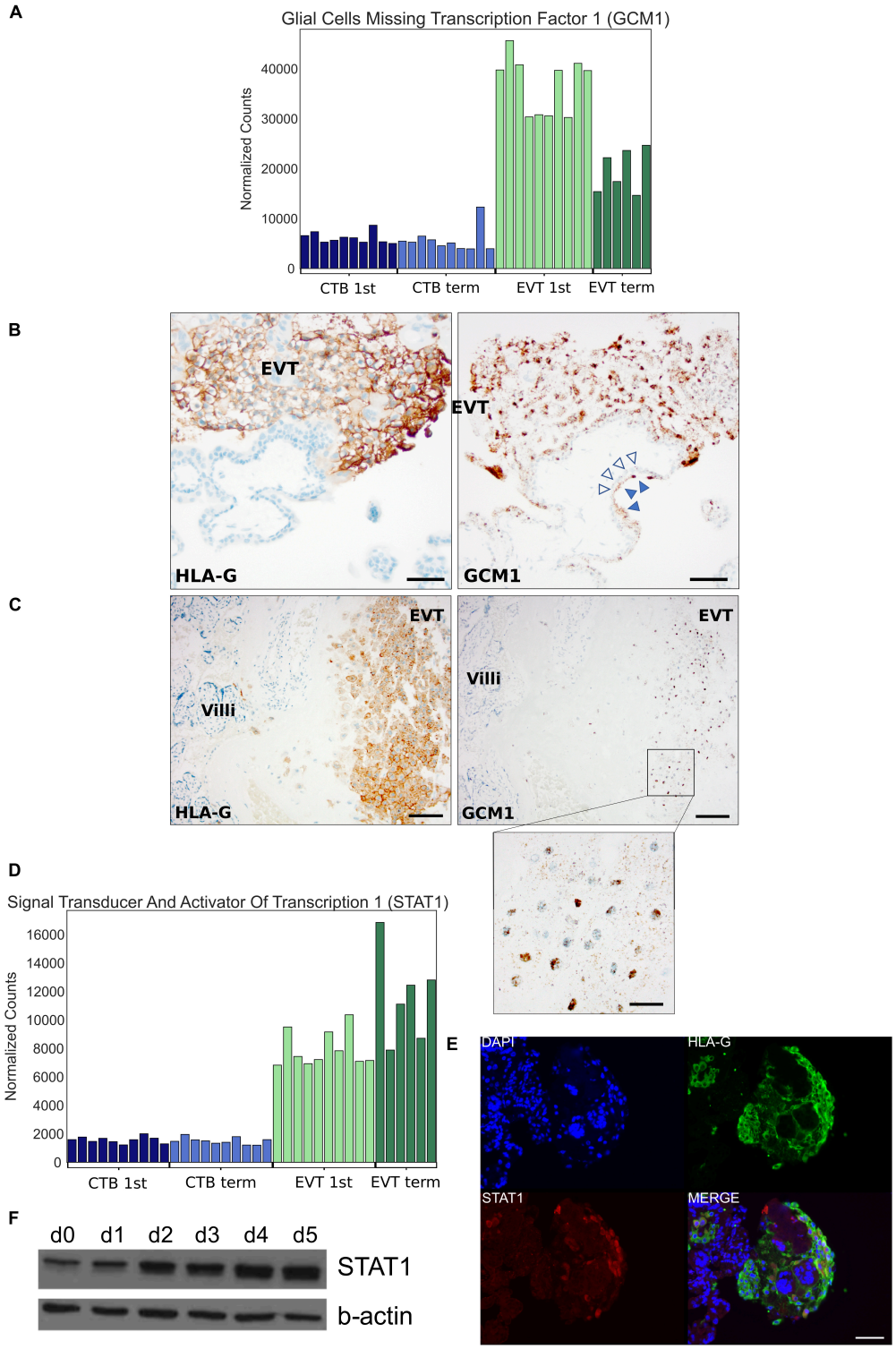

FIGURE 9 | Localization and expression of GCM1 and STAT1 transcription factors. **(A)** Bar graph depicting GCM1 expression in all 36 placental samples using RNA-seq. **(B)** *In situ* hybridization of GCM1 (right-side) and immunohistochemistry for HLA-G (left-side) in adjacent sections of first trimester EVT. Empty arrowheads point to CTB and filled arrowheads to syncytiotrophoblast, which also expresses GCM1. HLA-G staining highlights EVT. Scale bars = 50 μm. **(C)** *In situ* hybridization of GCM1 (right-side, with further magnification in inset) and immunohistochemistry for HLA-G (left-side) in adjacent sections of term EVT. HLA-G again highlights EVT at the basal plate. Scale bar = 100 μm in main panels and 25 μm in inset. **(D)** Bar graph depicting STAT1 expression in all 36 placental samples using RNA-seq. **(E)** Immunostaining of first trimester placenta with antibodies against HLA-G and STAT1 and counterstained with DAPI. Scale bars = 50 μm. **(F)** Western blot of STAT1 and beta-actin (control) during EVT differentiation of 1049 hTSC line.

polyploidy rate or widespread CNVs, we performed single-cell CNV analysis on a set of isolated samples and again found no evidence of polyploidy or cells with a large number of CNVs. Nevertheless, we suspect that the algorithms used in our analysis are poorly suited to calling polyploidy.

To validate previous reports of polyploidy in EVT, and to confirm the limitations of the algorithms applied to our genomic data, we determined the DNA content of our isolated placental cells by flow cytometry and found the majority (57%) of first trimester EVT and a lower percentage (44%) of term EVT to be tetraploid. FISH confirmed our flow cytometry results. As previously reported (Zybina et al., 2002), we also noted a population of EVT with > 4N status, with a slightly larger proportion of such cells at term. Interestingly, a similar proportion of term CTB (∼15%) had a >4N status, suggesting that this may be a feature of "aged" trophoblast, as recently reported (Coorens et al., 2021), rather than a unique feature of term EVT. Additionally, we differentiated primary hTSC cells to EVT, using established protocols (Okae et al., 2018) to assess how well current *in vitro* models recapitulate the polyploid phenotype seen in primary EVT. We found that *in vitro* differentiation did not increase the proportion of hyperdiploid cells, suggesting that perhaps *in vivo*, EVTs receive additional signals from their environment that lead to polyploidization. Additional work is thus needed to better recapitulate the *in vivo* EVT state *in vitro*.

The biological significance of polyploidization remains unclear, particularly in the placenta. In the liver, polyploidization has been hypothesized to be a hallmark of terminal differentiation, a mechanism through which a cell may shift energy usage from cell division to more important functions, and/or as a way to protect cells against oxidative stress and genotoxic damage (Wang et al., 2017). Oxygen tension in blood surrounding the placental villi has been reported to increase threefold during pregnancy causing oxidative stress (Jauniaux et al., 2000) and recently (Coorens et al., 2021) reported a substantial mutational burden in placental tissue. Thus, the onset of endoreduplication and senescence, which requires replication arrest in a previously proliferative cell type such as EVT, would lead to the acquisition of multiple sets of chromosomes and could function to buffer cells against harmful mutations. Our evaluation of EVT transcriptome, discussed below, may shed some light on this question; however, future studies examining transcriptomes of EVT subpopulations, separated based on different levels of ploidy, along with delineation of the spatial distribution of these subpopulations, are needed to more precisely define the function(s) of polyploid EVT.

Characterization of EVT Transcriptome

Pathways Involved in EVT Differentiation and Maturation

To help characterize the differences between the largely diploid CTB and the majority polyploid EVT, we profiled the transcriptomes of isolated first trimester and term CTB and EVT, using RNA-seq. Our RNA-seq dataset was well powered, consisting of 10 first trimester CTB, 10 first trimester EVT, 10 term CTB, and 6 term EVT samples at an average depth of over 40 million uniquely mapped reads, offering a detailed look at how these two trophoblast cell types differed at two different GAs. With respect to first trimester EVT, our GSEA results confirmed previously published microarray datasets (Apps et al., 2011; Telugu et al., 2013; Tilburgs et al., 2015; Wakeland et al., 2017) and added further evidence that EVT differentiation entails upregulation of EMT and hypoxia signaling, along with many inflammatory- and immune-mediated processes, and eventually a downregulation of proliferation and cell cycle pathways suggesting terminal differentiation. Perhaps surprisingly, many of the same pathways were up- or down-regulated when comparing CTB and EVT from term placenta, suggesting that, despite a previous report (McMaster et al., 1995), given the right conditions, it may be possible to differentiate term CTB to EVT. Interestingly, two pathways that were found to be up-regulated in first trimester EVT and not term EVT were the PI3K/AKT/mTOR signaling and UPR pathways. By inhibiting one arm of the UPR pathway during EVT differentiation of primary hTSC, we found that this pathway is important for surface expression of HLA-G, a molecule required for EVT crosstalk with maternal natural killer (NK) cells (Pollheimer et al., 2018). ER stress has been studied in the context of oxidative stress-induced placental dysfunction (i.e., in the setting of pre-eclampsia and intrauterine growth restriction; Burton et al., 2009; Mizuuchi et al., 2016). It is also known that enhanced induction of this pathway disrupts placental development (Yung et al., 2012), but, until now, it had not been studied specifically in the context of EVT. Interestingly, hypoxic conditions, known to promote EVT differentiation (Wakeland et al., 2017), induce adaptive cellular responses including the UPR pathway. It is tempting to speculate that hypoxia-induced EVT differentiation is partially mediated through the IRE1-alpha arm of UPR; further studies are needed to test this hypothesis.

At the same time, we also noted a large overlap in pathways that were significantly different in first trimester CTB vs. EVT and first trimester vs. term EVT. This suggests that these overlapping pathways may be essential for both differentiation and maturation of, or simply characteristic of both immature and mature, EVT. Many such pathways are likely to involve signals from the decidua and decidual immune cells, of which NK and macrophages are the most abundant (Vento-Tormo et al., 2018; Pique-Regi et al., 2019). Given the lack of polyploidy in our *in vitro*-differentiated EVT, it is worth exploring which, if any, of these pathways require further manipulation in order to optimize EVT differentiation of hTSC lines *in vitro*.

Finally, we evaluated gene expression differences between male and female EVTs and identified a relatively small number of DEGs between these groups; interestingly, the number of DEGs was higher at term (51) compared with first trimester (16). Although these DEGs were not enriched in any specific pathways, the findings correlate with those of Papuchova et al. (2020), showing that term (but not first trimester) EVTs showed higher levels of HLA-G if they came from placenta of a male fetus. Given this, and the well-known role of sexual dimorphism in placental development and disease (Kalisch-Smith et al., 2017), further study of these DEGs in EVT function is warranted.

Gene Expression Changes Associated With Polyploidy and Senescence

Polyploidy has long been intricately linked with cellular senescence (Campisi and d'Adda di Fagagna, 2007), and a recent report has suggested that first trimester EVTs exhibit both endoreduplication-induced polyploidy and senescence (Velicky et al., 2018). Therefore, we examined our RNA-seq data for genes involved in the cell cycle, endoreduplication, and cellular senescence. We found that term EVT did not express mitosis-linked genes, such as cyclin B, Ki67, and Aurora kinase A, but all three genes were expressed in first trimester EVT, in contrast to previous reports (Velicky et al., 2018). As discussed above, endoreduplication consists of DNA replication without cell or nuclear division and is triggered by p57 (CDKN1C) inhibition of CDK1 and p21 (CDKN1A) suppression of CHEK1, preventing induction of apoptosis (Ullah et al., 2008). Our term EVT showed marked decrease in CDK1 and CHEK1 and corresponding increases in p57 and p21, suggesting that, as in mouse TGCs, human term EVTs undergo endoreduplication. Interestingly, the G1–S transition promoting cyclin E1 was highly expressed in first trimester EVT, but nearly 3-fold lower in term EVT, whereas cyclin E2 progressively decreased between both CTB, first trimester EVT, and term EVT. Additionally, the mitosis-linked cyclin B gene was highly expressed in first trimester EVT but almost undetectable in term EVT. However, despite Velicky et al.'s claim that Cyclin $A^+/p57^-$ expression could be used as a marker for endoreduplicating HLA-G^+ trophoblast, we found very low levels of cyclin A in all of our samples despite relatively deep sequencing. We did observe that the genes encoding the RB protein and its E2F TF family targets also drop precipitously in term EVT, whereas SASP-associated genes were most highly expressed in term EVT. In the context of our FISH and flow cytometry data, these results suggest that cells may begin to undergo endoreduplication and senescence in the first trimester, but progress into a more fully senescent phenotype only at term. However, further studies, including evaluation of protein and phosphorylation levels (including RB protein phosphorylation; Giacinti and Giordano, 2006), should be conducted to more precisely evaluate the cell cycle during EVT formation.

It should be noted that, while Velicky et al. defined EVT spatially (as cells within the distal portion of the trophoblast cell column with larger nuclei), we defined EVT in this study based on surface HLA-G expression. Within first trimester samples, this likely led to a more heterogenous mixture of EVT in our samples, containing more proximal cell column trophoblasts, which are more proliferative and less mature, leading to some of the discrepancies between our two studies. More mature EVTs are found within decidual tissue strips (in first trimester samples) and deeper within the placental bed (in term samples). Though more difficult to obtain, future studies should attempt to include such samples and thus more thoroughly assess processes involved in EVT maturation.

TF Networks Regulating EVT Differentiation and Maturation

Using our RNA-seq data, we sought to identify TFs needed to drive EVT differentiation and maturation. We found that many TFs identified as being important in our protein-to-protein interaction networks were well-known regulators of processes previously identified as being vital in normal EVT development. During differentiation of first trimester CTB to EVT, we found the top four TFs with the highest importance scores in our largest clustered subnetwork to be TFEB, IRF7, IRF8, and STAT1, all of which are involved in immune response (Martina et al., 2012; Brady et al., 2018; Jefferies, 2019; Jung et al., 2020), correlating well with our GSEA findings (Zhang et al., 2015). We validated STAT1 as uniquely expressed in EVT within first trimester placental tissue, with its expression increasing during *in vitro* differentiation of hTSC into EVT; similar findings were recently reported by Chen et al. (2021), who have suggested that the signals leading to STAT1 induction are derived from decidual stromal cells. Additionally, we noted that this clustered subnetwork, and the largest subnetwork in the genes up-regulated in term EVT vs. CTB, was centered around FN1, which, we found to be linked with XBP1, a key part of the UPR pathway in mammals (Hetz and Papa, 2018). XBP1 was recently reported to initiate FN1 expression in colon cancer cells (Xie et al., 2019) and thus deserves further study as a possible link between hypoxia, UPR, and ECM remodeling in the context of EVT differentiation.

In our analysis of TFs involved in EVT maturation, we identified GCM1 as the TF with the highest importance score in the largest subnetwork of genes up-regulated in term, compared with first trimester, EVT, though its expression appeared to decrease in term, compared with first trimester, EVT; we validated these findings by ISH, using both first trimester and term placental tissues. GCM1 is a TF known best as a master regulator of labyrinthine or villous trophoblast differentiation in both mice and human (Cross et al., 2006; Baczyk et al., 2009). However, we and others have shown that GCM1 is also highly expressed in human EVT (Baczyk et al., 2004; Chiu and Chen, 2016; Wakeland et al., 2017). GCM1 has been shown to play a role in trophoblast invasion, acting through HTRA4, a serine protease that facilitates fibronectin cleavage, to suppress cell–cell fusion and promote invasion (Wang et al., 2012). However, while this describes a clear role for GCM1 in a basic function (invasion) of all EVT, including those in first trimester, its identification as a key TF involved in regulation of term EVT transcriptome requires further study.

Other TFs identified as controlling up-regulated genes during EVT maturation included NFAT5 and STAT4, both of which are involved in immune response, with the latter regulating response to IL-12 signaling (Morinobu et al., 2002; Lee et al., 2019). The IL-12 cytokine family, produced by EVT, is important in establishment of maternal–fetal tolerance through modulation of naïve conventional T cells and their conversion into induced regulatory T cells (Liu et al., 2019). Papuchova et al. (2020) has pointed to heterogeneity within term EVT, with subtypes showing differing capacities for modulating resident immune cells, including regulatory T cells. Future studies, including single-cell analysis, are warranted to further study EVT heterogeneity, based not just on ploidy and gene expression, but on functional capacities, in order to better understand the role

of these cells in establishment and maintenance of the maternal–fetal interface.

Summary

In summary, our study builds on earlier reports characterizing first trimester EVT, extending such genomic and transcriptomic studies to term EVT, and defining pathways and TF networks involved in both initial differentiation and maturation of this important trophoblast lineage at the maternal–fetal interface. Our results suggest that term EVTs lack high rates of CNVs, though studies using WGS with substantially larger sample sizes are needed to definitively identify or rule-out the presence of functionally relevant under- or over-represented genomic regions. Additionally, we have highlighted senescence and polyploidy-related genes, pathways, networks, and TFs that appeared to be important in EVT differentiation and maturation and have validated a critical role for the UPR in formation of functional EVT. Lastly, our results highlight the need for more optimized *in vitro* models of EVT differentiation, further research into functional differences among EVT subpopulations with different ploidy levels, and studies of placental diseases that may be associated with changes in cellular ploidy or dysfunctional EVT differentiation or maturation.

DATA AVAILABILITY STATEMENT

The datasets presented in this study can be found in online repositories. The names of the repository/repositories and accession number(s) can be found below: BioProject, accession: PRJNA724881, GEO accession: GSE173372 https://www.ncbi.nlm.nih.gov/geo/query/acc.cgi?acc=GSE173372.

ETHICS STATEMENT

The studies involving human participants were reviewed and approved by Human Research Protections Program Committee of the UCSD Institutional Review Board (IRB number: 181917X). The patients/participants provided their written informed consent to participate in this study. Written informed consent was obtained from the individual(s) for the publication of any potentially identifiable images or data included in this article.

AUTHOR CONTRIBUTIONS

RM, OF, DR, SK, FS, and MM performed the experiments. RM, OF, DR, and SK performed the data analysis. LL and MP supervised and designed the study. RM, LL, and MP wrote the manuscript. All authors contributed to the article and approved the submitted version.

FUNDING

This work was supported by funds from the National Institutes of Health (NIH)/National Institute of Child Health and Human Development (NICHD, R01-HD089537 and R21-HD094618 to MP). RM was also supported by a grant from the National Institutes of Health, United States (NIH grant T32GM8806). OF was also supported by a fellowship from the Lalor Foundation. SK, LL, and FS were also supported by the NIH/NICHD R01-HD096260 to FS. This publication includes data generated at the UC San Diego IGM Genomics Center utilizing an Illumina NovaSeq 6000 that was purchased with funding from a National Institutes of Health SIG grant (#S10 OD026929), and analysis was done using the Extreme Science and Engineering Discovery Environment (XSEDE) Comet for computational analysis, which is supported by the National Science Foundation grant number ACI-1548562 (allocation ID: TG-MCB140074).

ACKNOWLEDGMENTS

We would like to thank all patients who donated placental tissues for this study, as well as the UC San Diego Health Clinical Laboratories and specifically Marie Dell'Aquila and Graciela Resolme for their help with the cytogenetics experiment. We would also like to thank Donald Pizzo for help with the *in situ* hybridization experiment.

SUPPLEMENTARY MATERIAL

The Supplementary Material for this article can be found online at: https://www.frontiersin.org/articles/10.3389/fcell.2021.702046/full#supplementary-material

Supplementary Figure 1 | Ploidy determination of whole genome sequencing data and SNP genotyping array data. **(A)** Ploidy of two $HLAG^+$ samples (11- and 12-weeks gestational age) from BioProject accession PRJNA445189 (Velicky et al., 2018) as determined by PURPLE reanalysis. **(B)** Ploidy of SNP genotyping array of our term EVT samples as determined by ASCAT.

Supplementary Figure 2 | Differential gene expression between male and female samples in first trimester and term EVT. **(A)** Heatmap of all differentially expressed genes between male and female samples in first trimester EVT. Blue- and pink-highlighted dendrogram rows are genes up-regulated in male or female samples, respectively. **(B)** Heatmaps of differentially expressed genes between male and female samples in term EVT, with genes up-regulated in the female samples shown in top heatmap and those up-regulated in male samples in bottom heatmap. For both analyses, differentially expressed genes were determined by adj p-value < 0.05, Log_2 fold change > 1, mean normalized expression in group > 100; values were log transformed to create heatmap.

Supplementary Figure 3 | Common and unique pathways involved in EVT differentiation and maturation. **(A)** GSEA using only founder gene sets of the two common down-regulated pathways during EVT maturation (first trimester EVT → term EVT; E2F targets and G2M checkpoint pathways) showed down-regulation in term EVT for the neighborhood of CCNA2 (Cyclin A2), PCNA, and RRM2 in the GNF2 expression compendium. The three genes shown in the figure are representative genes from each of these gene sets. **(B)** GSEA enrichment score plot showing Hallmark pathway Unfolded Protein Response (UPR) gene set in first trimester EVT compared to term EVT. The UPR pathway is also enriched in first trimester EVT compared to first trimester CTB.

Supplementary Figure 4 | Principal component analysis of RNA-seq data comparing our three hTSC lines and those previously reported (Okae et al., 2018). Principal component analysis shows the first two components using all common genes between the two datasets post-filtering. The plot shows all 36 placenta samples from this study and 6 from Okae et al. (2018), triplicates of three hTSC

lines (1,048, 1,049, and 1,270) from this study, and duplicates of blastocyst derived hTSC and placental derived hTSC from Okae et al. (2018; see **Supplementary Table 1**).

Supplementary Figure 5 | The role of IRE1-alpha arm of the Unfolded Protein Response (UPR) pathway in EVT differentiation of hTSCs. Two different hTSC lines (1,048 and 1,049) were differentiated into EVT over 5 days in the presence or absence of the IRE1-alpha inhibitor, 4u8C. **(A)** qPCR for markers of CTB (ITGA6) or EVT (ITGA5 and ITGA1). **(B)** qPCR for markers of EVT (HLAG and ASCL2). **(C)** qPCR for UPR pathway genes, XBP1 (total and spliced) and ATF4. The decrease in spliced XBP1 following 4u8C treatment confirms inhibition of the IRE1-alpha arm of UPR. ddCT values were normalized to beta-actin and shown as fold change over day 0. * shows statistically significant difference from day 0, while # shows statistically significant difference from DMSO carrier alone treatment on the same day, based on *t*-test ($p < 0.05$).

Supplementary Figure 6 | Expression of cell cycle-associated genes in first trimester and term CTB and EVT. **(A)** Normalized gene expression in all samples for AURKA, CDK1, MKI67, and CCNB1. **(B)** Cell cycle scoring based on previously-identified cell cycle phase-specific gene expression (Macosko et al., 2015) on term single-cell RNA-seq data (Tsang et al., 2017) visualized in a UMAP representation. HLAG and EGFR expression are shown to identify EVT and CTB cell clusters, respectively. **(C)** Cell cycle and endoreduplication-associated gene expression (normalized counts) of Cyclin E1 (CCNE1).

Supplementary Table 1 | Details of all samples used in study. CTB, cytotrophoblast; EVT, extravillous trophoblast; MSC, umbilical cord-derived mesenchymal stem cells; and TSC, trophoblast stem cells (derived from first trimester placentae).

Supplementary Table 2 | List of primers used for qPCR.

REFERENCES

Apps, R., Sharkey, A., Gardner, L., Male, V., Trotter, M., Miller, N., et al. (2011). Genome-wide expression profile of first trimester villous and extravillous human trophoblast cells. *Placenta* 32, 33–43. doi: 10.1016/j.placenta.2010.10.010

Baczyk, D., Drewlo, S., Proctor, L., Dunk, C., Lye, S., and Kingdom, J. (2009). Glial cell missing-1 transcription factor is required for the differentiation of the human trophoblast. *Cell Death Differ.* 16, 719–727. doi: 10.1038/cdd.2009.1

Baczyk, D., Satkunaratnam, A., Nait-Oumesmar, B., Huppertz, B., Cross, J. C., and Kingdom, J. C. P. (2004). Complex patterns of GCM1 mRNA and protein in villous and extravillous trophoblast cells of the human placenta. *Placenta* 25, 553–559. doi: 10.1016/j.placenta.2003.12.004

Barlow, P. W., and Sherman, M. I. (1972). The biochemistry of differentiation of mouse trophoblast: studies on polyploidy. *J. Embryol. Exp. Morphol.* 27, 447–465. doi: 10.1242/dev.27.2.447

Basisty, N., Kale, A., Jeon, O. H., Kuehnemann, C., Payne, T., Rao, C., et al. (2020). A proteomic atlas of senescence-associated secretomes for aging biomarker development. *PLoS Biol.* 18:e3000599. doi: 10.1371/journal.pbio.3000599

Brady, O. A., Martina, J. A., and Puertollano, R. (2018). Emerging roles for TFEB in the immune response and inflammation. *Autophagy* 14, 181–189. doi: 10.1080/15548627.2017.1313943

Brosens, J. J., Pijnenborg, R., and Brosens, I. A. (2002). The myometrial junctional zone spiral arteries in normal and abnormal pregnancies: a review of the literature. *Am. J. Obstet. Gynecol.* 187, 1416–1423. doi: 10.1067/mob.2002.127305

Burton, G. J., Yung, H. W., Cindrova-Davies, T., and Charnock-Jones, D. S. (2009). Placental endoplasmic reticulum stress and oxidative stress in the pathophysiology of unexplained intrauterine growth restriction and early onset preeclampsia. *Placenta* 30 (Suppl A), S43–S48.

Cameron, D. L., Baber, J., Shale, C., Papenfuss, A. T., Valle-Inclan, J. E., Besselink, N., et al. (2019). GRIDSS, PURPLE, LINX: unscrambling the tumor genome via integrated analysis of structural variation and copy number. *bioRxiv* [Preprint] 781013

Campisi, J., and d'Adda di Fagagna, F. (2007). Cellular senescence: when bad things happen to good cells. *Nat. Rev. Mol. Cell Biol.* 8, 729–740. doi: 10.1038/nrm2233

Chen, C., Kang, X., Li, C., Guo, F., Wang, Q., and Zhao, A. (2021). Involvement of signal transducers and activators of transcription in trophoblast differentiation. *Placenta* 105, 94–103. doi: 10.1016/j.placenta.2021.01.021

Chiu, Y. H., and Chen, H. (2016). GATA3 inhibits GCM1 activity and trophoblast cell invasion. *Sci. Rep.* 6:21630.

Coorens, T. H. H., Oliver, T. R. W., Sanghvi, R., Sovio, U., Cook, E., Vento-Tormo, R., et al. (2021). Inherent mosaicism and extensive mutation of human placentas. *Nature* 592, 80–85. doi: 10.1038/s41586-021-03345-1

Cross, J. C., Nakano, H., Natale, D. R. C., Simmons, D. G., and Watson, E. D. (2006). Branching morphogenesis during development of placental villi. *Differentiation* 74, 393–401. doi: 10.1111/j.1432-0436.2006.00103.x

Dasilva-Arnold, S., James, J. L., Al-Khan, A., Zamudio, S., and Illsley, N. P. (2015). Differentiation of first trimester cytotrophoblast to extravillous trophoblast involves an epithelial-mesenchymal transition. *Placenta* 36, 1412–1418. doi: 10.1016/j.placenta.2015.10.013

Davies, J. P., Pollheimer, J., Yong, H., Kokkinos, M., Kalionis, B., Knöfler, M., et al. (2016). Epithelial-mesenchymal transition during extravillous trophoblast differentiation. *Cell Adh. Migr.* 10, 310–321. doi: 10.1080/19336918.2016.1170258

Dobin, A., Davis, C. A., Schlesinger, F., Drenkow, J., Zaleski, C., Jha, S., et al. (2013). STAR: ultrafast universal RNA-seq aligner. *Bioinformatics (Oxford, England)* 29, 15–21. doi: 10.1093/bioinformatics/bts635

Ferretti, C., Bruni, L., Dangles-Marie, V., Pecking, A. P., and Bellet, D. (2007). Molecular circuits shared by placental and cancer cells, and their implications in the proliferative, invasive and migratory capacities of trophoblasts. *Human Reprod. Update* 13, 121–141. doi: 10.1093/humupd/dml048

Fisher, S. J. (2015). Why is placentation abnormal in preeclampsia? *Am. J. obstet. Gynecol.* 213, S115–122.

Fox, D. T., and Duronio, R. J. (2013). Endoreplication and polyploidy: insights into development and disease. *Development (Cambridge, England)* 140, 3–12. doi: 10.1242/dev.080531

Giacinti, C., and Giordano, A. (2006). RB and cell cycle progression. *Oncogene* 25, 5220–5227. doi: 10.1038/sj.onc.1209615

Hannibal, R. L., and Baker, J. C. (2016). Selective amplification of the genome surrounding key placental genes in trophoblast giant cells. *Curr. Biol.* 26, 230–236. doi: 10.1016/j.cub.2015.11.060

Hannibal, R. L., Chuong, E. B., Rivera-Mulia, J. C., Gilbert, D. M., Valouev, A., and Baker, J. C. (2014). Copy number variation is a fundamental aspect of the placental genome. *PLoS Genet.* 10:e1004290. doi: 10.1371/journal.pgen.1004290

Hayflick, L. (1965). The limited in vitro lifetime of human diploid cell strains. *Exp. Cell Res.* 37, 614–636. doi: 10.1016/0014-4827(65)90211-9

Hetz, C., and Papa, F. R. (2018). The unfolded protein response and cell fate control. *Mol. Cell* 69, 169–181. doi: 10.1016/j.molcel.2017.06.017

Hustin, J., Jauniaux, E., and Schaaps, J. P. (1990). Histological study of the materno-embryonic interface in spontaneous abortion. *Placenta* 11, 477–486. doi: 10.1016/s0143-4004(05)80193-6

Ishige, I., Nagamura-Inoue, T., Honda, M. J., Harnprasopwat, R., Kido, M., Sugimoto, M., et al. (2009). Comparison of mesenchymal stem cells derived from arterial, venous, and Wharton's jelly explants of human umbilical cord. *Int. J. Hematol.* 90, 261–269. doi: 10.1007/s12185-009-0377-3

Jauniaux, E., Watson, A. L., Hempstock, J., Bao, Y. P., Skepper, J. N., and Burton, G. J. (2000). Onset of maternal arterial blood flow and placental oxidative stress. A possible factor in human early pregnancy failure. *Am. J. Pathol.* 157, 2111–2122. doi: 10.1016/s0002-9440(10)64849-3

Jefferies, C. A. (2019). Regulating IRFs in IFN driven disease. *Front. Immunol.* 10:325. doi: 10.3389/fimmu.2019.00325

Johmura, Y., and Nakanishi, M. (2016). Multiple facets of p53 in senescence induction and maintenance. *Cancer Sci.* 107, 1550–1555. doi: 10.1111/cas.13060

Jung, S. R., Ashhurst, T. M., West, P. K., Viengkhou, B., King, N. J. C., Campbell, I. L., et al. (2020). Contribution of STAT1 to innate and adaptive immunity during type I interferon-mediated lethal virus infection. *PLoS Pathog.* 16:e1008525. doi: 10.1371/journal.ppat.1008525

Kalisch-Smith, J. I., Simmons, D. G., Dickinson, H., and Moritz, K. M. (2017). Review: sexual dimorphism in the formation, function and adaptation of the placenta. *Placenta* 54, 10–16. doi: 10.1016/j.placenta.2016.12.008

Kasak, L., Rull, K., Vaas, P., Teesalu, P., and Laan, M. (2015). Extensive load of somatic CNVs in the human placenta. *Sci. Rep.* 5:8342.

Khong, T. Y. A. (1986). Inadequate maternal vascular response to placentation in pregnancies complicated by pre-eclampsia and by small-for-gestational age infants. *Br. J. Obstet. Gynaecol.* 93, 1049–1059. doi: 10.1111/j.1471-0528.1986.tb07830.x

Khong, T. Y., Liddell, H. S., and Robertson, W. B. (1987). Defective haemochorial placentation as a cause of miscarriage: a preliminary study. *Br. J. Obstet. Gynaecol.* 94, 649–655. doi: 10.1111/j.1471-0528.1987.tb03169.x

Knofler, M., Haider, S., Saleh, L., Pollheimer, J., Gamage, T. K. J. B., and James, J. (2019). Human placenta and trophoblast development: key molecular mechanisms and model systems. *Cell. Mol. Life Sci.* 76, 3479–3496. doi: 10.1007/s00018-019-03104-6

Kuleshov, M. V., Jones, M. R., Rouillard, A. D., Fernandez, N. F., Duan, Q., Wang, Z., et al. (2016). Enrichr: a comprehensive gene set enrichment analysis web server 2016 update. *Nucleic Acids Res.* 44, W90–W97.

Langmead, B., and Salzberg, S. L. (2012). Fast gapped-read alignment with Bowtie 2. *Nat. Methods* 9, 357–359. doi: 10.1038/nmeth.1923

Lee, N., Kim, D., and Kim, W.-U. (2019). Role of NFAT5 in the immune system and pathogenesis of autoimmune diseases. *Front. Immunol.* 10:270. doi: 10.3389/fimmu.2019.00270

Li, Y., Moretto-Zita, M., Soncin, F., Wakeland, A., Wolfe, L., Leon-Garcia, S., et al. (2013). BMP4-directed trophoblast differentiation of human embryonic stem cells is mediated through a ΔNp63 cytotrophoblast stem cell state. *Development* 140, 3965–3976. doi: 10.1242/dev.092155

Liao, Y., Smyth, G. K., and Shi, W. (2014). featureCounts: an efficient general purpose program for assigning sequence reads to genomic features. *Bioinformatics* 30, 923–930. doi: 10.1093/bioinformatics/btt656

Liberzon, A., Birger, C., Thorvaldsdttir, H., Ghandi, M., Mesirov, J. P., and Tamayo, P. (2015). The Molecular Signatures Database (MSigDB) hallmark gene set collection. *Cell Syst.* 1, 417–425. doi: 10.1016/j.cels.2015.12.004

Liu, J., Hao, S., Chen, X., Zhao, H., Du, L., Ren, H., et al. (2019). Human placental trophoblast cells contribute to maternal-fetal tolerance through expressing IL-35 and mediating iT(R)35 conversion. *Nat. Commun.* 10:4601.

Love, M. I., Huber, W., and Anders, S. (2014). Moderated estimation of fold change and dispersion for RNA-seq data with DESeq2. *Genome Biol.* 15:550.

Macosko, E. Z., Basu, A., Satija, R., Nemesh, J., Shekhar, K., Goldman, M., et al. (2015). Highly parallel genome-wide expression profiling of individual cells using nanoliter droplets. *Cell* 161, 1202–1214. doi: 10.1016/j.cell.2015.05.002

Martina, J. A., Chen, Y., Gucek, M., and Puertollano, R. (2012). MTORC1 functions as a transcriptional regulator of autophagy by preventing nuclear transport of TFEB. *Autophagy* 8, 903–914. doi: 10.4161/auto.19653

McMaster, M. T., Librach, C. L., Zhou, Y., Lim, K. H., Janatpour, M. J., Demars, R., et al. (1995). Human placental HLA-G expression is restricted to differentiated cytotrophoblasts. *J. Immunol.* 154, 3771–3778.

Meinhardt, G., Kaltenberger, S., Fiala, C., Knfler, M., and Pollheimer, J. (2015). ERBB2 gene amplification increases during the transition of proximal EGFR(+) to distal HLA-G(+) first trimester cell column trophoblasts. *Placenta* 36, 803–808. doi: 10.1016/j.placenta.2015.05.017

Mizuuchi, M., Cindrova-Davies, T., Olovsson, M., Charnock-Jones, D. S., Burton, G. J., and Yung, H. W. (2016). Placental endoplasmic reticulum stress negatively regulates transcription of placental growth factor via ATF4 and ATF6β: implications for the pathophysiology of human pregnancy complications. *J. Pathol.* 238, 550–561. doi: 10.1002/path.4678

Moerman, T. A. (2019). GRNBoost2 and Arboreto: efficient and scalable inference of gene regulatory networks. *Bioinformatics (Oxford, England)* 35, 2159–2161. doi: 10.1093/bioinformatics/bty916

Morinobu, A., Gadina, M., Strober, W., Visconti, R., Fornace, A., Montagna, C., et al. (2002). STAT4 serine phosphorylation is critical for IL-12-induced IFN-gamma production but not for cell proliferation. *Proc. Natl. Acad. Sci. U.S.A.* 99, 12281–12286. doi: 10.1073/pnas.182618999

Okae, H., Toh, H., Sato, T., Hiura, H., Takahashi, S., Shirane, K., et al. (2018). Derivation of human trophoblast stem cells. *Cell Stem Cell* 22, 50–63.e56.

Papuchova, H., Kshirsagar, S., and Xu, L. A. (2020). Three types of HLA-G+ extravillous trophoblasts that have distinct immune regulatory properties. *Proc. Natl. Acad. Sci. U.S.A.* 117, 15772–15777. doi: 10.1073/pnas.2000484117

Patel, A. P., Tirosh, I., Trombetta, J. J., Shalek, A. K., Gillespie, S. M., Wakimoto, H., et al. (2014). Single-cell RNA-seq highlights intratumoral heterogeneity in primary glioblastoma. *Science (New York, N.Y.)* 344, 1396–1401. doi: 10.1126/science.1254257

Pijnenborg, R., Dixon, G., Robertson, W. B., and Brosens, I. (1980). Trophoblastic invasion of human decidua from 8 to 18 weeks of pregnancy. *Placenta* 1, 3–19. doi: 10.1016/s0143-4004(80)80012-9

Pijnenborg, R., Vercruysse, L., and Hanssens, M. (2006). The uterine spiral arteries in human pregnancy: facts and controversies. *Placenta* 27, 939–958. doi: 10.1016/j.placenta.2005.12.006

Pique-Regi, R., Romero, R., Tarca, A. L., Sendler, E. D., Xu, Y., Garcia-Flores, V., et al. (2019). Single cell transcriptional signatures of the human placenta in term and preterm parturition. *ELife* 8:e52004.

Pluquet, O., Pourtier, A., and Abbadie, C. (2015). The unfolded protein response and cellular senescence. A review in the theme: cellular mechanisms of endoplasmic reticulum stress signaling in health and disease. *Am. J. physiol. Cell Physiol.* 308, C415–C425.

Pollheimer, J., and Knofler, M. (2005). Signalling pathways regulating the invasive differentiation of human trophoblasts: a review. *Placenta* 26 (Suppl A), S21–S30.

Pollheimer, J., Vondra, S., Baltayeva, J., Beristain, A. G., and Knfler, M. (2018). Regulation of placental extravillous trophoblasts by the maternal uterine environment. *Front. Immunol.* 9:2597. doi: 10.3389/fimmu.2018.02597

Priestley, P., Baber, J., Lolkema, M. P., Steeghs, N., De Bruijn, E., Shale, C., et al. (2019). Pan-cancer whole-genome analyses of metastatic solid tumours. *Nature* 575, 210–216. doi: 10.1038/s41586-019-1689-y

Sansregret, L., and Swanton, C. (2017). The role of aneuploidy in cancer evolution. *Cold Spring Harbor. Perspect. Med.* 7:a028373. doi: 10.1101/cshperspect.a028373

Shay, J. W., Pereira-Smith, O. M., and Wright, W. E. (1991). A role for both RB and p53 in the regulation of human cellular senescence. *Exp. Cell Res.* 196, 33–39. doi: 10.1016/0014-4827(91)90453-2

Soncin, F., Khater, M., To, C., Pizzo, D., Farah, O., and Wakeland, A. A. (2018). Comparative analysis of mouse and human placentae across gestation reveals species-specific regulators of placental development. *Development (Cambridge, England)* 145:dev156273.

Tacutu, R., Thornton, D., Johnson, E., Budovsky, A., Barardo, D., Craig, T., et al. (2018). Human ageing genomic resources: new and updated databases. *Nucleic Acids Res.* 46, D1083–D1090.

Telugu, B. P., Adachi, K., Schlitt, J. M., Ezashi, T., Schust, D. J., Roberts, R. M., et al. (2013). Comparison of extravillous trophoblast cells derived from human embryonic stem cells and from first trimester human placentas. *Placenta* 34, 536–543. doi: 10.1016/j.placenta.2013.03.016

Tilburgs, T., Crespo, N. C., Van Der Zwan, A., Rybalov, B., Raj, T., Stranger, B., et al. (2015). Human HLA-G+ extravillous trophoblasts: immune-activating cells that interact with decidual leukocytes. *Proc. Natl. Acad. Sci. U.S.A.* 112, 7219–7224. doi: 10.1073/pnas.1507977112

Trost, B., Walker, S., Wang, Z., Thiruvahindrapuram, B., Macdonald, J. R., Sung, W. W. L., et al. (2018). A comprehensive workflow for read depth-based identification of copy-number variation from whole-genome sequence data. *Am. J. Hum. Genet.* 102, 142–155. doi: 10.1016/j.ajhg.2017.12.007

Tsang, J. C. H., Vong, J. S. L., Ji, L., Poon, L. C. Y., Jiang, P., Lui, K. O., et al. (2017). Integrative single-cell and cell-free plasma RNA transcriptomics elucidates placental cellular dynamics. *Proc. Natl. Acad. Sci. U.S.A.* 114, E7786–E7795.

Turco, M. Y., and Moffett, A. (2019). Development of the human placenta. *Development (Cambridge, England)* 146:dev163428.

Ullah, Z., Kohn, M. J., Yagi, R., Vassilev, L. T., and Depamphilis, M. L. (2008). Differentiation of trophoblast stem cells into giant cells is triggered by p57/Kip2 inhibition of CDK1 activity. *Genes Dev.* 22, 3024–3036. doi: 10.1101/gad.1718108

Ullah, Z., Lee, C. Y., Lilly, M. A., and Depamphilis, M. L. (2009). Developmentally programmed endoreduplication in animals. *Cell Cycle (Georgetown, Tex.)* 8, 1501–1509. doi: 10.4161/cc.8.10.8325

Van Loo, P., Nordgard, S. H., Lingjærde, O. C., Russnes, H. G., Rye, I. H., Sun, W., et al. (2010). Allele-specific copy number analysis of tumors. *Proc. Natl. Acad. Sci. U.S.A.* 107, 16910–16915.

Velicky, P., Meinhardt, G., Plessl, K., Vondra, S., Weiss, T., Haslinger, P., et al. (2018). Genome amplification and cellular senescence are hallmarks of human placenta development. *PLoS Genet.* 14:e1007698. doi: 10.1371/journal.pgen.1007698

Vento-Tormo, R., Efremova, M., Botting, R. A., Turco, M. Y., Vento-Tormo, M., Meyer, K. B., et al. (2018). Single-cell reconstruction of the early maternal–fetal interface in humans. *Nature* 563, 347–353.

Viovac, L., and Aplin, J. D. (1996). Epithelial-mesenchymal transition during trophoblast differentiation. *Acta Anat.* 156, 202–216. doi: 10.1159/000147847

Wakeland, A. K., Soncin, F., Moretto-Zita, M., Chang, C.-W., Horii, M., Pizzo, D., et al. (2017). Hypoxia directs human extravillous trophoblast differentiation in a hypoxia-inducible factor-dependent manner. *Am. J. Pathol.*187, 767–780. doi: 10.1016/j.ajpath.2016.11.018

Wang, L.-J., Cheong, M.-L., Lee, Y.-S., Lee, M.-T., and Chen, H. (2012). High-temperature requirement protein A4 (HtrA4) suppresses the fusogenic activity of syncytin-1 and promotes trophoblast invasion. *Mol. Cell. Biol.* 32, 3707–3717. doi: 10.1128/mcb.00223-12

Wang, M.-J., Chen, F., Lau, J. T. Y., and Hu, Y.-P. (2017). Hepatocyte polyploidization and its association with pathophysiological processes. *Cell Death Dis.* 8:e2805. doi: 10.1038/cddis.2017.167

Weier, J. F., Weier, H.-U. G., Jung, C. J., Gormley, M., Zhou, Y., Chu, L. W., et al. (2005). Human cytotrophoblasts acquire aneuploidies as they differentiate to an invasive phenotype. *Dev. Biol.* 279, 420–432. doi: 10.1016/j.ydbio.2004.12.035

Wolf, F. A., Angerer, P., and Theis, F. J. (2018). SCANPY: large-scale single-cell gene expression data analysis. *Genome Biol.* 19:15.

Xie, Y., Liu, C., Qin, Y., Chen, J., and Fang, J. (2019). Knockdown of IRE1αsuppresses metastatic potential of colon cancer cells through inhibiting FN1-Src/FAK-GTPases signaling. *Int. J. Biochem. Cell Biol.* 114:105572. doi: 10.1016/j.biocel.2019.105572

Yang, P., Dai, A., Alexenko, A. P., Liu, Y., Stephens, A. J., Schulz, L. C., et al. (2014). Abnormal oxidative stress responses in fibroblasts from preeclampsia infants. *PLoS One* 9:e103110. doi: 10.1371/journal.pone.0103110

Yung, H. W., Hemberger, M., Watson, E. D., Senner, C. E., Jones, C. P., Kaufman, R. J., et al. (2012). Endoplasmic reticulum stress disrupts placental morphogenesis: implications for human intrauterine growth restriction. *J. Pathol.* 228, 554–564. doi: 10.1002/path.4068

Zhang, X.-J., Zhang, P., and Li, H. (2015). Interferon regulatory factor signalings in cardiometabolic diseases. *Hypertension (Dallas, Tex. : 1979)* 66, 222–247. doi: 10.1161/hypertensionaha.115.04898

Zhu, M., Need, A. C., Han, Y., Ge, D., Maia, J. M., Zhu, Q., et al. (2012). Using ERDS to infer copy-number variants in high-coverage genomes. *Am. J. Hum. Genet.* 91, 408–421. doi: 10.1016/j.ajhg.2012.07.004

Zybina, T. G., Frank, H. G., Biesterfeld, S., and Kaufmann, P. (2004). Genome multiplication of extravillous trophoblast cells in human placenta in the course of differentiation and invasion into endometrium and myometrium. II. Mechanisms of polyploidization. *Tsitologiia* 46, 640–648.

Zybina, T. G., Kaufmann, P., Frank, H. G., Freed, J., Kadyrov, M., and Biesterfeld, S. (2002). Genome multiplication of extravillous trophoblast cells in human placenta in the course of differentiation and invasion into endometrium and myometrium. I. Dynamics of polyploidization. *Tsitologiia* 44, 1058–1067.

Zybina, T. G., Stein, G. I., and Zybina, E. V. (2011). Endopolyploid and proliferating trophoblast cells express different patterns of intracellular cytokeratin and glycogen localization in the rat placenta. *Cell Biol. Int.* 35, 649–655. doi: 10.1042/cbi20100278

Conflict of Interest: The authors declare that the research was conducted in the absence of any commercial or financial relationships that could be construed as a potential conflict of interest.

Publisher's Note: All claims expressed in this article are solely those of the authors and do not necessarily represent those of their affiliated organizations, or those of the publisher, the editors and the reviewers. Any product that may be evaluated in this article, or claim that may be made by its manufacturer, is not guaranteed or endorsed by the publisher.

frontiers in Cell and Developmental Biology

BRIEF RESEARCH REPORT
published: 14 September 2021
doi: 10.3389/fcell.2021.704781

Characterization of the Primary Human Trophoblast Cell Secretome Using Stable Isotope Labeling With Amino Acids in Cell Culture

Fredrick J. Rosario[1], Sammy Pardo[2], Trond M. Michelsen[3], Kathryn Erickson[1,4], Lorna Moore[1], Theresa L. Powell[1,4], Susan T. Weintraub[2] and Thomas Jansson[1]*

[1] Division of Reproductive Sciences, Department of OB/GYN, University of Colorado Anschutz Medical Campus, Aurora, CO, United States, [2] Department of Biochemistry and Structural Biology, University of Texas Health Science Center at San Antonio, San Antonio, TX, United States, [3] Division of Obstetrics and Gynecology, Department of Obstetrics Rikshospitalet, Oslo University Hospital, Oslo, Norway, [4] Section of Neonatology, Department of Pediatrics, University of Colorado Anschutz Medical Campus, Aurora, CO, United States

OPEN ACCESS

Edited by:
Michael J. Soares, University of Kansas Medical Center Research Institute, United States

Reviewed by:
Evdokia Dimitriadis, University of Melbourne, Australia
Haijun Gao, Howard University, United States
Balaji Rao, North Carolina State University, United States

***Correspondence:**
Fredrick J. Rosario
fredrick.joseph@cuanschutz.edu

Specialty section:
This article was submitted to Developmental Epigenetics, a section of the journal Frontiers in Cell and Developmental Biology

Received: *03 May 2021*
Accepted: *16 August 2021*
Published: *14 September 2021*

Citation:
Rosario FJ, Pardo S, Michelsen TM, Erickson K, Moore L, Powell TL, Weintraub ST and Jansson T (2021) Characterization of the Primary Human Trophoblast Cell Secretome Using Stable Isotope Labeling With Amino Acids in Cell Culture. Front. Cell Dev. Biol. 9:704781. doi: 10.3389/fcell.2021.704781

The placental villus syncytiotrophoblast, the nutrient-transporting and hormone-producing epithelium of the human placenta, is a critical regulator of fetal development and maternal physiology. However, the identities of the proteins synthesized and secreted by primary human trophoblast (PHT) cells remain unknown. Stable Isotope Labeling with Amino Acids in Cell Culture followed by mass spectrometry analysis of the conditioned media was used to identify secreted proteins and obtain information about their relative rates of synthesis in syncytialized multinucleated PHT cells isolated from normal term placental villus tissue (n = 4/independent placenta). A total of 1,344 proteins were identified, most of which have not previously been reported to be secreted by the human placenta or trophoblast. The majority of secreted proteins are involved in energy and carbon metabolism, glycolysis, biosynthesis of amino acids, purine metabolism, and fatty acid degradation. Histone family proteins and mitochondrial proteins were among proteins with the slowest synthesis rate whereas proteins associated with signaling and the plasma membrane were synthesized rapidly. There was a significant overlap between the PHT secretome and proteins known be secreted to the fetal circulation by the human placenta *in vivo*. The generated data will guide future experiments to determine the function of individual secreted proteins and will help us better understand how the placenta controls maternal and fetal physiology.

Keywords: placenta, pregnancy, maternal-fetal exchange, mass spectrometry relative protein synthesis rates, proteomics

INTRODUCTION

The human placenta constitutes the interface between the maternal and fetal circulations and performs a wide array of functions, including nutrient and oxygen transport and secretion of hormones and exosomes (Costa, 2016). Hormones secreted by the placenta into the maternal circulation are believed to mediate maternal physiological adaptions to pregnancy. For example, animal studies have shown that placental lactogen promotes maternal β-cell proliferation and

increases glucose-stimulated insulin secretion (Brelje et al., 1994; Sorenson and Brelje, 1997; Kim et al., 2010; Baeyens et al., 2016), and placental growth hormone (pGH) induces skeletal muscle insulin resistance in the mother (Barbour et al., 2004). Moreover, normal fetal growth and development is critically dependent on a well-functioning placenta, and most common pregnancy complications, including intrauterine growth restriction (IUGR), stillbirth, and preeclampsia, are caused by abnormal development and/or function of the placenta (Sibley et al., 2005; Mifsud and Sebire, 2014; Fisher, 2015; Sircar et al., 2015). Thus, a better understanding of the mechanisms by which the human placenta regulates fetal development and maternal physiology will provide insights into the pathophysiology of pregnancy complications and how changes in placental function determines life-long health.

To allow early prediction of development of pregnancy complications caused by altered placental function and to design new intervention strategies targeting the placenta, sensitive biomarkers for placental function that can be measured using a minimally invasive approach, preferably in a maternal blood sample, are required. Unfortunately, no such approach is currently available, and the search for biomarkers for early detection of serious pregnancy complications has been disappointing. Indeed, recent systematic reviews and meta-analyses suggest that none of the currently available biomarkers predict IUGR or preeclampsia with sufficient sensitivity to be used in routine clinical practice (Conde-Agudelo et al., 2013; Chaiworapongsa et al., 2014; Wu et al., 2015; Zhong et al., 2015). One of the problems using maternal plasma proteomics to identify biomarkers for placental function is that the contribution of the placenta to the maternal plasma proteome is largely unknown. Characterization of the proteins synthesized and secreted by the placenta or primary human trophoblast (PHT) cells would help address this gap in knowledge and allow a more focused approach in the search for biomarkers for placental function.

To date, analyses of protein levels in the placenta have been performed primarily using two-dimensional (2D) PAGE (He et al., 2014) or surface-enhanced laser desorption/ionization (SELDI) mass spectrometry (Luciano-Montalvo et al., 2008). The SELDI results indicated alterations in protein expression patterns but were not able to provide comprehensive identification of individual proteins (Batorfi et al., 2003). Advances in technology have made it possible to apply mass spectrometry to a wide range of cell culture-based studies (Aebersold and Mann, 2003). Stable Isotope Labeling with Amino Acids in Cell Culture, or SILAC, has emerged as a valuable proteomic technique (Ong et al., 2002, 2003). Using SILAC, cells representing two or more biological conditions can be cultured in growth media supplemented with specific unlabeled ("light") or stable isotope-labeled ("heavy") amino acids (usually lysine and arginine). The proteins being synthesized in these cell populations incorporate the corresponding "light" or "heavy" amino acids. In cells that are dividing, essentially 100% amino acid incorporation can be readily achieved, permitting relative protein quantification for two experimental conditions using light/heavy-labeled cultures. For cells that do not divide, such as syncytiotrophoblasts, or cells that divide very slowly, incorporation of label depends on the rate of protein synthesis, and, thus, inclusion of stable isotope labeled amino acids provides a powerful approach to obtain a relative measure of the rate of protein synthesis while at the same time identifying the proteins in the cells. Recent studies in mice (Abdulghani et al., 2019; Napso et al., 2021) and humans (Michelsen et al., 2019) suggest that analysis of the placental secretome/proteome can provide information on candidate biomarkers for pregnancy complications, and placental secretome regulates maternal islet cell mass and functions (Drynda et al., 2018). In addition, the results from characterization of human placental macrophage secretome suggest that proteins secreted by placental macrophages at term pregnancy are essential for protecting fetuses against various viral infections (Garcia et al., 2009). However, no discovery approach has been used to identify the proteins secreted by cultured PHT cells isolated from term placenta. To assess trophoblast protein synthesis rate, inform efforts to find novel protein biomarkers for trophoblast function, and identify trophoblast proteins that regulate maternal physiological adaptations to pregnancy and influence fetal development and growth, we employed a SILAC-based mass spectrometric approach to characterize the secretome of PHT cells.

MATERIALS AND METHODS

Placental Collection

Healthy women with normal term pregnancies (>37 weeks of gestation) delivered by Cesarean section were recruited following written informed consent. The exclusion criteria were: smoking; use of illicit drugs; concurrent diseases, such as diabetes and hypertension; and development of pregnancy complications including gestational diabetes, pregnancy-induced hypertension and preeclampsia. The Institutional Review Board at the University of Texas Health Science Center at San Antonio approved the protocol (HSC20100262H); study personnel provided the de-identified samples and clinical information used in this study.

Stable Isotope Labeling With Amino Acids in Cell Culture

Primary human trophoblast cells were isolated using a well-established method involving sequential trypsin digestion and Percoll centrifugation (Kliman et al., 1986) as described in **Supplementary Material**. For SILAC labeling, PHT cells were cultured in DMEM/F12 media containing [$^{2}H_{4}$] L-lysine (700 μM) and [$^{13}C_{6}$] L-arginine (700 μM) (K4R6, Cambridge Isotope Laboratories, Inc., Andover, MA, United States) starting at 18 h following plating. In parallel, PHT cells were grown in the same media containing unlabeled L-lysine and L-arginine instead of isotopically labeled variants; media was refreshed every 24 h. At 90 h, cells were washed five times with phosphate-buffered saline to remove excess bovine serum proteins (Pellitteri-Hahn et al., 2006; Stastna and Van Eyk, 2012) and then incubated in serum-free labeled and unlabeled media for a

period of 24 h. At 114 h and following 24-h culture in serum-free media, the conditioned media was collected, and human chorionic gonadotropin (hCG) was measured (**Supplementary Figure 1**). In addition, conditioned media was processed and analyzed by mass spectrometry as described in detail in **Supplementary Material**.

Bioinformatics

Gene Ontology term enrichment analysis was performed using the DAVID bioinformatics resource (Huang da et al., 2009). The biological processes and molecular functions of secreted proteins were categorized by Ingenuity Pathway Analysis (IPA; Kramer et al., 2014). Prediction of subcellular localization and exosome comparison were obtained using Functional Enrichment Analysis Tool[1] and the Exo Carta database, [2] respectively.

Statistical Analysis

Analyses were performed using GraphPad Prism 6 software. Results were statistically significant if $p < 0.05$.

RESULTS

Proteins Identified in the PHT Cell Secretome

Proteins in the PHT cell conditioned media were separated by 1D SDS PAGE, and the gel lanes were excised into six slices and subjected to in-gel digestion followed by HPLC-electrospray ionization tandem mass spectrometry analysis. Four independent biological replicates (conditioned media of PHT cells isolated from four separate placentas) were analyzed. There were a total of 1,344 secreted proteins identified by at least one peptide spectrum match among the four samples (**Supplementary Table 1**). It is interesting to note that among the PHT secreted proteins were many related to nutrient transport, including phospholipid transfer protein (PTLP), vitamin D binding protein (GC), protein transport protein [SEC23A or B (Sec23 homolog A or B); COPII (Coat Complex Component); and phosphatidylinositol transfer protein (PITPN)] (**Supplementary Table 1**). In addition, numerous members of the serpin family were found in the PHT secretome (**Supplementary Table 2**).

Functional Characterization

Prediction of the subcellular localization of the secreted proteins indicated that the top-ranked cellular compartments for the PHT secretome were cytoplasm, extracellular vesicles, nucleus, and lysosomes (**Figure 1A**). Of the 1,344 identified proteins in the PHT cell secretome, 50% were predicted to be associated with extracellular vesicles (**Figure 1A**). These findings are consistent with recent reports that trophoblast-derived extracellular vesicles play a key role in placental orchestration of pregnancy and maternal immune sensing of the fetus (Stefanski et al., 2019). Furthermore, 68% of secreted proteins were associated with the cytoplasm. It cannot be excluded that some of these proteins represent unspecific leakage of PHT cell cytoplasmic proteins into the conditioned media. However, these proteins may be secreted via unconventional protein-secretory pathways, possibly mediated by Golgi or endosomal export mechanisms (Nickel and Rabouille, 2009). Alternatively, cytoplasmic proteins may be secreted after being incorporated into the membrane or the intravehicular space of extracellular vesicles released by PHT cells.

Gene Ontology Analysis

The results of gene ontology annotation for the molecular function of the PHT secretome revealed that catalytic activity and transporter activity were the two predominant functional groups (**Figure 1B**). Moreover, processes such as metabolism, energy pathways and cell communications were among the top-ranked biological functions (**Figure 1C**).

Using the UP TISSUE tool in DAVID, we compared the protein distribution of the PHT secretome with tissue expression databases (**Figure 1D**) and found that large subgroups of proteins in the PHT secretome are associated with the brain (50%), placenta (38%), liver (28%), and epithelium (27%). Furthermore, using the Kyoto Encyclopedia for Genes and Genomes (KEGG), we found enrichment for pathways related to carbon metabolism that can be linked to trophoblast function, including glycolysis, biosynthesis of amino acids, purine metabolism, and fatty acid degradation (**Figure 1E**). For example, triosephosphate isomerase (TPI1) was secreted by PHT cells. TPI1 is known to catalyze the reversible interconversion of dihydroxyacetone phosphate and D-glyceraldehyde 3-phosphate; it plays an important role in glycolysis and is essential for efficient ATP production. Other proteins in the PHT secretome related to the citric acid cycle and ATP production are dihydrolipoamide dehydrogenase precursor (DLD), isocitrate dehydrogenase 1 (IDH1) and aconitase 1 (ACO1).

Pathway Analysis

Pathway analysis of the PHT secretome revealed over-representation of various signaling mechanisms, including EIF2, eIF4, mTOR, and p70S6 kinases signaling and protein ubiquitination pathway (**Table 1**). IPA demonstrated that the PHT secretome was enriched for various physiological systems and functions (**Figure 1F**), including organismal survival (418 proteins), tissue development (306 proteins), cardiovascular system development and functions (263 proteins), organismal development (368 proteins) and connective tissue development and function (211 proteins). In the category "morphology of cardiovascular system," catenin alpha-3 (CTTNA-3), heat shock protein family B (HSPFB-8) and prolyl isomerase 1A (FKBP 1A) are associated with cardiovascular development, all of which were enriched in the PHT secretome.

Protein Synthesis Rate in the PHT Secretome

In addition to protein identification, the SILAC results provided information about the synthesis rate for 731 protein in the PHT

[1] www.funrich.org

[2] www.exocarta.org

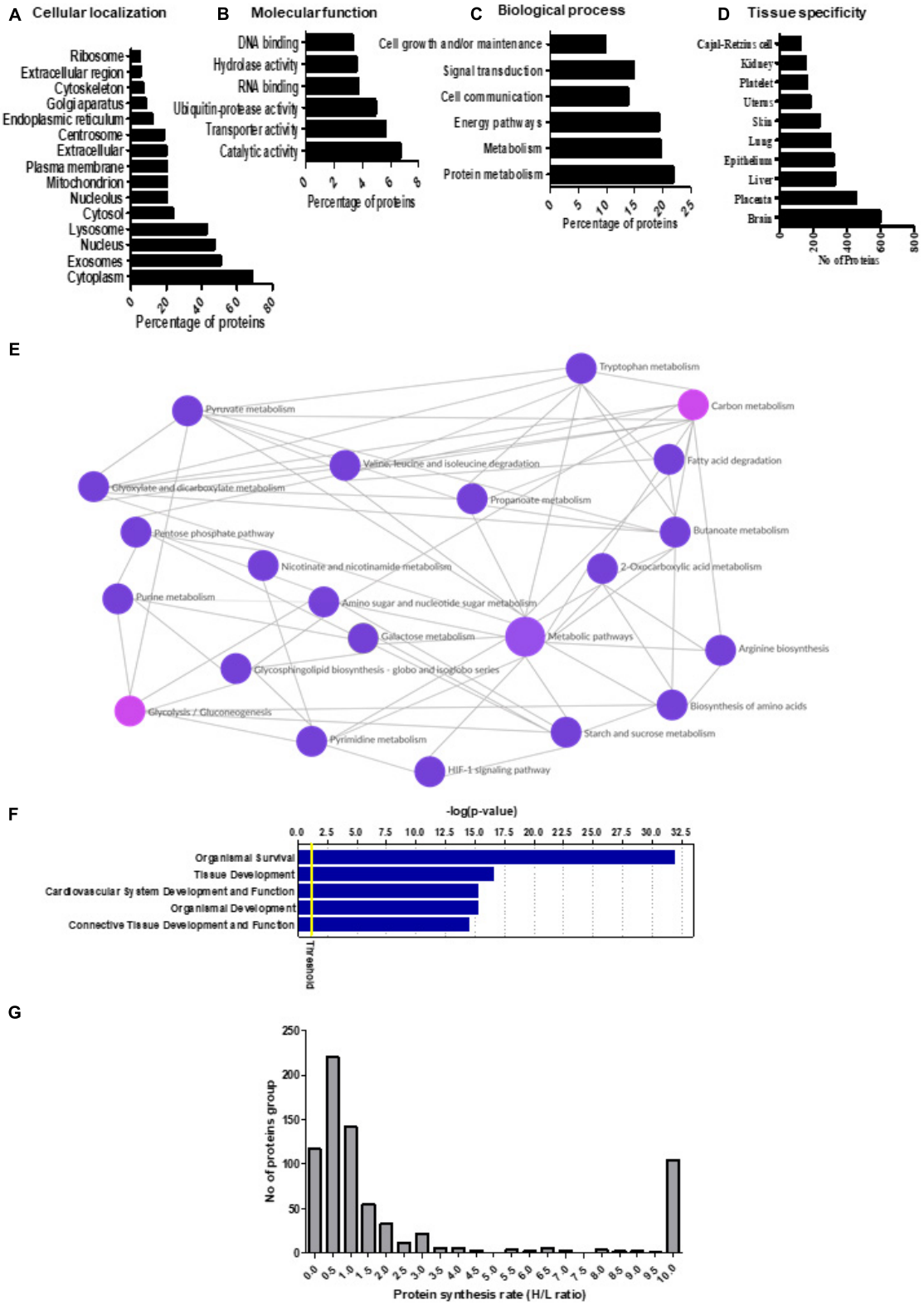

FIGURE 1 | (A–D) Gene ontology and Kyoto Encyclopedia of Genes and Genomes (KEGG) pathway analysis of the primary human trophoblast (PHT) secretome. The proteins identified in the PHT secretome were analyzed by Functional Enrichment Analysis Tool (www.funrich.org), which provides prediction of subcellular localization prediction software to predict the **(A)** cellular localization, **(B)** molecular function, and **(C)** biological processes of proteins in the secretome. **(D)** The

(Continued)

FIGURE 1 | (Continued)
identified proteins in the PHT secretome were analyzed by Gene Ontology term "tissue specificity" annotation using DAVID Bioinformatics Resources 6.8. **(E)** KEGG pathway analysis of the PHT secretome. The KEGG database was used to identify enriched pathways against the background of *Homo sapiens* for the PHT secreted proteins. KEGG pathway analysis shows enrichment of proteins related to carbon metabolism (including glycolysis, biosynthesis of amino acids), purine metabolism and fatty acid degradation in the PHT secretome. (Reprinted with permission from Kyoto Encyclopedia of Genes and Genomes, http://www.kegg.jp/kegg/kegg1.html). **(F)** Ingenuity Pathway Analysis (IPA) assignment of physiological process imputed from the PHT cell secretome. The list of PHT secreted proteins was submitted to IPA to find statistically enriched physiological functions. A function is significantly enriched when the percentage of proteins annotated with this function is above the proportion of annotated protein in the secretome (threshold p-value <0.05). The graph shows the top five enriched physiological functions reported by IPA according to the mapped secreted protein lists. Ordinates: -log (p-value) correspond to the p-values obtained by a Fisher test with Benjamini–Hochberg correction. **(G)** The distribution of relative protein synthesis rates in the PHT secretome. The ratio of "heavy" to "light" protein forms ranged from 10 to 0.01, with a median of 0.84. The protein synthesis rate distribution in the PHT secretome is skewed toward smaller values, reflecting the larger proportion of proteins with slower synthesis rates.

secretome (**Supplementary Table 3**). The ratio of "heavy" to "light" protein forms ranged from 0.01 to 10, with a median of 0.84 (**Figure 1G**). We arbitrarily defined proteins with an H/L ratio of $\geq$1 as fast synthesis proteins. The distribution of ratios is skewed toward lower ratios, reflecting a greater abundance of proteins with slower synthesis rates. This is likely related to the general slow synthesis of proteins that are components of non-dividing cells (Savas et al., 2012), including PHT cells. Twenty-two histone family proteins were among the slowest to incorporate label (**Supplementary Table 4**). The relationship between protein synthesis rate and subcellular location of the PHT secretome was examined using Functional Enrichment Analysis Tool (**Supplementary Figure 2**). Proteins in the cytoplasm, extracellular vesicles, lysosome and nucleus were found to be enriched in both the slow- and fast-synthesis classes (**Supplementary Figure 2**). A trend was apparent that proteins with a relatively slower synthesis rate were associated with mitochondria, nucleosomes, nucleoplasm, proteasome complex and ribosomes.

We found that secreted proteins from PHT cells associated with distinct biological processes exhibited similar trends with respect to protein synthesis rates (**Supplementary Figure 3**). For example, proteins involved in protein metabolism, signal transduction, cell communication, cell growth and maintenance were overrepresented in the group of proteins with fast rates of synthesis. In contrast, proteins involved in energy pathways, metabolism and regulation of gene expression and epigenetics were among those with slower synthesis. We also examined the relative synthesis rates of different subunits within the same protein complex. For most complexes, such as the proteasome and ATP synthase, subunits had similar synthesis rates. This suggests that the synthesis and degradation of the different subunits in the PHT secretome are coordinated. However, ribosomal subunits were synthesized at different rates. Ribosomal proteins are synthesized in the cytoplasm and subsequently assembled into the large and small ribosomal subunits in the nucleus and nucleolus where they interact with a variety of assembly proteins and ribosomal RNA before they are released back into the cytoplasm where they mediate protein synthesis. As shown in **Supplementary Table 3**, synthesis of 12 of 17 identified ribosomal proteins was relatively slow.

TABLE 1 | Canonical pathway analysis of primary human trophoblast (PHT) secretome by Ingenuity Pathway Analysis (IPA).

Top canonical pathways	p-value[1]	Overlap
EIF2 signaling	1.8 E-36	33%
Protein ubiquitination	3.8 E-35	29%
Regulation of eIF4 and p70S6K signaling	3.8 E-28	35%
mTOR signaling	1.7 E-20	26%
Clathrin mediated endocytosis signaling	1.0 E-17	25%

[1] *The p-values were calculated from hypergeometric tests based on the number of the overlapping molecular relations between the generated network and the canonical pathways stored in IPA.*

Associations Between the PHT Cell Secretome and the Placental Proteome Secreted Into the Fetal Circulation

Factors secreted from the human placenta are believed to be critical for fetal development (Bonnin et al., 2011; Behura et al., 2019a). Using an aptamer-based proteomic approach, we previously reported that 341 proteins are specifically secreted by the human term placenta into the fetal circulation, as evidenced by significantly higher concentrations in the umbilical vein compared to the umbilical artery (Michelsen et al., 2018). In the current study, we found that 47 of the 341 proteins secreted into the fetal circulation by the human placenta *in vivo* were also secreted by cultured PHT cells (**Table 2**). Moreover, as a proof of concept we quantified the abundance of legumain (one of the placental factors secreted by PHT cells) in paired serum samples collected from women during her pregnancy (36 weeks of pregnancy) and postpartum (3rd week of postpartum). We found that serum legumin level was higher in 36 weeks of pregnancy as compared to postpartum (**Figure 2**).

DISCUSSION

In the current study, we cultured PHT cells isolated from human term placenta using a widely-accepted standard protocol in which isolated cytotrophoblast cells form syncytial islands in culture (Kliman et al., 1986); and this is considered to be a physiologically relevant model to study the syncytiotrophoblast, the transporting epithelium of the human placenta. This is the first report of utilizing SILAC as a part of an effort to identify

TABLE 2 | Proteins secreted by PHT cells *in vitro* and by the human placenta into the fetal circulation *in vivo*.

Uni Prot ID	Target full name
O43278	Kunitz-type protease inhibitor 1
O43464	Serine protease HTRA2, mitochondrial
P00533	Epidermal growth factor receptor
P01023	Alpha-2-macroglobulin
P01024	Complement C3
P01034	Cystatin-C
P01215	Glycoprotein hormones alpha chain
P02649	Apolipoprotein E
P02751	Fibronectin
P04179	Superoxide dismutase [Mn], mitochondrial
P05155	Plasma protease C1 inhibitor
P05362	Intercellular adhesion molecule 1
P06396	Gelsolin
P07339	Cathepsin D
P0DMV8	Heat shock 70 kDa protein 1A
P12277	Creatine kinase B-type
P12830	Cadherin-1
P13987	CD59 glycoprotein
P15586	N-acetylglucosamine-6-sulfatase
P28799	Granulins
P30040	Endoplasmic reticulum resident protein 29
P33151	Cadherin-5
P36222	Chitinase-3-like protein 1
P36955	Pigment epithelium-derived factor
P42702	Leukemia inhibitory factor receptor
P61626	Lysozyme C
P61769	Beta-2-microglobulin
P68871	Hemoglobin subunit beta
P69905	Hemoglobin subunit alpha
Q02487	Desmocollin-2
Q03167	Transforming growth factor beta receptor type 3
Q07954	Prolow-density lipoprotein receptor-related protein 1
Q08380	Galectin-3-binding protein
Q12841	Follistatin-related protein 1
Q14126	Desmoglein-2
Q15582	Transforming growth factor-beta-induced protein ig-h3
Q15828	Cystatin-M
Q99988	Growth/differentiation factor 15
Q9NZ08	Endoplasmic reticulum aminopeptidase 1
Q9UBR2	Cathepsin Z

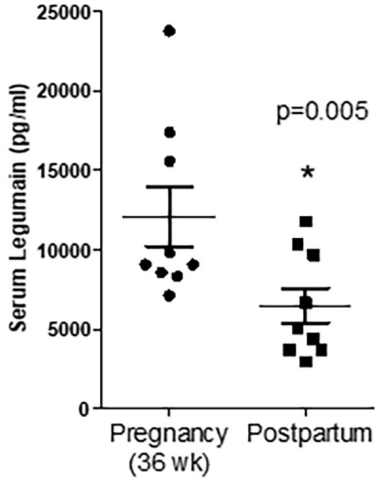

FIGURE 2 | Serum concentration of legumain at 36 weeks of pregnancy and the third week of postpartum. Values are mean + SEM. *$P < 0.05$ considered significant; Student's *t*-test, $n = 9$/each group.

proteins secreted by syncytialized PHT cells, which do not divide in culture. The majority of proteins in the PHT secretome have not previously been reported to be secreted by the human placenta or trophoblast. Our results demonstrate the feasibility of using SILAC to characterize the PHT cell secretome and we present novel information. Conventional SILAC requires extensive metabolic labeling of proteins, and, therefore, is difficult to apply to cells that do not divide in culture (Spellman et al., 2008).

The SILAC approach labels any protein that is newly synthesized during the time period when label is present without preference for certain subgroups of proteins. In cells that are dividing, essentially 100% amino acid incorporation/coverage can be readily achieved, for example it has been reported that complete label incorporation occurred after five doublings in a range of cell lines (Ong et al., 2002). On the other hand, in non-dividing cells, such as primary neurons, incorporation is slow (Zhang et al., 2014). Because PHT cells do not divide, in the current study we incubated PHT cells in label from 18 to 114 h in culture to maximize label incorporation. We collected conditioned media for characterization of the PHT cell secretome the last 24 h in culture when trophoblast cells have formed a syncytium. Thus, the secretome we report represents proteins secreted by the syncytiotrophoblast. Because the syncytiotrophoblast constitutes the transporting and hormone producing epithelium of the human placenta and is the predominant cell type in the human placenta at term, we believe that it is likely that secreted proteins from the human placenta *in vivo* predominantly originate from this cell type. This provided the rationale for focusing on the secretome of the syncytiotrophoblast in the current study.

The detection in the PHT secretome of chorionic gonadotrophin subunit alpha (CGA), one of the subunits of hCG, which is a well-known marker for trophoblast differentiation and function (Posillico et al., 1985; Fournier et al., 2015), validates our approach and confirms the trophoblast origin of the secreted proteins. hCG acts on the uterine environment via the luteinizing hormone/hCG receptor and exerts autocrine effects, promoting differentiation, and migration of trophoblasts, and paracrine effects on the maternal endometrium (Shi et al., 1993). Fibronectin (FN) was another of the 1,344 proteins in the PHT secretome, in agreement with previous reports (Yuehong et al., 2001). FN is a member of a family of high molecular weight extracellular matrix glycoproteins that has been characterized as "trophoblast glue" and is highly abundant in regions rich

in extravillous trophoblasts (Mercorio et al., 2006). Growing evidence suggests that placental and cord FN levels are elevated in preeclampsia (Uzun et al., 2010) and in recurrent pregnancy loss, and could be a potential candidate biomarker to assess placental function. PTLP secreted by trophoblasts is believed to be important for HDL assembly and regulation of maternal-fetal cholesterol transfer (Scholler et al., 2012). Also in the PHT secretome was Vitamin D binding protein, which is one of the key biomolecules involved in stimulation of calcium absorption for sufficient fetal bone mineral accrual and enhancing systemic and local maternal tolerance to paternal and fetal alloantigen (Karras et al., 2018). SEC23A and SEC23B are components of the coat protein complex II (COPII) which promotes the formation of transport vesicles from the endoplasmic reticulum; these proteins were found to be secreted by PHT cells. Both SEC23A and SEC23B are required for embryo morphogenesis, neural tube closure (Zhu et al., 2015), craniofacial chondrocyte maturation (Lang et al., 2006), and placental development.

Serpins are serine proteases that regulate an array of molecular pathways, such as inflammation, coagulation, fibrinolysis, complement activation, and phagocytosis; they can also be linked to trophoblast function. Serpin family members G1, B2, and E2 are necessary for proper circulatory function, and serpin deficiency is a risk factor for preeclampsia (Mondon et al., 2005; Severens-Rijvers et al., 2017). There are no reports in the literature of known function for SERPIN B9/E1/C1/B5/A1 and F1 in the placenta, even though they have been associated with inflammation, immune suppression, cell senescence, angiogenesis, coagulation, collagen biosynthesis, and invasion in other tissues (El Haddad et al., 2011; Heutinck et al., 2012; Jiang et al., 2017). Thus, secreted members of the serpin family of proteins are potentially novel regulators of trophoblast angiogenesis, invasion, cell senescence, and inflammation. Pathway analysis of the PHT secretome revealed over-representation of various signaling mechanisms, including EIF2, eIF4, mTOR, and p70S6 kinases signaling and protein ubiquitination pathway (**Table 1**). Possible interpretation of these findings is that mTOR signaling is involved in the regulation of trophoblast function or that the PHT secretome regulates mTOR signaling in other cells. There is a wealth of evidence demonstrating that the placental mTOR pathway responds to many growth-related signals, including amino acids, glucose, oxygen, folate, and growth factors, to regulate trophoblast mitochondrial respiration, nutrient transport, and protein synthesis, thereby influencing placental and fetal growth (Rosario et al., 2013, 2017, 2019).

Pathway analysis demonstrated that the PHT secretome was enriched for cardiovascular system development and function. These findings are consistent with the possibility that trophoblasts secrete proteins involved in maternal cardiovascular adaptation to pregnancy and/or fetal cardiovascular development. In support of this speculation, recent studies demonstrated that placental dysfunction may significantly contribute to the incidence of congenital heart diseases (Maslen, 2018). Moreover, defects in placentation are highly prevalent in embryonically lethal mouse mutants and placental defects correlate strongly with abnormal heart and vascular development (Perez-Garcia et al., 2018). However, a cause-and-effect relationship between placental secreted factors and cardiovascular development remains to be established.

Recent findings suggest that many proteins secreted from the trophoblast may remotely control the development of function of specific maternal and/or fetal tissues (Wu et al., 2017; Behura et al., 2019b). In support of this hypothesis, we recently found that 34 proteins were secreted by the placenta into the maternal circulation, as evidenced by significantly higher levels in uterine vein compared to radial artery (used to represent the uterine artery). The proteins secreted included placental growth factor, growth differentiation factor 15, and matrix metalloproteinase 12 (Michelsen et al., 2018). Similarly, 341 proteins were secreted by the placenta into the fetal circulation (Michelsen et al., 2018) based on significantly higher levels in the umbilical vein compared to the umbilical artery for samples collected simultaneously. It is also possible that the proteins identified in the PHT secretome reflect common functions between the placenta and other tissues. Both the liver and the placenta are tissues with high metabolic activity that share common pathways. For example, 1,4-alpha-glucan branching enzyme 1 (GBE1) identified in the PHT secretome is known to participate in glycogen biosynthesis by attaching a short glucosyl chain in an α-1,6-glucosidic link to a naked peripheral chain of nascent glycogen. GBE1 deficiency results in the accumulation of abnormal glycogen (polyglucosan) in placenta (Konstantinidou et al., 2008). The syncytiotrophoblast is the transporting and hormone-producing epithelium of the human placenta. Therefore, proteins that are associated with the tissue functional annotation term "epithelium" may have a role in placental transport, secretion, selective absorption, sensing, and protection similar to other epithelial cells.

The mechanisms by which proteins are secreted/released from the syncytiotrophoblast remain to be fully established but may involve any type of syncytiotrophoblast-derived extracellular vesicles, including small extracellular vesicles. Proteins in the PHT cell secretome may be secreted into the maternal and/or the fetal circulation. Whereas secretion of proteins synthesized by the syncytiotrophoblast into the maternal circulation is well established and includes hormones such as placental lactogen and pGH (Freemark, 2010), secretion of syncytial proteins into fetal blood is much less characterized. Although the fetal capillary endothelium is likely to restrict the passage of some proteins, there is ample evidence, including transfer of maternal IgG to the fetus and the transport of alpha fetoprotein into the maternal circulation, that large proteins do cross this barrier. Moreover, the observation that 50% of total exosomes in human fetal blood are of placental (syncytiotrophoblast) origin (Miranda et al., 2018) demonstrates that structures as large as ∼100 nm can cross the human placental capillary endothelium, although the mechanisms involved are largely unknown.

It is possible that the protein synthesis data can provide information on proteins that are subjected to short-term regulation because we speculate that a protein with a rapid synthesis rate is turned over rapidly and therefore more likely to be subjected to such regulation. It may be speculated that proteins involved in intracellular signaling and cell-to-cell

communication should be short-lived for efficient and rapid fine-tuned regulation, while proteins that serve more structural functions in the cell are longer-lived in order to save energy that would be required for protein synthesis and degradation. We found that histone family members as well as proteins associated with mitochondria, ribosomes, gene expression, and epigenetics exhibited the slowest synthesis rates in the PHT secretome. This agrees with previous studies that showed slow synthesis rates of histone proteins in mouse embryonic neurons (Toyama et al., 2013) and is consistent with the fact that cultured PHT cells are fully differentiated, non-dividing, cells. Of these, proteins associated with mitochondria had the slowest synthesis rates, consistent with previous reports (Price et al., 2012; Dai et al., 2014). These findings are in general agreement with reports that distinct mechanisms of degradation may cause systematic differences in protein synthesis between cytosolic (Tai and Schuman, 2008) and membrane proteins (Avci and Lemberg, 2015). Our observation that proteins involved in regulation of gene expression and epigenetics have slow synthesis rates is consistent with previous reports in primary neurons (Mathieson et al., 2018). This trend is in line with a previous study in mice, where ribosomal proteins were found to turn over at slower rates compared to many other proteins in complexes (Price et al., 2010). Several ribosomal proteins exhibited a relatively fast synthesis rate in our study, including proteins associated with both the large (60S acidic ribosomal protein P2) and small (40SRps28, 40SRps3, and ubiquitin 40SRps27a) subunits. These ribosomal proteins often do not assemble into stable large ribosome units; an unassembled ribosome unit is rapidly degraded by the ubiquitin proteasome degradation pathways (Boisvert et al., 2012).

Our study has some limitations. For example, cell lysis may contribute to the characterized secretome, which is difficult to control for. Moreover, the expression "rate of protein synthesis" is a simplification because, rather than representing the actual rate of synthesis, it corresponds to the difference between actual synthesis of new protein during the study period minus any newly synthesized protein that has been degraded. The goal of this study was to characterize the syncytiotrophoblast secretome at term. Given the major changes in uteroplacental blood flow and in placental function and morphology across gestation, the findings reported in this study may not be representative for the syncytiotrophopblast secretome earlier in gestation. For example, it is well established that the maternal circulating levels of hCG, a protein synthesized and secreted predominantly by the syncytiotrophoblast, are very high at the end of the first trimester and subsequently decline to low levels at term, consistent with the notion that the first trimester and term syncytiotrophoblast secretomes are distinct.

CONCLUSION

The placenta, and specifically the syncytiotrophoblast, is believed to release hormones into the maternal circulation that contribute to the maternal metabolic and cardiovascular adaptation to pregnancy. However, the identities of these hormones remain to be fully established. Emerging evidence in animal models demonstrates that specific placental factors secreted into the fetal circulation are critical for fetal development, however, it is not known if this occurs in humans. We demonstrate that SILAC-based mass spectrometry can be successfully applied to non-dividing PHT cells to characterize the human trophoblast secretome and obtain information about rates of protein synthesis. This dataset can be of value to identify novel placental proteins that regulate maternal physiology and/or fetal development. Identifying proteins in the PHT cell secretome does not provide information about whether these proteins are secreted into the maternal and/or fetal circulation. Additional studies of, for example, uteroplacental and umbilical concentrations gradients are needed to better understand what potential role these secreted proteins have *in vivo*. Although there is general consensus that factors in the maternal circulation that reflect placental function are ideal candidates for biomarkers for early diagnosis of pregnancy complications due to placental insufficiency, few, if any, maternal serum biomarkers are currently in clinical use. Our data defining the secretome of cultured PHT cells can serve as a starting point for a more targeted approach in the search for clinically useful maternal serum biomarkers for early detection of important pregnancy complications. The generated data will guide future experiments to gain insight into the function of individual secreted proteins and to better understand how the placenta controls maternal and fetal physiology. Moreover, because secreted proteins are often glycosylated, glycocapture-based proteomics for secretome analysis will allow a more focused approach to study classically secreted proteins from the trophoblast and the placenta, decreasing the complexity of the sample and circumventing the potential problem with proteins that have leaked out of the cells or released by ectodomain shedding.

DATA AVAILABILITY STATEMENT

The original contributions presented in the study are included in the article/**Supplementary Material**, further inquiries can be directed to the corresponding author/s.

ETHICS STATEMENT

The studies involving human participants were reviewed and approved by the University of Texas Health Science Center at San Antonio. The patients/participants provided their written informed consent to participate in this study.

AUTHOR CONTRIBUTIONS

FR, SP, TP, SW, and TJ researched the data, designed the experiments, and wrote the manuscript. LM performed and collected the human serum samples. TM was responsible for four vessel sample data analysis and presentation of the data.

FR, SP, and KE performed the experiments. All authors critically revised the manuscript for substantive content and approved the final version.

FUNDING

This study was supported by NIH grant HD068370. The UTHSCSA Institutional Mass Spectrometry Laboratory is supported in part by UTHSCSA and NIH grant 1S10RR025111-01 for purchase of the Orbitrap mass spectrometer (SW).

SUPPLEMENTARY MATERIAL

The Supplementary Material for this article can be found online at: https://www.frontiersin.org/articles/10.3389/fcell.2021.704781/full#supplementary-material

REFERENCES

Abdulghani, M., Song, G., Kaur, H., Walley, J. W., and Tuteja, G. (2019). Comparative analysis of the transcriptome and proteome during mouse placental development. *J. Proteome Res.* 18, 2088–2099. doi: 10.1021/acs.jproteome.8b00970

Aebersold, R., and Mann, M. (2003). Mass spectrometry-based proteomics. *Nature* 422, 198–207.

Avci, D., and Lemberg, M. K. (2015). Clipping or extracting: two ways to membrane protein degradation. *Trends Cell Biol.* 25, 611–622. doi: 10.1016/j.tcb.2015.07.003

Baeyens, L., Hindi, S., Sorenson, R. L., and German, M. S. (2016). Beta-cell adaptation in pregnancy. *Diabetes Obes. Metab.* 18(Suppl. 1), 63–70.

Barbour, L. A., Shao, J., Qiao, L., Leitner, W., Anderson, M., Friedman, J. E., et al. (2004). Human placental growth hormone increases expression of the p85 regulatory unit of phosphatidylinositol 3-kinase and triggers severe insulin resistance in skeletal muscle. *Endocrinology* 145, 1144–1150. doi: 10.1210/en.2003-1297

Batorfi, J., Ye, B., Mok, S. C., Cseh, I., Berkowitz, R. S., and Fulop, V. (2003). Protein profiling of complete mole and normal placenta using proteinchip analysis on laser capture microdissected cells. *Gynecol. Oncol.* 88, 424–428. doi: 10.1016/s0090-8258(02)00167-1

Behura, S. K., Dhakal, P., Kelleher, A. M., Balboula, A., Patterson, A., and Spencer, T. E. (2019a). The brain-placental axis: therapeutic and pharmacological relevancy to pregnancy. *Pharmacol. Res.* 149:104468. doi: 10.1016/j.phrs.2019.104468

Behura, S. K., Kelleher, A. M., and Spencer, T. E. (2019b). Evidence for functional interactions between the placenta and brain in pregnant mice. *FASEB J.* 33, 4261–4272. doi: 10.1096/fj.201802037r

Boisvert, F. M., Ahmad, Y., Gierlinski, M., Charriere, F., Lamont, D., Scott, M., et al. (2012). A quantitative spatial proteomics analysis of proteome turnover in human cells. *Mol. Cell Proteomics* 11:M11101 1429.

Bonnin, A., Goeden, N., Chen, K., Wilson, M. L., King, J., Shih, J. C., et al. (2011). A transient placental source of serotonin for the fetal forebrain. *Nature* 472, 347–350. doi: 10.1038/nature09972

Brelje, T. C., Parsons, J. A., and Sorenson, R. L. (1994). Regulation of islet beta-cell proliferation by prolactin in rat islets. *Diabetes* 43, 263–273. doi: 10.2337/diabetes.43.2.263

Chaiworapongsa, T., Chaemsaithong, P., Korzeniewski, S. J., Yeo, L., and Romero, R. (2014). Pre-eclampsia part 2: prediction, prevention and management. *Nat. Rev. Nephrol.* 10, 531–540.

Conde-Agudelo, A., Papageorghiou, A. T., Kennedy, S. H., and Villar, J. (2013). Novel biomarkers for predicting intrauterine growth restriction: a systematic review and meta-analysis. *BJOG* 120, 681–694. doi: 10.1111/1471-0528.12172

Costa, M. A. (2016). The endocrine function of human placenta: an overview. *Reprod. Biomed. Online* 32, 14–43. doi: 10.1016/j.rbmo.2015.10.005

Dai, D. F., Karunadharma, P. P., Chiao, Y. A., Basisty, N., Crispin, D., Hsieh, E. J., et al. (2014). Altered proteome turnover and remodeling by short-term caloric restriction or rapamycin rejuvenate the aging heart. *Aging Cell* 13, 529–539. doi: 10.1111/acel.12203

Drynda, R., Persaud, S. J., Bowe, J. E., and Jones, P. M. (2018). The placental secretome: identifying potential cross-talk between placenta and islet beta-cells. *Cell Physiol. Biochem.* 45, 1165–1171. doi: 10.1159/000487357

El Haddad, N., Moore, R., Heathcote, D., Mounayar, M., Azzi, J., Mfarrej, B., et al. (2011). The novel role of SERPINB9 in cytotoxic protection of human mesenchymal stem cells. *J. Immunol.* 187, 2252–2260. doi: 10.4049/jimmunol.1003981

Fisher, S. J. (2015). Why is placentation abnormal in preeclampsia? *Am. J. Obstet. Gynecol.* 213(4 Suppl), S115–S122.

Fournier, T., Guibourdenche, J., and Evain-Brion, D. (2015). Review: HCGS: different sources of production, different glycoforms and functions. *Placenta* 36(Suppl. 1), S60–S65.

Freemark, M. (2010). Placental hormones and the control of fetal growth. *J. Clin. Endocrinol. Metab.* 95, 2054–2057. doi: 10.1210/jc.2010-0517

Garcia, K., Garcia, V., Perez Laspiur, J., Duan, F., and Melendez, L. M. (2009). Characterization of the placental macrophage secretome: implications for antiviral activity. *Placenta* 30, 149–155. doi: 10.1016/j.placenta.2008.10.014

He, P., Wang, F., Jiang, Y., Zhong, Y., Lan, Y., and Chen, S. (2014). Placental proteome alterations in women with intrahepatic cholestasis of pregnancy. *Int. J. Gynaecol. Obstet.* 126, 256–259. doi: 10.1016/j.ijgo.2014.03.035

Heutinck, K. M., Kassies, J., Florquin, S., Ten Berge, I. J., Hamann, J., and Rowshani, A. T. (2012). SerpinB9 expression in human renal tubular epithelial cells is induced by triggering of the viral dsRNA sensors TLR3, MDA5 and RIG-I. *Nephrol. Dial. Transplant.* 27, 2746–2754. doi: 10.1093/ndt/gfr690

Huang da, W., Sherman, B. T., and Lempicki, R. A. (2009). Systematic and integrative analysis of large gene lists using DAVID bioinformatics resources. *Nat. Protoc.* 4, 44–57. doi: 10.1038/nprot.2008.211

Jiang, C., Liu, G., Luckhardt, T., Antony, V., Zhou, Y., Carter, A. B., et al. (2017). Serpine 1 induces alveolar type II cell senescence through activating p53-p21-Rb pathway in fibrotic lung disease. *Aging Cell* 16, 1114–1124. doi: 10.1111/acel.12643

Karras, S. N., Koufakis, T., Fakhoury, H., and Kotsa, K. (2018). Deconvoluting the biological roles of vitamin D-binding protein during pregnancy: a both clinical and theoretical challenge. *Front. Endocrinol.* 9:259. doi: 10.3389/fendo.2018.00259

Kim, H., Toyofuku, Y., Lynn, F. C., Chak, E., Uchida, T., Mizukami, H., et al. (2010). Serotonin regulates pancreatic beta cell mass during pregnancy. *Nat.Med.* 16, 804–808. doi: 10.1038/nm.2173

Kliman, H. J., Nestler, J. E., Sermasi, E., Sanger, J. M. and Strauss, J. F. III (1986). Purification, characterization, and in vitro differentiation of cytotrophoblasts from human term placentae. *Endocrinology* 118, 1567–1582. doi: 10.1210/endo-118-4-1567

Konstantinidou, A. E., Anninos, H., Dertinger, S., Nonni, A., Petersen, M., Karadimas, C., et al. (2008). Placental involvement in glycogen storage disease type IV. *Placenta* 29, 378–381.

Kramer, A., Green, J., Pollard, J. Jr., and Tugendreich, S. (2014). Causal analysis approaches in ingenuity pathway analysis. *Bioinformatics* 30, 523–530. doi: 10.1093/bioinformatics/btt703

Lang, M. R., Lapierre, L. A., Frotscher, M., Goldenring, J. R., and Knapik, E. W. (2006). Secretory COPII coat component Sec23a is essential for craniofacial

chondrocyte maturation. *Nat. Genet.* 38, 1198–1203. doi: 10.1038/ng1880

Luciano-Montalvo, C., Ciborowski, P., Duan, F., Gendelman, H. E., and Melendez, L. M. (2008). Proteomic analyses associate cystatin B with restricted HIV-1 replication in placental macrophages. *Placenta* 29, 1016–1023. doi: 10.1016/j.placenta.2008.09.005

Maslen, C. L. (2018). Recent advances in placenta-heart interactions. *Front. Physiol.* 9:735. doi: 10.3389/fphys.2018.00735

Mathieson, T., Franken, H., Kosinski, J., Kurzawa, N., Zinn, N., Sweetman, G., et al. (2018). Systematic analysis of protein turnover in primary cells. *Nat. Commun.* 9:689.

Mercorio, F., Mercorio, A., Di Spiezio Sardo, A., Votino, C., Barba, G. V., and Nappi, C. (2006). Cervical fetal fibronectin as a predictor of first trimester pregnancy outcome in unexplained recurrent miscarriage. *Eur. J. Obstet. Gynecol. Reprod. Biol.* 126, 165–169. doi: 10.1016/j.ejogrb.2005.08.007

Michelsen, T. M., Henriksen, T., Reinhold, D., Powell, T. L., and Jansson, T. (2018). The human placental proteome secreted into the maternal and fetal circulations in normal pregnancy based on 4-vessel sampling. *FASEB J.* 33:fj201801193R.

Michelsen, T. M., Henriksen, T., Reinhold, D., Powell, T. L., and Jansson, T. (2019). The human placental proteome secreted into the maternal and fetal circulations in normal pregnancy based on 4-vessel sampling. *FASEB J.* 33, 2944–2956. doi: 10.1096/fj.201801193r

Mifsud, W., and Sebire, N. J. (2014). Placental pathology in early-onset and late-onset fetal growth restriction. *Fetal. Diagn. Ther.* 36, 117–128. doi: 10.1159/000359969

Miranda, J., Paules, C., Nair, S., Lai, A., Palma, C., Scholz-Romero, K., et al. (2018). Placental exosomes profile in maternal and fetal circulation in intrauterine growth restriction–Liquid biopsies to monitoring fetal growth. *Placenta* 64, 34–43. doi: 10.1016/j.placenta.2018.02.006

Mondon, F., Mignot, T. M., Rebourcet, R., Jammes, H., Danan, J. L., Ferre, F., et al. (2005). Profiling of oxygen-modulated gene expression in early human placenta by systematic sequencing of suppressive subtractive hybridization products. *Physiol. Genomics* 22, 99–107. doi: 10.1152/physiolgenomics.00276.2004

Napso, T., Zhao, X., Lligona, M. I., Sandovici, I., Kay, R. G., George, A. L., et al. (2021). Placental secretome characterization identifies candidates for pregnancy complications. *Commun. Biol.* 4:701.

Nickel, W., and Rabouille, C. (2009). Mechanisms of regulated unconventional protein secretion. *Nat. Rev. Mol. Cell Biol.* 10, 148–155. doi: 10.1038/nrm2617

Ong, S. E., Blagoev, B., Kratchmarova, I., Kristensen, D. B., Steen, H., Pandey, A., et al. (2002). Stable isotope labeling by amino acids in cell culture, SILAC, as a simple and accurate approach to expression proteomics. *Mol. Cell Proteomics* 1, 376–386. doi: 10.1074/mcp.m200025-mcp200

Ong, S. E., Kratchmarova, I., and Mann, M. (2003). Properties of 13C-substituted arginine in stable isotope labeling by amino acids in cell culture (SILAC). *J. Proteome Res.* 2, 173–181. doi: 10.1021/pr0255708

Pellitteri-Hahn, M. C., Warren, M. C., Didier, D. N., Winkler, E. L., Mirza, S. P., Greene, A. S., et al. (2006). Improved mass spectrometric proteomic profiling of the secretome of rat vascular endothelial cells. *J. Proteome Res.* 5, 2861–2864. doi: 10.1021/pr060287k

Perez-Garcia, V., Fineberg, E., Wilson, R., Murray, A., Mazzeo, C. I., Tudor, C., et al. (2018). Placentation defects are highly prevalent in embryonic lethal mouse mutants. *Nature* 555, 463–468. doi: 10.1038/nature26002

Posillico, E. G., Handwerger, S., and Tyrey, L. (1985). Human chorionic gonadotropin alpha-subunit of normal placenta: characterization of synthesis and association with beta-subunit. *Biol. Reprod.* 32, 1101–1108. doi: 10.1095/biolreprod32.5.1101

Price, J. C., Guan, S., Burlingame, A., Prusiner, S. B., and Ghaemmaghami, S. (2010). Analysis of proteome dynamics in the mouse brain. *Proc. Natl. Acad. Sci. U.S.A.* 107, 14508–14513.

Price, J. C., Khambatta, C. F., Li, K. W., Bruss, M. D., Shankaran, M., Dalidd, M., et al. (2012). The effect of long term calorie restriction on in vivo hepatic proteostatis: a novel combination of dynamic and quantitative proteomics. *Mol. Cell Proteomics* 11, 1801–1814. doi: 10.1074/mcp.m112.021204

Rosario, F. J., Gupta, M. B., Myatt, L., Powell, T. L., Glenn, J. P., Cox, L., et al. (2019). Mechanistic target of rapamycin complex 1 promotes the expression of genes encoding electron transport chain proteins and stimulates oxidative phosphorylation in primary human trophoblast cells by regulating mitochondrial biogenesis. *Sci. Rep.* 9:246.

Rosario, F. J., Kanai, Y., Powell, T. L., and Jansson, T. (2013). Mammalian target of rapamycin signalling modulates amino acid uptake by regulating transporter cell surface abundance in primary human trophoblast cells. *J. Physiol.* 591, 609–625. doi: 10.1113/jphysiol.2012.238014

Rosario, F. J., Powell, T. L., and Jansson, T. (2017). mTOR folate sensing links folate availability to trophoblast cell function. *J. Physiol.* 595, 4189–4206. doi: 10.1113/jp272424

Savas, J. N., Toyama, B. H., Xu, T., Yates, J. R. III, and Hetzer, M. W. (2012). Extremely long-lived nuclear pore proteins in the rat brain. *Science* 335:942. doi: 10.1126/science.1217421

Scholler, M., Wadsack, C., Lang, I., Etschmaier, K., Schweinzer, C., Marsche, G., et al. (2012). Phospholipid transfer protein in the placental endothelium is affected by gestational diabetes mellitus. *J. Clin. Endocrinol. Metab.* 97, 437–445. doi: 10.1210/jc.2011-1942

Severens-Rijvers, C. A. H., Al-Nasiry, S., Ghossein-Doha, C., Marzano, S., Ten Cate, H., Winkens, B., et al. (2017). Circulating fibronectin and plasminogen activator inhibitor-2 levels as possible predictors of recurrent placental syndrome: an exploratory study. *Gynecol. Obstet. Invest.* 82, 355–360. doi: 10.1159/000449385

Shi, Q. J., Lei, Z. M., Rao, C. V., and Lin, J. (1993). Novel role of human chorionic gonadotropin in differentiation of human cytotrophoblasts. *Endocrinology* 132, 1387–1395. doi: 10.1210/endo.132.3.7679981

Sibley, C. P., Turner, M. A., Cetin, I., Ayuk, P., Boyd, C. A. R., Souza, S. W., et al. (2005). Placental phenotypes of intrauterine growth. *Pediatr. Res.* 58, 827–832.

Sircar, M., Thadhani, R., and Karumanchi, S. A. (2015). Pathogenesis of preeclampsia. *Curr. Opin. Nephrol. Hypertens* 24, 131–138.

Sorenson, R. L., and Brelje, T. C. (1997). Adaptation of islets of Langerhans to pregnancy: beta-cell growth, enhanced insulin secretion and the role of lactogenic hormones. *Horm. Metab. Res.* 29, 301–307. doi: 10.1055/s-2007-979040

Spellman, D. S., Deinhardt, K., Darie, C. C., Chao, M. V., and Neubert, T. A. (2008). Stable isotopic labeling by amino acids in cultured primary neurons: application to brain-derived neurotrophic factor-dependent phosphotyrosine-associated signaling. *Mol. Cell Proteomics* 7, 1067–1076. doi: 10.1074/mcp.m700387-mcp200

Stastna, M., and Van Eyk, J. E. (2012). Investigating the secretome: lessons about the cells that comprise the heart. *Circ Cardiovasc Genet* 5, o8–o18.

Stefanski, A. L., Martinez, N., Peterson, L. K., Callahan, T. J., Treacy, E., Luck, M., et al. (2019). Murine trophoblast-derived and pregnancy-associated exosome-enriched extracellular vesicle microRNAs: implications for placenta driven effects on maternal physiology. *PLoS One* 14:e0210675. doi: 10.1371/journal.pone.0210675

Tai, H. C., and Schuman, E. M. (2008). Ubiquitin, the proteasome and protein degradation in neuronal function and dysfunction. *Nat. Rev. Neurosci.* 9, 826–838. doi: 10.1038/nrn2499

Toyama, B. H., Savas, J. N., Park, S. K., Harris, M. S., Ingolia, N. T., Yates, J. R. III, et al. (2013). Identification of long-lived proteins reveals exceptional stability of essential cellular structures. *Cell* 154, 971–982. doi: 10.1016/j.cell.2013.07.037

Uzun, H., Konukoglu, D., Albayrak, M., Benian, A., Madazli, R., Aydin, S., et al. (2010). Increased maternal serum and cord blood fibronectin concentrations in preeclampsia are associated with higher placental hyaluronic acid and hydroxyproline content. *Hypertens. Pregnancy* 29, 153–162. doi: 10.3109/10641950902968619

Wu, P., van den Berg, C., Alfirevic, Z., O'Brien, S., Rothlisberger, M., Baker, P. N., et al. (2015). Early pregnancy biomarkers in pre-eclampsia: a systematic review and meta-analysis. *Int. J. Mol. Sci.* 16, 23035–23056. doi: 10.3390/ijms160923035

Wu, W. L., Hsiao, E. Y., Yan, Z., Mazmanian, S. K., and Patterson, P. H. (2017). The placental interleukin-6 signaling controls fetal brain development and behavior. *Brain Behav. Immun.* 62, 11–23.

Yuehong, M. A., D'Antona, D., LaChapelle, L., Ryu, J. S., and Guller, S. (2001). Role of the proteasome in the regulation of fetal fibronectin secretion in human placenta. *Ann. N. Y. Acad. Sci.* 943, 340–351. doi: 10.1111/j.1749-6632.2001.tb03814.x

Zhang, G., Deinhardt, K., and Neubert, T. A. (2014). Stable isotope labeling by amino acids in cultured primary neurons. *Methods Mol. Biol.* 1188, 57–64. doi: 10.1007/978-1-4939-1142-4_5

Zhong, Y., Zhu, F., and Ding, Y. (2015). Serum screening in first trimester to predict pre-eclampsia, small for gestational age and preterm delivery: systematic review and meta-analysis. *BMC Pregnancy Childbirth* 15:191. doi: 10.1186/s12884-015-0608-y

Zhu, M., Tao, J., Vasievich, M. P., Wei, W., Zhu, G., Khoriaty, R. N., et al. (2015). Neural tube opening and abnormal extraembryonic membrane development in SEC23A deficient mice. *Sci. Rep.* 5:15471.

Conflict of Interest: The authors declare that the research was conducted in the absence of any commercial or financial relationships that could be construed as a potential conflict of interest.

frontiers in Cell and Developmental Biology

REVIEW
published: 24 September 2021
doi: 10.3389/fcell.2021.723656

Transcriptomics and Other Omics Approaches to Investigate Effects of Xenobiotics on the Placenta

Cheryl S. Rosenfeld[1,2,3,4]*

[1] Biomedical Sciences, University of Missouri, Columbia, MO, United States, [2] MU Institute for Data Science and Informatics, University of Missouri, Columbia, MO, United States, [3] Thompson Center for Autism and Neurobehavioral Disorders, University of Missouri, Columbia, MO, United States, [4] Genetics Area Program, University of Missouri, Columbia, MO, United States

The conceptus is most vulnerable to developmental perturbation during its early stages when the events that create functional organ systems are being launched. As the placenta is in direct contact with maternal tissues, it readily encounters any xenobiotics in her bloodstream. Besides serving as a conduit for solutes and waste, the placenta possesses a tightly regulated endocrine system that is, of itself, vulnerable to pharmaceutical agents, endocrine disrupting chemicals (EDCs), and other environmental toxicants. To determine whether extrinsic factors affect placental function, transcriptomics and other omics approaches have become more widely used. In casting a wide net with such approaches, they have provided mechanistic insights into placental physiological and pathological responses and how placental responses may impact the fetus, especially the developing brain through the placenta-brain axis. This review will discuss how such omics technologies have been utilized to understand effects of EDCs, including the widely prevalent plasticizers bisphenol A (BPA), bisphenol S (BPS), and phthalates, other environmental toxicants, pharmaceutical agents, maternal smoking, and air pollution on placental gene expression, DNA methylation, and metabolomic profiles. It is also increasingly becoming clear that miRNA (miR) are important epigenetic regulators of placental function. Thus, the evidence to date that xenobiotics affect placental miR expression patterns will also be explored. Such omics approaches with mouse and human placenta will assuredly provide key biomarkers that may be used as barometers of exposure and can be targeted by early mitigation approaches to prevent later diseases, in particular neurobehavioral disorders, originating due to placental dysfunction.

Keywords: trophoblast, serotonin, bisphenol A, endocrine disruptors, environmental chemicals, placenta-brain axis, pharmaceutical agents, smoking

OPEN ACCESS

Edited by:
Michael J. Soares, University of Kansas Medical Center Research Institute, United States

Reviewed by:
Alina Maloyan, Oregon Health and Science University, United States
Khursheed Iqbal, University of Kansas Medical Center, United States

***Correspondence:**
Cheryl S. Rosenfeld
rosenfeldc@missouri.edu

Specialty section:
This article was submitted to Developmental Epigenetics, a section of the journal Frontiers in Cell and Developmental Biology

Received: *11 June 2021*
Accepted: *31 August 2021*
Published: *24 September 2021*

Citation:
Rosenfeld CS (2021) Transcriptomics and Other Omics Approaches to Investigate Effects of Xenobiotics on the Placenta. Front. Cell Dev. Biol. 9:723656. doi: 10.3389/fcell.2021.723656

INTRODUCTION

The placenta and uterine tissue directly interact, and thus, factors circulating in the maternal bloodstream easily transfer across the placenta, where they can affect this organ and secondarily the fetus. This close relationship between the placenta and maternal tissue is essential for nutrient, gas, and waste exchange. The placenta is also an endocrine organ that produces a range of hormones

and cytokine factors that exert local paracrine effects in the placenta but can also act upon maternal and fetal tissues. Many biomedical studies examine effects on mouse or rat placenta as rodents have an invasive hemochorial type of placentation with syncytiotrophoblast (syncytioTB) cells that are involved in nutrient and gas exchange and are bathed in maternal blood, analogous to structural components of the human placenta (Rosenfeld, 2015a). However, the fetal placental cells, trophoblasts (TB), may also be immersed in compounds percolating through the maternal blood. For this reason, TB cells have some ability to detoxify select xenobiotic chemicals, which may help buffer the fetus against such chemical assaults (Myllynen et al., 2005; Obolenskaya et al., 2010; Corbel et al., 2015; Nahar et al., 2015). However, being an endocrine organ in of itself, the placenta is vulnerable to a myriad of exogenous chemicals. The ability to respond to such environmental challenges is also likely sexually dimorphic in nature (Mao et al., 2010; Rosenfeld, 2015a).

Individual gene or protein expression patterns were used to ascertain the effects of such chemical exposures on the placenta. Microarray technology was the first method employed to relate such chemicals exposures and transcriptomic changes in the placenta (e.g., Imanishi et al., 2003; Avissar-Whiting et al., 2010; Bruchova et al., 2010; Votavova et al., 2011; Tait et al., 2015; Grindler et al., 2018). However, such studies were confined to genes included on the arrays, and microarrays were only developed for a few select species whose genome was sequenced and annotated. RNA sequencing (RNAseq) is a high throughput approach that has greatly expanded our knowledge of how EDC, other environmental toxicants and pharmaceutical agents affect global gene expression patterns in the placenta (e.g., Green et al., 2020; Mao et al., 2020). Herein, we will consider the studies to date that have shown such extrinsic factors can affect transcriptomic profiles or protein expression in the placenta as determined by microarray analyses, RNAseq, or candidate gene/protein approaches. Further, we will consider other omics approaches, including metabolomics, proteomics, and methylomics, that have been used to characterize the effects of xenobiotics on the human and rodent placenta. The importance of miRNAs (miRs) is gaining currency as such small RNAs have the ability to block translation by binding to target mRNA (Van Wynsberghe et al., 2011; Moreno-Moya et al., 2014). The miR/mRNA complexes can then be degraded prior to the mRNA entering the cytoplasm to be translated into a protein. In this way, miR represent the final epigenetic regulators. Studies have thus examined how some of the above factors can regulate miR and other non-coding RNA profiles by using small RNAseq. Lastly, we will consider some of the recently developed transcriptomic technology that will continue to advance our understanding in placental toxicology and allow for pinpointing transcriptomic changes in individual TB cell populations.

Endocrine Disrupting Chemicals

Endocrine disrupting chemicals (EDC) are synthetic and natural compounds that can mimic or antagonize endogenous hormone responses. BPA is a widely prevalent synthetic chemical that can act through steroid and non-steroid receptor pathways (Schug et al., 2011). Current production estimates for BPA are around 20 billion pounds (Grand View Research, 2014). Approximately 93% of the U.S. population unknowingly has measurable amounts of BPA in their urine (Calafat et al., 2008). Exposure to BPA and, its analog, bisphenol S (BPS) is primarily dietary (Galloway et al., 2010; Sieli et al., 2011), but other routes of exposure are known (Xue et al., 2016; Hines et al., 2018). BPA readily can be transmitted from the maternal tissue to the fetal placenta (Vandenberg et al., 2007; vom Saal et al., 2007). BPA substitutes, such as BPS, are increasingly being used in a range of consumer products labeled BPA-free. Yet, BPS may lead to similar and potentially even more pronounced effects compared to BPA (Rosenfeld, 2017; Wu et al., 2018).

BPA has been shown to affect placental gene expression patterns (Imanishi et al., 2003; Kang et al., 2011; Susiarjo et al., 2013; Tan et al., 2013; Tait et al., 2015; Xu et al., 2015; Lee et al., 2016; Lan et al., 2017). Most of these reports though only used a candidate gene expression approach (Kang et al., 2011; Susiarjo et al., 2013; Tan et al., 2013; Tait et al., 2015; Xu et al., 2015; Lee et al., 2016; Lan et al., 2017), in particular for those known to be imprinted (Kang et al., 2011; Susiarjo et al., 2013). More recent studies employed microarrays to examine thousands of genes in a single experiment (Imanishi et al., 2003; Tait et al., 2015), but such studies may have been under-powered. One study that used microarrays to examine the effects of BPA on the placenta found that the high dosage of BPA tested resulted in significant degeneration and necrosis of giant cells, vacuolization in the junctional zone, and overall reduction of the spongioTB layer (Tait et al., 2015). Nuclear accumulation of β-catenin was evident in TB within the labyrinthine and spongioTB layers, suggestive of Wnt/β-catenin pathway activation (Tait et al., 2015). The microarray studies revealed that the low dosage of BPA tested promoted blood vessel development and arborization, whereas the high dose inhibited such angiogenic changes.

We used RNAseq analyses to examine the global transcriptomic profile in embryonic age (E) 12.5 mouse placenta following dietary exposure to BPA or BPS. BPA and BPS altered the expression of an identical set of 13 genes (Mao et al., 2020). Of which, 11 were downregulated and two (*Actn2* and *Efcab2*) modestly upregulated. Four of the differentially expressed (DE) transcripts are typically enriched in the placenta (*Sfrp4*, *Coch*, *Gm9513,* and *Calm4*) as determined by the TissueEnrich program (Mao et al., 2020). Based on the DE gene-sets, WNT and chemokine signaling pathways, amino acid metabolism, and possibly neurotransmission are pathways predicted to be affected in the placental samples exposed to BPA/BPS.

In the same study, we examined for histopathological changes in the placenta following BPA and BPS exposure. Additionally, targeted and non-targeted metabolomics analyses were performed to determine the extent to which these EDCs affect other omics profiles and whether transcriptomics and metabolomic changes correlated with BPA/BPS-associated architectural modifications in the placenta (Mao et al., 2020). Both exposures reduced the area occupied by spongioTB relative to parietal trophoblast giant cells (pTGC) within

the junctional zone. Both BPA and BPS markedly reduced placental serotonin (5-HT) concentrations and lowered 5-HT pTGC immunoreactivity. Concentrations of dopamine and 5-hydroxyindoleacetic acid), the main metabolite of 5-HT, however, were increased. Dopamine-immunoreactivity in pTGC was increased in BPA and BPS exposed placentas. By using mixOmics analyses (Rohart et al., 2017), we found a strong positive correlation between 5-HT positive pTGC cells and reductions in spongioTB to pTGC area, indicative that 5-HT is essential for maintaining cells within the junctional zone. In contrast, an inverse correlation existed between dopamine positive pTGC cells and reductions spongioTB to pTGC area. The collective findings suggest that BPS exposure causes almost identical placental effects as BPA. A major target of BPA/BPS is either spongioTB or pTGC within the junctional zone. BPA/BPS induced disruptions in placental 5-HT and dopamine may affect fetal brain development through the placenta- brain axis. It is clear that 5-HT as a morphogen may be one of the primary conductors regulating early neural crest formation, metamorphosis, neurogenesis, cell motility, synaptogenesis, and development of the nociceptive system (Lauder, 1988; Lauder et al., 1988; Whitaker-Azmitia, 1991; Herlenius and Lagercrantz, 2001). Strong evidence exists that the initial source of 5-HT to orchestrate such neural changes is the placenta (Huang et al., 1998; Bonnin and Levitt, 2011; Hadden et al., 2017). By using such omics approaches in the placenta, it may also thus shed light on how EDC compromise early neural development and thereby increase the risk for neurobehavioral disorders.

BPA might also affect DNA methylation patterns in the placenta. One study examined BPA concentrations, gene expression patterns of BPA-specific metabolizing enzymes, and global DNA methylations in the placenta of 2nd trimester human fetuses (Nahar et al., 2015). Average LINE1 and CCGG global methylation in the placenta were 58.3 and 59.2%, respectively, Total BPA concentrations positively correlated with global methylation for the placenta based on the LINE1 assay. BPA-specific metabolizing enzymes, such as GUSB, UGT2B15, STS, and SULT1A1 were identified in these placenta samples. The findings suggest that maternal exposure to BPA might promote hypermethylation of select genes in the placenta.

Phthalates are another class of EDCs found in commonly used household items, including children's toys, plastic containers, and plastic wraps (Ferguson et al., 2011; Lioy et al., 2015; Schulz et al., 2015; Jo et al., 2018). They are associated with adverse pregnancy outcomes, including fetal loss and placental growth abnormalities (Zong et al., 2015; Gao et al., 2017; Mahaboob Basha and Radha, 2017), but the full range of mechanisms by which they induce such effects remains elusive. Examination of the DNA methylome (Illumina Infinium Human Methylation 850k BeadChip) and transcriptome (Agilent whole human genome array) in first-trimester human placenta revealed 39 genes that demonstrated altered methylation and gene expression patterns in women exposed to high amounts of phthalates with most showing reduced expression in this group (Grindler et al., 2018). The combined usage of methylomics and transcriptomics revealed epidermal growth factor receptor (EGFR) as a likely primary mediator of phthalates on placental function.

Another cohort study revealed that chorionic gonadotropin A (*CGA*) showed sex-dependent gene expression changes in the placenta that were linked to various phthalate concentrations detected in the urine of pregnant women (Adibi et al., 2017a). *CY19A1*, *CYP11A1*, *CGA* expression in the placenta correlated with maternal urinary concentrations of monobenzyl phthalate (MBzP), MnBP, mono-iso-butyl phthalate (MiBP), and conceptus sex (Adibi et al., 2017a).

In vitro culture approaches have aided our understanding of how EDCs affect placental cells. One study used TB stem cells from rhesus monkeys (*Macaca mulatta*) to screen global transcriptome changes induced by several EDCs, atrazine, tributyltin, bisphenol A, bis(2-ethylhexyl) phthalate, and perfluorooctanoic acid (PFOA) (Midic et al., 2018). Atrazine and tributylin, and to a lesser extent the other three EDCs, suppressed genes involved in cytokine signaling related to antiviral response, along with those involved in metabolism, DNA repair, and cell migration.

Another study isolated human TB progenitor cells at 7–14 weeks. of pregnancy from two female and three male concepti, as well as villous cytotTB cells (vCTBs) at 15–20 weeks. pregnancy from three female and four male concepti. Primary cell lines were cultured in the presence of one or more phthalates: mono-*n*-butyl (MnBP), monobenzyl (MBzP), mono-2-ethylhexyl (MEHP), and monoethyl (MEP) (Adibi et al., 2017b). Treatment of both TB lines with MnBP, MBzP and MEHP at concentrations that resemble those found in the urine of pregnant women altered *CGB* and *PPARG* expression in these primary placental cells, although the effects varied according to the sex from which the placental cells were derived (Adibi et al., 2017b).

Other Environmental Toxicants

Other environmental toxicants, including heavy metals, such as arsenic, and flame retardants can reach the placenta, whereupon they may induce transcriptomic changes. The earth's crust contains arsenic, and it can also be found in the water, land, and air. However, it is highly toxic in the inorganic form (WHO, 2018). Common routes of exposure to inorganic arsenic are through drinking contaminated groundwater, using such water in food preparation and irrigation of food crops, manufacturing of it, consumption of contaminated food, and smoking tobacco (WHO, 2018). As with the EDCs, the placenta can accumulate high concentrations of arsenic that can lead to placental alterations, including in the glucocorticoid receptor pathway, oxidative stress, inflammation, linkages to pre-eclampsia, and epigenetic changes (Ahmed et al., 2011; Caldwell et al., 2015; Cardenas et al., 2015; Li et al., 2015; Green et al., 2016; Konkel, 2016; Appleton et al., 2017; Rahman et al., 2018; Punshon et al., 2019; Winterbottom et al., 2019b; Meakin et al., 2020; Stone et al., 2021).

To examine whether exposure to arsenic results in global transcriptomic changes in the placenta, 46 pregnant women were selected from the New Hampshire Birth Cohort Study (NHBCS), which is a US cohort known to have low-to-moderate arsenic levels in drinking water because of unregulated private wells (Winterbottom et al., 2019a). Potential sex-dependent gene expression changes in the placenta were correlated with prenatal

exposure to arsenic, as determined by concentrations in the urine of pregnant mothers. While no genes were differentially expressed in female placenta based on arsenic exposure, several hundred genes were affected in the placenta of males. Two of the genes that showed the greatest downregulation in male placenta exposed to arsenic were *FIBIN* and *RANBP3L* (Ahmed et al., 2011; Caldwell et al., 2015; Cardenas et al., 2015; Li et al., 2015; Green et al., 2016; Konkel, 2016; Appleton et al., 2017; Rahman et al., 2018; Punshon et al., 2019; Winterbottom et al., 2019b; Meakin et al., 2020; Stone et al., 2021).

To understand how such gene expression patterns might originate in the placenta, a handful of studies have examined the expression of epigenetic regulator genes and DNA methylation profiles in the placenta of arsenic-exposed human cohorts. One study analyzed the expression of over a hundred epigenetic regulator genes, such as those that act as readers, writers and erasers of post-translational histone modifications, and chromatin remodelers (Winterbottom et al., 2019b). Several of these genes demonstrated differences based on the interaction between placental sex and arsenic exposure with the histone methyltransferase (*PRDM6*) negatively correlating with arsenic exposure. Placental glucocorticoid receptor (*NR3C1*) methylation positively associated with arsenic exposure (Appleton et al., 2017).

Global DNA methylation patterns based on CpG loci were examined in placental samples obtained from 343 individuals enrolled in the New Hampshire Birth Cohort Study and correlated based on arsenic levels in the urine and toenails samples of these pregnant mothers (Green et al., 2016). While no linkages were found based on arsenic in maternal urine, strong association were identified based on levels of this heavy metal in the toenail samples. Of the 163 differentially methylated loci, the primary one was for *LYRM2* (Green et al., 2016). This study also found that allocation of placental cell sub-populations changed based on arsenic exposure.

Another study linked arsenic exposure and DNA methylation patterns, as determined by Infinium HumanMethylation450 BeadChip array, in the placenta, in the umbilical artery, and human umbilical vein endothelial cells (HUVEC) (Cardenas et al., 2015). Genes regulating melanogenesis and insulin signaling pathways were differentially methylated in the placenta and umbilical artery based on arsenic exposure (Cardenas et al., 2015).

The flame-retardant mixture, Firemaster 550 (FM 550) contains organophosphate flame retardants that was hypothesized to disrupt placental function. To examine how this environmental toxicant affected the placenta, pregnant Wistar rats were treated with varying concentrations of this chemical (Rock et al., 2020). This treatment altered the expression of genes involved in transport and synthesis of 5-HT in the placenta (Rock et al., 2020). Additionally, metabolites of 5-HT and the kynurenine metabolic pathway were increased.

The cellular and transcriptomic effects of another flame retardant, BDE-47- a polybrominated diphenyl ethers (PBDEs), was tested in human placental cytotTB cells (CTBs) (Robinson et al., 2019). This compound suppressed migration and invasion by CTBs. BDE-47 induced transcriptome changes that were dose dependent with genes involved in stress, inflammation, lipid/cholesterol metabolism, differentiation, migration, and vascular morphogenesis affected (Robinson et al., 2019). Hypermethylation of CpG islands for genes involved in cell adhesion and migration occurred in response to this treatment.

Pharmaceutical Agents

Pregnant women are often prescribed pharmaceutical agents to regulate such conditions as depression, epilepsy, and pain. While such drugs may be beneficial to the mother, they can have untoward consequences on the conceptus, including the placenta. Transcriptomics and other gene expression approaches have been useful tools in understanding how such xenobiotics alter the genetic machinery in this organ. In this section, we will consider three such pharmaceutical agents, serotonin-reuptake inhibitors (SSRI) used to treat depression, valproic acid (VPA) used to treat seizures, and oxycodone (OXY) that is a commonly prescribed analgesic agent.

Approximately 8–10% of pregnant women are prescribed selective serotonin-reuptake inhibitors (SSRI) to combat depression (Mitchell et al., 2011; Huybrechts et al., 2013). Such drugs act by binding to SLC6A4/SERT within the intracellular membrane, which in the central nervous system prevents the presynaptic cells from accruing 5-HT. Inhibition of SLC6A4/SERT results in increased concentrations of 5-HT in the synaptic space that can continue to bind and activates its cognate receptors. Such drugs though can also inhibit SLC6A4/SERT within placental TB, namely the pTGC that use this transporter to uptake maternal 5-HT. *In vitro* studies reveal SSRIs disrupt various structural and hormonal properties of placental cell lines (Hudon Thibeault et al., 2017; Clabault et al., 2018a,b). In rats, *in utero* exposure to venlafaxine reduced fetal placental weight (Laurent et al., 2016). Two SSRI, fluoxetine and sertraline, reduced cell proliferation of extravillous TB (JEG-3) cells (Clabault et al., 2018a). Norfluoxetine, a metabolite of fluoxetine, increased MMP-9 activity by these TB cells but suppressed MMP-9 activity in another cell line, HIPEC, derived from extravillous TB. TIMP-1 and ADAM-10 showed increased expression in JEG-3 cells treated with sertraline. Venlafaxine, another SSRI, increased ADAM-10 in HIPEC cells (Clabault et al., 2018a). Sertraline and venlafaxine induced fusion of cultured primary villous TB cells (Clabault et al., 2018b). Both compounds affect human chorionic gonadotropin beta (β-HCG) secretion by BeWo TB-derived cells. Norfluoxetine stimulated increased gene expression of chorionic gonadotropin beta (*CGB*) and gap junction protein alpha 1 (*GJA1*) which are considered biomarkers of syncytialization for these TB cells. Pregnant mothers consuming SSRIs have been reported to deliver lower birthweight infants and exhibit higher rates of placental-fetal vascular malperfusion than controls (Levy et al., 2020).

Valproic acid (VPA) is a short-chain-fatty acid commonly used as an antiepileptic drug and mood stabilizer (Chateauvieux et al., 2010). Such beneficial effects are ascribed to its inhibition of gamma amino butyric acid (GABA), transaminobutyrate, and ion channels (Chateauvieux et al., 2010). More recently, it has been shown that VPA can act as an histone deacetylase (HDAC) inhibitor that increases transcription by preventing deacetylation

of histone proteins (Monti et al., 2009). Thus, some of the actions of VPA may be due to its epigenetic properties. Epilepsy is the most common neurological disorder in pregnant women, necessitating continued usage of antiepileptic drugs (AED) to prevent seizures. VPA is one of the primary AED prescribed to pregnant women, even though current data suggests that it may be associated with adverse fetal outcomes and behavioral deficits in children exposed *in utero* to this drug (Eadie, 2014; Elkjaer et al., 2018; Richards et al., 2019; Vajda et al., 2019; Daugaard et al., 2020). The placenta is also not immune to the effects of this AED (Khera, 1992; Meir et al., 2016; Tetro et al., 2019; Jinno et al., 2020; Shafique and Winn, 2021), and VPA-induced changes in the placenta may adversely affect fetal development, including the brain.

To examine the transcriptome changes in response to VPA, term placenta from women who delivered via cesarean were perfused with varying concentrations of VPA or vehicle. They were than analyzed with a customized gene array panel to examine the expression of carrier genes (Rubinchik-Stern et al., 2018). This drug treatment changed the mRNA expression patterns for transporters of folic acid, glucose, choline, thyroid hormone, and serotonin. Placental folate concentrations were also decreased with VPA treatment. VPA treatment to pregnant rats altered the expression of other transporter genes with *Abcc4* and *Slc22a4* reduced in late gestation, but *Abcc5* was increased by VPA during mid-gestation (Jinno et al., 2020). Whether such changes on transporter gene expression patterns in the human and rat placenta is due to HDAC inhibition or other biological effects of VPA remains uncertain.

Opioid drugs, especially oxycodone (OxyContin, OXY), are widely prescribed analgesic agents to control pain in pregnant women. This abuse is one of the leading non-infectious disease public health concerns and economic challenges facing the United States (Reinhart et al., 2018). Opioid use disorder (OUD), is a particular health concern in women of child-bearing age (SAMHSA, 2015) with OUD during pregnancy estimated to affect 5.6 per 1000 live birth infants (Patrick et al., 2012). Neonates exposed during gestation to opioids are at risk for neonatal abstinence syndrome (NAS) (Jones et al., 2019). Maternal OUD has been associated with poor fetal growth, increased risk for premature births, low birthweight offspring, and congenital defects (Yazdy et al., 2015; CDC, 2019). Adult-onset diseases due to developmental origin of health and disease (DOHaD) effects of these drugs are also possible (Grandjean et al., 2015; Rosenfeld, 2015b). The placenta may be bathed and affected by any opioids circulating in the maternal blood, whereupon it can affect this organ and be transmitted to the fetus.

An endogenous opioid system is present in the placenta that mediates several placental responses, including production of maternal recognition of pregnancy factors, such as HCG and placental lactogens (Cemerikic et al., 1991; Ahmed et al., 1992; Cemerikic et al., 1992; Petit et al., 1993; Cemerikic et al., 1994). Exogenous opioids that transit from the maternal blood to the placenta can thus impact this system. Effects of OXY and other opioids have been examined in cultured TB cells and shown to affect production of steroid hormones, HCG, and other placental factors (Cemerikic et al., 1988; Zharikova et al., 2007; Neradugomma et al., 2017; Serra et al., 2017).

We tested whether maternal OXY exposure affects the morphology and transcriptome profile as determined by RNAseq in E 12.5 mice placenta (Green et al., 2020). Maternal OXY treatment reduced pTGC area and maternal blood vessel area within the labyrinth region. OXY exposure altered placental gene expression profiles in a sexually dimorphic manner with female placenta exhibiting up-regulation of several placental enriched genes, including *Ceacam11*, *Ceacam14*, *Ceacam12*, *Ceacam13*, *Prl7b1*, *Prl2b1*, *Ctsq*, and *Tpbpa*. Placenta of OXY exposed males had alterations of many ribosomal proteins. Weighted correlation network analysis revealed that in OXY females vs. CTL females, select modules correlated with placental histological changes induced by OXY. Such associations were lacking in the male OXY vs. CTL male comparison. Pathways that are likely affected in OXY females based on gene-sets in these modules include extracellular matrix reorganization, VEGF signaling, and regulation of actin bioskeleton, collagen biosynthesis, peptide hormone signaling, interferon signaling, interferon gamma signaling, and triglyceride metabolism and catabolism.

Smoking

Inorganic arsenic in cigarettes can affect placental architecture and function as discussed below. Other chemicals within cigarettes may also act though upon the placenta. The placenta expresses nicotinic acetylcholine receptor (nAChR) subunits that regulate TB cell invasion but whose expression and signaling pathway can be usurped by nicotine contained within tobacco smoke (Lips et al., 2005; Machaalani et al., 2014, 2018; Aishah et al., 2017; Chen et al., 2020). For instance, nicotine acting through nAChR induced endoplasmic reticulum stress in rat pTGC (Wong et al., 2016). Maternal smoking has been linked with changes in gross placental weight and microanatomical structure, especially for the extravillous TB cells (Heidari et al., 2018a,b; Larsen et al., 2018). Metabolism of lipids, namely long-chain polyunsaturated fatty acids and transporters for glucose uptake transporters (*SLC2A1* and *SLC2A3*), amino acids (*SLC7A8*), and lipid gene expression patterns in the placenta correlate with maternal smoking (Walker et al., 2019; Weinheimer et al., 2020). Circulating levels of placental-associated proteins, pregnancy-associated plasma protein A (PAPP-A) and free (fβHCG) are reduced in the serum of pregnant mothers who smoke (Jauniaux et al., 2013).

Transcriptomic and DNA methylation studies have been undertaken to determine whether maternal smoking affects these parameters in the placenta. An Illumina Expression Beadchip v3 that contained 24,526 transcripts was used to survey placental samples and cord blood from women who smoked while pregnant vs. non-smokers (Votavova et al., 2011). Pathways that were likely affected in placental and cord blood samples included xenobiotic metabolism, oxidative stress, inflammation, immunity, hematopoiesis, and vascularization. An earlier array-based study by this same research group found that maternal smoking induced several

genes involved in xenobiotic metabolism (*CYP1A1, CYP1B1, CYB5A*, and *COX412*) collagen-associated genes (*COL6A3, COL1A1,* and *COL1A2*), coagulation genes (*F5* and *F13A1*), and thrombosis-related genes (*CD36*, *ADAMTS9*, and *GAS6*) (Bruchova et al., 2010). Another study that considered effects of maternal smoking on gene expression and the proteome in the placenta found that smoking down-regulated SERPINB2, FGA, and HBB but upregulated SERPINA1, EFHD1, and KRT8 (Huuskonen et al., 2016). Transcript expression for *CYP1A1* and *CYP4B1* were elevated, whereas *HSD17B2*, *NFKB*, and *TGFB1* were suppressed by maternal smoking (Huuskonen et al., 2016).

A handful of studies characterized DNA methylation changes in the placenta based on maternal smoking (Suter et al., 2011; Chhabra et al., 2014; Tsaprouni et al., 2014; Maccani and Maccani, 2015; Fa et al., 2016; Morales et al., 2016; Cardenas et al., 2019; Rousseaux et al., 2020). Exposure to maternal smoking during the first trimester increased methylation of the *AHRR* gene but did not alter its gene expression pattern (Fa et al., 2018). In contrast, maternal smoking during this period did not alter DNA methylation of *CYP1A1* but expression of this gene was upregulated (Fa et al., 2018). DNA methylation analyses with the Illumina HumanMethylation450 BeadChip for participants in the Infancia y Medio Ambiente (INMA) birth cohort revealed that maternal smoking decreased methylation levels of cg27402634 in the placenta, and this change was also associated with decreased birthweight (Morales et al., 2016). Another group that used this same BeadChip reported CpG sites mapping to *GTF2H2C* and *GTF2H2D* in the placental methylome strongly associated with maternal smoking (Chhabra et al., 2014). Usage of the Illumina HumanMethylation BeadChip technology in another cohort population showed that methylation patterns within the *RUNX3* gene were linked to maternal smoking during pregnancy with one of the loci correlating with decreased gestational age (Maccani et al., 2013).

One study considered whether maternal cessation of smoking prior to pregnancy would prevent some of the harmful DNA methylation marks relative to women who continued to smoke throughout their pregnancy (Rousseaux et al., 2020). The placenta from both groups of women showed similar epigenetic changes, including demethylation of LINE-1 sequences, enrichment in epigenetic marks for enhancer regions (H3K4me1 and H3K27ac), and regions in proximity or overlapping imprinted genes (*NNAT, SGCE, PEG10, H19.MIR675*). The persistence of DNA methylation changes in those women who quit smoking before becoming pregnant is worrying as it is suggests that events even during the periconception period can lead to a permanent stamp on the DNA methylome of the placenta. Further work is clearly needed to determine the extent to when such changes become irreversible and whether these same methylation alterations are conferred to the placenta of subsequent generations, i.e., potential transgenerational effects. In this aspect, another study reported that while cigarette smoking by pregnant mothers reduced DNA methylation for several genes, including *CPOX* near *GPR15, PRSS23, AVPR1B, PSEN2, LINC00299, RPS6KA2, and KIAA0087*, cessation of smoking 3 months prior to pregnancy partially reversed such methylation alterations in the placenta (Tsaprouni et al., 2014).

Air Pollution

Particular matter that is around 2.5 μm in diameter ($PM_{2.5}$) in air pollution easily crosses the maternal-placental interface. As such, the placenta is vulnerable to such environmental toxicants. We will consider the evidence to date that air pollution disrupts the placental transcriptome and methylome profiles. Culturing of JEG-3 human placental cells in the presence of such PM affected genes involved in immune response, apoptosis regulation, calcium signaling pathway, steroid hormone biosynthesis, and cytokine-cytokine receptor interaction (Kim et al., 2018). Protein levels for mitogen activated protein kinases (MAPK) and COX2 were reduced in the $PM_{2.5}$ exposed JEG-3 cells. A Rhode Island Child Health Study (RICHS) revealed two developmentally sensitive windows to $PM_{2.5}$, with 12 weeks prior to and 13 weeks into gestation also being associated with reduced infant birthweight (Deyssenroth et al., 2021). This same study analyzed effects of $PM_{2.5}$ on placental gene expression patterns and relation to birthweight. Two placental modules enriched for genes involved in amino acid transport and cellular respiration correlated with maternal $PM_{2.5}$ exposure and infant birthweight (Deyssenroth et al., 2021). Additional findings from this cohort revealed that maternal exposure to $PM_{2.5}$ or black carbon (based on proximity to major roadways) changed the placental expression if several imprinted genes with *CHD7* showing interactions between $PM_{2.5}$ exposure/black carbon and infant sex being linked to placental expression of *ZDBF2* (Kingsley et al., 2017). The ENVironmental Influences ON early AGEing birth cohort was used to examine placental DNA methylation patterns (via a bisulfite -PCR pyrosequencing approach) in response to exposure to $PM_{2.5}$ or black carbon (Neven et al., 2018). Promoter methylation for *APEX1, ERCC4, and p53* were positively linked with maternal $PM_{2.5}$ exposure, whereas *DAPK1* showed a negative association to this extrinsic factor (Neven et al., 2018). Maternal exposure to black carbon was associated with increased promoter methylation for *APEX1* and *ERCC4*.

MicroRNAs and Long Non-Coding RNAs

MicroRNAs (miR) and long non-coding (lnc)RNAs were once considered junk, but this "rubbish" RNA is now known to exhibit critical regulatory roles, including acting as the goalie as to which mRNAs are allowed to exist out of the nucleus and be translated to a protein vs. those that are instead targeted for degradation (Clancy et al., 2007; Van Wynsberghe et al., 2011; Moreno-Moya et al., 2014). Thus, increasing number of researchers are studying the expression of small and long non-coding RNAs in the placenta following maternal exposure to various xenobiotics. The expression pattern of such RNAs in the placenta might also provide key insights into infant diseases. For instance, several miRs, such as mR-379-3p, miR-335-3p, miR-4532, miR-519e-3p, miR-3065-5p, and miR-105-5p, were found to be down-regulated

in the placenta of infants born small for gestational age (Östling et al., 2019).

BPA exposure has been linked to changes in miR expression patterns in whole placenta and TB cell lines (Avissar-Whiting et al., 2010; De Felice et al., 2015; Gao et al., 2018; Kaur et al., 2021). BPA treatment of human immortalized cytoTB cell lines and subsequent microarray analysis showed that several miRs had altered expression following this treatment, in particular miR-146a expression was strongly upregulated by BPA (Avissar-Whiting et al., 2010). Overexpression of miR-146a in these cell lines reduced cellular proliferation and rendered the cells more vulnerable to a DNA mutagenic agent (Avissar-Whiting et al., 2010). Genome-wide miR expression profiling revealed that maternal exposure to BPA significantly correlated with overexpression of miR-146a in whole placenta (De Felice et al., 2015). In experiments with California mice exposed to BPA, genistein, or the combination of these two EDCs, we found that developmental exposure to one or both compounds upregulated miR-146 in the hypothalamus of males and females (Kaur et al., 2021). In the testes, BPA induced miR-146a-5p that in turn impaired steroidogenesis through negative regulation of Metastatic tumor antigen 3 (MTA3) signaling (Gao et al., 2018). Taken together, miR-146 might be a biomarker for xenoestrogen exposure in mammals.

Analyses of miR expression patterns in placenta derived from a National Children's Study (NCS) sought to link such profiles to maternal exposure to a variety of environmental toxicants, dichlorodiphenyldichloroethylene (DDE), bisphenol A (BPA), polybrominated diphenyl ethers (PBDEs), polychlorinated biphenyls (PCBs), arsenic (As), mercury (Hg), lead (Pb), and cadmium (Cd) (Li et al., 2015). PBDE 209 positively correlated with miR-188-5p but inversely associated with let-7c. PCBs and Cd positively associated with miR-1537 expression. Hg and Pb exposure were linked with down-regulation of several let-7 family members. However, maternal exposure to DDE or BPA levels were not associated with any changes in miR expression. The conflicting results between the one cohort study above that found a linkage between BPA and expression of miR-146a in the placenta and the NCS findings might relate to variation in BPA exposure for the cohort population of pregnant women examined, number of women enrolled, and sequencing technique, including depth of coverage.

The aforementioned Rhode Island Child Healthy Study explored the linkage between placental cadmium concentrations and lncRNA expression in the placenta (Hussey et al., 2020). MIR22HG and ERVH48-showed increasing expression corresponding to cadmium exposure and was linked with elevated odds of small for gesational age birth. In contrast, A114763.2 and LINC02595 demonstrated reduced expression relative to cadmium concentrations but increased odds for large for gestational age birth with increasing expression. In a Bangladesh cohort population with known exposure to arsenic, several placental miRs, miR-1290, miR-195, and miR27a, were negatively associated with birthweight, and miR-1290 expression varied based on arsenic exposure (Rahman et al., 2018).

One study explored whether maternal exposure to $PM_{2.5}$ air pollution during different pregnancy trimesters was linked with varying changes in placental miR (Tsamou et al., 2018). Accordingly, miR-21 and miR-222 expression in the placenta

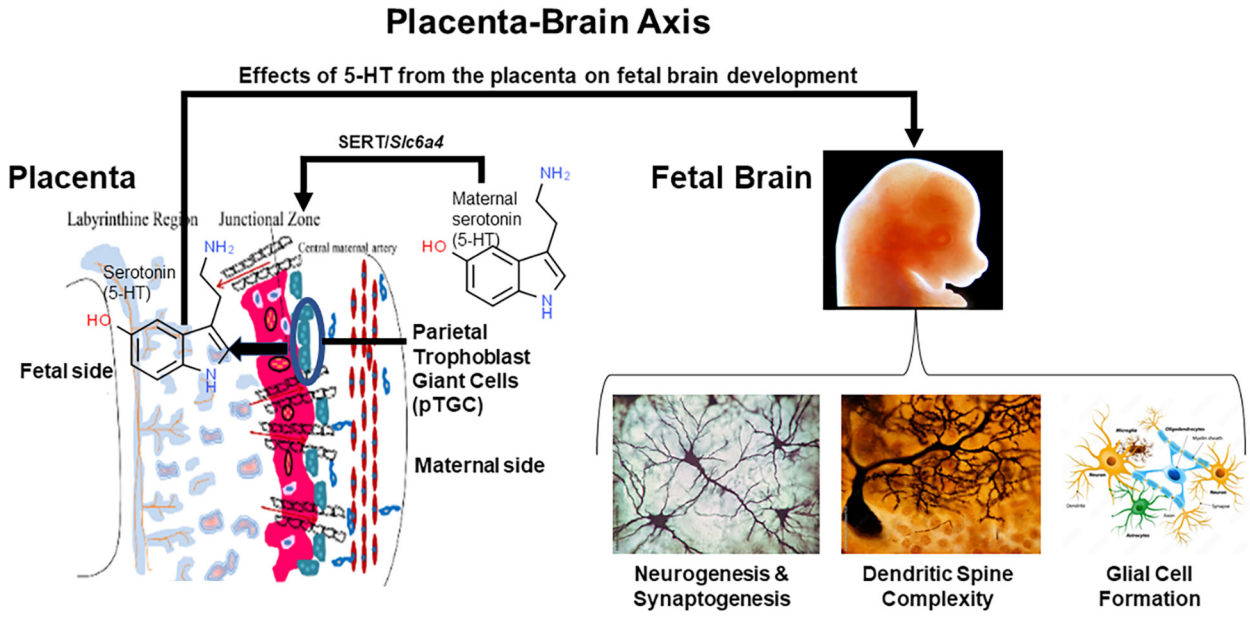

FIGURE 1 | The placenta-brain axis and effects of placental 5-HT on fetal brain development. The parietal trophoblast giant cells (pTGC) in the fetal placenta may amass maternal 5-HT via SERT or may synthesize this morphogen. Placental-derived 5-HT may then act upon the developing fetal brain to promote neurogenesis, synaptogenesis, increase dendritic spine complexity, and glial cell formation. In essence, early embryology and brain development may depend upon 5-HT originating from the placenta.

was inversely associated with $PM_{2.5}$ exposure during the 2nd trimester of pregnancy. However, exposure during the first trimester appeared to increase placental expression of miR-20a and miR-21. Based on the miR expression patterns, target mRNAs can be predicted, and the expression of tumor suppressor phosphatase and tensin homolog (*PTEN*) seems to be affected by the miRs that changed in response to maternal exposure to PM. Correspondingly, placental PTEN expression was positively associated with 3rd trimester $PM_{2.5}$ exposure (Tsamou et al., 2018).

CONCLUSION

In acting as the gatekeeper, the placenta is vulnerable to xenobiotics circulating in the maternal bloodstream, especially in rodents and humans who exhibit an invasive, hemochorial type of placentation. In this review, we have considered the impact of EDCs, other environmental toxicants, pharmaceutical agents, maternal smoking, and air pollution on the placental transcriptome and other omics, including miR profiles, along with associated changes such compounds induced on placental morphology. What emerges from many of these studies is that such xenobiotics act upon endogenous receptors and transporters, e.g., steroid receptors, SERT inhibitors, opioid receptors, and nicotinic acetylcholine receptor, naturally expressed by the placenta that when bound by their endogenous ligands are crucial in regulating placental responses. Binding of xenobiotics to such receptors or transporters evades normally homeostatic regulation and prevents the endogenous ligands from binding and activating their cognate receptors.

The placenta is an ephemeral organ but how it responds to such xenobiotics can lead to longstanding effects on fetal health. Such is particularly true in the case of the fetal brain that depends upon placental hormones, especially 5-HT, for initial forebrain development (Bonnin and Levitt, 2011; Rosenfeld, 2020, 2021). The current studies show that exposure to BPA, VPA, and flame retardants suppress placental 5-HT, dopamine, and likely other neurotransmitters (Rubinchik-Stern et al., 2018; Mao et al., 2020; Rock et al., 2020). Such changes assumingly disrupt paracrine actions that these factors would otherwise stimulate in the placenta, but such placental disturbances can also lead to ramifications on the fetal brain whose initial development depends upon placental transfer of such substances, in particular placental derived 5-HT (Bonnin and Levitt, 2011; Rosenfeld, 2020, 2021). 5-HT acting as a morphogen may be one of the primary conductors regulating early neural crest formation, metamorphosis, neurogenesis, cell motility, synaptogenesis, and development of the nociceptive system (Lauder, 1988; Lauder et al., 1988; Whitaker-Azmitia, 1991; Herlenius and Lagercrantz, 2001). Definitive evidence that the placenta is the initial source of 5-HT for the developing fetal brain comes from studies that blocked placental tryptophan hydroxylase 1 (TPH1) enzymatic activity by *in utero* injecting the TPH inhibitor p-chlorophenyalanine (PCPA) into the labyrinth region of E14.5 placentas (Bonnin and Levitt, 2011). Predictably, direct and short exposure to this pharmacological inhibitor suppressed 5-HT levels in the placenta, as well as notably in the fetal forebrain. Thus, factors that affect placental synthesis and ability to amass 5-HT can also dramatically shape early brain development that can result in longstanding neurobehavioral changes. This interconnection between the two organ systems, has been branded, the placenta-brain-axis (Rosenfeld, 2021). Placental transmission of 5-HT is likely one of many ways the placenta influences fetal brain development, as shown in **Figure 1**. Many neurobehavioral disorders likely trace their genesis to pathophysiological changes in the placenta (Marsit et al., 2012; Lesseur et al., 2014; Rosenfeld, 2015a).

One thing that also stands out in tracing the journey of discovery based on these omics approaches is that the experiments detailed herein employed techniques considered innovative for their time. However, ideas and technologies continue to evolve, and we must adapt our approaches accordingly. The studies described in this review were done with either whole placenta or isolated TB cell lines. Yet, the placenta in rodents and humans is a complex mixture of cells, and it is important to pinpoint how xenobiotics affect individual placental cell populations and how such changes may affect neighboring cells. The recently developed Visium spatial transcriptomics (ST) technology from 10X Genomics allows quantification of mRNA populations in the spatial context of intact tissue (Berglund et al., 2018; Maniatis et al., 2019). We have recently used this approach with mouse uteri (Mesa et al., 2021), but no studies to date have used novel method with placental samples. Single cell and single nuclei RNA-seq have been performed to understand human and mouse TB differentiation (Liu et al., 2018; Suryawanshi et al., 2018; Pique-Regi et al., 2019; West et al., 2019; Marsh and Blelloch, 2020). The architectural landscape of the placenta though is destroyed with both of these approaches. Thus, ST technology where the histoarchitecture is retained may complement these other techniques that allow for examination of gene expression patterns at the cellular or tissue level. Such approaches are predicted to become available to be able to characterize how varying extrinsic and intrinsic factors affect the DNA methylome, proteome, and global miR/other small RNA expression patterns down to the cellular level. MixOmics analyses (Rohart et al., 2017) and other integrative correlation analyses to be developed will permit integration of omics data and establish linkages between such molecular alterations to phenotypic changes in the placenta.

In conclusion, the studies to date provide strong evidence that xenobiotics affect placenta structure and molecular processes that assumingly affect placental morphology. The coming years will assuredly be devoted to tracing xenobiotic affects to individual TB cell populations and how such effects change over the course of pregnancy. How xenobiotics modify the placenta-brain axis is also predicted to become an important avenue of research. Identification of such placental changes may provide a mechanistic understanding of the fetal origin of neurobehavioral disorders in general and open up new avenues for early diagnosis and potential treatments for patients with autism spectrum disorders (ASD) caused by placental dysfunction during pregnancy.

AUTHOR CONTRIBUTIONS

CR researched, wrote, and edited the article.

FUNDING

CR is supported by 1R01ES025547.

REFERENCES

Adibi, J. J., Buckley, J. P., Lee, M. K., Williams, P. L., Just, A. C., Zhao, Y., et al. (2017a). Maternal urinary phthalates and sex-specific placental mRNA levels in an urban birth cohort. *Environ. Health* 16:35.

Adibi, J. J., Zhao, Y., Zhan, L. V., Kapidzic, M., Larocque, N., Koistinen, H., et al. (2017b). An investigation of the single and combined phthalate metabolite effects on human chorionic gonadotropin expression in placental cells. *Environ. Health Perspect.* 125:107010. doi: 10.1289/ehp1539

Ahmed, M. S., Cemerikic, B., and Agbas, A. (1992). Properties and functions of human placental opioid system. *Life Sci.* 50, 83–97. doi: 10.1016/0024-3205(92)90290-6

Ahmed, S., Mahabbat-E Khoda, S., Rekha, R. S., Gardner, R. M., Ameer, S. S., Moore, S., et al. (2011). Arsenic-associated oxidative stress, inflammation, and immune disruption in human placenta and cord blood. *Environ. Health Perspect.* 119, 258–264. doi: 10.1289/ehp.1102086

Aishah, A., Hinton, T., and Machaalani, R. (2017). Cellular protein and mRNA expression of β1 nicotinic acetylcholine receptor (nAChR) subunit in brain, skeletal muscle and placenta. *Int. J. Dev. Neurosci.* 58, 9–16. doi: 10.1016/j.ijdevneu.2017.01.011

Appleton, A. A., Jackson, B. P., Karagas, M., and Marsit, C. J. (2017). Prenatal exposure to neurotoxic metals is associated with increased placental glucocorticoid receptor DNA methylation. *Epigenetics* 12, 607–615. doi: 10.1080/15592294.2017.1320637

Avissar-Whiting, M., Veiga, K. R., Uhl, K. M., Maccani, M. A., Gagne, L. A., Moen, E. L., et al. (2010). Bisphenol A exposure leads to specific microRNA alterations in placental cells. *Reprod. Toxicol.* 29, 401–406. doi: 10.1016/j.reprotox.2010.04.004

Berglund, E., Maaskola, J., Schultz, N., Friedrich, S., Marklund, M., Bergenstrahle, J., et al. (2018). Spatial maps of prostate cancer transcriptomes reveal an unexplored landscape of heterogeneity. *Nat. Commun.* 9:2419.

Bonnin, A., and Levitt, P. (2011). Fetal, maternal, and placental sources of serotonin and new implications for developmental programming of the brain. *Neuroscience* 197, 1–7. doi: 10.1016/j.neuroscience.2011.10.005

Bruchova, H., Vasikova, A., Merkerova, M., Milcova, A., Topinka, J., Balascak, I., et al. (2010). Effect of maternal tobacco smoke exposure on the placental transcriptome. *Placenta* 31, 186–191. doi: 10.1016/j.placenta.2009.12.016

Calafat, A. M., Ye, X., Wong, L. Y., Reidy, J. A., and Needham, L. L. (2008). Exposure of the U.S. population to bisphenol A and 4-tertiary-octylphenol: 2003-2004. *Environ. Health Perspect.* 116, 39–44. doi: 10.1289/ehp.10753

Caldwell, K. E., Labrecque, M. T., Solomon, B. R., Ali, A., and Allan, A. M. (2015). Prenatal arsenic exposure alters the programming of the glucocorticoid signaling system during embryonic development. *Neurotoxicol. Teratol.* 47, 66–79. doi: 10.1016/j.ntt.2014.11.006

Cardenas, A., Houseman, E. A., Baccarelli, A. A., Quamruzzaman, Q., Rahman, M., Mostofa, G., et al. (2015). In utero arsenic exposure and epigenome-wide associations in placenta, umbilical artery, and human umbilical vein endothelial cells. *Epigenetics* 10, 1054–1063. doi: 10.1080/15592294.2015.1105424

Cardenas, A., Lutz, S. M., Everson, T. M., Perron, P., Bouchard, L., and Hivert, M. F. (2019). Mediation by Placental DNA Methylation of the association of prenatal maternal smoking and birth weight. *Am. J. Epidemiol.* 188, 1878–1886. doi: 10.1093/aje/kwz184

CDC (2019). *Basics About Opioid Use During Pregnancy*. Available online at: https://Www.Cdc.Gov/Pregnancy/Opioids/Basics.Html (accessed September 13, 2021).

Cemerikic, B., Cheng, J., Agbas, A., and Ahmed, M. S. (1991). Opioids regulate the release of human chorionic gonadotropin hormone from trophoblast tissue. *Life Sci.* 49, 813–824. doi: 10.1016/0024-3205(91)90246-8

Cemerikic, B., Genbacev, O., Sulovic, V., and Beaconsfield, R. (1988). Effect of morphine on hCG release by first trimester human trophoblast *in vitro*. *Life Sci.* 42, 1773–1779. doi: 10.1016/0024-3205(88)90044-6

Cemerikic, B., Schabbing, R., and Ahmed, M. S. (1992). Selectivity and potency of opioid peptides in regulating human chorionic gonadotropin release from term trophoblast tissue. *Peptides* 13, 897–903. doi: 10.1016/0196-9781(92)90047-7

Cemerikic, B., Zamah, R., and Ahmed, M. S. (1994). Opioids regulation of human chorionic gonadotropin release from trophoblast tissue is mediated by gonadotropin releasing hormone. *J. Pharmacol. Exp. Ther.* 268, 971–977.

Chateauvieux, S., Morceau, F., Dicato, M., and Diederich, M. (2010). Molecular and therapeutic potential and toxicity of valproic acid. *J. Biomed. Biotechnol.* 2010:479364.

Chen, J., Qiu, M., Huang, Z., Chen, J., Zhou, C., Han, F., et al. (2020). Nicotine suppresses the invasiveness of human trophoblasts by downregulation of CXCL12 expression through the alpha-7 subunit of the nicotinic acetylcholine receptor. *Reprod. Sci.* 27, 916–924. doi: 10.1007/s43032-019-00095-4

Chhabra, D., Sharma, S., Kho, A. T., Gaedigk, R., Vyhlidal, C. A., Leeder, J. S., et al. (2014). Fetal lung and placental methylation is associated with in utero nicotine exposure. *Epigenetics* 9, 1473–1484. doi: 10.4161/15592294.2014.971593

Clabault, H., Cohen, M., Vaillancourt, C., and Sanderson, J. T. (2018a). Effects of selective serotonin-reuptake inhibitors (SSRIs) in JEG-3 and HIPEC cell models of the extravillous trophoblast. *Placenta* 72-73, 62–73.

Clabault, H., Flipo, D., Guibourdenche, J., Fournier, T., Sanderson, J. T., and Vaillancourt, C. (2018b). Effects of selective serotonin-reuptake inhibitors (SSRIs) on human villous trophoblasts syncytialization. *Toxicol. Appl. Pharmacol.* 349, 8–20. doi: 10.1016/j.taap.2018.04.018

Clancy, J. L., Nousch, M., Humphreys, D. T., Westman, B. J., Beilharz, T. H., and Preiss, T. (2007). Methods to analyze microRNA-mediated control of mRNA translation. *Methods Enzymol.* 431, 83–111. doi: 10.1016/s0076-6879(07)31006-9

Corbel, T., Perdu, E., Gayrard, V., Puel, S., Lacroix, M. Z., Viguié, C., et al. (2015). Conjugation and deconjugation reactions within the fetoplacental compartment in a sheep model: a key factor determining bisphenol A fetal exposure. *Drug Metab. Dispos.* 43, 467–476. doi: 10.1124/dmd.114.061291

Daugaard, C. A., Pedersen, L., Sun, Y., Dreier, J. W., and Christensen, J. (2020). Association of prenatal exposure to valproate and other antiepileptic drugs with intellectual disability and delayed childhood milestones. *JAMA Netw. Open* 3:e2025570. doi: 10.1001/jamanetworkopen.2020.25570

De Felice, B., Manfellotto, F., Palumbo, A., Troisi, J., Zullo, F., Di Carlo, C., et al. (2015). Genome-wide microRNA expression profiling in placentas from pregnant women exposed to BPA. *BMC Med. Genomics* 8:56. doi: 10.1186/s12920-015-0131-z

Deyssenroth, M. A., Rosa, M. J., Eliot, M. N., Kelsey, K. T., Kloog, I., Schwartz, J. D., et al. (2021). Placental gene networks at the interface between maternal PM(2.5) exposure early in gestation and reduced infant birthweight. *Environ. Res.* 199:111342. doi: 10.1016/j.envres.2021.111342

Eadie, M. J. (2014). Treating epilepsy in pregnant women. *Expert Opin. Pharmacother.* 15, 841–850. doi: 10.1517/14656566.2014.896902

Elkjaer, L. S., Bech, B. H., Sun, Y., Laursen, T. M., and Christensen, J. (2018). Association between prenatal valproate exposure and performance on standardized language and mathematics tests in school-aged children. *JAMA Neurol.* 75, 663–671. doi: 10.1001/jamaneurol.2017.5035

Fa, S., Larsen, T. V., Bilde, K., Daugaard, T. F., Ernst, E. H., Lykke-Hartmann, K., et al. (2018). Changes in first trimester fetal CYP1A1 and AHRR DNA methylation and mRNA expression in response to exposure to maternal cigarette smoking. *Environ. Toxicol. Pharmacol.* 57, 19–27. doi: 10.1016/j.etap.2017.11.007

Fa, S., Larsen, T. V., Bilde, K., Daugaard, T. F., Ernst, E. H., Olesen, R. H., et al. (2016). Assessment of global DNA methylation in the first trimester fetal tissues exposed to maternal cigarette smoking. *Clin. Epigenetics* 8:128.

Ferguson, K. K., Loch-Caruso, R., and Meeker, J. D. (2011). Urinary phthalate metabolites in relation to biomarkers of inflammation and oxidative stress: NHANES 1999-2006. *Environ. Res.* 111, 718–726. doi: 10.1016/j.envres.2011.02.002

Galloway, T., Cipelli, R., Guralnick, J., Ferrucci, L., Bandinelli, S., Corsi, A. M., et al. (2010). Daily bisphenol A excretion and associations with sex hormone

concentrations: results from the InCHIANTI adult population study. *Environ. Health Perspect.* 118, 1603–1608.

Gao, G. Z., Zhao, Y., Li, H. X., and Li, W. (2018). Bisphenol A-elicited miR-146a-5p impairs murine testicular steroidogenesis through negative regulation of Mta3 signaling. *Biochem. Biophys. Res. Commun.* 501, 478–485. doi: 10.1016/j.bbrc.2018.05.017

Gao, H., Zhang, Y. W., Huang, K., Yan, S. Q., Mao, L. J., Ge, X., et al. (2017). Urinary concentrations of phthalate metabolites in early pregnancy associated with clinical pregnancy loss in Chinese women. *Sci. Rep.* 7:6800.

Grand View Research (2014). *Global Bisphenol A (BPA) Market by Appliation (Appliances, Automotive, Consumer, Construction, Electrical & Electronics) Expected to Reach USD 20.03 Billion by 2020*. Available online at: http://www.digitaljournal.com/pr/2009287 (accessed September 13, 2021).

Grandjean, P., Barouki, R., Bellinger, D. C., Casteleyn, L., Chadwick, L. H., Cordier, S., et al. (2015). Life-long implications of developmental exposure to environmental stressors: new perspectives. *Endocrinology* 156, 3408–3415.

Green, B. B., Karagas, M. R., Punshon, T., Jackson, B. P., Robbins, D. J., Houseman, E. A., et al. (2016). Epigenome-wide assessment of DNA methylation in the placenta and arsenic exposure in the New Hampshire birth cohort study (USA). *Environ. Health Perspect.* 124, 1253–1260. doi: 10.1289/ehp.1510437

Green, M. T., Martin, R. E., Kinkade, J. A., Schmidt, R. R., Bivens, N. J., Tuteja, G., et al. (2020). Maternal oxycodone treatment causes pathophysiological changes in the mouse placenta. *Placenta* 100, 96–110. doi: 10.1016/j.placenta.2020.08.006

Grindler, N. M., Vanderlinden, L., Karthikraj, R., Kannan, K., Teal, S., Polotsky, A. J., et al. (2018). Exposure to phthalate, an endocrine disrupting chemical, alters the first trimester placental methylome and transcriptome in women. *Sci. Rep.* 8:6086.

Hadden, C., Fahmi, T., Cooper, A., Savenka, A. V., Lupashin, V. V., Roberts, D. J., et al. (2017). Serotonin transporter protects the placental cells against apoptosis in caspase 3-independent pathway. *J. Cell. Physiol.* 232, 3520–3529. doi: 10.1002/jcp.25812

Heidari, Z., Mahmoudzadeh-Sagheb, H., and Sheibak, N. (2018a). Placenta structural changes in heavy smoking mothers: a stereological aspect. *Curr. Med. Res. Opin.* 34, 1893–1897. doi: 10.1080/03007995.2018.1444590

Heidari, Z., Mahmoudzadeh-Sagheb, H., and Sheibak, N. (2018b). Quantitative changes of extravillous trophoblast cells in heavy smoker mothers compared with healthy controls. *Reprod. Fertil. Dev.* 30, 409–414. doi: 10.1071/rd17041

Herlenius, E., and Lagercrantz, H. (2001). Neurotransmitters and neuromodulators during early human development. *Early Hum. Dev.* 65, 21–37. doi: 10.1016/s0378-3782(01)00189-x

Hines, C. J., Christianson, A. L., Jackson, M. V., Ye, X., Pretty, J. R., Arnold, J. E., et al. (2018). An evaluation of the relationship among urine, air, and hand measures of exposure to bisphenol A (BPA) in US manufacturing workers. *Ann. Work Expo. Health* 62, 840–851. doi: 10.1093/annweh/wxy042

Huang, W. Q., Zhang, C. L., Di, X. Y., and Zhang, R. Q. (1998). Studies on the localization of 5-hydroxytryptamine and its receptors in human placenta. *Placenta* 19, 655–661. doi: 10.1016/s0143-4004(98)90027-3

Hudon Thibeault, A. A., Laurent, L., Vo Duy, S., Sauve, S., Caron, P., Guillemette, C., et al. (2017). Fluoxetine and its active metabolite norfluoxetine disrupt estrogen synthesis in a co-culture model of the feto-placental unit. *Mol. Cell. Endocrinol.* 442, 32–39. doi: 10.1016/j.mce.2016.11.021

Hussey, M. R., Burt, A., Deyssenroth, M. A., Jackson, B. P., Hao, K., Peng, S., et al. (2020). Placental lncRNA expression associated with placental cadmium concentrations and birth weight. *Environ. Epigenet.* 6:dvaa003.

Huuskonen, P., Amezaga, M. R., Bellingham, M., Jones, L. H., Storvik, M., Häkkinen, M., et al. (2016). The human placental proteome is affected by maternal smoking. *Reprod. Toxicol.* 63, 22–31. doi: 10.1016/j.reprotox.2016.05.009

Huybrechts, K. F., Palmsten, K., Mogun, H., Kowal, M., Avorn, J., Setoguchi-Iwata, S., et al. (2013). National trends in antidepressant medication treatment among publicly insured pregnant women. *Gen. Hosp. Psychiatry* 35, 265–271. doi: 10.1016/j.genhosppsych.2012.12.010

Imanishi, S., Manabe, N., Nishizawa, H., Morita, M., Sugimoto, M., Iwahori, M., et al. (2003). Effects of oral exposure of bisphenol A on mRNA expression of nuclear receptors in murine placentae assessed by DNA microarray. *J. Reprod. Dev.* 49, 329–336. doi: 10.1262/jrd.49.329

Jauniaux, E., Suri, S., and Muttukrishna, S. (2013). Evaluation of the impact of maternal smoking on ultrasound and endocrinological markers of first trimester placentation. *Early Hum. Dev.* 89, 777–780. doi: 10.1016/j.earlhumdev.2013.06.005

Jinno, N., Furugen, A., Kurosawa, Y., Kanno, Y., Narumi, K., Kobayashi, M., et al. (2020). Effects of single and repetitive valproic acid administration on the gene expression of placental transporters in pregnant rats: an analysis by gestational period. *Reprod. Toxicol.* 96, 47–56. doi: 10.1016/j.reprotox.2020.04.077

Jo, S. H., Lee, M. H., Kim, K. H., and Kumar, P. (2018). Characterization and flux assessment of airborne phthalates released from polyvinyl chloride consumer goods. *Environ. Res.* 165, 81–90. doi: 10.1016/j.envres.2018.04.007

Jones, H. E., Kaltenbach, K., Benjamin, T., Wachman, E. M., and O'grady, K. E. (2019). Prenatal opioid exposure, neonatal abstinence syndrome/neonatal opioid withdrawal syndrome, and later child development research: shortcomings and solutions. *J. Addict. Med.* 13, 90–92. doi: 10.1097/adm.0000000000000463

Kang, E. R., Iqbal, K., Tran, D. A., Rivas, G. E., Singh, P., Pfeifer, G. P., et al. (2011). Effects of endocrine disruptors on imprinted gene expression in the mouse embryo. *Epigenetics* 6, 937–950. doi: 10.4161/epi.6.7.16067

Kaur, S., Kinkade, J. A., Green, M. T., Martin, R. E., Willemse, T. E., Bivens, N. J., et al. (2021). Disruption of global hypothalamic microRNA (miR) profiles and associated behavioral changes in California mice (*Peromyscus californicus*) developmentally exposed to endocrine disrupting chemicals. *Horm. Behav.* 128:104890. doi: 10.1016/j.yhbeh.2020.104890

Khera, K. S. (1992). Valproic acid-induced placental and teratogenic effects in rats. *Teratology* 45, 603–610. doi: 10.1002/tera.1420450605

Kim, W., Cho, Y., Song, M. K., Lim, J. H., Kim, J. Y., Gye, M. C., et al. (2018). Effect of particulate matter 2.5 on gene expression profile and cell signaling in JEG-3 human placenta cells. *Environ. Toxicol.* 33, 1123–1134. doi: 10.1002/tox.22591

Kingsley, S. L., Deyssenroth, M. A., Kelsey, K. T., Awad, Y. A., Kloog, I., Schwartz, J. D., et al. (2017). Maternal residential air pollution and placental imprinted gene expression. *Environ. Int.* 108, 204–211. doi: 10.1016/j.envint.2017.08.022

Konkel, L. (2016). Arsenic and the placental epigenome: unlocking the secrets of prenatal exposure. *Environ. Health Perspect.* 124:A148.

Lan, X., Fu, L. J., Zhang, J., Liu, X. Q., Zhang, H. J., Zhang, X., et al. (2017). Bisphenol A exposure promotes HTR-8/SVneo cell migration and impairs mouse placentation involving upregulation of integrin-beta1 and MMP-9 and stimulation of MAPK and PI3K signaling pathways. *Oncotarget* 8, 51507–51521. doi: 10.18632/oncotarget.17882

Larsen, S., Haavaldsen, C., Bjelland, E. K., Dypvik, J., Jukic, A. M., and Eskild, A. (2018). Placental weight and birthweight: the relations with number of daily cigarettes and smoking cessation in pregnancy. A population study. *Int. J. Epidemiol.* 47, 1141–1150. doi: 10.1093/ije/dyy110

Lauder, J. M. (1988). Neurotransmitters as morphogens. *Prog. Brain Res.* 73, 365–387. doi: 10.1016/s0079-6123(08)60516-6

Lauder, J. M., Tamir, H., and Sadler, T. W. (1988). Serotonin and morphogenesis. I. Sites of serotonin uptake and -binding protein immunoreactivity in the midgestation mouse embryo. *Development* 102, 709–720. doi: 10.1242/dev.102.4.709

Laurent, L., Huang, C., Ernest, S. R., Berard, A., Vaillancourt, C., and Hales, B. F. (2016). In utero exposure to venlafaxine, a serotonin-norepinephrine reuptake inhibitor, increases cardiac anomalies and alters placental and heart serotonin signaling in the rat. *Birth Defects Res. A Clin. Mol. Teratol.* 106, 1044–1055. doi: 10.1002/bdra.23537

Lee, J. H., Ahn, C., Kang, H. Y., Hong, E. J., Hyun, S. H., Choi, K. C., et al. (2016). Effects of octylphenol and bisphenol A on the metal cation transporter channels of mouse placentas. *Int. J. Environ. Res. Public Health* 13:965. doi: 10.3390/ijerph13100965

Lesseur, C., Armstrong, D. A., Murphy, M. A., Appleton, A. A., Koestler, D. C., Paquette, A. G., et al. (2014). Sex-specific associations between placental leptin promoter DNA methylation and infant neurobehavior. *Psychoneuroendocrinology* 40, 1–9. doi: 10.1016/j.psyneuen.2013.10.012

Levy, M., Kovo, M., Miremberg, H., Anchel, N., Herman, H. G., Bar, J., et al. (2020). Maternal use of selective serotonin reuptake inhibitors (SSRI) during pregnancy-neonatal outcomes in correlation with placental histopathology. *J. Perinatol.* 40, 1017–1024. doi: 10.1038/s41372-020-0598-0

Li, Q., Kappil, M. A., Li, A., Dassanayake, P. S., Darrah, T. H., Friedman, A. E., et al. (2015). Exploring the associations between microRNA expression profiles and environmental pollutants in human placenta from the National Children's Study (NCS). *Epigenetics* 10, 793–802. doi: 10.1080/15592294.2015.1066960

Lioy, P. J., Hauser, R., Gennings, C., Koch, H. M., Mirkes, P. E., Schwetz, B. A., et al. (2015). Assessment of phthalates/phthalate alternatives in children's toys and childcare articles: review of the report including conclusions and recommendation of the Chronic Hazard Advisory Panel of the Consumer Product Safety Commission. *J. Expo. Sci. Environ. Epidemiol.* 25, 343–353. doi: 10.1038/jes.2015.33

Lips, K. S., Brüggmann, D., Pfeil, U., Vollerthun, R., Grando, S. A., and Kummer, W. (2005). Nicotinic acetylcholine receptors in rat and human placenta. *Placenta* 26, 735–746. doi: 10.1016/j.placenta.2004.10.009

Liu, Y., Fan, X., Wang, R., Lu, X., Dang, Y. L., Wang, H., et al. (2018). Single-cell RNA-seq reveals the diversity of trophoblast subtypes and patterns of differentiation in the human placenta. *Cell Res.* 28, 819–832. doi: 10.1038/s41422-018-0066-y

Maccani, J. Z., and Maccani, M. A. (2015). Altered placental DNA methylation patterns associated with maternal smoking: current perspectives. *Adv. Genomics Genet.* 2015, 205–214. doi: 10.2147/agg.s61518

Maccani, J. Z., Koestler, D. C., Houseman, E. A., Marsit, C. J., and Kelsey, K. T. (2013). Placental DNA methylation alterations associated with maternal tobacco smoking at the RUNX3 gene are also associated with gestational age. *Epigenomics* 5, 619–630. doi: 10.2217/epi.13.63

Machaalani, R., Ghazavi, E., Hinton, T., Makris, A., and Hennessy, A. (2018). Immunohistochemical expression of the nicotinic acetylcholine receptor (nAChR) subunits in the human placenta, and effects of cigarette smoking and preeclampsia. *Placenta* 71, 16–23. doi: 10.1016/j.placenta.2018.09.008

Machaalani, R., Ghazavi, E., Hinton, T., Waters, K. A., and Hennessy, A. (2014). Cigarette smoking during pregnancy regulates the expression of specific nicotinic acetylcholine receptor (nAChR) subunits in the human placenta. *Toxicol. Appl. Pharmacol.* 276, 204–212. doi: 10.1016/j.taap.2014.02.015

Mahaboob Basha, P., and Radha, M. J. (2017). Gestational di-n-butyl phthalate exposure induced developmental and teratogenic anomalies in rats: a multigenerational assessment. *Environ. Sci. Pollut. Res. Int.* 24, 4537–4551. doi: 10.1007/s11356-016-8196-6

Maniatis, S., Aijo, T., Vickovic, S., Braine, C., Kang, K., Mollbrink, A., et al. (2019). Spatiotemporal dynamics of molecular pathology in amyotrophic lateral sclerosis. *Science* 364, 89–93.

Mao, J., Jain, A., Denslow, N. D., Nouri, M. Z., Chen, S., Wang, T., et al. (2020). Bisphenol A and bisphenol S disruptions of the mouse placenta and potential effects on the placenta-brain axis. *Proc. Natl. Acad. Sci. U.S.A.* 117, 4642–4652. doi: 10.1073/pnas.1919563117

Mao, J., Zhang, X., Sieli, P. T., Falduto, M. T., Torres, K. E., and Rosenfeld, C. S. (2010). Contrasting effects of different maternal diets on sexually dimorphic gene expression in the murine placenta. *Proc. Natl. Acad. Sci. U.S.A.* 107, 5557–5562. doi: 10.1073/pnas.1000440107

Marsh, B., and Blelloch, R. (2020). Single nuclei RNA-seq of mouse placental labyrinth development. *eLife* 9:e60266.

Marsit, C. J., Lambertini, L., Maccani, M. A., Koestler, D. C., Houseman, E. A., Padbury, J. F., et al. (2012). Placenta-imprinted gene expression association of infant neurobehavior. *J. Pediatr.* 160, 854–860.e2.

Meakin, C. J., Szilagyi, J. T., Avula, V., and Fry, R. C. (2020). Inorganic arsenic and its methylated metabolites as endocrine disruptors in the placenta: mechanisms underpinning glucocorticoid receptor (GR) pathway perturbations. *Toxicol. Appl. Pharmacol.* 409:115305. doi: 10.1016/j.taap.2020.115305

Meir, M., Bishara, A., Mann, A., Udi, S., Portnoy, E., Shmuel, M., et al. (2016). Effects of valproic acid on the placental barrier in the pregnant mouse: optical imaging and transporter expression studies. *Epilepsia* 57, e108–e112.

Mesa, A. M., Mao, J., Medrano, T. I., Bivens, N. J., Jurkevich, A., Tuteja, G., et al. (2021). Spatial transcriptomics analysis of uterine gene expression in enhancer of zeste homolog 2 (Ezh2) conditional knockout mice. *Biol. Reprod.* ioab147. doi: 10.1093/biolre/ioab147

Midic, U., Goheen, B., Vincent, K. A., Vandevoort, C. A., and Latham, K. E. (2018). Changes in gene expression following long-term *in vitro* exposure of *Macaca mulatta* trophoblast stem cells to biologically relevant levels of endocrine disruptors. *Reprod. Toxicol.* 77, 154–165. doi: 10.1016/j.reprotox.2018.02.012

Mitchell, A. A., Gilboa, S. M., Werler, M. M., Kelley, K. E., Louik, C., and Hernandez-Diaz, S. (2011). Medication use during pregnancy, with particular focus on prescription drugs: 1976-2008. *Am. J. Obstet. Gynecol.* 205, 51.e1–51.e8.

Monti, B., Polazzi, E., and Contestabile, A. (2009). Biochemical, molecular and epigenetic mechanisms of valproic acid neuroprotection. *Curr. Mol. Pharmacol.* 2, 95–109. doi: 10.2174/1874467210902010095

Morales, E., Vilahur, N., Salas, L. A., Motta, V., Fernandez, M. F., Murcia, M., et al. (2016). Genome-wide DNA methylation study in human placenta identifies novel loci associated with maternal smoking during pregnancy. *Int. J. Epidemiol.* 45, 1644–1655. doi: 10.1093/ije/dyw196

Moreno-Moya, J. M., Vilella, F., and Simon, C. (2014). MicroRNA: key gene expression regulators. *Fertil. Steril.* 101, 1516–1523. doi: 10.1016/j.fertnstert.2013.10.042

Myllynen, P., Pasanen, M., and Pelkonen, O. (2005). Human placenta: a human organ for developmental toxicology research and biomonitoring. *Placenta* 26, 361–371. doi: 10.1016/j.placenta.2004.09.006

Nahar, M. S., Liao, C., Kannan, K., Harris, C., and Dolinoy, D. C. (2015). In utero bisphenol A concentration, metabolism, and global DNA methylation across matched placenta, kidney, and liver in the human fetus. *Chemosphere* 124, 54–60. doi: 10.1016/j.chemosphere.2014.10.071

Neradugomma, N. K., Liao, M. Z., and Mao, Q. (2017). Buprenorphine, norbuprenorphine, R-methadone, and S-methadone upregulate BCRP/ABCG2 expression by activating aryl hydrocarbon receptor in human placental trophoblasts. *Mol. Pharmacol.* 91, 237–249. doi: 10.1124/mol.116.107367

Neven, K. Y., Saenen, N. D., Tarantini, L., Janssen, B. G., Lefebvre, W., Vanpoucke, C., et al. (2018). Placental promoter methylation of DNA repair genes and prenatal exposure to particulate air pollution: an ENVIRONAGE cohort study. *Lancet Planet Health* 2, e174–e183.

Obolenskaya, M. Y., Teplyuk, N. M., Divi, R. L., Poirier, M. C., Filimonova, N. B., Zadrozna, M., et al. (2010). Human placental glutathione S-transferase activity and polycyclic aromatic hydrocarbon DNA adducts as biomarkers for environmental oxidative stress in placentas from pregnant women living in radioactivity- and chemically-polluted regions. *Toxicol. Lett.* 196, 80–86. doi: 10.1016/j.toxlet.2010.03.1115

Östling, H., Kruse, R., Helenius, G., and Lodefalk, M. (2019). Placental expression of microRNAs in infants born small for gestational age. *Placenta* 81, 46–53. doi: 10.1016/j.placenta.2019.05.001

Patrick, S. W., Schumacher, R. E., Benneyworth, B. D., Krans, E. E., Mcallister, J. M., and Davis, M. M. (2012). Neonatal abstinence syndrome and associated health care expenditures: United States, 2000-2009. *J. Am. Med. Assoc.* 307, 1934–1940.

Petit, A., Gallo-Payet, N., Bellabarba, D., Lehoux, J. G., and Belisle, S. (1993). The modulation of placental lactogen release by opioids: a role for extracellular calcium. *Mol. Cell. Endocrinol.* 90, 165–170. doi: 10.1016/0303-7207(93)90148-d

Pique-Regi, R., Romero, R., Tarca, A. L., Sendler, E. D., Xu, Y., Garcia-Flores, V., et al. (2019). Single cell transcriptional signatures of the human placenta in term and preterm parturition. *eLife* 8:e52004.

Punshon, T., Li, Z., Jackson, B. P., Parks, W. T., Romano, M., Conway, D., et al. (2019). Placental metal concentrations in relation to placental growth, efficiency and birth weight. *Environ. Int.* 126, 533–542. doi: 10.1016/j.envint.2019.01.063

Rahman, M. L., Liang, L., Valeri, L., Su, L., Zhu, Z., Gao, S., et al. (2018). Regulation of birthweight by placenta-derived miRNAs: evidence from an arsenic-exposed birth cohort in Bangladesh. *Epigenetics* 13, 573–590. doi: 10.1080/15592294.2018.1481704

Reinhart, M., Scarpati, L. M., Kirson, N. Y., Patton, C., Shak, N., and Erensen, J. G. (2018). The economic burden of abuse of prescription opioids: a systematic literature review from 2012 to 2017. *Appl. Health Econ. Health Policy* 16, 609–632. doi: 10.1007/s40258-018-0402-x

Richards, N., Reith, D., Stitely, M., and Smith, A. (2019). Developmental outcomes at age four following maternal antiepileptic drug use. *Epilepsy Behav.* 93, 73–79. doi: 10.1016/j.yebeh.2019.01.018

Robinson, J. F., Kapidzic, M., Hamilton, E. G., Chen, H., Puckett, K. W., Zhou, Y., et al. (2019). Genomic profiling of BDE-47 effects on human placental cytotrophoblasts. *Toxicol. Sci.* 167, 211–226. doi: 10.1093/toxsci/kfy230

Rock, K. D., St Armour, G., Horman, B., Phillips, A., Ruis, M., Stewart, A. K., et al. (2020). Effects of prenatal exposure to a mixture of organophosphate flame retardants on placental gene expression and serotonergic innervation in the fetal rat brain. *Toxicol. Sci.* 176, 203–223. doi: 10.1093/toxsci/kfaa046

Rohart, F., Gautier, B., Singh, A., and Le Cao, K.-A. (2017). mixOmics: an R package for 'omics feature selection and multiple data integration. *PLoS Comp. Biol.* 13:e1005752. doi: 10.1371/journal.pcbi.1005752

Rosenfeld, C. S. (2015a). Sex-specific placental responses in fetal development. *Endocrinology* 156, 3422–3434. doi: 10.1210/en.2015-1227

Rosenfeld, C. S. (2015b). *The Epigenome and Developmental Origns of Health and Disease*. Cambridge, MA: Academic Press.

Rosenfeld, C. S. (2017). Neuroendocrine disruption in animal models due to exposure to bisphenol A analogues. *Front. Neuroendocrinol.* 47, 123–133. doi: 10.1016/j.yfrne.2017.08.001

Rosenfeld, C. S. (2020). Placental serotonin signaling, pregnancy outcomes, and regulation of fetal brain development. *Biol. Reprod.* 102, 532–538. doi: 10.1093/biolre/ioz204

Rosenfeld, C. S. (2021). The placenta-brain-axis. *J. Neurosci. Res.* 99, 271–283. doi: 10.1002/jnr.24603

Rousseaux, S., Seyve, E., Chuffart, F., Bourova-Flin, E., Benmerad, M., Charles, M. A., et al. (2020). Immediate and durable effects of maternal tobacco consumption alter placental DNA methylation in enhancer and imprinted gene-containing regions. *BMC Med.* 18:306. doi: 10.1186/s12916-020-01736-1

Rubinchik-Stern, M., Shmuel, M., Bar, J., Kovo, M., and Eyal, S. (2018). Adverse placental effects of valproic acid: studies in perfused human placentas. *Epilepsia* 59, 993–1003. doi: 10.1111/epi.14078

SAMHSA (2015). *"Behavioral Health Barometer: United States, 2015 Report*. Rockville, MD: SAMHSA.

Schug, T. T., Janesick, A., Blumberg, B., and Heindel, J. J. (2011). Endocrine disrupting chemicals and disease susceptibility. *J. Steroid Biochem. Mol. Biol.* 127, 204–215.

Schulz, S., Wagner, S., Gerbig, S., Wächter, H., Sielaff, D., Bohn, D., et al. (2015). DESI MS based screening method for phthalates in consumer goods. *Analyst* 140, 3484–3491. doi: 10.1039/c5an00338e

Serra, A. E., Lemon, L. S., Mokhtari, N. B., Parks, W. T., Catov, J. M., Venkataramanan, R., et al. (2017). Delayed villous maturation in term placentas exposed to opioid maintenance therapy: a retrospective cohort study. *Am. J. Obstet. Gynecol.* 216, 418.e1–418.e5.

Shafique, S., and Winn, L. M. (2021). Gestational valproic acid exposure induces epigenetic modifications in murine decidua. *Placenta* 107, 31–40. doi: 10.1016/j.placenta.2021.03.004

Sieli, P. T., Jasarevic, E., Warzak, D. A., Mao, J., Ellersieck, M. R., Liao, C., et al. (2011). Comparison of serum bisphenol A concentrations in mice exposed to bisphenol A through the diet versus oral bolus exposure. *Environ. Health Perspect.* 119, 1260–1265. doi: 10.1289/ehp.1003385

Stone, J., Sutrave, P., Gascoigne, E., Givens, M. B., Fry, R. C., and Manuck, T. A. (2021). Exposure to toxic metals and per- and polyfluoroalkyl substances and the risk of preeclampsia and preterm birth in the United States: a review. *Am. J. Obstet. Gynecol. MFM* 3:100308. doi: 10.1016/j.ajogmf.2021.100308

Suryawanshi, H., Morozov, P., Straus, A., Sahasrabudhe, N., Max, K. E. A., Garzia, A., et al. (2018). A single-cell survey of the human first-trimester placenta and decidua. *Sci. Adv.* 4:eaau4788. doi: 10.1126/sciadv.aau4788

Susiarjo, M., Sasson, I., Mesaros, C., and Bartolomei, M. S. (2013). Bisphenol a exposure disrupts genomic imprinting in the mouse. *PLoS Genet.* 9:e1003401. doi: 10.1371/journal.pgen.1003401

Suter, M., Ma, J., Harris, A., Patterson, L., Brown, K. A., Shope, C., et al. (2011). Maternal tobacco use modestly alters correlated epigenome-wide placental DNA methylation and gene expression. *Epigenetics* 6, 1284–1294. doi: 10.4161/epi.6.11.17819

Tait, S., Tassinari, R., Maranghi, F., and Mantovani, A. (2015). Toxicogenomic analysis of placenta samples from mice exposed to different doses of BPA. *Genom. Data* 4, 109–111. doi: 10.1016/j.gdata.2015.04.004

Tan, W., Huang, H., Wang, Y., Wong, T. Y., Wang, C. C., and Leung, L. K. (2013). Bisphenol A differentially activates protein kinase C isoforms in murine placental tissue. *Toxicol. Appl. Pharmacol.* 269, 163–168. doi: 10.1016/j.taap.2013.03.016

Tetro, N., Imbar, T., Wohl, D., Eisenberg, I., Yagel, S., Shmuel, M., et al. (2019). The effects of valproic acid on early pregnancy human placentas: pilot *ex vivo* analysis in cultured placental villi. *Epilepsia* 60, e47–e51.

Tsamou, M., Vrijens, K., Madhloum, N., Lefebvre, W., Vanpoucke, C., and Nawrot, T. S. (2018). Air pollution-induced placental epigenetic alterations in early life: a candidate miRNA approach. *Epigenetics* 13, 135–146. doi: 10.1080/15592294.2016.1155012

Tsaprouni, L. G., Yang, T. P., Bell, J., Dick, K. J., Kanoni, S., Nisbet, J., et al. (2014). Cigarette smoking reduces DNA methylation levels at multiple genomic loci but the effect is partially reversible upon cessation. *Epigenetics* 9, 1382–1396.

Vajda, F. J. E., O'brien, T. J., Graham, J. E., Hitchcock, A. A., Lander, C. M., and Eadie, M. J. (2019). Valproate-associated foetal malformations-rates of occurrence, risks in attempted avoidance. *Acta Neurol. Scand.* 139, 42–48. doi: 10.1111/ane.13005

Van Wynsberghe, P. M., Chan, S. P., Slack, F. J., and Pasquinelli, A. E. (2011). Analysis of microRNA expression and function. *Methods Cell Biol.* 106, 219–252.

Vandenberg, L. N., Hauser, R., Marcus, M., Olea, N., and Welshons, W. V. (2007). Human exposure to bisphenol A (BPA). *Reprod. Toxicol.* 24, 139–177.

vom Saal, F. S., Akingbemi, B. T., Belcher, S. M., Birnbaum, L. S., Crain, D. A., Eriksen, M., et al. (2007). Chapel Hill bisphenol A expert panel consensus statement: integration of mechanisms, effects in animals and potential to impact human health at current levels of exposure. *Reprod. Toxicol.* 24, 131–138. doi: 10.1016/j.reprotox.2007.07.005

Votavova, H., Dostalova Merkerova, M., Fejglova, K., Vasikova, A., Krejcik, Z., Pastorkova, A., et al. (2011). Transcriptome alterations in maternal and fetal cells induced by tobacco smoke. *Placenta* 32, 763–770. doi: 10.1016/j.placenta.2011.06.022

Walker, N., Filis, P., O'shaughnessy, P. J., Bellingham, M., and Fowler, P. A. (2019). Nutrient transporter expression in both the placenta and fetal liver are affected by maternal smoking. *Placenta* 78, 10–17. doi: 10.1016/j.placenta.2019.02.010

Weinheimer, C., Wang, H., Comstock, J. M., Singh, P., Wang, Z., Locklear, B. A., et al. (2020). Maternal tobacco smoke exposure causes sex-divergent changes in placental lipid metabolism in the rat. *Reprod. Sci.* 27, 631–643.

West, R. C., Ming, H., Logsdon, D. M., Sun, J., Rajput, S. K., Kile, R. A., et al. (2019). Dynamics of trophoblast differentiation in peri-implantation-stage human embryos. *Proc. Natl. Acad. Sci. U.S.A.* 116, 22635–22644. doi: 10.1073/pnas.1911362116

Whitaker-Azmitia, P. M. (1991). Role of serotonin and other neurotransmitter receptors in brain development: basis for developmental pharmacology. *Pharmacol. Rev.* 43, 553–561.

WHO (2018). Available online at: https://Www.Who.Int/News-Room/Fact-Sheets/Detail/Arsenic (accessed February 15, 2018).

Winterbottom, E. F., Ban, Y., Sun, X., Capobianco, A. J., Marsit, C. J., Chen, X., et al. (2019a). Transcriptome-wide analysis of changes in the fetal placenta associated with prenatal arsenic exposure in the New Hampshire Birth Cohort Study. *Environ. Health* 18:100.

Winterbottom, E. F., Moroishi, Y., Halchenko, Y., Armstrong, D. A., Beach, P. J., Nguyen, Q. P., et al. (2019b). Prenatal arsenic exposure alters the placental expression of multiple epigenetic regulators in a sex-dependent manner. *Environ. Health* 18:18.

Wong, M. K., Holloway, A. C., and Hardy, D. B. (2016). Nicotine directly induces endoplasmic reticulum stress response in rat placental trophoblast giant cells. *Toxicol. Sci.* 151, 23–34. doi: 10.1093/toxsci/kfw019

Wu, L. H., Zhang, X. M., Wang, F., Gao, C. J., Chen, D., Palumbo, J. R., et al. (2018). Occurrence of bisphenol S in the environment and implications for human exposure: a short review. *Sci. Total Environ.* 615, 87–98. doi: 10.1016/j.scitotenv.2017.09.194

Xu, X., Chiung, Y. M., Lu, F., Qiu, S., Ji, M., and Huo, X. (2015). Associations of cadmium, bisphenol A and polychlorinated biphenyl co-exposure in utero with placental gene expression and neonatal outcomes. *Reprod. Toxicol.* 52, 62–70. doi: 10.1016/j.reprotox.2015.02.004

Xue, J., Wan, Y., and Kannan, K. (2016). Occurrence of bisphenols, bisphenol A diglycidyl ethers (BADGEs), and novolac glycidyl ethers (NOGEs) in indoor air from Albany, New York, USA, and its implications for inhalation exposure. *Chemosphere* 151, 1–8. doi: 10.1016/j.chemosphere.2016.02.038

Yazdy, M. M., Desai, R. J., and Brogly, S. B. (2015). Prescription opioids in pregnancy and birth outcomes: a review of the literature. *J. Pediatr. Genet.* 4, 56–70.

Zharikova, O. L., Deshmukh, S. V., Kumar, M., Vargas, R., Nanovskaya, T. N., Hankins, G. D., et al. (2007). The effect of opiates on the activity of human placental aromatase/CYP19. *Biochem. Pharmacol.* 73, 279–286. doi: 10.1016/j.bcp.2006.08.019

Zong, T., Lai, L., Hu, J., Guo, M., Li, M., Zhang, L., et al. (2015). Maternal exposure to di-(2-ethylhexyl) phthalate disrupts placental growth and development in pregnant mice. *J. Hazard. Mater.* 297, 25–33. doi: 10.1016/j.jhazmat.2015.04.065

Conflict of Interest: The author declares that the research was conducted in the absence of any commercial or financial relationships that could be construed as a potential conflict of interest.

Publisher's Note: All claims expressed in this article are solely those of the authors and do not necessarily represent those of their affiliated organizations, or those of the publisher, the editors and the reviewers. Any product that may be evaluated in this article, or claim that may be made by its manufacturer, is not guaranteed or endorsed by the publisher.

frontiers in Cell and Developmental Biology

ORIGINAL RESEARCH
published: 04 November 2021
doi: 10.3389/fcell.2021.670980

Mechanistic Target of Rapamycin Complex 2 Regulation of the Primary Human Trophoblast Cell Transcriptome

Fredrick J. Rosario[1], Amy Catherine Kelly[1], Madhulika B. Gupta[2], Theresa L. Powell[1,3], Laura Cox[4] and Thomas Jansson[1]*

[1] Division of Reproductive Sciences, Department of OB/GYN University of Colorado Anschutz Medical Campus, Aurora, CO, United States, [2] Children's Health Research Institute and Department of Pediatrics and Biochemistry, University of Western Ontario, London, ON, Canada, [3] Section of Neonatology, Department of Pediatrics, University of Colorado Anschutz Medical Campus, Aurora, CO, United States, [4] Section of Molecular Medicine, Department of Internal Medicine, Center for Precision Medicine, Wake Forest School of Medicine, Winston-Salem, NC, United States

OPEN ACCESS

Edited by:
Geetu Tuteja, Iowa State University, United States

Reviewed by:
Amanda Sferruzzi-Perri, University of Cambridge, United Kingdom
Joseph Mauro Calabrese, University of North Carolina at Chapel Hill, United States

***Correspondence:**
Fredrick J. Rosario
fredrick.joseph@cuanschutz.edu

Specialty section:
This article was submitted to Developmental Epigenetics, a section of the journal Frontiers in Cell and Developmental Biology

Received: *22 February 2021*
Accepted: *23 September 2021*
Published: *04 November 2021*

Citation:
Rosario FJ, Kelly AC, Gupta MB, Powell TL, Cox L and Jansson T (2021) Mechanistic Target of Rapamycin Complex 2 Regulation of the Primary Human Trophoblast Cell Transcriptome. Front. Cell Dev. Biol. 9:670980. doi: 10.3389/fcell.2021.670980

Mechanistic Target of Rapamycin Complex 2 (mTORC2) regulates placental amino acid and folate transport. However, the role of mTORC2 in modulating other placental functions is largely unexplored. We used a gene array following the silencing of rictor to identify genes regulated by mTORC2 in primary human trophoblast (PHT) cells. Four hundred and nine genes were differentially expressed; 102 genes were down-regulated and 307 up-regulated. Pathway analyses demonstrated that inhibition of mTORC2 resulted in increased expression of genes encoding for pro-inflammatory IL-6, VEGF-A, leptin, and inflammatory signaling (SAPK/JNK). Furthermore, down-regulated genes were functionally enriched in genes involved in angiogenesis (Osteopontin) and multivitamin transport (SLC5A6). In addition, the protein expression of leptin, VEGFA, IL-6 was increased and negatively correlated to mTORC2 signaling in human placentas collected from pregnancies complicated by intrauterine growth restriction (IUGR). In contrast, the protein expression of Osteopontin and SLC5A6 was decreased and positively correlated to mTORC2 signaling in human IUGR placentas. In conclusion, mTORC2 signaling regulates trophoblast expression of genes involved in inflammation, micronutrient transport, and angiogenesis, representing novel links between mTOR signaling and multiple placental functions necessary for fetal growth and development.

Keywords: placenta, maternal-fetal exchange, human, nutrient sensor, gene array

INTRODUCTION

The intrauterine environment impacts the lifelong health of the fetus (Barker et al., 1993; Gluckman and Hanson, 2004a,b; Gluckman et al., 2008). The placenta plays a critical role in regulating the intrauterine environment and orchestrating fetal growth and organ-specific development (Burton and Jauniaux, 2015; Burton et al., 2016). The placenta mediates the transport of nutrients and

oxygen from the mother to the fetus, provides immune protection, and secretes hormones into the maternal and fetal circulations. Emerging evidence suggests that the placenta functions as a nutrient sensor which integrates maternal and fetal nutritional cues with information from intrinsic nutrient-sensing signaling pathways to regulate placental nutrient transport and fetal growth (Jansson and Powell, 2007; Burton and Jauniaux, 2015). Therefore, changes in the maternal compartment or in the intrauterine environment caused by various intrinsic and extrinsic stressors modulate placental function, including nutrient transport, blood flow, metabolism, and hormone secretion. These changes in placental function may adversely impact the developing fetus with potential health consequences across the lifespan (Sandovici et al., 2012). However, the molecular mechanisms regulating the function of the human placenta are poorly understood (Guttmacher et al., 2014).

The mechanistic target of rapamycin (mTOR) is an evolutionarily conserved signaling hub that belongs to the phosphatidylinositol kinase-related kinase (PIKK) family (Wullschleger et al., 2006). mTOR exists as two functionally and structurally different complexes, mTORC1 and mTORC2 (Wullschleger et al., 2006). One key difference between the two complexes is that the protein Raptor is associated with mTORC1 and the protein Rictor constitutes a part of mTORC2 (Kim et al., 2002; Sarbassov et al., 2004). Pharmacological and gene silencing studies have demonstrated that the activation of mTORC1 phosphorylates S6K1 and 4E-BP1, and promotes gene transcription and protein translation (Yang and Guan, 2007). mTORC2 is known to phosphorylate Akt, SGK1, and PKCα and regulates metabolism and cytoskeletal trafficking (Guertin et al., 2006). Placental mTOR signaling activity has been reported to be inhibited in human (Chen et al., 2015) and animal models of IUGR (Rosario et al., 2011; Kavitha et al., 2014). Moreover, activation of placental mTOR signaling is positively associated with fetal overgrowth in obese women (Jansson et al., 2013), and in a diet-induced mouse model of maternal obesity with increased fetal growth (Rosario et al., 2015b). Importantly, mTOR has emerged as a master regulator of placental function. Specifically, both mTORC1 and 2 are positive regulators of trophoblast amino acid and folate transport (Rosario et al., 2015a, 2016a,b) and O-linked N-acetylglucosamine (O-GlcNAc) transferase (OGT) protein expression (Kelly et al., 2020), whereas mTORC1 activation promotes placental mitochondrial biogenesis/respiration (Rosario et al., 2013). We also demonstrated that mTORC 2 signaling is a negative regulator of trophoblast serotonin synthesis (Kelly et al., 2020). However, mTORC2 regulation of other trophoblast functions remains largely unknown.

We recently reported that mTORC1 regulates > 700 genes in cultured primary human trophoblast (PHT) cells (Rosario et al., 2020). Specifically, inhibition of mTORC1 down-regulates trophoblast genes involved in ribosome subunits, protein synthesis, and molecular transport (Rosario et al., 2020). In contrast, mTORC2 regulation of the trophoblast transcriptome has not been previously explored. In the present study, we employed an unbiased discovery approach to find regulatory networks and novel regulators that can help us decipher mTORC2 regulation of gene expression in PHT cells.

MATERIALS AND METHODS

Ethical Approval

The Institutional Review Board at the University of Texas Health Science Center, San Antonio, approved all the experimental protocols. For the gene expression profiling experiment, placentas of uncomplicated term pregnancies were collected with informed consent at the Labor and Delivery Unit at the University Hospital San Antonio. Selected clinical characteristics of the study subjects are provided in **Table 1**.

Isolation and Culture of Primary Human Trophoblast Cells

Placentas were collected immediately following delivery by cesarean section at term without labor. As described previously, primary PHT cells were isolated by trypsin digestion followed by discontinuous Percoll gradient separation (Rosario et al., 2016a). PHT cells were plated in 60 mm culture dishes (∼7.5 × 10^6 cells/dish) and cultured in 5% CO2, 95% atmosphere air at 37°C for 90 h. Cell culture media (DMEM/Hams F-12) containing L-glutamine, penicillin, streptomycin, gentamycin, and 10% fetal bovine serum was changed daily.

RNA Interference-Mediated Silencing in Primary Human Trophoblast Cells

RNA interference-mediated silencing of the target gene was performed in PHT cells as previously described (Rosario et al., 2013). Briefly, Dharmafect 2 transfection reagent (Thermo Fisher Scientific, Rockford, IL) and small interfering RNAs (siRNAs) (Sigma-Aldrich, St. Louis, MO) targeting *RICTOR* (100 nM: sense, 5' CGAUCAUGGGCAGGUAUUA) were used (**Supplementary Figure 1**). First, we searched BLASTn to ensure that the designed *RICTOR* siRNA sequences would not target any other gene transcript. Then, control PHT cells were transfected with a non-coding scrambled sequence (100 nM; sense: 5'GAUCAUACGUGCGAUCAGATT). The *RICTOR* or non-coding scrambled sequence siRNAs, synthesized by Sigma-Aldrich, were used according to the manufacturer's instructions (with the final concentration of 100 nM). According to the manufacturer's instructions, after 18 h in culture, PHT cells were transfected with siRNAs using Dharmafect 2 transfection reagent. PHT cells were incubated in siRNA for 24 h and then removed, fresh medium was added to wells (Forbes et al., 2009). At 90 h in culture, *RICTOR* silencing efficiency was assessed at the protein (expression of rictor) and functional levels (phosphorylation of mTORC2 downstream target; AKT-Serine-473) using Western blot.

Assessment of Biochemical Differentiation and Viability

The human chorion gonadotropin (hCG) is a marker of trophoblast cell differentiation and viability. Using the

TABLE 1 | Selected clinical data of the mothers and newborns from whom placental samples were obtained for the transcriptomics analysis.

	Placenta 1	Placenta 2	Placenta 3	Placenta 4
Maternal age (years)	26.0	27.0	25.0	28.0
BMI (kg/m^2) *	24.5	23.5	22.5	23.0
Gestational age (weeks)	37.1	37.2	37.3	37.5
Birth weight (g)	2,500	2,645	2,589	2,679
Placental weight (g)	645	680	595	604
Fetal sex (M/F)	M	F	M	F
Mode of delivery (C/V)	C	C	C	C

*F, female; M, male; C, cesarean section; V, vaginal delivery. *Maternal BMI (kg/m2) was calculated using maternal weight and height measurements taken during the first (10–12 weeks) trimesters.*

commercially available ELISA kit from Immuno Biological Labs, we quantified the secretion of hCG (kit designed to detects the beta subunit of hCG) in conditioned media collected at 18, 42, 66, and 90 h after plating PHT cells. Using Western blot, we also measured the protein expression of caspase-3 (a marker of apoptosis) in the cell lysates of scramble and Rictor silenced PHT cells.

RNA Isolation From Primary Human Trophoblast Cells

According to the manufacturer's instructions, RNA was isolated from cultured PHT cells at 90 h in culture using TRIzol Reagent (Invitrogen, Carlsbad, CA). RNA was resuspended in 100 μl DEPC-treated water. RNA quality was determined using an Agilent 2100 Bioanalyzer (Agilent Technologies, Inc., Santa Clara, CA), and RNA concentrations were confirmed by quantitation using a NanoDrop^{TM} 8000 spectrophotometer (Thermo Fisher Scientific, Wilmington, DE).

Gene Expression Profiling in Primary Human Trophoblast Cells

Whole-genome expression profiling was performed using gene arrays (HumanHT-12 v4 Expression BeadChips, Illumina Inc., San Diego, CA). cRNA was synthesized and biotin-labeled according to the manufacturer's instructions (cat. no. 1750, Ambion, Austin, TX). Total RNA was used for first and second-strand cDNA synthesis, followed by *in vitro* transcription to synthesize biotin-labeled cRNA. cRNA was quality checked and then hybridized to Human HT-12 v4 Expression BeadChips (Illumina Inc.). Individual cRNA samples were used to interrogate each BeadChip (Scramble siRNA, $n = 4$; *RICTOR* siRNA, $n = 4$). Gene expression was detected and cleaned using GenomeStudio software (Illumina Inc.) and filtered using a quality score (>0.95). Gene array data were all-median normalized and $\log_2$ transformed (GeneSifter), and differentially expressed genes were identified by *t*-test ($p < 0.05$).

Pathway Analysis

Using GeneSifter, genes with significantly different expression levels were superimposed on Kyoto Encyclopedia of Genes and Genomes (KEGG) pathways (Kanehisa and Goto, 2000; Kanehisa et al., 2016, 2017). In addition, GeneSifter was used to compute Z-scores, which is described in detail in **Supplementary Methods**.

Network Analysis

The networks were generated through the use of IPA (QIAGEN Inc.)[1] (Kramer et al., 2014). Network analysis (Ingenuity Pathway Analysis (IPA), Ingenuity® Systems, Redwood City, CA) was performed using differentially expressed genes ($p < 0.05$) from each pairwise comparison (RICTOR vs. Scramble). Networks were built using the IPA Knowledge Base, using expression profiles from this dataset and requiring direct connections between molecules based on experimental evidence (Kramer et al., 2014). Network significance was calculated in IPA using Fisher exact *t*-test (Ingenuity® Systems). The *p*-value for a given network takes into account the number of eligible molecules (differentially expressed genes) in the selected reference set (defined by the Ingenuity Knowledge Base); the total number of molecules in the selected reference set known to be associated with that function; the total number of eligible molecules in the selected reference set; and the total number of molecules in the reference set (Ingenuity® Systems). This analysis considered networks are containing > 25 differentially expressed genes and a *p*-value $< 10^{-20}$ as significant.

Placental Mechanistic Target of Rapamycin Complex 2 Signaling and Expression of Leptin, VEGF-A, IL-6, Osteopontin, and Sodium-Dependent Multivitamin Transporter (SLC5A6) in Intrauterine Growth Restriction

Placentas from pregnancies complicated by IUGR and women delivering appropriate-for-gestational age (AGA) infants were collected within 15 min of delivery as described (Chen et al., 2015). The study was approved by the University of Western Ontario Health Sciences Research Ethics Board. Pregnant women attending St. Joseph's Health Care Centre, London, Ontario, Canada, were enrolled after informed consent was obtained. The decidua basalis and chorionic plate were removed, and villous tissue was dissected and rinsed in cold physiological saline. The villous tissue was transferred

[1]https://www.qiagenbioinformatics.com/products/ingenuity-pathway-analysis

to cold buffer D (250 mM sucrose, 10 mM HEPES, pH 7.4) containing 1:100 dilution of protease and phosphatase inhibitors (Sigma–Aldrich, St. Louis, MO, United States) and homogenized on ice with a Polytron (Kinematica, Luzern, Switzerland). Placental homogenates were frozen in liquid nitrogen and stored at −80°C until further processing. The phosphorylation of key proteins in the mTORC2 (Chen et al., 2015) and leptin, VEGF-A, IL-6, osteopontin, and SLC5A6 expression in placental homogenates of IUGR and AGA groups were determined using Western blots as described previously (Rosario et al., 2016a).

Statistics

The number of experiments (n) denotes the number of placentas studied. Data are represented as means ± S.E.M. All the array data from each sample were all-median normalized and $\log_2$ transformed. Box plots were tested to ensure that each group's median was 0 and variance among groups was similar. Statistical analyses of array data were performed by *t*-test using GeneSifter software (Geospiza, Inc.) for pairwise comparisons. Statistical significance of differences between control and experimental groups in protein expression studies were assessed using Student's *t*-test. A *P*-value < 0.05 was considered significant.

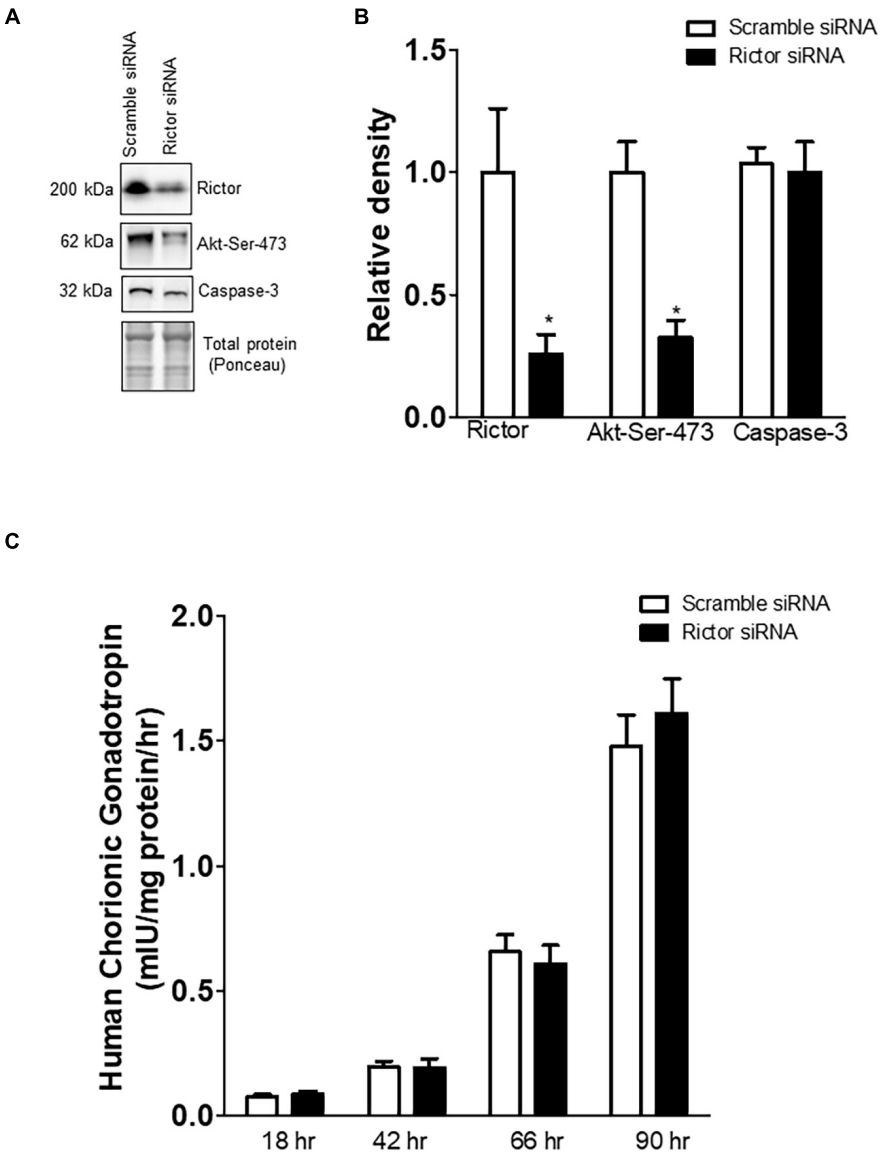

FIGURE 1 | Effect of rictor silencing on rictor protein expression, mTORC2 signaling activity, and trophoblast differentiation and viability. **(A)** Representative western blots of rictor, phosphorylated Akt-Ser-473 and caspase-3 expression in cell lysates of scramble siRNA and rictor siRNA silenced PHT cells. Equal loading was performed. **(B)** Summary of the western blot data of rictor, Akt-Ser-473, and caspase-3 protein. **(C)** Secretion of human chorionic gonadotropin (hCG) from PHT cells transfected with scramble or rictor siRNA. Values are given as means + SEM. *$P < 0.05$ vs. scramble siRNA; unpaired Student's *t*-test; $n = 5$/each group.

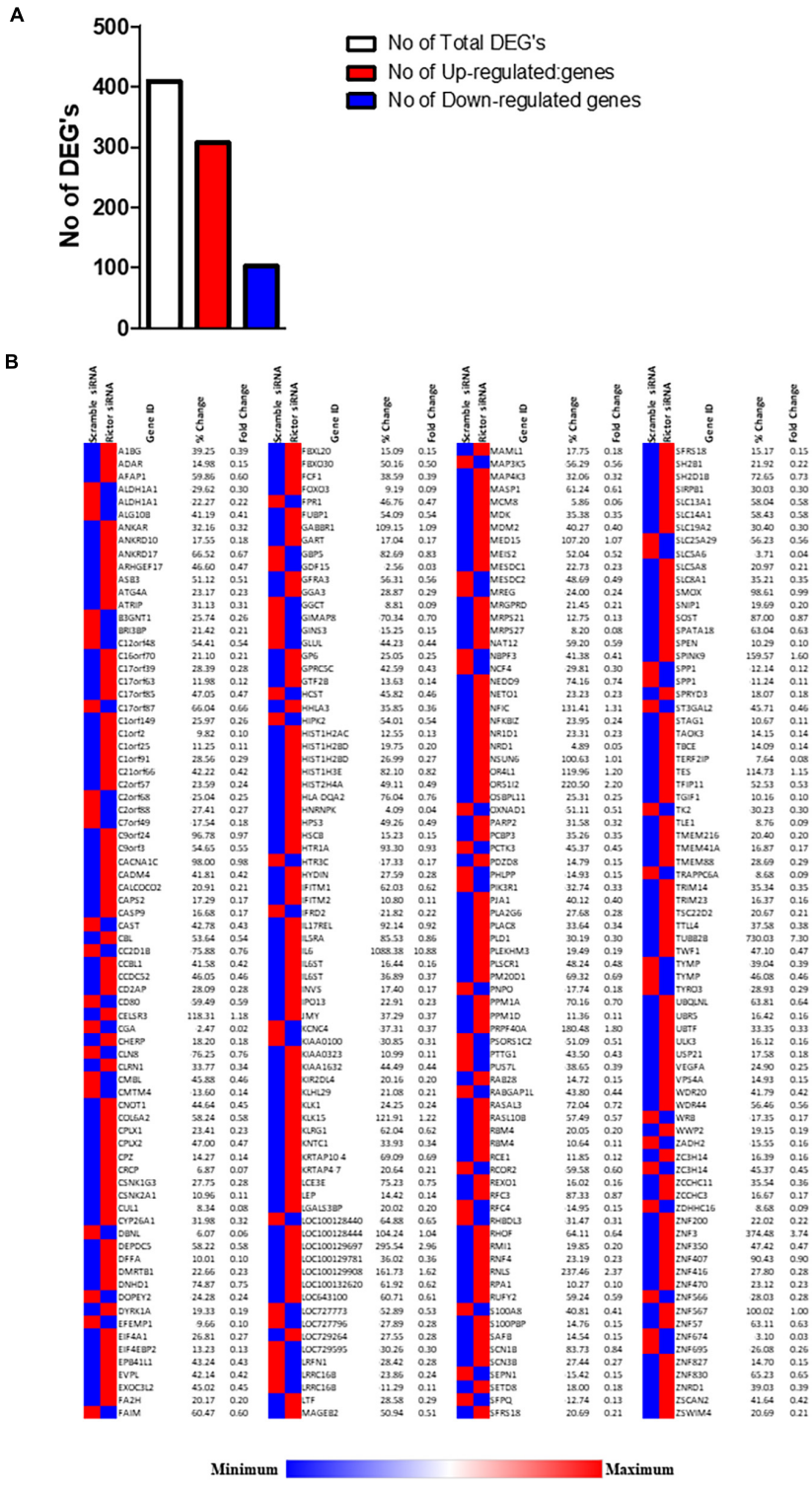

FIGURE 2 | Differentially expressed genes in rictor siRNA vs. scramble siRNA silenced PHT cells. **(A)** The number of differentially expressed genes in rictor siRNA vs. scramble siRNA silenced PHT cells. The red represents up-regulated genes and blue represents down-regulated genes in rictor silenced PHT cells as compared to cells transfected with scramble siRNA. **(B)** Heatmap of expression data for the differentially expressed genes in rictor siRNA vs. scramble siRNA silenced PHT cells. Color index represents gene expression changes, the red represents up-regulated genes, and the blue represent down-regulated genes in rictor silenced PHT cells as compared to cells transfected with scramble siRNA.

RESULTS

Rictor Silencing in Primary Human Trophoblast Cells Inhibits mTORC2 Signaling

Rictor siRNA markedly decreased the protein expression of rictor (–75%, $p = 0.001$; $n = 5$/each group) and decreased the phosphorylation of Akt-Ser-473 (–68%, $p = 0.003$; $n = 5$/each group), a functional readout for mTORC2 signaling (**Figure 1**). However, total Akt protein expression was comparable between scramble and Rictor siRNA silenced PHT cells (Rosario et al., 2013). The hCG secretion profiles and caspase-3 protein expression were comparable between PHT cells transfected with scrambled or rictor siRNA (**Figure 1**, $n = 5$/each group). These findings indicate that mTORC2 inhibition did not affect differentiation/syncytialization and viability of cultured PHT cells and suggest that rictor silencing effects on the trophoblast transcriptome were not caused by unspecific effects on differentiation. We previously demonstrated that there is no cross talk between mTORC1 and mTORC2 signaling in PHT cells (Rosario et al., 2013).

Analysis of Differentially Expressed Genes in Response to mTORC2 Inhibition Signaling in Primary Human Trophoblast Cells

We analyzed DEGs following *rictor* siRNA silencing (mTORC2 inhibition), all sequenced genes were compared between rictor and scramble siRNA silenced (Rictor vs. scramble). We identified a total of 409 DEGs between rictor and scramble siRNA treated PHT cells, comprising 307 up-regulated and 102 downregulated

TABLE 2 | Gene Ontology biological process classification of up-regulated genes in rictor silenced PHT cells.

N	High level GO category	Genes
66	Response to stress	MAP4K3 ERCC8 DEPDC5 UBR5 VEGFA MASP1 SEM1 PARP2 RPA1 ANKRD17 CASP9 TAOK3 EVPL LEP RMI1 IFITM2 IFITM1 ZNF830 PARG TFIP11 IL6ST LTF TRIM14 MCM8 MDM2 IL6 CALCOCO2 TRPM2 SPATA18 RBM4 PLA2G6 KIR2DL4 NCBP3 IL5RA FBXL20 CBL MDK TRIM23 FOXO3 KLRG1 NFKBIZ PLAC8 JMY DYRK1A ADAR ATRIP HNRNPK TERF2IP PPM1D HTR1A SLC8A1 RNLS PLSCR1 TSC22D2 SH2D1B CRCP GP6 NR1D1 KMT5A CUL1 LGALS3BP CNOT1 RFC3 ULK3 SH2B1 HLA-DQA2
62	Regulation of response to stimulus	PPM1A DEPDC5 CBL VEGFA MASP1 ZSWIM4 IL6ST TAOK3 CSNK1G3 TMEM88 LEP TLE1 PARG IL6 LTF INVS CNOT1 ANKRD17 MDM2 ULK3 NETO1 SOST RASGRP4 KIR2DL4 MAP4K3 ARHGEF17 MDK FOXO3 NR1D1 PARP2 TUT4 TRPM2 NFKBIZ TWF1 DYRK1A NPR2 HNRNPK TERF2IP SH2B1 PLA2G6 AFAP1 CHERP CSNK2A1 UBR5 RASAL3 CASP9 TUBB2B ADAR KMT5A PLSCR1 CD2AP TFIP11 SH2D1B CYP26A1 RPA1 RHOF JMY MAML1 MEAF6 IFITM1 WWP2 HLA-DQA2
53	Regulation of biological quality	LTF ZC3H14 SCN1B FOXO3 RPA1 RHOF CPLX2 TWF1 JMY SCN3B TERF2IP KLK1 CPLX1 LEP PLSCR1 TFIP11 SLC8A1 CHERP CYP26A1 VEGFA GGA3 MDM2 IL6 CACNA1C PDZD8 RNLS WWP2 NR1D1 TRPM2 PLAC8 EIF4EBP2 SAFB PM20D1 NETO1 HTR1A RMI1 PLA2G6 ZNF830 GABBR1 RASL10B GP6 TMEM88 FA2H MCM8 OSBPL11 ADAR CLRN1 PRPF40A NRDC CUL1 RFC3 NPR2 SH2B1
41	Response to external stimulus	OPN3 DEPDC5 VEGFA ZSWIM4 LEP IFITM2 IFITM1 IL6ST IL6 LTF ANKRD17 ADAR RASGRP4 PLA2G6 CELSR3 ERCC8 NCBP3 CYP26A1 SCN1B CBL FOXO3 CASP9 MEIS2 TUT4 MDM2 TRPM2 PLAC8 GFRA3 PPM1D KYAT1 RMI1 SLC8A1 PLSCR1 CRCP SOST NR1D1 CALCOCO2 TUBB2B NFKBIZ RBM4 PLD1
13	Cytokine-mediated signaling pathway	ADAR IL5RA IFITM1 CUL1 CBL HLA-DQA2 LEP IL6ST IL17REL FOXO3 IFITM2 IL6

The ShinyGO application (version 0.66) (Ge et al., 2020) was used for exploring enrichment in Gene Ontology (GO) categories for biological processes using the 150 top genes obtained from the gene-based association analyses. Multiple testing correction was applied using the Benjamini–Hochberg method implemented in the application. We considered significant those processes with false discovery rate (FDR) p-value < 0.05. Only categories with a minimum of 10 overlapping genes were selected. N: is the total number of genes the total numbers of genes included on the array and giving a signal in the primary trophoblast cultures. The number of experiments (n) denotes the number of placentas studied, n = 4 placenta/each group, rictor siRNA and scramble siRNA.

TABLE 3 | Gene Ontology biological process classification of down-regulated genes in rictor silenced (mTORC2 inhibited) PHT cells.

N	High level GO category	Genes
22	Regulation of signaling	PHLPP1 HCST GDF15 NEK10 MAP3K5 SFPQ SPP1 CGA S100A8 SCIMP CRLF2 TYMP TYRO3 EFEMP1 KCNC4 GLUL PIK3R1 HIPK2 SELENON CD80 DBNL FPR1
21	Regulation of molecular function	PIK3R1 RABGAP1L CAST NEK10 MAP3K5 GDF15 CGA S100A8 RFC4 TRAPPC6A TYMP HIPK2 NCF4 EFEMP1 SPP1
14	Immune system process	CD80 FPR1 SFPQ S100A8 PHLPP1 TYRO3 HCST DBNL PIK3R1 GBP5 MAP3K5 CRLF2 HIPK2 NCF4
11	Immune response	CD80 FPR1 SFPQ TYRO3 HCST DBNL S100A8 GBP5 MAP3K5 NCF4 PIK3R1
10	Regulation of immune system process	CD80 FPR1 SFPQ PHLPP1 TYRO3 HCST PIK3R1 GBP5 CRLF2 S100A8

The ShinyGO application (version 0.66) (Ge et al., 2020) was used for exploring enrichment in Gene Ontology (GO) categories for biological processes using the 150 top genes obtained from the gene-based association analyses. Multiple testing correction was applied using the Benjamini–Hochberg method implemented in the application. We considered significant those processes with false discovery rate (FDR) p-value < 0.05. Only categories with a minimum of 10 overlapping genes were selected. N: is the total number of genes the total numbers of genes included on the array and giving a signal in the primary trophoblast cultures. The number of experiments (n) denotes the number of placentas studied, n = 4 placenta/each group, rictor siRNA and scramble siRNA.

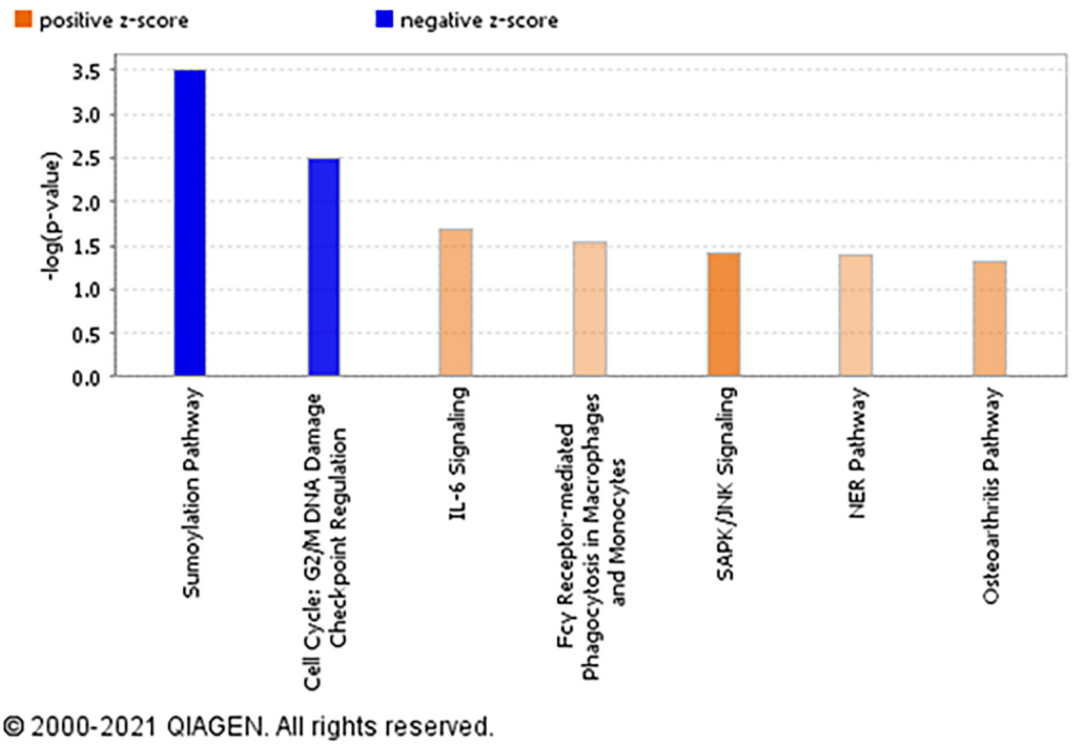

FIGURE 3 | Overall functional analysis. Analysis of the top molecular and cellular functions determined by IPA for the rictor siRNA silenced (mTORC2 inhibited) PHT cells. Ingenuity Pathway Analyses (IPA) of array data identified canonical pathways significantly affected by rictor silencing in PHT cells. Color index represents pathway expression changes, the orange represents up-regulated pathways, and the blue represent down-regulated pathways in rictor silenced PHT cells as compared to cells transfected with scramble siRNA.

DEGs (**Figure 2** and **Supplementary Table 1**). Differentially expressed genes are displayed in the heat map in **Figure 2**.

Interestingly, we found several ubiquitin-conjugating E2 transcripts, such as UBE2D3 and E3 ubiquitin-protein ligase (UBR5, UBE2D3, PJA2, RBCK1, RNF38, TRIM5, TRIM27, TRIM23, TRIM9, and TRIM28) were up-regulated following rictor silencing (**Supplementary Table 1**). Furthermore, mTORC2 inhibition increased the expression of ubiquitin-specific proteases such as USP21, USP2, USP9X, USP53, USP5, and USP49.

Functional Analysis of Differentially Expressed Genes

Next, we identified the Gene Ontology (GO) terms enriched with differentially expressed genes in the biological process (BP). Separate GO enrichment analyses for up-regulated and down-regulated genes were performed. GO analysis revealed that up-regulated genes were mainly involved in biological processes, including response to stress, regulation of response to the stimulus, response to an external stimulus, regulation of biological quality, and cytokine-mediated signaling pathway (**Table 2**). In contrast, down-regulated genes primarily played a role in regulating signaling, regulation of molecular function, immune system process, immune response, and immune system regulation (**Table 3**).

Ingenuity Pathway Analysis

The top significantly enriched canonical signaling pathways up-regulated in rictor-silenced PHT cells were IL-6 (Interleukin-6), SAPK/JNK (Stress-activated protein kinase/c-Jun NH(2)-terminal kinase), and NER (Nucleotide excision repair) signaling (**Figure 3**). Conversely, we found that sumoylation and cell cycle G2/M DNA damage checkpoint regulation pathways were down-regulated in mTORC2 inhibited PHT cells (**Figure 3**).

In greater detail, we used IPA-canonical pathway analysis to study mTORC2 regulation of genes encoding for IL-6 signaling proteins. We found that five genes were identified as significantly activated in rictor silenced PHT cells. Specifically, IL6, IL6ST, CSNK2A1, VEGFA, and PIK3R1 were up-regulated (**Figure 4**), suggesting that inhibition of mTORC2 results in a broad and coordinated up-regulation of genes encoding proteins involved in IL-6 signaling.

Kyoto Encyclopedia of Genes and Genomes Pathway Analysis

KEGG pathway analysis comparing rictor/mTORC2 siRNA with scramble siRNA revealed 53 down-regulated and 63 up-regulated pathways. Down-regulated trophoblast pathways in response to mTORC2 inhibition included alanine, aspartate and glutamate metabolism, carbohydrate digestion and

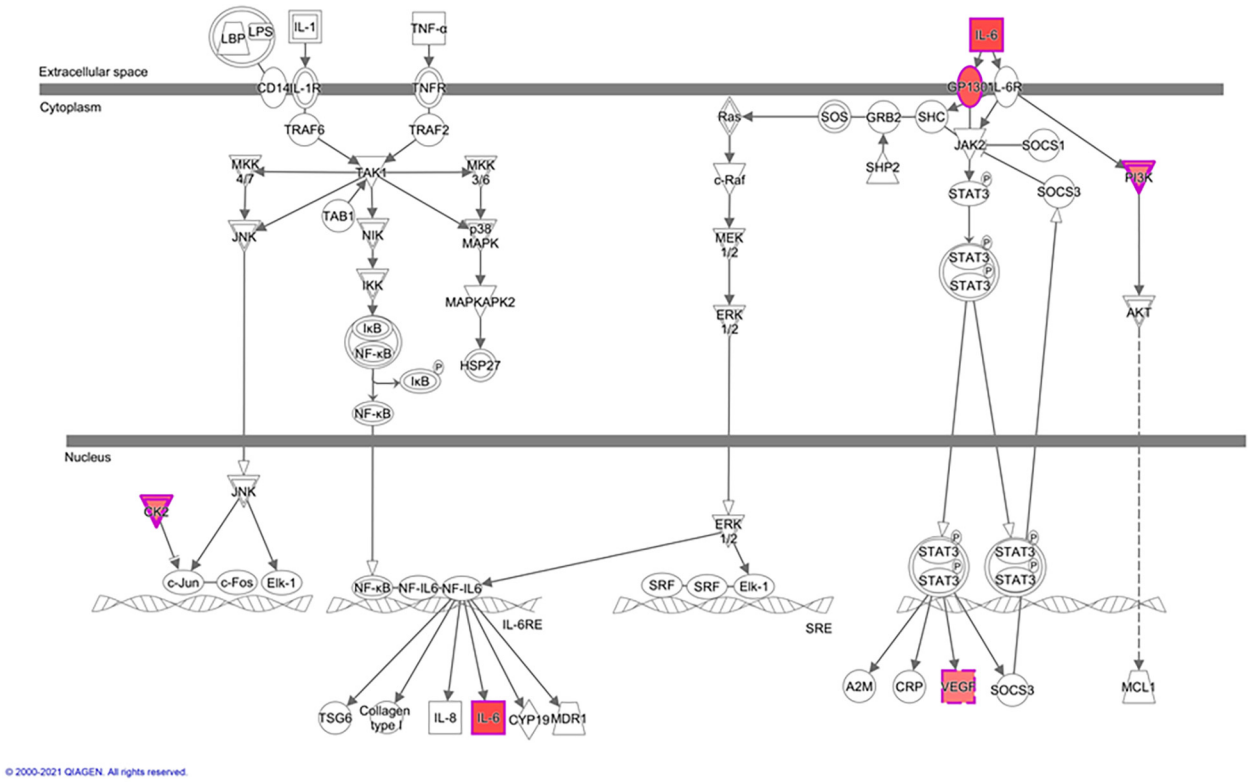

FIGURE 4 | Rictor silencing up regulated components of IL-6 signaling in PHT cells. Graphical representation of PHT cell IL-6 signaling networks identified by Ingenuity Pathway Analysis (IPA) following rictor silencing. Molecular relationships between genes up-regulated (red) or no change (white) in expression after rictor silencing are shown; CSNK2A1, Casein kinase 2 alpha 1; IL6, Interleukin 6; IL6ST, Interleukin 6 signal transducer; PIK3R1, Phosphoinositide-3-kinase regulatory subunit 1; VEGFA, Vascular endothelial growth factor A.

absorption, DNA replication, drug metabolism, leukocyte trans-endothelial migration, metabolic pathways, N-Glycan biosynthesis, neurotrophin signaling pathway, nitrogen metabolism, nucleotide excision repair, pyrimidine metabolism, toll-like receptor signaling pathway, type I diabetes mellitus, type II diabetes mellitus, and vitamin B6 metabolism (**Table 4**). Jak-STAT signaling pathway, mismatch repair, nucleotide excision repair, p53 signaling pathway, regulation of autophagy, ubiquitin-mediated proteolysis, and VEGF signaling pathways are examples of pathways up-regulated in response to mTORC2 inhibition (**Table 5**).

Network Analysis

Network analysis of RNA expression from PHT cells with mTORC2 inhibition (rictor silencing) compared with control cells (scramble) revealed three networks (**Supplementary Figures 4–6**). The top annotated functions of the genes composing the networks included: RNA post-transcriptional modification, post-translational modification, tissue development, cell morphology, cellular function and maintenance, cancer, lipid metabolism, molecular transport, small molecule biochemistry, DNA replication, recombination, and repair, cell cycle, gene expression, cellular movement, inflammatory response, endocrine system disorders. Evaluation of these networks showed a coordinated response to Rictor silencing with the majority of genes up-regulated.

Comparison Between mTORC1 and mTORC2 Transcriptome

Despite how clear it is that mTOR has diverse functions in placenta, the comparative roles of both mTOR complexes in PHT cells gene expression regulation specifically are poorly understood. Next, we compared it with the mTORC1 transcriptome (Rosario et al., 2020). The common differential expressed genes between mTORC1 and mTORC2 inhibition are listed in **Table 6**. GO analysis of common DEG's identified the categories molecular function regulator (DEPDC5 SCN1B ARHGEF17 RABGAP1L SCN3B IL6 SPINK9 TYMP RASAL3 SPP1 PTTG1 ALDH1A1), transporter activity (SLC13A1 KCNC4 SLC5A6 SCN1B SCN3B SLC5A8), and transmembrane transporter activity (SLC13A1 KCNC4 SLC5A6 SCN1B SCN3B SLC5A8). In addition, sodium-dependent multivitamin transporter (SLC5A6) and osteopontin transcripts regulated transport activity and molecular function and were down-regulated in response to both mTORC1 and mTORC2 inhibition. It is interesting to observe that the two mTOR complexes have distinct and overlapping roles in transcription regulation.

TABLE 4 | Down-regulated KEGG pathways in PHT cells in response to rictor siRNA silencing.

KEGG Pathways Down	Diff regulated genes	Up	Down	Gene set	Z-score
Alanine, aspartate and glutamate metabolism	1	0	1	31	2.72
Aldosterone-regulated sodium reabsorption	1	0	1	41	2.27
Allograft rejection	2	1	1	33	2.62
Autoimmune thyroid disease	3	1	2	48	4.5
Bladder cancer	3	2	1	41	2.27
Carbohydrate digestion and absorption	1	0	1	42	2.24
DNA replication	3	2	1	35	2.52
Drug metabolism—other enzymes	2	0	2	41	4.93
Glycosaminoglycan biosynthesis—keratan sulfate	2	0	2	15	8.53
Glycosphingolipid biosynthesis—ganglio series	1	0	1	15	4.15
Glycosphingolipid biosynthesis—globo series	1	0	1	14	4.31
Glycosphingolipid biosynthesis—lacto and neolacto series	1	0	1	25	3.1
Graft-vs.-host disease	3	2	1	35	2.52
Intestinal immune network for IgA production	3	2	1	44	2.17
Leukocyte transendothelial migration	2	0	2	115	2.55
Metabolic pathways	14	5	9	1,080	2.99
Mucin type O-Glycan biosynthesis	1	0	1	30	2.78
N-Glycan biosynthesis	1	0	1	49	2.01
Natural killer cell mediated cytotoxicity	4	2	2	133	2.28
Neurotrophin signaling pathway	4	2	2	127	2.37
Nitrogen metabolism	1	0	1	23	3.25
Nucleotide excision repair	4	3	1	43	2.2
Osteoclast differentiation	3	1	2	127	2.37
Pyrimidine metabolism	3	1	2	95	2.92
Toll-like receptor signaling pathway	4	1	3	102	4.47
Type I diabetes mellitus	2	1	1	38	2.39
Type II diabetes mellitus	2	1	1	47	2.07
Vitamin B6 metabolism	1	0	1	5	7.45

Table lists KEGG pathways that were significantly downregulated in PHT cells with rictor silencing as compared to control cells; "List" denotes the total number of differentially expressed genes on the array. "Up" denotes the number of up-regulated genes; "Down" denotes the number of down-regulated genes; "Gene set" denotes the total number of genes in this pathway that are included on the array and give a signal with PHT cell RNA; and "Z-score" denotes the z-score for the list pathway. The significance of identified KEGG pathways was determined by Z-score. Pathways were considered significantly different between scramble and Rictor siRNA groups if the Z-score for that pathway was > 2.00. The number of experiments (n) denotes the number of placentas studied, n = 4 placenta/each group, rictor siRNA and scramble siRNA.

Placental mTORC2 Signaling Is Associated With the Protein Expression of Leptin, VEGF-A, IL-6, Osteopontin, and Sodium-Dependent Multivitamin Transporter (SMVT, SLC5A6) Protein in Human Pregnancy

To explore the clinical relevance of our findings, we examined the relationship between placental mTORC2 signaling and protein expression of leptin, VEGF-A, IL-6, Osteopontin, and sodium-dependent multivitamin transporter (SLC5A6) in placentas collected from AGA and IUGR pregnancies. Selected clinical data for the AGA and IUGR groups are provided in **Table 7**. There was no significant difference in maternal age, body mass index (BMI), or gestational age between the control and the IUGR groups. However, birth weight was 28% lower ($P < 0.01$), and placental weight was reduced by 36% ($P < 0.001$) in the IUGR group compared with AGAs.

The leptin, VEGF-A, and IL-6 protein expression were significantly increased in IUGR placentas (**Figure 5**). However, osteopontin and sodium-dependent multivitamin transporter protein expression were significantly decreased in IUGR placentas (**Figure 6**). We previously reported phosphorylated Akt (Ser-473), a placental mTORC2 signaling functional readout, was reduced considerably in IUGR placentas compared to AGA (Chen et al., 2015). The protein expression of mTORC2 signaling was negatively correlated with leptin, VEGF-A, IL-6 in AGA, and IUGR placentas (**Figure 5**). In addition, we further validated the protein expression of leptin, VEGF-A, IL-6 in PHT cells silenced with scrmble and rictor siRNA by Western blotting as described in **Supplementary Methods**. As shown in **Figure 6**, silencing of rictor increased the protein expression of leptin ($p = 0.003$), VEGF-A ($p = 0.01$), IL-6 ($p = 0.04$) in PHT cells as compared to control (Scramble siRNA). This findings validate the transcriptome findings and also reinforce the translation of those findings with those from AGA and IUGR human placenta.

TABLE 5 | Up-regulated KEGG pathways in PHT cells in response to rictor silencing.

KEGG pathways up	List	Up	Down	Gene set	z-score (Up)
Circadian rhythm—mammal	2	2	0	22	3.36
Ether lipid metabolism	2	2	0	33	2.53
Jak-STAT signaling pathway	6	5	1	154	2.31
Mismatch repair	3	2	1	22	3.36
Nucleotide excision repair	4	3	1	43	3.44
p53 signaling pathway	3	3	0	68	2.41
Pancreatic cancer	4	3	1	70	2.34
Regulation of autophagy	2	2	0	33	2.53
Systemic lupus erythematosus	6	5	1	130	2.75
Ubiquitin mediated proteolysis	6	6	0	135	3.44
VEGF signaling pathway	4	3	1	73	2.26

Table lists KEGG pathways that were significantly up regulated in PHT cells with rictor silencing as compared to control cells; "List" denotes the total number of differentially expressed genes on the array. "Up" denotes the number of up-regulated genes; "Down" denotes the number of down-regulated genes; "Gene set" denotes the total number of genes in this pathway that are included on the array and give a signal with PHT cell RNA; and "Z-score" denotes the z-score for the list pathway. The significance of identified KEGG pathways was determined by Z-score. Pathways were considered significantly different between scramble and Rictor siRNA groups if the Z-score for that pathway was > 2.00. The number of experiments (n) denotes the number of placentas studied, n = 4 placenta/each group, rictor siRNA and scramble siRNA.

Additionally, the protein expression of mTORC2 signaling readout was positively associated with osteopontin and SLC5A6 in AGA and IUGR placentas (**Figure 6**).

DISCUSSION

Using gene silencing approaches, we report mTORC2 regulation of the trophoblast transcriptome in cultured primary human trophoblast cells, an experimental model system considered to be highly relevant to human pregnancy. mTORC2 inhibition predominantly resulted in up-regulation of genes (75% of the differentially expressed genes), and these genes encode primarily for pro-inflammatory (IL-6) and inflammatory signaling (SAPK/JNK). In contrast, genes involved in multivitamin transport were enriched among down-regulated genes following rictor silencing. Furthermore, placental gene expression of leptin, VEGF-A, and IL-6 were increased, whereas osteopontin and sodium-dependent multivitamin transporter were decreased following mTORC2 inhibition. To further demonstrate the clinical relevance of these findings, we show that mTORC2 signaling activity was negatively correlated to protein expression of leptin, VEGF-A, and IL-6 in placentas from pregnancies complicated by IUGR. In contrast, mTORC2 signaling activity was positively associated with osteopontin and sodium-dependent multivitamin transporter protein expression in placentas from pregnancies complicated by IUGR. This suggests that our findings in genetically manipulated cultured trophoblast cells have relevance to clinically important pregnancy complications.

Protein ubiquitination, which functions as a signal for trafficking proteins to the proteasome for subsequent degradation, appears to activate PHT cells following mTORC2 inhibition. Recent studies suggest that ubiquitin-specific proteases act as novel mTORC1 and −2 binding partners that negatively regulate mTOR activity (Agrawal et al., 2012). In addition, it has been previously shown that protein ubiquitination is altered in IUGR, specifically as a cause of increased oxidative stress, with accelerated degradation of p53 and Mcl-1 proteins, possibly contributing to placental insufficiency in IUGR (Rolfo et al., 2012).

We found increased LEP (leptin) gene expression among the most highly up-regulated genes by rictor siRNA silencing. IUGR is associated with increased placental leptin mRNA and leptin protein expression (Tzschoppe et al., 2011). Previous studies demonstrated that hypoxia is a potent stimulatory factor for placental leptin mRNA up−regulation (Grosfeld et al., 2002), mediated through a transcriptional mechanism likely to involve the HIF−1−dependent mechanism (Grosfeld et al., 2001). Leptin regulates placental growth, angiogenesis, and immune tolerance. The gene expression of *VEGF-A* (Vascular Endothelial Growth Factor A), which is known to play a role in vasculogenesis and angiogenesis, was up-regulated in response to mTORC2 inhibition. Previous studies demonstrated an elevated placental VEGF-A expression in IUGR pregnancy (Szentpeteri et al., 2013), which could be a secondary response to persistent hypoxia (Szentpeteri et al., 2013). Increased VEGF-A expression is associated with elevated placental syncytial knots (Azliana et al., 2017), a defining feature of maternal vascular mal-perfusion (Parks, 2018).

Moreover, global overexpression of VEGF-A resulted in severe abnormalities in heart development and embryonic lethality in mice (Miquerol et al., 2000). We demonstrated that protein expression of VEGF-A was higher in human IUGR placentas. It is possible that elevated VEGF-A expression in the IUGR placenta may decrease vascularization in placental villi and lead to reduced blood flow. Abnormal vascular development in the placental villi ultimately causes inadequate oxygen and nutrient transfer between mother and fetus. mTORC2 inactivation failed to mediate VEGF stimulated angiogenesis in endothelial cells (Farhan et al., 2015). Thus, mTORC2 signaling inhibition in IUGR placentas (Chen et al., 2015; Rosario et al., 2016a) is associated with elevated VEGF-A and leptin expression, which could be potentially responsible for the impaired angiogenesis

TABLE 6 | List of common DEG's between mTORC1 and mTORC2 inhibited PHT cells.

Gene ID	Gene name	Expression	
		mTORC1 inhibition	mTORC2 inhibition
ALDH1A1	Aldehyde dehydrogenase 1 family member A1	Down	Down
ARHGEF17	Rho guanine nucleotide exchange factor 17	Up	Up
BRI3BP	BRI3-binding protein	Down	Down
C16ORF70	Chromosome 16 open reading frame 70	Up	Up
C9ORF24	Chromosome 9 open reading frame 24	Up	Up
CADM4	Cell adhesion molecule 4	Up	Up
CMBL	Carboxymethylenebutenolidase	Down	Down
CMTM4	CKLF like MARVEL transmembrane domain containing 4	Down	Down
CPLX2	Complexin 2	Up	Up
CPZ	Carboxypeptidase Z	Up	Up
DEPDC5	DEP domain containing 5, GATOR1 subcomplex subunit	Up	Up
DNHD1	Dynein heavy chain domain 1	Up	Up
EXOC3L2	Exocyst complex component 3-like 2	Up	Up
FA2H	Fatty acid 2-hydroxylase	Up	Up
FPR1	Formyl peptide receptor 1	Down	Down
GBP5	Guanylate-binding protein 5	Up	Up
GGCT	Gamma-glutamylcyclotransferase	Down	Down
GLUL	Glutamate-Ammonia Ligase	Down	Down
HLA-DQA2	Major histocompatibility complex, class II, DQ alpha 2	Up	Up
IL17REL	Interleukin 17 receptor E like	Up	Up
IL6	Interleukin 6	Up	Up
KCNC4	Potassium voltage-gated channel subfamily C member 4	Down	Down
KLK1	Kallikrein 1	Up	Up
KLK15	Kallikrein related peptidase 15	Up	Up
LGALS3BP	Galectin-3-binding protein	Up	Up
LRRC16B	Leucine rich repeat containing 1	Down	Down
MASP1	Mannan binding lectin serine peptidase 1	Up	Up
MCM8	Minichromosomal maintenance 8 homologous recombination repair factor	Up	Up
MDM2	Murine double minute 2	Up	Up
MREG	Melanoregulin	Down	Down
NETO1	Neuropilin and tolloid like 1	Up	Up
NFKBIZ	NFKB inhibitor zeta	Up	Up
OR4L1	Olfactory receptor family 4 subfamily L member 1	Up	Up
OXNAD1	Oxidoreductase NAD binding domain containing 1	Down	Down
PJA1	Praja ring finger ubiquitin ligase 1	Up	Up
PPM1A	Protein phosphatase 1A	Down	Up
PTTG1	PTTG1 Regulator of sister chromatid separation, securin	Down	Down
RABGAP1L	RAB GTPase activating protein 1 like	Down	Down
RASAL3	RAS protein activator like 3	Up	Up
RASL10B	RAS like family 10 member B	Up	Up
RCE1	Ras converting enzyme 1	Up	Up
SCN1B	Sodium voltage-gated channel beta subunit 1	Up	Up
SCN3B	Sodium voltage-gated channel beta subunit 3	Up	Up
SH2B1	SH2B adaptor protein 1	Up	Up
SLC13A1	Solute carrier family 13 (sodium/sulfate symporters)	Up	Up
SLC5A6	Solute carrier family 5 member 6	Down	Down
SLC5A8	Sodium-coupled monocarboxylate transporter 1	Up	Up
SMOX	Spermine Oxidase	Up	Up
SPINK9	Serine peptidase inhibitor kazal type 9	Up	Up
SPP1	Osteopontin	Down	Down
TYMP	Thymidine phosphorylase	Down	Down

(Continued)

TABLE 6 | (Continued)

Gene ID	Gene name	Expression	
		mTORC1 inhibition	mTORC2 inhibition
UBQLNL	Ubiquitin like	Up	Up
ZC3H14	Zinc finger CCCH-type containing 14	Down	Down
ZNRD1	Zinc ribbon gene	Down	Up
SEPN1	Selenoprotein N, 1	Down	Down
PCTK3	PCTAIRE protein kinase 3	Down	Down
DOPEY2	Dopey family member 2	Down	Down
WRB	Tryptophan rich basic protein	Down	Down
MESD	Mesoderm development candidate 2	Down	Down

in IUGR placentas. Collectively, these data implicate trophoblast mTORC2 in the regulation of placental angiogenesis.

We observed a significant increase in the transcript levels of genes encoding IL-6 signaling pathways in response to mTORC2 inhibition in PHT cells, which confirms previous findings demonstrating that loss of *rictor* in monocytes/macrophages activated IL-6 signaling (Babaev et al., 2018). Placental IL-6 mRNA and corresponding peptide levels were reported to be increased in IUGR pregnancy (Street et al., 2006). Additionally, IL-6 transcript increased in pregnancy complications associated with placental infection (Fedorka et al., 2020). Recent studies demonstrate that IL-6 activation in the placenta is necessary to relay inflammatory signals to the fetal brain and impact behaviors and neuropathologies relevant to neurodevelopmental disease (Wu et al., 2017). However, the lack of IL-6 signaling in trophoblasts effectively blocks maternal immune activation-induced inflammatory responses in the placenta and the fetal brain (Wu et al., 2017; Aguilar-Valles et al., 2020). Moreover, placental AKT/mTOR signaling is a possible mechanistic link to impaired neural circuit development and neurocognitive function (Howell and Law, 2020). We observed a negative correlation between placental mTORC2 signaling and IL-6 expression in placentas of IUGR pregnancies. Furthermore, we demonstrated that protein expression of IL-6 was higher in human IUGR placentas. We have previously shown that placental mTORC2 signaling is reduced in pregnancies complicated by IUGR (Chen et al., 2015) and speculate that the placenta's aberrant mTORC2/IL6 signaling pathway may impair the fetal brain development in IUGR infants.

Osteopontin (SPP1), which belongs to the small integrin-binding ligand N-linked glycoprotein (SIBLING) family of extracellular matrix proteins and cytokines, has been reported to play multiple functions including cell proliferation, cell invasion, cell adhesion (Wu and Wang, 2016). It plays an essential role in embryo development in the mouse (Weintraub et al., 2004). Furthermore, osteopontin promotes invasion (Ke et al., 2020) and angiogenesis in the trophoblast and other cells (Li et al., 2021). Phosphatidylinositol 3-kinase (PI3K) is a heterodimer containing a regulatory subunit (p85) and a catalytic subunit (p110). The p85 regulatory subunit is essential for the p110 catalytic subunit's stability and mediates the binding, activation, and localization of the PI3K enzyme (Luo et al., 2005). PI3K regulates growth in relation to nutrient supply (Engelman et al., 2006). In mice, inactivating p110α kinase causes growth-restriction at term (Foukas et al., 2006). Lopez-Tello et al. (2019) demonstrated that silencing of trophoblast p110α resulted in abnormal placental and fetal development. Furthermore, p110α kinase deficiency impairs the placenta from transporting nutrients to match fetal demands for growth. We also compared our current study pathway analysis with the existing transcriptome of trophoblast silenced with PI3K signaling (Lopez-Tello et al., 2019). Interestingly, pathways regulating immune function were down-regulated in both mTORC2 (current study) and PI3K signaling inhibited trophoblast cells (Lopez-Tello et al., 2019). These data suggest that mTORC2 and PI3K signaling may cause an immune imbalance in the placenta and result in fetal growth restriction (Wang et al., 2020; McColl and Piquette-Miller, 2021). We observed a decreased gene expression of the Osteopontin and PIK3R1 in *rictor* silenced cells. We have shown that mTORC2 signaling (Chen et al., 2015) and osteopontin (current study) expression is reduced in human IUGR placentas. We speculate that osteopontin and PI3K inhibition, mediated by reduced mTORC2 activity, may contribute to placental insufficiency and reduced fetal growth in IUGR.

Biotin is essential for normal fetal development and is provided to the fetus by transport across the placenta from

TABLE 7 | Selected clinical data.

	AGA (*n* = 19)	IUGR (*n* = 25)
Maternal age (years)	25.9 ± 1.29	28.7 ± 1.23
BMI (kg/m^2) *	28.3 ± 2.6	26.8 ± 2.0
Gestational age (weeks)	33.9 ± 0.95	35.7 ± 0.61
Birth weight (g)	2,493 ± 236	1,804 ± 110†
Birth weight percentile‡	55.9 ± 4.6	2.4 ± 0.3§
Placental weight (g)	566 ± 42.0	394 ± 18.4$^{\|}$
Fetal sex (M/F)	7/12	8/17
Mode of delivery (C/V)	6/13	15/10

*Data are presented as means ± SEM. AGA, appropriate grown for gestational age; IUGR, intrauterine growth restriction; F, female; M, male; C, cesarean section; V, vaginal delivery. *Data from n = 10 AGA and 18 IUGR; ‡by corresponding gestational age; $^{\dagger}P < 0.05$; $^{\|}P < 0.01$; $^{\S}P < 0.0001$.*

Maternal BMI (kg/m^2) was calculated using maternal weight and height measurements taken during the first (10–12 weeks) trimesters.

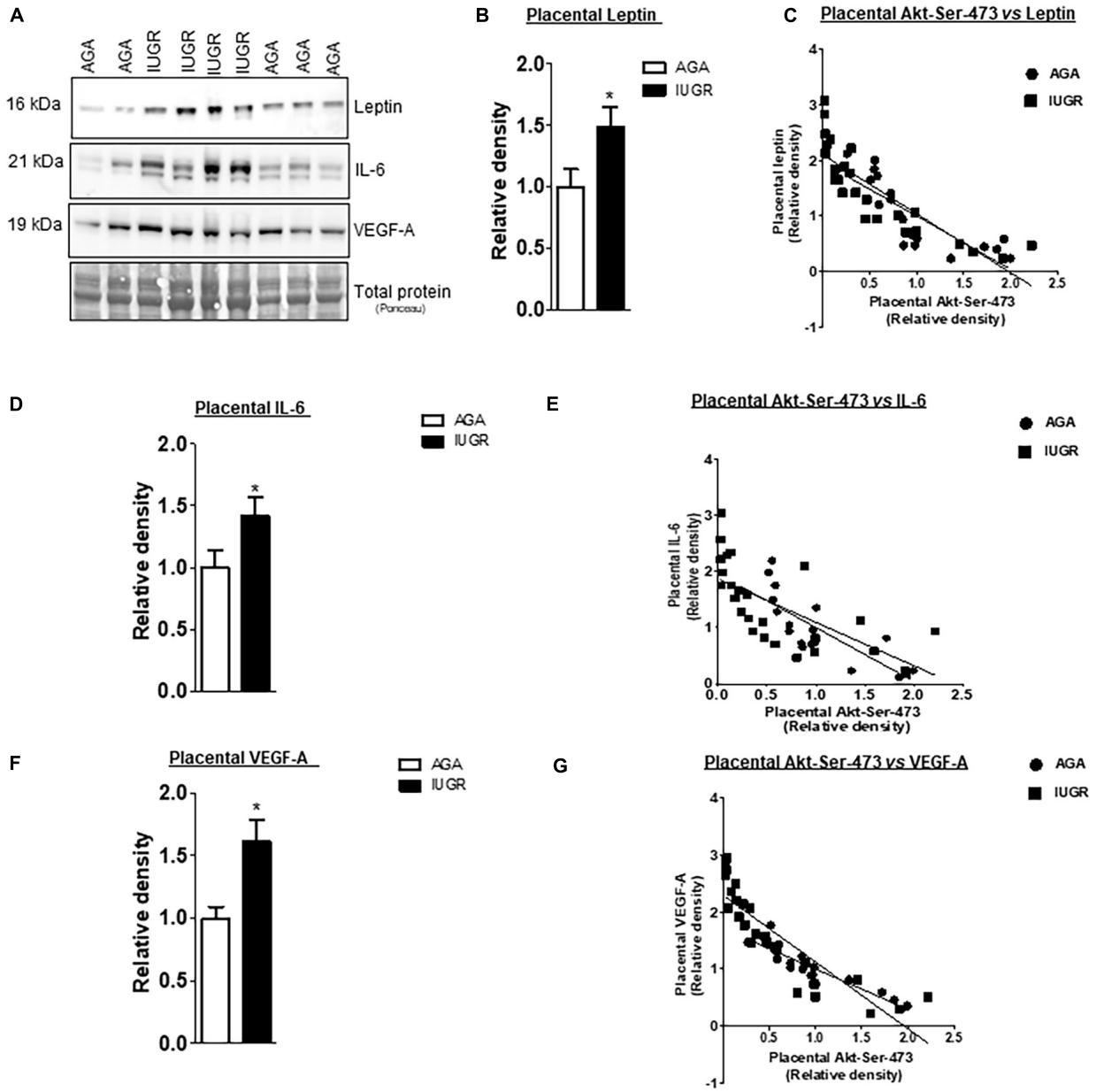

FIGURE 5 | Correlation between placental mTORC2 functional readouts and the protein expression of leptin, VEGF-A and IL-6. **(A)** Representative western blots of leptin, IL-6 and VEGF-A expression in homogenates of AGA and IUGR placentas. Equal loading was performed. **(B,D,F)** Relative expression of leptin, VEGF-A and IL-6 in homogenates of AGA and IUGR placentas. *$P < 0.05$ vs. AGA, unpaired Student's *t*-test. **(C,E,G)** Correlation between placental mTORC2 functional readouts $AKT^{Ser-473}$ and leptin, VEGF-A and IL-6 expression. r = Pearson correlation coefficient, n = AGA, 19; IUGR, 25. Pearson correlation analysis was used to examine the relation among the investigated factors (GraphPad Prism version 5). Leptin, AGA, $r = 0.6403$, $p = 0.0001$; IUGR $r = 0.7121$, $p = 0.0001$. VEGF-A, AGA, $r = 0.8569$, $p = 0.0001$; IUGR $r = 0.7706$, $p = 0.0001$. IL-6, AGA, $r = 0.6560$, $p = 0.0001$; IUGR $r = 0.4379$, $p = 0.0001$.

the mother. Biotin transport in the human placenta is mediated by Na^+-dependent multivitamin transporter (encoded by SLC5A6 gene) (Noam et al., 2020). Fetuses of biotin deficient mouse dams demonstrate fetal growth restriction (Levin et al., 1985). In the present study, we found a positive correlation between mTORC2 signaling and the protein expression of SLC5A6 in the IUGR placenta. We have also recently demonstrated that placental mTOR signaling regulates trophoblast folate transporter expression at the post-translational level by modulating the plasma membrane trafficking of specific transporter isoforms (Rosario et al., 2016b). Together with the demonstration in the current study that mTORC2 regulates specific trophoblast nutrient transporters at the transcriptional level, these findings suggest that trophoblast mTOR is a master regulator of a range of placental nutrient transporters mediated by distinct molecular mechanisms.

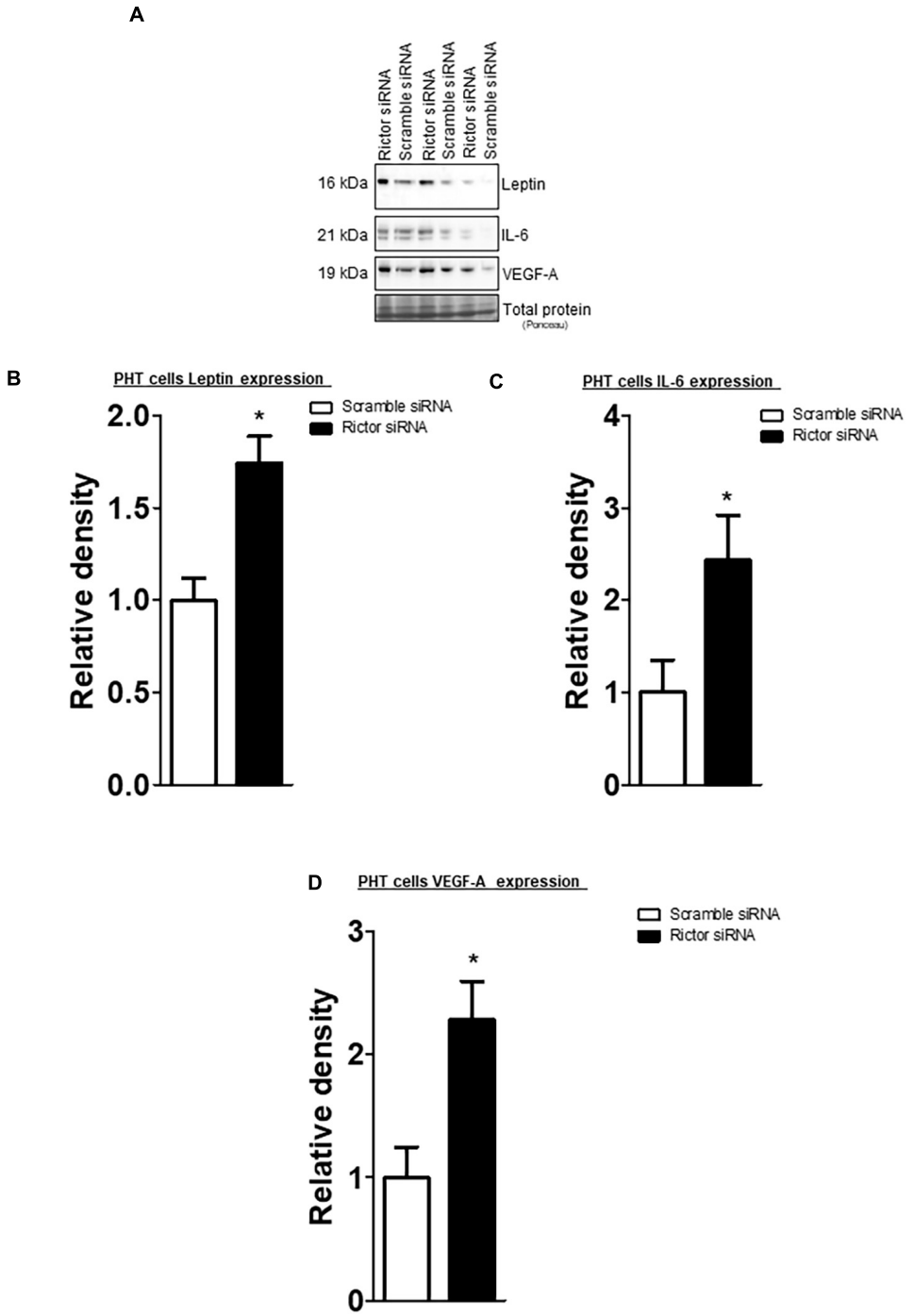

FIGURE 6 | Effect of rictor silencing on leptin, IL-6 and VEGF-A protein expression in PHT cells. **(A)** Representative western blots of leptin, IL-6 and VEGF-A expression in cell lysates of scramble siRNA and rictor siRNA silenced PHT cells. Equal loading was performed. **(B–D)** Summary of the western blot data leptin, IL-6 and VEGF-A protein. Values are given as means + SEM. *$P < 0.05$ vs. scramble siRNA; unpaired Student's *t*-test; $n = 5$/each group.

One potential limitation of using a single Rictor siRNA to inhibit the mTORC2 signaling could lead to off-target consequences as described elsewhere (Gagnon and Corey, 2019). On the other hand, BlastN analysis revealed that our Rictor siRNA sequence did not complement another gene sequence. In addition, we previously showed that inhibition of mTORC2 signaling by utilizing a single Rictor siRNA sequence in PHT cells did not alter mTORC1 signaling (Rosario et al., 2013), implying that Rictor silencing is highly specific in targeting mTORC2 signaling. Furthermore, we showed that co-transfection of Raptor

siNA (to silence mTORC1 signaling) with DEPTOR siRNA (endogenous inhibitor of mTORC1 and mTORC2 signaling) to activate mTORC2 signaling in PHT cells. Notably, activating the mTORC2 signaling stimulated the PHT cell function, such as amino acid transport, which our Rictor siRNA decreases. These findings strongly suggest that the Rictor siRNA employed suppresses mTORC2 signaling specifically, with no substantial off-target effects.

CONCLUSION

We demonstrate that mTORC2 signaling regulates the expression of trophoblast genes involved in pro-inflammatory, inflammatory, and micronutrient transport and angiogenesis, representing novel links between mTOR signaling and placental functions critical for normal fetal growth and development. Furthermore, because placental mTOR signaling is inhibited in IUGR and activated in fetal overgrowth, we propose regulating the placental transcriptome by mTOR signaling directly contributes to altered placental function and fetal growth in common pregnancy complications. Thus, our findings provide clues for the underlying etiology of IUGR, which ultimately could translate into a novel therapeutic approach.

DATA AVAILABILITY STATEMENT

The datasets presented in this study can be found in online repositories. The names of the repository/repositories and accession number(s) can be found in the article/**Supplementary Material**.

ETHICS STATEMENT

The studies involving human participants were reviewed and approved by the University of Texas Health Science Center. The patients/participants provided their written informed consent to participate in this study.

AUTHOR CONTRIBUTIONS

FR, LC, TJ, MG, and TP contributed to the experiments' conception and design and performed collection, analysis, and data interpretation. ACK and FR performed bioinformatics analysis. FR, ACK, TJ, and TP wrote the manuscript. All authors approved the final version of the manuscript.

FUNDING

This study was supported by the grants from NIH (R01HD68370).

ACKNOWLEDGMENTS

We thank Kathryn Erickson for her support in making graphs.

SUPPLEMENTARY MATERIAL

The Supplementary Material for this article can be found online at: https://www.frontiersin.org/articles/10.3389/fcell.2021.670980/full#supplementary-material

REFERENCES

Agrawal, P., Chen, Y. T., Schilling, B., Gibson, B. W., and Hughes, R. E. (2012). Ubiquitin-specific peptidase 9, X-linked (USP9X) modulates activity of mammalian target of rapamycin (mTOR). *J. Biol. Chem.* 287, 21164–21175. doi: 10.1074/jbc.m111.328021

Aguilar-Valles, A., Rodrigue, B., and Matta-Camacho, E. (2020). Maternal immune activation and the development of dopaminergic neurotransmission of the offspring: relevance for schizophrenia and other psychoses. *Front. Psychiatry* 11:852. doi: 10.3389/fpsyt.2020.00852

Azliana, A. F., Zainul-Rashid, M. R., Chandramaya, S. F., Farouk, W. I., Nurwardah, A., Wong, Y. P., et al. (2017). Vascular endothelial growth factor expression in placenta of hypertensive disorder in pregnancy. *Indian J. Pathol. Microbiol.* 60, 515–520. doi: 10.4103/ijpm.ijpm_376_16

Babaev, V. R., Huang, J., Ding, L., Zhang, Y., May, J. M., and Linton, M. F. (2018). Loss of rictor in monocyte/macrophages suppresses their proliferation and viability reducing atherosclerosis in LDLR null mice. *Front. Immunol.* 9:215. doi: 10.3389/fimmu.2018.00215

Barker, D. J., Gluckman, P. D., Godfrey, K. M., Harding, J. E., Owens, J. A., and Robinson, J. S. (1993). Fetal nutrition and cardiovascular disease in adult life. *Lancet* 341, 938–941. doi: 10.1016/0140-6736(93)91224-a

Burton, G. J., Fowden, A. L., and Thornburg, K. L. (2016). Placental origins of chronic disease. *Physiol. Rev.* 96, 1509–1565. doi: 10.1152/physrev.00029.2015

Burton, G. J., and Jauniaux, E. (2015). What is the placenta? *Am. J. Obstet. Gynecol.* 213, S6–S8.

Chen, Y. Y., Rosario, F. J., Shehab, M. A., Powell, T. L., Gupta, M. B., and Jansson, T. (2015). Increased ubiquitination and reduced plasma membrane trafficking of placental amino acid transporter SNAT-2 in human IUGR. *Clin. Sci.* 129, 1131–1141. doi: 10.1042/cs20150511

Engelman, J. A., Luo, J., and Cantley, L. C. (2006). The evolution of phosphatidylinositol 3-kinases as regulators of growth and metabolism. *Nat. Rev. Genet.* 7, 606–619. doi: 10.1038/nrg1879

Farhan, M. A., Carmine-Simmen, K., Lewis, J. D., Moore, R. B., and Murray, A. G. (2015). Endothelial cell mTOR complex-2 regulates sprouting angiogenesis. *PLoS One* 10:e0135245. doi: 10.1371/journal.pone.0135245

Fedorka, C. E., Scoggin, K. E., El-Sheikh Ali, H., Loux, S., Dini, P., Troedsson, M. H. T., et al. (2020). Interleukin-6 pathobiology in equine placental infection. *Am. J. Reprod. Immunol.* 85:e13363.

Forbes, K., Desforges, M., Garside, R., Aplin, J. D., and Westwood, M. (2009). Methods for siRNA-mediated reduction of mRNA and protein expression in human placental explants, isolated primary cells and cell lines. *Placenta* 30, 124–129. doi: 10.1016/j.placenta.2008.10.003

Foukas, L. C., Claret, M., Pearce, W., Okkenhaug, K., Meek, S., Peskett, E., et al. (2006). Critical role for the p110alpha phosphoinositide-3-OH kinase in growth and metabolic regulation. *Nature* 441, 366–370. doi: 10.1038/nature04694

Gagnon, K. T., and Corey, D. R. (2019). Guidelines for experiments using antisense oligonucleotides and double-stranded RNAs. *Nucleic Acid Ther.* 29, 116–122. doi: 10.1089/nat.2018.0772

Ge, S. X., Jung, D., and Yao, R. (2020). ShinyGO: a graphical gene-set enrichment tool for animals and plants. *Bioinformatics* 36, 2628–2629. doi: 10.1093/bioinformatics/btz931

Gluckman, P. D., and Hanson, M. A. (2004a). Living with the past: evolution, development, and patterns of disease. *Science* 305, 1733–1736. doi: 10.1126/science.1095292

Gluckman, P. D., and Hanson, M. A. (2004b). The developmental origins of the metabolic syndrome. *Trends Endocrinol. Metab.* 15, 183–187.

Gluckman, P. D., Hanson, M. A., Cooper, C., and Thornburg, K. L. (2008). Effect of in utero and early-life conditions on adult health and disease. *N. Engl. J. Med.* 359, 61–73. doi: 10.1056/nejmra0708473

Grosfeld, A., Turban, S., Andre, J., Cauzac, M., Challier, J. C., Hauguel-de Mouzon, S., et al. (2001). Transcriptional effect of hypoxia on placental leptin. *FEBS Lett.* 502, 122–126. doi: 10.1016/s0014-5793(01)02673-4

Grosfeld, A., Zilberfarb, V., Turban, S., Andre, J., Guerre-Millo, M., and Issad, T. (2002). Hypoxia increases leptin expression in human PAZ6 adipose cells. *Diabetologia* 45, 527–530. doi: 10.1007/s00125-002-0804-y

Guertin, D. A., Stevens, D. M., Thoreen, C. C., Burds, A. A., Kalaany, N. Y., Moffat, J., et al. (2006). Ablation in mice of the mTORC components raptor, rictor, or mLST8 reveals that mTORC2 is required for signaling to Akt-FOXO and PKCalpha, but not S6K1. *Dev. Cell* 11, 859–871. doi: 10.1016/j.devcel.2006.10.007

Guttmacher, A. E., Maddox, Y. T., and Spong, C. Y. (2014). The Human Placenta Project: placental structure, development, and function in real time. *Placenta* 35, 303–304. doi: 10.1016/j.placenta.2014.02.012

Howell, K. R., and Law, A. J. (2020). Neurodevelopmental concepts of schizophrenia in the genome-wide association era: AKT/mTOR signaling as a pathological mediator of genetic and environmental programming during development. *Schizophr. Res.* 217, 95–104. doi: 10.1016/j.schres.2019.08.036

Jansson, N., Rosario, F. J., Gaccioli, F., Lager, S., Jones, H. N., Roos, S., et al. (2013). Activation of placental mTOR signaling and amino acid transporters in obese women giving birth to large babies. *J. Clin. Endocrinol. Metab.* 98, 105–113. doi: 10.1210/jc.2012-2667

Jansson, T., and Powell, T. L. (2007). Role of the placenta in fetal programming: underlying mechanisms and potential interventional approaches. *Clin. Sci.* 113, 1–13. doi: 10.1042/cs20060339

Kanehisa, M., Furumichi, M., Tanabe, M., Sato, Y., and Morishima, K. (2017). KEGG: new perspectives on genomes, pathways, diseases and drugs. *Nucleic Acids Res.* 45, D353–D361.

Kanehisa, M., and Goto, S. (2000). KEGG: kyoto encyclopedia of genes and genomes. *Nucleic Acids Res.* 28, 27–30.

Kanehisa, M., Sato, Y., Kawashima, M., Furumichi, M., and Tanabe, M. (2016). KEGG as a reference resource for gene and protein annotation. *Nucleic Acids Res.* 44, D457–D462.

Kavitha, J. V., Rosario, F. J., Nijland, M. J., McDonald, T. J., Wu, G., Kanai, Y., et al. (2014). Down-regulation of placental mTOR, insulin/IGF-I signaling, and nutrient transporters in response to maternal nutrient restriction in the baboon. *FASEB J.* 28, 1294–1305. doi: 10.1096/fj.13-242271

Ke, R., Zheng, L., Zhao, F., and Xia, J. (2020). Osteopontin promotes trophoblast invasion in the smooth muscle cell-endothelial co-culture at least via targeting integrin alphavbeta3. *Cell Transplant.* 29:963689720965979.

Kelly, A. C., Kramer, A., Rosario, F. J., Powell, T. L., and Jansson, T. (2020). Inhibition of mechanistic target of rapamycin signaling decreases levels of O-GlcNAc transferase and increases serotonin release in the human placenta. *Clin. Sci.* 134, 3123–3136. doi: 10.1042/cs20201050

Kim, D. H., Sarbassov, D. D., Ali, S. M., King, J. E., Latek, R. R., Erdjument-Bromage, H., et al. (2002). mTOR interacts with raptor to form a nutrient-sensitive complex that signals to the cell growth machinery. *Cell* 110, 163–175. doi: 10.1016/s0092-8674(02)00808-5

Kramer, A., Green, J., Pollard, J. Jr., and Tugendreich, S. (2014). Causal analysis approaches in ingenuity pathway analysis. *Bioinformatics* 30, 523–530. doi: 10.1093/bioinformatics/btt703

Levin, S. W., Roecklein, B. A., and Mukherjee, A. B. (1985). Intrauterine growth retardation caused by dietary biotin and thiamine deficiency in the rat. *Res. Exp. Med.* 185, 375–381. doi: 10.1007/bf01851917

Li, Y., Guo, S., Zhao, K., Conrad, C., Driescher, C., Rothbart, V., et al. (2021). ADAM8 affects glioblastoma progression by regulating osteopontin-mediated angiogenesis. *Biol. Chem.* 402, 195–206. doi: 10.1515/hsz-2020-0184

Lopez-Tello, J., Perez-Garcia, V., Khaira, J., Kusinski, L. C., Cooper, W. N., Andreani, A., et al. (2019). Fetal and trophoblast PI3K p110alpha have distinct roles in regulating resource supply to the growing fetus in mice. *eLife* 8:e45282.

Luo, J., Field, S. J., Lee, J. Y., Engelman, J. A., and Cantley, L. C. (2005). The p85 regulatory subunit of phosphoinositide 3-kinase down-regulates IRS-1 signaling via the formation of a sequestration complex. *J. Cell Biol.* 170, 455–464. doi: 10.1083/jcb.200503088

McColl, E. R., and Piquette-Miller, M. (2021). Viral model of maternal immune activation alters placental AMPK and mTORC1 signaling in rats. *Placenta* 112, 36–44. doi: 10.1016/j.placenta.2021.07.002

Miquerol, L., Langille, B. L., and Nagy, A. (2000). Embryonic development is disrupted by modest increases in vascular endothelial growth factor gene expression. *Development* 127, 3941–3946. doi: 10.1242/dev.127.18.3941

Noam, B. E., Marina, L., Inbal, B. E., Ofra, G., Jennifer, B. L., Solana, F. R., et al. (2020). Novel multimodal molecular imaging of Vitamin H (Biotin) transporter activity in the murine placenta. *Sci. Rep.* 10:20767.

Parks, W. T. (2018). "Increased syncytial knot formation," in *Pathology of the Placenta*, eds T. Khong, P. Nikkels, T. Morgan, and S. Gordijn (Cham: Springer), 131–137. doi: 10.1007/978-3-319-97214-5_17

Rolfo, A., Garcia, J., Todros, T., Post, M., and Caniggia, I. (2012). The double life of MULE in preeclamptic and IUGR placentae. *Cell Death Dis.* 3:e305. doi: 10.1038/cddis.2012.44

Rosario, F. J., Kanai, Y., Powell, T. L., and Jansson, T. (2015b). Increased placental nutrient transport in a novel mouse model of maternal obesity with fetal overgrowth. *Obesity* 23, 1663–1670. doi: 10.1002/oby.21165

Rosario, F. J., Dimasuay, K. G., Kanai, Y., Powell, T. L., and Jansson, T. (2015a). Regulation of amino acid transporter trafficking by mTORC1 in primary human trophoblast cells is mediated by the ubiquitin ligase Nedd4-2. *Clin Sci* 130, 499–512. doi: 10.1042/cs20150554

Rosario, F. J., Dimasuay, K. G., Kanai, Y., Powell, T. L., and Jansson, T. (2016a). Regulation of amino acid transporter trafficking by mTORC1 in primary human trophoblast cells is mediated by the ubiquitin ligase Nedd4-2. *Clin. Sci.* 130, 499–512.

Rosario, F. J., Powell, T. L., and Jansson, T. (2016b). Mechanistic target of rapamycin (mTOR) regulates trophoblast folate uptake by modulating the cell surface expression of FR-alpha and the RFC. *Sci. Rep.* 6:31705.

Rosario, F. J., Jansson, N., Kanai, Y., Prasad, P. D., Powell, T. L., and Jansson, T. (2011). Maternal protein restriction in the rat inhibits placental insulin, mTOR, and STAT3 signaling and down-regulates placental amino acid transporters. *Endocrinology* 152, 1119–1129. doi: 10.1210/en.2010-1153

Rosario, F. J., Kanai, Y., Powell, T. L., and Jansson, T. (2013). Mammalian target of rapamycin signalling modulates amino acid uptake by regulating transporter cell surface abundance in primary human trophoblast cells. *J. Physiol.* 591, 609–625. doi: 10.1113/jphysiol.2012.238014

Rosario, F. J., Powell, T. L., Gupta, M. B., Cox, L., and Jansson, T. (2020). mTORC1 transcriptional regulation of ribosome subunits, protein synthesis, and molecular transport in primary human trophoblast cells. *Front. Cell Dev. Biol.* 8:583801. doi: 10.3389/fcell.2020.583801

Sandovici, I., Hoelle, K., Angiolini, E., and Constancia, M. (2012). Placental adaptations to the maternal-fetal environment: implications for fetal growth and developmental programming. *Reprod. Biomed. Online* 25, 68–89. doi: 10.1016/j.rbmo.2012.03.017

Sarbassov, D. D., Ali, S. M., Kim, D. H., Guertin, D. A., Latek, R. R., Erdjument-Bromage, H., et al. (2004). Rictor, a novel binding partner of mTOR, defines a rapamycin-insensitive and raptor-independent pathway that regulates the cytoskeleton. *Curr. Biol.* 14, 1296–1302. doi: 10.1016/j.cub.2004.06.054

Street, M. E., Seghini, P., Fieni, S., Ziveri, M. A., Volta, C., Martorana, D., et al. (2006). Changes in interleukin-6 and IGF system and their relationships in placenta and cord blood in newborns with fetal growth restriction compared with controls. *Eur. J. Endocrinol.* 155, 567–574. doi: 10.1530/eje.1.02251

Szentpeteri, I., Rab, A., Kornya, L., Kovacs, P., and Joo, J. G. (2013). Gene expression patterns of vascular endothelial growth factor (VEGF-A) in human placenta from pregnancies with intrauterine growth restriction. *J. Matern. Fetal Neonatal Med.* 26, 984–989. doi: 10.3109/14767058.2013.766702

Tzschoppe, A., Struwe, E., Rascher, W., Dorr, H. G., Schild, R. L., Goecke, T. W., et al. (2011). Intrauterine growth restriction (IUGR) is associated with increased leptin synthesis and binding capability in neonates. *Clin. Endocrinol.* 74, 459–466. doi: 10.1111/j.1365-2265.2010.03943.x

Wang, X., Zhu, H., Lei, L., Zhang, Y., Tang, C., Wu, J. X., et al. (2020). Integrated analysis of key genes and pathways involved in fetal growth restriction and their associations with the dysregulation of the maternal immune system. *Front. Genet.* 11:581789. doi: 10.3389/fgene.2020.581789

Weintraub, A. S., Lin, X., Itskovich, V. V., Aguinaldo, J. G., Chaplin, W. F., Denhardt, D. T., et al. (2004). Prenatal detection of embryo resorption in osteopontin-deficient mice using serial noninvasive magnetic resonance microscopy. *Pediatr. Res.* 55, 419–424. doi: 10.1203/01.pdr.0000112034.98387.b2

Wu, J., and Wang, Z. (2016). Osteopontin improves adhesion and migration of human primary renal cortical epithelial cells during wound healing. *Oncol. Lett.* 12, 4556–4560. doi: 10.3892/ol.2016.5219

Wu, W. L., Hsiao, E. Y., Yan, Z., Mazmanian, S. K., and Patterson, P. H. (2017). The placental interleukin-6 signaling controls fetal brain development and behavior. *Brain Behav. Immun.* 62, 11–23. doi: 10.1016/j.bbi.2016.11.007

Wullschleger, S., Loewith, R., and Hall, M. N. (2006). TOR signaling in growth and metabolism. *Cell* 124, 471–484.

Yang, Q., and Guan, K. L. (2007). Expanding mTOR signaling. *Cell Res.* 17, 666–681.

Conflict of Interest: The authors declare that the research was conducted in the absence of any commercial or financial relationships that could be construed as a potential conflict of interest.

Publisher's Note: All claims expressed in this article are solely those of the authors and do not necessarily represent those of their affiliated organizations, or those of the publisher, the editors and the reviewers. Any product that may be evaluated in this article, or claim that may be made by its manufacturer, is not guaranteed or endorsed by the publisher.

Advantages of publishing in Frontiers

OPEN ACCESS
Articles are free to read for greatest visibility and readership

FAST PUBLICATION
Around 90 days from submission to decision

HIGH QUALITY PEER-REVIEW
Rigorous, collaborative, and constructive peer-review

TRANSPARENT PEER-REVIEW
Editors and reviewers acknowledged by name on published articles

Frontiers
Avenue du Tribunal-Fédéral 34
1005 Lausanne | Switzerland

Visit us: www.frontiersin.org
Contact us: frontiersin.org/about/contact

REPRODUCIBILITY OF RESEARCH
Support open data and methods to enhance research reproducibility

DIGITAL PUBLISHING
Articles designed for optimal readership across devices

FOLLOW US
@frontiersin

IMPACT METRICS
Advanced article metrics track visibility across digital media

EXTENSIVE PROMOTION
Marketing and promotion of impactful research

LOOP RESEARCH NETWORK
Our network increases your article's readership